MONASH University

BIASED AGONISM AT THE μ-OPIOID RECEPTOR

Georgina Thompson

Bachelor of Science (Honours)

A thesis submitted for the degree of Doctor of Philosophy

Drug Discovery Biology Theme

Monash Institute of Pharmacology

2016

COPYRIGHT NOTICE

CONTENTS

ABSTRACT

The μ opioid receptor (MOP) is the main therapeutic target for the most clinically useful class of analgesics for treating severe acute and chronic pain, despite the numerous associated side effects that limit their use. The property of G protein-coupled receptors (GPCRs) where different ligands stabilise the receptor into unique active conformations, which can result in differential activation of cell signalling pathways and, eventually, in different physiological outcomes is known as biased agonism. Biased agonism is a natural phenomenon that has been observed at other neuropeptide receptors that, like the opioid system, have multiple endogenous ligands targeting the same receptor. This property of GPCRs can be exploited to design drugs that selectively activate signalling pathways that lead to the desired physiological effects whilst minimising side effects that are elicited by activation of other signalling pathways.

Quantification of biased agonism of endogenous opioids at MOP across multiple different signalling pathways using the transduction coefficient ratio [$\Delta\Delta\log(\tau/K_A)$] method was performed in a common cellular background. This has revealed that this family of peptides possess a diverse range of signalling profiles. Met-enk-RF, endomorphin-1 and α-neoendorphin in particular showed unique bias profiles when compared to the synthetic ligand DAMGO, whereas most other endogenous peptides showed bias profiles more similar to DAMGO. This diversity in bias among endogenous opioids, may enable the endogenous opioid system to have an unprecedented level of control to fine-tune MOP mediated physiology.

There are a number of factors that need to be taken into consideration when quantifying biased agonism, such as the spatiotemporal kinetics of the signalling pathways. The spatiotemporal kinetics of extracellular signal regulated kinase (ERK) activation by morphine and DAMGO was examined in dorsal root ganglia neurons. This showed that morphine stimulates sustained activation of cytosolic ERK via a PKC dependent pathway, whereas DAMGO stimulates transient activation of cytosolic and nuclear ERK. Similarly, examination of the kinetics of cAMP inhibition in CHO-MOP cells revealed that the cAMP kinetic profile of Met-enk-RF is distinct from that of DAMGO and other endogenous ligands, which results in a significant change in bias of Met-enk-RF depending on the time point chosen to measure cAMP inhibition. Additionally, bias between activation of different G protein subtypes was quantified at different time

points, which showed that the bias of Met-enk-RF and α-neoendorphin changed over time. Overall, the spatiotemporal characteristics of the signalling pathways can have a significant impact on the observed bias of a ligand.

The impact of the cellular background on the quantification of bias was also investigated by quantifying biased agonism of the same ligands in different cell backgrounds. This revealed that even altering the expression level of a single signalling protein can change the observed bias of a ligand, where overexpression of GRK2 in CHO-MOP cells altered the bias of endomorphin-1 between inhibition of cAMP and β-arrestin recruitment. However, when biased agonism was quantified across multiple signalling pathways in different cell types, CHO-MOP and AtT20-MOP, despite the fact the overall bias profiles changed significantly between cell lines, ligands with unique bias profiles retained uniqueness. Thus suggesting that these pluridimensional bias profiles can be used to predict *in vivo* bias indirectly via ligand clustering.

GENERAL DECLARATION

Monash University

Declaration for thesis based or partially based on conjointly published or unpublished work

In accordance with Monash University Doctorate Regulation 17.2 Doctor of Philosophy and Research Master's regulations the following declarations are made:

I hereby declare that this thesis contains no material which has been accepted for the award of any other degree or diploma at any university or equivalent institution and that, to the best of my knowledge and belief, this thesis contains no material previously published or written by another person, except where due reference is made in the text of the thesis.

This thesis includes 4 original papers published in peer reviewed journals and 1 unpublished publication. The core theme of the thesis is quantification of biased agonism at the μ-opioid receptor. The ideas, development and writing up of all the papers in the thesis were the principal responsibility of myself, the candidate, working within the Drug Discovery Biology Laboratory under the supervision of Dr Meritxell Canals.

[The inclusion of co-authors reflects the fact that the work came from active collaboration between researchers and acknowledges input into team-based research.]

In the case of chapters 1-4 my contribution to the work involved the following:

Thesis chapter	Publication title	Publication status*	Nature and extent of candidate's contribution
1	Biological redundancy of the endogenous GPCR ligands in the gut and the potential for endogenous functional selectivity	Published	Contributed to writing of the manuscript
1	Novel GPCR Paradigms at the μ-opioid receptor	Published	Performed data analysis and wrote the manuscript
2	Biased agonism of endogenous opioid peptides at the μ-opioid receptor	Published	Participated in the design of the study, performed all experiments and analysis, and wrote the manuscript.
3	Systematic analysis of factors influencing observations of biased agonism at the μ-opioid receptor	Published	Participated in the design of the study, performed all experiments and analysis, and wrote the manuscript.
4	Plasma membrane localisation of MOP controls spatiotemporal signalling	Published	Performed and analysed FRET sensor experiments in dorsal root ganglia neurons.

I have / ~~have not~~ (circle that which applies) renumbered sections of submitted or published papers in order to generate a consistent presentation within the thesis.

Signed: … [redacted] ……

Date: …… 9 May 2016 ……

PUBLICATIONS DURING ENROLMENT

Thompson GL, Canals M and Poole DP (2014) Biological redundancy of endogenous GPCR ligands in the gut and the potential for endogenous functional selectivity. *Frontiers in pharmacology* **5**:262.

Thompson GL, Kelly E, Christopoulos A and Canals M (2015) Novel GPCR paradigms at the mu-opioid receptor. *Br J Pharmacol* **172**:287-296.

Thompson GL, Lane JR, Coudrat T, Sexton PM, Christopoulos A and Canals M (2015) Biased agonism of endogenous opioid peptides at the mu-opioid receptor. *Mol Pharmacol.* **88**:335-346.

Thompson GL, Lane JR, Coudrat T, Sexton PM, Christopoulos A and Canals M (2016) Systematic analysis of factors influencing observations of biased agonism at the mu-opioid receptor *Biochem. Pharmacol*. **113**:70–87

Halls ML, Yeatman HR, Nowell CJ, Thompson GL, Gondin AB, Civciristov S, Bunnett NW, Lambert NA, Poole DP and Canals M (2016) Plasma membrane localization of the μ-opioid receptor controls spatiotemporal signaling. *Science Signaling* **9**:ra16

ACKNOWLEDGEMENTS

I would like to acknowledge all those who provided assistance and support throughout my PhD. Firstly, I would particularly like to thank my supervisor Dr Merixell Canals for being the ideal mentor I've always needed, and for her patience, motivation, expertise and confidence in me. And also Prof. Arthur Christopoulos for his incredible knowledge, unfailing enthusiasm and uncanny ability to make everything much clearer.

I would like to express my gratitude to my PhD advisors: Prof. MacDonald Christie and Prof. Nigel Bunnett, as well as Dr Rob Lane, Dr Daniel Poole and Dr Michelle Halls who provided essential insight and expertise which kept my research on the right path.

I would also like to acknowledge the Bunnett group for their assistance with DRG culturing and providing entertainment during the long hours in the primary lab, as well as all the DDB staff and students for their enthusiastic assistance whenever I needed it (and putting up with me on occasion) and making the lab such an enjoyable place to work.

Finally, I'd like to thank my colleagues from DST Group, David Mawdsley, Kate Shields and Peter Gray for granting me the opportunity and support to undertake this study.

CHAPTER 1

INTRODUCTION

1.1 G Protein-Coupled Receptors

1.1.1 Structural Characteristics and Classification

G protein-coupled receptors (GPCRs), also known as 7 transmembrane receptors, are a superfamily of cell surface receptors that are ubiquitously expressed throughout the body. There are over 800 members, and they detect very specific stimuli, or “ligands”, and transmit this information into the cell. GPCRs can detect a diverse array of extracellular stimuli, including neurotransmitters, metabolites, peptides, hormones, ions and photons. This versatility in “ligands” enables GPCRs to be involved in control of virtually every physiological process.

GPCRs are divided into 5 major families based on sequence similarity: A (rhodopsin), B (secretin), C (glutamate), F (frizzled) and G (adhesion) [1] (Figure 1.1). All GPCRs have the same basic structure: a single peptide that forms a bundle of 7 α-helical transmembrane domains (7TMD) joined by alternating intracellular (IL1-3) and extracellular loops (EL1-3), with an intracellular C-terminal domain (CT) which, in many GPCRs, contains a small α-helix (helix-8) tethered to the plasma membrane via a palmitoylation moiety, and an extracellular N-terminal domain (ECD) [2-4] (Figure 1.2). The most distinctive difference between families is in the size, structure and function of the ECD. Family A GPCRs are the largest group, with the widest variety of ligand types, and is further divided into 4 subfamilies and numerous subgroups [1]. They have small ECDs which mainly function to assist receptor folding and trafficking to the plasma membrane [5, 6], and in the case of the protease activated receptor subfamily, the ECD contains the ligand for the receptor [7, 8].

All the remaining families of GPCRs have large ECDs. The structures of these large ECDs have been determined using crystallography and nuclear magnetic resonance spectroscopy (NMR). The structure of family B ECDs is highly conserved between members, and is comprised of an N-terminal α-helix and 2 anti-parallel β-sheets which are joined together by three disulphide bonds [9, 10]. The ECD acts as the primary recognition site for the endogenous peptide ligands in order to facilitate ligand binding [9, 11, 12]. Family C have very large and distinctive ECDs containing a “venus flytrap” domain, which contains the endogenous ligand binding site [13-15]. Similarly the ECD of family F GPCRs contains a cysteine rich “frizzled” domain, which serves as the ligand binding site [16]. GPCRs of family G possess a variety of different types of ECDs, which are very large and contain various structural domains that facilitate cell interactions [17].

The structure and function of the non-canonical GPCRs of family F and G are very different and poorly understood compared to the other GPCR families and will not be discussed further.

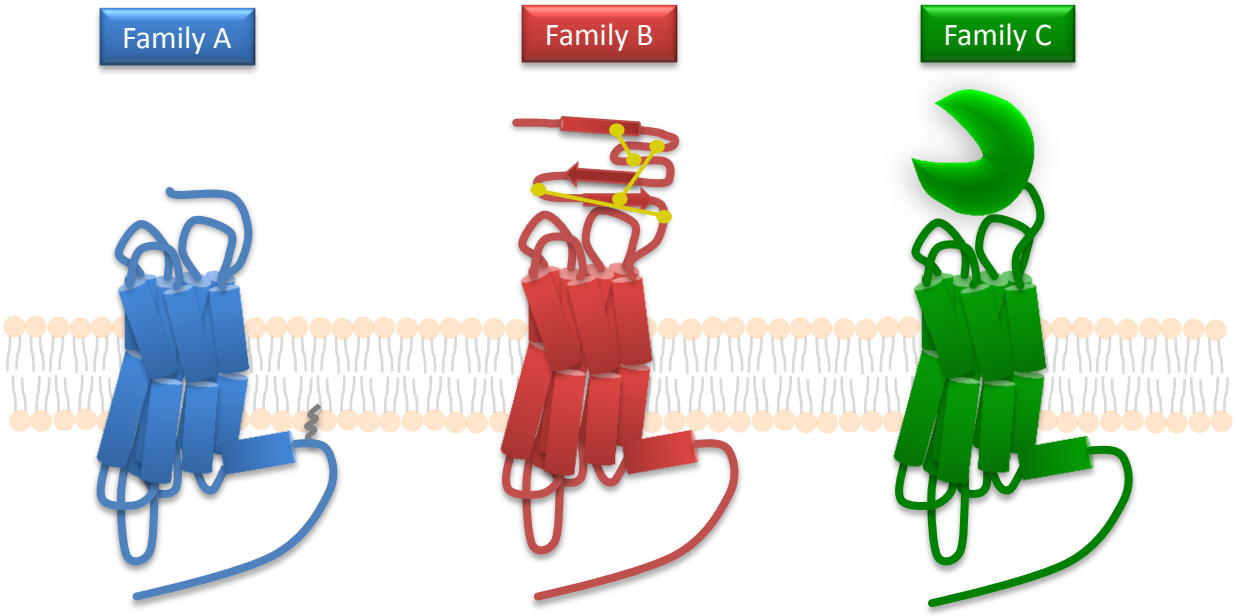

Figure 1.1: Structural model of the main 3 GPCR families, Family A, B and C.
Family A GPCRs, which include the opioid receptor family, detect the widest variety of ligands and have small extracellular domains (ECDs). Family B GPCRs have large ECDs for recognition of peptide hormones. The ECD has a highly conserved structure that is stabilised by 3 disulfide bonds. Family C GPCRs have very large ECDs which contains the "venus flytrap" domain that acts as the ligand binding site for ions and small molecules, and forms a disulphide bond within dimers.

The arrangement of the 7TMD is more similar between the different families. Advances in crystallography techniques have enabled the generation of high resolution structures of the 7TMD of a wide variety of GPCRs, including members of family A, B, C and F [3, 18-20]. The 7TMD is ordered in a circular arrangement, anticlockwise when observed from the extracellular surface, forming a core which is impermeable to ions [21-23]. The 7TMD is held together by the plasma membrane surrounding the hydrophobic residue core, as well as by a network of polar interactions and hydrogen bonds within the core [3, 4, 23]. The extracellular ends of the TM domains along with the ELs of the receptor form a cavity that, in the majority of GPCRs, serves as the binding site for the endogenous ligand, also known as the orthosteric binding site [24-26]. The main exception is the family C receptors, where the orthosteric binding site is within the ECD [15]. The distinct physical and chemical properties of this binding cavity in each GPCR determine the ligand specificity of the receptor. The arrangement of the TM domains,

the residues that form the binding site and ELs in different receptors is highly variable, forming binding sites of a range of sizes and properties to accommodate ligands of any size from small molecules to whole proteins. TM domains have different lengths and can be arranged at different angles, and some contain proline residues which bend the α-helix [27]. The ELs form secondary structures using salt bridges and disulphide bonds, and in some cases form a lid over the orthosteric binding pocket [28]. The arrangement of the 7TMD and the residues that make up the orthosteric binding pocket determine the shape and electrostatic properties of the cavity, ensuring the GPCR only detects its specific endogenous ligands.

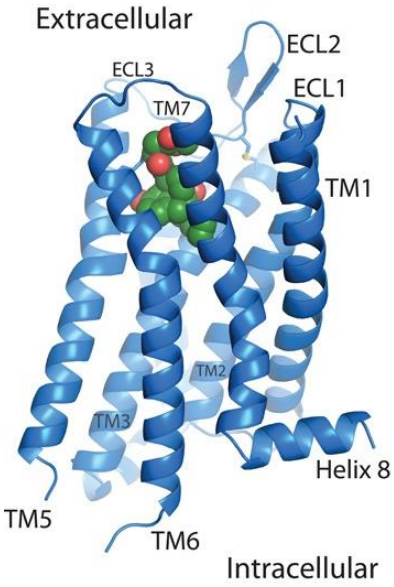

Figure 1.2: Crystal structure of the μ-opioid receptor (MOP) from Manglik, Kruse, Kobilka, Thian, Mathiesen, Sunahara, Pardo, Weis, Kobilka and Granier [29].
View of MOP crystal structure (blue) bound to an antagonist β-funaltrexamine (β-FNA) (green) from within the membrane plane. TM – transmembrane domain, ECL – extracellular loop.

Similarly, an intracellular cavity formed by the intracellular ends of the TMDs, the ILs and the CT serve as the site of interaction with intracellular signalling proteins. GPCRs "transduce" the extracellular signals they receive in the form of ligands, into intracellular signals by interacting with these intracellular proteins. The family of heterotrimeric Guanine nucleotide binding proteins known as G proteins, which give the receptors their name, are the main family of intracellular signalling effectors activated by GPCRs. The major interaction site between a GPCR and the G protein is IL-2 and intracellular ends of TM-V and TM-IV [30-33]. However, IL-3 has been shown to be involved in control of G protein subtype specificity [26, 34]. Additionally, initial recognition of the active receptor by the G protein is thought to involve changes in conformation of Helix-8 [35-38].

The structural changes behind how ligand binding to a GPCR leads to activation of the G protein are complex. GPCRs do not simply switch between the inactive and active state upon ligand binding; they are highly flexible and can adopt a range of different conformations. Unbound receptors, before ligand or G protein binding, exist in equilibrium between multiple conformations by switching between several low energy states [39-43]. Some GPCRs are even known to have “constitutive activity” by spontaneously adopting active conformations in the absence of ligand [44-46]. Ligand binding changes the energy landscape of the receptor, resulting in stabilisation of the receptor into a different range of conformations, depending on the type of ligand. Inverse agonists stabilise the receptor into the inactive conformation, preventing constitutive activity. Conversely, full agonists and partial agonists, which activate intracellular signalling maximally and sub-maximally respectively, shift the equilibrium towards intermediate and active states of the receptor [41, 43, 47].

Biophysical studies [48] and comparison of active conformations of rhodopsin, β_2 adrenergic receptor (β2AR), muscarinic acetylcholine receptor 2 (M2) and μ opioid receptor (MOP) [32, 49-51] bound to an agonist and a G protein and or a G protein mimetic nanobody have revealed several conserved structural changes upon receptor activation. Changes in the structural arrangement of the ligand binding site are relatively small and different for each receptor and ligand [52-55]. These small rearrangements disrupt the forces holding the GPCR in the inactive conformation, triggering much larger structural changes at the intracellular regions of the receptors. GPCR activation requires disruption of the salt bridges, hydrophobic interactions and hydrogen bonds that exist in the basal state to enable the GPCR to adopt the active state conformation [3, 4, 23]. GPCR activation universally involves disruption of a number of interactions between TM-III and TM-VI which lock the receptor in its inactive conformation [56-58]. These disrupted interactions include rearrangement of the hydrophobic core residues to allow movement between TM-II and TM-VI [59], and similarly restructuring of a “polar network” formed by water molecules hydrogen-bonded to TM-III, TM-VI and TM-VII [49, 59, 60]. Receptor activation also typically involves reorganisation of several highly conserved motifs known as “microswitches”. One such mircoswitch is the “ionic lock”, which is a highly conserved ionic interaction between a Glu residue in TM-VI and the Asp-Arg-Tyr motif (E/DRY) located on the intracellular end of TM-III of most family A GPCRs [61]. The Arg on TM-III forms a salt bridge with a Glu/Asp on TM-VI, or in some cases a hydrogen bond with a polar residue on TM-VI [49]. Other conserved

microswitches include the NPxxY motif on TM-VII [62] and the CWxP motif on TM-VI [40, 42, 53]. Disruption of all these forces holding the receptor in its inactive state, allows movement of the TM domains. The most highly conserved intracellular TM domain movements are the large outward movement of TM-VI, with smaller displacements of TM-III, TM-V and TM-VII [32, 49-51, 55, 56]. In the active β2AR structure TM-V and TM-VI interact directly with the co-crystallised G protein [32]. As these rearrangements of TM-V and TM-VI are so highly conserved among the active receptor structures described to date, they are considered essential for G protein activation.

However, agonist binding alone is not enough to achieve stabilisation of the active conformation [52-55, 63], as the intracellular regions of the receptor, in particular TM-V and TM-VI, continue to shift between inactive and active states [35, 55, 64-66]. To achieve stabilisation the active conformation the receptor must form a ternary complex with its cognate G protein, which increases the affinity of the receptor for its ligand [67]. Upon G protein binding, the equilibrium between receptor states shifts further towards the active conformations, stabilising the receptor in the active state [35, 68, 69].

The range of conformations of the receptor is not only dependent on the presence of ligand and G proteins. Virtually everything that interacts with the receptor will influence the conformations and activity of the receptor. Molecules that modulate receptor activity via interactions with the receptor at “allosteric sites”, which are spatially distinct from the orthosteric binding site, are known as “allosteric modulators”. There are numerous endogenous allosteric modulators in the cellular environment which have been shown to modulate GPCR activity, including ions [70-72], amino acids [73, 74], membrane lipids and cholesterols [75-77] and intracellular signalling proteins [69, 78]. The plasma membrane is composed of a mixture of lipids, cholesterol and other proteins and molecules, which may alter the conformation of the GPCR within different membrane compartments. For instance GPCR activity has been shown to be highly dependent on the presence of cholesterol, which is important for the formation of lipid rafts [75, 79, 80]. Crystal structures have shown that cholesterol interacts directly with the receptor [4, 70, 76], potentially modulating receptor conformational dynamics and activity [77, 81, 82]. The receptor conformation is also dependent on the concentration of Na^{2+} ions in the extracellular environment. In the inactive conformation, a Na^{2+} ion binds within the central polar network of water molecules, which inhibits agonist binding and receptor activation and enhances antagonist affinity [70, 72].

GPCRs were originally thought to function exclusively as monomers. However, there is now substantial evidence that GPCRs can function as dimers or even higher order oligomers. Dimerisation is essential for family C GPCRs, as only dimerised receptors are fully functional and trafficked to the cell surface [83-85]. They form homodimers and heterodimers via interactions between the ECDs (usually by formation of a disulphide bond) and the CT [86, 87]. Whilst monomers of family C GPCRs have been shown to be capable of activating G proteins, only the dimer is capable of stimulating intracellular signalling in response to an orthosteric ligand [88]. Evidence for dimerisation of family A and B GPCRs is less clear [89]. These receptors can fully function as monomers [90, 91], however they are clearly capable of forming homo and heterodimers [29, 92-98]. Unlike family C receptors however, they do not form a covalent bond between the receptors, hence the dimers most likely form transiently [97, 99-101]. The functional purpose of GPCR dimerisation in family A receptors is also uncertain, however several explanations have been proposed. GPCR oligomerisation may be a requirement for successful folding and trafficking of the receptor [102]. Additionally, there is substantial evidence that dimerised GPCRs act as allosteric modulators of one another, where ligand binding to the first receptor modulates the binding affinity and or the intrinsic efficacy of the ligand for the second receptor [103-107].

1.1.2 Signalling Mechanisms

GPCRs transduce the extracellular signals they receive in the form of ligands into intracellular signals via activation of “signalling pathways” involving a plethora of intracellular proteins known as “signalling effectors”. The initial step in activation of most known GPCR signalling pathways is the activation of G proteins, which are formed by the heterotrimer of 3 different subunits, Gα, Gβ and Gγ. In its inactive state the Gα subunit is bound to a guanosine diphosphate (GDP) nucleotide, which is exchanged for guanosine triphosphate (GTP) when the G protein is activated [108, 109]. The GDP is bound to the Ras-like GTPase domain, and held in place by the other half of the Gα, the helical domain [110, 111]. When the G protein binds to the agonist bound receptor, the two halves of the protein open, changing the conformation of the Ras domain to release the GDP and allow GTP to bind [111, 112]. This triggers separation of the Gα subunit from the Gβγ dimer [113], and the two parts of the G protein subsequently activate other intracellular signalling effectors. The Gα is inactivated when the GTP is hydrolysed into GDP by the Gα Ras domain [109], which can be assisted by GTPase activating proteins (GAPs) such as regulators of G protein signalling (RGS) and other GTPases [114, 115], allowing reassembly of the heterotrimeric G protein.

Gα subunits are divided into four classes, $G\alpha_s$, $G\alpha_{q/11}$ ($G\alpha_q$, $G\alpha_{11}$, $G\alpha_{14}$ and $G\alpha_{16}$), $G\alpha_{i/o}$ ($G\alpha_i$, $G\alpha_o$, $G\alpha_z$, $G\alpha_g$ and $G\alpha_t$) and $G\alpha_{12/13}$ ($G\alpha_{12}$ and $G\alpha_{13}$) [116]. $G\alpha_S$, $G\alpha_{q/11}$, $G\alpha_{i/o}$ and $G\alpha_{12/13}$ are ubiquitously expressed, whereas the other subtypes have tissue specific expression and functions and will not be discussed further. Most GPCRs predominantly couple selectively to a subset of Gα subunits, often within a single class, however many can couple G proteins belonging to multiple classes. Each Gα class is associated with activation of different signalling pathways (Figure 1.3). The characteristic signalling pathway activated by $G\alpha_s$ is 3,5-Cyclic adenosine monophosphate (cAMP) signalling. $G\alpha_s$ activates adenylyl cyclase (AC) which generates the second messenger cAMP from ATP [117, 118]. Likewise the defining signalling pathway of $G\alpha_i$ coupled receptors is the inhibition of cAMP signalling through inhibition of AC [119]. cAMP signalling is tightly controlled and compartmentalised in a cell and receptor specific manner by phosphodiesterases (PDE) and A-kinase anchoring proteins (AKAP) [120, 121]. There are a number of downstream targets of cAMP including cyclic nucleotide-gated ion channels and the small G protein guanine nucleotide exchange factor (Epac) [122, 123], however the most notable target is protein kinase A (PKA), also known as the cAMP-dependent protein kinase [124]. PKA executes the cellular effects of cAMP by

phosphorylating numerous targets, including GPCRs, Ca^{2+} channels and other kinases [125, 126].

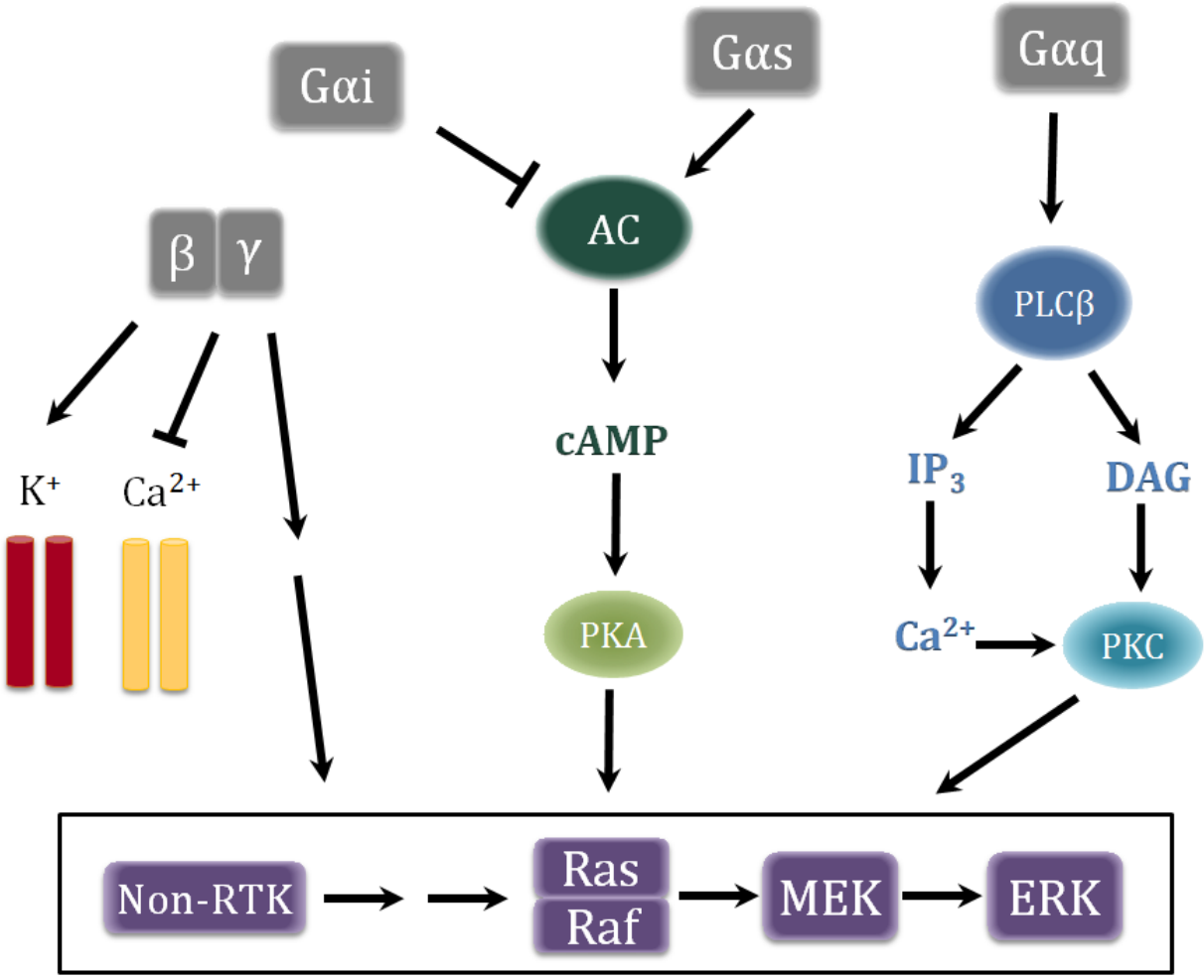

Figure 1.3: Classical GPCR signalling pathways.
Canonical $G\alpha_{i/o}$, $G\alpha_s$, $G\alpha_q$, and $G\beta\gamma$ signalling pathways. $G\alpha_s$ and $G\alpha_{i/o}$ stimulate and inhibit cAMP signalling respectively, $G\alpha_q$ activates phospholipid and C^{a2+} signalling, and $G\beta\gamma$ stimulate GIRKs and inhibit VGCCs. ERK activation can be mediated by $G\beta\gamma$ and all $G\alpha$ subtypes via multiple different pathways.

$G\alpha_q$ coupled receptors typically activate phosphoinositide signalling. $G\alpha_q$ activates phospholipase Cβ (PLCβ), which hydrolyses a plasma membrane lipid, phosphatidylinositol 4,5-bisphosphate (PIP_2), generating two second messengers, inositol 1,4,5-trisphosphate (IP_3) and 1,2-diacylglycerol (DAG) [127]. IP_3 stimulates release of Ca^{2+} from intracellular stores in the endoplasmic reticulum (ER) via IP_3 receptors [128], and can be further converted into other inositol phosphates by various kinases, which participate in other signalling pathways [129, 130]. Ca^{2+} is important for the control of an enormous number of cellular processes through regulating the activity of a myriad of enzymes, channels, receptors and other cellular proteins [131]. Similarly

DAG activates protein kinase C (PKC), a Ser/Thr protein kinase which also has numerous downstream targets including various cation channels, cytoskeletal proteins, enzymes and even the GPCRs themselves [132-135]. Many $G\alpha_q$ coupled receptors are also coupled to $G\alpha_{12/13}$, which regulate Rho signalling. $G\alpha_{12/13}$ directly activates guanine nucleotide exchange factors for Rho (RhoGEF), which facilitate exchange of GDP for GTP on Rho GTPases [136]. The most well characterised function of Rho signalling is the regulation of cytoskeletal changes required for cell growth, differentiation and migration, through activation of a number of downstream targets including Rho kinase [137, 138].

G protein mediated signalling is not limited to the signalling pathways described here, Gα subunits and their downstream effectors can activate a multitude of different cell-dependent and receptor specific signalling pathways in order to generate a particular cellular response. Additionally, many other signalling pathways are stimulated by the free Gβγ dimer that is released when it dissociates from the Gα. There are 5 Gβ subtypes and 12 subtypes of Gγ which can form heterotrimers of nearly every combination of Gαβγ [116]. Only small differences in coupling to downstream effectors between the various Gβγ combinations have been observed to date [139-141]. Gβγ activates inwardly rectifying K^+ channels (GIRKs) through direct interaction with the channel [142] and similarly Gβγ directly inhibits N and P/Q type voltage gated Ca^{2+} channels (VGCCs) [143, 144]. These actions are most often associated with activation of $G\alpha_{i/o}$-coupled receptors [145, 146]. Several canonical Gα signalling pathways can also be modulated by Gβγ, including inositol phosphate signalling, via stimulation of PLCβ, primarily via $G\alpha_{i/o}$-coupled receptors [147], and activation phosphoinositide-3 kinase (PI3K) [148], as well as modulate cAMP signalling by direct inhibition of certain AC isoforms [149]. Additionally, Gβγ is involved in activation of G protein-coupled receptor kinases (GRK) [150], which play an important role in receptor regulation as described later.

Gβγ is also known to mediate activation of mitogen activated protein kinases (MAPK), such as extracellular signal regulated kinase (ERK). There are numerous complex and intertwined signalling pathways which lead to ERK1/2 activation in a cell specific and receptor-dependent manner [151, 152]. However, the classical signalling pathway that leads to activation of ERK involves transactivation of receptor tyrosine kinase (RTK) growth factor receptors. Gβγ and $G\alpha_q$ have been shown to activate non-receptor tyrosine kinases (non-RTK) such as Src either directly or via PI3K (Gβγ), and PLC

and/or PKC ($G\alpha_q$) [153-158] which then stimulates phosphorylation and activation of the RTK, either directly or via stimulation of matrix metalloproteases (MMP), which proteolytically cleaves and releases a tethered growth factor, which stimulates auto phosphorylation of the RTK [159-161]. The activated RTK, in complex with a number of adaptor proteins and a guanine nucleotide exchange factor, SOS, stimulates activation of the small GTPase Ras, which in turn triggers activation of the MAPK cascade Raf-Mek-ERK [162, 163]. $G\beta\gamma$ and $G\alpha$ subunits can also stimulate ERK activation via many other pathways that do not require transactivation of RTKs [164-166], including non G protein-mediated pathways as described later.

Termination of these signalling pathways is achieved by many processes, including specific feedback mechanisms within signalling pathways as well as switching off G protein activity by GTP hydrolysis and reassembly of the heterotrimer [109, 112]. However, the primary mechanism for regulation of signalling at the receptor level, occurs through phosphorylation of the receptor and subsequent uncoupling from the G protein and binding of arrestins [167]. This process, known as desensitisation, was originally shown with rhodopsin and β2AR, but has since been shown to be widely applicable among GPCRs. Desensitisation renders the GPCR unable to respond to further stimulation by the agonist, preventing further activation of G protein-mediated signalling [168-170]. Residues within the ILs and CT of GPCRs can be basally phosphorylated or undergo agonist-induced phosphorylation [168, 171]. There are numerous kinases that have been shown to be capable of phosphorylating GPCRs including PKC, PKA, CaMIIK and ERK, usually associated with heterologous desensitisation of receptors [172, 173], however it is the GRK family that is most commonly associated with agonist-induced phosphorylation and homologous desensitisation [174]. There are 7 GRKs divided into 3 subfamilies, visual GRKs (GRK1 and 7), GRK2 (GRK2 and 3), and GRK4 (GRK4, 5 and 6), of which GRK2, 3, 5 and 6 are expressed ubiquitously [174-178]. Most GRKs are localised at the membrane, except for GRK2 and 3, which interact with free $G\beta\gamma$ subunits to stimulate translocation from the cytoplasm to the plasma membrane upon receptor activation [150, 179, 180]. Binding of the GRK to the receptor inhibits further interaction of G proteins with their intracellular targets [180-182], and activates the Ser/Thr kinase domain of the GRK which phosphorylates specific residues of the GPCR, particularly on the CT and IL-3 [183-185].

The final step in this desensitisation process is the recruitment of arrestins to the receptor. There are 4 members of the arrestin family, 2 visual arrestins (arrestin-1 and arrestin-4), and 2 non visual arrestins (β-arrs) β-arrestin 1 (β-arr1) and β-arrestin 2 (β-arr2). The phosphorylated form of the receptor has an enhanced affinity for arrestins, which compete with the G protein for binding to the receptor, preventing further activation of the G protein [186-190]. However, the role of arrestins in receptor regulation and signalling extends beyond decoupling of G proteins from the receptor. Arrestins act as scaffolds for numerous other proteins to form complexes, which when recruited to the receptor trigger activation of other receptor regulatory processes and signalling pathways [191]. Receptor activity can be regulated by removal from the plasma membrane and sequestration into endosomes [192]. Arrestins target GPCRs for internalisation into clathrin coated pits by forming a complex with components of the clathrin/dynamin-dependent internalisation machinery including clathrin and AP-2 [193-197]. Once internalised, GPCRs can be downregulated by targeting for degradation in lysosomes, in which case restoration of activity requires synthesis of new receptors [198]. Alternatively, receptors can be resensitised by dephosphorylation of the receptor, and returned to the plasma membrane [192, 199].

β-Arrs are also known to mediate activation of numerous G protein-independent signalling pathways. The most well-known β-arr mediated signalling pathway is ERK activation [200-202]. β-arrs have been shown to mediate ERK activation from clathrin coated pits and endosomes [203, 204] by forming a complex with ERK signalling pathway components including Src and Raf [201, 202, 205]. ERK activated via this pathway shows a different spatiotemporal profile to that of ERK activated via G protein-dependent signalling pathways. β-arr-dependent ERK activation typically shows a delayed onset and is more sustained [206, 207], shows differential localisation within the cell [205, 206, 208] and is associated with different downstream targets of ERK [208, 209]. β-arrs are also involved in activation of a myriad of other signalling pathways including JNK [210, 211], p38 MAP kinase [212-214], RhoA [215], Akt [216-218] and NF-κB [219, 220]. Additionally, other signalling pathways such as cAMP, can also be activated from receptors located in endosomes resulting in differential downstream effects when compared to activation of the same signalling pathways at the plasma membrane [221-223].

1.1.3 Biased Agonism at G Protein-Coupled Receptors

GPCRs were traditionally thought of as simple on/off switches, where the receptor exists in equilibrium between an inactive and an active conformation. Agonists shift the equilibrium towards the single active conformation, and inverse agonists shift the equilibrium towards the inactive conformation whereas neutral antagonists have no effect on the receptor conformation but simply block the binding site [67, 224, 225]. In this 2-state model, agonists simply vary in their ability to shift the equilibrium towards the active state. However, over the last two decades it has been shown that the efficacy of a ligand can vary between different signalling pathways [226-230]. In the most extreme cases, a ligand can effectively have no activity at some signalling pathways while activating other atypical signalling pathways [231, 232]. In such cases the 2-state model of receptor activation is not sufficient to explain this flexibility in signalling responses. Instead, it has been proposed that GPCRs can adopt multiple active states, where different ligands stabilise the receptor in distinct active conformations. This phenomenon is known as “biased agonism”, and is also referred to as “functional selectivity”, “ligand-biased signalling” or “stimulus trafficking” [233]. Biased agonism is a natural phenomenon that has been observed at receptors that possess multiple endogenous ligands, including β2AR [234], the somatostatin receptor 2A (SSTR2A) [235], chemokine receptors [236-238] and the melanocortin MC4 receptor [239]. As a result, biased agonism has been suggested to play an important role in the control of the physiological effects mediated by the receptor. This is because activation of particular signalling pathways is linked to specific physiological effects [240-246]. For example, at the M3 muscarinic acetylcholine receptor (M3R) receptor phosphorylation and β-arr recruitment have been shown to be important for learning and memory function [245]. Therefore, biased ligands that selectively activate certain signalling pathways would be expected to induce different physiological effects, and this has been widely observed with biased ligands for multiple GPCRs [237, 247-252].

There is a wealth of evidence in support of the multi-state theory of GPCR activation. The structural changes that are observed upon agonist stimulation have been shown to be ligand-dependent at numerous GPCRs including the cannabinoid CB_1 receptor [253], δ opioid receptor (DOP) [47], ghrelin receptor [69], α_2A adrenergic receptor (α2AR) [43], β1-adrenergic receptor (β1AR) [254], β2AR [68, 234, 255, 256] and the parathyroid hormone type 1 receptor (PTH1R) [257] to name a few. Furthermore, it is becoming increasingly apparent that the ligand-induced conformations of the receptor are unique

for every ligand. Comprehensive analysis of the structural movements induced by a large range of ligands at the β2AR showed that even among ligands with similar structure and activity, there were several conformational rearrangements that were highly ligand specific, showing that the overall conformation of the receptor is unique for each ligand [255]. Each distinct conformation of the receptor will have varying propensities for activation of particular signalling effectors, potentially resulting in activation of a unique signalling pattern.

Specific structural rearrangements have been shown to be associated with activation of particular signalling effectors. The ability of a ligand to stabilise these conformations of the G protein coupling domains of the receptor is separate from its ability to stimulate β-arr recruitment [256-262], hence different ligands will have differing efficacies for activation of G proteins and recruitment of β-arrs. For instance, efficacy for G protein activation has been linked to stabilisation of the G protein coupling domain on IL-3 of the receptor [65, 263]. At the α2AR, partial agonists have been shown to stabilise the IL-3 into a partially active conformation at a different rate compared to full agonists [43, 263]. Similarly, at the β2AR, highly conserved structural rearrangements around the NPxxY motif, which are required for G protein coupling, have been shown to correlate with the efficacy of the ligand for activation of G proteins [62, 255]. Overall, this shows that the efficacy of a ligand for activation of G proteins depends on the ability of the ligand to induce the active conformation of these particular regions of the receptor. In contrast, conformational rearrangements of the receptor that are associated with recruitment of β-arrs are distinct from those connected with G protein activation [69, 256-258, 260, 261, 264-267]. This has been clearly demonstrated by studies at the angiotensin type 1A (AT_{1A}) receptor [265], β2AR [207] and PTH1R [258], which have shown that certain mutations can selectively inhibit G protein activation but not recruitment of β-arrs, and also by the discovery of ligands that stimulate β-arr recruitment and receptor internalisation but not G protein activation [268-270]. The conformational requirements for recruitment of β-arrs have been less well defined than those required for G protein activation. However, enhanced β-arr recruitment has been frequently associated with conformational changes in TM-VII [260, 271, 272]. For example, at the vasopressin V2 receptor (V2R), the degree of conformational change around TM-VII and helix 8 has been shown to correspond with the efficacy of the ligand for recruitment of β-arrs. Conformational changes around EL-3 [255], TM-III [259, 264]

and the sodium binding site [273] have also been implicated in regulation of β-arr recruitment.

Biased agonism between G protein activation and β-arr recruitment is the most widely known form of bias that was first observed at MOP [274] and has since been observed at numerous GPCRs [206, 234, 269, 275-279]. Several ligands have been discovered which do not stimulate β-arr recruitment [257, 274, 280] and others that stimulate β-arr recruitment in the absence of G protein activation [247, 265, 266, 270, 280]. Biased agonism between G proteins and β-arrs has also been shown to result in differential activation of β-arr-dependent regulation and signalling pathways including receptor desensitisation, trafficking and MAP kinase activation [266, 274, 276, 277, 280-282].

Recruitment of β-arr is not only dependent on the conformation of the receptor, it is also dependent on the activation of GRKs and subsequent phosphorylation of the CT of the receptor [187, 189]. However, ligands activating the same receptor have been shown to induce different phosphorylation patterns via activation of different GRKs [34, 236, 276, 283-286]. For example, at the chemokine receptor CCR7, the chemokines CCL19 and CCL21 both stimulate CCR7 phosphorylation via GRK6, however only CCL19 stimulates CCR7 phosphorylation via GRK2 [285]. The combination of unique receptor conformations and phosphorylation patterns results in stabilisation of different active states of the β-arr that have been linked to activation of distinct functional outcomes [262, 284, 285, 287-289]. Specific receptor phosphorylation patterns have frequently been associated with the ability of a ligand to stimulate desensitisation, internalisation of the receptor and ERK activation [284, 285, 290-292]. In addition to this, recently Yang, Yu, Liu, Qu, Gong, Liu, Li, Wang, He, Yi, Song, Tian, Xiao, Wang and Sun [288], showed that the V2R is able to stabilise β-arr1 in a distinct active conformation that was able interact with clathrin when phosphorylated by GRK2 but not GRK6 [288]. Consequently, the phosphorylation pattern plays a vital role in determining the functions of the β-arrs recruited to the GPCR [207, 284, 285, 293-298]. Furthermore, this means that even though multiple ligands may stimulate β-arr recruitment, they may show divergent activation of subsequent β-arr-dependent signalling pathways [299, 300].

A similar principle applies to activation of G proteins. Most GPCRs can couple to multiple G protein subtypes [301-305], and different ligands can preferentially activate particular G protein subtypes [286, 301, 306-310]. For example, at the β2AR, most agonists are able to activate both $G\alpha_s$ and $G\alpha_{i/o}$, whereas another β2AR agonist,

fenoterol, only activates $G\alpha_s$ [309]. Additionally, agonists for receptors that primarily couple to $G\alpha_{i/o}$, such as the relaxin family peptide receptor 3 (RXFP3) [311], DOP [63], the serotonin 5-HT_{1A} receptor [312] and the dopamine D2 receptor (D2) [310], have shown differential coupling to specific $G\alpha_{i/o}$ subtypes. Such differential G protein coupling is associated with divergent activation of downstream signalling pathways [249, 301, 309, 313]. This has been clearly demonstrated at the 5-HT_{2A} receptor, where PLC activation and arachidonic acid release are mediated by $G\alpha_q$ and $G\alpha_{i/o}$ or $G\alpha_{12/13}$ respectively [314, 315]. In addition to bias between G protein subtypes, there is also the potential for bias between $G\alpha$ and $G\beta\gamma$ signalling. This has been observed at the oxoeicosanoid receptor (OXE-R), where an allosteric modulator Gue1654 inhibited 5-oxo-ETE stimulation of $G\beta\gamma$ but not $G\alpha_{i/o}$ signalling [316]. Overall, this differential activation of different G protein subunits means that ligands which induce similar levels of overall G protein activation, may stimulate activation of distinct G protein-mediated signalling pathways.

Biased agonism is not necessarily limited to differential activation of G protein and β-arr-dependent signalling pathways. GPCRs are known to directly interact with numerous other intracellular proteins including GRKs and other kinases, phosphatases, regulators of G protein signalling (RGS), receptor activity modifying proteins (RAMPS), scaffolding proteins, calmodulin and more [317-322]. The activity of many of these receptor interacting proteins is agonist-induced, and they are known to modulate the activity of G protein and or β-arr-dependent signalling pathways, and in some cases, can actually activate other signalling pathways which are independent of G protein and β-arrs [323-326]. For instance, at the $AT_{1A}R$, agonist-induced phosphorylation and activation of janus kinase 2 (JAK2) requires direct interaction between JAK2 and the CT of the receptor, and occurs even in the absence of G protein activation [325, 327, 328]. Therefore, since GPCRs can directly modulate the activity of such signalling proteins, biased agonism may also be applicable to activation of these signalling effectors. Altogether, the diverse range of signalling pathways which are subject to differential activation implies that there is a multitude of potential signalling patterns which can be activated by each unique conformation of the ligand-receptor complex.

1.1.4 Quantification of Biased Agonism

For a review of quantification of bias at GPCRs please refer to Chapter 1.3 Novel GPCR Paradigms at the μ-Opioid Receptor

1.2 Opioid Receptors

1.2.1 The Endogenous Opioid System

Opioid receptors are members of the large family of G protein-coupled receptors (GPCRs). There are 3 classical subtypes of opioid receptor; δ-opioid receptor (DOR, DOP, or OP1), κ-opioid receptor (KOR, KOP, OP2) and μ-opioid receptor (MOR, MOP, OP3). The fourth member of the opioid subfamily, the nociception receptor (orphanin FQ peptide receptor, NOP), has high sequence similarity to the other opioid receptors and some similar physiological roles. Despite these similarities, the binding site of NOP is structurally very different from the other opioid receptors [329, 330] and as a result recognises different endogenous and synthetic ligands [331], hence will not be further discussed. The classical opioid receptors are expressed widely throughout the nervous system as well as in numerous other tissues. They have a number of physiological roles that include control of respiration, modulation of addiction and reward pathways, control of bowel motility and modulation of nociception.

The endogenous ligands for opioid receptors are small peptides that are synthesised by cleavage of precursor proteins; pro-enkephalin (pENK), pro-dynorphin (pDYN) and pro-opiomelanocortin (pOMC). These peptides all have the same N-terminal tetrapeptide sequence Tyr-Gly-Gly-Phe, and have varying affinities for all three opioid receptors, but none are significantly selective for one receptor subtype Table 1.1 [332, 333]. There are also two additional putative endogenous peptides; endomorphin-1 (endo-1) and endo-2. These are structurally unrelated to the typical opioid peptides and are the most selective and potent for MOP [334]. The gene or genes encoding the precursor proteins of these peptides are unknown [335], although a *de novo* synthesis mechanism has been proposed as an alternative source [336].

Table 1.1: Endogenous opioid peptide sequences

Peptide	Sequence
pENK derived opioids	
Leu-enkephalin (Leu-enk)	Tyr-Gly-Gly-Phe-Leu
Met-enkephalin (Met-enk)	Tyr-Gly-Gly-Phe-Met
Met-enkephalin-RF (Met-enk-RF)	Tyr-Gly-Gly-Phe-Met-Arg-Phe
Met-enkephalin-RGL (Met-enk-RGL)	Tyr-Gly-Gly-Phe-Met-Arg-Gly-Leu
Metorphamide	Tyr-Gly-Gly-Phe-Met-Arg-Arg-Val
BAM 12	Tyr-Gly-Gly-Phe-Met-Arg-Arg-Val-Gly-Arg-Pro-Glu
BAM 18	Tyr-Gly-Gly-Phe-Met-Arg-Arg-Val-Gly-Arg-Pro-Glu-Trp-Trp-Met-Asp-Tyr-Gln
BAM 22	Tyr-Gly-Gly-Phe-Met-Arg-Arg-Val-Gly-Arg-Pro-Glu-Trp-Trp-Met-Asp-Tyr-Gln-Lys-Arg-Tyr-Gly
Peptide E	Tyr-Gly-Gly-Phe-Met-Arg-Arg-Val-Gly-Arg-Pro-Glu-Trp-Trp-Met-Asp-Tyr-Gln-Lys-Arg-Tyr-Gly-Gly-Phe-Leu
Peptide F	Tyr-Gly-Gly-Phe-Met-Lys-Lys-Met-Asp-Glu-Leu-Tyr-Pro-Leu-Glu-Val-Glu-Glu-Glu-Ala-Asn-Gly-Gly-Glu-Val-Leu-Gly-Lys-Arg-Tyr-Gly-Gly-Phe-Met
pDYN derived opioids	
Dynorphin A (DynA)	Tyr-Gly-Gly-Phe-Leu-Arg-Arg-Ile-Arg-Pro-Lys-Leu-Lys-Trp-Asp-Asn-Gln
Dynorphin B	Tyr-Gly-Gly-Phe-Leu-Arg-Arg-Gln-Phe-Lys-Val-Val-Thr
Big Dynorphin (Dyn A/B 1-32)	Tyr-Gly-Gly-Phe-Leu-Arg-Arg-Ile-Arg-Pro-Lys-Leu-Lys-Trp-Asp-Asn-Gln-Lys-Arg-Tyr-Gly-Gly-Phe-Leu-Arg-Arg-Gln-Phe-Lys-Val-Val-Thr
Dynorphin A 1-13 (DynA 1-13)	Tyr-Gly-Gly-Phe-Leu-Arg-Arg-Ile-Arg-Pro-Lys-Leu-Lys
Dynorphin A 1-8 (DynA 1-8)	Tyr-Gly-Gly-Phe-Leu-Arg-Arg-Ile
Dynorphin A 1-6 (DynA 1-6)	Tyr-Gly-Gly-Phe-Leu-Arg
Leumorphin	Tyr-Gly-Gly-Phe-Leu-Arg-Arg-Gln-Phe-Lys-Val-Val-Thr-Arg-Ser-Gln-Glu-Asp-Pro-Asn-Ala-Tyr-Tyr-Glu-Glu-Leu-Phe-Asp-Val
α-Neoendorphin (α-Neo)	Tyr-Gly-Gly-Phe-Leu-Arg-Lys-Tyr-Pro-Lys
β-Neoendorphin	Tyr-Gly-Gly-Phe-Leu-Arg-Lys-Tyr-Pro
pOMC derived opioids	
α-Endorphin	Tyr-Gly-Gly-Phe-Met-Thr-Ser-Glu-Lys-Ser-Gln-Thr-Pro-Val-Thr-Leu
β-Endorphin (β-Endo)	Tyr-Gly-Gly-Phe-Met-Thr-Ser-Glu-Lys-Ser-Gln-Thr-Pro-Val-Thr-Leu-Phe-Lys-Asn-Ile-Ile-Lys-Asn-Ala-Tyr-Lys-Lys-Gly-Glu
Unknown precursor	
Endomorphin 1 (Endo-1)	Tyr-Pro-Trp-Phe
Endomorphin 2 (Endo-2)	Tyr-Pro-Phe-Phe

1.2.2 Declaration for Thesis Chapter 1.2.2

Monash University

Declaration for Thesis Chapter 1.2.2

Declaration by candidate

In the case of Chapter 1.2.2, the chapter contains an excerpt from Thompson et al. (2014) "Biological redundancy of the endogenous GPCR ligands in the gut and the potential for endogenous functional selectivity" *Front Neurosci*. (For full article see Appendix B) The nature and extent of my contribution to the work was the following:

Nature of contribution	**Extent of contribution (%)**
Contributed to writing of the manuscript – Only sections of the manuscript written by myself are included in thesis, for which my contribution was 95%.	30%

The following co-authors contributed to the work. If co-authors are students at Monash University, the extent of their contribution in percentage terms must be stated:

Name	**Nature of contribution**	**Extent of contribution (%)** for student co-authors only
Meritxell Canals	Contributed to writing of the manuscript	N/A
Daniel Poole	Contributed to writing of the manuscript	N/A

The undersigned hereby certify that the above declaration correctly reflects the nature and extent of the candidate's and co-authors' contributions to this work*.

Candidate's Signature	[redacted]	**Date 9 May 2016**
Main Supervisor's Signature	[redacted]	**Date 9 May 2016**

1.2.3 Opioid physiology of nociception and gastrointestinal motility

The endogenous opioid system is an integral component of the nociceptive system, which acts throughout the entire nociception network to provide analgesia by inhibiting transmission of pain signals [337, 338]. All opioid receptors play important roles in the control of nociception, however this review is focussed on MOP, as MOP is the main target of the most effective and widely used analgesics that are currently available, as shown by the lack of effects in MOP-/- mice [339]. The analgesic effects of MOP are naturally mediated via stimulation by the endogenous opioids. Identifying regions where endogenous opioids are expressed and released under normal physiological conditions is challenging due to the high susceptibility of the peptides to degradation, and also the high similarity between different peptides. Nonetheless, endogenous opioids have been shown to be expressed and released from many different tissues, including throughout nociceptive pathways.

Opioid-induced analgesia is predominantly mediated via receptors in the central nervous system (CNS), both at the level of the spinal cord (spinal analgesia) and in the brain (supraspinal analgesia). MOP receptor expression in the spinal cord is highest in presynaptic C fibre primary afferents (dorsal root ganglia neurons, DRGs) [340-343] and postsynaptic terminals in laminae I and II of the dorsal horn (DH) [344-346]. MOP activation in the DH neurons inhibits spinal withdrawal reflexes, typically measured in rodents using tail-flick assays [347-349], and modulates transmission of ascending and descending nociceptive signals to the brain [350-355]. Endogenous opioids including Dynorphin A (DynA), α-neoendorphin (α-neo), β-endorphin (β-endo) and enkephalins show overlapping expression with MOP in the DH, and are released in response to painful stimuli [344, 356-360]. A number of studies have also shown release of endogenous opioids in the spinal cord indirectly by observing MOP internalisation induced by endogenous opioids in response to noxious stimuli [361-363]. Endo-1 and Endo-2 have also been detected in the spinal cord by both immunohistochemical methods [364-367] and by electrochemical HPLC [368], and is possibly generated extracellularly [336].

MOP is also involved in supraspinal control of analgesia. MOP is highly expressed in in numerous areas of the brain [345, 346, 369-371]. These include several regions involved in descending nociception inhibition pathways, such as the periaqueductal gray area (PAG) [372-374], the nucleus raphe magnus (NRM) in the rostral ventral medulla (RVM) [375, 376] and the locus coeruleus (LC) [377, 378] among others [379], which

have been shown to specifically mediate opioid-induced analgesia. Activation of these brain regions, which is simulated by MOP via inhibition of inhibitory interneurons in these regions (disinhibition), results in stimulation of neurons projecting to the DH, which triggers release of endogenous opioids and inhibition of DH neurons [338, 355, 380, 381]. Similar to the DH, the expression of endogenous opioids overlaps the expression of MOP in descending inhibition pathways. Enk containing neurons project between the PAG, NRM, LC and other descending inhibition nuclei as well as neurons projecting to the spinal cord [344, 358, 382-385]. Enkephalins appear to be the most highly expressed endogenous peptides in these regions [370, 386], and microinjection of enkephalins in these areas produces strong analgesia [387], suggesting they are the predominant peptides mediating opioid-induced descending inhibition. However, both β-endo and dynorphin derived peptides also play important and distinct roles in descending control of analgesia [388-390]. There are high levels of β-endo in the PAG and the LC in terminals of neurons originating the hypothalamus [391, 392]. Similarly endo-1 and endo-2 are also found in the PAG, as well as neurons of the RVM that project to the DH of the spinal cord [364, 393, 394]. Furthermore, dynorphins are found in many of the same regions as the enkephalins, predominantly in neurons distinct from those expressing enkephalins, however it is unknown if MOP is involved in dynorphin mediated analgesia [386, 395-397].

MOP is also believed to provide analgesia via direct actions on sensory neurons in the peripheral nervous system. MOP is expressed on the peripheral terminals of primary afferent neurons [341, 398-400], and endogenous opioids are released from the peripheral terminals of primary afferent neurons in tissues in response to noxious stimuli [399, 401-403]. Endogenous opioids appear to play a particularly important role in peripheral analgesia for inflammatory, neuropathic and cancer pain, as MOP expression on the terminals is increased in response to inflammation [404-409] and the large molecular weight opioid peptides also have better access to the nerve terminals under these conditions [410, 411]. Additionally, immune cells including macrophages, leukocytes and lymphocytes, synthesise enkephalins, endomorphins and β-endo [412-415], which when recruited in response to inflammation, release the peptides to provide natural analgesia [398, 416-418]. For example, T lymphocytes have been shown to be important in control of visceral pain by releasing β-endo in the gastrointestinal tract (GIT), and increasing β-endo expression in the myenteric plexus [419, 420] . Surgery

has also been shown to increase dynorphin expression in DRGs of mice [421], and elevate levels of opioid peptides after abdominal surgery in guinea pigs [422].

The involvement of the MOP at every level of nociceptive control is what endows MOP agonists with such powerful analgesic properties. Unfortunately, the use of opioids as analgesics is associated with a large number of side effects that limit their usefulness. A major issue is the development of tolerance to the analgesic effects after prolonged or repeated exposure to opioids limits their long term use. Additionally, there are other undesirable side effects elicited by activation of opioid receptors in other tissues including respiratory depression, nausea, euphoria, addiction, itch and constipation. The constipating effects of opioids are the most common and debilitating side effects [423, 424], and unlike most other side effects of opioids, tolerance does not develop to opioid-induced constipation [425-427]. MOP expression in the GIT varies between species, but in humans is expressed by both myenteric and submucosal neurons throughout the small and large intestine [428]. Activation of these receptors inhibits GIT motility by suppressing longitudinal muscle contractions and fluid secretion from the submucosa [429-431].

The following is an excerpt from Thompson, Canals and Poole [432] "Biological redundancy of the endogenous GPCR ligands in the gut and the potential for endogenous functional selectivity" *Front Pharmacol.* 5:262 For full article see Appendix B.

The enkephalins have been the most widely studied opioid peptides in the GIT. Pro-enk contains four copies of Met-enk and one each of Leu-enk, Met-enk-RF and Met-enk-RGL, and several additional opioid peptides may be formed by partial processing of the precursor protein (see **Table 1.1**) [433]. Expression of at least four enk peptides (Leu-enk, Met-enk, Met-enk-RF and Met-enk-RGL) in the GIT has been confirmed [434-437]. Immunohistochemical studies demonstrate expression throughout the human GIT, with highest levels detected in the muscularis externa [438-440]. A similar expression pattern has been observed in rodents [441]. PENK-derived peptides are mainly found in the cell bodies of myenteric neurons and in nerve fibers within the myenteric plexus and circular muscle [358, 442-444]. There is evidence that immunoreactivities for Leu-enk and Met-enk are expressed by distinct neuronal populations within the enteric nervous system [435, 445, 446]. The morphology and distribution of Enk-containing myenteric neurons has been examined in detail. Approximately 23% of myenteric neurons express Enk-immunoreactivity [442]. These are morphologically Dogiel Type I inhibitory or excitatory

motor neurons and are also immunoreactive for ChAT and/ or substance P [442, 447-449]. Leu-enk-positive myenteric neurons of the human intestine have been described morphologically as ‘stubby neurons’ and are proposed to represent motor neurons or ascending interneurons [450]. Examples of opioid receptor and enkephalin labeling in the intestine are presented in Figure 1.4.

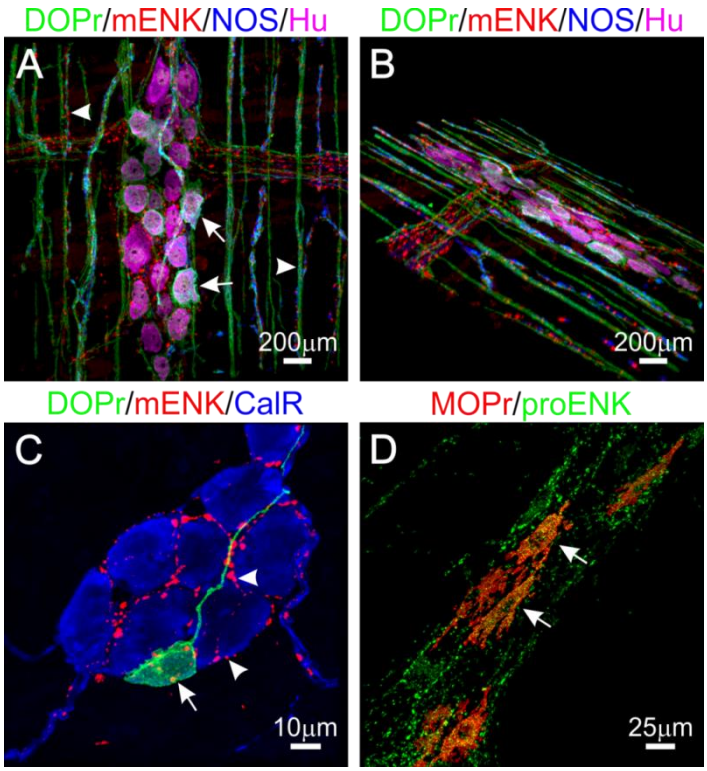

Figure 1.4: Expression of opioid receptors and enkephalin in the enteric nervous system.
(A-B) Distribution of DOP (green), Met-enk (mENK, red), nitric oxide synthase (NOS, blue) and the pan-neuronal marker HuC/D (Hu, magenta) in the myenteric plexus (arrows) and circular muscle nerve fibers (arrowheads) of the mouse distal colon. (C) Example of a DOP-positive submucosal neuron (arrow) and association with mENK-immunoreactive nerve varicosities (arrowheads) in the mouse distal colon. (D) Overlap between immunoreactivities for MOP (red) and pENK (proENK, green) in myenteric neurons of the guinea pig ileum. Images have been modified using Imaris 7.4.2 software (Bitplane). Scale bars are as indicated.

There are a small number of neurons that express enkephalin-immunoreactivity in the submucosal plexus and fibers in the mucosa [441, 449, 451], and in enteroendocrine cells [452]. However, it is possible that the enkephalin detected in these regions is due to detection of dynorphins or dynorphin derived Leu-enk which is highly expressed in these regions as discussed later in this review. Expression of other enkephalin derivatives including Met-enk-RF [453] and Met-enk-RGL [454] by enteric neurons has also been demonstrated. Other sites where proENK and its derivatives are expressed include enteroendocrine cells [453, 455, 456], extrinsic afferents [457] and immune cells including CD4+ T cells [458].

There is good evidence that opioid peptides derived from pro-dynorphin (dynorphins), are present in the GIT. Pre-pro-dynorphin mRNA is expressed in the myenteric and mucosal layers to varying levels throughout the GIT [459]. Prodynorphin contains three opioid peptides, dynA, dynB and α-neo, which can all be further processed to shorter opioid peptides including Leu-Enk (Table 1.1) [460]. Dynorphins have been detected in

the GIT of various species, including the full length dynA 1-17, dynA 1-13, dynA 1-8), dynB and α-neo [461-465]. Dynorphins are present in all layers of the GIT wall throughout the entire human GIT, although information regarding cellular sites of expression is lacking [466]. Immunohistochemistry studies performed mainly in guinea pigs indicate that dynorphins are widely expressed by submucosal and myenteric neurons [457, 461, 462]. Dynorphins are co-expressed with enkephalins in a subpopulation of Dogiel type I myenteric neurons [448, 451, 457]. It is possible that this may reflect conversion of dynorphin to Leu-enk in these neurons rather than co-expression of pro-ENK. There are also reports of pro-DYN expression by enterochromaffin cells [467].

The endorphins are formed from the precursor peptide POMC, which also contains several other non-opioid peptide hormones [468]. POMC contains only one opioid peptide, β-endo, which can be cleaved to form α-endo. Although β-endo has been detected in the GIT [469, 470], the localisation of β-endo expression still remains uncertain. There is some evidence of β-endo expression, and of other POMC peptides, by myenteric neurons, nerve fibers within the circular muscle and enteroendocrine cells [430, 444, 456, 471, 472]. Another major source of β-endo in the GIT are immune cells, particularly those associated with inflammatory bowel disease or irritable bowel syndrome [473, 474]. It should be noted that the distribution of β-endo in the GIT is controversial, as the specificity of the antisera used in many of these studies has been questioned [475]. Hence whilst there is certainly β-endo present in the GIT, the question of its origin remains unresolved.

Even though the distribution of the different classes of endogenous opioids in the GIT has been fairly well established, there is very little known about individual levels of the different peptides within each class. The expression of proteases that synthesize and degrade endogenous opioids may have varying levels of expression in different cell types, which would result in different production and degradation rates. As such, the mixture of opioid peptides derived from the same precursor will be variable in different cell populations. Differential proteolytic processing of proENK and proDYN peptides occurs in various regions of the brain and other tissues, leading to variations in the relative proportions of peptides derived from the same precursors [476-478]. Differential processing of precursors may also occur in the different cell populations within the GIT. In rat duodenum, specific antisera against DynA 1-17 and DynA 1-8 stain two distinct populations of neurons, one which contains both peptides and one with only DynA 1-8,

indicating that DynA 1-8 may be synthesized via distinct proteases or at varying rates in distinct neuronal populations [479].

Endogenous opioids play an important regulatory role in normal GIT physiology, primarily through activation of opioid receptors on enteric neurons [480]. When applied exogenously, the physiological effects of endogenous opioids are the same as the effects of other opioids, they hyperpolarize enteric neurons leading to inhibition of GIT motility and secretion and ultimately cause constipation [430]. On the other hand, the effects of endogenous peptides when released intrinsically under normal physiological conditions are unclear. Release of enkephalin- and dynorphin-derived peptides has been detected in intestinal tissue preparations during peristalsis or after electrical stimulation. These include Leu-enk, Met-enk, Met-enk-RF, Met-enk-RGL, metorphamide [481, 482], α-neo [483] and DynA [484, 485]. In addition, studies using opioid antagonists, mainly naloxone, have shown that inhibition of opioid activity increases non-propagating intestinal motility [486]. Altogether, this shows that endogenous opioids play a subtle but important role in control of GIT motility by suppressing activity. There is also evidence that the endogenous peptides either contribute to, or protect against, the development of pathophysiological conditions. Levels of endogenous opioids in the GIT have been shown to increase under pathological conditions, including inflammatory bowel disease, and not only inhibit gastrointestinal motility, but also provide visceral antinociception. β-endo levels have been shown to increase in a model of chronic inflammatory bowel disease in mice, suppressing inflammation-associated hyperexcitability of colonic primary spinal afferents [420, 474]. In addition, T lymphocytes can release β-endo and induce expression of β-endo in the myenteric plexus in mice with immunodeficiency-related visceral hyperalgesia [419, 473]. Surgical intervention has also been shown to increase dynorphin expression in the dorsal root ganglia of mice [421], and stimulate release of opioid peptides from enteric neurons after abdominal surgery in guinea pigs [422]. This may contribute in part to post-operative ileus, although sympathetic pathways are likely to play a more significant role. A greater understanding of the involvement of endogenous opioids in GIT pathophysiology is important as the opioid system is not only a potential target for treatment, but the enhanced production and release of endogenous opioids may also alter the effectiveness of opioid-based therapeutics.

End of excerpt from Thompson et al. (2014) "Biological redundancy of the endogenous GPCR ligands in the gut and the potential for endogenous functional selectivity" ***Front Pharmacol.*** **5:262**

1.2.4 μ-Opioid Receptor Signalling

MOP is known to couple to a wide range of intracellular signalling effectors, a summary of the classical MOP signalling pathways is shown in Figure 1.5. MOPs primarily couple to most members of the $G\alpha_{i/o}$ class ($G\alpha_{i1-3}$, $G\alpha_{o1-2}$ and $G\alpha_z$) [302, 487-490], thereby inhibiting AC [491]. Additionally, the released $G\beta\gamma$ subunit stimulates K^+ conductance predominantly via GIRKs [146] and inhibits Ca^{2+} conductance via N and P/Q type VGCCs [492-494], resulting in hyperpolarisation of the cell and inhibition of synaptosomal release of neurotransmitters [495-499].

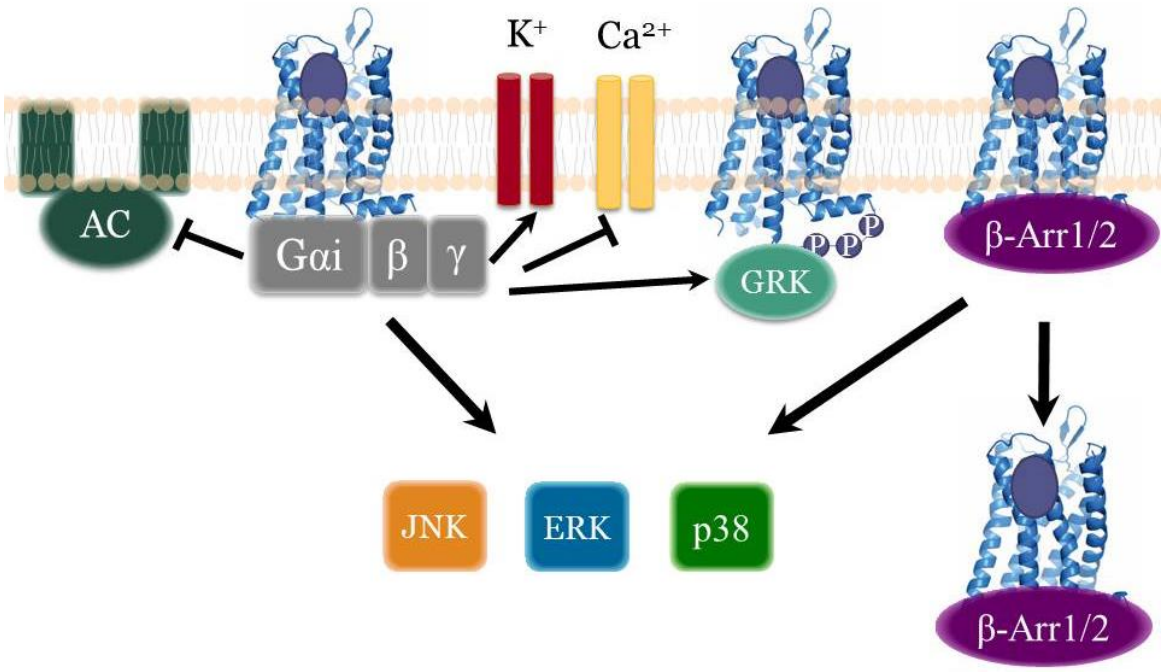

Figure 1.5: Classical opioid signalling pathways.
MOP activates G protein-gated inward rectifying K^+ channels (GIRKs, K^+) inhibits voltage-gated Ca^{2+} channels (VGCCs, Ca^{2+}) and inhibits adenylyl cyclase (AC). MOP regulation involves phosphorylation by GPCR kinases (GRKs), recruitment of β-Arr1/2 and internalisation of the receptor. MOP can also activate MAP kinases (JNK, ERK and p38) via both G protein and β-arr-mediated signalling pathways.

MOP can stimulate the activation of MAP kinases including ERK [500] [501], JNK [502-505] and p38 [506-508]. MOP mediated ERK activation has been studied in the most detail, but there are only a few examples of ERK activation by MOP in endogenously expressing cells or tissue [509-512]. However it has been shown in heterologous cell lines that like other $G\alpha_{i/o}$ coupled receptors, MOP mediates ERK activation primarily via $G\beta\gamma$, and PKC-dependent transactivation of RTKs [512-514]. Belcheva *et al* have found

in HEK293 and astrocytes that MOP mediated ERK phosphorylation requires PLC, PKCε and calmodulin [515, 516], whereas other groups have found in CHOs that ERK phosphorylation is via a PKC independent pathway that requires PI3K [154, 517]. MOP has been shown to stimulate β-arr-dependent ERK activation in heterologous cell lines, striatal neurons and astrocytes, and in some cases this pathway has been shown to require MOP internalisation [518], but not in others [501, 519, 520]. More recently, it has been shown that ERK activation is actually dependent on translocation of MOP from lipid rafts [520] into clathrin coated pits, where β-arrs mediate ERK activation from the clathrin coated pits and not endosomes [203]. JNK has also been shown to be activated by MOP via several different pathways. MOP stimulated JNK activation has been shown to be by a β-arr2-dependent pathway, which requires activation of Gβγ, GRK3, Src kinase and PI3K [502, 521]. However, MOP has also been shown to activate JNK via a β-arr independent pathway, which requires PKC activation and Src [503, 504, 521]. Finally, very little is known about MOP-induced p38 activation. However p38 activation appears to be β-arr2-dependent [508], and has been shown to be activated by chronic treatment with morphine in DRGs [506], and to mediate morphine-induced apoptosis in macrophages [507, 508, 522, 523]. Finally, MOP internalisation and resensitisation has been shown to be dependent on PLD activation, production of DAG and p38 activation [507, 523, 524].

Similar to most GPCRs, MOP desensitisation typically involves phosphorylation of the CT and ILs by GRKs and or second messenger kinases [171, 525-529], which facilitates recruitment of β-arr1 and 2 [274, 530, 531], preventing further signalling by G proteins. Subsequently MOPs can undergo clathrin/dynamin-dependent internalisation [532-535]. Internalised receptors are then either resensitised (i.e. dephosphorylated) and returned to the surface, or downregulated by degradation in lysosomes [536]. Recruitment of different β-arrs can have differential downstream effects, as they can act as scaffolds for different signalling complexes. β-arr1 has been shown to promote MOP dephosphorylation more rapidly than β-arr2, and has also been shown to be required for MOP ubiquitination [536], which is in turn required for trafficking of MOP to lysosomes [537].

Receptor phosphorylation patterns play a vital role in receptor desensitisation, internalisation, trafficking and resensitisation, as well as activation of β-arr-dependent signalling pathways [283, 284, 538]. There are numerous phosphorylation sites located on the intracellular loops and the CT of MOP which have been implicated in control of

these regulatory and signalling functions (Figure 1.6). Early investigations into MOP phosphorylation used mutagenesis studies to identify 3 key resides in the CT of mouse MOP; S^{363}, T^{370} and S^{375}, which are involved in MOP desensitisation [292]. S^{375} phosphorylation, in particular, has been shown to be vital for receptor desensitisation and β-arr recruitment, as it has been shown to undergo agonist-induced phosphorylation, and mutation of this residue to alanine reduces [D-Ala2, NMe-Phe4, Gly-ol5]-enkephalin (DAMGO) -induced desensitisation and MOP internalisation [292, 539-541]. More recently, phosphorylation of CT residues has been examined in more detail by several groups, confirming previous findings *in vivo* [542], and revealing numerous other residues in the intracellular regions which are involved in MOP regulation [184, 543-546]. Apart from the three residues above, these include several motifs in the CT such as S^{375}TANT [184, 545], T^{354}SST [544, 547-549] and T^{394} [550-552], most of which have shown agonist-induced phosphorylation and/or constitutive phosphorylation, and have also been implicated in MOP desensitisation. Lau, Trester-Zedlitz, Trinidad, Kotowski, Krutchinsky, Burlingame and von Zastrow [545] used quantitative mass spectrometry to examine phosphorylation of CT residues, and concluded that it is not just S^{375} phosphorylation, but rather overall phosphorylation of the S^{375}TANT motif that is required for recruitment of β-arrs and MOP internalisation. Subsequently, Just, Illing, Trester-Zedlitz, Lau, Kotowski, Miess, Mann, Doll, Trinidad, Burlingame, von Zastrow and Schulz [184], showed that MOP internalisation requires sequential phosphorylation of the S^{375}TANT motif and T^{370}, firstly S^{375} is phosphorylated, which is required for successive phosphorylation of T^{370}, T^{376} and T^{379}. In contrast, phosphorylation of the T^{354}SST motif does not appear to facilitate desensitisation via β-arrs, but rather this motif has been shown to promote desensitisation by altering ligand affinity and binding kinetics [549, 553]. Additionally, it is still uncertain whether T^{394} undergoes agonist-induced or constitutive phosphorylation. Nonetheless this residue and the surrounding glutamate residues are clearly vital for desensitisation [527, 550-552], and this region of the CT also been shown to be involved in delaying receptor internalisation and resensitisation [552].

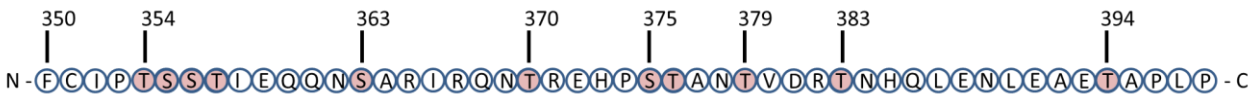

Figure 1.6: Mouse MOP CT phosphorylation sites.
There are 11 Ser and Thr residues on the CT of MOP which can be phosphorylated, and are known to be involved in MOP regulatory processes.

Most agonist-induced phosphorylation of MOP has been attributed to the activity of GRKs. GRK2 and 3, and to a lesser extent GRK5 and 6, have been shown to phosphorylate S^{375} [184, 541, 544, 546], whereas only GRK2 and 3 can phosphorylate T^{370} [184]. However, other kinases such as PKC, PKA, calcium/calmodulin kinase (CaMKII) and ERK have also been shown to be capable of phosphorylating the receptor either constitutively or in an agonist-induced manner [529, 530, 543, 544, 546, 554-556]. PKC can stimulate both constitutive and agonist-induced phosphorylation of MOP [546, 554, 557], as well as phorbol ester-dependent phosphorylation of T^{370} [557]. Additionally, CaMIIK, which is believed to be involved in desensitisation and the development of opioid tolerance [558, 559], has also been shown to phosphorylate T^{370} [544], and also two Ser residues on IL3 [529]. There is also substantial evidence that suggests that whilst receptor phosphorylation and β-arr recruitment are clearly involved in MOP desensitisation, they are not necessarily essential for MOP desensitisation [527, 560-562]. MOP desensitisation has been shown to occur via alternative pathways. These mechanisms include possible desensitisation via direct interaction of GRKs with $G\beta\gamma$ [563], inactivation of $G\alpha_i$ via phosphorylation by PKC [564] as well as an ERK-dependent desensitisation pathway [517, 556, 562].

MOP has also been shown to activate numerous other, less well characterised, signalling pathways under certain conditions. Prolonged agonist exposure has been shown to increase cAMP above basal levels, known as AC superactivation [565]. MOPs are also known to stimulate PLC activity and inositol phosphate turnover via $G\beta\gamma$ or $G\alpha_{15/16}$, potentiating $G\alpha_q$ mediated Ca^{2+} release from intracellular stores and PKC activation [566-569]. Additionally, MOP has been shown to stimulate PLA_2 and arachidonic acid release [514], and activate Akt signalling [570].

1.2.5 Biased Agonism at the μ-Opioid Receptor

Opioid receptors have a large binding site [29] and hence different ligands potentially interact with different components of the binding site, stabilising unique conformations of the receptor. This has been shown by mutagenesis studies of binding site residues that identified residues that disrupt binding of some ligands but not others [571-575]. However, it is yet to be shown if these unique ligand-receptor interactions result in stabilisation of unique receptor conformations and biased agonism. Whilst there is limited direct evidence of agonist-dependent receptor conformations at the MOP to date, there is an abundance of indirect evidence to show ligand-dependent signalling at the MOP. Ligand directed signalling of MOPs was first observed in experiments that demonstrated agonist-dependent phosphorylation and internalisation of MOP, where DAMGO, but not morphine, stimulated robust MOP phosphorylation and internalisation [171, 533]. This was subsequently demonstrated *in vivo* [535, 576]. Since this discovery, research in the opioid field has largely focussed on understanding the mechanisms behind agonist-dependent MOP regulation and its role in desensitisation and development of opioid tolerance. In addition to agonist-dependent MOP phosphorylation and internalisation, differential activation of numerous other signalling events has been observed including β-arr recruitment, receptor trafficking and resensitisation, MAP kinase activation, receptor movement between plasma membrane domains, as well as activation of several other second messenger kinases. Whilst there is increasing evidence that shows that biased agonism at the MOP is pluridimensional, most descriptions of bias at the MOP to date have been limited to ligands which show a preference between activation of either G protein-mediated or β-arr-mediated signalling.

It is now widely accepted that morphine, under most conditions, stimulates little to no internalisation of MOP, whereas most other agonists including DAMGO and endogenous opioids promote robust receptor internalisation [533, 535, 577, 578]. Similarly, differential activation of other related cellular events has also been observed between “internalising” and “non-internalising” agonists. Translocation of MOP from lipid rafts to non-raft domains has only been observed with internalising ligands such as DAMGO and etorphine [520]. Furthermore, since p38 MAPK and PLD activation are required for MOP internalisation, morphine would be expected to induce little p38 MAPK phosphorylation. In agreement with this, Tan, Walwyn, Evans and Xie [508] have shown that in mouse DRG neurons β-arr2-dependent p38 MAPK activation is required for DAMGO but not morphine-induced receptor internalisation and desensitisation of VGCC

inhibition [508]. Similarly, PLD activation in HEK293 cells has been observed in response to DAMGO but not morphine [524]. Internalisation is also dependent on the recruitment of β-arrs, hence internalising ligands such as DAMGO stimulate robust recruitment of β-arr1 and 2. Conversely, non-internalising agonists promote very little β-arr recruitment [579-581]; there is very little β-arr2 recruitment in response to morphine and β-arr1 recruitment is undetectable [579]. More recently, several novel ligands have been discovered which stimulate little to no β-arr recruitment or MOP internalisation. These include herkinorin, an analogue of the potent KOP agonist salvinorin A, which does not promote any β-arr recruitment or receptor internalisation [580], and TRV130, which stimulates less β-arr2 recruitment compared to morphine [581]. Overall there is a clear distinction between the ability of internalising and non-internalising ligands to activate several signalling processes, however even among ligands with a similar ability to internalise MOP, there are differences in the subsequent trafficking and resensitisation of the receptor. DAMGO desensitised receptors are readily internalised, dephosphorylated and recycled back to the surface, whereas etonitazene treated receptors are readily internalised, but are not dephosphorylated nor returned to the surface [541, 543]. Even though receptors desensitised to morphine remain at the surface, they are still dephosphorylated efficiently at the plasma membrane [543]. Altogether, differential activation of these regulatory events; receptor phosphorylation, β-arr recruitment and receptor internalisation and trafficking, can have significant effects on the activation of downstream signalling pathways as well as desensitisation and the development of tolerance.

Differential β-arr recruitment and MOP internalisation has been linked to stimulation of different phosphorylation patterns on the CT of the receptor. Agonists that robustly stimulate receptor internalisation, DAMGO, etonitazene and fentanyl, strongly stimulate multi-site phosphorylation of the CT motif required for MOP internalisation (T^{370} and the S^{375}TANT motif), whereas the weakly internalising morphine only stimulates weak phosphorylation of S^{375} and little to no phosphorylation of T^{370}, T^{376} and T^{379} [184, 543, 544]. In line with this, mutation of these residues inhibits agonist-induced β-arr2 recruitment to clathrin coated pits and MOP internalisation [184, 545]. Differences in agonist-induced receptor phosphorylation are mainly a result of selective engagement of different kinases. MOP phosphorylation on the S^{375}TANT motif stimulated by DAMGO, etonitazene and fentanyl is mediated by GRK2 and 3 but not GRK5 [184, 530, 546]. Conversely morphine appears to poorly stimulate MOP phosphorylation by GRK2

or 3, and instead induces S^{375} phosphorylation via GRK5 [546]. The lack of morphine-induced GRK2 activation appears to underlie the inability of morphine to stimulate β-arr1 recruitment and MOP internalisation, as overexpression of GRK2 enables morphine to stimulate β-arr1 recruitment and MOP internalisation [274, 525, 579, 582]. There is also the potential for differential receptor phosphorylation to be mediated by activation of second messenger kinases. This has been observed in membrane preparations, where morphine and β-endo stimulated MOP phosphorylation in the presence of PKA whereas DAMGO and Met-enk did not [555]. Altogether, the differential activation of multiple kinases by MOP ligands results in stimulation of different receptor phosphorylation patterns, which regulates internalisation and potentially regulates activation of other signalling pathways.

In addition to differential receptor phosphorylation, numerous studies have shown that desensitisation and the development of tolerance to DAMGO, morphine and other agonists is also dependent on activation of different kinases [503, 583, 584]. For instance, tolerance to fentanyl but not morphine appears to be GRK3-dependent, as acute analgesic tolerance to fentanyl is attenuated in GRK3 -/- mice, whereas tolerance to morphine is unaffected [503, 585], except in the hippocampus where tolerance to morphine is attenuated [585]. Similarly, DAMGO and Met-enk utilise a GRK2/β-arr2-dependent desensitisation pathway in LC neurons [562, 583, 584, 586], and other cell types [526, 531]. However, activation of GRK2/β-arr2 in response to morphine is only associated with the development of tolerance in response to chronic treatment, but not acute desensitisation in LC neurons [584, 587]. Instead, desensitisation and tolerance induced by morphine have been shown to be dependent on activation of PKC [503, 530, 588-592]. Morphine stimulates activation of PKC [564, 593], which phosphorylates $G\alpha_{i2}$ to prevent further G protein mediated signalling [564]. Numerous studies have shown that morphine-induced desensitisation and tolerance is attenuated by inhibition of PKC activity in LC neurons and HEK293 cells, and is enhanced by PKC activation [530, 590]. Surprisingly, not all ligands which normally induce GRK2/β-arr2-dependent desensitisation show the same propensity for activation of the PKC-dependent pathway. Fentanyl has been shown to activate PKC, and stimulate desensitisation simultaneously via both PKC and GRK2/β-arr2-dependent mechanisms. However, desensitisation to Met-enk is unaffected by PKC inhibition but is enhanced by PKC activation [590].

MAP kinases ERK and JNK have also been implicated in agonist-dependent mechanisms of MOP desensitisation and tolerance. DAMGO, but not fentanyl-induced

nociceptive tolerance has been shown to be dependent on ERK activation [594]. MOP agonists have been shown to preferentially activate ERK via different pathways. DAMGO, fentanyl and etorphine have been shown to stimulate ERK activation via a GRK2/3 and β-arr2-dependent pathway, [208, 511, 593], whereas morphine and methadone activate ERK via a G protein mediated pathway that is dependent on PKC [208]. ERK activated via these different pathways was also shown to target different substrates. ERK activated via the G protein-dependent pathway remained in the cytosol and activated 90RSK and CREB, whereas ERK activated via the β-arr-dependent pathway translocated to the nucleus where it activated ELK-1 [208]. DAMGO has been shown to activate JNK via the Gβγ/PI3K pathway [502], whereas morphine activation of JNK is PKC-dependent [503, 504]. However, only JNK activated in response to morphine appears to contribute to desensitisation, as JNK inhibition prevents desensitisation and the development of tolerance to morphine, but not to fentanyl or DAMGO [503, 504, 589]. Furthermore, this JNK-mediated desensitisation mechanism is also potentially dependent on β-arr2, as JNK-mediated desensitisation to morphine is absent in β-arr2-/- mice [504]. Overall, MOP ligands differentially activate multiple desensitisation pathways, including both receptor phosphorylation-dependent and -independent mechanisms, via activation of various kinases and other signalling effectors.

Most biased agonism at the MOP receptor observed so far has been between G protein and β-arr mediated signalling, or in some cases differential activation of various β-arr-dependent events. The potential for bias between activation of multiple G protein-mediated signalling pathways has remained largely unexplored. This is due to the fact that the G protein activation efficacy of a ligand has always been assumed to equate to its efficacy for activation of G protein-mediated signalling. However this is not necessarily the case, as changes in the rank order of efficacy between G protein activation and G protein-mediated signalling in different studies has been observed [595-601], although these have not yet been confirmed by quantification of bias. Additionally, agonists have been shown to display different profiles of intracellular Ca^{2+} flux in HEK293 cells [602], which most likely occurs via G protein-dependent mechanisms [566]. Furthermore, differential activation of $G\alpha_{i/o}$ subtypes at MOP has also been examined by several groups, and several MOP agonists have shown preferences, albeit small, for activation of specific subtypes [603-606], which may lead to differential activation of G protein mediated signalling pathways.

Altogether, studies of biased agonism at the MOP have shown that MOP ligands display an assorted array of signalling patterns. However, up till now, all studies examining biased agonism at the MOP have been limited to examination of a small number of signalling endpoints and only a handful of synthetic opioids, and have predominantly based their conclusions on the responses of ligands at a single concentration. Extending biased agonism studies to include a more diverse range of MOP ligands will likely uncover even more variety in MOP signalling patterns. One class of opioids that has been largely omitted from biased agonism studies is the endogenous peptides. All endogenous opioids possess an identical pharmacophore, the Tyr-Gly-Gly-Phe tetrapeptide, which is essential for opioid receptor binding and activation [332, 607]. Similarly the putatively endogenous ligands, endo-1 and endo-2 have tripeptide pharmacophores, Tyr-Pro-Trp and Tyr-Pro-Phe respectively [332]. Ligands with identical pharmacophores would normally be expected to stabilise the receptor into similar conformations, however this is not necessarily the case. The highly variable C-terminal residues of the endogenous opioids, which determine the selectivity between opioid receptor subtypes [607], may also enable endogenous opioids to stabilise unique conformations of the receptor. The CT residues may achieve this either via unique interactions with other residues in the orthosteric binding site or other extracellular regions of the receptor, and/or by altering the conformation of the tetrapeptide pharmacophore. Interactions with the extracellular loops have been shown to be particularly important for binding and selectivity of peptide ligands but not other ligands [608-610], however unique interactions between particular endogenous opioids are yet to be discovered. The potential for the tetrapeptide to adopt multiple conformations at the same receptor has been shown recently. The potential binding pose of Leu-enk has been determined by docking Leu-enk into the recently published crystal structures of MOP and DOP in the inactive state [29, 611]. This revealed two potential conformations of Leu-enk when bound to DOP. Thus it is clear that the endogenous opioid pharmacophore is capable of adopting multiple conformations, which, if they can be differentially adopted by different endogenous opioids, could each stabilise the receptor in unique active conformations resulting in biased agonism. With the exception of Met-enk, relatively very little is known about the signalling pathways activated by endogenous opioids at the MOP. Not surprisingly however, endogenous opioid signalling tends to mimic that of the Met-enk analog DAMGO, rather than that of morphine [597]. Only a handful of studies have examined biased agonism of a small number of endogenous opioids [596, 612-614], and so far have observed very little

diversity in biased agonism. The only exception is endo-2 which has been shown to be biased towards recruitment of β-arr2 over G protein activation and stimulate stronger MOP phosphorylation [596, 615, 616]. In addition to this, Yu, Zhang, Yin, Sun, Uhl and Wang [597] discovered that α-neo does not stimulate detectable MOP phosphorylation, which is in contrast to most other endogenous ligands that stimulate robust MOP phosphorylation and internalisation [576, 596, 597, 617, 618].

To enable design of a novel biased opioid that selectively activates signalling pathways that produce analgesia with minimal activation of pathways responsible for producing side effects, the contribution of each signalling pathway to specific physiological effects needs to be established. It is well established that the MOP exerts its acute analgesic effects primarily through the inhibition of neurotransmitter release, which, depending on the cell type, is achieved via G protein-mediated effects on AC, K^+ and Ca^{2+} channels [123, 498, 619, 620]. For instance, in LC neurons MOP is predominantly coupled to GIRKs and VGCCs [620-623], whereas as in DRGs MOP couples to VGCCs and AC [123, 624-627]. In line with this, the efficacy of an agonist to activate G proteins correlates well with its analgesic efficacy [601]. However, there is evidence that MOP ligands produce analgesia at least partly via divergent signalling pathways [628-631]. For example, the analgesic effects of morphine, levorphanol and buprenorphine, but not fentanyl or methadone, have been shown to be dependent on stimulation of Na^+,K^+-ATPase activity, possibly via inhibition of AC which results in less PKA phosphorylation of Na^+,K^+-ATPase [629]. This indicates that there may be the potential for increasing analgesic efficacy by tweaking ligand bias towards particular G protein-mediated signalling pathways. Precise determination of the physiological roles of other signalling pathways activated by MOP has proved to be difficult. Since MAP kinases have so many potential downstream targets, they appear to have multiple physiological roles. Apart from their involvement in the development of tolerance already described, MAP kinase activation has also been associated with reduced analgesia in response to morphine [632, 633], but also enhanced analgesia in response to DAMGO [594].

Unfortunately, most side effects to MOP analgesics, including respiratory depression and inhibition of GIT motility, are also mediated via activation of the same G protein-mediated signalling pathways in different tissues [429, 634, 635], so simply designing ligands that are biased towards G protein activation may not result in generation of fewer side effects. However, this is not necessarily the case with activation of signalling pathways that are involved in desensitisation and the development of tolerance. This is

in part because these signalling events appear to be highly tissue specific. Some MOP ligands have been shown to stimulate MOP desensitisation via different mechanisms in some cell types. For instance morphine, which does not stimulate GRK2/3 or MOP internalisation, does stimulate MOP internalisation in dendrites of neurons of the nucleus accumbens (NA) [636], and morphine-induced tolerance is reduced in the hippocampus of GRK3-/- mice [585]. Oxycodone has also been shown to stimulate MOP internalisation in HEK293 cells [503] but not in LC neurons [618]. Furthermore, the development of tolerance to morphine appears to be independent of ERK activation [503, 637], except tolerance is inhibited in the PAG [638] and enhanced in the spinal cord and DRGs by ERK activation [639]. Additionally, increased expression or activity of kinases involved in MOP desensitisation, have also been shown to alter desensitisation mechanism induced by some ligands. Overexpression of GRK2 enhances the ability of morphine to stimulate recruitment of β-arrs and internalise the receptor and reduces AC inhibition [525]. Likewise, increased PKC activity induced by phorbol esters or concomitant activation of a $G\alpha_q$ coupled receptor, enhances desensitisation to Met-enk [590]. Overall this suggests that the natural variations in expression and activity of these kinases in different cell types will alter the mechanisms of desensitisation used by these ligands.

Tissue specific regulation induced by morphine has been demonstrated by the effects of morphine in β-arr2-/- mice [640]. These mice are more resistant to morphine-induced respiratory depression and constipation, but conversely morphine-induced analgesia is enhanced and analgesic tolerance is reduced [579, 640-643]. Interestingly, the attenuation of analgesic tolerance was greater for supraspinal analgesia than for spinal analgesia [643]. Overall this suggests that β-arr2 may play differential roles in desensitisation and the development of tolerance to morphine in different tissues. Additionally, these effects are not observed with other agonists such as methadone, fentanyl, etorphine and oxycodone [579, 640-642], which shows that activation of the same signalling effector by different ligands may not necessarily result in activation of the same downstream signalling events. Nonetheless, several groups have begun searching for ligands which stimulate less β-arr2 recruitment compared to morphine in the hope that they will mimic the effects of morphine in β-arr2-/- mice and produce enhanced analgesia with reduced side effects. This has led to the development of a G protein biased compound TRV130, which has been shown to produce less respiratory

and gastrointestinal side effects, and is currently in phase III clinical trials [581, 644, 645].

For a review on quantification of bias at MOP please refer to chapter 1.3 Novel GPCR Paradigms at the μ-Opioid Receptor

Declaration for Thesis Chapter 1.3

Monash University

Declaration by candidate

In the case of Chapter 1.3, the nature and extent of my contribution to the work was the following:

Nature of contribution	**Extent of contribution (%)**
Data analysis and writing of the manuscript	80%

The following co-authors contributed to the work. If co-authors are students at Monash University, the extent of their contribution in percentage terms must be stated:

Name	**Nature of contribution**	**Extent of contribution (%)** for student co-authors only
Meritxell Canals	Contributed to data analysis and writing of the manuscript	N/A
Arthur Christopoulos	Contributed to writing of the manuscript	N/A
Eamonn Kelly	Contributed to data analysis and writing of the manuscript	N/A

The undersigned hereby certify that the above declaration correctly reflects the nature and extent of the candidate's and co-authors' contributions to this work*.

Candidate's Signature	[redacted]	**Date 9 May 2016**
Main Supervisor's Signature	[redacted]	**Date 9 May 2016**

1.3 Novel GPCR Paradigms at the μ-Opioid Receptor

Georgina L. Thompson [1,2], Eamonn Kelly[3], Arthur Christopoulos[1] and Meritxell Canals[1]

Published in Br J Pharmacol. 2015;172(2):287-96

[1]Drug Discovery Biology and Department of Pharmacology, Monash Institute of Pharmaceutical Sciences, Monash University, 399 Royal Parade, Parkville, Victoria 3052, Australia; [2]Defence Science and Technology Group, Australian Department of Defence, Australia; [3] School of Physiology and Pharmacology, University of Bristol, Bristol, UK

1.3.1 Abstract

Opioids, such as morphine, are the most clinically useful class of analgesic drugs for the treatment of acute and chronic pain. However, the use of opioids is greatly limited by the development of severe adverse side effects. Consequently, drug discovery efforts have been directed towards improving the therapeutic profile of opioid-based treatments. Opioid receptors are members of the family of GPCRs. As such, the recent GPCR paradigms of biased agonism and allosterism may provide novel avenues for more effective analgesics. Biased agonism (or functional selectivity) has been described for all the opioid receptor family members. Furthermore, the first allosteric modulators of opioid receptors have very recently been described. However, identification and quantification of biased agonism in a manner that is informative to medicinal chemists and drug discovery programmes still remains a challenge. In this review, we examine the progress, to date, towards identification and quantification of biased agonism and allosterism at the μ-opioid receptor in the context of its implications for the discovery of better and safer analgesics.

1.3.2 Introduction

GPCRs can mediate a spectrum of acute signalling and longer-term regulatory behaviours that can be modulated in a ligand-specific manner. Such functional versatility cannot be explained by a simple ‘on–off’ switch model of receptor activation, and is more compatible with dynamic and flexible structures. Indeed, during the last decade, we have witnessed the experimental confirmation of previously theoretical concepts demonstrating that GPCRs exist in many, temporally related, micro-conformations [646, 647]. Approaches such as NMR spectroscopy have provided evidence that GPCRs are highly dynamic proteins that exist in several functionally relevant conformational states [52, 647]. Two paradigms that are fundamentally linked to such inherent plasticity of GPCRs are biased agonism (or functional selectivity) and allosterism.

Biased agonism describes the phenomenon whereby the binding of different ligands to the same receptor in an identical cellular background results in differential activation of cell signalling pathways and, eventually, in different physiological outcomes [233]. At a molecular level, this is a consequence of the fact that different agonists do not activate receptors through stabilisation of the same active state; rather, they can stabilise different functionally active states that lead to the engagement of a limited subset of intracellular effectors, and in turn, the activation of specific signalling pathways. The ability of distinct GPCR-agonist complexes to differentially activate intracellular signals provides new avenues for the development of drugs that are not only receptor-specific, but also ‘pathway-specific’, and has opened the way to the discovery of ligands that selectively activate signalling pathways mediating the desired physiological effects while minimizing ‘on-target’ side effects that are elicited by activation of other signalling pathways via the same receptor. However, although this concept is very attractive, there are significant challenges to its translation from the field of medicinal chemistry into effective therapies. On the one hand, the identification of the signalling pathways responsible for therapeutic effects and of those responsible for the deleterious side effects is not straightforward; on the other hand, analytical tools for the detection and quantification of biased agonism are becoming available for drug development efforts aimed in this direction [648].

The phenomenon of allosterism is also a consequence of the conformational plasticity of GPCRs. Allosteric ligands influence receptor activity by binding to sites that are topographically distinct from the site where the endogenous (orthosteric) ligand binds.

Classical models of allosterism already postulated the need for multiple conformational states in the absence of ligand as a fundamental characteristic of allosteric proteins [649]. These states exist in a dynamic equilibrium, and the binding of a ligand to an allosteric protein stabilises some states at the expense of others [650]. As such, allosteric ligands mediate their effects by promoting conformational changes in the GPCR protein that are transmitted from the allosteric binding pocket to the orthosteric site, or directly to the effector sites. In terms of drug development, allosteric GPCR ligands offer significant advantages over targeting of the orthosteric site. First, because of the lack of evolutionary pressure on sites other than that where the endogenous ligand binds, allosteric sites have not necessarily been conserved and therefore offer greater potential for receptor subtype selectivity. Second, in the absence of intrinsic efficacy, allosteric modulators will only exert their effect when and where the endogenous ligand is present, therefore tuning cellular responses and maintaining the temporal and spatial characteristics of endogenous signals. Furthermore, as the effect of an allosteric ligand is limited by its cooperativity, such class of ligands may become safer therapies with fewer on-target overdosing risks.

Studies on opioid receptors have provided prototypical examples of ligand-dependent signalling and regulation [651], and recently, allosteric modulators of the MOP have been described [652]. In this review, we examine the progress, to date, towards identification and quantification of biased agonism and allosterism at the MOP, in the context of its implications for the discovery of better and safer analgesics.

1.3.3 Ligand-Dependent Effects at the μ-Opioid Receptor

Opioids have been used for millennia for the treatment of moderate to severe pain, and remain the most effective and widely used analgesics to date. Of the four subtypes of opioid receptors, the MOP subtype is the therapeutic target for most currently used opioids as the analgesic effects of morphine were abolished in a MOP knockout mouse [339]. However, it is well known that opioid analgesics, including morphine, oxycodone and fentanyl, suffer from very limiting side effects such as tolerance, dependence and addiction, respiratory depression, and constipation, which severely limit their clinical use. Therefore, there is a need for new compounds that provide effective analgesia, but without the serious side effects.

As mentioned previously, biased agonism offers such potential, and there are clear indications of the existence of ligand-specific effects on MOP signalling and regulation

[see 651, 653]. Two key observations on the actions of morphine triggered most of the studies on biased agonism at the MOP. First, morphine induces relatively less MOP internalisation, in spite of its efficacy in mediating G-protein activation [533, 535]. Second, morphine-induced respiratory depression and constipation are dramatically attenuated in a β-arr2 knockout mouse while analgesia is enhanced [640]. This latter result also provided clear evidence of the tissue-specific mechanisms of receptor activity and regulation. Taken together, these reports have sparked the search for the potentially different signalling mechanisms that mediate the diverse physiological actions of MOP agonists as well as for ligands that exploit such mechanisms. However, most descriptions of biased agonism at the MOP have been based on qualitative comparisons between ligands. The number of studies quantifying bias is still very low (see later). Yet, in order to apply biased agonism therapeutically and effectively, it is necessary to incorporate parameters that describe the degree of bias in a manner that can inform future drug development.

1.3.4 Quantifying Biased Agonism

Although biased agonism is now widely accepted, the majority of studies to date on biased agonism have used largely qualitative observations, such as reversals in agonist potency orders or maximal agonist effects between different pathways, as indicators of biased agonism. However, such approaches are not optimal. The observed response of an agonist at a given pathway is not only the result of unique ligand-induced receptor conformations, but is also affected by ‘system bias’, which reflects the differing coupling efficiencies of the receptor to a given signalling pathway, and by ‘observation bias’, which results from differing assay sensitivity and conditions [648]. It is the bias imposed by the ligand on the receptor that is the only source of bias that can be chemically optimised to improve the therapeutic profile of a drug. It is therefore important to quantify signalling bias in such a way that it excludes system and observation bias, in order to reveal the unique signalling profile that is induced by the ligand.

The potency of a ligand is determined by both its affinity for the receptor state coupled to that particular pathway, as well as its intrinsic efficacy for generating a response in that pathway. In contrast, the maximal effect of a ligand at saturating concentrations is only determined by intrinsic efficacy. In addition, contributors to system bias, signal amplification and receptor expression need to be taken into account as they have markedly different effects on potencies and efficacies of differently efficacious ligands.

Therefore, a rigorous and useful analysis of bias should take into account both potency and maximal effect of a ligand, eliminate the effects of system and observation bias, and should be broadly applicable to routinely derived concentration–response data. Such analysis would not only allow the signalling bias profiles of ligands in different cell types to be compared, but would also aid the efforts of medicinal chemists to discover new biased ligands.

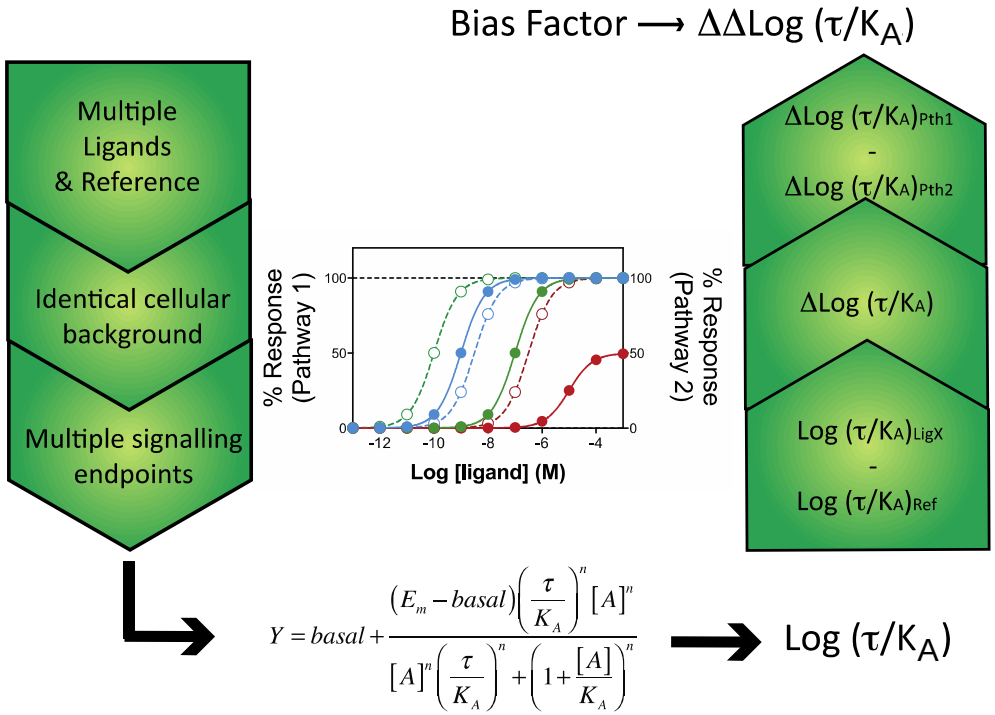

Figure 1.7: Quantification of biased agonism using relative transduction ratios.
In order to quantify the signalling bias of a set of ligands, it is necessary to measure bias in an identical cellular background across several signalling end points. Full concentration–response curves for each pathway are fitted to the Black–Leff operational model to estimate a transduction coefficient (log[τ/K_A]) for each agonist (in the example, solid lines for pathway 1 and dotted lines for pathway 2). Next, the effects of system and observation bias are removed by adjusting these values to a reference ligand to yield the $\Delta\log[\tau/K_A]$. Finally, the relative transduction ratio ($\Delta\Delta\log[\tau/K_A]$) is obtained by subtraction of the $\Delta\log[\tau/K_A]$ value of two pathways one from another. The $\Delta\Delta\log[\tau/K_A]$ values represent ligand bias on a linear scale, which is amenable to statistical analysis. [A], agonist concentration; K_A, operational affinity; τ, efficacy; n, slope of the fitting parameter; Em, maximal response of the system. For a step-by-step method to measure bias, see van der Westhuizen, Breton, Christopoulos and Bouvier [654].

Several analytical approaches have been described to quantify biased agonism [see 648]. Of these, the relative transduction ratio [$\Delta\Delta\log(\tau/K_A)$] is one of the most robust

and widely applicable method for bias quantification. This method applies the operational model of agonism first derived by Black and Leff [655]. Application of this model to concentration–response curves estimates a 'transduction coefficient' $\log(\tau/K_A)$ which is comprised of the functional equilibrium dissociation constant (operational affinity, K_A), a measure of the affinity for the receptor coupled to a particular effector protein or signalling pathway, which is different from the affinity of the ligand for the bare receptor determined in radioligand binding experiments (see later); and τ which encompasses both the intrinsic efficacy of the agonist in activating a particular signalling response and receptor density. The $\log(\tau/K_A)$ is thus an overall measure of the relative 'power' of an agonist to induce a response. In order to eliminate the effects of system and observation bias, the $\log(\tau/K_A)$ is normalised to a reference agonist, yielding values of $\Delta\log(\tau/K_A)$. Finally, these values can be compared across two signalling pathways for a given agonist to obtain the relative transduction ratio $\Delta\Delta\log(\tau/K_A)$ as measures of agonist bias (Figure 1.7).

1.3.5 Quantification of Biased Agonism at the μ-Opioid Receptor

The effects of morphine in the β-arr2 knockout mice [640] together with the substantial evidence of the distinct effects of morphine in MOP desensitisation and internalisation [530, 587] suggest that ligands that display bias towards G-protein-mediated pathways and away from β-arr2 recruitment, may have improved therapeutic profiles as analgesics. Such ligands offer the potential to provide pain relief with less adverse effects normally associated with the opioid agonists, including tolerance, dependence and addiction, constipation, nausea, and respiratory depression. For this reason, most of the studies focused on detection and quantification of biased agonism have utilised these two pathways, G-protein activation and β-arr2 recruitment, albeit using different approaches for such determinations [596, 598, 612, 615, 656].

Using bioluminescence resonance energy transfer (BRET) approaches, Molinari, Vezzi, Sbraccia, Gr, Riitano, Ambrosio, Casella and Costa [612] investigated the ability of MOP and DOP to activate G proteins and recruit β-arrs [612]. G protein activation by a wide range of opioid ligands was measured as changes in the BRET signal in between the receptor and the β1 subunit of the G protein in cell membranes while arrestin recruitment to the receptor was performed in whole cells. Plotting the relative intrinsic activities (i.e. the maximal response of a given ligand relative to the maximal response of a reference agonist) of all ligands in the two signalling endpoints revealed a

hyperbolic relationship between the two. This is in line with the fact that most of the tested ligands displayed full agonism for G protein activation and intrinsic activities fail to differentiate between full agonists [657]. A number of ligands including morphine, oxymorphone and ethylketocyclazocine clustered as ligands with low intrinsic activities for β-arr2 recruitment and high intrinsic activities for G protein activation. Indeed, this result is also expected when the coupling efficiency of different pathways is taken into consideration, as the response of partial agonists will be lower in less efficiently coupled signalling pathways such as β-arr2 recruitment. Estimation of the bias factor $\Delta\Delta\log(\tau/K_A)$ relative to etorphine of the corresponding concentration–response curves reveals that different intrinsic activities (such as oxymorphone vs. etorphine, endo-2 or lofentanyl) do not necessarily translate into significant ligand bias (Figure 1.8A).

As bias is an intrinsic characteristic of a ligand, it follows that metabolites of a given ligand do not necessarily have to mimic the bias of the original compound. Interestingly, this has been evaluated *in vitro* for morphine and its metabolites [656] using Förster Resonance Energy Transfer (FRET) approaches to detect $G\alpha_{i1}$ activation and β-arr2 recruitment. Comparison of relative efficacies of all the metabolites to morphine, suggested that only 3 metabolites (normorphine, 6-acetylmorphine, morphine-6-glucuronide) showed bias towards β-arr2 recruitment. However, when using morphine as the reference ligand to estimate $\Delta\Delta\log(\tau/K_A)$ values, nearly all the metabolites are significantly biased towards β-arr2 compared with morphine (Figure 1.8B). This illustrates additional information that can be obtained by application of the operational model of agonism to detect and quantify bias because, as mentioned previously, comparison of relative efficacies fails to distinguish between full agonists as their activity is limited by the system. In this case, the signalling bias of higher-efficacy agonists may be overlooked or may be mistakenly considered as biased when they are in fact not. Therefore, in the case of the higher-efficacy agonists, a scale that incorporates both the maximal response and potency, such as the transduction coefficient, is required. Such results also suggest that morphine metabolites possess divergent signalling bias, an aspect that will need to be taken into consideration when interpreting the effects of morphine signalling *in vivo*. Finally, it should be noted that in these experiments, GRK2 was only overexpressed when measuring β-arr2 recruitment, and as described later, the cellular content of relevant proteins or other agents can also play a role in the direction of bias. It would therefore be very informative to quantify bias of morphine metabolites under similar conditions across different signalling pathways.

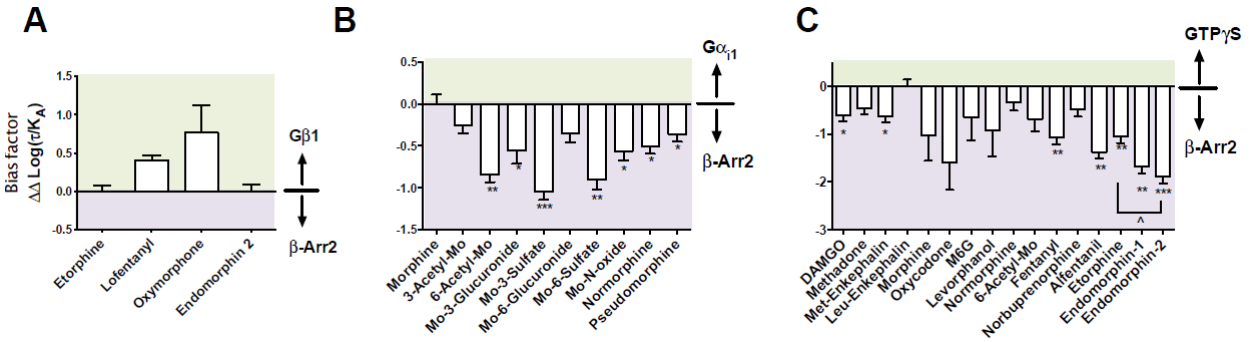

Figure 1.8: Quantification of signalling bias between G protein and β-arr interactions at MOP.

(A) Relative transduction ratios estimated for data from Molinari, Vezzi, Sbraccia, Gr, Riitano, Ambrosio, Casella and Costa [612] between assays for Gβ1 and β-arr2 interactions using etorphine as the reference ligand showed no significant bias between ligands (B) Relative transduction ratios between Gαi1 and β-arr2 recruitment estimated using data from Frolich, Dees, Paetz, Ren, Lohse, Nikolaev and Zenk [656] using morphine as the reference ligand shows that most morphine metabolites are significantly biased towards recruitment of β-arr2 compared with morphine (C) Relative transduction ratios between GTPγS binding and β-arr2 recruitment from McPherson, Rivero, Baptist, Llorente, Al-Sabah, Krasel, Dewey, Bailey, Rosethorne, Charlton, Henderson and Kelly [596] estimated using Leu-enk as the reference ligand show that in addition to endo-2, endo-1, etorphine and several other ligands are biased towards β-arr2 recruitment. The two-tailed t-test was used to determine whether transduction ratios were statistically different from the reference ligand * P≤0.05, **P≤0.01, ***P≤0.001, ∧P≤0.05.

In a systematic approach to evaluate biased agonism at the MOP, McPherson, Rivero, Baptist, Llorente, Al-Sabah, Krasel, Dewey, Bailey, Rosethorne, Charlton, Henderson and Kelly [596] examined the signalling bias of a wide range of ligands including endogenous opioid peptides and synthetic opioids [596, 615]. As in the previous reports, G-protein activation and β-arr2 recruitment were measured by [^{35}S]GTPγS binding, and an enzymatic complementation assay respectively. In these studies, endo-2 was the only ligand that showed statistically significant bias towards β-arr2 recruitment. Agonist bias was determined by fitting concentration–response curves to the Black–Leff operational model to estimate the efficacy parameter τ. However, instead of estimating the functional affinity of the ligand-bound receptor in each particular pathway, the affinity parameter in these calculations remained constant across pathways and was determined from radioligand binding experiments [658]. Given that a ligand can have differing affinities for distinct receptor states (e.g., for the G-protein-bound and unbound states), such differing affinities have to be taken into account when measuring biased agonism. Although in some situations, the binding affinity and the functional affinity can be very similar, this will not always be the case [see 648, 659]. When the dissociation constant is obtained from concentration–response curves using

the Black–Leff operational model and bias factors are estimated, it becomes apparent that other ligands, apart from endo-2 also show significant bias towards β-arr2 recruitment when compared with Leu-enk as a reference ligand (Figure 1.8C). Interestingly, some ligands used in this analysis had previously been used in other studies. However, the relative transduction ratio analysis suggests that morphine-6-glucuronide, 6-acetyl-morphine and normorphine did not show significant bias towards β-arr2 recruitment when compared with morphine in contrast to previous reports Frolich, Dees, Paetz, Ren, Lohse, Nikolaev and Zenk [656]. Similarly, this analysis also revealed a significant difference between etorphine and endo-2 that had not been detected by Molinari, Vezzi, Sbraccia, Gr, Riitano, Ambrosio, Casella and Costa [612] (Figure 1.8).

Finally, the ability of different ligands to mediate G-protein activation, receptor desensitisation and receptor internalisation has been examined using inhibition of calcium channel currents (I_{Ca}) and immunocytochemistry, respectively, as functional readouts [598]. The relative efficacies of DAMGO, morphine, methadone and pentazocine were measured for acute inhibition of calcium currents, for homologous desensitisation of these currents and for receptor endocytosis. Importantly, relative efficacies were calculated using functional affinity constants determined experimentally from receptor depletion experiments. These experiments revealed that the efficacy for I_{Ca} inhibition did not correlate with the efficacy of desensitisation or receptor internalisation, suggesting that morphine and, potentially, pentazocine are biased, relative to DAMGO, and that acute desensitisation is not dependent on receptor internalisation.

Overall, these studies have provided valuable insight into biased signalling of opioids at MOP although it still remains to be seen whether they are able to predict differential responses *in vivo*. These studies also illustrate the importance of a number of factors that influence the identification and quantification of biased agonism such as cellular content, the pluridimensionality of efficacy and the choice of a reference agonist. It is important to consider these key aspects when interpreting information obtained from studying biased signalling *in vitro*.

1.3.6 Effect of Cellular Content on Biased Agonism

The content of signalling effectors among different cells is not identical. As a consequence, biased agonism across different cellular systems is likely to change. This has important implications *in vivo* as, for instance, the effect of the same ligand in primary cells isolated from different tissues can show opposite bias. One relevant example in the case of the MOP-biased agonism is the effect of the levels of GRK2 expression. Overexpression of GRK2 has sometimes been used as a strategy to increase the sensitivity of the detection of β-arr2 recruitment to several GPCRs including the MOP [656, 660, 661]. However, there is substantial evidence to demonstrate that receptor phosphorylation is also subject to bias (ligand-dependent) and that this phosphorylation can have downstream consequences such as differential engagement of signalling kinases or differential receptor regulation [184, 283, 538, 546]. Thus, overexpressing a particular kinase may have differential effects on the efficacy of distinct ligands, thus changing the bias profile of the entire set of ligands. One approach to minimize such artificial introduction of bias is to evaluate all the signalling end points under exactly the same cellular conditions and content, for example overexpressing GRK2 when investigating all the pathways in addition to β-arr2 recruitment.

However, the issue of differential contents of effector and regulatory proteins in different tissues still remains. For example, high levels of GRK2 are found in brain, leukocytes, heart and spleen, followed by lung and kidney [662]. Thus, quantification of signalling bias in recombinant cells can be used to reveal ligands with unique signalling profiles that can then be used as pharmacological tools for studying the consequences of biased agonism *in vivo*. It is therefore important to adopt a global perspective on the concept of bias, that is as an indicator of differential behaviours, fingerprints or activity profiles across ligands at the same receptor that can ultimately translate to different physiological outcomes.

1.3.7 Efficacy is Pluridimensional

Most of the descriptions of biased agonism to date have focused on the differential activation of G-protein-mediated events and β-arr2 recruitment. However, it is evident that most GPCRs pleiotropically couple to a myriad of signalling effectors. The ability of compounds to promote unique, ligand-selective conformations of GPCRs that are able to engage different transduction pathways or regulatory events underlies the mechanism for the pluridimensionality of efficacy [663]. As such, the detection of bias

should be extended beyond differences between G protein activation and β-arr2 recruitment. Additionally, it is now clear that signalling efficacy through GPCRs is not linear, and that multiple mechanisms control the responsiveness of receptor systems such as desensitisation and internalisation, resulting from receptor phosphorylation [664]. It is now established in several GPCR models, including the MOP, that not all ligands with similar apparent efficacy towards a given signalling pathway display a similar propensity to trigger these regulatory events [535].

The MOP has been shown to couple to many signalling effectors via G proteins and β-arrs [see 319, 651, 665]. Furthermore, the MOP has also been shown to directly interact with phospholipase D2 [666], and with proteins that control its localisation in lipid raft microdomains [667]. As such, limiting bias studies to these two proximal events directly limits the detection of biased agonism. In addition, there is now evidence of biased activation of G protein subunits by the MOP, which is not detected in proximal G protein activation assays (such as cAMP inhibition), but may differentially affect downstream signalling [603-605]. Similarly, biased effects on β-arr activity are not completely captured in β-arr recruitment assays. β-arrs have a diverse range of functions that affect signalling and receptor regulation, which are dependent on both cellular content and the ligand itself. The strength of interaction between the receptor and β-arr, as measured in a β-arr recruitment assay, is not necessarily indicative of the subsequent effects on downstream signalling and receptor regulation.

The systematic analysis of many signalling end points will maximize the information obtained from biased signalling studies *in vitro* as such approaches will provide 'textures' of ligands in cellular models. Different 'textures' *in vitro* may be indicative of distinct physiological fingerprints when translating bias into physiologically relevant systems.

1.3.8 Relevance of the Reference Ligand

As mentioned earlier, signalling bias is a relative measure; it is always in comparison with another ligand. As such, choosing a reference ligand is a key aspect of the quantification. The reference ligand itself is not unbiased (there is no such thing), but ideally, the reference ligand should show activity in most pathways as well as possess a signalling profile similar to the endogenous ligand or to most ligands that target that particular GPCR. It can be misleading to use a reference agonist such as morphine, which is known to exhibit differential signalling when compared with most endogenous

opioid peptides. Under most conditions, morphine will be biased towards G-protein-mediated signalling, so if it is used as a reference agonist, most other ligands will be clustered as β-arr biased. This is illustrated in Figure 1.9 where bias between G-protein activation and β-arr2 recruitment measured by [656], is quantified using two different reference ligands. As shown earlier, when morphine is used as the reference ligand to estimate values of $\Delta\Delta\log(\tau/K_A)$, nearly all the morphine metabolites are biased towards β-arr2 recruitment. However, when an agonist with higher efficacy in the β-arr2 recruitment assay, such as normorphine, is used as the reference agonist, the calculated bias for many of the metabolites appears to change. This shows that the majority of the metabolites are similar to normorphine, whereas morphine becomes significantly G-protein-biased and there are now only three metabolites that are biased towards β-arr2 recruitment. However, it is important to note that while the absolute bias factors ascribed to an agonist will change depending upon the ligand designated as reference, whether or not a significant difference exists between any ligand pair will not change regardless of which ligand is designated as reference. In order to make direct comparisons of signalling bias among different studies, it is important that the same ligand is used as a reference for quantification. The reference ligand is also very important when attempting to predict bias *in vivo*. As mentioned earlier, ligand bias is cell-dependent, making predictions of *in vivo* bias difficult. However, extensive knowledge of the physiological activity and signalling by the reference ligand, will allow links between signalling profiles and physiological effects to be made. Hence, the reference should ideally be a ligand that has been very widely studied. The obvious choice in most cases would be to use the endogenous ligand however, that is not straightforward with opioid receptors because of the existence of many endogenous opioid peptides. As DAMGO and Met-enk have been the ligands most widely studied in MOP biology, these two ligands would potentially be ideal ‘universal’ candidates. However, the choice of reference ligands will always depend on the question that a particular study is trying to address.

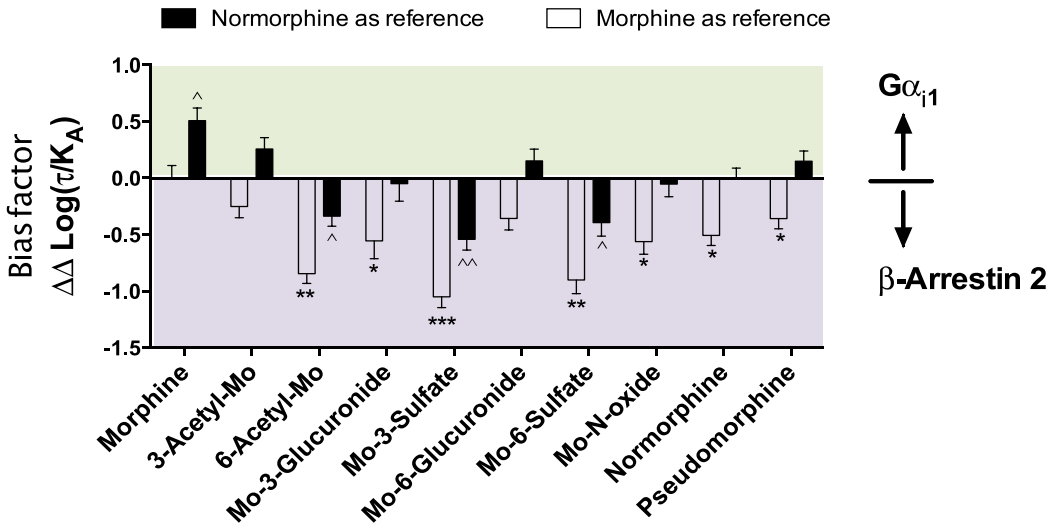

Figure 1.9: Quantification of bias using different reference ligands.
Concentration–response curves from Frolich, Dees, Paetz, Ren, Lohse, Nikolaev and Zenk [656] for G-protein activation and β-arr2 recruitment were fitted to the operational model to estimate values of $\Delta\Delta\log(\tau/K_A)$ between the two pathways using either morphine or normorphine as the reference ligand. When morphine is used as the reference ligand most morphine metabolites are biased towards β-arr2 recruitment. When normorphine is used as the reference, morphine becomes G-protein-biased and its derivatives, 6-acetyl-morphine (6-acetyl-Mo), Mo-3-sulfate and Mo-6-sulfate are β-arr2-biased. The two-tailed t test was used to determine whether transduction ratios were statistically different from the reference ligand, morphine *P ≤ 0.05, **P ≤ 0.01, ***P ≤ 0.001 or normorphine ∧P ≤ 0.05, ∧∧P ≤ 0.01.

1.3.9 Use of Biased Agonism in Drug Discovery to Improve Pharmacological Profiles of Analgesics

Quantification and determination of bias *in vitro* can guide medicinal chemists towards the design of biased GPCR ligands for those receptors where the signalling cascades responsible for therapeutic versus side effects are known. Structure–activity relationship (SAR) studies at the angiotensin AT1 receptor have resulted in a β-arr2-biased ligand (TRV120027) that is currently in clinical trials for acute decompensated heart failure [668]. Similarly, at the dopamine D2 receptor, biased partial agonists have been identified by exploring the structure of the antipsychotic aripiprazole through a combinatorial chemistry approach [661] and, more recently, by classical SAR studies supplemented with parameters of bias and functional affinity determined using the transduction coefficient method [659].

Given the phenotype of the β-arr2 knockout mouse and the accumulated evidence of ligand-directed signalling at the MOP, SAR approaches for the biased activation of this receptor have also been developed and have yielded promising compounds with analgesic function and improved side effect profile [581, 669]. Recently, new MOP

ligands (low MW compounds and endo-1 derivatives) that produce analgesia with less gastrointestinal dysfunction and respiratory depression have been reported. One of these compounds, TRV130, is the result of SAR screening studies by Trevena, Inc. focused on the discovery of G-protein-biased (as opposed to β-arr2 biased) ligands at the MOP [670]. *In vitro*, and compared with morphine, TRV130 displayed markedly different responses when assessed by two different signalling end points – inhibition of forskolin-induced cAMP and β-arr2 recruitment. Additionally, TRV130 showed decreased phosphorylation of the receptor at Ser375 and failed to internalise receptors. The authors examined bias between adenylate cyclase inhibition and β-arr2 recruitment by comparison of relative intrinsic activities [658] of TRV130 and morphine, and showed that TRV130 was biased towards adenylate cyclase inhibition. However, statistical comparison of bias using this method was hampered by the low efficacy of TRV130 in β-arr2 recruitment. As an alternative approach, the authors constructed a 'bias plot', where the normalised responses as changes in cAMP were shown as a function of the corresponding response in β-arr recruitment [648, 671]. Bias plots are useful graphical tools for visualizing bias of ligands between two pathways, but they incorporate all three types of bias, observation, system bias and ligand bias. This means ligand bias can only be observed when there are extreme differences between ligands, and also makes bias plots unsuitable for quantifying bias. Estimation of the bias factor using the operational model of agonism described above showed that the relative transduction ratio of TRV130 was not statistically different from morphine. The reduced β-arr2 recruitment observed with TRV130 in HEK cells could be attributed to the fact that it is a low-efficacy agonist and hence, poorly stimulates signalling pathways with low coupling efficiency. However, this moderate difference in the bias factors is very likely to be more relevant *in vivo*, which accounts for the improved pharmacological profile of TRV130. A more comprehensive analysis of bias of TRV130 across many signalling pathways, and compared with other opioid ligands will reveal more information about its unique bias profile, and provide insight into how TRV130 exerts its effects *in vivo*.

Finally, it is worth noting that most of the SAR studies performed so far that were focused on the discovery of biased ligands, have utilised differences between G-protein and β-arr-mediated pathways. However, it is tempting to anticipate that, in the coming years, there will be an increase in the number of studies that investigate a more diverse array of signalling end points that will reveal differential 'textures' of GPCR ligands.

1.3.10 Allosterism at the μ-Opioid Receptor

Although topographically distinct, druggable, allosteric sites have been postulated to be present in all GPCRs [672, 673], the discovery of allosteric ligands that bind to the opioid receptors has remained a challenge until recently. Allosteric ligands induce conformational changes that are transmitted from the allosteric binding pocket to the orthosteric binding site. They offer the potential of improved subtype selectivity, decreased risk of overdose and maintained spatial and temporal activity of the target receptor [674]. All these pharmacological characteristics are of particular relevance for opioid-based therapies, as they may offer the potential to overcome the tolerance and dependence developed upon chronic/prolonged receptor activation. However, several considerations need to be taken into account regarding the effects of allosteric modulators on GPCRs.

The classical view of GPCR allosterism has focused on the change elicited on the properties of the orthosteric ligand; however, the conformational changes induced by the binding of an allosteric modulator can have similar consequences when considering the cytosolic proteins that interact with the receptor and mediate signal transduction. More importantly, this effect can vary depending on the different intracellular effectors. Macroscopically, this translates in some pathways being modulated, in either a positive or negative direction, at the expense of others. Finally, allosteric ligands can also display efficacy in their own right, and as such, they can potentially activate signalling pathways that are distinct from those activated by the orthosteric ligands. It is therefore important that the characterisation of allosteric ligands includes the assessment of many relevant signalling pathways as well as the intrinsic efficacy of allosteric ligands on their own.

Interestingly, compared with other family A GPCRs, there have been significantly fewer allosteric ligands discovered for the opioid receptors. This is in contrast with the several descriptions of ‘allosteric interactions’ across opioid receptor dimers, whether homodimers or heterodimers [675-678]. With regards to the MOP subtype, the crystal structure of the MOP already suggests an oligomeric arrangement of this receptor [29], and allosteric interactions have been described between MOP and mGluR5, CB1, DOP and KOP [678-681].

In terms of – low MW allosteric modulators, Burford *et al* 2013 [652] recently discovered the first allosteric modulators of the MOP using high throughput screening with a

complementation approach to measure β-arr2 recruitment. This screening resulted in the identification of two positive allosteric modulators (PAMs) and two silent allosteric modulators (which bind to the allosteric site of the receptor but have neutral cooperativity with the orthosteric ligand). BMS-986121 and BMS-986122 positively modulated the binding of DAMGO to the MOP and potentiated the effects of endo-1, DAMGO and morphine in β-arr2 recruitment, G-protein activation and cAMP inhibition. This exciting discovery has provided the tools to investigate the effects of allosterism on ligand-dependent effects at the MOP. For example, how do PAMs affect MOP regulation by different agonist? Do PAMs differently affect synthetic versus endogenous opioid ligands? It will also be extremely interesting to investigate whether PAMs can potentiate the analgesic effects of current opioid drugs or endogenous opioids, without potentiation of the side effects.

1.3.11 Concluding Comments

Although GPCRs are coupled to a plethora of signalling pathways, most descriptions of biased agonism have been based on the comparison of two signalling events across different ligands. It is therefore quite likely that the 'relevant' signalling event has been omitted by the initial selection of signalling end points. Additionally, it is unlikely that a response derives from the activation of a very distinct signalling pathway. Rather, physiological responses are likely to reflect complex outputs from a tightly controlled and selective activation of a particular group of intracellular signals. Such a holistic view represents a major challenge for pharmacologists and medicinal chemists. One potential approach to predict physiological outcomes is the thorough investigation of many signalling end points in simple cellular models to generate ligand activity profiles. Subsequently these specific fingerprints can be related to more complex physiological responses. This approach requires not only a robust and systematic quantification method, but also the validation of signalling profiles in more relevant systems. However, once obtained, these fingerprints will represent a framework that will offer the potential to predict the physiological outcome from a novel drug.

Parallel with the discovery of new biased MOP ligands with improved therapeutic windows, the discovery of opioid receptor allosteric modulators will also open new avenues to overcome the current limitations of opioid ligands as analgesics. As such, the evaluation of this new class of compounds *in vivo* will be extremely informative in terms of whether allosterism can be exploited to generate better and safer analgesics.

1.4 Summary and Aims

The MOP receptor remains one of the key targets for management of pain, despite the numerous side effects associated with their use. The therapeutic profile of MOP agonists could be improved by optimisation of their biased agonism profile, enabling maximisation of the analgesic effects with minimal the side effects. The improved side effect profile of the recently described biased MOP ligand TRV130 as well as the reduced side effects of morphine in β-arr2 knockout mice certainly indicates that this is possible. However, despite extensive research into biased signalling at MOP both in recombinant cell lines and primary cells using predominantly synthetic opioids, clear links between activation of particular signalling pathways and specific physiological effects are yet to be established, hence the bias profile required to produce analgesia with reduced side effects is unknown. Whilst there is evidence that the therapeutic profile of opioids can be improved by optimising ligand bias towards G protein activation over β-arr2 recruitment, there is also clear evidence of the existence of multiple mechanisms of desensitisation and tolerance which are both ligand and tissue specific. Futhermore, there is also a number of discrepancies between studies examining bias of the same ligands between the same or similar signalling pathways. This has raised the question whether *in vitro* studies of biased agonism can truly predict bias *in vivo*. Consequently, a more comprehensive, and quantitative, approach to bias optimisation is required. To date, studies of biased agonism at MOP have been predominantly qualitative assessments of biased agonism by small number of synthetic ligands, the endogenous opioids have been largely overlooked. As a receptor with multiple endogenous ligands, bias is highly likely to play an important role in the normal control of MOP-mediated physiological processes. Additionally, the endogenous opioids have been shown to be able to produce analgesia with fewer side effects. Hence these peptides are ideal candidates for studies of biased signalling at MOP, as they are likely to possess novel biased agonism profiles which may assist in establishing the ideal bias profile required for optimisation of the therapeutic profile of opioid analgesics. Accordingly, the aims of the work described in this thesis are:

1. Characterise the biased agonism profile of endogenous ligands at MOP across multiple different signalling pathways

2. Determine the factors that affect the quantification of biased agonism at MOP

CHAPTER 2

BIASED AGONISM OF ENDOGENOUS OPIOID PEPTIDES AT THE μ-OPIOID RECEPTOR

Georgina L. Thompson[1,2], J. Robert Lane[1], Thomas Coudrat[1], Patrick M. Sexton[1], Arthur Christopoulos[1] and Meritxell Canals[1]

PUBLISHED IN MOL PHARMACOL. 2015;88(2):335-46

[1]Drug Discovery Biology and Department of Pharmacology, Monash Institute of Pharmaceutical Sciences, Monash University, 399 Royal Parade, Parkville, Victoria 3052, Australia; [2]Defence Science and Technology Group, Australian Department of Defence, Australia

Declaration for Thesis Chapter 2

Monash University

Declaration for Thesis Chapter 2

Declaration by candidate

In the case of Chapter 2, the nature and extent of my contribution to the work was the following:

Nature of contribution	**Extent of contribution (%)**
Participated in research design, performed all experiments and analysis, and wrote the manuscript.	90%

The following co-authors contributed to the work. If co-authors are students at Monash University, the extent of their contribution in percentage terms must be stated:

Name	**Nature of contribution**	**Extent of contribution (%)** for student co-authors only
Meritxell Canals	Participated in research design, contributed to data analysis and writing of the manuscript	N/A
Arthur Christopoulos	Participated in research design, contributed to data analysis and writing of the manuscript	N/A
J. Robert Lane	Participated in research design, contributed to data analysis and writing of the manuscript	N/A
Thomas Coudrat,	Performed data analysis	2%
Patrick M. Sexton	Contributed to writing of the manuscript	N/A

The undersigned hereby certify that the above declaration correctly reflects the nature and extent of the candidate's and co-authors' contributions to this work*.

Candidate's Signature	[redacted]	**Date 9 May 2016**
Main Supervisor's Signature	[redacted]	**Date 9 May 2016**

2.1 Abstract

Biased agonism is having a major impact on modern drug discovery and describes the ability of distinct GPCR ligands to activate different cell signalling pathways, and to result in different physiological outcomes. To date, most studies of biased agonism have focussed on synthetic molecules targeting various GPCRs, however many of these receptors have multiple endogenous ligands, suggesting that "natural" bias may be an unappreciated feature of these GPCRs. MOP is activated by numerous endogenous opioid peptides, remains an attractive therapeutic target for the treatment of pain, and exhibits biased agonism in response to synthetic opiates. The aim of this study was to rigorously assess the potential for biased agonism in the actions of endogenous opioids at MOP in a common cellular background, and compare these to the effects of the agonist DAMGO. We investigated activation of G proteins, inhibition of cAMP production, ERK1/2 phosphorylation, β-arr1/-2 recruitment and MOP trafficking, and applied a novel analytical method to quantify biased agonism. Whilst many endogenous opioids displayed signalling profiles similar to that of DAMGO, α-neo, Met-enk-RF and the putatively endogenous peptide, endo-1, displayed particularly distinct bias profiles. These may represent examples of natural bias if it can be shown that they have different signalling properties and physiological effects *in vivo* compared to other endogenous opioids. Understanding of how endogenous opioids control physiological processes through biased agonism can reveal vital information required to enable design of biased opioids with improved pharmacological profiles and treat diseases involving dysfunction of the endogenous opioid system.

2.2 Introduction

Opioids are the most widely used and most effective analgesics available. However, their use is associated with a large array of side effects [682]. Opioids that are currently used as therapeutics, such as morphine, predominantly exert both their analgesic effects and undesirable effects through activation of MOP [683, 684]. It is now accepted that chemically distinct ligands binding to the same GPCR can stabilise the receptor in multiple active conformations, which result in differential activation of cell signalling pathways and, eventually, in different physiological outcomes, a phenomenon known as biased agonism [685]. Biased agonism can be exploited to design drugs that selectively activate signalling pathways leading to the desired physiological effects whilst minimising on-target side effects elicited by activation of other signalling pathways via the same receptor subtype [248, 686, 687].

Biased agonism at the MOP has been extensively studied [596, 615, 616, 651, 653, 688-690]. However, evidence of biased agonism at the MOP is mostly limited to qualitative analyses of two signalling events with a limited number of ligands. Evidence of the involvement of β-arr2 in the mediation of the adverse effects of morphine has prompted the search for opioids that do not induce β-arr2 recruitment. Indeed, enhanced morphine analgesia with reduced respiratory and gastrointestinal side effects was reported in β-arr2 knockout mice [640, 641, 691]. Recently, ligands with impaired β-arr2 recruitment have been reported to provide potent analgesia with less severe side effects [580, 581, 644]. However, the improved pharmacological profiles of these ligands may still be due to their partial agonism, with lower overall efficacy than morphine, rather than true “bias” away from β-arr2 recruitment [616].

In order to guide discovery efforts to generate drugs with therapeutically relevant biased agonism profiles, it is necessary to quantify this phenomenon. In any system, the observed biased agonism can be confounded by “system bias”, which reflects the differing coupling efficiencies of the receptor for each signalling pathway, and by “observational bias”, which results from differing assay sensitivities and conditions [648]. Bias imposed by the ligand on the conformation of the receptor is the only source of bias that can be chemically optimised to improve its therapeutic profile. Therefore, it is important to quantify biased agonism in such a way that excludes system and observational bias, to reveal the unique signalling profile that is induced by the ligand. Several analytical methods to quantify biased agonism have been developed. The method recently described by Kenakin, Watson, Muniz-Medina, Christopoulos and

Novick [685], based on the Black and Leff (1983) operational model can be applied to concentration-response curves to obtain a single parameter that describes bias between signalling pathways in a system independent manner.

Several studies have quantified biased agonism at the MOP, but these have been limited to comparison of efficacies for G protein activation versus β-arr2 recruitment [596, 612, 615, 656]. However, differential activation of other signalling events including receptor internalisation, MAP kinase and PKC activation has been reported [653], but these signalling events are rarely considered when describing bias of the MOP, or when attempting to link biased agonism with physiological effects. Moreover, bias between G protein activation and β-arr recruitment may not necessarily predict differential activation of such downstream signalling events. Therefore, it is important to study biased agonism at multiple signalling pathways in order to encompass multiple aspects of the signalling properties of a ligand.

To date, descriptions of biased agonism have mainly focused upon the actions of synthetic ligands. However, the existence of multiple endogenous ligands targeting the same GPCR suggests the potential for “endogenous” biased agonism. Indeed, biased agonism by endogenous peptide ligands has been observed at several GPCRs [235, 237, 692]. Such observations may explain, in part, the apparent redundancy of such systems. However, the potential for bias within the endogenous opioid system has not been explored extensively. The endogenous ligands for opioid receptors are small peptides generated by cleavage of precursor proteins; pENK, pOMC and pDYN. PENK and pOMC derived peptides, enkephalins and endorphins respectively, are generally localised to regions with MOP or DOP expression and are involved in the numerous physiological processes mediated by these receptors. Similarly, the pDYN-derived peptides, the dynorphins and neoendorphins, are generally localised to similar regions as the KOP, however it is likely that in some regions dynorphins may also activate MOP. All the opioid peptides have varying affinities for all three opioid receptors, and none are significantly selective for one receptor subtype [332, 333]. Finally, the precursor genes for endo-1 and endo-2 are still unknown and therefore these two ligands remain “putatively endogenous”, however, they are the most selective and potent opioid peptides for MOP [334]. Such diversity in the endogenous opioid system suggests that biased agonism may play a role in control of normal MOP mediated

physiological processes. The understanding of the fundamental basis for ligand bias at the MOP and determining whether differences in the expression and release of endogenous opioids can underlie the development and maintenance of disease may offer promising avenues to address and to provide mechanistic insight for the development of safer opioid-based therapies.

In the current study we investigated the existence of biased agonism at the MOP by endogenous and putatively endogenous opioids. The ability to activate several signal transduction pathways for a range of opioid peptides and three reference ligands was assessed. Bias between each signalling pathway was quantified to obtain unique biased agonism profiles for these ligands. The results show that whilst most endogenous opioids possess similar biased agonism profiles to one another, α-neo and the putative endogenous opioid endo-1 display unique biased agonism profiles. Our studies also provide a foundation for future studies aimed at linking these profiles to physiology of the opioid system.

2.3 Materials and Methods

2.3.1 Materials

Chinese hamster ovary (CHO) FlpIn cells and Dulbecco's modified Eagle's medium (DMEM) were purchased from Invitrogen (Mulgrave, VIC, Australia). Foetal bovine serum (FBS) was purchased from ThermoTrace (Melbourne, Australia). Hygromycin-B was purchased from Roche Applied Science (Dee Why, NSW, Australia). Sure-Fire cellular ERK1/2 assay kits were a generous gift from TGR BioSciences (Adelaide, SA, Australia). AlphaScreen reagents for ERK1/2 assays, [^{35}S]Guanosine 5′-O-[γ-thio]triphosphate ([^{35}S]GTPγS; >1000 Ci/mmol), [^{3}H] Diprenorphine and Ultima Gold scintillation cocktail were purchased from PerkinElmer Life Sciences (Melbourne, Australia). All endogenous opioid peptides were purchased from Mimotopes (Melbourne, Australia). All other chemicals were purchased from SigmaAldrich. Morphine HCl was from GlaxoSmithKline (Boronia, Victoria, Australia). *Renilla* luciferase tagged MOP (MOP-RLuc) was a kind gift of Prof. Laura Bohn (Scripps Research Institute, Florida, USA).

2.3.2 Cell Culture and Generation of Stable Cell Line

Cells were maintained and cultured in high-glucose DMEM containing 10% FBS and 600 μg/ml hygromycin B at 37°C under a humidified atmosphere containing 5% CO_2. cDNA encoding the wild-type human MOP was obtained from the Missouri University of Science and Technology (http://www.cdna.org) and was provided in pcDNA3.1+. Sequence of the human MOP was amplified by polymerase chain reaction and cloned into the Gateway entry vector pENTR/D-TOPO, using the pENTR directional TOPO cloning kit, according to the manufacturer's instructions (Mulgrave, VIC, Australia). The construct was subsequently transferred into the Gateway destination vector pEF5/frt/V5/dest using the LR Clonase enzyme mix (Invitrogen), and the constructs were used to transfect FlpIn CHO cells (Invitrogen) which ensure constant expression of MOP across a cell population Cells were selected using 600 μg/ml hygromycin B to generate cell lines stably expressing MOP.

2.3.3 Membrane Preparation

Cells from 10 175cm^2 flasks were grown until approximately 90% confluence and harvested using 2mM EDTA in phosphate-buffered saline (PBS, 137mM NaCl, 2.7mM

KCl, 4.3mM Na_2HPO_4, and 1.5mM KH_2PO_4). Cells were pelleted by centrifugation for 10 minutes at 1200g, and the pellets resuspended in 20ml of PBS containing 20mM HEPES and 10mM EDTA at pH 7.4. All subsequent steps were performed at 4°C. The cell suspension was homogenized using a Polytron homogenizer (PT 1200 CL; Kinematica, Basel, Switzerland), with three 10-second bursts separated by cooling on ice. The cell homogenate was centrifuged for 5 minutes at 1700g, and the supernatant was transferred to new tubes and further centrifuged (90 minutes, 38000g). The pellet was resuspended in 5ml of buffer (20mM HEPES and 0.1mM EDTA, pH 7.4) and briefly homogenized to ensure uniform consistency. Membranes were aliquoted and stored at -80°C. The protein concentration was determined using a Bradford assay and bovine serum albumin as a standard.

2.3.4 Saturation Radioligand Binding Assay

Cell membranes (20μg) were incubated in buffer (50mM Tris, 100mM NaCl, 3mM $MgCl_2$, pH7.4) containing increasing concentrations of [^{3}H] Diprenorphine (0.01-10nM), at 25°C for 60min. The reaction was terminated by rapid filtration through glass fibre filters (GF/B) with a Brandel cell harvester and washing with cold saline. Non-specific binding was determined using 1mM naloxone and radioactivity was determined by liquid scintillation counting using Ultima Gold scintillation cocktail, and a Tri-Carb 2900TR liquid scintillation counter (Perkin Elmer).

2.3.5 [^{35}S]GTPγS Binding Assay

Cell membranes (10μg) were incubated in buffer (20 mM HEPES, 100 mM NaCl, 4 mM $MgCl_2$, pH7.4) containing 1μm GDP, 0.01% bovine serum albumin (BSA), protease inhibitors (1μM captopril, 1μM phosphoramidon and 1μM amastatin) and increasing concentrations of agonist for 30min at 30°C. A 100μl volume of [^{35}S]GTPγS (0.1nM final concentration) was then added, and the incubation was continued for a further 30min. The reaction was terminated by rapid filtration through glass fibre filters (GF/B) with a Brandel cell harvester and washing with cold saline. Radioactivity was determined by liquid scintillation counting using Ultima Gold scintillation cocktail, and a Tri-Carb 2900TR liquid scintillation counter (Perkin Elmer). All experiments were performed in triplicate.

2.3.6 Inhibition of Forskolin-Induced cAMP Levels

The ability of ligands to inhibit forskolin-induced cAMP production was assessed in FlpIn CHO-MOP cells transiently transfected to express the CAMYEL cAMP bioluminescence resonance energy transfer (BRET) biosensor [693]. FlpIn CHO-MOP cells were grown overnight in 10cm dishes. Transient transfection was performed using polyethylenimine (PEI) at a 6:1 ratio of DNA. 24h after transfection FlpIn CHO-MOP cells were seeded in white 96-well plates (Culturplates, Perkin Elmer) and incubated overnight. The following day cells were rinsed and pre-incubated in Hank's Balanced Saline Solution (HBSS) with 0.01% BSA and protease inhibitors (1μM captopril, 1μM phosphoramidon and 1μM amastatin) for 30min at 37°C. Cells were then incubated with the RLuc substrate coelenterazine-h, final concentration 5μM, for 5min, followed by a further 5min incubation with increasing concentrations of agonists. Forskolin was added to a final concentration of 10μM. After 5min the YFP and the RLuc emissions were measured using a LumiSTAR Omega instrument (BMG Labtech, Ortenberg, Germany) that allows for sequential integration of the signals detected at 475 ± 30 and 535 ± 30nm, using filters with the appropriate band pass. Data are presented as a BRET ratio, calculated as the ratio of YFP to RLuc signals, and expressed as the percentage of the forskolin-induced signal.

2.3.7 Bioluminescence Resonance Energy Transfer Assays

Agonist-induced recruitment of β-arrs to the MOP and MOP proximity to the plasma membrane maker KRas were examined using a BRET-based method. Parental FlpIn CHO cells were transfected to co-express MOP C-terminally tagged with RLuc, and β-arr1-, β-arr2-YFP or KRas-Venus at a 1:4 DNA ratio. The assay was performed as described above for the cAMP BRET-based assay. For β-arr recruitment assays, agonists were added after 5min of pre-incubation with coelenterazine-h, and then incubated for an additional 5min and the BRET ratio was determined. For receptor trafficking (KRas BRET) assays, cells were incubated with agonists for 60mins in the presence of protease inhibitors, and coelenterazine h added 10mins prior to detection of BRET. Data is expressed as DAMGO response for β-arr assays, and % vehicle response for KRas assays.

2.3.8 ERK 1/2 Phosphorylation Assay

Cells were seeded at $4x10^4$ cells/well in clear 96 well plates and grown for 5hr. Cells were washed twice with 200μl of phosphate-buffered saline and incubated in serum-free DMEM overnight at 37°C in 5% CO_2. ERK1/2 phosphorylation (pERK) was detected

using the AlphaScreen ERK1/2 SureFire protocol (TGR Biosciences). The assay was performed at 37°C, cells were preincubated with 0.01% BSA and protease inhibitors (1μM captopril, 1μM phosphoramidon and 1μM amastatin) followed by addition of ligands to a final volume of 200 μl. Time course experiments were initially performed to determine the time at which maximal pERK was detected following agonist stimulation (5min). Ligand-stimulated pERK was terminated by removal of media and drugs, followed by the addition of 100μl of SureFire lysis buffer per well and agitation of lysates for 5min at room temperature. 5μl of lysate were added in a 384-well white ProxiPlate (PerkinElmer). A mixture of SureFire activation buffer, SureFire reaction buffer, and AlphaScreen beads was prepared in a ratio of 100:600:3 (v/v/v) and added to the lysate for a lysate:mixture ratio of 5:8 (v/v). Plates were incubated for 1–1.5 hr. at 37°C before the florescence signal was measured on a Fusion-α plate reader (PerkinElmer) using standard AlphaScreen settings. For all experiments, 10μM DAMGO (100%) and vehicle (0%) were used to normalise pERK curves**.**

2.3.9 Data Analysis

Agonist concentration−response curves were fitted empirically to a three-parameter logistic equation using Prism 6.0 (GraphPad Software Inc.) where bottom and top are the lower and upper plateaus, respectively, of the concentration−response curve, [A] is the molar concentration of agonist, and EC_{50} is the molar concentration of agonist required to generate a response halfway between the top and the bottom.

$$Y = bottom + \frac{top - bottom}{1 + 10^{(\log EC_{50} - \log[A])}} \quad (1)$$

To compare agonist profiles and to quantify stimulus bias, agonist concentration−response data were fitted to the following form of the operational model of agonism [655]

$$Y = basal + \frac{(E_m - basal)\left(\frac{\tau}{K_A}\right)^n [A]^n}{[A]^n\left(\frac{\tau}{K_A}\right)^n + \left(1 + \frac{[A]}{K_A}\right)^n} \quad (2)$$

where E_m is the maximal possible response of the system, *basal* is the basal level of response, K_A denotes the functional equilibrium dissociation constant of the agonist (A) for the receptor , τ is an index of the signalling efficacy of the agonist and is defined as R_T/K_E, where R_T is the total number of receptors and K_E is the coupling efficiency of

each agonist-occupied receptor, and *n* is the slope of the transducer function that links occupancy to response. The analysis assumes that the maximal system responsiveness (E_m) and the transduction machinery utilised for a given cellular pathway are the same for all agonists, such that the E_m and transducer slope (n) are shared between agonists. Data for all compounds for each pathway were fit globally to determine values of K_A and τ.

The ratio τ/K_A was determined as a logarithm (i.e., $\log(\tau/K_A)$) and is referred to herein as the transduction coefficient which represents a single fitted parameter sufficient to describe agonism and bias for a given pathway (i.e., biased agonism can result from either a selective affinity (K_A) of an agonist for a given receptor state(s) and/or a differential coupling efficacy (τ) toward certain pathways).

To cancel the impact of cell-dependent effects on the observed agonism at each pathway, the $\log(\tau/K_A)$ values were then normalised to that determined for DAMGO at each pathway to yield a normalised transduction coefficient, $\Delta\log(\tau/K_A)$, which was calculated as follows

$$\Delta \log\left(\frac{\tau}{K_A}\right) = \log\left(\frac{\tau}{K_A}\right)_{\substack{test \\ compound}} - \log\left(\frac{\tau}{K_A}\right)_{DAMGO} \tag{3}$$

Finally, to determine the actual bias of each agonist between different signalling pathways, the $\Delta\log(\tau/K_A)$ values were evaluated statistically between the pathways. The ligand bias of an agonist for one pathway, j1, over another, j2, is given as

$$\Delta\Delta\log\left(\tau/K_A\right)_{j1-j2} = \Delta\log\left(\frac{\tau}{K_A}\right)_{j1} - \Delta\log\left(\frac{\tau}{K_A}\right)_{j2} \tag{4}$$

A lack of biased agonism as compared to the reference agonist DAMGO will result in values of $\Delta\Delta\log(\tau/K_A)$ not significantly different from 0 between pathways. To account for the propagation of error associated with the determination of composite parameters using eqs 3 and 4, the following equation was used

$$Pooled\_SEM = \sqrt{\left(SEj1\right)^2 + \left(SEj2\right)^2} \tag{5}$$

All potency (pEC_{50}) and transduction ratio ($\Delta\Delta\log(\tau/K_A)$) parameters were estimated as logarithms. When fold-changes in bias are described, this was calculated by first converting values of $\Delta\Delta\log(\tau/K_A)$ to the corresponding antilog value.

$$Bias = 10^{\Delta\Delta \log\left(\frac{\tau}{K_A}\right)} \quad (6)$$

The distribution of antilog values does not conform to a normal (Gaussian) distribution, whereas the logarithm of the measure is approximately Gaussian [694-696]. Thus, as the application of t tests and analyses of variance assume Gaussian distribution, estimating the parameters as logarithms allows valid statistical comparison. All results are expressed as the mean ± SEM. Statistical analysis was performed using a two-way unpaired Student's t test to make pairwise comparisons between bias factors for a given ligand and DAMGO, where $P<0.05$ was considered to be statistically significant.

To visualise bias between multiple pathways at once, webs of bias were constructed. $\Delta\Delta\tau/K_A$ values between a reference pathway, cAMP, and all other pathways were obtained using DAMGO as the reference ligand as follows

$$\Delta\tau/K_A = \frac{\tau/K_A \ \ test\ compound}{\tau/K_A \ \ DAMGO} \quad (7)$$

$$\Delta\Delta\tau/K_A = \frac{\Delta\tau/K_{A_{j1}}}{\Delta\tau/K_{A_{j2}}} \quad (8)$$

2.3.10 Principal Component Analysis

Principal component analysis (PCA) is a dimensionality reduction method that uses transformations to project a high-dimensional set of data into a lower dimensional set of variables called principal components (PCs). The PCs extract the important information from the data, revealing its internal structure in a way that best explains its variance [697]. PCs are ranked according to the percentage of total variance in the data they explain. The first PC explains a maximal amount of total variance in the data. Each succeeding PC explains a maximal amount of the remaining variation, without being correlated with the preceding components. PCA was applied using singular value decomposition as implemented in the package scikit-learn [698], the script used for the analysis and plotting can be found at https://github.com/thomas-coudrat/pca_analysis.

2.4 Results

The ability of MOP to activate several signal transduction pathways in response to ten endogenous opioid peptides, endo-1, endo-2 and three synthetic ligands was assessed in FlpIn CHO cells stably expressing the human MOP. Receptor expression levels were determined by saturation binding assays with [^{3}H]diprenorphine (B_{max} 0.72 ±0.04 pmol/mg protein, Figure A.1). The selected opioid peptides included members of all 3 of the main classes of endogenous opioids; enkephalins, dynorphins and endorphins, as well as the putative endogenous ligands the endomorphins (Table 2.1). Quantification of bias between each pathway was performed using DAMGO as the reference ligand. Morphine was included as an additional control ligand, as the literature suggests that it may be a biased agonist at MOP compared to DAMGO [651, 653, 690] and, finally, the signalling profile of the peripherally restricted MOP agonist, loperamide, was also investigated. All incubations in the different signalling assays were performed in the presence of endopeptidase inhibitors (see Materials and Methods), to prevent peptide degradation.

Table 2.1: Endogenous peptides used in this study

Peptide	Sequence
Enkephalins	
Leu-enk	Tyr-Gly-Gly-Phe-Leu
Met-enk	Tyr-Gly-Gly-Phe-Met
Met-enk-RF	Tyr-Gly-Gly-Phe-Met-Arg-Phe
Dynorphins	
DynA	Tyr-Gly-Gly-Phe-Leu-Arg-Arg-Ile-Arg-Pro-Lys-Leu-Lys-Trp-Asp-Asn-Gln
DynB	Tyr-Gly-Gly-Phe-Leu-Arg-Arg-Gln-Phe-Lys-Val-Val-Thr
DynA 1-13	Tyr-Gly-Gly-Phe-Leu-Arg-Arg-Ile-Arg-Pro-Lys-Leu-Lys
DynA 1-8	Tyr-Gly-Gly-Phe-Leu-Arg-Arg-Ile
DynA 1-6	Tyr-Gly-Gly-Phe-Leu-Arg
α-neoendorphin	Tyr-Gly-Gly-Phe-Leu-Arg-Lys-Tyr-Pro-Lys
Endorphins	
β-endorphin	Tyr-Gly-Gly-Phe-Met-Thr-Ser-Glu-Lys-Ser-Gln-Thr-Pro-Val-Thr-Leu-Phe-Lys-Asn-Ile-Ile-Lys-Asn-Ala-Tyr-Lys-Lys-Gly-Glu
Endomorphins	
Endo-1	Tyr-Pro-Trp-Phe
Endo-2	Tyr-Pro-Phe-Phe

2.4.1 Endogenous Opioids Differentially Inhibit AC and Recruit β-Arrestin 2

MOPs are primarily coupled to $G\alpha_i$ G proteins that mediate inhibition of adenylyl cyclase (AC), resulting in a decrease in the levels of intracellular cAMP. The ability of ligands to inhibit forskolin-induced cAMP production was assessed in FlpIn CHO-MOP cells transiently transfected to express the CAMYEL cAMP BRET-based biosensor (Figure 2.1A-B, Table A.1). All ligands inhibited forskolin-induced cAMP stimulation. Such inhibition was abolished by incubation of the cells with pertussis toxin (data not shown) demonstrating the $G\alpha_i$-dependence of this effect. However, concentration-response curves could not be obtained for dynA and dynA 1-13. Although these two peptides stimulated the production of cAMP at high concentrations (Figure 2.1B), this effect was not mediated by MOP as it was not blocked by the MOP antagonist naloxone, and was still observed in untransfected FlpIn CHO cells (Figure A.2). We then examined recruitment of β-arr2 to MOP using a BRET assay. CHO FlpIn cells were co-transfected with MOP-RLuc and YFP-tagged β-arr2 (β-arr2-YFP). All endogenous opioids as well as DAMGO and loperamide stimulated recruitment of β-arr2. In contrast, morphine displayed partial agonism by only stimulating 28% of the DAMGO-mediated response (Figure 2.1C-D, Table A.1). In order to quantify biased agonism at these two signalling pathways, bias factors were calculated as described in Materials and Methods (Figure 2.1E,Table A.2). Both loperamide and the endogenous opioid, α-neo, showed significant bias towards inhibition of AC over recruitment of β-arr2 compared to the reference ligand DAMGO. Morphine and all the other opioid peptides tested were not significantly biased compared to DAMGO.

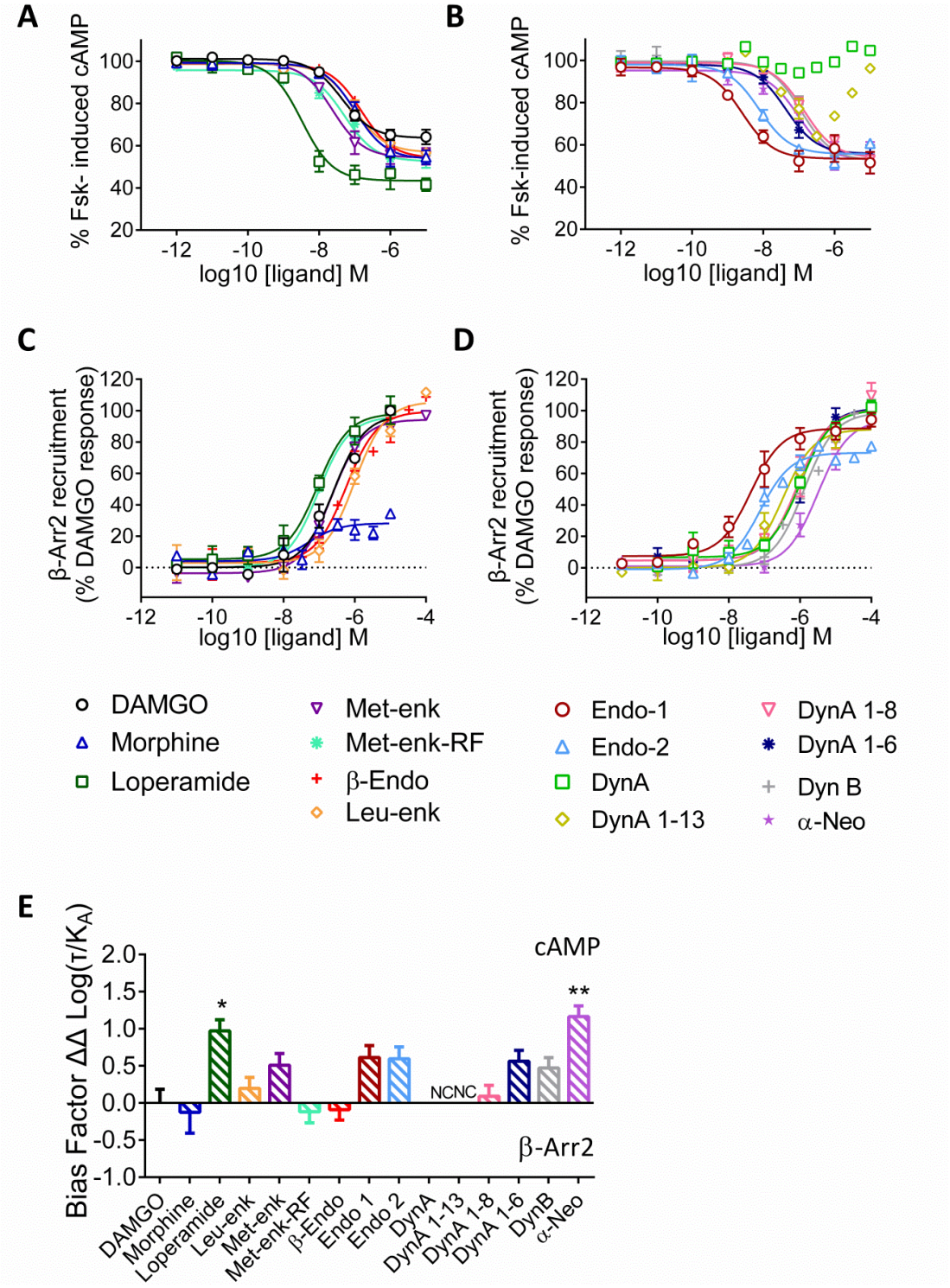

Figure 2.1: Biased agonism of endogenous opioids between inhibition of forskolin-induced cAMP and β-arr2 recruitment.

(A-B) Inhibition of forskolin-induced cAMP in CHO-MOP cells. (C-D) Recruitment of β-arr2 in FlpIn CHO cells. Data normalised to the 10μM DAMGO response. Data expressed as mean ± SEM of at least 3 separate experiments. (E) Bias factors for all agonists between cAMP and β-arr2 recruitment (Table A.2). *p≤0.05 **p≤0.005, different from DAMGO, as determined by two-tailed t-test. Bias factors for dynA and dynA 1-13 not shown as log[τ/K_A] values could not be calculated for the cAMP assay (NC= not calculable)

2.4.2 Differential Recruitment of β-Arrestin Isoforms by Opioid Ligands

Morphine has previously been shown to preferentially stimulate recruitment of β-arr2 over β-arr1 [579]. Differential recruitment of arrestins may have significant effects on downstream signalling as different β-arr isoforms have different functions [284, 699]. We examined the potential for endogenous opioids to stimulate differential recruitment of β-arr isoforms to MOP. For this, β-arr recruitment assays were repeated using YFP-tagged β-arr1. All the ligands tested stimulated recruitment of β-arr1, with the exception of morphine, which did not stimulate any detectable recruitment (Figure 2.2A-B, Table A.1). Of note, the BRET signal was much lower for the β-arr1 assays compared to the BRET signal obtained for β-arr2. Although this could be interpreted as a compromised recruitment of β-arr1 for all the ligands, we cannot exclude the possibility that this is due to lower BRET efficiency between the different arrestin isoforms and MOP-RLuc. Bias factors between recruitment of β-arr1 and β-arr2 showed that in addition to morphine, endo-1 differentially recruits β-arrs in comparison to the reference ligand DAMGO (Figure 2.2C,). Endo-1 showed significant bias towards recruitment of β-arr2 over β-arr1. Since morphine did not stimulate any detectable β-arr1 recruitment, a bias factor could not be calculated. However, this does not necessarily indicate that morphine is biased towards β-arr2 recruitment. Since all the ligands showed a lower response in the β-arr1 assay than for β-arr2, a partial agonist such as morphine is expected to stimulate little to no response in the β-arr1 assay. Hence our results suggest that bias between β-arr isoforms can be due to the lower sensitivity of β-arr1 assays and/or lower coupling efficiency of β-arr1 recruitment to MOP.

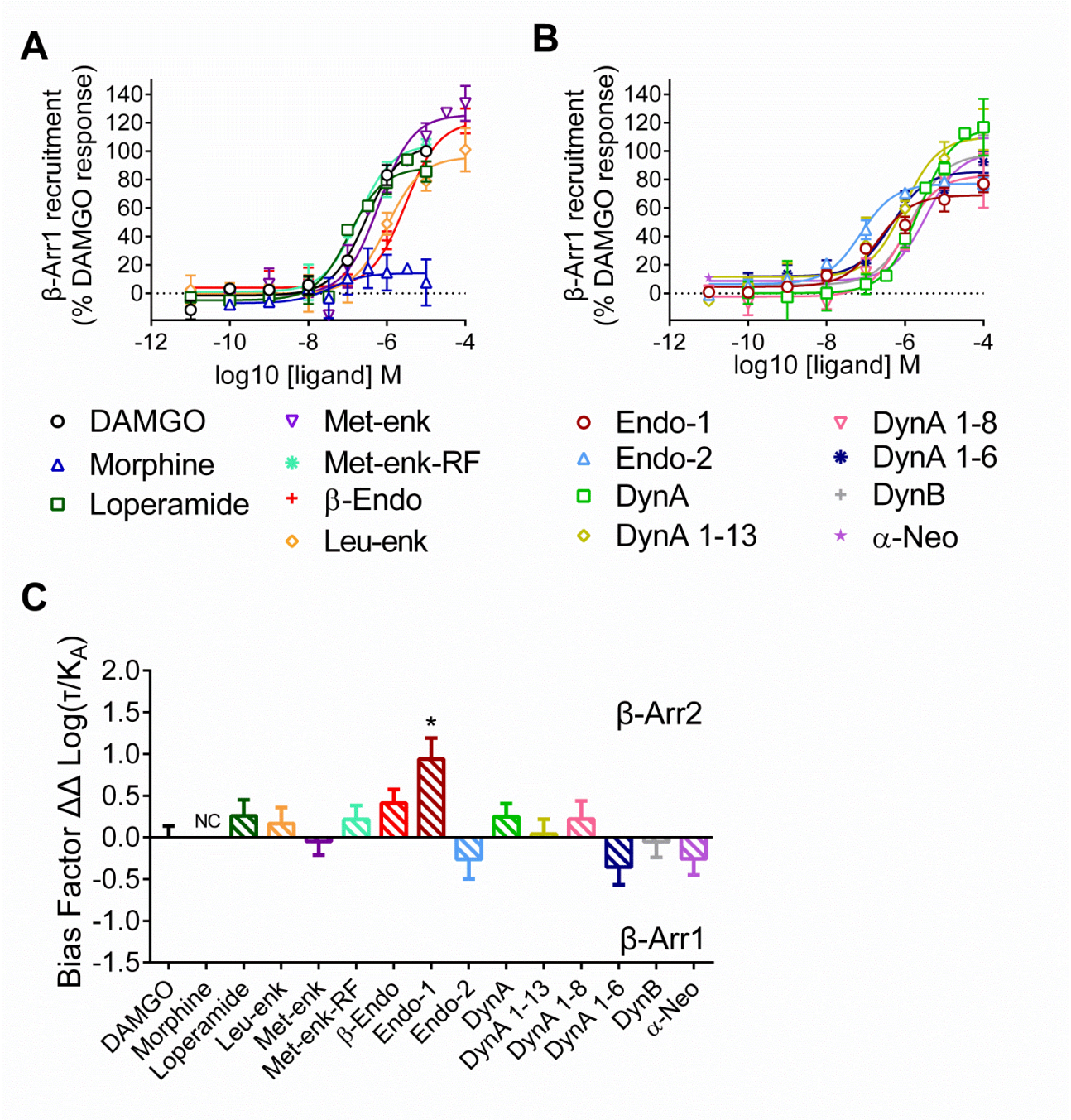

Figure 2.2: Bias between β-arr1 and β-arr2 recruitment.
(A-B) Recruitment of β-arr1 in FlpIn CHO cells. Data normalised to the 10μM DAMGO response and expressed as means ± SEM of 3 separate experiments. (C) Bias factors for all agonists between β-arr1 and β-arr2. *p ≤0.05 **p≤0.005, different from DAMGO as determined by two-tailed t-test. NC = not calculable

2.4.3 Biased ERK1/2 Phosphorylation Correlates with Bias Between cAMP and β-Arrestin Recruitment

Next, we examined activation of extracellular regulated kinases 1 and 2 (ERK1/2). Agonist-induced stimulation of ERK1/2 phosphorylation (pERK) was measured in FlpIn CHO-MOP cells using the Alpha-Screen phospho ERK1/2 assay. All agonists strongly stimulated pERK in CHO-MOP cells (Figure 2.3, A and B,Table A.1). This effect was blocked by naloxone and was absent in untransfected CHO cells (data not shown). Bias factors between pERK and all the previous signalling pathways (inhibition of cAMP production, β-arr1 and β-arr2 recruitment) were calculated (Figure 2.3, C and D, Table A.2). There were several ligands that displayed biased agonism towards cAMP inhibition over pERK compared to DAMGO, including morphine, loperamide, endo-1, α-neo and dynB. In line with this result, there was also a strong correlation between bias towards cAMP inhibition over pERK and the bias toward cAMP inhibition over β-arr2 recruitment (Pearson $r = 0.893$, $p < 0.0001$; Figure 2.3E). However, β-arr-dependent pERK may not be specifically mediated via β-arr2 only, as a similar correlation was observed for bias between pERK and β-arr1 recruitment (Figure A.3). The lack of bias between pERK and β-arr1 or 2 recruitment for nearly all of the ligands suggests that a component of pERK in CHO cells is β-arr-dependent. The only exception to this was morphine, which was biased towards β-arr2 and cAMP and away from pERK.

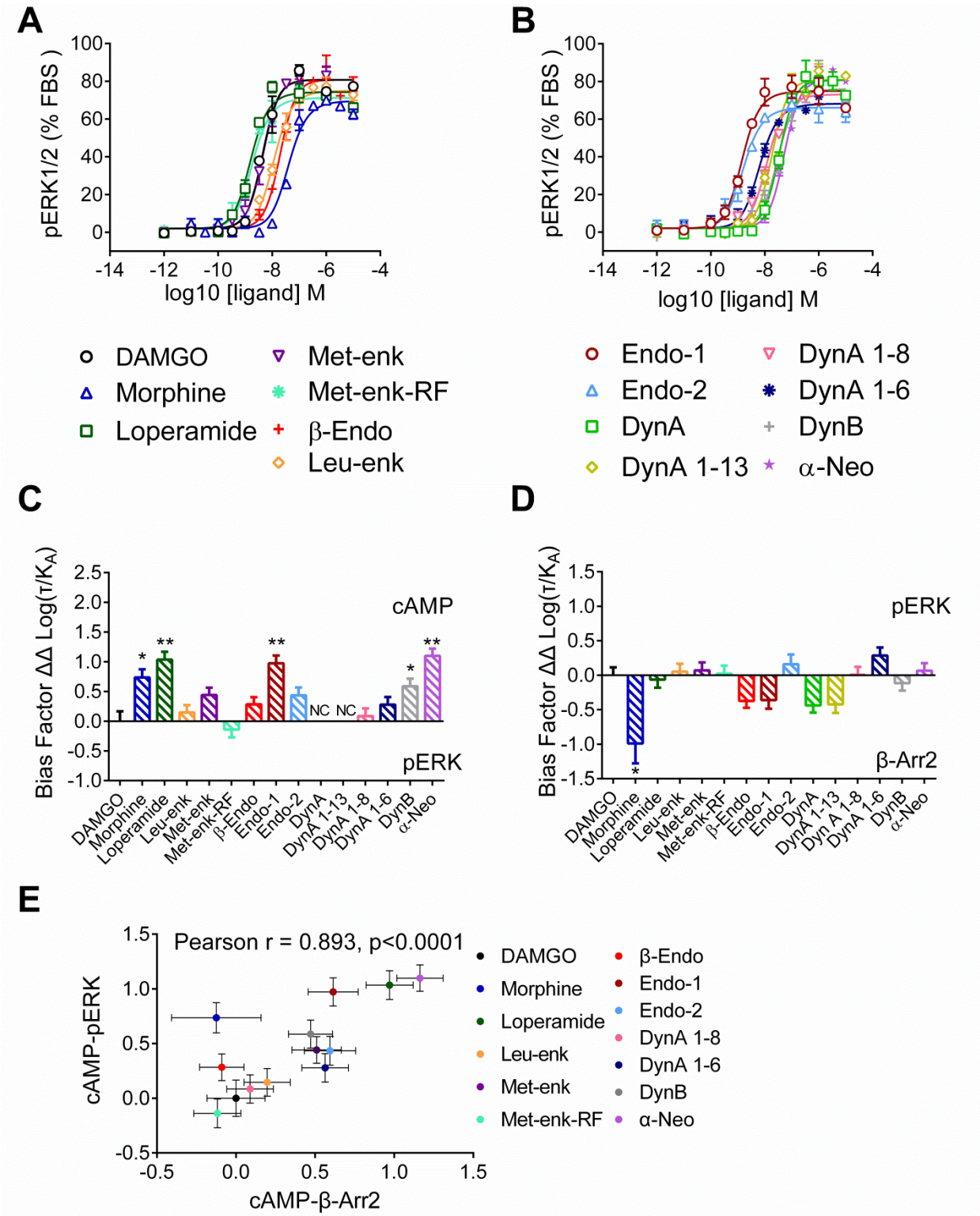

Figure 2.3: Bias towards β-arr recruitment determines pERK bias.
(A-B) pERK in FlpIn CHO-MOP cells. Data normalised to the 10% FBS response and expressed as means ± SEM of at least 3 separate experiments. Bias factors between pERK and cAMP (C) and β-arr2 (D). *p≤0.05 **p≤0.005, as determined by two-tailed t-test compared to DAMGO. (E) Two-tailed Pearson correlation was calculated between bias factors for cAMP-β-arr2 in Figure 1E and cAMP-pERK excluding morphine. NC = not calculable

2.4.4 Differential Activation of G Protein-Mediated Signalling

Although we used the inhibition of AC as a measure of G protein-mediated signalling, AC activity is regulated by numerous other signalling effectors in addition to $G\alpha_i$ subunits. These include Ca^{2+}, $G\beta\gamma$ subunits and A-kinase anchoring protein (AKAP). In addition to this, AC is differentially regulated by various $G\alpha$ subunits [700], which in turn are differentially modified by regulators of G protein signalling (RGS) [701]. We measured direct G protein activation in FlpIn CHO-MOP membrane preparations using [^{35}S]GTPγS binding assays and quantified bias between [^{35}S]GTPγS binding and inhibition of forskolin-induced cAMP (Figure 2.4). Several ligands showed bias towards cAMP over [^{35}S]GTPγS binding in comparison to DAMGO, including morphine, Met-enk, endo-1, endo-2 and α-neo. Interestingly some of these, endo-1 and α-neo, consistently showed bias towards cAMP over all other signalling pathways, whereas Met-enk and endo-2 did not. This suggests that bias towards cAMP by these two sets of ligands may be driven by different effectors. Modulation of AC activity by $G\beta\gamma$ subunits and AKAP did not contribute to bias between the cAMP and [^{35}S]GTPγS binding as inhibitors for these proteins had no effect on endo-1 or DAMGO inhibition of cAMP stimulation (Figure A.4).

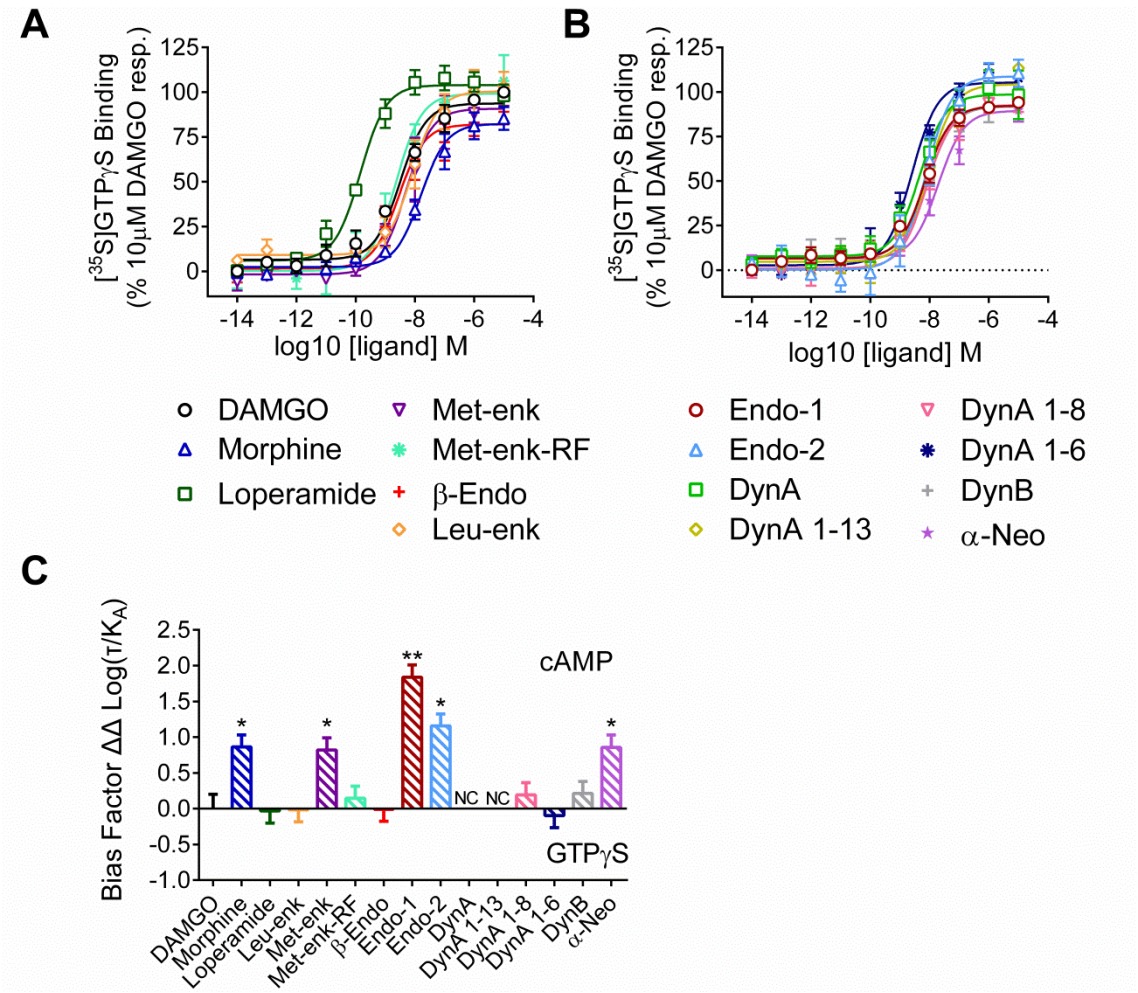

Figure 2.4: Bias between G protein activation and AC inhibition.
(A-B) Agonist-induced [^{35}S]GTPγS binding in CHO-MOP membrane preparations. Data normalised to the 10μM DAMGO response and expressed as means ± SEM of 3 separate experiments. (C) Bias factors between cAMP and GTPγS assays. *p ≤0.05 **p≤0.005, as determined by two-tailed t-test compared to DAMGO. NC = not calculable

2.4.5 Receptor Localisation/Trafficking

The inability of morphine to induce MOP internalisation was the first indication of differential actions of MOP agonists [171, 533]. It is now apparent that this compromised internalisation is associated with different modes of desensitisation for internalising vs non-internalising agonists. MOP trafficking was examined using BRET to measure the proximity between MOP-RLuc and a Venus-KRas construct, used as a plasma membrane marker. Before stimulation with agonists, MOP and KRas are in close proximity allowing BRET to occur. Upon MOP activation, receptor redistribution, clustering and internalisation the distance between these two proteins increases and result in a reduction in the BRET signal. A time course experiment was initially performed to determine the time at which a maximal reduction in BRET was observed following agonist stimulation, which occurred at 60min (data not shown). All ligands except morphine induced a reduction in BRET between MOP and KRas at 60min, (Figure 2.5, Table A.1).

Bias between receptor trafficking and the other signalling pathways for Met-enk-RF could not be quantified since a full concentration response curve could not be obtained for this ligand in the KRas BRET assay. As Met-enk-RF gave similar responses to Met-enk in all the signalling pathways interrogated previously, this result suggests that Met-enk-RF is biased away from this pathway. Since receptor trafficking is dependent on recruitment of β-arrs, bias factors were calculated between KRas BRET and β-arr1 and 2 recruitment. No ligands showed bias between KRas BRET and recruitment of β-arr1. Only endo-1 showed significant bias towards recruitment of β-arr2 and away from receptor trafficking. This result is in line with the fact that this ligand had previously shown significant bias towards β-arr2 over β-arr1 when these two pathways were compared (Figure 2.2)

We next compared the bias between KRas BRET and other signalling pathways. Endo-1 and α-neo, which previously showed bias towards cAMP inhibition over β-arr1 and 2 recruitment, now displayed significant bias towards cAMP over receptor trafficking (Figure 2.5E). Surprisingly, endo-2, which previously showed no bias between cAMP and recruitment of β-arrs, was now biased towards cAMP over KRas BRET. This shows that endo-2 is slightly biased towards β-arr recruitment over receptor trafficking, and this has significant consequences on downstream signalling. Bias between recruitment of β-arrs and KRas BRET indicates that the β-arrs recruited to endo-2 activated MOP

receptors may be mediating activation of an alternative signalling pathway that has not been captured by the signalling pathways interrogated in this study. Interestingly, the differences in bias between cAMP and KRas BRET or [^{35}S]GTPγS and KRas BRET track with the bias between cAMP and [^{35}S]GTPγS binding (Figure 2.5, E and F, Figure 2.4C). Therefore these results highlight that the bias between G protein signalling and receptor trafficking depends on the endpoint measured for G protein signalling.

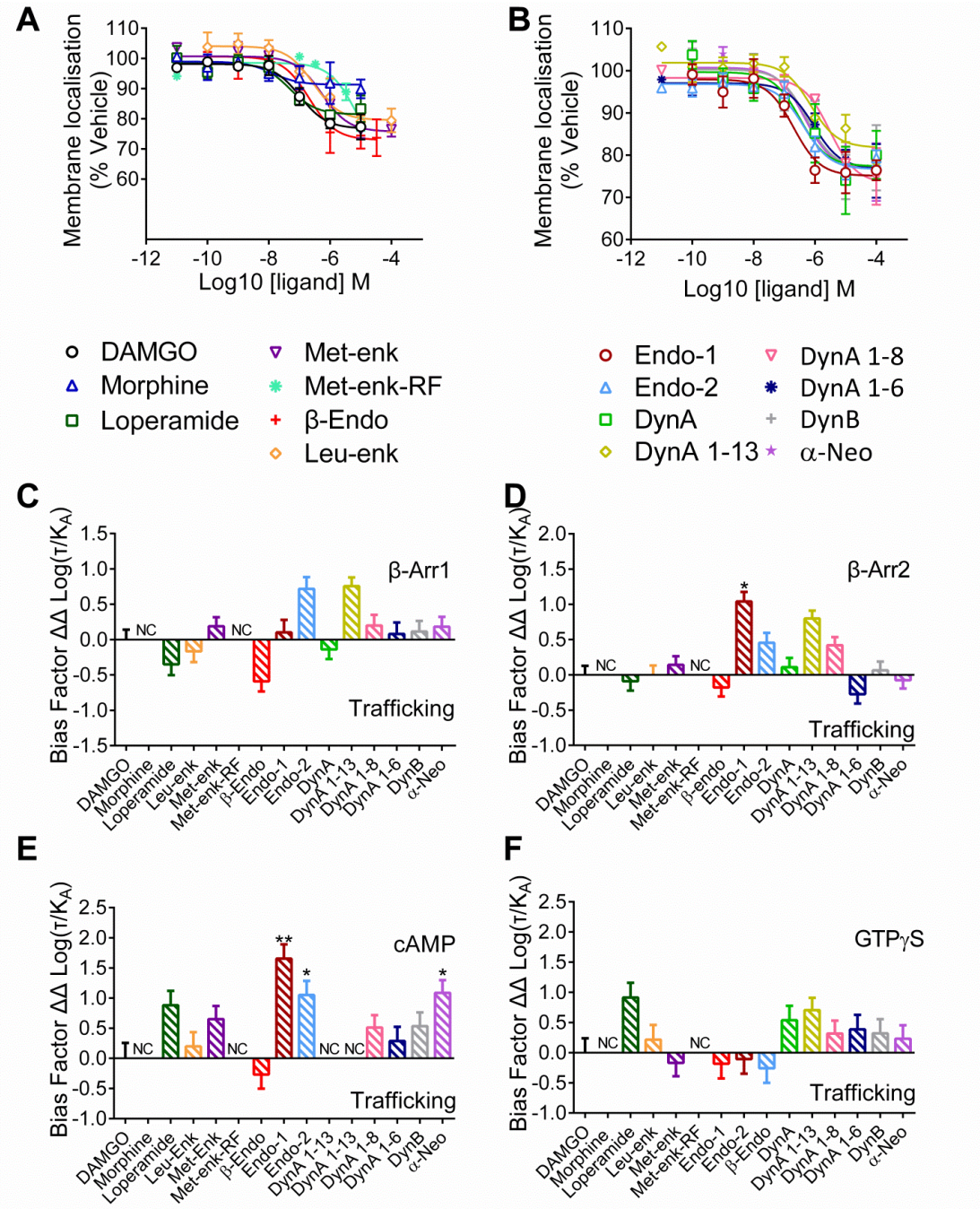

Figure 2.5: Endogenous opioids decrease the association of MOP with KRas.
(A-B) BRET between MOP-Rluc and KRas-Venus. Data expressed as percentage of vehicle, and expressed as means ± SEM of at least 3 separate experiments. Bias factors between KRas BRET (trafficking) and (C) β-arr1, (D) β-arr2, (E) cAMP and (F) GTPγS. *p ≤0.05 **p≤0.005, as determined by two-tailed t-test compared to DAMGO. NC = not calculable

2.4.6 Comprehensive Biased Agonism Profiles

In the context of biased agonism, given the complex signalling pathways that lie downstream of the MOP, it is evident that the comparison of ligand action between two pathways gives only a limited picture of drug action. Thus, to allow visualisation of the action of different ligands across all the pathways tested in this study, “webs of bias” were generated. These webs of bias allow the clustering of ligands into different activity profiles across the entire data set. For this, bias factors between cAMP and all other pathways were calculated using DAMGO as the reference ligand ($\Delta\Delta\tau/K_A$) and represented in a single multi-axial graph. Morphine and loperamide are already known to possess different signalling properties compared to DAMGO, hence they were included in this study as positive controls to validate our analytical tools. As expected, morphine, and loperamide each showed characteristic fingerprints, different to that of DAMGO (Figure 2.6A). Importantly, two additional opioids, endo-1 and α-neo also displayed unique signalling profiles, and showed bias across multiple different signalling pathways when compared to DAMGO. Met-enk and endo-2 also showed bias compared to DAMGO, but were similar to one another. Met-enk-RF also displayed a unique signalling profile. Despite its bias profile being very similar to DAMGO at most signalling pathways, Met-enk-RF only stimulated a very small response in the KRas BRET assay, which indicates that Met-enk-RF is biased away from receptor trafficking, however the degree of bias could not be quantified. All other endogenous ligands displayed activity profiles that were very similar to DAMGO (Figure 2.6B).

Another method to visualise and evaluate the overall signalling profiles is to perform principal component analysis (PCA) (see Materials and Methods). PCA identifies values in the data set that contribute the most variability, the principal components, which in this case are the bias factors that reveal the largest differences between ligands. Ligands that show similar biased agonism to one another will cluster together. PCA of all the bias factors (Figure 2.6C, Table A.2) showed that most of the endogenous ligands cluster closely with DAMGO. In contrast, loperamide, α-neo and endo-1, and to a smaller extent Met-enk and endo-2, are separated, indicating that these ligands display an overall unique pattern of bias, consistent with their signalling profiles in the webs of bias. Of note, the first principal component (PC1) of the analysis, which accounts for the greatest source of variability between ligands, only accounts for 56% of the variability (Figure 2.6C,Table A.3). PC2 contributes 26%, to the variability between ligands. Indeed, PC1 and PC2 together only account for 82% of the variability.

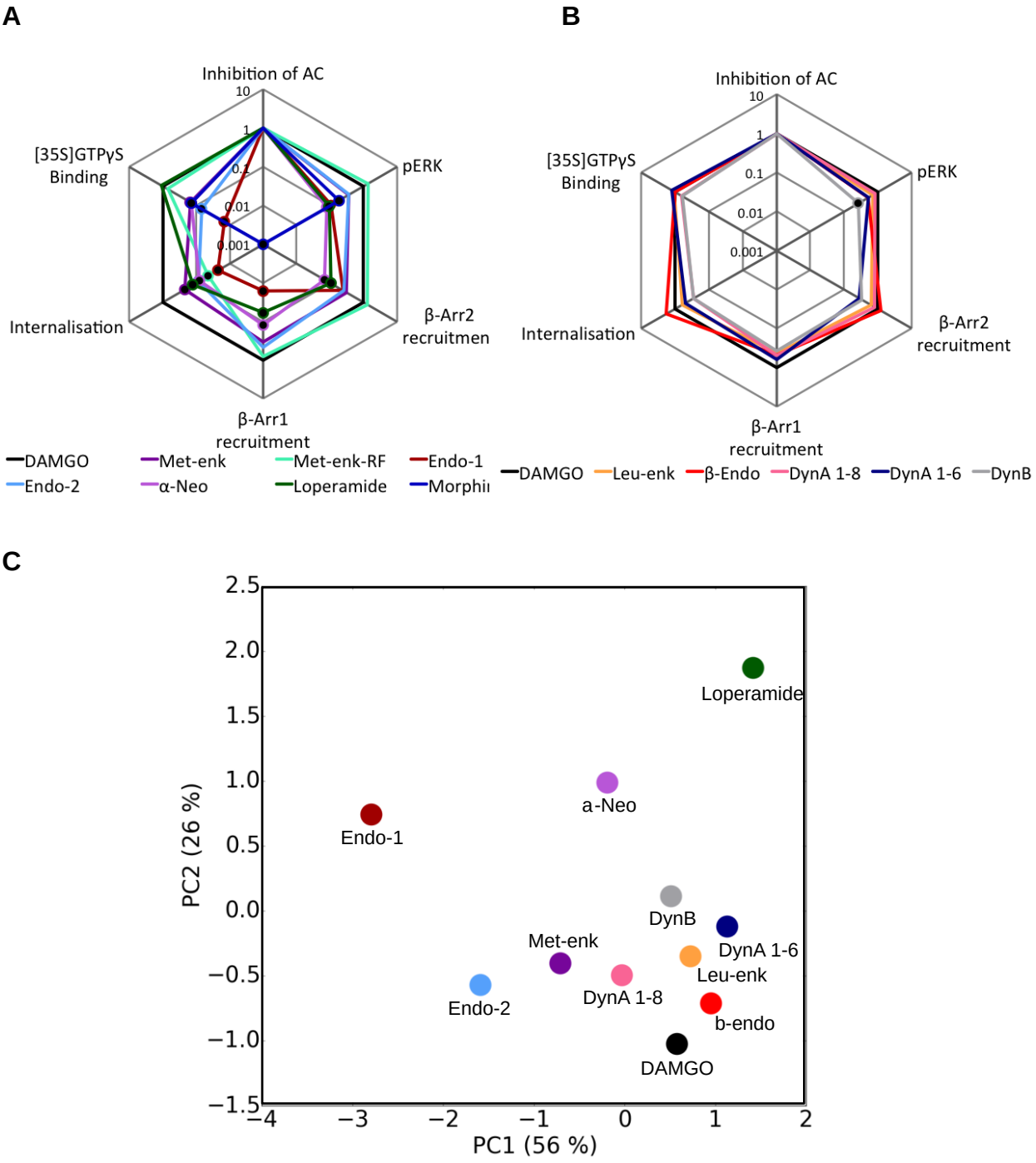

Figure 2.6: Webs of bias of endogenous opioid peptides and reference ligands at the MOP.

(A) Ligands with profiles similar to DAMGO (B) ligands with profiles that differ from that of DAMGO. τ/K_A values were normalised to the reference ligand DAMGO, and to the cAMP assay. Statistically significant differences ($p<0.05$) are denoted by black circles as determined by two-tailed t-test. For the purposes of visualisation only, a τ/K_A for Met-enk-RF in the internalisation assay was estimated using the incomplete KRas concentration response curve. (C) Principal component analysis (PCA) of all bias factors excluding morphine, DynA, DynA 1-13 and Met-enk-RF.

Interestingly, both the first two principal components are comprised mainly of bias factors between G protein and β-arr-mediated signalling endpoints (Table A.4). This

shows that bias between G protein activation and β-arr recruitment is a major determinant of the biased agonism characteristics of a ligand. However, as these bias factors are separated into two uncorrelated principal components, this also means that there is a diverse spectrum of bias between G protein and β-arr mediated signalling pathways. Altogether this highlights the multidimensional nature of biased agonism and the fact that quantification of bias should be expanded beyond examination of only two pathways such as G proteins vs β-arrs, in order to cover the whole spectrum of possible signalling characteristics.

2.5 Discussion

The data presented here show that endogenous opioids acting on the MOP can exhibit diverse signalling profiles. Examining bias across multiple pathways has highlighted the complex nature of biased agonism at MOP, and has revealed another level of complexity of bias that extends beyond differential activation of G proteins and β-arr recruitment. Several endogenous opioids including α-neo, Met-enk, Met-enk-RF, and the putative endogenous opioids endo-1 and endo-2, displayed biased agonism compared to DAMGO across multiple signalling pathways, whereas the rest of the endogenous ligands displayed profiles that were similar to that of DAMGO. In particular, endo-1 and α-neo displayed markedly different signalling profiles. α-Neo is considered a KOP agonist and, as such, no studies have examined its actions at the MOP. The physiological actions and signalling of endo-1 at MOP, conversely, have been extensively studied [702]. Endo-1 produces similar physiological effects to most opioids, such as analgesia, inhibition of gut motility, respiratory depression and the development of tolerance [703-706]. Differences between the physiological effects of endo-1 and endo-2 have been described. However, these differences are usually small and it cannot be ruled out that they are due to different degradation rates of the peptides rather than biased agonism [707, 708]. Interestingly, endo-1 has been shown to produce antinociceptive cross-tolerance to morphine whereas endo-2 does not, suggesting potential differences in the mechanisms of tolerance produced by these two ligands. As both endo-1 and 2 stimulate receptor internalisation [578], they would both be expected to produce tolerance via a similar mechanism to that of DAMGO. This suggests that tolerance produced by endo-1 and 2 may involve differential activation of signalling pathways unrelated to receptor internalisation, or alternatively, that the mechanisms of development of tolerance to these ligands are cell type-dependent.

Few other studies have examined biased agonism of endogenous opioids, and the results from these different studies are not consistent. Morse, Tran, Sun, Levenson and Fang [613] examined a range of endogenous and exogenous opioids in HEK293 cells using dynamic mass redistribution to measure MOP global responses. In that study, all endogenous opioids, except dynA 1-13, exhibited similar profiles. Our analysis suggests that whilst dynA 1-13 displayed some bias compared to the other endogenous ligands, this is limited evidence to suggest that dynA 1-13 is particularly unique compared to the other endogenous opioids. Rivero, Llorente, McPherson, Cooke, Mundell, McArdle, Rosethorne, Charlton, Krasel, Bailey, Henderson and Kelly [615] quantified bias

between [^{35}S]GTPγS binding and β-arr2 recruitment in HEK293 cells for some endogenous ligands, and found that endo-1 and endo-2 were biased towards β-arr2 recruitment compared to leu-enk [596, 615, 616]. In our study only endo-1 was biased towards β-arr2 over [^{35}S]GTPγS binding (Figure A.5). Various reasons can explain the different results. First, the different methodologies and time points used to measure β-arr2 recruitment may affect bias, since at later time points differential rates and modes of desensitisation may affect the level of β-arr2 recruitment. In addition, the different cell backgrounds used in each study may also change the bias of a ligand, as the expression levels of the various proteins involved in the activation of the signalling pathways examined may differ across cell lines and have an impact in the measures of bias [616].

Morphine is often described as a ligand with compromised ability to recruit β-arrs [274, 525, 544, 579, 612]). As a partial agonist, morphine is expected to give a lower response in signalling pathways with low coupling efficiency and/or assays with low sensitivity. However, to understand whether these observations refer to a biased action, requires systematic quantification of biased agonism. In our study, morphine did not show significant bias between β-arr2 and cAMP, although it was significantly biased towards β-arr2 when compared to [^{35}S]GTPγS binding. This is similar to results obtained by Rivero, Llorente, McPherson, Cooke, Mundell, McArdle, Rosethorne, Charlton, Krasel, Bailey, Henderson and Kelly [615], where morphine was slightly biased towards β-arr2, although not significantly [616].

We observed a correlation between pERK and β-arr recruitment, suggesting that β-arr recruitment is involved in pERK in CHO cells. This correlation was seen with both β-arr1 and β-arr2, indicating that both β-arrs are capable of mediating a component of ERK activation. β-arr-dependent pERK has also been shown previously in transgenic cell lines and primary cells [510, 511]. The one exception to this correlation was morphine. This indicates that morphine stimulates pERK via different pathway that is independent of β-arrs. A likely candidate is PKC, as morphine stimulated pERK in HEK293 cells has a been suggested to be PKC-dependent [208]. However, to date this has not been demonstrated in CHO cells.

In our study, endo-1 preferentially recruited β-arr2 over β-arr1. Differential recruitment of β-arrs to the MOP by endo-1 has not been shown previously, but has been demonstrated for morphine, which promotes recruitment of β-arr2 and little or no

recruitment of β-arr1 [525, 579, 580]. However, as mentioned previously, as all ligands gave a lower response in the β-arr1 assay, a partial agonist is expected to have very low to undetectable signal. Biased activation of β-arrs may result in differential activation of downstream signalling, as different β-arrs can act as scaffolds for different signalling complexes [284, 699]. β-arr1 but not 2 is required for MOP ubiquitination, and has also been shown to promote MOP dephosphorylation more rapidly than β-arr2 [536]. In addition, the downstream functions of β-arrs may vary with different ligands. Differential engagement of G protein receptor-coupled kinases (GRKs) and different patterns of ligand-induced MOP phosphorylation have been demonstrated previously [511, 525, 541, 543-545, 585]. These receptor phosphorylation patterns play a vital role in determining receptor interactions with β-arrs and may direct β-arr functions [285]. The differential role of β-arr2 recruitment in response to morphine compared to other opioids has been shown in the β-arr2 KO mice, where the improved pharmacological profile is only observed with morphine [640, 641]. Whilst morphine-induced β-arr recruitment results in activation of different signalling pathways, whether the differential recruitment of β-arrs induced by endo-1 mediates biased activation of signalling pathways downstream of β-arr is still unknown.

Agonists were assessed for bias between G protein activation and inhibition of AC, a classical downstream G protein-mediated effect. Several ligands showed bias towards inhibition of AC over [^{35}S]GTPγS binding in comparison to DAMGO, indicating differential activation of G protein-mediated signalling pathways. There are not many examples where [^{35}S]GTPγS assays have been performed in conjunction with cAMP assays in the same cellular background to assess MOP function [595, 709]. Zaki, Keith, Brine, Carroll and Evans [595] reported differing relative potencies of some agonists between the two assays but concluded that this was due to the different coupling efficiencies. There is also some evidence of ligand dependent engagement of different Gα subunits with MOP [603-605, 710]. However, these differences are small and since most methods used in these studies require overexpression or addition of purified G proteins, the real preferences for different subunits may be masked by differences in stoichiometry between receptor and G proteins. It is also possible that the bias observed between these signalling effectors is due to differences in signalling kinetics. As measurements for [^{35}S]GTPγS binding assays are usually taken after longer incubations with the ligand than for cAMP assays, ligands with slower association kinetics or that stimulate different rates of desensitisation can display bias between two

signalling endpoints. Further experiments are required to elucidate whether bias between [^{35}S]GTPγS binding and AC inhibition or other signalling pathways is due to differential regulation of G protein-mediated signalling pathways, different signalling kinetics or different ligand association/dissociation rates.

The bias between cAMP inhibition and [^{35}S]GTPγS also correlates with the bias observed between MOP trafficking and these signalling pathways. Several ligands showed bias between trafficking and cAMP, but not between trafficking and [^{35}S]GTPγS. Morphine and possibly Met-enk-RF may also be biased towards cAMP inhibition and [^{35}S]GTPγS binding over trafficking. However as bias factors could not be quantified for morphine and Met-enk-RF between trafficking and other signalling pathways, we cannot exclude the possibility that these ligands simply have lower efficacy, in which case the lower response in a low sensitivity assay, such as trafficking, is to be expected. There were no ligands showing significant bias between trafficking and recruitment of β-arr1, and only endo-1 was biased towards β-arr2 over receptor trafficking. This result is in line with the fact that receptor trafficking is highly dependent on recruitment of β-arrs.

In summary, we have performed a systematic quantitative analysis of biased agonism at the MOP by endogenous and putatively endogenous opioid peptides across multiple different signalling pathways. This work has revealed that opioid peptides display a variety of different biased agonism profiles, some of which are unique. α-Neo and endo-1 display particularly distinct biased agonism profiles, and may have different signalling properties and physiological effects *in vivo* compared to other endogenous opioids. Biased agonism profiles, combined with different degradation rates, expression patterns in the body, and differing selectivities for opioid receptor subtypes, may engender tremendous diversity in endogenous opioid activity and lead to finely tuned physiological processes. Although the impact of MOP biased agonism in the control of normal physiological processes still remains to be explored, our findings provide a pharmacological framework to progress our understanding on ligand redundancy of the opioid system. A greater understanding of how endogenous opioids control physiological processes through biased agonism will reveal vital information required to enable design of biased opioids with improved pharmacological profiles.

CHAPTER 3

SYSTEMATIC ANALYSIS OF FACTORS INFLUENCING OBSERVATIONS OF BIASED AGONISM AT THE μ-OPIOID RECEPTOR

Georgina L. Thompson[1,2], J. Robert Lane[1], Thomas Coudrat[1], Patrick M. Sexton[1], Arthur Christopoulos[1] and Meritxell Canals[1]

PUBLISHED IN BIOCHEM. PHARMACOL. 2016;113, 70–87

[1]Drug Discovery Biology and Department of Pharmacology, Monash Institute of Pharmaceutical Sciences, Monash University, 399 Royal Parade, Parkville, Victoria 3052, Australia; [2]Defence Science and Technology Group, Australian Department of Defence, Australia

3.1 Declaration for Thesis Chapter 3

Monash University

Declaration by candidate

In the case of Chapter 3, the nature and extent of my contribution to the work was the following:

Nature of contribution	**Extent of contribution (%)**
Participated in research design, performed all experiments and analysis, and wrote the manuscript.	90%

The following co-authors contributed to the work. If co-authors are students at Monash University, the extent of their contribution in percentage terms must be stated:

Name	**Nature of contribution**	**Extent of contribution (%)** for student co-authors only
Meritxell Canals	Participated in research design, contributed to data analysis and writing of the manuscript	N/A
Arthur Christopoulos	Participated in research design, contributed to data analysis and writing of the manuscript	N/A
J. Robert Lane	Participated in research design, contributed to data analysis and writing of the manuscript	N/A
Thomas Coudrat,	Performed data analysis	2%
Patrick M. Sexton	Contributed to writing of the manuscript	N/A

The undersigned hereby certify that the above declaration correctly reflects the nature and extent of the candidate's and co-authors' contributions to this work*.

Candidate's Signature	[redacted]	**Date 9 May 2016**
Main Supervisor's Signature	[redacted]	**Date 9 May 2016**

3.2 Abstract

Biased agonism describes the ability of distinct G protein–coupled receptor (GPCR) ligands to stabilise distinct receptor conformations leading to the activation of different cell signalling pathways that can deliver different physiologic outcomes. This phenomenon is having a major impact on modern drug discovery as it offers the potential to design ligands that selectively activate or inhibit the signalling pathways linked to therapeutic effects with minimal activation or blockade of signalling pathways that are linked to the development of adverse on-target effects. However, the explosion in studies of biased agonism at multiple GPCR families in recombinant cell lines has revealed a high degree of variability on descriptions of biased ligands at the same GPCR and raised the question of whether biased agonism is a fixed attribute of a ligand in all cell types. The current study addresses this question at the MOP. Here we have systematically assessed the impact of differential cellular protein complement (and cellular background), signalling kinetics and receptor species on our previous descriptions of biased agonism at MOP by several opioid peptides and synthetic opioids. Our results show that all these factors need to be carefully determined and reported when considering biased agonism. Nevertheless, our studies also show that, despite changes in overall signalling profiles, ligands that previously showed distinct bias profiles at MOP retained their uniqueness across different cell backgrounds.

3.3 Introduction

GPCRs are involved in the control of virtually every physiological process. They are a major target of currently used medicines, and represent valuable targets for the design of new therapeutics. However, most GPCRs are ubiquitously expressed in multiple tissues and exert their effects through activation of wide variety of signalling pathways. Many drugs that target GPCRs produce side effects mediated through the activation of "unwanted" signalling pathways by the GPCR of interest, or by the activation of the same GPCR in different non-target tissues. The former "on-target" side effects can be minimised by designing drugs that selectively activate the signalling pathways required to produce the therapeutic response. This pathway-specific drug design is based on a property of GPCRs known as "biased agonism", "ligand-directed signalling" or "functional selectivity" [711]. Biased agonism describes how chemically distinct ligands targeting the same GPCR in an identical cellular background, stabilise the receptor in different conformations, resulting in differential activation of downstream signalling, which in turn can induce different physiological effects. Therefore, biased agonism offers the potential to design ligands that selectively activate or inhibit the signalling pathways linked to the desired therapeutic effects with minimal activation or blockade of signalling pathways that are linked to the development of side effects.

In order to develop strategies to design a biased ligand with the desired selectivity for particular signalling pathways, methods for quantifying biased agonism are essential. To achieve this, it is important to consider that the observed response that is induced by a ligand at a particular signalling pathway is not solely determined by the affinity and intrinsic efficacy of such ligand. Rather, the differing coupling efficiencies of the signalling pathways, and the different conditions and sensitivities of the detection methods, also contribute to the overall observed response, and are termed "system bias" and "observational bias", respectively [648]. Therefore, biased agonism engendered solely by conformational effects of the ligand-receptor interaction, must be quantified using a method that excludes both system and observational bias. Although several analytical methods to quantify biased agonism have been developed, most can only be applied in specific circumstances (as reviewed in [648]). The method recently described by Kenakin, Watson, Muniz-Medina, Christopoulos and Novick [685], or "transduction coefficient" method, based on the Black and Leff (1983) operational model of agonism, can be applied to concentration-response curves to obtain a single

parameter that describes bias between signalling pathways in a system independent manner [648].

In the last decade, biased agonism has been quantified at numerous GPCRs including; opioid receptors [615, 712-714], chemokine receptors [237, 238, 685], adrenoceptors [654, 715], and many others [716-719]. Most studies have focused on discovery of ligands with differential receptor signalling versus regulation characteristics, specifically by quantifying bias between G protein-mediated signalling and β-arr recruitment or receptor internalisation [237, 615, 712, 714]. However, it has become increasingly apparent that biased agonism can result in the differential activation of a plethora of signalling pathways downstream of receptor activation, not only G protein activation and β-arr recruitment, supporting the concept of the pluridimensionality of efficacy [229]. For this reason, more recent studies are extending assessment of bias to a wider array of signalling pathways to obtain comprehensive descriptions of ligand action that can predict the differential effects of ligands [238, 654, 713, 717].

Most descriptions of biased agonism have been initially based on studies in recombinant cell systems, where consistent and robust responses of different signalling pathways can be obtained, ensuring a high degree of accuracy and sensitivity. However, it is still unclear whether quantification of biased agonism in recombinant cell lines can truly predict biased agonism *in vivo* [720]. The potential for inconsistencies in biased agonism determinations is exemplified by conflicting results reported in different studies of the same GPCR that have examined this phenomenon in different cell backgrounds. At the MOP, for instance, several studies have examined bias between G protein activation and β-arr recruitment [612, 615, 616, 713]. Most notably, endo-2 may exhibit differential bias towards β-arr2 recruitment and away from G protein activation in different studies [615, 616, 713]. Similar discrepancies have been observed for bias of aripiprazole between extracellular signal regulated ERK1/2 phosphorylation and AC inhibition at the dopamine D_2 receptor [719, 721], and bias between receptor internalisation and G protein-mediated signalling pathways mediated by CCL4 and CCL3L1 at CCR5 receptors [237, 685]. Altogether, such discrepancies between studies raise important questions about the determination and quantification of biased agonism, specifically, is biased agonism a fixed attribute of a ligand in all cell types?

Because GPCR function is determined by at least three molecular partners, i.e. ligand, receptor, and transducer or effector protein, it follows that an agonist-bound active

receptor state cannot be defined outside the context of a specific receptor–transducer interaction [722]. Such an active receptor state will be dependent on the cellular complement of transducers (or intracellular effector proteins) of a particular cell type. Thus, altering the cellular complement of intracellular binding proteins by overexpressing specific signalling components, or changing cell background, will likely affect bias. When the change in expression of a signalling effector(s) has equal effects on the agonism of all ligands, this results in a change in “system bias” which is eliminated when quantifying bias relative to the reference ligand using the “transduction coefficient method” (see above and [685]). However, altered expression of signalling effectors may have unequal effects on different ligands and, as a consequence, the observed biased agonism will not necessarily be maintained in different systems. Ligands may preferentially activate different isoforms of signalling effectors that are expressed in different cell types such as G protein subunits or GRKs). Moreover, in addition to potentially altering ligand bias, the cell background also dictates which signalling pathways can be practically used to quantify bias. GPCRs will be more efficiently coupled to some signalling pathways more than others (system bias). This may require alterations of assay conditions to optimise detection of poorly coupled signalling pathways, and may entail changing the signalling effectors examined altogether. This makes it prohibitively difficult to measure the same signalling events under identical conditions in different cells, increasing the likelihood of obtaining different results when quantifying bias in different cell backgrounds. Alterations in the assays conditions may include overexpression of a signalling effector to enhance detection of the desired signalling pathway, such as the overexpression of a GRK to enhance β-arr recruitment [660, 661]. Altering the balance between signalling effectors that are in competition with each other, such as G proteins and β-arrs or different GRK isoforms, may enhance interactions with signalling effectors that a ligand-receptor complex naturally has little affinity for. This change in signalling effector expression may again affect the descriptions of biased agonism.

Quantifying bias in a different cell background may alternatively require substitution of a poorly coupled signalling pathway for another closely related signalling pathway, such as different G protein-mediated signalling pathways. However, even closely related signalling pathways are differentially regulated by distinct signalling effectors, and therefore are subject to the same limitations in determining biased agonism. For example, differential activation of G protein-mediated signalling pathways can occur as

a result of differential activation of G protein subunits [723], which may preferentially activate some signalling pathways, and may in turn be differentially controlled by RGS [724-726]. Additionally, different G protein-mediated signalling pathways, such as AC stimulation or inhibition, are regulated by numerous other signalling effectors [120].

Finally, another factor that may alter observed bias when measured under different experimental conditions is the kinetics of all processes involved; ligand binding, activation and desensitisation of the signalling pathways [727]. Biased agonism is generally described as a difference in the magnitude of activation of signalling pathways compared to a reference ligand, when measured at its peak or steady state activation. However, this limited measure of biased agonism largely excludes the differential effects biased agonists may have on the spatiotemporal properties of the signalling pathways. Every signalling pathway has different activation and desensitisation kinetics that will be differentially regulated by different ligands, i.e ligands may have similar bias when considering the maximal response of the signalling pathway, but due to differential desensitisation their bias may change at later time points. This means that the observed bias of a ligand will be time dependent, and consequently different results may be obtained when measuring the same signalling pathway using different assay techniques that require different incubation times [727].

Altogether, cell background and signalling kinetics add additional layers of complexity to defining the biased agonism of a ligand, and to ascertain the profile that is required to produce the desired therapeutic effects. Previously, we systematically quantified biased agonism of a range of both exogenous and endogenous opioids at MOP across multiple different signalling pathways in CHO cells [713]. This study revealed a number of ligands that possess unique biased agonism profiles, including the endogenous ligands Met-enk-RF and α-neo. Here, we have used this initial characterisation to extend our studies towards understanding the impact of cell background and signalling dynamics on the detection and quantification of bias. Our results illustrate that when assessing biased agonism, both of these factors need to be taken under consideration. However, our studies at MOP also show that, despite changes in directions of bias, and overall signalling profiles, ligands with distinct bias profiles retained their differentiation across different cell backgrounds.

3.4 Methods

3.4.1 Materials

Chinese hamster ovary (CHO) FlpIn cells and Dulbecco's modified Eagle's medium (DMEM) were purchased from Invitrogen (Mulgrave, VIC, Australia). Foetal bovine serum (FBS) was purchased from ThermoTrace (Melbourne, Australia). Hygromycin-B was purchased from Roche Applied Science (Dee Why, NSW, Australia). All endogenous opioid peptides were purchased from Mimotopes (Melbourne, Australia). Morphine HCl was from GlaxoSmithKline (Boronia, Victoria, Australia). All other chemicals were purchased from SigmaAldrich (Castle Hill, NSW, Australia). AtT20 and AtT20-FLAG-MOP cells were a gift from Prof. Macdonald Christie (University of Sydney, Australia). MOP-RLuc was a gift of Prof. Laura Bohn (Scripps Research Institute, Florida, USA).

3.4.2 Cell Culture and Generation of Stable Cell Line

Cells were maintained and cultured in high-glucose DMEM containing 10% FBS and 600 μg/ml hygromycin B for CHO-MOP cells, and 500μg/ml G418 for AtT20-MOP, at 37°C under a humidified atmosphere containing 5% CO_2. cDNA encoding the wild-type human MOP was obtained from the Missouri University of Science and Technology (http://www.cdna.org) and was provided in pcDNA3.1+. Sequence of the human MOP was amplified by polymerase chain reaction and cloned into the Gateway entry vector pENTR/D-TOPO, using the pENTR directional TOPO cloning kit, according to the manufacturer's instructions (Invitrogen, Mulgrave, Australia). The construct was subsequently transferred into the Gateway destination vector pEF5/frt/V5/dest using the LR Clonase enzyme mix (Invitrogen), and the constructs were used to transfect FlpIn CHO cells (Invitrogen). Cells were selected using 600 μg/ml hygromycin B to generate cell lines stably expressing MOP. AtT20 cells stably expressing a FLAG tagged MOP were generated as described previously [598].

3.4.3 Inhibition of Forskolin-Induced cAMP Levels

The ability of ligands to inhibit forskolin-induced cAMP production was assessed in AtT20-MOP and FlpIn CHO-MOP cells transiently transfected to express the CAMYEL cAMP BRET biosensor [693]. CHO-MOP cells were grown overnight in white 96-well plates (Culturplates, Perkin Elmer, Melbourne Australia). Transient transfection of FlpIn

CHO-MOP cells was performed using polyethylenimine (PEI, Polysciences, Warrington, PA, USA) at a 6:1 ratio of DNA. AtT20-MOP cells were grown in 10cm dishes and transient transfection of cells was performed using lipofectamine (Invitrogen). After 24h AtT20-MOP cells were transferred to white 96-well plates. 48h after transfection cells were rinsed and pre-incubated in Hank's Balanced Saline Solution (HBSS) with 0.01% BSA and protease inhibitors (1μM captopril, 1μM phosphoramidon, 1μM amastatin, 1μM actinonin and 1μM Diprotin A) for 30min at 37°C. Cells were then incubated with the Rluc substrate coelenterazine-h, final concentration 5μM, for 5min, followed by a further 5min incubation with increasing concentrations of agonists. Forskolin was then added to a final concentration of 10μM. After 5min the YFP and the Rluc emissions were measured using a LumiSTAR Omega (BMG Labtech, Ortenberg, Germany) that allows for sequential integration of the signals detected at 475 ± 30 and 535 ± 30nm, using filters with the appropriate band pass. For cAMP kinetic experiments baseline readings were taken every 30s for 3min before addition of forskolin, and measurements taken every 30s for 30min after addition of forskolin. Data are presented as a BRET ratio, calculated as the ratio of YFP to Rluc signals, and expressed as the percentage of the forskolin-induced signal.

3.4.4 Bioluminescence Resonance Energy Transfer Assays

Agonist-induced recruitment of β-arrs to the MOP was examined using a BRET-based method. AtT20 cells and parental FlpIn CHO cells were transfected as described above to co-express MOP C-terminally tagged with Rluc, G protein coupled receptor kinase 2 (GRK2) and β-arr1- or β-arr2-YFP, at a 1:2:4 DNA ratio. To measure G protein activation in FlpIn CHO cells, $1x10^6$ cell were seeded in white 96 well plates. The next day cells were transfected using PEI as above with 1μg MOP, 1.2 μg Gβ1, and either 1.35μg Gγ-Venus with 0.6μg of $G\alpha_{i1}$-Rluc8, $G\alpha_{i2}$-Rluc8 or $G\alpha_{i3}$-Rluc8, or 0.6 μg Gγ2-Venus with 0.14 μg $G\alpha_{ob}$-Rluc8. For β-arr recruitment assays, agonists were added after 5min of pre-incubation with coelenterazine-h, and then incubated for an additional 5min before the BRET ratio was determined. For G protein assays, agonists were added after 10min pre-incubation with coelenterazine-h, and readings were taken after 5min incubation with the ligand. For G protein assays with 60min agonist stimulation, coelenterazine-h was added 10min prior to detection. Data is expressed as the percentage of the maximum DAMGO response for β-arr assays, and the maximum Loperamide response for G protein assays.

3.4.5 Membrane Potential

Agonist-induced membrane hyperpolarisation in AtT20-MOP cells was measured using the FLIPR membrane potential assay kit (Molecular devices, CA, USA). AtT20-MOP cells were plated in clear bottom black half area 96-well plates (Corning, Clayton, Australia). Cells were allowed to adhere, the media was changed to low serum media (1% FBS), and cells allowed to grow overnight. 1 bottle of red membrane potential dye was dissolved in 10ml K^+ free HBSS (0.388mM $NaHPO_4$, 4.17mM $NaHCO_3$, 0.441mM KH_2PO_4, 145mM NaCl, 22mM HEPES, 0.407mM $MgSO_4$, 0.493mM $MgCl_2$, 1.26mM $CaCl_2$ and 5.56mM glucose). Dye was added to cells to a 1:1 ratio of dye to low serum media, and cells allowed to recover for 30min. Membrane hyperpolarisation was measured at 37°C using a Flexstation®3 (Molecular Devices; Sunnyvale, CA, USA). Fluorescence was detected for every 2s for 90s at 530 nm excitation and 565 nm emission. Baseline readings were taken for 30s before addition of agonists. Data is expressed as ΔMP, which is the area under the curve units normalised to the maximum response obtained with DAMGO.

3.4.6 Receptor Internalisation

AtT20-MOP cells were plated and grown overnight in 48-well culture plates. Cells were incubated with increasing concentrations of agonists in DMEM for 30min, then washed gently 3 times with TBS and fixed in 3.7% v/v paraformaldehyde. Surface or total FLAG-MOP receptors were detected in intact or (Nonidet P-40 equivalent)-detergent permeabilised cells, respectively, using the mouse anti-FLAG antibody (1:2000) followed by HRP-conjugated goat anti-mouse IgG (1:2000). After washing with TBS, the peroxidase substrate (SIGMAFAST™ OPD, SigmaAldrich) was added at a final concentration of 0.4 mg/ml, and the reaction was terminated by the addition of 1 M HCl. The coloured reaction product was detected at 490 nm in a multi-label plate reader (EnVision, PerkinElmer Life Sciences). The absorbance values for transfected cells were normalised to those of mock-transfected cells, and receptor density was reported relative to vehicle-treated wells.

3.4.7 Data Analysis

Quantification of bias was performed as described in section 2.3.9.

3.4.8 Principal Component Analysis

Principal component analysis (PCA) is a dimensionality reduction method that uses transformations to project a high-dimensional set of data into a lower dimensional set of variables called principal components (PCs). The PCs extract the important information from the data, revealing its internal structure in a way that best explains its variance [697]. PCs are ranked according to the percentage of total variance in the data they explain. The first PC explains a maximal amount of total variance in the data. Each succeeding PC explains a maximal amount of the remaining variation, without being correlated with the preceding components. PCA was applied using singular value decomposition as implemented in the package scikit-learn [698], the script used for the analysis and plotting can be found at https://github.com/thomas-coudrat/pca_analysis.

3.5 Results

We recently quantified biased agonism at the MOP in FlpIn CHO cells stably expressing the human MOP [713] and identified several opioids that display unique biased agonism profiles compared to the reference ligand DAMGO. These include morphine, endo-1 and endo-2, which had previously been reported to display biased agonism at MOP [615, 616], the peripherally restricted MOP agonist, loperamide, as well as three endogenous opioids, Met-enk, Met-enk-RF and α-neo. In the current study, we investigated whether the biased agonism profiles for these eight MOP ligands remain consistent across different cell lines, examined the effect of different cellular protein complement on bias, and assessed the time dependency of biased agonism.

3.5.1 Opioids Show Differential Gα Subunit Activation

To investigate the effect of the different G protein complement on biased agonism we have examined the activation of different G proteins. MOPs are primarily coupled to G proteins containing $G\alpha_i$ or $G\alpha_o$ subunits, and there is some evidence that opioid ligands show differential preference for some subtypes [603-605]. The ability of ligands to activate G proteins was assessed using a BRET-based assay. CHO FlpIn MOP cells were co-transfected with $G\gamma_2$-Venus, $G\beta_1$ and either RLuc8-tagged $G\alpha_{i1}$, $G\alpha_{i2}$, $G\alpha_{i3}$ or $G\alpha_{ob}$. All ligands activated the four G protein subtypes after 5min in a concentration-dependent manner (Figure 3.1). The greatest changes in BRET were observed with $G\alpha_{i1}$ and $G\alpha_{ob}$ (data not shown), which may indicate that MOP has a greater ability to couple to G proteins containing $G\alpha_{i1}$ or $G\alpha_{ob}$ subunits, however we cannot exclude the possibility that this is due to differences in BRET efficiency between the different RLuc8-Gα constructs and the Gγ-Venus. DAMGO and Met-enk stimulated most Gα subtypes to at least 80% of the response to loperamide at 5min, whereas morphine, endo-1, endo-2, Met-enk-RF and α-neo were, in general, less efficacious than loperamide (Figure 3.1).

Bias factors ($\Delta\Delta\log(\tau/K_A)$, see materials and methods) between activation of different Gα subtypes were quantified for all ligands using DAMGO as the reference ligand (Figure 3.2, Table 3.1). When compared to DAMGO, Met-enk-RF and α-neo were biased away from $G\alpha_{i1}$ activation relative to at least one of the other Gα subunits (Figure 3.2A-C). This is largely due to the fact that DAMGO-stimulated MOP is more efficiently coupled to $G\alpha_{i1}$ than to the other Gα subunits, which is apparent when comparing the

log(τ/K_A) values of DAMGO vs other ligands for each Gα subunit (Table 3.1). Additionally, Met-enk-RF, which exhibited similar activation of $G\alpha_{i1}$, $G\alpha_{i2}$ and $G\alpha_{ob}$ relative to DAMGO, showed increased $G\alpha_{i3}$ activation when compared to DAMGO at 5min, resulting in bias towards $G\alpha_{i3}$ over $G\alpha_{i1}$ (Figure 3.2B). This bias is partly attributable to a small increase in the K_A of Met-enk-RF for $G\alpha_{i3}$ (Table 1). Interestingly, no ligands showed bias between $G\alpha_{i2}$ and $G\alpha_{i3}$, $G\alpha_{i3}$ and $G\alpha_{ob}$ or $G\alpha_{i2}$ and $G\alpha_{ob}$ (Figure 3.2D-F).

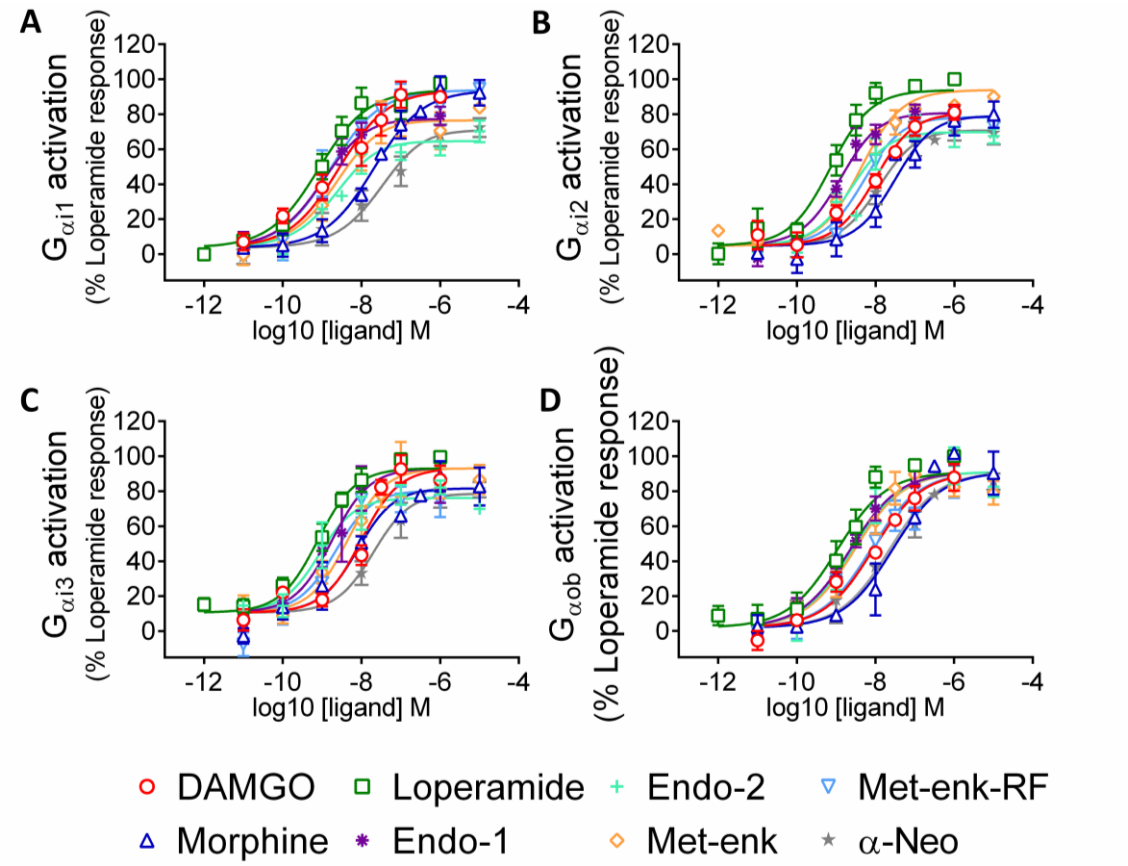

Figure 3.1: Activation of $G\alpha_{i/o}$ subunits by MOP agonists.
(A-D) Activation of $G\alpha_{i1}$, $G\alpha_{i2}$, $G\alpha_{i3}$ and $G\alpha_{ob}$ in FlpIn CHO cells after 5min of agonist stimulation. Data normalised to the 1μM Loperamide response. Data expressed as mean ± SEM of at least 3 separate experiments.

We next quantified bias between activation of the Gα subunits and recruitment of β-arr2 (Figure 3.2G). α-neo showed bias towards $G\alpha_{i2}$ which is in line with previous results that showed α-neo was biased towards inhibition of cAMP production when compared to β-arr2 [713]. In addition to this, morphine and endo-1 were biased towards β-arr2 over $G\alpha_{i1}$ and $G\alpha_{i3}$ respectively. This was unexpected since morphine and endo-1 previously showed no bias between inhibition of cAMP production and β-arr2. The different bias observed when comparing β-arr2 to either inhibition of cAMP production or G protein

activation illustrates that the level of G protein activation is not always indicative of the level of activation of downstream G protein-mediated signalling.

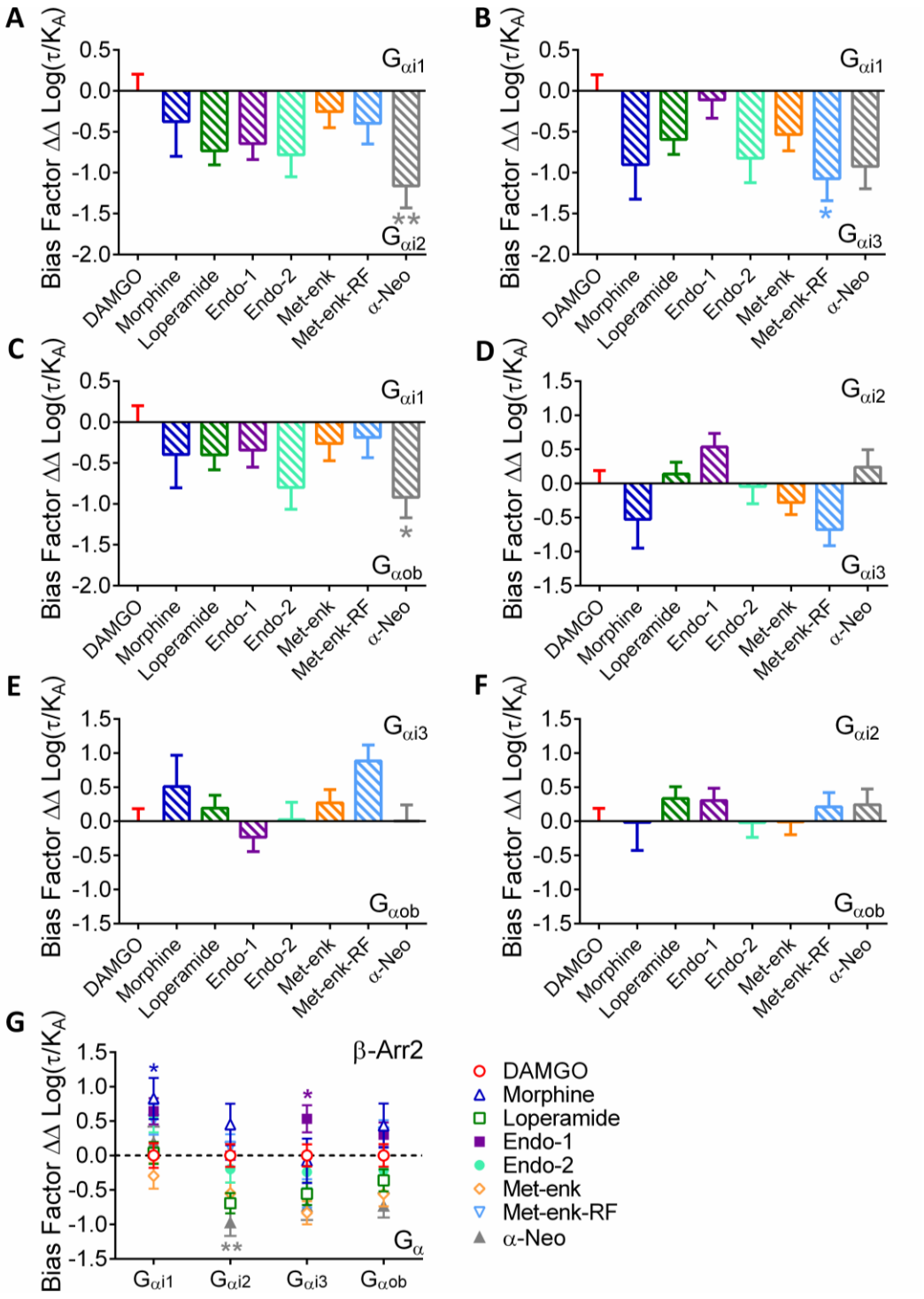

Figure 3.2: Quantification of biased agonism of MOP agonists between activation of different $G\alpha_{i/o}$ subunits.

(A-F) Bias factors for all agonists between $G\alpha_{i1}$, $G\alpha_{i2}$, $G\alpha_{i3}$ and $G\alpha_{ob}$ activation after 5min of agonist stimulation. (G) Bias factors between β-arr2 recruitment and $G\alpha_{i1}$, $G\alpha_{i2}$, $G\alpha_{i3}$ and $G\alpha_{ob}$ activation after 5min agonist stimulation. Data expressed as means ± SEM of at least 3 separate experiments. *p≤0.05 **p≤0.005, different from DAMGO as determined by one-way ANOVA with Dunnett's multiple comparison test.

Table 3.1: Quantification of biased agonism between activation of different G protein subtypes at two time points.

Transduction coefficients [Log(τ/K_A)], normalised transduction coefficients [ΔLog(τ/K_A)] and Log(bias factors) [$\Delta\Delta$Log(τ/K_A)]. Values represent the mean ± SEM of three to five independent experiments. *p ≤0.05 **p≤0.005, different from DAMGO as determined by ANOVA with Dunnett's multiple comparison test. † p ≤0.05 as determined by two-tailed t-test compared to same ligand at 5min. NC: not calculated due to full agonism.

		5mins						60mins					
		$\log K_A$	SEM	$\log\tau/K_A$	SEM	$\Delta\log\tau/K_A$	SEM	$\log K_A$	SEM	$\log\tau/K_A$	SEM	$\Delta\log\tau/K_A$	SEM
$G_{\alpha i1}$	DAMGO	NC	NC	8.575	0.150	0.000	0.212	-6.89	0.29	7.759†	0.110	0.000	0.155
	Morphine	NC	NC	7.686	0.149	-0.889	0.211	-6.76	0.26	7.445	0.157	-0.315	0.191
	Loperamide	NC	NC	9.082	0.128	0.507	0.197	NC	NC	8.948	0.092	1.189	0.143
	Endo-1	-7.89	0.32	8.813	0.157	0.239	0.217	NC	NC	8.516	0.107	0.756	0.153
	Endo-2	-7.85	0.29	8.309	0.221	-0.266	0.267	NC	NC	8.328	0.153	0.569	0.188
	Met-enk	-7.56	0.36	8.781	0.153	0.207	0.214	-7.21	0.32	8.001†	0.151	0.242	0.187
	Met-enk-RF	NC	NC	8.448	0.200	-0.127	0.250	-6.78	0.33	7.543†	0.138	-0.217	0.176
	α-Neo	-6.58	0.32	7.238	0.201	-1.336	0.251	-6.79	0.30	7.767†	0.140	0.007	0.178
$G_{\alpha i2}$	DAMGO	-7.01	0.36	7.908	0.138	0.000	0.195	-6.74	0.40	7.619	0.120	0.000	0.170
	Morphine	-6.57	0.31	7.396	0.149	-0.512	0.203	NC	NC	7.293	0.112	-0.326	0.164
	Loperamide	NC	NC	9.147	0.113	1.239	0.178	NC	NC	8.816	0.096	1.198	0.154
	Endo-1	-7.89	0.28	8.790	0.115	0.883	0.179	-7.85	0.28	8.599	0.135	0.980	0.181
	Endo-2	-7.91	0.22	8.424	0.156	0.516	0.208	-7.74	0.28	8.428	0.171	0.809	0.209
	Met-enk	NC	NC	8.368	0.119	0.460	0.182	NC	NC	8.517	0.133	0.898	0.179
	Met-enk-RF	-7.38	0.31	8.178	0.153	0.270	0.206	-7.08	0.31	7.589†	0.171	-0.030	0.209
	α-Neo	-7.19	0.26	7.734	0.177	-0.174	0.224	-6.75	0.33	7.226†	0.218	-0.392	0.249
$G_{\alpha i3}$	DAMGO	NC	NC	8.006	0.128	0.000	0.181	-7.30	0.33	7.970	0.167	0.000	0.237
	Morphine	-7.15	0.36	8.021	0.192	0.015	0.231	-7.22	0.27	7.627	0.196	-0.343	0.258
	Loperamide	NC	NC	9.107	0.132	1.102	0.184	NC	NC	8.969	0.132	0.999	0.213
	Endo-1	NC	NC	8.746	0.131	0.741	0.183	-7.65	0.29	8.224	0.157	0.254	0.230
	Endo-2	-8.31	0.27	8.952	0.181	0.946	0.222	-8.08	0.34	8.369†	0.278	0.399	0.324
	Met-enk	NC	NC	8.354	0.161	0.348	0.206	-7.47	0.35	8.107	0.193	0.137	0.255
	Met-enk-RF	-7.76	0.39	8.564	0.205	0.559	0.242	-7.30	0.39	7.835†	0.218	-0.135	0.275
	α-Neo	-6.86	0.33	7.593	0.184	-0.413	0.225	-7.35	0.31	7.691	0.235	-0.279	0.289
$G_{\alpha ob}$	DAMGO	NC	NC	8.037	0.128	0.000	0.181	-6.94	0.38	8.099	0.145	0.000	0.204
	Morphine	NC	NC	7.546	0.179	-0.491	0.220	-6.73	0.29	7.460	0.185	-0.639	0.235
	Loperamide	NC	NC	8.946	0.126	0.910	0.180	NC	NC	8.959	0.140	0.860	0.201
	Endo-1	NC	NC	8.626	0.134	0.590	0.186	-7.47	0.28	8.300	0.152	0.201	0.209
	Endo-2	NC	NC	8.584	0.147	0.547	0.195	-7.85	0.23	8.423	0.179	0.324	0.230
	Met-enk	NC	NC	8.508	0.139	0.471	0.189	-7.62	0.27	8.525	0.160	0.426	0.216
	Met-enk-RF	NC	NC	8.289	0.182	0.252	0.223	-7.00	0.32	7.905	0.149	-0.194	0.208
	α-Neo	NC	NC	7.622	0.145	-0.415	0.193	-6.77	0.26	7.542	0.169	-0.557	0.223

		$G_{\alpha i1}$ - $G_{\alpha i2}$		$G_{\alpha i1}$ - $G_{\alpha i3}$		$G_{\alpha i1}$ - $G_{\alpha ob}$		$G_{\alpha i2}$ - $G_{\alpha i3}$		$G_{\alpha i2}$ - $G_{\alpha ob}$		$G_{\alpha i3}$ - $G_{\alpha ob}$	
		$\Delta\Delta\log\tau/K_A$	SEM	$\Delta\Delta\log\tau/K_A$	SEM	$\Delta\Delta\log\tau/K_A$	SEM	$\Delta\Delta\log\tau/K_A$	SEM	$\Delta\Delta\log\tau/K_A$	SEM	$\Delta\Delta\log\tau/K_A$	SEM
5mins	DAMGO	0.000	0.288	0	0.279	0.000	0.279	0.000	0.266	0.000	0.266	0.000	0.256
	Morphine	-0.377	0.293	-0.904	0.313	-0.398	0.305	-0.527	0.307	-0.021	0.299	0.506	0.319
	Loperamide	-0.732	0.266	-0.594	0.270	-0.402	0.267	0.138	0.256	0.330	0.253	0.192	0.257
	Endo-1	-0.644	0.282	-0.109	0.284	-0.351	0.286	0.535	0.274	0.293	0.258	-0.242	0.261
	Endo-2	-0.782	0.338	-0.824	0.347	-0.813	0.330	-0.043	0.317	-0.031	0.285	0.012	0.295
	Met-enk	-0.254	0.281	-0.534	0.297	-0.264	0.286	-0.280	0.256	-0.011	0.262	0.270	0.279
	Met-enk-RF	-0.397	0.323	-1.073*	0.347	-0.379	0.335	-0.676	0.304	0.018	0.303	0.694	0.329
	α-Neo	-1.162**	0.337	-0.923	0.337	-0.921*	0.317	0.239	0.317	0.241	0.296	0.002	0.296
60mins	DAMGO	0.000	0.230	0.000	0.283	0.000	0.257	0.000	0.292	0.000	0.266	0.000	0.313
	Morphine	0.011	0.252	0.028	0.321	0.324	0.303	0.017	0.306	0.313	0.287	0.296	0.349
	Loperamide	-0.009	0.210	0.190	0.257	0.329	0.247	0.199	0.263	0.338	0.253	0.139	0.293
	Endo-1	-0.224	0.237	0.502	0.276	0.555	0.260	0.726	0.292	0.779	0.277	0.053	0.311
	Endo-2	-0.241	0.281	0.169	0.375	0.245	0.297	0.410	0.386	0.485	0.311	0.076	0.397
	Met-enk	-0.657	0.259	0.104	0.316	-0.184	0.285	0.761	0.312	0.473	0.280	-0.288	0.334
	Met-enk-RF	-0.187	0.273	-0.082	0.327	-0.023	0.272	0.105	0.345	0.164	0.295	0.059	0.344
	α-Neo	0.400	0.306	0.286	0.339	0.564	0.285	-0.114	0.381	0.164	0.334	0.278	0.364

3.5.2 Changes in GRK2 Expression Levels Alter the Bias Between β-Arrestin 1 and β-Arrestin 2

Recruitment of β-arrs to MOP is dependent on preceding phosphorylation of the receptor. Different GRKs and other kinases such as PKC have been shown to phosphorylate different residues on the receptor, and several studies have demonstrated that phosphorylation of the CT of MOP is ligand-dependent [184, 546]. As diverse cell types express different kinase levels, this may, in turn, change the ability of ligands to recruit β-arrs in different cells. Indeed, overexpression of GRK2 has been shown to enhance recruitment of β-arrs to MOP [525]. We have found that endo-1 is biased towards recruitment of β-arr2 over β-arr1 in CHO-MOP cells with endogenous levels of GRKs [713]. To investigate whether this bias was altered upon changes in GRK expression levels, we repeated this experiment with overexpression of GRK2. CHO FlpIn cells were co-transfected with GRK2, RLuc-tagged MOP and YFP-tagged β-arr1 or β-arr2. Upon overexpression of GRK2, all the ligands tested stimulated recruitment of β-arr1 and β-arr2 in CHO-MOP-GRK2 cells (Figure 3.3A-B, Table 3.2), and all stimulated greater β-arr recruitment than measured previously in CHO-MOP cells with endogenous levels of GRKs [713]. In agreement with previous reports, even the weak partial agonist morphine was now able to significantly recruit β-arrs to MOP. Quantification of bias factors between recruitment of β-arr1 and β-arr2 upon GRK2 overexpression showed that under these conditions, endo-1 no longer differentially recruits β-arrs when compared to the reference ligand DAMGO (Figure 3.3C).

Next, we investigated whether different levels of GRK2 expression affect the biased agonism between recruitment of β-arrs and G protein-mediated signalling that we had previously observed for some opioid ligands (loperamide, endo-1 and α-neo). Enhancing β-arr recruitment would be expected to correlate with a decrease in G protein activation. However, this change may not affect all ligands equally. To test this we measured the MOP-induced inhibition of AC in CHO-MOP-GRK2 cells using a cAMP BRET biosensor and compared this to our results upon endogenous GRK2 expression levels [713](Figure 3.3D-F). All ligands inhibited forskolin induced cAMP production, however, the maximum response was greatly reduced upon GRK2 overexpression, when compared to endogenous levels of GRK2 (less than 30% inhibition compared to 58% inhibition by DAMGO) (Figure 3.3D, Table 3.2). Despite this, calculation of bias factors between cAMP and β-arr1 and β-arr2 in CHO-MOP-GRK2 cells showed that the bias of most ligands in these cells was similar to the bias they

showed in CHO-MOP cells (Figure 3.3E-F, Table 3.2). The only exception was endo-1, which showed a significant reduction in the bias between cAMP and β-arr1 in the CHO-MOP-GRK2 cells (Figure 3.3E). This means that overexpression of GRK2 caused a greater reduction in the inhibition of cAMP induced by endo-1 than expected. This could, in part, be due to the enhanced recruitment of β-arr1 detected upon GRK2 overexpression.

Table 3.2: Quantification of biased agonism upon overexpression of GRK2.
Transduction coefficients [$Log(\tau/K_A)$], normalised transduction coefficients [$\Delta Log(\tau/K_A)$] and bias factors [$\Delta\Delta Log(\tau/K_A)$]. Values represent the mean ± SEM of three to five independent experiments.

	β-Arr1 + GRK2				β-Arr2 + GRK2				cAMP + GRK2			
	$Log\tau/K_A$	SEM	$\Delta log\tau/K_A$	SEM	$Log\tau/K_A$	SEM	$\Delta log\tau/K_A$	SEM	$Log\tau/K_A$	SEM	$\Delta log\tau/K_A$	SEM
DAMGO	7.410	0.113	0.000	0.160	7.599	0.097	0.000	0.137	7.309	0.267	0.000	0.377
Morphine	6.437	0.205	-0.973	0.234	6.721	0.131	-0.878	0.163	6.943	0.363	-0.366	0.450
Loperamide	7.458	0.128	0.048	0.171	7.831	0.096	0.232	0.137	8.251	0.227	0.942	0.351
Endo-1	7.381	0.128	-0.029	0.170	7.529	0.111	-0.070	0.147	7.783	0.105	0.474	0.287
Endo-2	7.587	0.128	0.177	0.171	7.755	0.110	0.156	0.146	7.818	0.105	0.509	0.287
Met-enk	7.564	0.128	0.154	0.171	7.564	0.097	-0.035	0.137	7.664	0.262	0.355	0.374
Met-enk-RF	7.370	0.128	-0.040	0.170	7.875	0.109	0.276	0.146	7.674	0.105	0.365	0.287
α-Neo	6.530	0.128	-0.880	0.171	6.703	0.110	-0.896	0.147	7.263	0.215	-0.047	0.343

	β-Arr2 + GRK2 - β-Arr1 + GRK2		cAMP + GRK2 - β-Arr1 + GRK2		cAMP + GRK2 - β-Arr2 + GRK2	
	$\Delta\Delta Log\tau/K_A$	SEM	$\Delta\Delta Log\tau/K_A$	SEM	$\Delta\Delta Log\tau/K_A$	SEM
DAMGO	0.000	0.211	0.000	0.410	0.000	0.402
Morphine	0.095	0.285	0.607	0.508	0.512	0.479
Loperamide	0.184	0.218	0.894	0.390	0.710	0.376
Endo-1	-0.041	0.225	0.503	0.334	0.544	0.322
Endo-2	-0.021	0.225	0.332	0.334	0.353	0.322
Met-enk	-0.189	0.219	0.201	0.411	0.390	0.399
Met-enk-RF	0.316	0.224	0.405	0.334	0.089	0.322
α-Neo	-0.016	0.225	0.833	0.383	0.849	0.373

	β-Arr1 + GRK2				β-Arr2 + GRK2				cAMP + GRK2			
	LogEC50	SEM	Emax	SEM	LogEC50	SEM	Emax	SEM	LogEC50	SEM	Emax	SEM
DAMGO	-7.39	0.12	93.3	4.2	-7.59	0.09	95.4	2.9	-7.00	0.24	16.2	1.8
Morphine	-6.73	0.16	58.4	4.0	-6.92	0.13	72.4	3.8	-6.73	0.28	12.5	1.8
Loperamide	-7.73	0.16	81.3	4.5	-7.73	0.12	103.6	4.0	-7.92	0.32	19.6	2.8
Endo-1	-7.34	0.14	88.3	4.3	-7.65	0.13	88.0	3.8	-7.88	0.13	29.7	1.6
Endo-2	-7.54	0.17	93.0	5.4	-7.81	0.08	88.1	2.2	-7.86	0.18	28.9	2.1
Met-enk	-7.77	0.16	78.5	3.9	-7.78	0.11	87.9	3.3	-7.19	0.31	16.8	2.3
Met-enk-RF	-7.30	0.13	93.5	4.3	-7.90	0.12	88.9	3.1	-7.80	0.23	27.0	2.9
α-Neo	-6.63	0.15	86.5	5.2	-6.74	0.11	88.7	3.4	-7.20	0.26	16.9	2.2

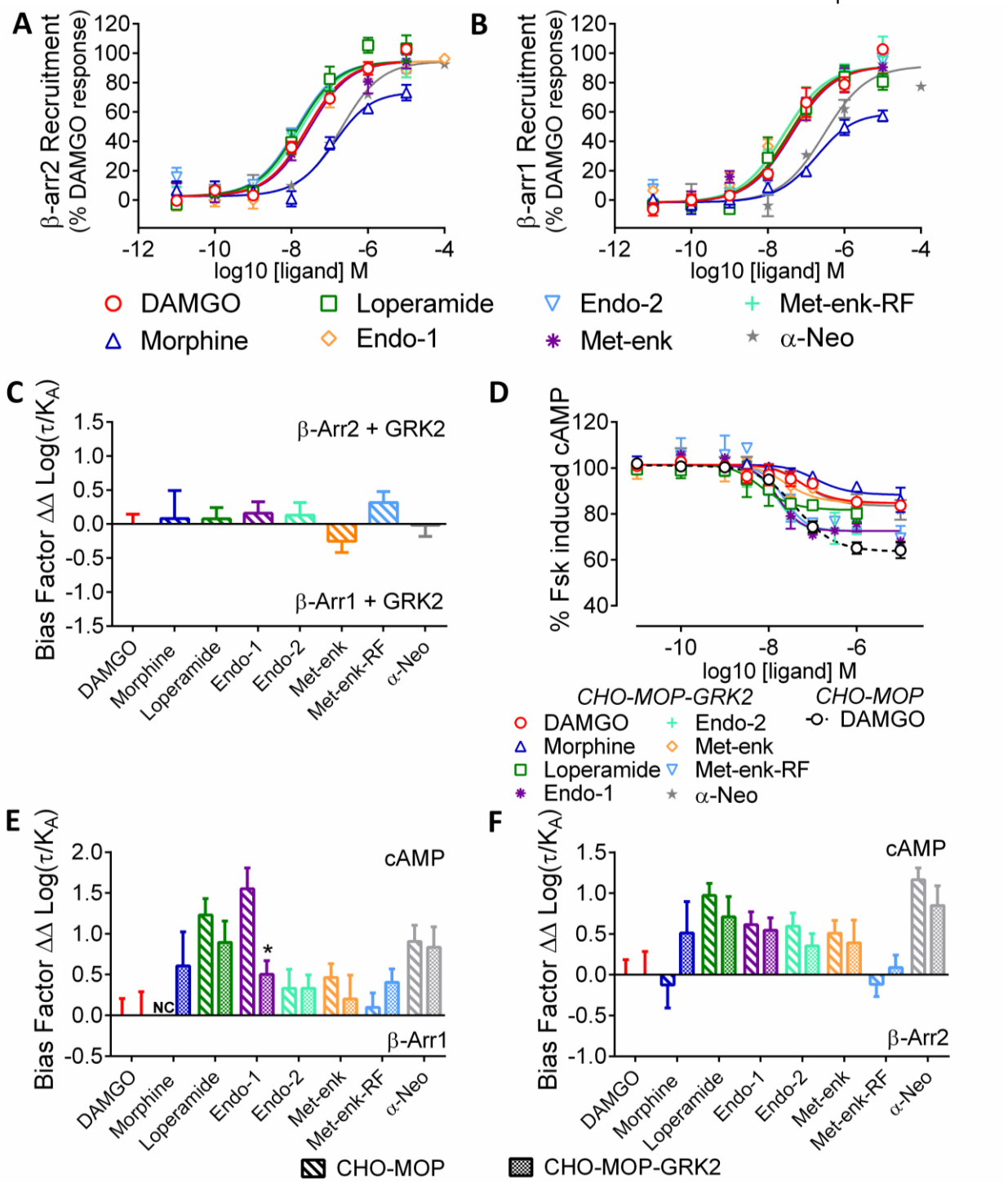

Figure 3.3: Overexpression of GRK2 changes bias between recruitment of β-arrs and AC inhibition.

Recruitment of (A) β-arr2 and (B) β-arr1 in FlpIn CHO-MOP-GRK2 cells. Data normalised to the 10μM DAMGO response and expressed as means ± SEM of at least 3 separate experiments. (C) Bias factors between recruitment of β-arr1 and β-arr2 in CHO-MOP-GRK2 cells. (D) Inhibition of fsk- induced cAMP in FlpIn CHO-MOP-GRK2 cells. Data expressed as the % fsk-induced cAMP response in the absence of agonist, and expressed as means ± SEM of 2-3 separate experiments. Bias factors between cAMP and (E) β-arr1 and (F) β-arr2 in CHO-MOP [713] and CHO-MOP-GRK2 cells. *p ≤0.05, as determined by one-way ANOVA with Dunnett's multiple comparison test compared to bias factor for same ligand in CHO-MOP. NC = not calculable

3.5.3 The Differential Kinetics of AC Inhibition by Opioids Changes Bias

Most quantifications of biased agonism are calculated at a single time point for each signalling pathway which usually corresponds to the maximum activation of that pathway, or when the signal reaches a steady state. As such, this time point can significantly vary across different signalling pathways. However, it is now apparent that ligands can elicit differential kinetics of activation and deactivation of each signalling pathway. MOP activation results in inhibition of AC which is detectable within minutes, and is also known to produce prolonged inhibition of AC [728, 729]. Inhibition of cAMP production is usually measured using accumulation assays, requiring long incubation times, up to 60min, thereby detecting both acute and prolonged signalling. However, the kinetics of AC inhibition over this time period may vary significantly for different agonists, which means bias between cAMP and other signalling pathways can also change over time. To test this we examined the inhibition of AC using the CAMYEL BRET biosensor for 30min. An initial experiment using EC_{50} concentrations of the ligands (Figure 2.1) showed that most ligands inhibit AC with a similar profile to that of DAMGO, where maximum AC inhibition is reached 5 to 10min after forskolin (fsk) addition, and remains constant for up to 30min (Figure 3.4A). However, we observed that whilst Met-enk-RF also reached maximum AC inhibition between 5 and 10min, by 30min such inhibition was no longer detected (Figure 3.4A). This effect was not due to degradation of the peptide, as protease inhibitors used in all experiments (see Materials and Methods) provided adequate protection from proteases, and the same effect was observed in the presence of a protease inhibitor cocktail (Figure 3.4A).

We then examined the AC inhibition kinetics for Met-enk-RF, DAMGO, loperamide and endo-1 at a full range of concentrations (Figure 3.4C-F). DAMGO, loperamide and endo-1 showed the same cAMP kinetic profiles regardless of concentration, they all reached their maximum signal at 5min and remained constant for the duration of the experiment. However, Met-enk-RF only displayed this profile at the highest concentrations tested (1-10μM), and at lower concentrations the AC inhibition was gradually lost over time. This difference in the kinetics of AC inhibition could impact the quantification of bias between AC inhibition and other signalling pathways, especially if AC inhibition is measured at different times and/or by different methods. We plotted concentration response curves using the BRET values obtained at 5min and 30min, and quantified bias between these two time points (Figure 3.4G-H). As expected from its

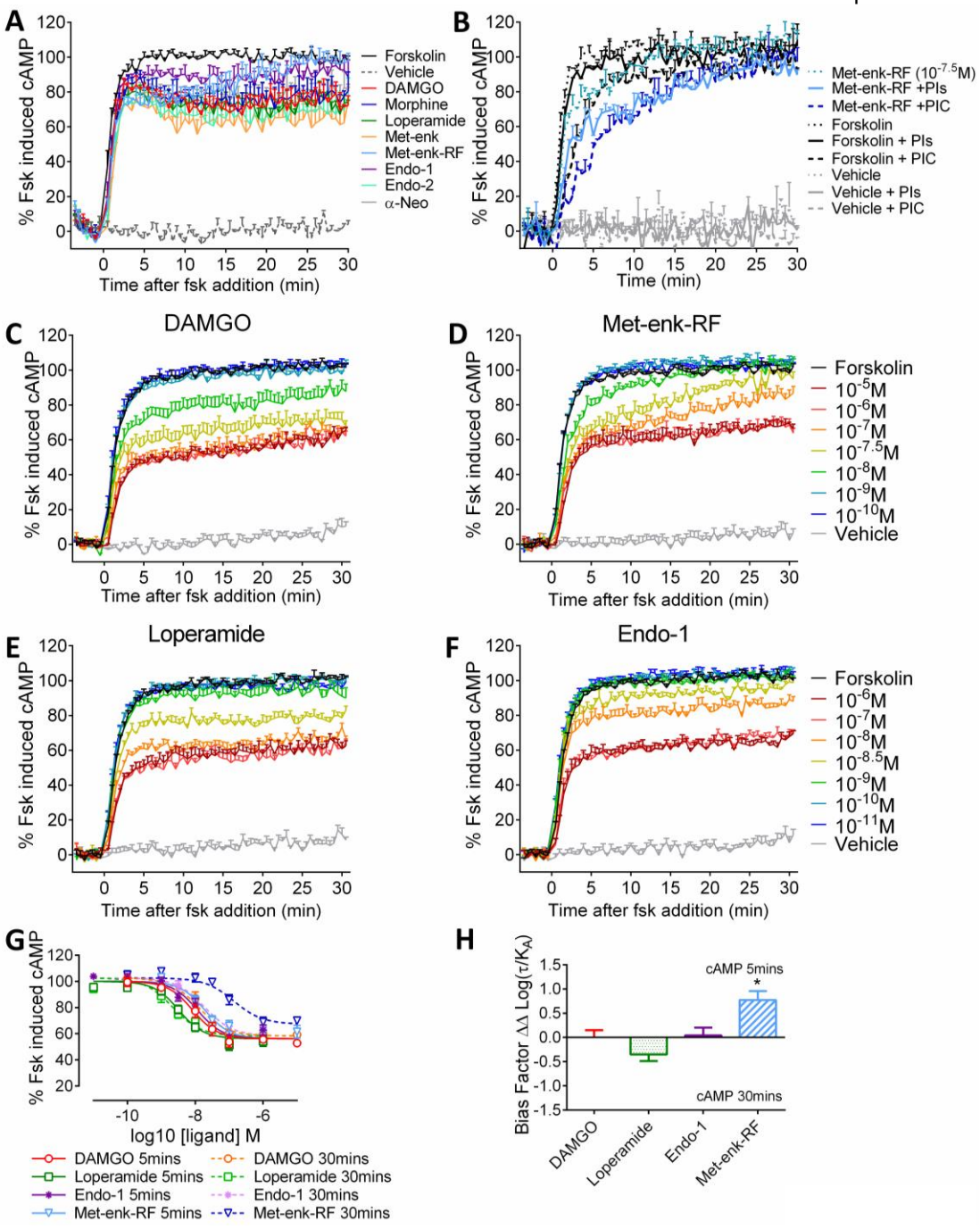

Figure 3.4: Kinetics of AC inhibition.

(A-F) Kinetic profiles of agonist-induced inhibition of fsk-induced cAMP production in FlpIn CHO-MOP up to 30min after fsk addition. Kinetic traces of ligands at (A) EC50 concentrations, (B) Met-enk-RF in the presence of protease inhibitor mix (PIs; See Materials and Methods) or protease inhibitor cocktail (PIC, SigmaAldrich) and (C-F) increasing concentrations of DAMGO, Met-enk-RF, Loperamide and endo-1. Data expressed as the %fsk induced cAMP response (mean fsk response between 10-30min) in the absence of agonist, and expressed as means ± SEM of 3 separate experiments. (G) Concentration response curves of inhibition of fsk-induced cAMP production at 5min and 30min post fsk addition constructed from kinetic profiles. (H) Bias factors between inhibition of fsk-induced cAMP production at 5min and 30min. *p≤0.05, as determined by one-way ANOVA with Dunnett's multiple comparison test compared to DAMGO.

observed kinetic profile, Met-enk-RF demonstrated relatively greater efficacy for inhibition of AC at 5min versus 30min that lead to altered bias with respect to DAMGO for this pathway across the two time points. Consequently, the bias of Met-enk-RF, but not the other ligands, will change when quantifying bias between cAMP and other signalling pathways, depending on the time point chosen to measure AC inhibition.

3.5.4 Differential G Protein Desensitisation Alters Bias

Since the kinetics of a G protein-mediated signalling pathway are ligand dependent, it follows that G protein activation kinetics may also be ligand dependent. It is also well established that neither the initial level of G protein activation, nor the level of desensitisation of G protein-mediated signalling of MOP correlate with the level β-arr recruitment and receptor internalisation [598]. Therefore, quantifying bias between acute G protein activation and receptor regulatory events reveals only limited information about the differential desensitisation mechanisms initiated by different ligands. Alternatively, quantifying bias between G protein activation and regulatory events at the same time point can reveal ligands that have divergent mechanisms of receptor regulation. Additionally, the divergent mechanisms of receptor desensitisation and regulation initiated by different ligands can potentially have differential effects on Gα subtypes thereby altering bias between various Gα subtypes at different time points. To examine this, the G protein assays described above were repeated after 60min of agonist stimulation (Figure 3.5). As expected, most ligands stimulated less Gα subunit activation at 60min compared to 5min, which is apparent in the reduction of $\log(\tau/K_A)$ values at 60min (Table 3.1), however only small changes were observed with $G\alpha_{ob}$. Interestingly, the greatest reductions in relative efficacy between 5 and 60min for all Gα subunits were observed for Met-enk-RF. This enhanced desensitisation of Met-enk-RF induced Gα subunit activation is in line with the increased desensitisation of the inhibition of cAMP production observed at later time points (Figure 3.4G). DAMGO and Met-enk also showed a significant reduction in activation of $G\alpha_{i1}$ at 60min, whereas α-neo surprisingly showed an increase in activation of $G\alpha_{i1}$. Calculation of bias factors between each G protein at 60min showed that α-neo and Met-enk-RF were no longer biased between $G\alpha_{i1}$ and $G\alpha_{i2}$, $G\alpha_{i3}$ or $G\alpha_{ob}$. (Figure 3.6, Table 3.1). Together these results show the variability in the level of desensitisation of different Gα subunits by different ligands.

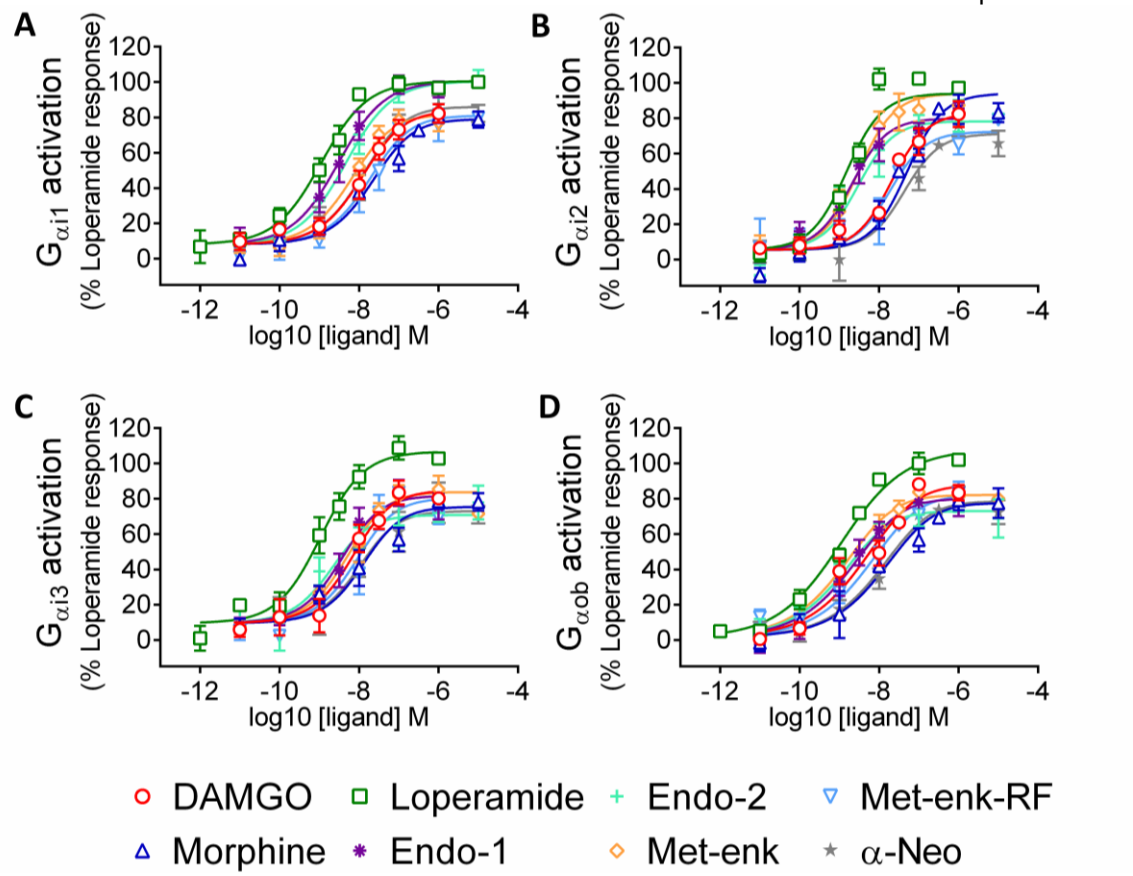

Figure 3.5: Activation of $G\alpha_{i/o}$ subunits by MOP agonists at 60min.
Activation of (A) $G\alpha_{i1}$, (B) $G\alpha_{i2}$, (C) $G\alpha_{i3}$ and (D) $G\alpha_{ob}$ in FlpIn CHO cells after 60min agonist stimulation. Data normalised to the 1μM Loperamide response. Data expressed as mean ± SEM of at least 3 separate experiments.

Next we examined the effect of G protein desensitisation on bias between G protein activation and receptor trafficking. Previously, we measured MOP trafficking at 60min using a BRET assay to measure the reduction in MOP proximity to the membrane marker KRas, which revealed that endo-1, endo-2 and α-neo were all biased towards the acute inhibition of cAMP production (at 10min) over MOP trafficking at 60min [713]. In order to identify whether these ligands are still G protein biased after desensitisation of G protein activation, we quantified bias between G protein activation and receptor trafficking when both pathways were measured at 60min. Endo-1, and Met-enk showed bias towards activation of $G\alpha_{i2}$ over receptor trafficking (Figure 3.6E). Surprisingly, Met-enk-RF, which showed the greatest reductions in G protein activation at 60min, also stimulated very little receptor trafficking, as a result a bias factor could not be quantified. This may suggest that desensitisation and trafficking induced by Met-enk-RF are completely independent mechanisms. Alternatively, the rapid desensitisation of cAMP inhibition by Met-enk-RF observed at 30min (Figure 3.4), suggests that the kinetics of receptor trafficking induced by Met-enk-RF may also be more rapid than for the other

ligands, and no longer detectable at 60min due to rapid receptor recycling. Altogether, quantifying bias between the G protein activation and receptor trafficking at the same time point has revealed ligands that may have differential desensitisation mechanisms or kinetics.

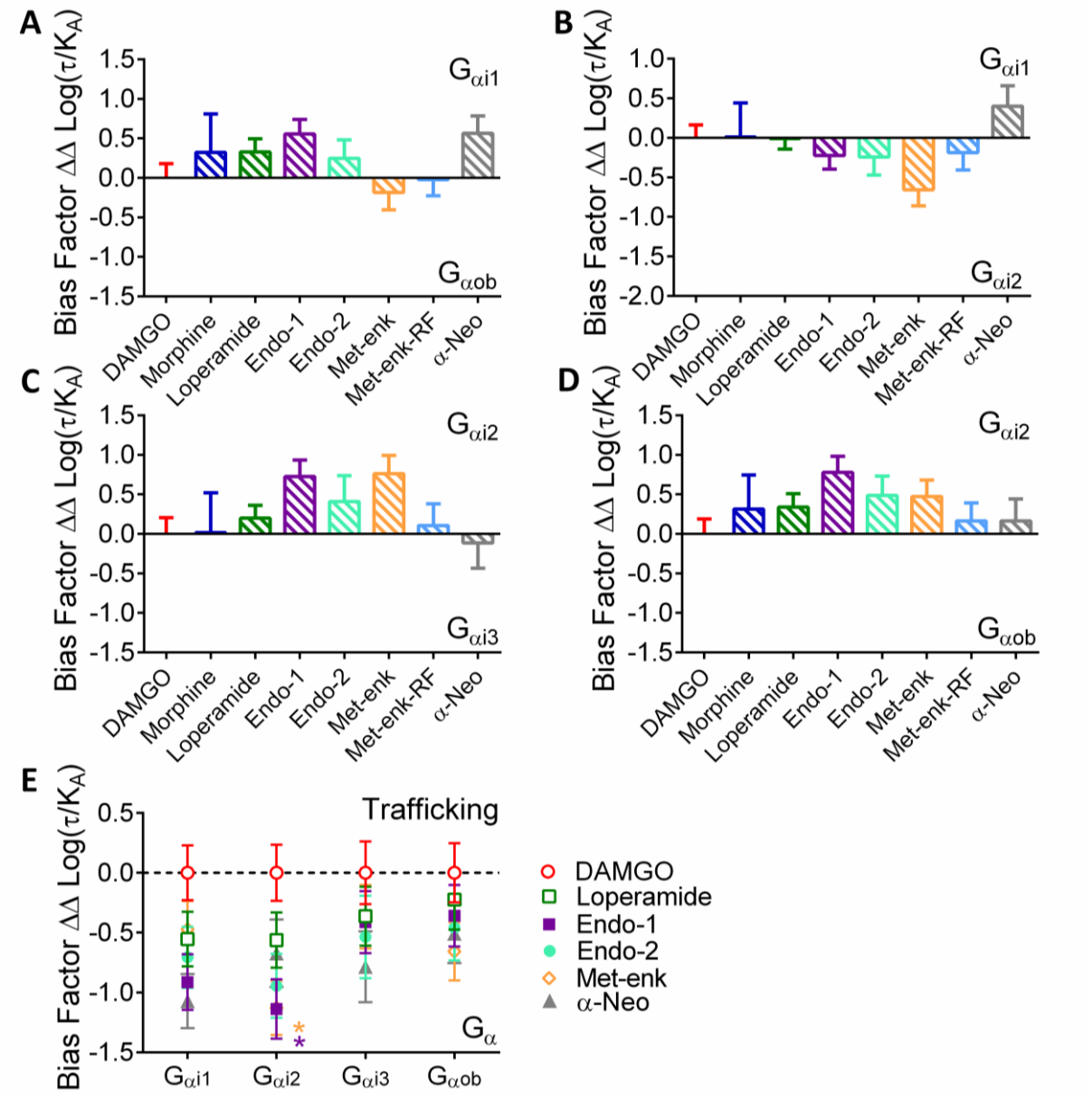

Figure 3.6: Quantification of biased agonism of MOP agonists between activation of different $G\alpha_{i/o}$ subunits at 60min.

(A-D) Bias factors for all agonists between activation of $G\alpha_{i1}$, $G\alpha_{i2}$, $G\alpha_{i3}$ and $G\alpha_{ob}$ after 60min agonist stimulation (Table 3.1). (E) Bias factors between MOP trafficking measured using BRET between MOP-Rluc and KRas-Venus [713] and activation of $G\alpha_{i1}$, $G\alpha_{i2}$, $G\alpha_{i3}$ and $G\alpha_{ob}$ after 60min agonist stimulation. Data expressed as means ± SEM of at least 3 separate experiments.

3.5.5 Impact of Cell Background in Determinations of Biased Agonism at MOP

We next investigated whether the biased agonism detected in CHO FlpIn hMOP cells was retained at the mMOP, and whether such biased agonism changes in a different cell background, where different endpoints and assay conditions may be necessary to obtain robust signals. For this we determined comprehensive biased agonism profiles for the same eight ligands in AtT20 mouse pituitary tumour cells stably expressing mMOP.

We first quantified bias between inhibition of AC and recruitment of β-arr1 and β-arr2. β-arr1 and β-arr2 recruitment was measured using BRET in cells co-transfected with GRK2 (Figure 3.7A-B), as β-arr recruitment in AtT20-mMOP cells was barely detectable in the absence of this kinase. Loperamide, endo-1, endo-2 and α-neo stimulated less β-arr1 recruitment compared to DAMGO and the other ligands (75-85%). Morphine only stimulated 39.9% of DAMGO induced β-arr1 recruitment. All ligands stimulated a similar level of β-arr2 recruitment as DAMGO, except α-neo and morphine, which only stimulated 81% and 62%, respectively. In agreement with the bias profiles obtained in CHO MOP cells overexpressing GRK2, no ligands were biased between the two β-arrs (Figure 3.7C, Table 3.3).

Inhibition of cAMP production was measured using the CAMYEL BRET-based biosensor (Figure 3.7D), without additional co-transfection of GRK2 as this would compromise the cAMP response as shown in the CHO cells. All ligands produced between 55%-65% inhibition of forskolin-induced cAMP production. Our previous study in CHO-hMOP cells showed that endo-1 was biased towards cAMP over recruitment of β-arr1, while loperamide and α-neo were biased towards cAMP over β-arr1 and β-arr2 when compared to the reference ligand DAMGO (Thompson et al., 2015). In contrast, in AtT20-mMOP cells, no ligands showed significant bias towards cAMP over β-arr1 or β-arr2 (Figure 3.7E.F, Table 3.3). This may be due, in part, to the fact that GRK2 needed to be overexpressed in β-arr recruitment assays but not the cAMP assays. Moreover, in AtT20 cells and relative to DAMGO, loperamide, endo-1 and α-neo are less efficacious at inhibiting cAMP production than in CHO cells (which is apparent when comparing the $\Delta\log(\tau/K_A)$ values for the cAMP assays between these cell lines). Such changes in efficacy, thus, may explain the loss of bias towards cAMP of these ligands in AtT20 cells.

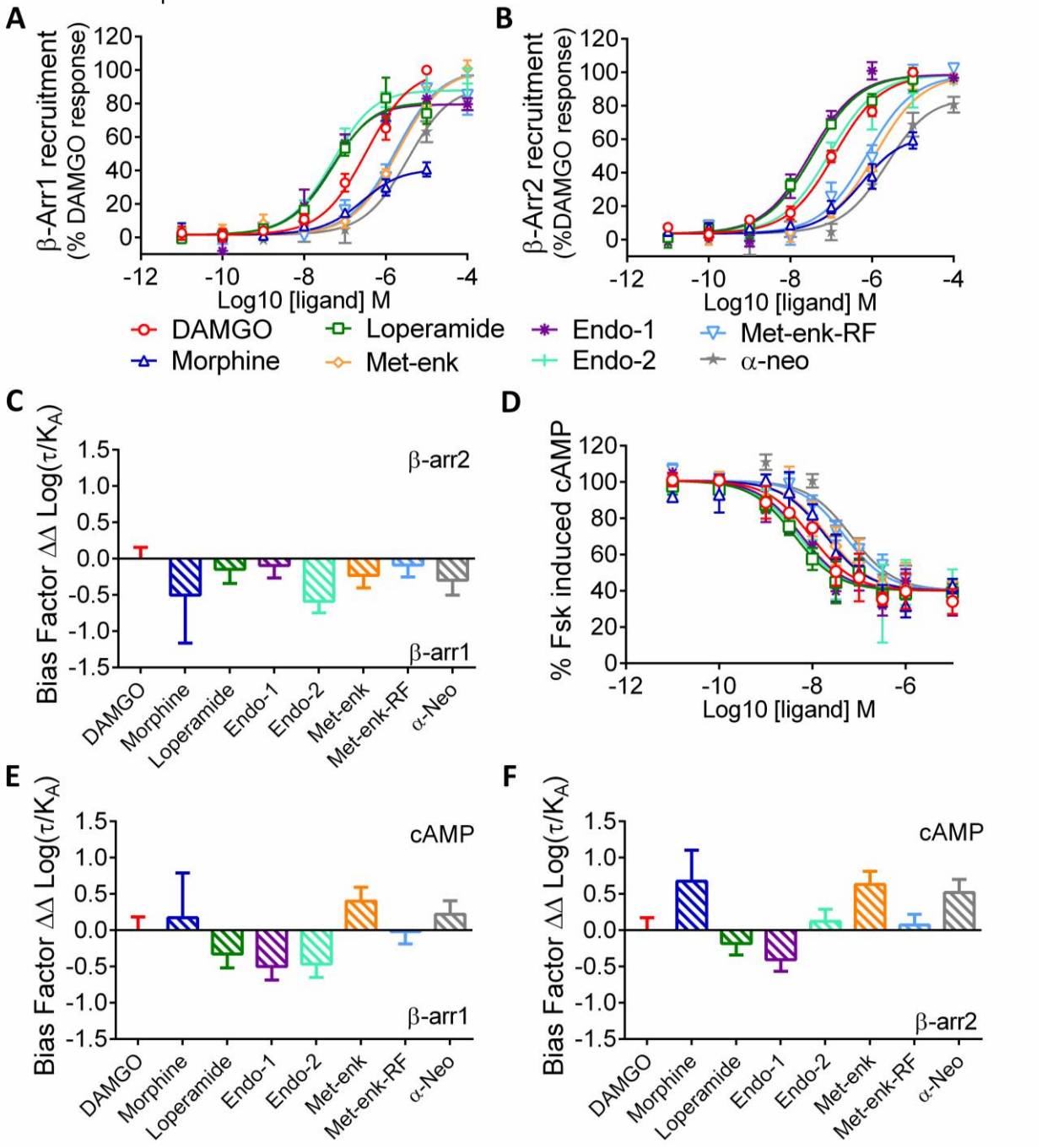

Figure 3.7: Bias between AC inhibition and recruitment of β-arrs is cell dependent.
Recruitment of (A) β-arr1 and (B) β-arr2 in AtT20-mMOP-GRK2 cells. Data normalised to the 10μM DAMGO response and expressed as means ± SEM of 3 separate experiments. (C) Bias factors for all agonists between β-arr1 and β-arr2 (Table 3.4). (D) Inhibition of fsk-induced cAMP in AtT20-mMOP cells. Data expressed as the %fsk-induced cAMP response in the absence of agonist, and expressed as means ± SEM of at least 3 separate experiments. Bias factors for all agonists between cAMP and (E) β-arr1 and (F) β-arr2 in AtT20 cells is shown in (Table 3.4).

Table 3.4: Quantification of biased agonism in AtT20-mMOP cells. Transduction coefficients [Log(τ/K_A)], normalised transduction coefficients [ΔLog(τ/K_A)] and Log(bias factors) [$\Delta\Delta$Log(τ/K_A)]. Values represent the mean ± SEM of three to five independent experiments. *p≤0.05 **p≤0.005 ***p≤0.005, different from DAMGO as determined by ANOVA with Dunnett's multiple comparison test. NC: not calculated due to full agonism.

	cAMP				Membrane potential				β-Arr1				β-Arr2				Internalisation			
	Logτ/K_A	SEM	Δlogτ/K_A	SEM	Logτ/K_A	SEM	Δlogτ/K_A	SEM	Logτ/K_A	SEM	Δlogτ/K_A	SEM	Logτ/K_A	SEM	Δlogτ/K_A	SEM	Logτ/K_A	SEM	Δlogτ/K_A	SEM
DAMGO	8.041	0.139	0.000	0.197	8.282	0.086	0.000	0.121	6.475	0.120	0.000	0.170	6.912	0.100	0.000	0.142	5.106	0.130	0.000	0.000
Morphine	7.718	0.145	-0.323	0.201	7.806	0.086	-0.476	0.122	5.979	0.326	-0.495	0.347	5.914	0.201	-0.998	0.225	NC	NC	NC	NC
Loperamide	8.385	0.109	0.344	0.176	8.165	0.100	-0.117	0.132	7.149	0.156	0.674	0.196	7.439	0.115	0.527	0.152	6.864	0.135	1.758	1.758
Endo-1	8.232	0.121	0.192	0.184	8.334	0.096	0.052	0.129	7.168	0.138	0.693	0.183	7.511	0.101	0.599	0.143	5.675	0.128	0.570	0.570
Endo-2	8.299	0.134	0.259	0.193	8.342	0.085	0.060	0.121	7.201	0.124	0.726	0.172	7.049	0.101	0.137	0.142	5.584	0.103	0.479	0.479
Met-enk	7.676	0.139	-0.365	0.196	8.135	0.099	-0.147	0.131	5.709	0.132	-0.766	0.178	5.916	0.114	-0.996	0.152	5.592	0.099	0.487	0.487
Met-enk-RF	7.316	0.110	-0.725	0.177	8.134	0.132	-0.148	0.157	5.768	0.132	-0.707	0.178	6.117	0.100	-0.795	0.142	5.388	0.099	0.283	0.283
α-Neo	7.172	0.117	-0.869	0.182	7.265	0.073	-1.017	0.113	5.387	0.149	-1.087	0.191	5.526	0.142	-1.387	0.174	4.505	0.121	-0.601	-0.601

	MP-cAMP		cAMP - β-Arr1		cAMP - β-Arr2		cAMP - Int		MP - β-Arr1		MP - β-Arr2		MP - Int		β-Arr2 - β-Arr1		Int - β-Arr1		Int - β-Arr2	
	ΔΔLogτ/K_A	SEM	ΔΔLogτ/K_A	SEM	ΔΔLogτ/K_A	SEM	ΔΔLogτ/K_A	SEM	ΔΔLogτ/K_A	SEM	ΔΔLogτ/K_A	SEM	ΔΔLogτ/K_A	SEM	ΔΔLogτ/K_A	SEM	ΔΔLogτ/K_A	SEM	ΔΔLogτ/K_A	SEM
DAMGO	0.000	0.231	0.000	0.260	0.000	0.243	0.000	0.197	0.000	0.209	0.000	0.187	0.000	0.121	0.000	0.221	0.000	0.170	0.000	0.142
Morphine	-0.153	0.235	0.172	0.401	0.675	0.301	NC	NC	0.020	0.368	0.522	0.256	NC	NC	-0.503	0.414	NC	NC	NC	NC
Loperamide	-0.4614	0.220	-0.330	0.264	-0.183	0.233	-1.414***	1.767	-0.791	0.237	-0.644	0.202	-1.875***	1.763	-0.147	0.249	1.084**	1.769	1.231***	1.765
Endo-1	-0.140	0.225	-0.502	0.260	-0.407	0.233	-0.3781	0.599	-0.642	0.224	-0.547	0.192	-0.518	0.584	-0.094	0.232	-0.124	0.598	-0.029	0.587
Endo-2	-0.199	0.228	-0.467	0.259	0.122	0.240	-0.2198	0.516	-0.666	0.211	-0.077	0.187	-0.419	0.494	-0.589	0.223	-0.248	0.509	0.342	0.499
Met-enk	0.218	0.236	0.401	0.265	0.631	0.248	-0.852*	0.525	0.618	0.221	0.849**	0.200	-0.633*	0.504	-0.230	0.234	1.252**	0.518	1.482***	0.510
Met-enk-RF	0.577	0.237	-0.018	0.251	0.070	0.227	-1.007**	0.333	0.559	0.238	0.648	0.212	-0.430	0.323	-0.089	0.228	0.989**	0.334	1.078**	0.316
α-Neo	-0.148	0.214	0.218	0.263	0.518	0.251	-0.268	0.628	0.070	0.222	0.370	0.207	-0.416	0.612	-0.299	0.258	0.486	0.631	0.786*	0.626

FLAG-MOP internalisation after 30min of agonist exposure was measured using anti-FLAG ELISA. All ligands, except morphine, induced a reduction in MOP at the cell surface after 30min in AtT20 cells (Figure 3.8A). Bias factors were calculated between internalisation and inhibition of cAMP production, β-arr1 and β-arr2 (Figure 3.8B-C, Table 3.4). Loperamide, Met-enk and Met-enk-RF all showed significant bias towards receptor internalisation over inhibition of cAMP, β-arr1 and β-arr2. This is in contrast to our previous results in CHO-MOP cells where these ligands showed no bias towards receptor trafficking. The bias towards internalisation of Met-enk-RF is particularly surprising, since Met-enk-RF stimulated very little receptor trafficking in CHO-MOP cells. However, this result is difficult to interpret as this discrepancy may be due to the use of different methods (membrane localisation vs ELISA) or time points in the two cells types.

We next examined the bias between activation of two canonical G protein-mediated signalling pathways; inhibition of cAMP production (predominantly $G\alpha_{i/o}$-mediated) and cell hyperpolarisation (predominantly $G\beta\gamma$-mediated) [146]. Hyperpolarisation in AtT20-mMOP cells was measured using the FLIPR membrane potential assay [730]. Opioids hyperpolarise AtT20 cells primarily through G protein mediated activation of G protein-gated inwardly rectifying K^+ channels (GIRKs). In agreement with this, all ligands stimulated AtT20-mMOP hyperpolarisation (Figure 3.8-E). Quantification of bias factors between hyperpolarisation (ΔMP) and inhibition of cAMP production showed that no ligands were significantly biased between these two signalling pathways compared to DAMGO (Figure 3.8F, Table 3.4). In agreement with this, the bias between receptor internalisation and ΔMP was very similar to bias between internalisation and cAMP (Table 3.4), with loperamide and Met-enk being significantly biased towards internalisation. The only exception was Met-enk-RF, which was no longer significantly biased towards internalisation when compared to ΔMP.

Finally, we assessed whether biased agonism between hyperpolarisation and β-arr1or β-arr2 recruitment also reflected the results obtained when using inhibition of cAMP as a G protein-mediated pathway (Figure 3.7E-F, Figure 3.8G and Table 3.4). Interestingly, Met-enk was biased towards cell hyperpolarisation (Figure 3.8G and Table 3.4).

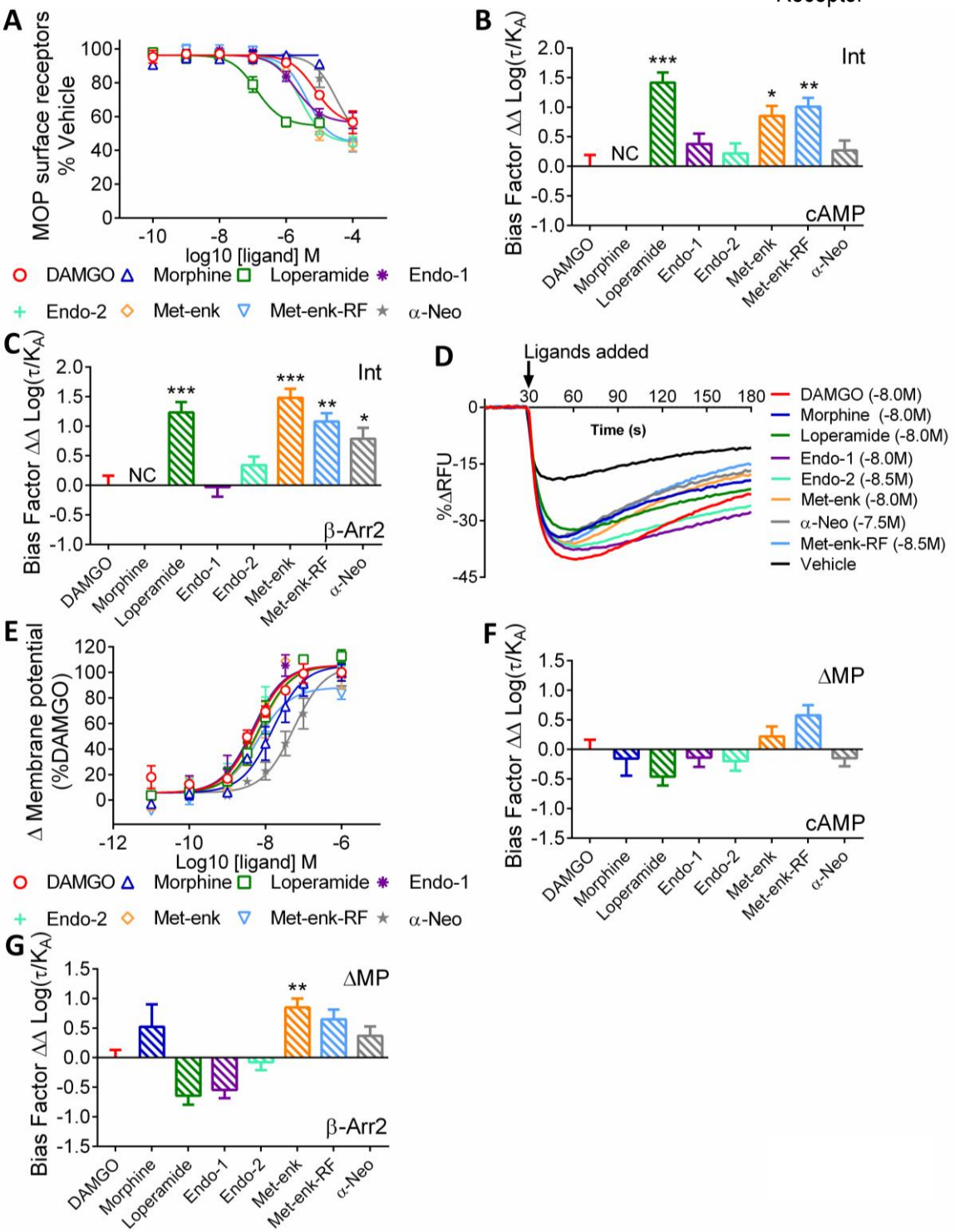

Figure 3.8: Quantification of biased agonism in AtT20 cells.

(A) FLAG-mMOP internalisation in AtT20 cells. Data expressed as percentage of vehicle, as means ± SEM of at least 3 separate experiments. Bias factors between internalisation (Int) and (B) cAMP and (C) β-arr2. (D) Representative kinetic trace of AtT20 cell hyperpolarisation measured using FLIPR membrane potential kit. Data expressed as %change in relative fluorescence units. (E) Concentration-response curves of cell hyperpolarisation (ΔMP) in AtT20-mMOP cells. Data normalised to the area under the curve of the 1μM DAMGO response and expressed as means± SEM of at least 3 separate experiments. Bias factors between ΔMP and (F) cAMP and (G) β-arr2. *p≤0.05, **p≤0.005, ***p≤0.001 one-way ANOVA with Dunnett's multiple comparison test compared to DAMGO. NC = not calculable

3.5.6 Ligand Clustering by Biased Agonism Profiles in AtT20 Cells

As shown above, quantification of bias in different cell lines requires the use of different assay conditions and signalling endpoints. Thus, directly comparing individual bias factors between two pathways obtained in two different cell lines can be difficult to interpret. For this reason, an overall bias profile of the ligands across all of the signalling pathways can provide information about ligand clustering and, consequently allow the comparison of different clusters across cell lines. To obtain an overall picture of the bias profiles of the ligands in AtT20-mMOP cells we constructed webs of bias. For this, the bias factors between ΔMP and all of the other signalling pathways were calculated ($\Delta\Delta\tau/K_A$) and plotted on a single multiaxial graph (Figure 3.9A). This shows that morphine, loperamide and Met-enk are biased compared to DAMGO at one or more signalling pathways, and that no ligands under study show the same pattern of bias as one another. Importantly, these results also highlight that although the bias of each ligand between individual signalling pathways has changed compared to the bias that we had previously determined in CHO cells [713], the clustering of ligands with unique bias profiles remains across different cell lines.

The overall bias profile of a ligand can also be visualised using Principal Component Analysis (PCA). PCA identifies which bias factors are correlated with one another, and collectively contribute the greatest variation in bias between the ligands, called principal components. PCA of all the bias factors revealed that the bias between receptor internalisation and recruitment of β-arr1 and β-arr2 contributes the greatest variability in bias between all the ligands, contributing to 54% of the overall observed bias. Bias between G protein-mediated signalling and β-arr recruitment and internalisation only contributed to ~37% of the observed bias. When these principal components are plotted against one another ligands with similar bias will cluster together (Figure 3.9B). PCA analysis of our data in AtT20 cells showed that loperamide, Met-enk and Met-enk-RF are separated from DAMGO, and hence have unique patterns of bias, whereas endo-1, endo-2 and α-neo cluster more closely to DAMGO. These results are in contrast to our previous data in CHO cells, where endo-1 and α-neo did not cluster with DAMGO, while Met-enk did. This illustrates that biased agonism profiles have not changed uniformly across the group of ligands, but, rather, that the impact of cell background on bias determinations is different for each agonist.

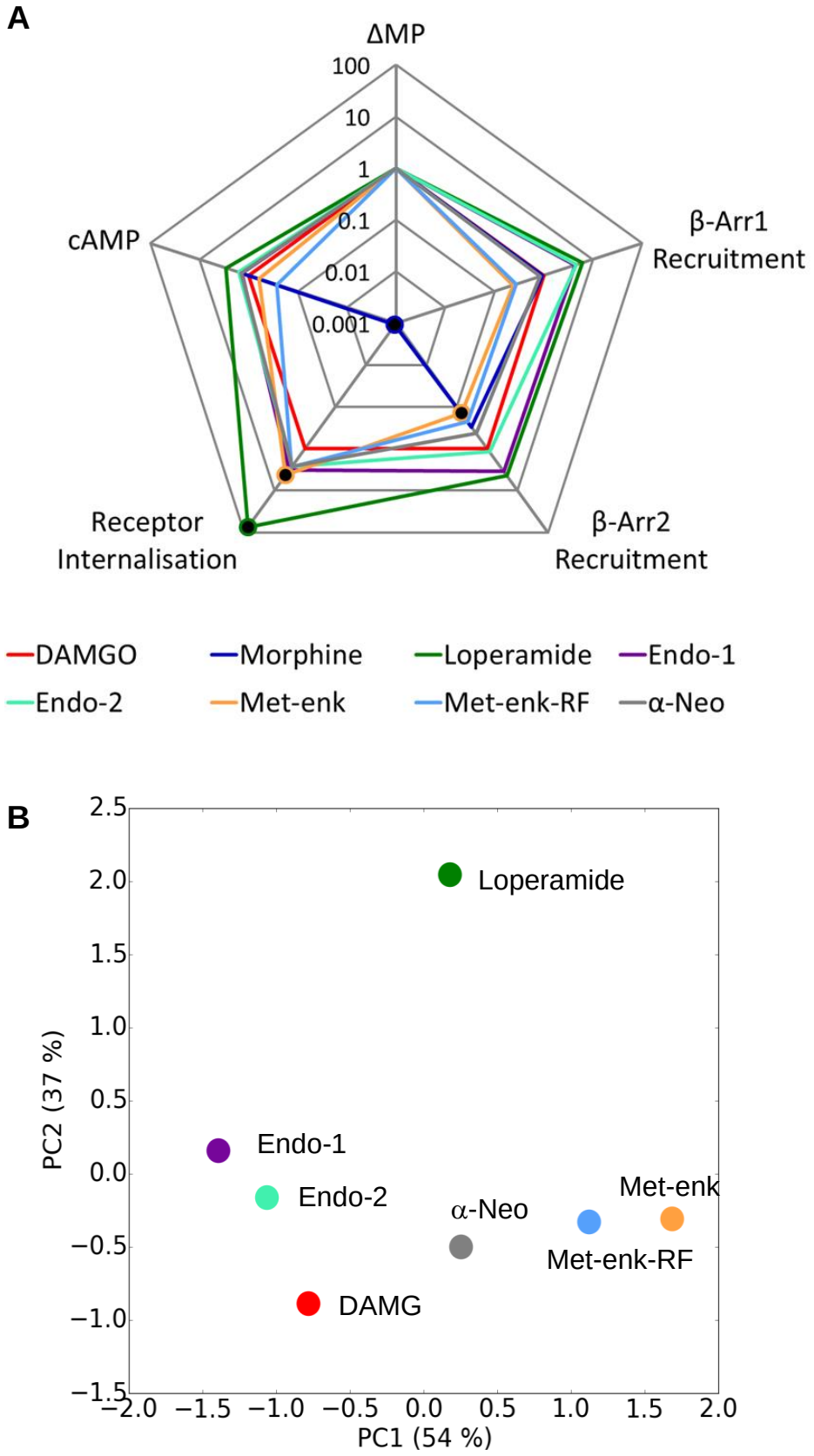

Figure 3.9: Biased agonism profiles of MOP agonists in AtT20-mMOP cells.
(A) Webs of bias for all ligands. τ/K_A values were normalised to the reference ligand DAMGO, and to the cAMP assay. Statistically significant differences ($p<0.05$) are denoted by black circles as determined by two-tailed t-test. (B) Principal component analysis (PCA) of all bias factors.

3.6 Discussion

In the present study we have extended our determinations of biased agonism at MOP to systematically assess the impact of differential cellular protein complement, signalling kinetics and receptor species. We show that despite changes in directions of bias and overall signalling profiles, ligands with distinct bias profiles at MOP in CHO cells (e.g. endo-1, met-enk-RF and α-neo) still displayed unique bias fingerprints, different from that of DAMGO, when evaluated in a different cell background. However, our results also highlight the importance of the experimental conditions used for the measurement of activation of various signalling pathways and show that these conditions need to be carefully and systematically determined when reporting biased agonism at GPCRs.

Examination of biased agonism at MOP across multiple different signalling pathways in two different cell backgrounds, one expressing hMOP and the other mMOP, has shown that although the biased agonism profiles of most ligands changed dramatically between the different cell types, ligands that displayed distinct bias profiles were still unique across different cell backgrounds. Our previous study in CHO cells showed that ligands such as loperamide, endo-1, Met-enk-RF and α-neo displayed signalling profiles different to that of DAMGO [713]. In the present study, such ligands still generate signalling profiles that are different from the same reference agonist. This is illustrated by the individual bias factors across different pathways (Figures 3.2, 3.3, 3.6 and 3.8) as well as by the web of bias presented in Figure 3.9.

We illustrate how biased agonism is influenced by the cellular protein complement by altering the expression of receptor kinases involved in the regulation of MOP. The bias of endo-1 between inhibition of cAMP and β-arr1/2 recruitment changed when the levels of GRK2 expression were increased in CHO cells. In addition to this, all ligands tested showed bias compared to DAMGO between activation of different $G\alpha_{i/o}$ subunits, indicating that the overall level of G protein activation, and consequently bias between G protein-mediated signalling and other signalling pathways will change depending on the G protein subunit content in a particular cell type. This shows that changes in the expression of a single protein can change the relative bias of a set of ligands, hence the direction of biased agonism can change in different cell types. Notably, changes in proteins other than intracellular signalling effectors can also determine changes in biased agonism. For instance, opioid receptors and other GPCRs have been shown to form homo- or heterodimers. It could be envisaged that the formation of oligomeric

structures in specific cell types, could lead to differences in the observed biased agonism.

The temporal dependence of biased agonism is demonstrated by the unusually rapid desensitisation of cAMP inhibition induced by Met-enk-RF. Whilst the different cAMP kinetic profile may not directly result in significantly different physiological effects, the differential kinetics may be an indicator of differential activation of other signalling pathways that will produce distinctive physiological effects. There are numerous factors that could contribute to the altered cAMP kinetics of Met-enk-RF. Different signalling kinetics could result from differing association and dissociation rates of the ligand (which is currently unexplored at MOP) or from unique conformations of the receptor induced by the ligand which possess altered receptor-effector activation dynamics. As mentioned earlier, differential receptor trafficking may also alter the cAMP kinetic profile. Indeed, receptor endocytosis has been shown to affect the initial cAMP inhibition kinetics at DOP [731].

Another factor that can affect the kinetic profile of cAMP signalling is the activation of other signalling effectors that regulate or desensitise cAMP signalling. Such signalling effectors include Ca^{2+}, PKC and several other kinases [120]. Differential activation of these signalling pathways by Met-enk-RF has not been examined to date, however Ca^{2+} mobilisation and PKC activation have been shown to be differentially activated by MOP ligands [530, 602]. In addition to this, cAMP assays typically measure total AC activity throughout the whole cell, but cAMP signalling can occur selectively in spatially distinct regions of the cell such as at the membrane or cytosol or even from internalised receptors in endosomes [221, 732]. Regulation of AC activity, and consequently the kinetics of cAMP signalling, can vary between different areas of the cell [733], hence differential activation of cAMP in different cellular compartments may also result in different cAMP signalling kinetics.

To quantify bias between G protein activation and other signalling pathways, measuring G protein activation directly using GTPγS or BRET/FRET based assays is thought to be the most direct approach that avoids complex signalling kinetics of downstream signalling effectors. However, nearly all ligands examined in this study, showed a change in bias between activation of different Gα subunits in CHO-MOP, when comparing acute activation of G proteins at 5min to G protein activation at 60min (time point at which substantial levels of receptor regulatory processes can be detected). This

suggests that G protein activation and deactivation kinetics are also ligand-dependent, hence measuring G protein activation directly instead of measuring downstream signalling pathways may only provide a partial picture of the differential signalling mechanisms. Altogether, the ligand-dependent kinetics of G protein activation and downstream G protein-mediated signalling indicate that bias is likely to be frequently observed between these two signalling endpoints. This was observed previously between cAMP and G protein-activation measured by [^{35}S]GTPγS binding assays in CHO-MOP [713], and to a lesser extent between cAMP and ΔMP in AtT20-MOP, in the current study. This has shown that the level of G protein activation does not necessarily have to be indicative of the level of activation of G protein-mediated downstream signalling, and that the level of activation of one G protein-mediated pathway is not necessarily representative of all G protein-mediated signalling.

Another factor that may contribute to bias between G protein activation and G protein-mediated signalling pathways is the bias between activation of different subtypes of G protein subunits. All ligands showed some bias compared to DAMGO between activation of different $G\alpha_{i/o}$ subtypes in CHO-MOP after 5min or 60min of agonist stimulation. Small differences in the level of activation of different $G\alpha_{i/o}$ subtypes at MOP by endo-1, endo-2 and morphine have also been reported previously [603-606], however none of these reports are consistent with the bias observed in this study. Such inconsistencies could be due to differences in the cell background, measurement of G protein activation at different time points, or factors related to the different experimental conditions. Selective G protein activation could cause unequal activation of downstream signalling pathways, as not all Gα subtypes have the same downstream effectors. Different $G\alpha_{i/o}$ subtypes have been shown to differentially inhibit AC isoforms [734-736], and are more susceptible to inactivation by different RGS subtypes [724-726]. Altogether, the differential activity and regulation of $G\alpha_{i/o}$ subunits could contribute to bias between G protein-mediated signalling pathways. Additionally, selective activation of particular $G\alpha_{i/o}$ subtypes and differential interactions with signalling effector isoforms will depend on the expression of specific subtypes/isoforms and their localisation in signalling complexes.

The dependence of biased agonism on the cellular protein content was also clearly demonstrated by the change in bias of endo-1 between cAMP and β-arr1/2 recruitment in CHO-MOP when GRK2 was overexpressed. As a consequence, biased agonism of endo-1 is likely to change in different tissues which express different levels of GRK2,

and be cAMP biased in some tissues and β-arr biased in others. It remains to be seen whether this change in bias is significant enough to produced marked differences in physiological effects. However, different cell types typically show altered expression of numerous signalling effectors, since changing the expression of a single protein can cause such a notable change in bias, it is likely that the cumulative effects of all changes in protein expression could induce considerable differences in bias across different cell types.

Altogether, the impact of the cellular complement on determinations of biased agonism, combined with the kinetics of the signalling pathways suggest that caution must be taken when interpreting bias quantifications in different cell backgrounds. The altered expression and localisation of proteins in a different cell background can result in changes in signalling kinetics, as well as changes in experimental conditions required to obtain concentration-response curves. Microarray analysis of genes expressed in AtT20 cells have shown that these cells have a very limited range of signalling proteins compared to other commonly used cell lines [737]. AtT20 cells only express detectable levels of GRK2, β-arr2, and $G\alpha_{i2}$, and also a very limited number of RGS subtypes and AC isoforms. With only a single GRK isoform and no endogenously expressed β-arr1, there will be less variation in receptor phosphorylation patterns that govern subsequent MOP regulation and trafficking events. Additionally, the expression of a single $G\alpha_{i/o}$ subtype, $G\alpha_{i2}$, and the low levels of a small subset of AC isoforms and RGS subtypes indicates that the level AC inhibition induced by the ligands and regulation of AC activity in these cells is likely to be different from that observed in the CHO cells. Overall, this may account for many of the changes in bias compared to CHO-MOP observed for endo-1, loperamide and α-neo between cAMP, β-arr1/2 recruitment and receptor internalisation. Moreover, the difference between biased agonism in AtT20 and CHO cells may also be due to the difference in species, mouse and human MOP, as has been recently observed at KOP [738]. Overall, this indicates that ligands will not only exhibit different biased agonism characteristics in different tissues, but that this can also change due to cellular adaptions that cause changes in protein expression and localisation, such as during the development of opioid tolerance.

Since the unique conformations of the receptor induced by the ligand are more likely to be consistent between cell types, some studies have bypassed the complications of signalling kinetics and cell background by directly measuring receptor conformational changes using BRET or FRET-based sensors [739]. Whilst this approach can identify

novel biased ligands that stabilise the receptor into unique conformations, there is still a requirement to link these unique conformations to specific signalling characteristics, and hence cell specific complications of biased agonism remain. However, the cell-dependent aspect of biased agonism may be an advantage in some cases, such as when the therapeutic effects and the side effects are mediated by activation of the same signalling pathways in different tissues. In such cases, a ligand that displays a distinct bias profile in different cells can selectively activate the desired signalling pathways in the desired tissue. In the case of MOP, a ligand which shows marked cell-dependent bias may produce less desensitisation and tolerance in cells involved in nociception and more in other cell types which are linked to limited side effects (those controlling respiration or gut motility), even if the mechanisms of desensitisation and tolerance are the same in different cells.

In summary the data presented here demonstrate the complex nature of biased agonism. Biased agonism is not an absolute quality, it is a dynamic and multi-faceted phenomenon; it is always relative to a reference ligand, and it is dependent on both cellular protein complement as well as the spatiotemporal properties of the different signalling pathways [727]. Our results highlight that biased agonism cannot be described in isolation of conformational, kinetic and cellular context. As mentioned above, it is vital to use a reference ligand that is likely to be subject to the same kinetic and cellular context than the other ligands. Ideally, such reference ligand is an endogenous agonist, although when multiple endogenous agonists exist, one may need to consider the potential of biased agonism and the effect of the so-called conformational and kinetic context among these.

Nevertheless, quantification of biased agonism in different cell backgrounds has also shown that despite the dramatic changes in the biased agonism profiles of the ligands between the cell backgrounds, the ligands under study still possessed distinct biased agonism profiles. This shows that despite such caveats, the diversity of biased agonism characteristics can be captured by examining bias across several signalling pathways. Ultimately, in order to establish links between distinct biased agonism traits and specific physiological responses, a greater understanding about biased signalling in native tissue and *in vivo* is essential. This complexity in biased agonism determinations presents a significant challenge when attempting to predict biased signalling *in vivo*. However the cell-dependent characteristics of biased agonism may prove to be an

advantage in the development of biased ligands, as this facilitates the design of drugs that are more targeted to specific tissues.

CHAPTER 4

PLASMA MEMBRANE LOCALISATION OF THE μ-OPIOID RECEPTOR CONTROLS SPATIOTEMPORAL SIGNALLING

Michelle L. Halls[1], Holly R. Yeatman[1], Cameron J. Nowell[1], Georgina L. Thompson[12], Arisbel Batista Gondin[1], Srgjan Civciristov[1], Nigel W. Bunnett[1,3,4,5] Nevin A. Lambert[6], Daniel P. Poole[1,7] & Meritxell Canals[1,2]

PUBLISHED IN SCI. SIGNAL. 2016 9;9(414)

[1]Drug Discovery Biology Theme, Monash Institute of Pharmaceutical Sciences, Monash University, Australia; [2]Defence Science and Technology Group, Australian Department of Defence, Australia; [3]ARC Center of Excellence in Convergent Bio-Nano Science and Technology, Monash Institute of Pharmaceutical Sciences, and [4]Department of Anesthesia and Perioperative Medicine, Monash University, Australia; [5]Department of Pharmacology, The University of Melbourne, Australia; [6]Georgia Regents University, Georgia, USA; [7]Department of Anatomy and Neuroscience, The University of Melbourne, Australia.

Monash University

Declaration by candidate

In the case of Chapter 4, the nature and extent of my contribution to the work was the following:

Nature of contribution	**Extent of contribution (%)**
Performed and analysed FRET sensor experiments in dorsal root ganglia neurons (Figure 4.6A-F of thesis) – For which my contribution to this work was 90%	15%

The following co-authors contributed to the work. If co-authors are students at Monash University, the extent of their contribution in percentage terms must be stated:

Name	**Nature of contribution**	**Extent of contribution (%)** for student co-authors only
Meritxell Canals	Contributed to research design, performed and analysed experiments, and wrote the manuscript	N/A
Michelle L. Halls	Contributed to research design, performed and analysed experiments, and wrote the manuscript	N/A
Holly R. Yeatman	Performed experiments, and contributed to writing of the manuscript	N/A
Cameron J. Nowell	Technical assistance with microscopy	N/A
Arisbel Batista Gondin	Performed experiments, and contributed to writing of the manuscript	5%
Srgjan Civciristov	Performed experiments, and contributed to writing of the manuscript	N/A
Nigel W. Bunnett	Contributed to writing of the manuscript	N/A
Nevin A. Lambert	provided essential materials for the project	N/A
Daniel P. Poole	Performed experiments, and contributed to writing of the manuscript	N/A

The undersigned hereby certify that the above declaration correctly reflects the nature and extent of the candidate's and co-authors' contributions to this work*.

Candidate's Signature	[redacted]	**Date 9 May 2016**
Main Supervisor's Signature	[redacted]	**Date 9 May 2016**

4.1 Abstract

Differential regulation of MOP contributes to the clinically limiting effects of opioid analgesics, such as morphine. However, whether differential regulation of MOP impacts on the spatiotemporal characteristics of receptor activation is unclear. Here we used biophysical approaches to quantify MOP spatiotemporal signalling. Morphine caused a $G_{\beta\gamma}$-dependent increase in membrane-localised PKC activity, which restricted the distribution of MOP within the plasma membrane and induced sustained cytosolic ERK. In contrast, DAMGO allowed receptor redistribution, transient increases in cytosolic and nucERK, and then receptor internalisation. Following inhibition of $G\beta\gamma$-subunits, PKCα or mutation of a key phosphorylation site, the morphine-activated MOP is released from its restricted localisation and stimulates a transient increase in cytosolic and nucERK in the absence of β-arr recruitment and internalisation. Thus, ligand-induced redistribution of MOP at the plasma membrane, and not internalisation, controls its spatiotemporal signalling.

4.2 Introduction

GPCRs are the largest family of cell surface signalling proteins encoded by the human genome. They allow cells to respond to structurally diverse endogenous and environmental signals, and are the target of over 30% of marketed drugs. It is increasingly recognised that the uniform elevation of second messengers throughout the cell cannot explain the diversity of GPCR-mediated effects. Rather, spatial (location) and temporal (duration) control of signalling plays an important role [221, 740]. Spatial compartmentalisation of signalling can be achieved by the formation of GPCR-dependent protein complexes, which ultimately restrict second messenger diffusion to induce extremely localised signals [741]. In addition, multiple regulatory mechanisms (including receptor phosphorylation, desensitisation and internalisation) control the duration of GPCR activation. Therefore, the spatial and temporal distribution of both receptors and signalling effectors are critical for the generation of distinct and highly specialised GPCR-mediated responses.

MOP has been extensively studied due to its physiological importance in mediating the effects of endogenous opioids, and its prominence as the target of opioid analgesics, such as morphine. Despite this, chronic use of opioid analgesics is still clinically limited by the development of tolerance, addiction, constipation and respiratory depression [742]. At a cellular level, stimulation of MOP by all opioids activates the same G protein-dependent signalling pathways. MOP activates $G\alpha_{i/o}$ proteins leading to an inhibition of cAMP, increased ERK phosphorylation, activation of G protein-regulated inwardly rectifying potassium channels, and inhibition of voltage-gated calcium channels [688]. However, different MOP agonists induce distinct patterns of receptor regulation and internalisation. In particular, morphine causes limited receptor phosphorylation and β-arr recruitment, which results in compromised receptor internalisation and resensitisation [184, 274, 525, 533, 561]. These observations have prompted intensive studies of the ability of MOP ligands to differentially activate G proteins and β-arrs, in an effort to explain their divergent biological effects [580, 581, 641].

It is now apparent that the spatiotemporal characteristics of a signal can specify the outcome of receptor activation [221, 740]. Most opioids, including morphine, elicit cytosolic ERK phosphorylation (cytoERK) [208, 520, 593]. However, unlike other opioids, morphine is unable to promote nucERK phosphorylation (nucERK) [208]. Taken together with its impaired internalisation of MOP, this suggests that morphine may

stimulate a unique spatiotemporal cellular response. To investigate this, we used complimentary biophysical techniques and super-resolution microscopy. We report that morphine and DAMGO activate distinct spatial and temporal signalling profiles that are controlled by the plasma membrane localisation of MOP induced by the two ligands. Subcellular-targeted FRET biosensors showed that only morphine stimulation of MOP induced sustained cytoERK and plasma membrane-localised PKC activation, which restricted MOP localisation. In contrast, DAMGO caused MOP redistribution within the plasma membrane and transient activation of cytosolic and nucERK. Thus, not only do morphine and DAMGO stimulate different signalling pathways, they activate signals in distinct subcellular compartments with unique temporal profiles. Importantly, we can alter the spatiotemporal signalling profile of morphine to mimic that of DAMGO, by allowing redistribution of MOP within the plasma membrane in the absence of β-arr recruitment or receptor internalisation. Thus, receptor localisation within the plasma membrane determines the spatiotemporal signals activated by MOP in response to different ligands.

4.3 Materials and methods

4.3.1 Materials

DAMGO was from Mimotopes (Victoria, Australia); Morphine and M2-anti-FLAG antibody were from Sigma Aldrich; Coelenterazine h was from Promega; β-arr1 and β-arr2 siRNA were from GE-Dharmacon; mouse anti-EEA1 antibody was from BD Transduction Laboratories; rabbit anti-MOP (UMB-3) was from Abcam, mouse anti-β-tubulin for confocal imaging was from Merck Millipore, Alexa-conjugated goat anti-mouse secondary antibodies were from Jackson ImmunoResearch; anti-caveolin 1, anti-β-actin and anti-clathrin heavy chain antibodies were from Abcam; anti-β-tubulin antibody for immunoblotting was from Santa Cruz Biotechnology; anti-β-arr1/2 antibodies were from Cell Signalling Technology; fluorescent IRDye-conjugated goat anti-rabbit (800 channel) and anti-mouse (680 channel) secondary antibodies were from LI-COR Biotechnology.

KRas-Venus, Rab5a-Venus, GFP-dynamin and GFP-dynamin K44E have been previously described [743-745]. MOP-RLuc was from L. Bohn, FLAG-MOP was from M. Christie, β-arr2-YFP was from M. Caron and FLAG-MOP 11ST/A was from S. Schulz. The following constructs were obtained from Addgene: cytoEKAR GFP/RFP (plasmid 18680), cytoEKAR Cerulean/Venus (plasmid 18679), nucEKAR GFP/RFP (plasmid 18681) and nucEKAR Cerulean/Venus (plasmid 18681) [746]; cytoCKAR (plasmid 14870) and pmCKAR (plasmid 14862) [747]. MOPr S375A has a mutation of the essential site governing hierarchical phosphorylation (human S377A, mouse S375A) [184], and was generated using QuikChange. RLuc8-tagged MOPr were generated by subcloning into the pcDNA3-RLuc8 vector.

4.3.2 Cell Culture and Inhibitors

HEK293 cells were grown in DMEM supplemented with 5% v/v FBS. Cells were transfected using linear polyethyleneimine (PEI) [745]. For siRNA, cells were transfected with 25 nM scrambled or combined β-arr1 and β-arr2 SMARTpool ON-TARGETplus siRNA with Lipofectamine 2000 24 h prior to transfection with receptor and biosensors.

Cells were pre-treated with inhibitors for 30min at 37°C, except for Filipin III, MβCD or MβCD/cholesterol complexes (45min) or PTx (16h). MβCD/cholesterol complexes were

formed as described previously [748]. Inhibitors were used at the following concentrations: 30μM PitStop2 or inactive PitStop2, 10μM NF023, 100ng/mL PTx, 5μM mSIRK or mSIRK L9A, 1μM GF109203X or Gö6983, 10nM Gö6976, 10μM Myr-EAVSLKPT-OH (inhibitory PKCε peptide, iPKCε), 1μg/mL Filipin III, 10mM MβCD, 2mM MβCD with 0.2mM cholesterol (MβCD/cholesterol complexes).

All experiments were performed in live cells at 37°C. For all regulation and trafficking experiments cells were stimulated with an EC_{50} concentration of DAMGO or morphine (both 1μM) defined by β-arr2 concentration-response curves (Figure A.7A). For all signalling experiments cells were stimulated with an EC_{50} concentration of DAMGO (10nM) or morphine (100nM) defined by AlphaScreen pERK assays (Figure A.6).

4.3.3 DRG Isolation and Culture

All procedures involving mice were approved by the Monash Institute of Pharmaceutical Sciences animal ethics committee. DRG neurons were isolated and nucleofected with 600ng of cytoEKAR Cerulean/Venus, nucEKAR Cerulean/Venus or pmCKAR using the Nucleofector system (Lonza) (see [749] for detailed protocols of DRG isolation and nucleofection).

4.3.4 Bioluminescence Resonance Energy Transfer

HEK293 cells were transfected with 1μg MOP-RLuc and 4μg KRas-Venus, Rab5a-Venus or β-arr2-YFP. For co-expression, cells were transfected with an additional 2μg of βARKct, GFP-dynamin or GFP-dynamin K44E. After 24h cells were plated in poly-D-lysine-coated 96-well plates (CulturPlate, PerkinElmer) and allowed to adhere. 48h post-transfection, cells were equilibrated in HBSS then stimulated with vehicle (0.1% DMSO), DAMGO or morphine for 30min. Coelenterazine h (Promega) was added at a final concentration of 5μM and cells were incubated for 10min. BRET measurements were obtained using a PHERAstar Omega (BMG Labtech, Germany) that allows sequential integration of the signals detected at 475±30 and 535±30nm using filters with the appropriate band pass. Data are presented as a BRET ratio (calculated as the ratio of YFP to RLuc signals) corrected for vehicle.

4.3.5 FRET

HEK293 cells were transfected with 55ng/well MOP and 40ng/well cytoEKAR GFP/RFP, nucEKAR GFP/RFP, cytoCKAR or pmCKAR. For co-expression, cells were transfected with an additional 50ng/well βARKct, GFP-dynamin or GFP-dynamin K44E. Experiments co-expressing GFP-dynamin or GFP-dynamin K44E used the Cerulean/Venus FRET sensors. FRET was measured using a high-content GE Healthcare INCell 2000 Analyzer (see [749] for detailed protocols). Briefly, fluorescence imaging was performed using a Nikon Plan Fluor ELWD 40x (NA 0.6) objective and FRET module. For GFP/RFP emission ratio analysis, cells were sequentially excited using a FITC filter (490/20) with emission measured using dsRed (605/52) and FITC (525/36) filters, and a polychroic optimised for the FITC/dsRed filter pair (Quad4). For CFP/YFP or Cerulean/Venus emission ratio analysis, cells were sequentially excited using a CFP filter (430/24) with emission measured using YFP (535/30) and CFP (470/24) filters, and a polychroic optimised for the CFP/YFP filter pair (Quad3). HEK293 cells were imaged every 1min, allowing image capture of 14 wells per min; DRG neurons were imaged every 1min with four fields of view per well, allowing capture of 3 wells per min. At the end of every experiment, the same cells were stimulated with the positive control (200nM phorbol 12,13-dibutyrate for ERK or 200nM phorbol 12,13-dibutyrate with phosphatase inhibitor cocktail 2 (Sigma Aldrich) for PKC) for 10min to generate a maximal FRET change, and positive emission ratio images were captured for 4min.

Data were analyzed using the FIJI distribution of ImageJ [750]. The three emission ratio image stacks (baseline, stimulated, positive) were collated and aligned using the StackCreator script [749]. Cells were selected and fluorescence intensity measured over the combined stack. Background intensity was subtracted, then FRET data plotted as the change in FRET emission ratio relative to the maximal response for each cell (FRET ratio/maximum FRET ratio; F/F_{Max}). For HEK293, only cells that showed more than a 10% change relative to baseline following stimulation with the positive control were considered for analysis. For DRG neurons, all cells that showed more than a 3% change relative to baseline following stimulation with the positive control were considered for analysis.

Ratiometric pseudocolour images were generated according to [751]. The Green Fire Blue LUT was applied, and the Brightness and Contrast range was set to the minimum and maximum FRET ratios within the image stack (0.13-0.23).

4.3.6 GSD/TIRF Microscopy

HEK293 cells and DRG neurons were stimulated with vehicle (0.1% DMSO), DAMGO or morphine as indicated, fixed in 4% paraformaldehyde (20min, 4°C), washed for 15min with PBS, blocked in PBS with 1% Normal goat serum and 0.1% saponin (1h, RT), and incubated overnight at 4°C with mouse anti-FLAG antibody (1:1000) for HEK293 or rabbit anti-MOP (UMB-3, 1:250) and anti-tubulin βIII (1:1000) for DRG neurons. Cells were washed and incubated with Alexa568- or Alexa647-conjugated goat anti-mouse or anti-rabbit secondary antibodies (1:400, 2 hours, RT). Coverslips were mounted on a concave slide containing 100mM cysteamine (MEA) and sealed. Cells were observed with a Leica GSD microscope with HCX PL APO 160x (NA 1.43) objective, SuMo stage, Andor iXon Ultra 897 camera and LAS AF software. Pumping occurred at 100% laser power until the frame correlation dropped to 0.25. Data were acquired at 50% laser power, and up to 30,000 frames captured. TIRF penetration was at 110nm. Only neurons with positive staining for β-tubulin were analysed. Images were analysed in FIJI [750]. Individual particles were selected using Find Maxima (noise tolerance 5) to generate a binary output of the single points. The average distance between events was calculated by creating a centroid list using the Analyse Particles command, and processed by the Nearest Neighbour Distance (NND) macro (Yuxiong Mao). Euclidean distance maps were generated from the single point binary

4.4 Results

4.4.1 Ligand-Dependent Spatiotemporal Signalling of MOP

To gain spatial and temporal resolution of MOP signalling in live cells, we used FRET biosensors for ERK and PKC (EKAR and CKAR, respectively) localised to different subcellular compartments [746, 747]. In HEK293 cells co-transfected with MOP and either a cytosolic or nucERK biosensor (cytoEKAR, nucEKAR), EC_{50} concentrations of DAMGO (10nM) or morphine (100nM; Figure A.6A) caused distinct temporal ERK profiles. DAMGO caused a transient increase in cytoERK, whereas morphine induced a sustained increase (Figure 4.1A *and* B). Moreover, only DAMGO caused a transient increase in nucERK (Figure 4.1C *and* D). Ligand-dependent responses were also observed when assessing direct activation of PKC. In cells co-transfected with MOP and a plasma membrane PKC biosensor (pmCKAR) only morphine caused a sustained increase in PKC activity (Figure 4.1E). DAMGO did not affect plasma membrane PKC activity, even at maximal concentrations (1μM; Figure A.6B), and neither ligand affected cytosolic PKC (Figure 4.1F).

The distinct internalisation profiles of MOP in response to DAMGO and morphine [274, 533], were quantified using a BRET assay that detects the proximity between BRET partners in defined subcellular compartments in live cells [743, 752]. In agreement with previous reports, incubation with DAMGO (1μM, Figure A.7A) induced MOP internalisation as shown by the increase in the BRET signal between MOP-RLuc and a Venus-tagged marker of early endosomes (Rab5a-Venus) (Figure 4.1A). In contrast, morphine produced no detectable change in BRET (Figure 4.2*A* and Figure A.7B). These results were validated by automated, high-content image analysis (Figure A.7C). DAMGO-mediated MOP endocytosis was unaffected by $G\alpha_{i/o}$ inhibition using NF023 or pertussis toxin (PTx) [753, 754] but was abolished by the clathrin-dependent endocytosis inhibitor PitStop2 [755], expression of a dominant negative dynamin (K44E) [756] or by knockdown of β-arrs (combined β-arr1 and β-arr2 siRNA; Figure 4.1A and B and Figure A.7 D and H). This shows that β-arr recruitment and MOP endocytosis are independent of $G\alpha_{i/o}$ coupling.

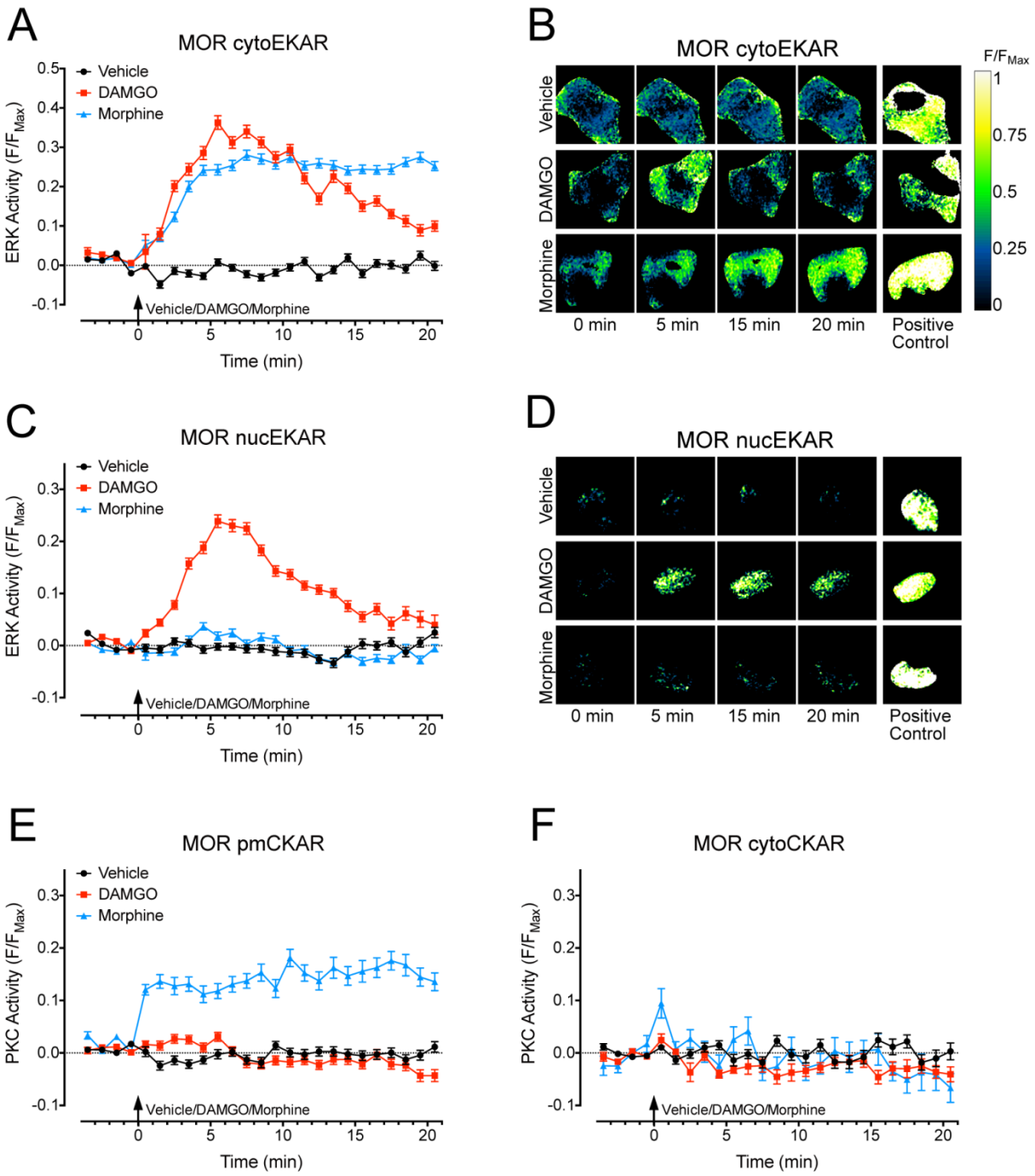

Figure 4.1: Ligand-dependent spatiotemporal signalling of MOP.
(A-D) Spatiotemporal activation of ERK following vehicle, DAMGO or morphine stimulation. (A) CytoERK (416-606 cells). (B) Representative pseudocolour ratiometric images of cytoEKAR. (C) NucERK (561-810 cells). (D) Representative pseudocolour ratiometric images of nucEKAR. Pseudocolour scale as in B. (E-F) Spatiotemporal activation of PKC following vehicle, DAMGO or morphine stimulation. (E) Plasma membrane-localised PKC (155-220 cells). (F) Cytosolic PKC (45-115 cells). Symbols represent means, error bars SEM.

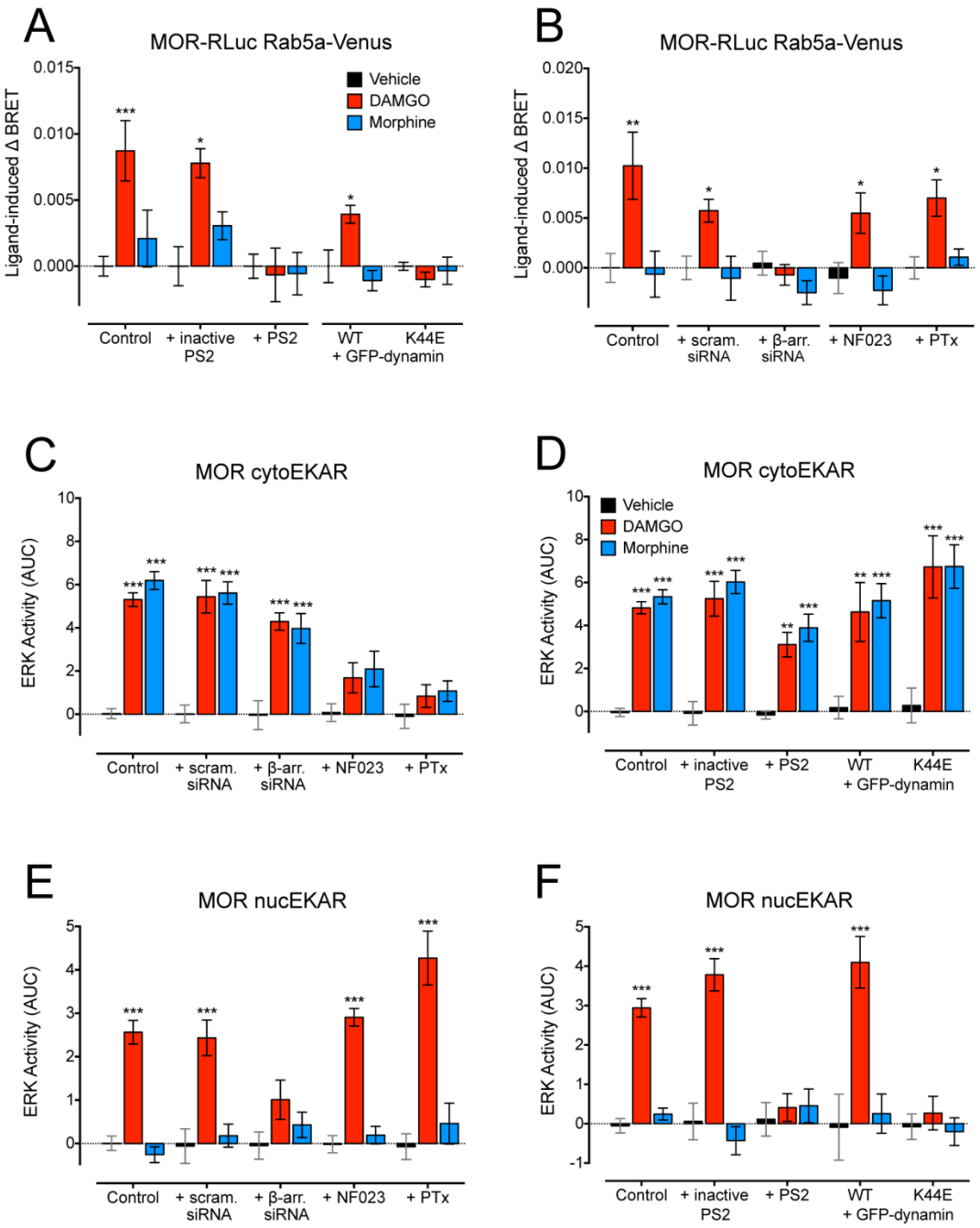

Figure 4.2: Effect of $G\alpha_{i/o}$ protein inhibition, β-arr knockdown or inhibition of endocytosis on cytosolic and nucERK activation by MOP.

(A-B) MOP trafficking to early endosomes (n≥3) in response to 30min vehicle, DAMGO or morphine in the presence of (A) the clathrin-mediated endocytosis inhibitor PitStop2 (PS2) or inactive control, or upon expression of wild-type (WT) dynamin or dominant negative dynamin K44E or (B) with and without knockdown of β-arrs or pre-incubation with Gαi/o protein inhibitors. (C-F) Spatial activation of ERK following vehicle, DAMGO or morphine stimulation, with and without knockdown of β-arrs, Gαi/o protein inhibition, in the presence of PS2 or inactive control, or upon expression of WT or K44E dynamin. (C) CytoERK (19-168 cells) with Gαi/o protein inhibition or knockdown of β-arrs. (D) CytoERK (35-245 cells) following inhibition of endocytosis. (E) NucERK (52-258 cells) with Gαi/o protein inhibition or knockdown of β-arrs. (F) NucERK (51-306 cells) following inhibition of endocytosis. Bars/symbols represent means, error bars SEM. *p<0.05, **p<0.01, ***p<0.001 versus vehicle control, two-way ANOVA with Tukey's multiple comparison test. AUC, area under the curve; scram., scrambled

Previous studies have linked activation of PKC to cytoERK, and β-arr to increased nucERK, to conclude that G protein- and β-arr-dependent pathways activate distinct ERK signalling [208]. By inhibiting $G\alpha_{i/o}$ proteins, we now directly demonstrate that cytoERK in response to DAMGO and morphine is dependent on $G\alpha_{i/o}$ (Figure 4.2C). In agreement with previous studies, cytoERK was unaffected by knockdown of β-arrs (Figure 4.2C). However, inhibition of receptor endocytosis by PitStop2 or dynamin K44E transformed the profile of DAMGO-induced cytoERK from a transient to a sustained signal, consistent with MOP retention at the plasma membrane (Figure 4.2D and Figure A.7I to J). As expected, the increase in nucERK in response to DAMGO was dependent on β-arrs and receptor internalisation (Figure 4.2E and F).

Thus, our results show that $G\alpha_{i/o}$ activation by MOP mediates increases in cytoERK in response to DAMGO and morphine, and confirm that the increases in nucERK in response to DAMGO are dependent on β-arrs and receptor endocytosis.

4.4.2 PKC Activation Controls the ERK Spatiotemporal Profile of Morphine

Inhibition of $G\alpha_{i/o}$ (NF023 or PTx) or Gβγ (mSIRK or expression of βARKct) [757, 758] abolished the plasma membrane PKC response to morphine (Figure 4.3A, Figure A.8A) There was no effect of knockdown of β-arrs, or negative controls (inactive mSIRK L9A, scrambled siRNA; Figure 4.3A, Figure A.8A).

Thus, the sustained increase in plasma membrane PKC induced by morphine is mediated by $G\alpha_{i/o}$-Gβγ. Previous studies have reported that PKC activity mediates increased cytoERK in response to morphine [208]. We therefore investigated whether the $G\alpha_{i/o}$-Gβγ-PKC pathway influences the unique ERK spatiotemporal signalling profiles of MOP. Rather than decreasing ERK, and in contrast to previous reports, inhibition of Gβγ or PKC (GF109203X, Gö6983) [759, 760] transformed the temporal profile of morphine-stimulated cytoERK to resemble the transient response induced by DAMGO (Figure 4.3B, Figure A.8A and C). Moreover, inhibition of the Gβγ-PKC pathway also allowed morphine to increase nucERK (Figure 4.3C and D). Previous studies have implicated PKCα, γ and ε as the isoforms that contribute to morphine signalling and the development of morphine tolerance [557, 584, 592, 593, 761]. Of these, only PKCα and PKCε are expressed in our HEK293 cell line (Figure 4.3D).

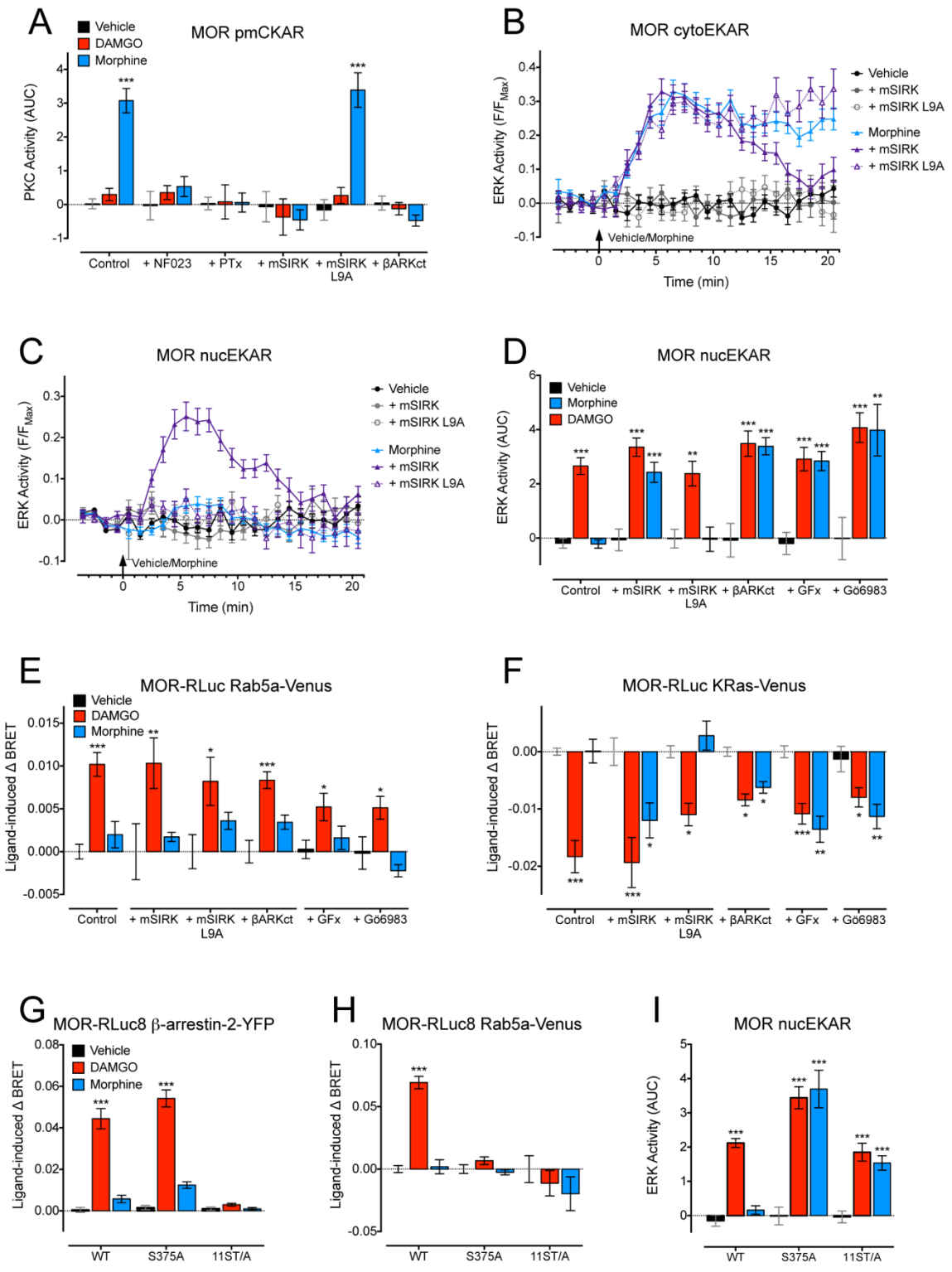

Figure 4.3: Role of PKC activation by morphine in the spatiotemporal control of ERK activity.

(A) The effect of G protein inhibitors or inactive controls on plasma membrane PKC activity in HEK293 cells determined with the pmCKAR FRET biosensor. Data are means ± SEM of 39 to 229 cells from 3 experiments. (B-D) Analysis of MOP-stimulated spatiotemporal activation of ERK in cells in which Gβγ or PKC signalling was inhibited. (B) Analysis of cytoERK (31 to 101 cells) and (C) nucERK (74 to 126 cells) activity over time. Data are means ± SEM from 3 experiments. (D) NucERK activity was analysed as the AUC. Data are means ± SEM of 22 to

360 cells from 3 experiments. (E and F) MOP trafficking was monitored in HEK293 cells in the presence or absence of the indicated Gβγ and PKC inhibitors. (E) Analysis of BRET between MOP-RLuc and Rab5a-Venus. Data are means ± SEM of 3-7 experiments. (F) Analysis of BRET between MOP-RLuc and KRas-Venus. Data are means ± SEM of 3-7 experiments. (G-I) Effect of the indicated phosphorylation site mutations on MOP trafficking and nucERK activity. (G) Analysis of BRET between MOP-RLuc8 and β-arr2–YFP. Data are means ± SEM of three to seven experiments. (H) Analysis of BRET between MOP-RLuc8 and Rab5a-Venus. Data are means ± SEM of 3 or 4 experiments. (I) Analysis of nucERK activity over time. Data are means ± SEM of 87 to 359 cells from 3-5 experiments. *P<0.05, **P<0.01, and ***P<0.001 versus vehicle control. Data were analysed by two-way ANOVA with Tukey's (A and D) or Dunnett's (E-I) multiple comparison tests. GFx, GF109203X

Inhibition of PKCα (Gö6976: targets PKCα and PKCβ_1) [762] but not PKCε (iPKCε, a cell-permeable PKCε-inhibitory peptide) [763] transformed the temporal profile of morphine-stimulated cytoERK and facilitated an increase in nucERK (Figure A.8E and F). There was no effect of inactive controls or of these inhibitors on the response to DAMGO (Figure 4.3B to D, Figure A.8C and F).

As expected, inhibition of Gβγ or PKC had no effect on DAMGO induced β-arr2 recruitment or MOP internalisation, determined by BRET (Figure 4.3E, Figure A.8G to I). In contrast, upon inhibition of Gβγ or PKC, morphine activation of MOP resulted in a decrease in BRET between MOP-RLuc and the plasma membrane marker KRas-Venus (Figure 4.3F) suggesting an increase in the distance between these two proteins. In the absence of MOP internalisation (Figure 4.3E, Figure A.8G and H), the morphine-stimulated change in MOP- KRas BRET may indicate movement of the receptor away from KRas within the plasma membrane. Thus, the transient activation of cyto and nucERK elicited by morphine does not require MOP internalisation but may instead depend on MOP translocation within the plasma membrane.

The importance of MOP localisation within the plasma membrane for the control of spatiotemporal signalling was also supported by the effects observed upon expression of a phosphorylation-impaired MOP mutant (S375A) [541]. MOP S375A still recruited β-arr2 in response to DAMGO, but was unable to internalise as determined by high-content imaging or Rab5a BRET (Figure 4.3G to H, Figure A.8G and H). There was no change in MOP S375A-KRas BRET in response to DAMGO or morphine (Figure A.8J). However, stimulation of MOP S375A by both DAMGO and morphine induced transient increases in cytosolic and nucERK (Figure 4.3I, Figure A.8K). To confirm that receptor phosphorylation was key for the control of MOP plasma membrane localisation and spatiotemporal signalling, we used a phosphorylation-deficient MOP mutant in which all the CT Ser and Thr residues have been mutated to Ala (11ST/A) [184]. Consistent with

previous reports, MOP 11ST/A was unable to internalise as determined by Rab5a BRET, or recruit β-arr2 in response to DAMGO (Figure 4.3G and H). However, stimulation of MOP 11ST/A by both DAMGO and morphine induced a transient increase in nucERK, with no change in KRas BRET (Figure 4.3I, Figure A.8J). Phosphorylation of Ser375 therefore appears critical for the control of MOP spatiotemporal signalling in response to morphine. Taken together, these data show that the impaired trafficking of MOP mutants results in an altered signalling profile and support the hypothesis that the plasma membrane localisation of MOP, and not β-arr recruitment or receptor internalisation, plays a key role in the spatiotemporal control of receptor signalling.

4.4.3 Ligand-Dependent Redistribution of MOP Within the Plasma Membrane

To investigate the changes in MOP distribution elicited by morphine upon inhibition of the Gβγ-PKCα pathway, we assessed receptor localisation at the plasma membrane by confocal microscopy and subcellular fractionation. After 10min stimulation of MOP (which causes activation of all signalling pathways) there was no colocalisation between the receptor and immunolabeled clathrin by confocal microscopy under any condition tested (Figure A.9A and B). However, after 60min, stimulation with DAMGO but not morphine caused significant colocalisation between MOP and clathrin (Figure A.9C). In contrast, activation of the fast internalising β2AR by isoprenaline caused significant receptor-clathrin colocalisation after 10min (Figure A.9A to C). Similarly, there was no effect of DAMGO or morphine stimulation on the location of FLAG-MOP within non-lipid-rich (Triton X-100 soluble) plasma membrane domains using basic lipid fractionation (Figure A.9D). Therefore, the distinct spatiotemporal signalling profiles of morphine and DAMGO do not reflect ligand-dependent MOP clustering in clathrin-coated pits nor translocation to different lipid domains.

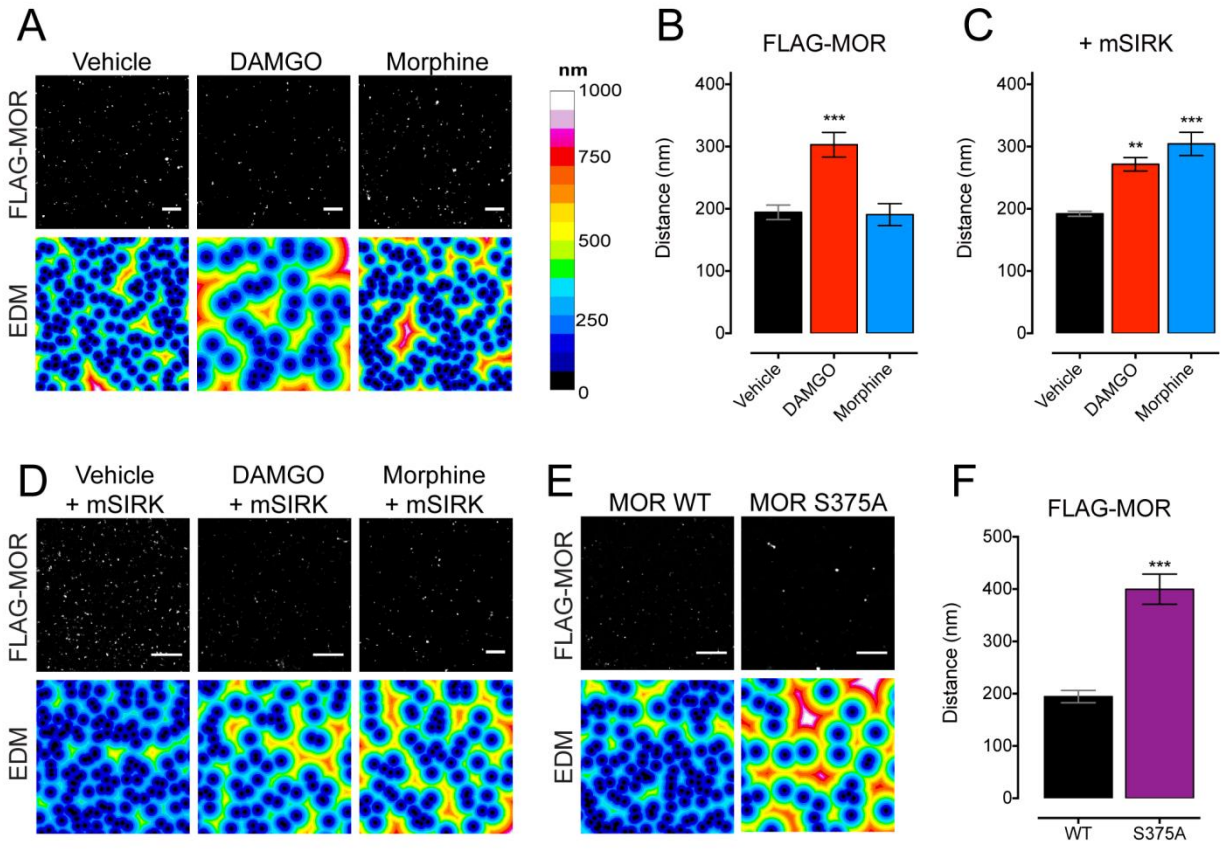

Figure 4.4: DAMGO induces a unique MOP distribution at the plasma membrane.
Plasma membrane distribution of FLAG-MOP in response to 10min vehicle, DAMGO or morphine using GSD/TIRF (n=3-9). (A) Representative GSD/TIRF images and Euclidean distance maps (EDM) under control conditions. Scale bar 1μm. (B) Average distance to nearest neighbour under control conditions and (C) following Gβγ inhibition. (D) Representative GSD/TIRF images and EDM following Gβγ inhibition. Scale bar 1μm, pseudocolour scale as in A. (E) Representative GSD/TIRF images and EDM of wild-type MOP (WT) or MOP S375A under basal conditions. Scale bar 1μm, pseudocolour scale as in A. (F) Average distance to nearest neighbour. Bars represent means, error bars SEM. ***p<0.001 versus vehicle control, one-way ANOVA with Dunnett's multiple comparison test (B,C) or unpaired t-test (E).

To investigate MOP localisation within the plasma membrane with increased resolution, we used ground state depletion (GSD) super-resolution microscopy in total internal reflection fluorescence (TIRF) mode. GSD/TIRF allows the detection of events within the plane of the plasma membrane to an axial resolution of 100nm. This approach can measure the distance between an event (receptor or receptor clusters) and its nearest neighbour across a population. Stimulation of FLAG-MOP with DAMGO (10min) increased the average distance between detected events (Figure 4.4A-B), suggesting MOP redistribution within the plasma membrane. This increase in distance occurs prior to and is independent of receptor internalisation, as there was no effect of expression of dominant negative dynamin K44E (Figure A.9E to F). Morphine stimulation of FLAG-MOP (10min) did not change the average distance between events (Figure 4.4A-B).

However, following inhibition of Gβγ morphine increased the distance between detected MOP events (Figure 4.4C-D, Figure A.9E to G), suggesting that activation of this pathway by morphine normally restricts MOP localisation. Interestingly, the distance between MOP events under basal conditions following expression of MOP S375A was also increased when compared to the wild-type receptor (Figure 4.4E-F). This increase in distance between events was not due to decreased receptor expression at the plasma membrane (MOP S375A 570,000 sites per cell, MOP wild-type 140,000 sites per cell measured by whole cell [^{3}H]-diprenorphine binding), confirming that MOP S375A was differentially distributed compared to the wild-type receptor. Thus, our results suggest that activation of MOP by morphine restricts receptor localisation, whereas DAMGO stimulation allows MOP redistribution within the plasma membrane. Disruption of the Gβγ-PKCα-phosphorylation pathway allows morphine to stimulate a DAMGO-like redistribution of MOP but does not result in receptor internalisation. This receptor redistribution precedes (DAMGO), or can occur independently of (morphine), endocytosis and appears to control the ability of MOP to transiently activate cytoERK and nucERK.

4.4.4 Disruption of Plasma Membrane Organisation Alters MOP Spatiotemporal Signalling

To confirm the importance of membrane organisation in the control of compartmentalised MOP signalling, we depleted cholesterol from the plasma membrane using methyl-β-cyclodextrin (MβCD) [764] or Filipin III [765]. There was no effect of these treatments on MOP internalisation, as determined by high-content imaging (Figure A.10A and B). However, both MβCD and Filipin III abolished the distinct spatiotemporal signalling profiles of morphine and DAMGO (Figure 4.5, Figure A.10). Upon cholesterol depletion, both morphine and DAMGO increased PKC activity at the plasma membrane and caused a transient increase in cytosolic and nucERK (Figure 4.5, Figure A.10C to F). Importantly, membrane cholesterol replenishment by incubation of the cells with MβCD/cholesterol complexes, completely restored the original spatiotemporal signalling profiles of DAMGO and morphine (Figure 4.5, Figure A.10). Thus, disruption of membrane organisation alters the spatiotemporal signalling profiles of MOP, with no change in the ability of the receptor to internalise, confirming that plasma membrane localisation of MOP plays an important role in determining its spatiotemporal signalling.

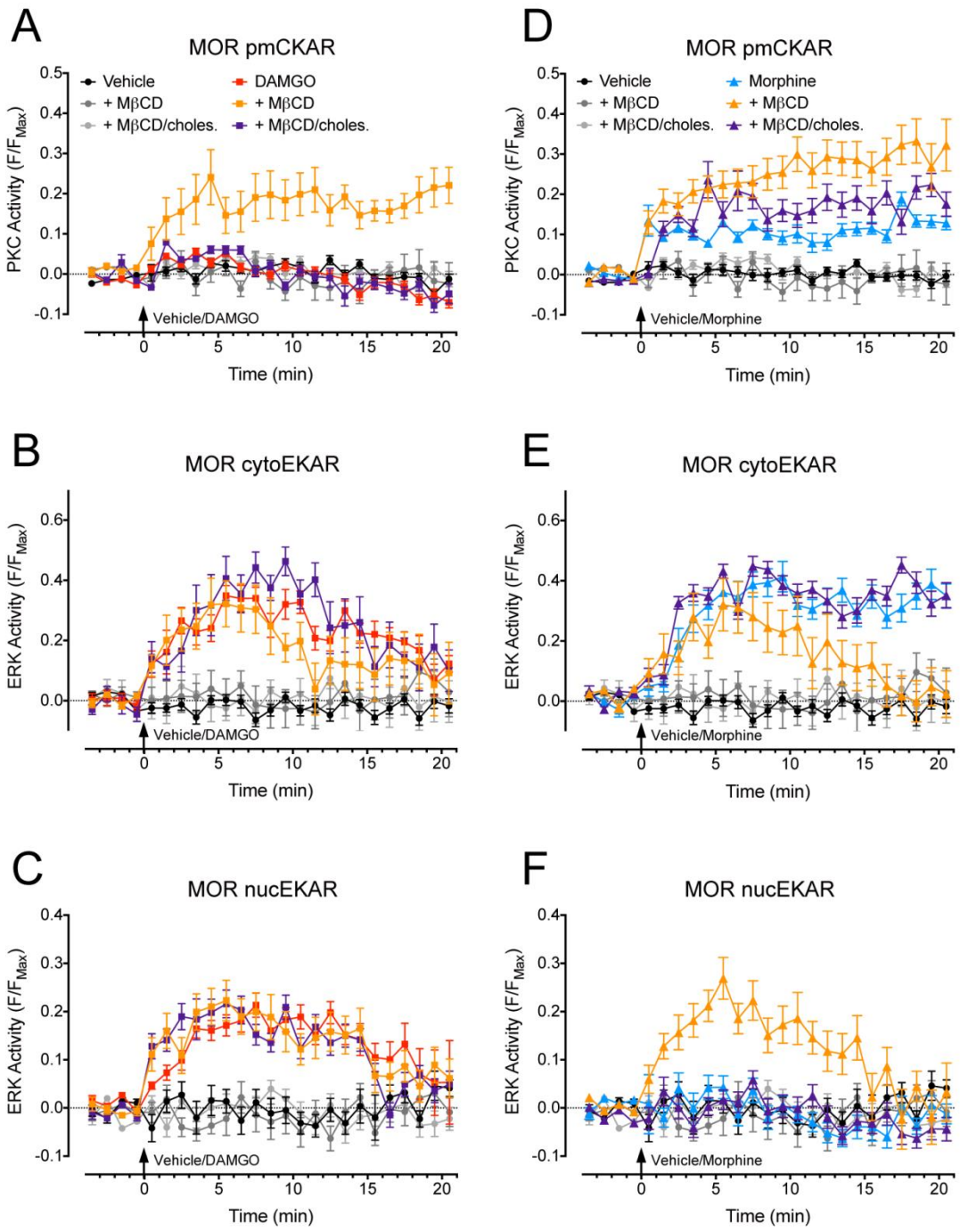

Figure 4.5: Disruption of membrane architecture alters MOP signalling profiles. Spatiotemporal activation of PKC and ERK following vehicle, DAMGO or morphine stimulation, with and without pre-treatment with MβCD or MβCD/cholesterol complexes (MβCD/choles.). (A) Plasma membrane PKC in response to DAMGO (40-174 cells). (B) CytoERK in response to DAMGO (30-167 cells). (C) NucERK in response to DAMGO (68-230 cells). (D) Plasma membrane PKC in response to morphine (41-195 cells). (E) CytoERK (32-194 cells) and (F) NucERK (80-217 cells) in response to morphine. Symbols represent means, error bars SEM.

4.4.5 MOP Compartmentalised Signalling in Dorsal Root Ganglia Neurons

To confirm the physiological relevance of the spatiotemporal signalling patterns of MOP when expressed in HEK293 cells, we nucleofected isolated neurons from mouse DRG with the FRET biosensors. DRG neurons are the principal mediators of nociception from the periphery to the spinal cord and activation of endogenous MOP in these neurons partially mediates the analgesic actions of opioids [766].

Activation of MOP in DRG neurons stimulated ERK and PKC activity with spatiotemporal profiles that were identical to those observed in HEK293 cells. DAMGO caused a transient increase in both cytosolic and nucERK, whereas morphine elicited a sustained increase in cytoERK and plasma membrane PKC (Figure 4.6A-B). Inhibition of PKC decreased the percentage of neurons that exhibited a sustained cytoERK response to morphine (from 75% to 49%), and increased the percentage of neurons that exhibited a transient cytoERK response (from 25% to 51%) (Figure 4.6D-E). There was no effect of PKC inhibition on the temporal profile of cytoERK following stimulation with DAMGO (Figure 4.6D-E). As observed in HEK293 cells, inhibition of PKC allowed morphine to activate nucERK (Figure 4.6F).

We also assessed the distribution of endogenous MOP at the plasma membrane of DRG neurons (Figure 4.6G) using GSD/TIRF microscopy. As in HEK293 cells, stimulation of endogenous MOP in DRG neurons with DAMGO increased the distance between detected events at the plasma membrane (Figure 4.6H-I). In contrast, there was no change in the distance between MOP events in response to morphine.

Thus, in DRG neurons, as in HEK293 cells, receptor redistribution at the plasma membrane correlates with transient increases in cytosolic and nucERK in response to DAMGO. Moreover, inhibition of PKC allows morphine to cause transient increases in cytosolic and nucERK. As such, the spatiotemporal regulation of MOP activation and signalling identified in recombinant expression systems also occurs in DRG neurons endogenously expressing this receptor.

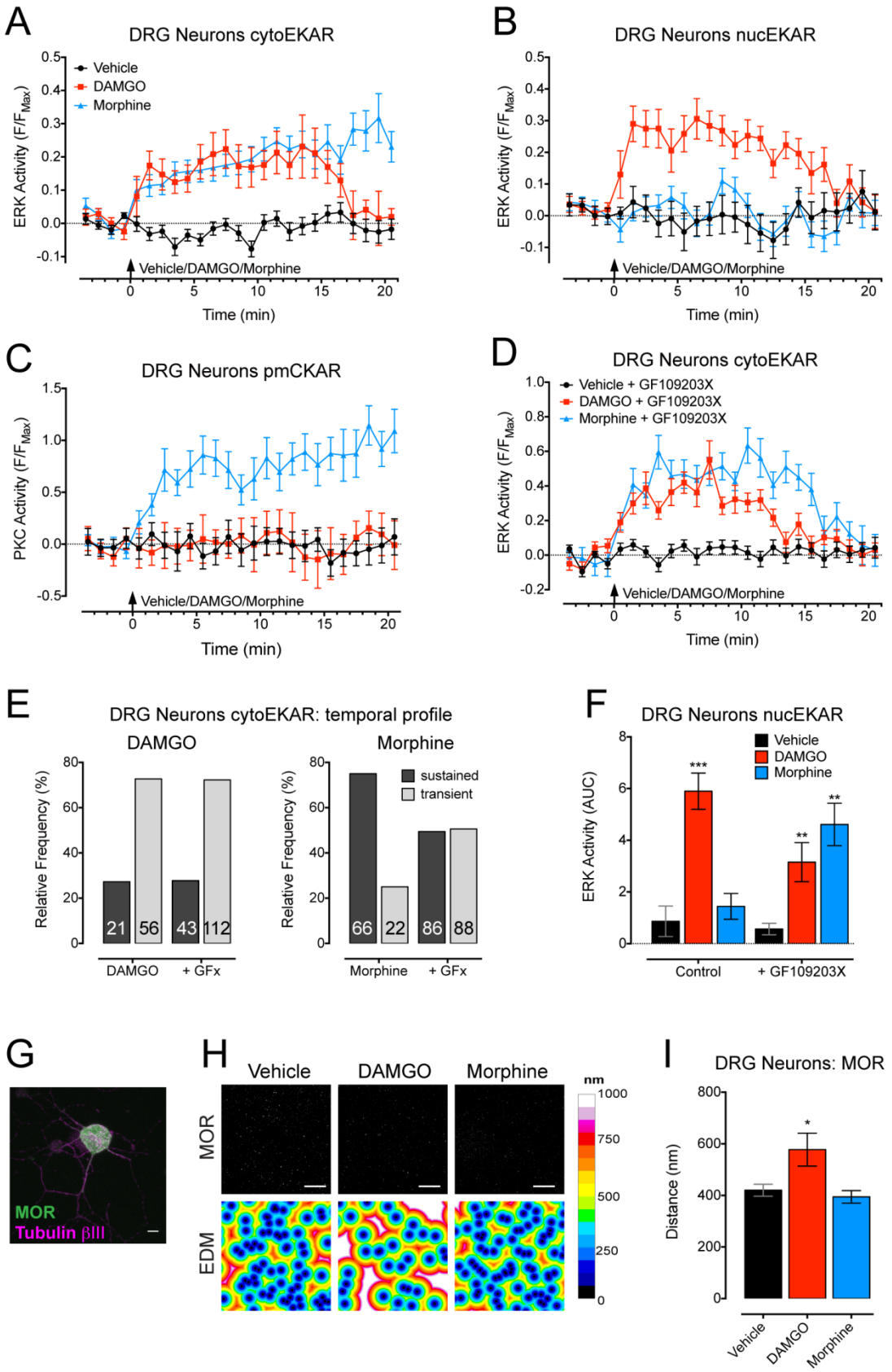

Figure 4.6: Spatiotemporal signalling of endogenous MOP in DRG neurons.
Spatiotemporal activation of (A) CytoERK (56-120 neurons), (B) NucERK (45-64 neurons) and (C) Plasma membrane-localised PKC (40-55 neurons) following vehicle, DAMGO or morphine stimulation. (D) Effect of PKC inhibition on cytoERK (86-99 neurons). (E) Population analysis of the temporal profile of cytoERK, with the number of neurons in each group indicated. (F) Effect of PKC inhibition on nucERK (25-73 neurons). (G-I) Plasma membrane distribution of

endogenous MOP in response to 10min vehicle, DAMGO or morphine using GSD/TIRF (n=9-15). (G) Isolated DRG neuron immunostained for MOP (green) and tubulin βIII (magenta). Scale bar 10μm. (H) Representative GSD/TIRF images and Euclidean distance maps (EDM). Scale bar 1μm. (I) Average distance to nearest neighbour. Bars/symbols represent means, error bars SEM. *p<0.05; **p<0.01 and ***p<0.001 versus vehicle control, two-way ANOVA with Tukey's multiple comparison test (F) or one-way ANOVA with Dunnett's multiple comparison test (I). AUC, area under the curve.

4.5 Discussion

The use of biophysical approaches to assess MOP signalling in real time and in live cells has revealed a new mechanism that contributes to the control of differential MOP activation. Here we show that DAMGO activation of MOP triggers receptor translocation within the plasma membrane. This translocation precedes receptor trafficking to clathrin-containing domains and internalisation and is likely dependent on receptor phosphorylation (Figure 4.7A). This MOP translocation, not receptor internalisation, determines the transient cytoERK profile and the activation of nucERK (Figure 4.7A). In contrast, morphine activates plasma membrane-localised PKCα, via $G_{\beta\gamma}$-subunits, which prevents receptor translocation within the plasma membrane. This results in sustained cytoERK and no nucERK activity (Figure 4.7B). Inhibition of this Gβγ-PKCα-phosphorylation pathway allows the morphine-activated MOP to translocate within the plasma membrane and transforms its spatiotemporal signalling profile (Figure 4.7B). Importantly, this new signalling profile mimics that of the internalising ligand DAMGO (i.e. transient cytosolic and nucERK) but occurs in the absence of β-arr2 recruitment and without receptor internalisation.

These results add essential detail to previous descriptions of ligand-dependent differences in ERK signalling [208, 520, 593]. Previous studies using immunoblotting showed that etorphine-induced ERK phosphorylation was dependent on β-arrs, whereas morphine activated ERK via a PKC-dependent pathway [208]. However, we show that upon PKC inhibition, morphine can still induce ERK phosphorylation, although this signal has different temporal dynamics and occurs both in the cytosol and the nucleus (Figure 4.3 and Figure 4.7B). Therefore, the activation of cytoERK by morphine is not PKC-dependent but rather PKC, by controlling MOP localisation, dictates the dynamics and location of this response. It is interesting to consider that in the context of a whole cell following solubilisation (with a relatively greater contribution of cytosolic compared to nucERK), this altered temporal profile could appear as an apparent *decrease* in morphine stimulated ERK. This illustrates the extra mechanistic detail that can be obtained by resolving spatial and temporal signalling dynamics in live cells. We therefore propose that plasma membrane organisation of MOP, not just β-arr recruitment and internalisation, dictates the spatiotemporal outcome of receptor activation. Importantly, these mechanisms operate in nociceptive neurons, and may thus contribute to the analgesic actions of opioids.

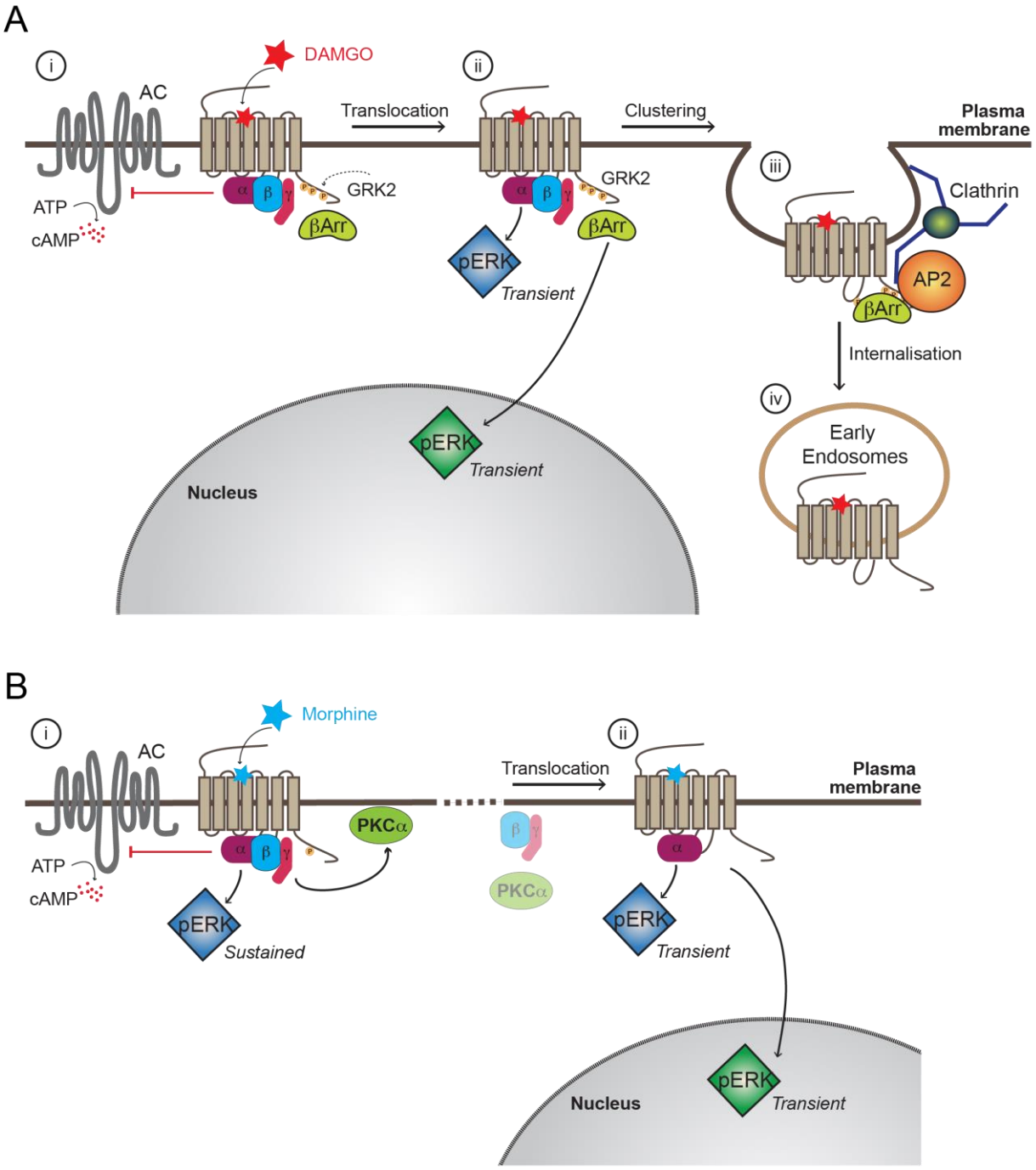

Figure 4.7: Plasma membrane localisation controls MOP spatiotemporal signalling.
(A) DAMGO causes recruitment of GRK2 and β-arr2 (i), facilitating MOP redistribution across the plasma membrane and transient activation of $G\alpha_{i/o}$-mediated cytoERK and $G\alpha_{i/o}$-independent nucERK (ii). Upon prolonged stimulation of MOP, DAMGO triggers MOP clustering and receptor internalisation via clathrin-coated pits (iii) to early endosomes (iv). (B) Morphine stimulates plasma membrane-localised Gβγ-PKCα that prevents receptor translocation within the plasma membrane. This causes a sustained activation of $G\alpha_{i/o}$-mediated cytoERK (i). Inhibition of the Gβγ-PKCα-pathway, or alteration of plasma membrane organisation facilitates MOP translocation and activation of nucERK by morphine (ii) without receptor internalisation.

The ability of DAMGO, but not morphine, to cause receptor redistribution may relate to differential patterns of MOP phosphorylation. While all opioids cause phosphorylation of MOP at Ser375, this is mediated by different kinases depending on the ligand [184, 543]. Previous studies have shown that the DAMGO-activated MOP is phosphorylated by GRKs 2 and 3 and that internalising ligands drive higher-order phosphorylation of flanking residues that result in efficient β-arr recruitment and receptor internalisation [184]. Here we show that recruitment of β-arr2, MOP translocation and activation of nucERK in response to DAMGO precede receptor internalisation. As such, we hypothesise that differential recruitment of regulatory proteins (GRKs, β-arrs) to MOP may underlie receptor redistribution at the plasma membrane, and thus indirectly control spatiotemporal signalling. This is supported by the fact that mutation of the key hierarchical phosphorylation site of MOP (MOP S375A) affects the localisation of the receptor within the plasma membrane and its spatiotemporal signalling. In this context, β-arrs are increasingly recognised as scaffolding proteins for signalling complexes, in addition to their traditional roles in the regulation of receptor desensitisation and internalisation [767]. Furthermore, recent evidence suggests that GRKs can also have important scaffolding functions, particularly for the control of ERK activation [768, 769]. We hypothesise that differential assembly of receptor kinases and other signalling mediators in response to morphine versus DAMGO stimulation of MOP determines receptor redistribution, transient signalling profiles and activation of nucERK. Importantly, this entails that the responses of opioid ligands will be highly dependent on the specific protein content of opioid-responsive cells [274, 525, 636, 770].

Our results also highlight the importance of PKCα in governing MOP spatiotemporal signalling profiles. Previous studies have shown that phosphorylation and desensitisation of MOP following morphine stimulation is partially dependent upon PKC [530, 543, 771]. Moreover, there are strong indications that PKC plays a significant role in the initiation and maintenance of tolerance to morphine analgesia [772, 773]. To date, evidence for morphine-induced activation of PKC comes from co-immunoprecipitation studies showing recruitment of over-expressed PKCε to MOP [593] and increased PKC activity in cell lysates [774]. By measuring endogenous PKC activity at the subcellular level, we directly demonstrate that morphine, but not DAMGO, stimulates a sustained activation of PKC at the plasma membrane. While PKC can phosphorylate MOP directly [554, 557], it can also phosphorylate proteins that participate in MOP signalling such as $G\alpha_i$ [564] or GRK2 [775] and could therefore restrict receptor redistribution by

modulating the function and/or association of such signalling and scaffolding proteins with MOP.

It is clear that plasma membrane organisation plays a critical role in the control of MOP spatiotemporal signalling. Whether MOP resides within biochemically-defined lipid-rich plasma membrane regions is controversial [776-778]. However, and in line with our findings, previous studies have provided evidence for a restricted plasma membrane localisation, and agonist-regulated plasma membrane diffusion of the MOP [779-782]. Protein-protein interactions were hypothesised to mediate the restricted and slow diffusion of agonist-stimulated non-internalising MOP [783]. Together with the results presented here, this suggests that the dynamic organisation of MOP within the plasma membrane, rather than MOP association with a pre-defined lipid-rich domain, may control ligand-dependent receptor redistribution and unique spatiotemporal signalling profiles. The dependence of MOP signalling on plasma membrane localisation extends recent studies demonstrating distinct control of spatiotemporal signalling by endosomally-localised GPCRs [221, 744]. In the context of MOP, mechanistic insight into the actions of morphine at the cellular level is of particular therapeutic relevance due to the severe side-effects induced by this opiate. Whether chronic exposure to opiates differentially alters spatiotemporal signalling and/or the plasma membrane distribution of MOP remains to be investigated.

CHAPTER 5

FINAL DISCUSSION

The phenomenon of biased agonism at GPCRs presents an invaluable approach for designing drugs with fewer “on-target” side effects. Design of a biased ligand requires delineation of the signalling pathways that produce the desired and unwanted physiological effects. Unfortunately, at the MOP this has proven to be an incredibly complicated task. These processes are both ligand-dependent and tissue-dependent, making it difficult to precisely establish the optimal pharmacological profile required to produce an improved analgesic devoid of side effects and with limited analgesic tolerance. Whilst there is evidence that the therapeutic profile of opioids can be improved by optimising ligand bias towards G protein activation over β-arr2 recruitment, a more comprehensive approach to bias optimisation, involving multiple signalling pathways, is required to truly maximise the benefits of a biased MOP ligand. Hence, a clearer understanding of how biased agonism can be used to fine tune MOP mediated physiological processes is required.

Up till now, studies of biased agonism have predominantly focussed on synthetic opioids, whereas the potential for bias within the endogenous opioid system has been overlooked. With such a large number of ligands targeting a few classical opioid receptors, the endogenous opioid peptides are ideal candidates for establishing how MOP naturally employs biased agonism to control the normal functioning of opioid-mediated physiological processes. A comprehensive analysis of biased agonism of the endogenous ligands at the MOP was examined in chapter 2. The most diversity in biased agonism profiles, compared to the reference ligand DAMGO, is seen in the enkephalins and endomorphins, whereas the dynorphins and β-endo showed very little diversity in biased agonism profiles at the MOP, compared to DAMGO. This is not surprising since pharmacological and anatomical evidence clearly points to the enkephalins and the putatively endogenous endomorphins as being the primary mediators of MOP physiology. These endogenous peptides have the highest affinities and selectivities for the MOP [333, 334], and their distribution in the CNS and PNS overlaps very closely with the expression of the MOP [702, 784, 785]. With such variability between only a few enkephalins, it is likely that the other pENK derived peptides that were not included in this study, such as Met-enk-RGL and metorphamide (Table 1.1) may also possess unique biased agonism profiles at the MOP.

Interestingly, nearly all the Leu-enk based endogenous peptides, including Leu-enk and all pDYN derived peptides except α-neo, showed the same biased agonism profile compared to DAMGO. This is possibly due to the fact that, as shown by Wieberneit,

Korste, Albada, Metzler-Nolte and Stoll [611], Leu-enk may only be able to bind to the MOP in a single conformation. This is in contrast to the DOP, where Leu-enk was shown to adopt two conformations, suggesting that these opioids may display unique bias profiles at DOP. Additionally, since the distribution of the pDYN derived peptides mainly overlaps with the expression of KOP, dynorphins are also likely to show more diversity at this receptor subtype. Whilst pDYN is predominantly expressed in regions distinct from those expressing MOP, there are areas where MOP and pDYN expression overlap, such as in the medulla, the DH of the spinal cord and myenteric neurons in the GI tract [338, 448, 784, 786], where dynorphins, and in particular α-neo with its unique bias profile, may play a distinctive role in control of MOP mediated physiology. A similar study to that presented here examining biased agonism of endogenous peptides at DOP and KOP needs to be performed to establish a complete picture of biased agonism within the opioid system.

Altogether, the heterogeneity in biased agonism profiles within the endogenous opioid peptides, combined with their differing selectivities and potencies for the various opioid receptors, discrete expression patterns, different degradation rates and the potential of differential proteolytic processing of precursor proteins in different tissues [476, 478], indicates that particular endogenous opioids may play specific roles in regulating opioid receptor-mediated physiology. To validate this, and establish links between specific signalling pathways and physiological effects, the biased agonism profiles of endogenous opioids need to be confirmed *in vivo*. However, there are many difficulties involved in *in vivo* validation of biased agonism profiles obtained in recombinant cell lines [720]. These difficulties include variables that can affect the quantification of biased agonism in different systems and were explored in detail in chapter 3. Quantification of biased agonism in different cell backgrounds revealed the cell-dependent nature of biased agonism, where even alteration of the expression of a single signalling effector altered the biased agonism profile of a ligand. This feature of biased agonism will be particularly problematic when attempting to optimise the bias profile of a ligand, as the bias profile may change in different tissues due to different expression of effector and regulatory proteins. Despite this added complexity, the cell-dependent nature of biased agonism could also be an advantage. When both the desired physiological effects and the side effects are produced via the same or similar signalling pathways in different tissues, a ligand with a highly cell-dependant bias profile may be exactly what is required to obtain a tissue-specific response.

In some cases, changes in bias between cell backgrounds were relatively small, such as the bias observed between activation of different Gα subtypes, where bias factors of around 0.5 $\Delta\Delta\log(\tau/K_A)$ ie ~3-fold, were common for most ligands. Although this still remains to be tested, a ligand with such a small bias factor would not be expected to produce significantly different physiological effects compared to the reference ligand *in vivo* [247, 251, 719]. However, it needs to be considered that these experiments required overexpression of individual G protein subunits in recombinant cells. Since, in similar experiments where GRK2 overexpression resulted in loss of endo-1 bias between AC inhibition and β-arr, this suggests that overexpression of a signalling effector may artificially obscure the bias of a ligand. In addition to this, small differences in G protein subtype activation may be amplified in some cell types due to the G protein subtype specific regulation, such as subtype specific AC inhibition or deactivation by distinct RGSs [701, 787]. Consequently biased G protein-activation may have a more significant impact on downstream signalling in primary cell types than anticipated, although to date there is very little evidence to support this [710, 723, 788]. Thus, the potential for differential activation of downstream signalling effectors by G protein subtypes needs further investigation. In any case, the small degree of bias observed between activation of Gα subtypes in this study may be enough to have a significant impact on the quantification of bias in different cell backgrounds, thereby influencing the selection of lead compounds when screening for biased ligands.

Another factor that may significantly affect the physiological outcomes of biased agonism is the spatiotemporal characteristics of the distinct signalling pathways. “When” and “where” a signalling effector is activated has a significant effect on the overall cellular response. The spatiotemporal activation of ERK and PKC by morphine and DAMGO previously characterised in HEK293 cells [789] was validated in cultured DRGs in chapter 4. Since ERK activation in different cellular compartments is associated with phosphorylation of different ERK substrates [208], and is also involved in ligand-dependent and tissue specific MOP desensitisation and tolerance [594, 633, 638], these differential patterns of ERK activation are likely to have a significant impact on the physiological effects of the ligands. This clearly demonstrates that the activation of the same signalling effector by different ligands doesn’t necessarily result in production of the same overall cellular effects. The same principle may also apply to the activation of other signalling pathways where ligands show differential spatiotemporal signalling, such as the differential cAMP inhibition kinetics by Met-enk-RF observed in chapter 3.

As biased agonism is most commonly examined at single time-points, the ligand-dependent spatiotemporal patterns of bias may be obscured. Such an important facet of the consequences of biased agonism is generally overlooked.

Biased agonism and signalling kinetics are also known to be dependent on the binding kinetics of the ligand [727, 790-792]. Unfortunately there is very limited information about binding kinetics of endogenous opioids for MOP, hence any connection between differential binding kinetics and biased agonism by endogenous opioids remains to be established. Of particular interest, will be the effect of binding kinetics on receptor trafficking and endosomal signalling. Efficient MOP recycling has been proposed as a potential mechanism that protects against the development of tolerance [653, 793, 794]. Receptor recycling requires dissociation of the ligand-receptor-β-arr complex [795, 796], and it has been well established that ligands with slow dissociation rates stimulate prolonged receptor internalisation and signalling [222, 797, 798], which is most likely the explanation for the prolonged duration of action and MOP internalisation that is observed with loperamide [799].

It is unknown whether all endogenous opioids are co-internalised with the receptor, however since endo-1 and synthetic opioid peptides are internalised with the receptor, this is most likely to be the case [800-802]. At other neuropeptide receptors endosomal trafficking of the receptor has been shown to be controlled by the membrane metalloendopeptidase endothelin-converting enzyme 1 (ECE-1) which degrades the neuropeptide ligand enabling recycling and resensitisation of the receptor [235, 803, 804]. Furthermore, at the SSTR2A the endogenous ligands somatostatin-14 and -28 have been shown to stimulate different rates of SSTR2A recycling as a result of differential susceptibility to degradation by ECE-1 [235]. Therefore, differential degradation of endogenous opioids by ECE-1 or other endosomal peptidases to control MOP recycling and resensitisation may be another mechanism for controlling MOP function.

There are also several aspects of biased agonism at MOP which remain to be explored that may further complicate translation of *in vitro* bias studies *in vivo*. These aspects include the potential for species specificity of biased agonism, such as that observed at KOP [738]. Another important aspect of biased agonism at MOP that remains to be established is how the development of cellular tolerance affects biased agonism. Since ligands differentially stimulate mechanisms of tolerance, potentially in a tissue specific

manner, the bias of a ligand is likely to change significantly in tolerant cells and tissue. In addition to this, some MOP splice variants show different signalling properties, for instance MOP1, MOP1A, and MOP1B recycle at different rates [729, 805], hence the presence of different MOP splice variants in various tissues may alter observations of biased agonism. Similarly, MOP is reported to form heterodimers with several GPCRs including DOP and α2AR among others in specific tissues [806, 807], and these interactions have been shown to alter MOP ligand binding and signalling properties [807-809]. As a result, the presence of these heterodimers in different tissues may affect biased agonism.

There are currently other strategies being explored in addition to biased agonism to achieve MOP-mediated analgesia with fewer side effects. These strategies include agonists that specifically target MOP heterodimers involved in nociception, such as the MOP/DOP heterodimer specific ligand CYM51010, which produces similar analgesic properties to morphine but with less analgesic tolerance [810]. Similarly, mixed efficacy ligands such as those with MOP agonist and DOP antagonist activity also show the potential to produce analgesia with less dependence and tolerance [811, 812]. Another alternative being investigated is to directly inhibit signalling pathways that mediate the side effects. For example, it has been demonstrated in knock-in mice expressing a RGS-insensitive $G\alpha_o$ that inhibition of RGS GAP activity may enhance morphine-induced analgesia [813]. Finally, the recent discovery of allosteric modulators of MOP presents another promising strategy to improve opioid therapeutics. Allosteric modulators at MOP could reduce the unwanted side effects by selectively enhancing (or inhibiting) particular signalling pathways activated by orthosteric drugs, or by enhancing the activity of the endogenous opioid system [652, 814]. In any case, biased agonism should always be an important consideration when designing improved opioid analgesics using each of these approaches.

Altogether, these aspects considered above will make it very complex to predict the actions of biased ligands *in vivo*. One way to minimise complications arising from many of these factors that affect biased agonism observations is to expand the number signalling pathways examined when quantifying biased agonism. With such pluridimensional bias profiles, the unique signalling characteristics of a ligand are far more likely to be captured in the study. Unfortunately, the cell-dependent nature of biased agonism means we cannot directly predict biased agonism *in vivo* in every tissue from *in vitro* assays in recombinant cells. However, whilst pluridimensional bias profiles

change in different cell backgrounds and under different experimental conditions, the uniqueness of the ligands can be maintained across different systems. Therefore, bias profiles can instead be used to predict *in vivo* bias indirectly through ligand clustering. To do this, the *in vivo* bias of ligands that produce enhanced analgesia with less side effects need to be clearly established. The endogenous opioids are ideal candidates for this as they have shown great diversity in biased agonism profiles, further investigation into how endogenous opioids naturally use biased agonism to control opioid physiology will hopefully reveal an endogenous ligand that mainly mediates analgesia with little activation of side effects. Such a ligand could then be used as a reference ligand to screen for new compounds with similar bias profiles, enabling optimisation of safer and more effective opioid analgesics.

In summary, this study has illustrated that the opioid family of peptides possess a diverse range of signalling profiles at MOP. The diversity in bias among endogenous opioids may enable the endogenous opioid system to have an unprecedented level of control to fine-tune MOP mediated physiology. This enhanced understanding of biased agonism within the endogenous opioid family will assist with identification of the optimal biased agonism profile required to design improved opioid analgesics. This study has also provided valuable insights into the complexities involved in quantification of biased agonism at GPCRs, including the spatiotemporal kinetics of the signalling pathways and cell-dependant nature of biased agonism, which will have implications on the design of future studies of biased agonism at GPCRs.

APPENDIX A SUPPLEMENTARY DATA

A.1 Supplementary Data From "Biased Agonism of Endogenous Opioid Peptides at the μ-Opioid Receptor"

Table A.1: Summary of potencies for reference ligands and endogenous opioids in CHO-MOP

	[^{35}S] GTPγS		cAMP		pERK		β-Arr1		β-Arr2		KRas	
	LogEC50	SEM	LogEC50	SEM	LogEC50	SEM	LogEC50	SEM	LogEC50	SEM	LogEC50	SEM
DAMGO	-8.50	0.11	-7.37	0.10	-8.39	0.10	-6.54	0.11	-6.60	0.13	-6.98	0.21
Morphine	-7.80	0.12	-8.49	0.14	-7.40	0.12	NC	NC	-7.29	0.35	NC	NC
Loperamide	-9.84	0.10	-6.99	0.13	-8.85	0.10	-6.96	0.11	-7.04	0.15	-7.32	0.30
Leu-enk	-8.09	0.14	-7.03	0.11	-7.89	0.06	-5.99	0.21	-6.01	0.10	-6.55	0.30
Met-enk	-8.31	0.16	-7.62	0.12	-8.34	0.08	-6.21	0.13	-6.65	0.08	-6.26	0.27
Met-enk-RF	-8.71	0.16	-7.29	0.13	-8.86	0.10	-6.73	0.16	-7.02	0.07	NC	NC
Endo-1	-8.16	0.07	-6.81	0.08	-8.87	0.10	-6.47	0.22	-7.38	0.15	-6.69	0.30
Endo-2	-8.11	0.14	-7.03	0.19	-8.75	0.10	-7.13	0.11	-7.13	0.09	-6.36	0.21
α-Neo	-7.71	0.12	-8.59	0.16	-7.25	0.05	-5.47	0.15	-5.50	0.11	-6.34	0.41
β-Endo	-8.55	0.17	-8.11	0.14	-7.71	0.09	-5.52	0.15	-6.24	0.10	-6.68	0.30
DynA	-8.33	0.15	NC	NC	-7.52	0.08	-5.65	0.17	-5.99	0.12	-6.48	0.46
DynA 1-13	-8.04	0.11	NC	NC	-7.66	0.07	-6.03	0.22	-6.48	0.12	-6.14	0.26
DynA 1-8	-8.10	0.12	-6.86	0.12	-7.88	0.07	-6.04	0.21	-6.07	0.16	-5.52	0.24
DynA 1-6	-8.60	0.10	-7.37	0.12	-8.16	0.07	-6.34	0.17	-6.04	0.12	-6.04	0.22
DynB	-8.06	0.11	-6.94	0.12	-7.50	0.10	-5.82	0.13	-5.89	0.08	-6.27	0.40

NC = LogEC50 value for not calculated as a full concentration response curve could not be obtain

Table A.2: Summary of bias factors in CHO-MOP. *p ≤0.05 **p≤0.005 as determined by two-tailed t-test compared to DAMGO

	cAMP				pERK				[^{35}S]GTPγS				β-Arr1				β-Arr2				Internalisation			
	$LogτK_A$	SEM	$ΔLogτK_A$	SEM	$LogτK_A$	SEM	$ΔLogτK_A$	SEM	$LogτK_A$	SEM	$ΔLogτK_A$	SEM	$LogτK_A$	SEM	$ΔLogτK_A$	SEM	$LogτK_A$	SEM	$ΔLogτK_A$	SEM	$LogτK_A$	SEM	$ΔLogτK_A$	SEM
DAMGO	7.117	0.156	0.000	0.221	8.354	0.058	0.000	0.082	8.437	0.126	0.000	0.178	6.183	0.137	0.000	0.194	6.473	0.097	0.000	0.137	6.824	0.202	0.000	0.286
Morphine	6.932	0.110	-0.185	0.191	7.433	0.084	-0.921	0.102	7.388	0.126	-1.049	0.178	NC	NC	NC	NC	6.413	0.260	-0.060	0.278	NC	NC	NC	NC
Loperamide	8.634	0.113	1.517	0.193	8.837	0.068	0.483	0.089	9.987	0.126	1.550	0.178	6.470	0.167	0.287	0.216	7.019	0.096	0.546	0.137	7.460	0.210	0.636	0.291
Leu-enk	6.876	0.110	-0.241	0.191	7.968	0.061	-0.386	0.084	8.213	0.126	-0.224	0.178	5.580	0.167	-0.603	0.216	6.035	0.096	-0.438	0.137	6.385	0.208	-0.439	0.290
Met-enk	7.538	0.114	0.421	0.193	8.334	0.045	-0.020	0.073	8.037	0.126	-0.400	0.178	6.141	0.127	-0.042	0.187	6.384	0.107	-0.089	0.144	6.594	0.184	-0.230	0.273
Met-enk-RF	7.396	0.113	0.279	0.193	8.772	0.068	0.418	0.089	8.571	0.126	0.134	0.178	6.365	0.138	0.182	0.195	6.870	0.097	0.397	0.137	NC	NC	NC	NC
β-Endo	6.750	0.112	-0.367	0.192	7.704	0.050	-0.650	0.077	8.079	0.126	-0.358	0.178	5.495	0.139	-0.688	0.195	6.196	0.085	-0.277	0.129	6.725	0.206	-0.099	0.289
Endo-1	8.613	0.113	1.496	0.193	8.877	0.062	0.523	0.085	8.095	0.129	-0.342	0.180	6.127	0.228	-0.056	0.266	7.355	0.111	0.882	0.147	6.666	0.208	-0.158	0.290
Endo-2	8.031	0.110	0.914	0.191	8.834	0.073	0.480	0.093	8.194	0.126	-0.243	0.178	6.764	0.204	0.581	0.246	6.793	0.120	0.320	0.154	6.688	0.207	-0.136	0.289
DynA	NC	NC	NC	NC	7.465	0.043	-0.889	0.072	8.413	0.126	-0.024	0.178	5.484	0.125	-0.699	0.186	6.022	0.096	-0.451	0.137	6.263	0.205	-0.561	0.288
DynA 1-13	NC	NC	NC	NC	7.727	0.056	-0.627	0.080	8.139	0.126	-0.298	0.178	5.937	0.140	-0.246	0.196	6.268	0.111	-0.205	0.147	5.820	0.160	-1.004	0.258
DynA 1-8	6.794	0.111	-0.323	0.192	7.946	0.067	-0.408	0.088	7.920	0.126	-0.517	0.178	5.550	0.196	-0.633	0.239	6.061	0.096	-0.412	0.137	5.991	0.174	-0.833	0.267
DynA 1-6	7.275	0.112	0.158	0.192	8.234	0.066	-0.120	0.088	8.692	0.126	0.255	0.178	6.134	0.190	-0.049	0.234	6.068	0.096	-0.405	0.137	6.694	0.207	-0.130	0.289
DynB	6.905	0.110	-0.212	0.191	7.556	0.067	-0.798	0.089	8.011	0.126	-0.426	0.178	5.551	0.167	-0.632	0.216	5.790	0.085	-0.683	0.129	6.078	0.200	-0.746	0.284
α-Neo	7.140	0.110	0.023	0.191	7.279	0.049	-1.075	0.076	7.603	0.136	-0.834	0.185	5.301	0.168	-0.882	0.217	5.333	0.097	-1.140	0.137	5.760	0.179	-1.064	0.270

	cAMP - pERK		cAMP - [^{35}S]GTPγS		cAMP - β-Arr1		cAMP - β-Arr2		[^{35}S]GTPγS - pERK		cAMP - Int		[^{35}S]GTPγS - Int		pERK - β-Arr1		pERK - β-Arr2		[^{35}S]GTPγS - Barr1		[^{35}S]GTPγS - β-Arr2		β-Arr1 - β-Arr2		Int - pERK		Int - β-Arr1		Int - β-Arr2	
	$ΔΔLogτK_A$	SEM	$ΔΔLogτK_A$	SEM	$ΔΔLogτK_A$	SEM	$ΔΔLogτK_A$	SEM	$ΔΔLogτK_A$	SEM	$ΔΔLogτK_A$	SEM	$ΔΔLogτK_A$	SEM	$ΔΔLogτK_A$	SEM	$ΔΔLogτK_A$	SEM	$ΔΔLogτK_A$	SEM	$ΔΔLogτK_A$	SEM	$ΔΔLogτK_A$	SEM	$ΔΔLogτK_A$	SEM	$ΔΔLogτK_A$	SEM	$ΔΔLogτK_A$	SEM
DAMGO	0.000	0.235	0.000	0.284	0.000	0.294	0.000	0.260	0.000	0.196	0.000	0.361	0.000	0.337	0.000	0.211	0.000	0.160	0.000	0.264	0.000	0.225	0.000	0.238	0.000	0.298	0.000	0.346	0.000	0.317
Morphine	0.736*	0.216	0.864*	0.261	NC	NC	-0.125	0.337	-0.128	0.205	NC	NC	NC	NC	NC	NC	0.861	0.296	NC	NC	-0.989*	0.330	NC	NC	NC	NC	NC	NC	NC	NC
Loperamide	1.034**	0.212	-0.033	0.262	1.23*	0.289	0.971*	0.236	1.067**	0.199	0.881	0.349	0.914	0.341	0.196	0.234	0.063	0.163	1.263*	0.280	1.004**	0.225	0.259	0.256	-0.153	0.305	-0.349	0.363	-0.090	0.322
Leu-enk	0.145	0.209	-0.017	0.261	0.362	0.289	0.197	0.235	0.162	0.197	0.198	0.348	0.215	0.341	0.217	0.232	-0.052	0.160	0.379	0.280	0.214	0.225	0.165	0.256	0.053	0.302	-0.164	0.362	0.001	0.321
Met-enk	0.441	0.206	0.821*	0.263	0.463	0.269	0.510	0.241	-0.380	0.192	0.651	0.335	-0.170	0.326	0.022	0.201	-0.069	0.162	-0.358	0.258	-0.311	0.229	-0.047	0.236	0.210	0.283	0.188	0.331	0.141	0.309
Met-enk-RF	-0.139	0.212	0.145	0.263	0.097	0.274	-0.118	0.236	-0.284	0.199	NC	NC	NC	NC	0.236	0.214	-0.021	0.163	-0.048	0.264	-0.263	0.225	0.215	0.238	NC	NC	NC	NC	NC	NC
β-Endo	0.283	0.207	-0.009	0.262	0.321	0.274	-0.090	0.231	0.292	0.194	-0.268	0.347	-0.259	0.339	0.038	0.210	0.373	0.150	0.330	0.264	-0.081	0.220	0.411	0.234	-0.551	0.299	-0.589	0.348	-0.178	0.316
Endo-1	0.973	0.211	1.838**	0.264	1.552*	0.329	0.614	0.243	-0.865*	0.200	1.654**	0.348	-0.184	0.341	0.579	0.280	0.359	0.170	-0.286	0.322	-1.224**	0.233	0.938*	0.304	0.681	0.302	0.102	0.394	1.040*	0.325
Endo-2	0.434**	0.212	1.157*	0.261	0.333	0.311	0.594	0.245	-0.723*	0.201	1.05*	0.347	-0.107	0.340	-0.101	0.263	-0.160	0.180	-0.824	0.304	-0.563	0.235	-0.261	0.290	0.616	0.304	0.717	0.380	0.456	0.328
DynA	NC	NC	NC	NC	NC	NC	NC	NC	0.865*	0.192	NC	NC	0.537	0.338	-0.190	0.199	0.438	0.155	0.675	0.257	0.427	0.225	0.248	0.231	-0.328	0.297	-0.138	0.342	0.110	0.319
DynA 1-13	NC	NC	NC	NC	NC	NC	NC	NC	0.329	0.195	NC	NC	0.706	0.313	-0.381	0.212	0.422	0.168	-0.052	0.265	-0.093	0.231	0.041	0.245	0.377	0.270	0.758	0.324	0.799	0.297
DynA 1-8	0.085	0.211	0.194	0.262	0.310	0.307	0.089	0.235	-0.109	0.199	0.510	0.329	0.316	0.321	0.225	0.255	-0.004	0.163	0.116	0.298	-0.105	0.224	0.221	0.276	0.425	0.281	0.200	0.359	0.421	0.300
DynA 1-6	0.278	0.211	-0.097	0.262	0.207	0.303	0.563	0.236	0.375	0.199	0.288	0.347	0.385	0.340	-0.071	0.250	-0.285	0.163	0.304	0.294	0.660*	0.225	-0.356	0.271	0.010	0.302	0.081	0.372	-0.275	0.320
DynB	0.586*	0.211	0.214	0.261	0.420	0.288	0.471	0.231	0.372	0.199	0.534	0.343	0.320	0.336	-0.166	0.234	0.115	0.157	0.206	0.280	0.257	0.220	-0.051	0.252	-0.052	0.298	0.114	0.357	0.063	0.312
α-Neo	1.098**	0.206	0.857*	0.266	0.905**	0.289	1.163**	0.235	0.241	0.200	1.087*	0.331	0.230	0.328	-0.193	0.230	-0.065	0.157	0.048	0.286	0.306	0.231	-0.258	0.257	-0.011	0.280	0.182	0.347	-0.076	0.303

Table A.3: Percentage contribution to the overall variance by principle components

PC1 = 56.09 %

PC2 = 25.83 %

PC3 = 12.82 %

PC4 = 4.55 %

PC5 = 0.69 %

PC6 = 0.0 %

Table A.4: Summary of the contribution by each bias factor to the principle components

	cAMP-pERK	cAMP-GTPyS	cAMP-β-arr1	cAMP-β-arr2	GTPyS-pERK	cAMP-Kras	KRas-GTPyS	KRas-β-arr2	pERK-β-arr1	pERK-β-arr2	GTPyS-β-arr1	GTPyS-β-arr2	β-arr1-β-arr2	KRas-pERK	KRas-β-arr1
PC1	-0.091	-0.481	-0.161	-0.058	0.390	-0.323	0.158	-0.070	-0.034	0.320	0.424	-0.104	-0.232	-0.162	-0.266
PC2	0.407	0.146	0.464	0.375	0.260	0.396	0.250	0.057	0.032	0.318	0.228	0.089	-0.010	-0.067	0.022
PC3	0.042	0.056	-0.226	0.322	-0.013	0.170	0.114	-0.268	-0.280	-0.282	0.267	-0.548	0.127	0.396	-0.153
PC4	-0.324	-0.259	-0.054	-0.160	-0.065	0.175	0.434	0.270	-0.164	0.205	0.099	0.106	0.499	0.229	0.335
PC5	-0.230	0.101	0.195	0.245	-0.330	-0.111	-0.211	0.425	-0.475	0.094	0.145	-0.051	0.119	-0.305	-0.356
PC6	0.675	0.224	-0.250	-0.446	-0.052	-0.204	0.074	0.092	-0.273	0.089	0.113	-0.034	0.259	-0.103	-0.027
PC7	0.373	-0.612	0.129	0.098	-0.533	0.012	0.149	-0.009	-0.074	0.046	-0.274	-0.046	-0.225	0.121	-0.057
PC8	-0.066	0.370	0.001	0.235	-0.172	-0.540	0.145	-0.083	-0.045	0.447	-0.050	0.055	-0.200	0.420	0.175
PC9	-0.037	0.032	-0.539	0.233	-0.184	0.312	-0.123	-0.245	0.020	0.476	-0.138	-0.093	0.044	-0.402	0.169
PC10	0.110	-0.159	0.040	0.461	0.138	-0.452	0.126	-0.211	-0.037	-0.296	-0.127	0.137	0.422	-0.330	0.234
PC11	-0.050	-0.084	0.466	-0.233	-0.092	-0.099	-0.310	-0.368	0.196	0.312	0.005	-0.390	0.423	0.020	-0.034

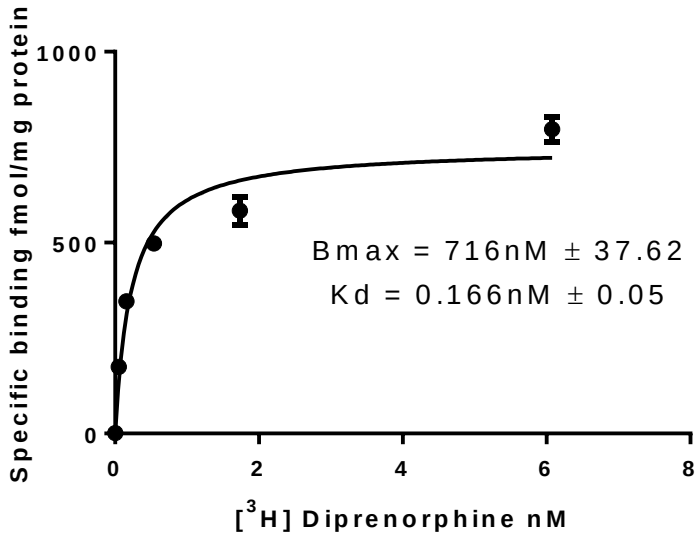

Figure A.1: [^{3}H] Diprenorphine saturation binding in FlpIn CHO-MOP membrane

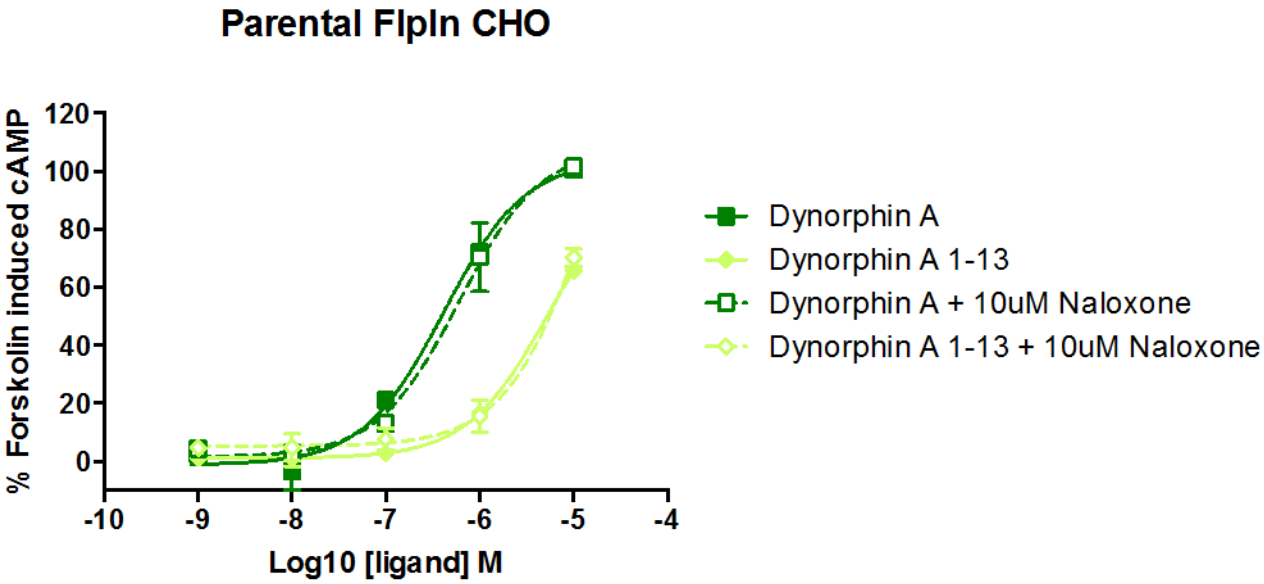

Figure A.2: DynA and DynA 1-13 increase cAMP production in Parental FlpIn CHO cells and this response is not blocked by Naloxone.

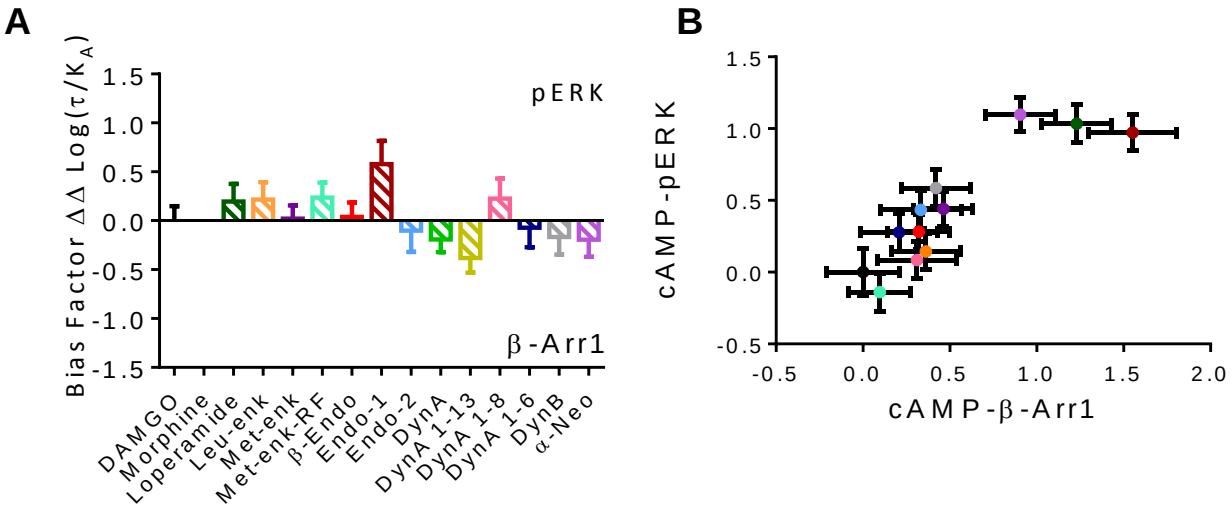

Figure A.3: Bias towards β-arr recruitment determines pERK bias.
(A) BIAS FACTORS BETWEEN PERK AND B-ARR1 IN CHO-MOP. NC = NOT CALCULABLE (B) TWO-TAILED PEARSON CORRELATION WAS CALCULATED BETWEEN BIAS FACTORS FOR CAMP-B-ARR1 AND CAMP-PERK EXCLUDING MORPHINE.

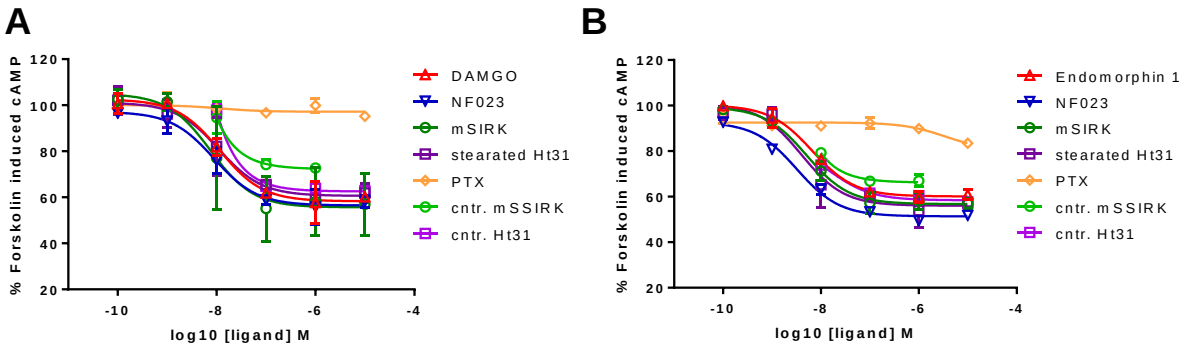

Figure A.4: cAMP assays in FlpIn CHO-MOP.
Cells were pre incubated with inhibitors for 45mins with 20μM Stearated Ht31 (AKAP inhibitor) or control peptide, 30mins with 5μM mSIRK (Gβγ inhibitor) or control peptide, or overnight with 25ng/ml PTx. n=1 in triplicate

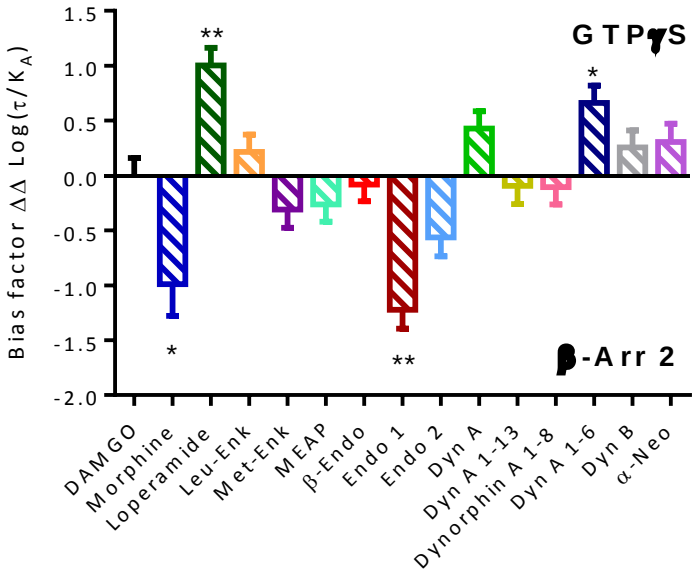

Figure A.5: Bias factors between β-arr2 recruitment and [^{35}S]GTPγS binding in CHO-MOP

A.2 Supplementary Data From "Plasma Membrane Localisation of the μ-Opioid Receptor Controls Spatiotemporal Signalling"

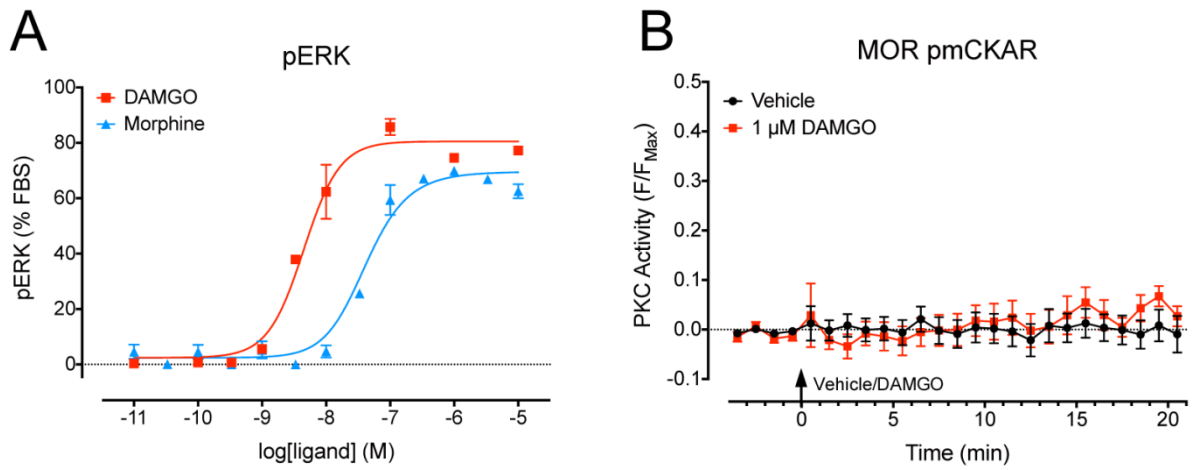

Figure A.6: (A) Concentration-response curves for activation of pERK using the AlphaScreen assay (n=3). (B) Plasma membrane-localised PKC activity in response to a high concentration of DAMGO (71-79 cells). Symbols represent means, error bars SEM; vehicle is shown in black, DAMGO in red, morphine in blue.

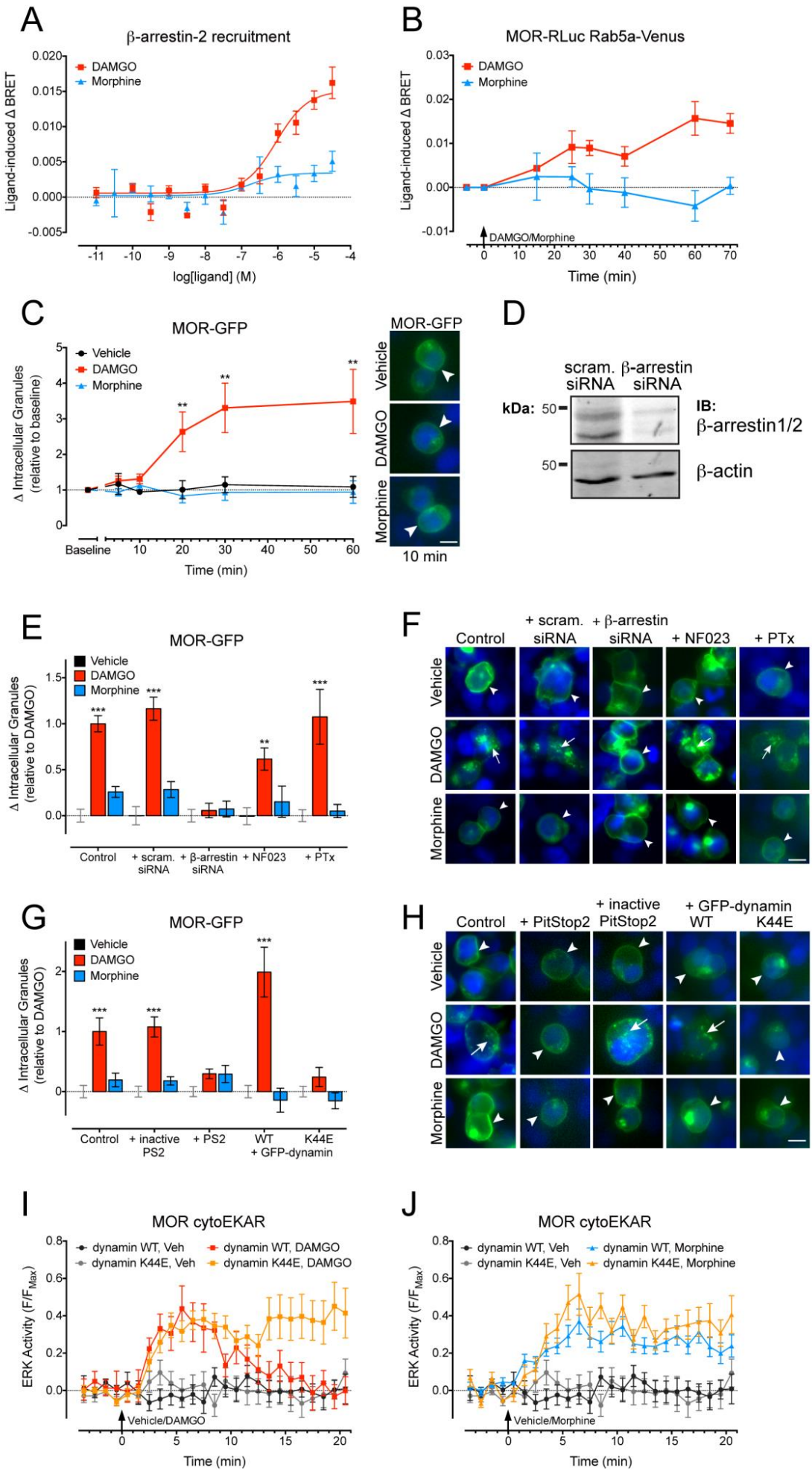
A
β-arrestin-2 recruitment
DAMGO
Morphine
Ligand-induced Δ BRET
log[ligand] (M)
B
MOR-RLuc Rab5a-Venus
DAMGO
Morphine
Ligand-induced Δ BRET
DAMGO/Morphine
Time (min)
C
MOR-GFP
Vehicle
DAMGO
Morphine
Δ Intracellular Granules (relative to baseline)
Baseline
Time (min)
MOR-GFP
Vehicle
DAMGO
Morphine
10 min
D
scram. siRNA
β-arrestin siRNA
kDa:
IB:
β-arrestin1/2
β-actin
E
MOR-GFP
Vehicle
DAMGO
Morphine
Δ Intracellular Granules (relative to DAMGO)
Control
+ scram. siRNA
+ β-arrestin siRNA
+ NF023
+ PTx
F
Control
+ scram. siRNA
+ β-arrestin siRNA
+ NF023
+ PTx
Vehicle
DAMGO
Morphine
G
MOR-GFP
Vehicle
DAMGO
Morphine
Δ Intracellular Granules (relative to DAMGO)
Control
+ inactive PS2
+ PS2
WT + GFP-dynamin
K44E
H
Control
+ PitStop2
+ inactive PitStop2
+ GFP-dynamin WT
K44E
Vehicle
DAMGO
Morphine
I
MOR cytoEKAR
dynamin WT, Veh
dynamin WT, DAMGO
dynamin K44E, Veh
dynamin K44E, DAMGO
ERK Activity (F/F_Max)
Vehicle/DAMGO
Time (min)
J
MOR cytoEKAR
dynamin WT, Veh
dynamin WT, Morphine
dynamin K44E, Veh
dynamin K44E, Morphine
ERK Activity (F/F_Max)
Vehicle/Morphine
Time (min)

Figure A.7: (A) Concentration-response curves for β-arr2 recruitment (n=3). Timecourse of (B) BRET between MOP-RLuc and Rab5a-Venus (n=3). And (C) MOP-GFP internalisation (n = 4-6). Inset: representative images. Scale bar 10μm. (D) Knockdown of β-arrs using siRNA. (E) MOP-GFP internalisation following knockdown of β-arrs or $G\alpha_{i/o}$ protein inhibition (n=4-6). (F) Representative images from E. Scale bar 10μm. (G) MOP-GFP internalisation following inhibition of endocytosis (n=4-12). (H) Representative images from G. Scale bar 10μm. (I) Effect of inhibition of dynamin on the cytoERK response to DAMGO (22-57 cells). (J) Effect of inhibition of dynamin on the cytoERK response to morphine (22-61 cells). Bars/symbols represent means, error bars SEM; vehicle is shown in black, DAMGO in red, morphine in blue. Arrowheads indicate cell surface MOP, arrows intracellular MOP. **p<0.01 and ***p<0.001 versus vehicle control, two-way ANOVA with multiple comparison tests. Scram., scrambled; IB, immunoblot; PS2, PitStop2.

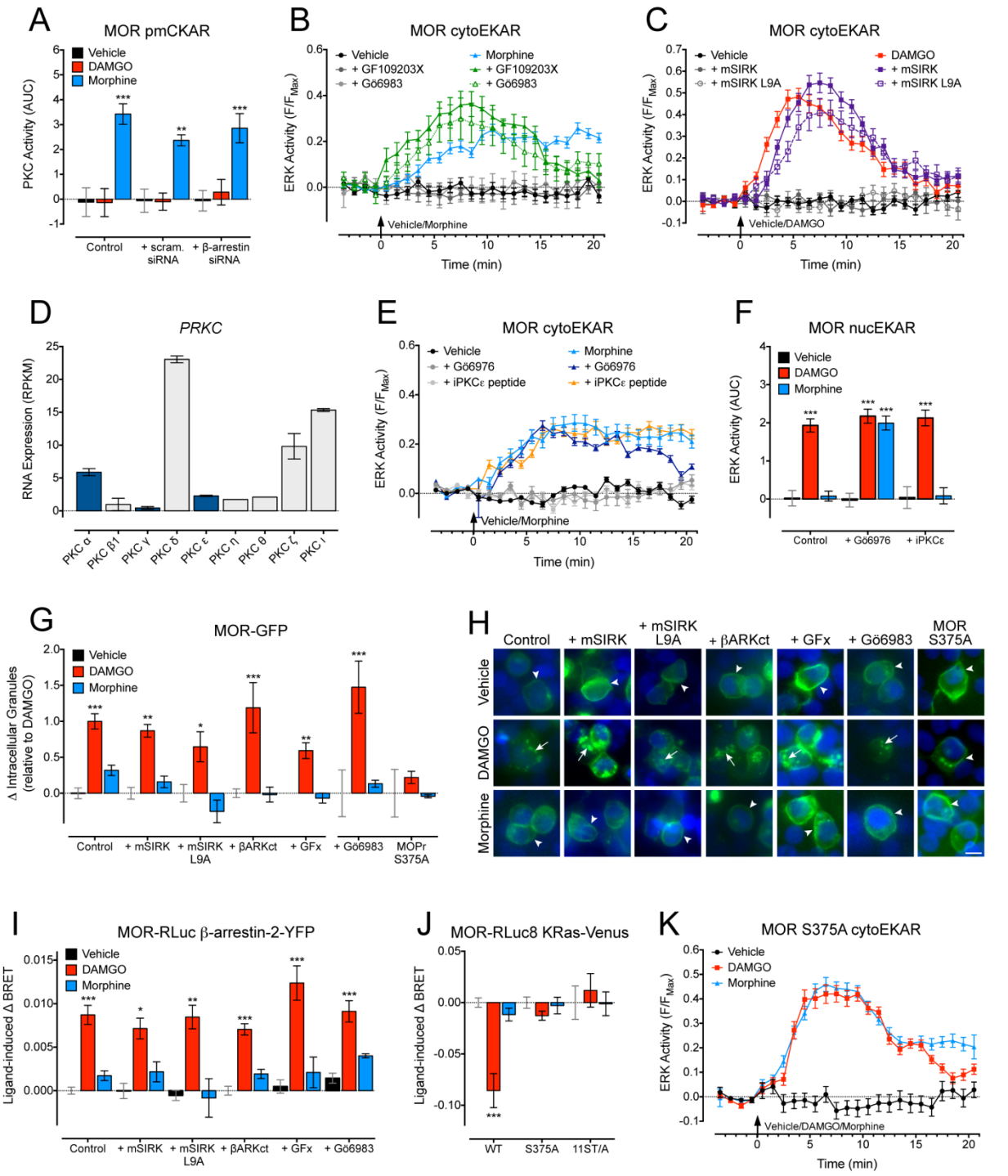

Figure A.8: (A) Effect of β-arr knockdown on plasma membrane PKC activity (37-86 cells). (B) Effect of PKC inhibition on the cytoERK response to morphine (22-108 cells). (C) Effect of Gβγ inhibition on the cytoERK response to DAMGO (26-69 cells). (D) MOP-GFP internalisation following inhibition of Gβγ or PKC, or over-expression of MOPphos (n=3). (E) MOP-RLuc β-arr2-YFP BRET following inhibition of Gβγ or PKC, or over-expression of MOPphos-RLuc (n=3). (F) Representative images from D. Scale bar 10μm. (G) CytoERK activation by MOPphos (63-116 cells). Bars/symbols represent means, error bars SEM; vehicle is shown in black, DAMGO in red, morphine in blue. Arrowheads indicate cell surface MOPr, arrows intracellular MOPr. *p<0.05, **p<0.01 and ***p<0.001 versus vehicle control, two-way ANOVA with multiple comparison tests. Scram., scrambled; GFx, GF109203X.

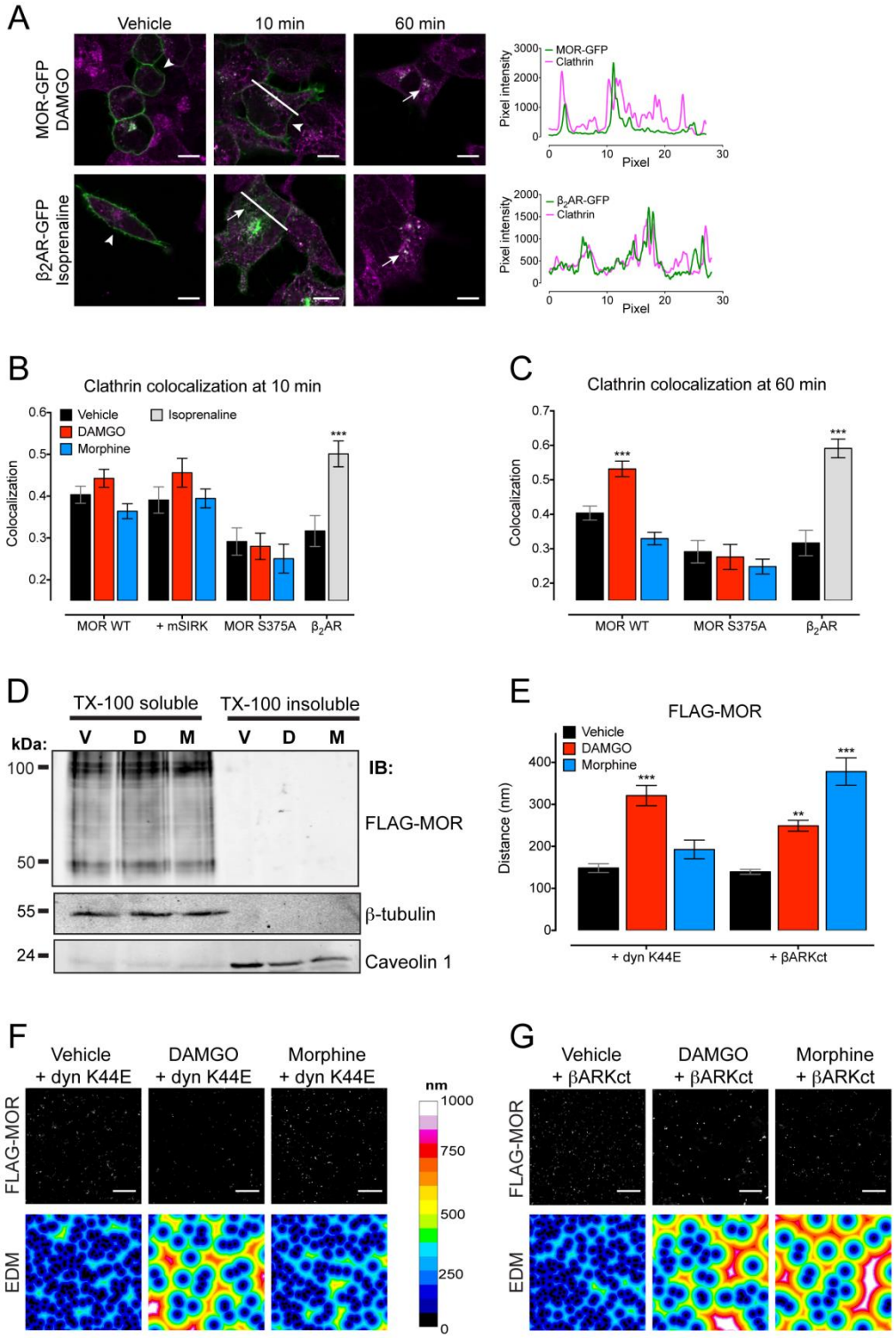

Figure A.9: (A) Representative images showing colocalisation of MOP-GFP or β2AR-GFP (green) with clathrin (purple). Scale bar 10μm. Inset line scan showing pixel intensity across the indicated section following 10min stimulation with 1μM DAMGO or Isoprenaline. (B) Colocalisation of MOP-GFP or β2AR-GFP with clathrin following 10min stimulation. (C) Colocalisation of MOP-GFP or β2AR-GFP with clathrin following 60min stimulation. (D) FLAG-MOP localisation in Triton X-100 soluble or insoluble membrane domains following fractionation and western blotting. Caveolin 1 and β-tubulin were used as markers for Triton X-100 insoluble and soluble domains, respectively. (E-G) FLAG-MOPr distribution at the plasma membrane using GSD/TIRF. (E) Average distance to nearest neighbour following inhibition of dynamin-

dependent endocytosis or Gβγ-subunits (n=3). (F) Representative GSD/TIRF images and Euclidean Distance maps following inhibition of dynamin-dependent endocytosis. Scale bar 1µm. (G) Representative GSD/TIRF images and Euclidean Distance maps following inhibition of Gβγ-subunits. Scale bar 1µm. Pseudocolour scale as in E. Bars/symbols represent means, error bars SEM; vehicle is shown in black, DAMGO in red, morphine in blue. Arrowheads indicate cell surface MOPr, arrows intracellular MOPr. ***$p<0.001$ versus vehicle control, two-way ANOVA with multiple comparison tests. TX-100, triton X-100; V, vehicle; D, DAMGO; M, morphine; IB, immunoblot; Dyn, dynamin; EDM, Euclidean distance map.

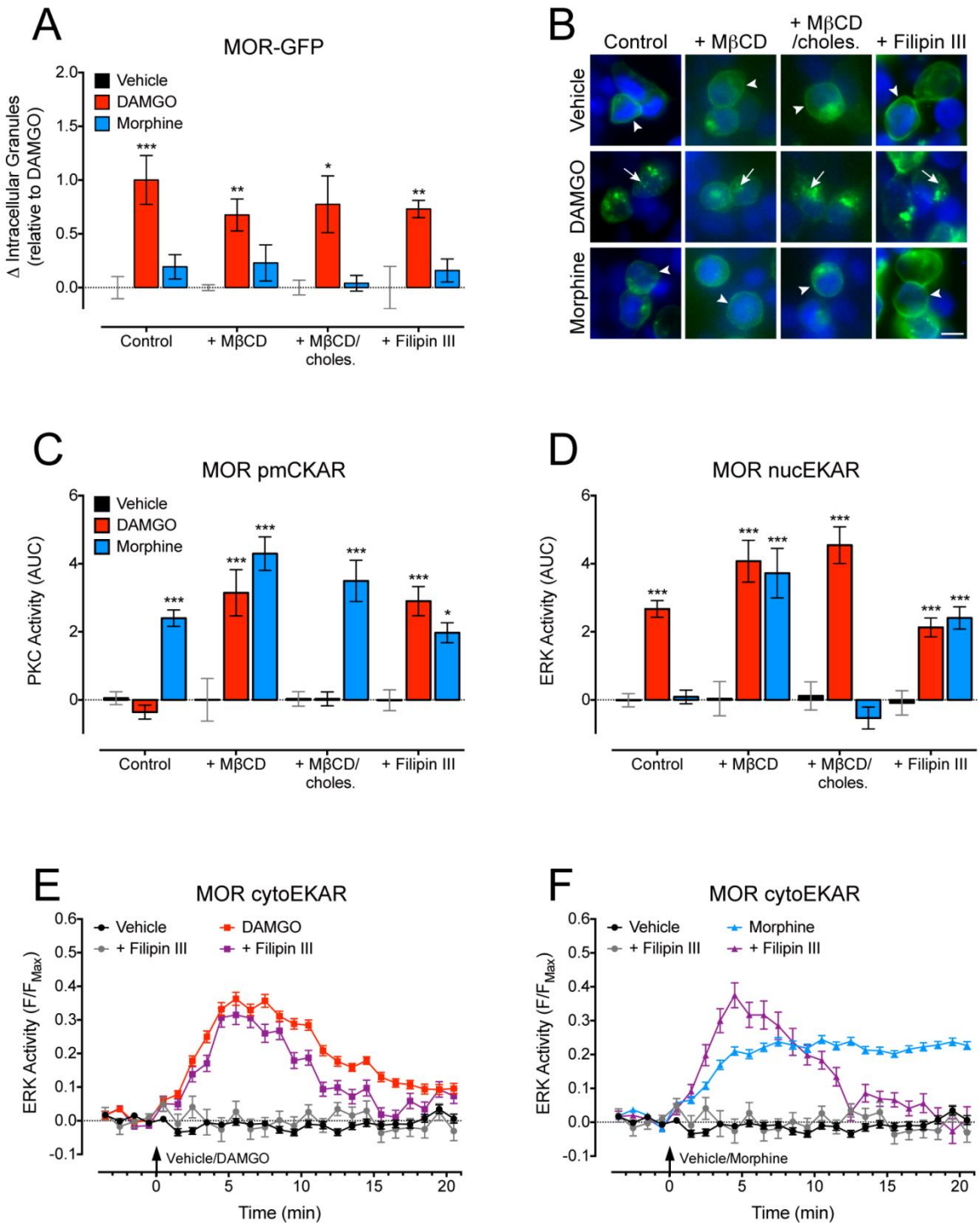

Figure A.10: (A) MOPr-GFP internalisation following disruption of the plasma membrane architecture (n=3). (B) Representative images from A. Scale bar 10μm. (C) Plasma membrane-localised PKC activation following disruption of the plasma membrane architecture (44-192 cells). (D) NucERK activity following disruption of the plasma membrane architecture (80-233 cells). (E) CytoERK activity in response to DAMGO in the presence of Filipin III (30-167 cells). (F) CytoERK activity in response to morphine in the presence of Filipin III (32-194 cells). Bars/symbols represent means, error bars SEM; vehicle is shown in black, DAMGO in red and morphine in blue. Arrowheads indicate cell surface MOPr, arrows intracellular MOP. *p<0.05, **p<0.01 and ***p<0.001 versus vehicle control, two-way ANOVA with multiple comparison tests. AUC, area under the curve; MβCD/choles., MβCD/cholesterol complexes.

APPENDIX B PUBLICATIONS

B.1 Biological redundancy of the endogenous GPCR ligands in the gut and the potential for endogenous functional selectivity

frontiers in PHARMACOLOGY

REVIEW ARTICLE
published: 28 November 2014
doi: 10.3389/fphar.2014.00262

Biological redundancy of endogenous GPCR ligands in the gut and the potential for endogenous functional selectivity

Georgina L. Thompson[1], Meritxell Canals[1] and Daniel P. Poole[1,2] *

[1] Drug Discovery Biology, Monash Institute of Pharmaceutical Sciences, Parkville, VIC, Australia
[2] Department of Anatomy and Neuroscience, The University of Melbourne, Parkville, VIC, Australia

Edited by:
Dominique Massotte, Institut des Neurosciences Cellulaires et Intégratives, France

Reviewed by:
Jakub Fichna, Medical University of Lodz, Poland
Pamela J. Hornby, Johnson & Johnson, USA

***Correspondence:**
Daniel P. Poole, Drug Discovery Biology, Monash Institute of Pharmaceutical Sciences, 381 Royal Parade, Parkville, VIC 3052, Australia
e-mail: daniel.poole@monash.edu

This review focuses on the existence and function of multiple endogenous agonists of the somatostatin and opioid receptors with an emphasis on their expression in the gastrointestinal tract. These agonists generally arise from the proteolytic cleavage of prepropeptides during peptide maturation or from degradation of peptides by extracellular or intracellular endopeptidases. In other examples, endogenous peptide agonists for the same G protein-coupled receptors can be products of distinct genes but contain high sequence homology. This apparent biological redundancy has recently been challenged by the realization that different ligands may engender distinct receptor conformations linked to different intracellular signaling profiles and, as such the existence of distinct ligands may underlie mechanisms to finely tune physiological responses. We propose that further characterization of signaling pathways activated by these endogenous ligands will provide invaluable insight into the mechanisms governing biased agonism. Moreover, these ligands may prove useful in the design of novel therapeutic tools to target distinct signaling pathways, thereby favoring desirable effects and limiting detrimental on-target effects. Finally we will discuss the limitations of this area of research and we will highlight the difficulties that need to be addressed when examining endogenous bias in tissues and in animals.

Keywords: biased agonism, enteric nervous system, G protein-coupled receptor, somatostatin, somatostatin receptor, opioid, opioid receptor

ENDOGENOUS BIASED AGONISM

The last decade has witnessed the experimental confirmation of previous theoretical concepts demonstrating that GPCRs exist in many temporally related micro-conformations (Deupi and Kobilka, 2010). Mechanistically, this inherent plasticity is in line with recent biophysical studies indicating that GPCRs can adopt multiple active states that can be differentially stabilized by chemically distinct classes of ligands (Hofmann et al., 2009; Bokoch et al., 2010). Such plasticity allows GPCRs to mediate a spectrum of acute signaling and longer-term regulatory behaviors that can be activated in a ligand-specific manner. Indeed, it is now established that different agonists do not uniformly activate all cellular signaling pathways linked to a given receptor. Rather, different ligands binding to the same receptor stabilize distinct receptor conformations linked to different signaling pathways and physiological outcomes. This paradigm whereby different ligands, binding to the same GPCR in an identical cellular background, promote distinct receptor conformational states linked to a different functional outcome has been termed *biased agonism* or *functional selectivity*. Therapeutically, biased agonism provides new avenues for the development of drugs that are not only receptor-specific but also 'pathway-specific.' As such it has opened the field to the discovery of ligands that selectively activate signaling pathways mediating desired physiological effects whilst minimizing 'on-target' side-effects that are elicited by activation of other signaling pathways *via* the same receptor.

To date, most descriptions of biased agonism have focused on the differential effects of synthetic drugs. However, there are several functionally important GPCR families that bind to multiple endogenous agonists [for example chemokine, somatostatin (SST), and opioid receptors (ORs)]. Although this has been traditionally attributed to the redundancy of some biological systems, biased agonism could represent an added layer of control to engender finely tuned physiological responses. Indeed, recent reports have already highlighted the potential for functional selectivity across the chemokine receptor family (Rajagopal et al., 2013; Zweemer et al., 2014).

In this focused review we provide an overview of the existing literature regarding two of these GPCR families with multiple endogenous peptide ligands, opioids and SST, in the context of the gastrointestinal tract (GIT). The opioid system is a prototypical example of potential biological redundancy, and it also represents one of the first examples where functional selectivity of synthetic drugs has been reported in the context of gut physiology. On the other hand, SST receptors are therapeutic targets in treating GI disease (e.g., diarrhea, bleeding varices, neuroendocrine tumors) and SSTs and related peptides also represent a well-characterized system where multiple endogenous ligands of the same receptor exist within the GIT (Zhao et al., 2013). Importantly, these two receptor systems also reveal different mechanisms that can explain distinct physiological outcomes derived from activation of the same receptor by different ligands.

THE SOMATOSTATIN SYSTEM OF THE GUT

There are five members of the SST receptor family ($SSTR_{1-5}$) and their distribution in the GIT has been recently reviewed (Van Op den Bosch et al., 2009).

Somatostatin, originally known as somatotropin release-inhibiting factor (SRIF), was first identified and characterized as a cyclic tetradecapeptide (Brazeau et al., 1973). It was predicted that SST-14 was a product of a larger peptide precursor and that other forms with potential biological activity were likely to exist. Indeed, it is now known that SST arises from maturation of preprosomatostatin (PPSST), and that all PPSST derivatives originate from the *SST* gene. The removal of a 24 amino acid signal sequence forms prosomatostatin (PSST), which is further C-terminally cleaved to form the biologically active peptides SST-14, SST-25, and SST-28 (Bohlen et al., 1980; Esch et al., 1980; Brazeau et al., 1981). SST-28, the longest peptide, was identified and characterized as an N-terminally extended variant of SST-14 (Pradayrol et al., 1978, 1980; Bohlen et al., 1980) and biological conversion of SST-28 to SST-14 was later confirmed (Zingg and Patel, 1983). Other cleavage products arising from PSST processing include PSST(1–32; Schmidt et al., 1985) and PSST(1–64; Bersani et al., 1989), for which little information regarding function and expression is available.

N-terminal cleavage of PSST also occurs, but the resulting peptides do not contain the SST-14 sequence and are therefore not considered to be SSTs (Benoit et al., 1990). These include SST-28(1–12) and antrin, which contains amino acids 1–10 of PSST [PPSST(25–34)]. Antrin, first identified in the gastric antrum (Benoit et al., 1987), is present in all SST-producing tissues. However, a functional role for this peptide has yet to be ascribed. Most recently, a bioinformatics approach predicted the existence of a novel 13mer PPSST cleavage product [PPSST(31–43)], which was subsequently confirmed by immunoaffinity purification and called neuronostatin (Samson et al., 2008). Neuronostatin is encoded by PSST and is highly conserved across vertebrates. Unlike SST and cortistatin (CST, see below), neuronostatin is not cyclic and is amidated at the C-terminus.

Biological activity of SST variants is conferred through a common Phe-Trp-Lys-Thr (FWKT) motif within the C-terminus (amino acids 7–10; Patel and Srikant, 1997). This sequence is also present in non-SST peptides that share a high-degree of sequence homology with SST. These include CST and thrittene. CST and SST are encoded by distinct genes, and genetic deletion of SST has no effect on the expression of CST. CST is a derivative of the 112 amino acid preproCST (PPCST) precursor (de Lecea et al., 1996), which is converted to proCST by signal peptide cleavage, resulting in the formation of hCST17 and hCST29 (Puebla et al., 1999). CST shares 11 amino acids in common with SST-14 including residues required for interaction with SSTRs and two key cysteines that enable formation of the cyclic peptide structure (Francis et al., 1990). Although they share sequence homology, structure, and affinity for SSTRs, there are clear differences in the ability of CST and SST-14 to stimulate SSTR2 endocytosis and signaling (Liu et al., 2005). Notably, CST is significantly less effective at inhibiting cAMP production and promoting SSTR2 endocytosis. Furthermore, CST does not exclusively interact with SST receptors and can also activate the MrgX2 and GHS-R1a receptors. Whether there are CST variants or a CST-specific GPCR is unknown. Another endogenous peptide that shares extensive sequence homology with SST is thrittene [SST28(1–13)]. As with CST, thrittene is not derived from PSST and is a product of a distinct gene, as supported by the presence of thrittene-like immunoreactivity in PSST deficient mice (Ensinck et al., 2003). Moreover, thrittene and SST are expressed by distinct cell populations and their release is triggered in response to different stimuli (Ensinck et al., 2002). With the exception of these initial studies nothing is known of the functional role of thrittene, nor if thrittene plays an analogous or discrete role to that of SST. A summary of SST and SST-like peptides is presented in **Table 1**.

DISTRIBUTION OF ENDOGENOUS SSTR LIGANDS IN THE GI TRACT

The GIT is the major source of SST and SST is a regulator of many digestive functions. SSTRs are an important therapeutic target in the treatment of digestive disease. In addition to its established role as a neurotransmitter, SST also acts in a hormonal and paracrine manner to regulate gut function (Low, 2004; Van Op den Bosch et al., 2009).

Somatostatin is expressed by D-cells of the stomach and plays a well-defined role in the control of acid secretion. SST negatively regulates gastrin release from antral G cells and histamine release from enterochromaffin-like cells, and acts directly on parietal cells leading to an SSTR2-dependent inhibition of acid release (Walsh, 1988; Lloyd et al., 1997; Low, 2004). SST-14 within the intestinal wall is mainly expressed by enteric neurons and potentially by extrinsic primary spinal afferents (Traub et al., 1999), although this is still debated (Keast and De Groat, 1992). SST-14 is also produced by macrophages during infection or inflammation as part of an immunoregulatory circuit with SSTR2 (Weinstock and Elliott, 2000). SST-28- distribution appears to be more restricted and is primarily expressed by enteroendocrine D-cells (Ravazzola et al., 1983; Baskin and Ensinck, 1984), consistent with the predominant release of SST-28 from the mucosa (Baldissera et al., 1985).

Myenteric SST-immunoreactivity is localized to a subclass of descending inhibitory interneuron, where it is co-expressed with choline acetyltransferase (Portbury et al., 1995; Song et al., 1997). Physiologically, SST is involved in the migrating myoelectric complex in the jejunum (Abdu et al., 2002) and propagating contractions of the colon (Grider, 2003). These actions are mediated through the SSTR2 receptor, which is expressed by NOS-positive inhibitory motor neurons or descending interneurons (Allen et al., 2002). SST is also an inhibitor of gastric emptying and of gall bladder contractility. SST is expressed by submucosal cholinergic secretomotor/ non-vasodilator neurons (Mongardi Fantaguzzi et al., 2009) and hyperpolarizes submucosal neurons (Shen and Surprenant, 1993) probably *via* SSTR1 and SSTR2 (Foong et al., 2010). In the human intestine SST is expressed by putative intrinsic primary afferent neurons of the submucosal plexus (Beyer et al., 2013).

There is limited information regarding the distribution of 'non-SST' peptides in the gut. Relatively high mRNA expression for CST has been detected through the human GIT (Dalm et al., 2004). However, it should be noted that with the exception of pancreatic delta islet cells (Papotti et al., 2003) and potentially

Table 1 | Endogenous somatostatin (SST) peptide sequences (*sequence not confirmed).

Precursor	Peptide	Sequence
Prosomatostatin (PSST)	SST-28	Ser-Ala-Asn-Ser-Asn-Pro-Ala-Met-Ala-Pro-Arg-Glu-Arg-Lys-Ala-Gly-Cys-Lys-Asn-Phe-Phe-Trp-Lys-Thr-Phe-Thr-Ser-Cys
	SST-14	Ala-Gly-Cys-Lys-Asn-Phe-Phe-Trp-Lys-Thr-Phe-Thr-Ser-Cys-OH
	Neuronostatin (PPSST(31-43))	Leu-Arg-Gln-Phe-Leu-Gln-Lys-Ser-Leu-Ala-Ala-Ala-Ala-NH2
	Antrin (SST-25-34)	Ala-Pro-Ser-Asp-Pro-Arg-Leu-Arg-Gln-Phe-OH
	SST-25	Ser-Asn-Pro-Ala-Met-Ala-Pro-Arg-Glu-Arg-Lys-Ala-Gly-Cys-Lys-Asn-Phe-Phe-Trp-Lys-Thr-Phe-Thr-Ser-Cys
	SST-28(1–14)	Ser-Ala-Asn-Ser-Asn-Pro-Ala-Met-Ala-Pro-Arg-Glu-Arg-Lys
	SST-28(1–12)	Ser-Ala-Asn-Ser-Asn-Pro-Ala-Met-Ala-Pro-Arg-Glu
	PPST 1–64	Ala-Pro-Ser-Asp-Pro-Arg-Leu-Arg-Gln-Phe-Leu-Gln-Lys-Ser-Leu-Ala-Ala-Ala-Ala-Gly-Lys-Gln-Glu-Leu-Ala-Lys-Tyr-Phe-Leu-Ala-Glu-Leu-Leu-Ser-Glu-Pro-Asn-Gln-Thr-Glu-Asn-Asp-Ala-Leu-Glu-Pro-Glu-Asp-Leu-Ser-Gln-Ala-Ala-Glu-Gln-Asp-Glu-Met-Arg-Leu-Glu-Leu-Gln-Arg
	PSST 1–32	Ala-Pro-Ser-Asp-Pro-Arg-Leu-Arg-Gln-Phe-Leu-Gln-Lys-Ser-Leu-Ala-Ala-Ala-Ala-Gly-Lys-Gln-Glu-Leu-Ala-Lys-Tyr-Phe-Leu-Ala-Glu-Leu
Preprocortistatin	Cortistatin-14 (rat)	Pro-Cys-Lys-Asn-Phe-Phe-Trp-Lys-Thr-Phe-Ser-Ser-Cys-Lys
	Cortistatin-17 (human)	Asp-Arg-Met-Pro-Cys-Arg-Asn-Phe-Phe-Trp-Lys-Thr-Phe-Ser-Ser-Cys-Lys
	Cortistatin-29	H-Glu-Gly-Ala-Pro-Pro-Gln-Gln-Ser-Ala-Arg-Arg-Asp-Arg-Met-Pro-Cys-Arg-Asn-Phe-Phe-Trp-Lys-Thr-Phe-Ser-Ser-Cys-Lys-OH
Unknown	Thrittene (SST28(1–13))	Ser-Ala-Asn-Ser-Asn-Pro-Ala-Met-Ala-Pro-Arg-Glu-Arg*

activated inflammatory cells (Gonzalez-Rey et al., 2006), the distribution of CST within the gut remains unknown. Thrittene-like immunoreactivity has been detected in enteroendocrine cells and enteric neurons and this distribution is distinct to that for SST-14 and SST-28 (Ensinck et al., 2002). This is supported by the differential release of thrittene and SST in response to feeding (Ensinck et al., 2003). Antrin expression was originally believed to be restricted to gastric D-cells, where it is localized to SST-28(1–12) containing secretory granules (Ravazzola et al., 1989; Benoit et al., 1990). However, this was contradicted by Rabbani and Patel (1990), who demonstrated comparable expression of antrin in the jejunal mucosa and pancreas by radioimmunoassay and HPLC.

EVIDENCE FOR DIFFERENCES IN FUNCTION

At present there is little evidence for significant differences in the effects of endogenous SSTs on GI function, although this may reflect the limited endpoints that have been assayed. Exposure of enteric neurons to SST results in activation of inwardly rectifying K^+ currents and to hyperpolarization, leading to inhibition of contractile and secretory activity (Van Op den Bosch et al., 2009). Direct electrophysiological recordings demonstrate no apparent difference in the acute effects of SST-14 and SST-28 on submucosal neurons, with exposure to either agonist leading to hyperpolarization and to rapid desensitization of responses (Shen and Surprenant, 1993). Similarly, there was no significant difference in the SST-14, SST-25, and SST-28 mediated inhibition of contractile activity. These agonists cross-desensitized responses to each other, but not to acetylcholine, suggesting actions at the same receptor (McIntosh et al., 1986). However, there is evidence for differences in the *in vivo* effects of SST-14 and SST-28 on both the stomach and intestine. For example, studies examining the direct effects of SSTR activation on gut function showed that SST-14 is significantly more potent at inhibiting gastric acid secretion than SST-28, despite the longer plasma half-life of SST-28 (Hirst et al., 1982; Seal et al., 1982). Zhao et al. (2013) recently demonstrated that although SST-14 and SST-28 both stimulated endocytosis of SSTR2A in myenteric neurons, there were clear differences in receptor recycling. The apparent retention of SSTR2A following treatment of neurons with SST-28 was attributed to the greater resistance of this peptide to degradation by the endosomal endopeptidase endothelin-converting enzyme 1 (ECE-1). This study did not determine the consequences of this retention or prolonged endosomal SSTR2A signaling on gut function. Moreover, the possible biological activity of SST cleavage products resulting from ECE-1 activity was not examined. Intermediate products of both SST-14 (SST-1–10) and SST-28 (SST-1–24) retained the Phe-Trp-Lys-Thr motif at the extreme N-terminus and may represent novel SSTR agonists produced locally within endosomes. However, absence of a key N-terminal Cys residue suggests that these peptides lack the cyclopeptide structure characteristic of SSTs.

The existence of endogenous ligand bias has been examined at the SSTR2A. Comparison of the responses of SST-14, SST-28 and cortistatin has not showed any evidence of functional selectivity at this receptor. However, potential ligand bias has been suggested for the small molecule ligands that bind SSTR2A, albeit the quantification of this bias is lacking (Nunn et al., 2004; Liu et al., 2008;

Cescato et al., 2010). More recently, we have shown that SST-14 and SST-28 show distinct profiles of receptor trafficking upon internalization (Zhao et al., 2013). After incubation with SST-14, SSTR2A recycled to the plasma membrane, which required the activity of the endosomal peptidase ECE-1, and an intact Golgi. In contrast, SSTR2A activated by SST-28, octreotide, lanreotide, or vapreotide was retained within the Golgi and did not recycle. Although ECE-1 rapidly degraded SST-14, SST-28 was resistant to degradation, and ECE-1 did not degrade the synthetic SST analogs. Thus, although no apparent bias was observed at the level of receptor signaling events, SST-14 and SST-28 differ in the trafficking of the receptor upon internalization. The differential regulation of SSTR2A may explain the different physiological effects of endogenous agonists and could account for the long-lasting therapeutic actions and side effects of clinically used agonists.

THE OPIOID SYSTEM IN THE GUT

Opioids and opiates are agonists of the mu, delta and kappa ORs (MOPr, DOPr, and KOPr). The nociceptin receptor (NOPr) was the last ORs to be cloned and is grouped with the ORs based on their high degree of sequence homology and its low level binding of opioids. The pharmacology and function of ORs has been reviewed extensively and will not be covered in detail in this review (Waldhoer et al., 2004). All receptors are expressed by enteric neurons and other cell types in the GIT and are major regulators of gut function (Wood and Galligan, 2004; Galligan and Akbarali, 2014)

The endogenous ligands for ORs are a large family of at least 20 different small peptides. The endogenous peptides have been detected throughout the central and peripheral nervous system as well as in other tissues, with similar distribution to the ORs. They are involved in numerous physiological processes including nociception, reward processing, and GIT motility and secretion. The distribution and physiological effects of endogenous opioids in the GIT have been the most extensively studied. However, identifying regions where endogenous opioids are expressed and released under normal physiological conditions has been challenging due to the high susceptibility of the peptides to degradation. Additionally, most studies have used antibody-based methods that may not reliably distinguish between different opioid peptides due to their high structural similarity, or HPLC-based methods which provide no detail of the specific cell types that express these peptides. Further complications arise due to interspecific differences and region-dependent variations in expression along the GIT. Nonetheless, most of the endogenous opioids are present in the GIT, and in some cases the distribution and release from discrete regions of the GIT has been thoroughly characterized.

There are three major classes of endogenous opioids (enkephalins, dynorphins, and endorphins), which are synthesized by proteolytic cleavage of precursor proteins; pro-enkephalin, pro-dynorphin, and pro-opiomelanocortin (POMC), respectively. The peptides range from 5 to 30 amino acids in length, and share a common N-terminal tetrapeptide sequence Tyr-Gly-Gly-Phe, with either a Leu or Met in the fifth position. These peptides have varying affinities for all three ORs, but none are highly selective for one receptor subtype (Mansour et al., 1995; Janecka et al., 2004). There are also two additional putative endogenous peptides; endomorphin-1, and endomorphin-2, which are structurally unrelated to the typical opioid peptides and are most selective and potent for MOPr (Zadina et al., 1997). The gene or genes encoding the precursor proteins of endomorphins are unknown (Terskiy et al., 2007), although a *de novo* synthesis mechanism has been proposed as an alternative source (Ronai et al., 2009). The presence of endomorphins in the GIT has not been reported and will not be discussed further in this review.

DISTRIBUTION OF ENDOGENOUS OPIOID RECEPTOR LIGANDS IN THE GI TRACT

Screening of the longitudinal muscle-myenteric plexus of the guinea pig ileum by HPLC identified expression of enkephalins (enk: Leu-enk, Met-enk, Met-enk-Arg-Gly-Leu, Met-enk-Arg-Phe, Metorphamide, and BAM-18) and dynorphins [α-neoendorphin, β-neoendorphin, dynorphin A(1–8), and dynorphin B]. No detectable beta endorphin was present in these preparations (Corbett et al., 1988).

Enkephalins

The enkephalins have been the most widely studied opioid peptides in the GIT. Pro-enkephalin contains four copies of Met-enk and one each of Leu-enk, Met-enk-Arg-Phe, and Met-enk-Arg-Gly-Leu, and several additional opioid peptides may be formed by partial processing of the precursor protein (see **Table 2**; Noda et al., 1982). Expression of at least four enkephalin peptides (Leu-enk, Met-enk, Met-enk-Arg-Phe, and Met-enk-Arg-Gly-Leu) in the GIT has been confirmed (Hughes et al., 1977; Linnoila et al., 1978; Tang et al., 1982; Giraud et al., 1984). Immunohistochemical studies demonstrate expression throughout the human GIT, with highest levels detected in the *muscularis externa* (Polak et al., 1977; Ferri et al., 1986, 1988). A similar expression pattern has been observed in rodents (Keast et al., 1985). Enkephalin-derived peptides are mainly found in the cell bodies of myenteric neurons and in nerve fibers within the myenteric plexus and circular muscle (Elde et al., 1976; Jessen et al., 1980; Schultzberg et al., 1980; Furness et al., 1983). There is evidence that immunoreactivities for Leu-enk and Met-enk are expressed by distinct neuronal populations within the enteric nervous system (Linnoila et al., 1978; Larsson et al., 1979; Larsson and Stengaard-Pendersen, 1982). The morphology and distribution of Enk-containing myenteric neurons has been examined in detail. Approximately 23% of myenteric neurons express Enk-immunoreactivity (Furness et al., 1983). These are morphologically Dogiel Type I inhibitory or excitatory motor neurons and are also immunoreactive for ChAT and/or substance P (Furness et al., 1983; Bornstein et al., 1984; Costa et al., 1985; Pfannkuche et al., 1998). Leu-enk-positive myenteric neurons of the human intestine have been described morphologically as 'stubby neurons' and are proposed to represent motor neurons or ascending interneurons (Brehmer et al., 2005). Examples of OR and enkephalin labeling in the intestine are presented in **Figure 1**.

There are a small number of neurons that express enkephalin-immunoreactivity in the submucosal plexus and fibers in the mucosa (Furness et al., 1985; Keast et al., 1985; Pfannkuche

Table 2 | Endogenous opioid peptide sequences.

Precursor	Peptide	Sequence
Pro-Enkephalin	Leu-enkephalin	Tyr-Gly-Gly-Phe-Leu
	Met-enkephalin	Tyr-Gly-Gly-Phe-Met
	Met-enkephalin-Arg-Phe	Tyr-Gly-Gly-Phe-Met-Arg-Phe
	Met-enkephalin-Arg-Gly-Leu	Tyr-Gly-Gly-Phe-Met-Arg-Gly-Leu
	Metorphamide	Tyr-Gly-Gly-Phe-Met-Arg-Arg-Val
	BAM 12	Tyr-Gly-Gly-Phe-Met-Arg-Arg-Val-Gly-Arg-Pro-Glu
	BAM 18	Tyr-Gly-Gly-Phe-Met-Arg-Arg-Val-Gly-Arg-Pro-Glu-Trp-Trp-Met-Asp-Tyr-Gln
	BAM 22	Tyr-Gly-Gly-Phe-Met-Arg-Arg-Val-Gly-Arg-Pro-Glu-Trp-Trp-Met-Asp-Tyr-Gln-Lys-Arg-Tyr-Gly
	Peptide E	Tyr-Gly-Gly-Phe-Met-Arg-Arg-Val-Gly-Arg-Pro-Glu-Trp-Trp-Met-Asp-Tyr-Gln-Lys-Arg-Tyr-Gly-Gly-Phe-Leu
	Peptide F	Tyr-Gly-Gly-Phe-Met-Lys-Lys-Met-Asp-Glu-Leu-Tyr-Pro-Leu-Glu-Val-Glu-Glu-Glu-Ala-Asn-Gly-Gly-Glu-Val-Leu-Gly-Lys-Arg-Tyr-Gly-Gly-Phe-Met
Pro-Dynorphin	Dynorphin A	Tyr-Gly-Gly-Phe-Leu-Arg-Arg-Ile-Arg-Pro-Lys-Leu-Lys-Trp-Asp-Asn-Gln
	Dynorphin B	Tyr-Gly-Gly-Phe-Leu-Arg-Arg-Gln-Phe-Lys-Val-Val-Thr
	Big Dynorphin (Dyn A/B 1-32)	Tyr-Gly-Gly-Phe-Leu-Arg-Arg-Ile-Arg-Pro-Lys-Leu-Lys-Trp-Asp-Asn-Gln-Lys-Arg-Tyr-Gly-Gly-Phe-Leu-Arg-Arg-Gln-Phe-Lys-Val-Val-Thr
	Dynorphin A 1–13	Tyr-Gly-Gly-Phe-Leu-Arg-Arg-Ile-Arg-Pro-Lys-Leu-Lys
	Dynorphin A (1–8)	Tyr-Gly-Gly-Phe-Leu-Arg-Arg-Ile
	Dynorphin A (1–6)	Tyr-Gly-Gly-Phe-Leu-Arg
	Leumorphin	Tyr-Gly-Gly-Phe-Leu-Arg-Arg-Gln-Phe-Lys-Val-Val-Thr-Arg-Ser-Gln-Glu-Asp-Pro-Asn-Ala-Tyr-Tyr-Glu-Glu-Leu-Phe-Asp-Val
	α-neoendorphin	Tyr-Gly-Gly-Phe-Leu-Arg-Lys-Tyr-Pro-Lys
	β-neoendorphin	Tyr-Gly-Gly-Phe-Leu-Arg-Lys-Tyr-Pro
Pro-Opiomelanocortin	α-endorphin	Tyr-Gly-Gly-Phe-Met-Thr-Ser-Glu-Lys-Ser-Gln-Thr-Pro-Val-Thr-Leu
	β-endorphin	Tyr-Gly-Gly-Phe-Met-Thr-Ser-Glu-Lys-Ser-Gln-Thr-Pro-Val-Thr-Leu-Phe-Lys-Asn-Ile-Ile-Lys-Asn-Ala-Tyr-Lys-Lys-Gly-Glu
Unknown	Endomorphin 1	Tyr-Pro-Trp-Phe
	Endomorphin 2	Tyr-Pro-Phe-Phe

et al., 1998), and in enteroendocrine cells (Mimoda et al., 1998). However, it is possible that the enkephalin detected in these regions is due to detection of dynorphins or dynorphin derived Leu-enk which is highly expressed in these regions as discussed later in this review. Expression of other enkephalin derivatives including Met-enk-Arg-Phe (Bu'Lock et al., 1983) and Met-enk-Arg-Gly-Leu (Wang and Lindberg, 1986) by enteric neurons has also been demonstrated. Other sites where preproenkephalin and its derivatives are expressed include enteroendocrine cells (Bu'Lock et al., 1983; Nihei and Iwanaga, 1985; Kokrashvili et al., 2009), extrinsic afferents (Steele and Costa, 1990) and immune cells including CD4+ T cells (Boue et al., 2014).

Dynorphins

There is good evidence that opioid peptides derived from pro-dynorphin (dynorphins), are present in the GIT. Pre-pro-dynorphin mRNA is expressed in the myenteric and mucosal layers to varying levels throughout the GIT (Yuferov et al., 1998). Pro-dynorphin contains three opioid peptides, dynorphin A, dynorphin B, and α-neoendorphin, which can all be further processed to shorter opioid peptides including Leu-Enk (see **Table 2**; Horikawa et al., 1983). Dynorphins have been detected in the GIT of various species, including the full length Dyn A (1–17), Dyn A (1–13), Dyn A (1–8), Dyn B, and α-neoendorphin (Vincent et al., 1984; Wolter, 1986; Steele et al., 1989; Murphy and Turner, 1990; Spampinato et al., 1992). Dynorphins are present in all layers of the gut wall throughout the entire human GIT, although information regarding cellular sites of expression is lacking (Spampinato et al., 1988). Immunohistochemistry studies performed mainly in guinea pigs indicate that dynorphins are widely expressed by submucosal and myenteric neurons (Vincent et al., 1984; Wolter, 1986; Steele and Costa, 1990). Dynorphins are co-expressed with enkephalins in a subpopulation of Dogiel type I myenteric neurons (Costa et al., 1985; Furness et al., 1985; Steele and Costa, 1990). It is possible that this may reflect conversion of dynorphin to Leu-enk in these

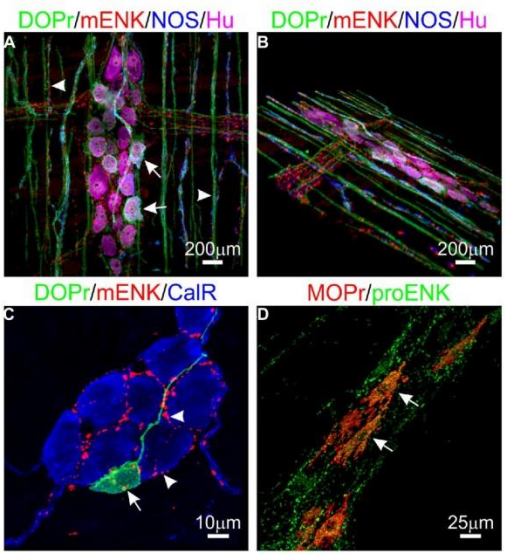

FIGURE 1 | Expression of opioid receptors (ORs) and enkephalin in the enteric nervous system. (A,B) Distribution of the delta opioid receptor (DOPr, green), met-enkephalin (mENK, red), nitric oxide synthase (NOS, blue), and the pan-neuronal marker HuC/D (Hu, magenta) in the myenteric plexus (arrows) and circular muscle nerve fibers (arrowheads) of the mouse distal colon. **(C)** Example of a DOPr-positive submucosal neuron (arrow) and association with mENK-immunoreactive nerve varicosities (arrowheads) in the mouse distal colon. **(D)** Overlap between immunoreactivities for the Mu opioid receptor (MOPr, red) and proenkephalin (proENK, green) in myenteric neurons of the guinea pig ileum. Images have been modified using Imaris 7.4.2 software (Bitplane). Scale bars are as indicated.

neurons rather than co-expression of pro-enkephalin. There are also reports of dynorphin expression by enterochromaffin cells (Cetin, 1988).

Endorphins

The endorphins are formed from the precursor peptide POMC, which also contains several other non-opioid peptide hormones (Eipper and Mains, 1978). POMC contains only one opioid peptide, β-endorphin, which can be cleaved to form α-endorphin. Although β-endorphin has been detected in the GIT (Orwoll and Kendall, 1980; DeBold et al., 1988), the localization of endorphin expression still remains uncertain. There is some evidence of β-endorphin expression, and of other POMC peptides, by myenteric neurons, nerve fibers within the circular muscle and enteroendocrine cells (Schultzberg et al., 1980; Leander et al., 1984; Wolter, 1985b; Kokrashvili et al., 2009; Miller and Hirning, 2010). Another major source of β-endorphin in the gut are immune cells, particularly those associated with inflammatory bowel disease or irritable bowel syndrome (Verma-Gandhu et al., 2006; Hughes et al., 2013). It should be noted that the distribution of β-endorphin in the GIT is controversial, as the specificity of the antisera used in many of these studies has been questioned (Sundler et al., 1981). Hence whilst there is certainly β-endorphin present in the GIT, the question of its origin remains unresolved.

Other OR agonists are also produced endogenously in the GIT. These include morphine and codeine-like compounds (Schulz et al., 1977; Laux-Biehlmann et al., 2013) and the pre-dermorphin derivatives dermorphin and dermenkephalin (Mor et al., 1989, 1990).

Even though the distribution of the different classes of endogenous opioids in the GIT has been fairly well established, there is very little known about individual levels of the different peptides within each class. The expression of proteases that synthesize and degrade endogenous opioids may have varying levels of expression in different cell types, which would result in different production and degradation rates. As such, the mixture of opioid peptides derived from the same precursor will be variable in different cell populations. Differential proteolytic processing of pro-enkephalin and pro-dynorphin peptides occurs in various regions of the brain and other tissues, leading to variations in the relative proportions of peptides derived from the same precursors (Cone et al., 1983; Zamir et al., 1984; Yakovleva et al., 2006). Differential processing of precursors may also occur in the different cell populations within the GIT. In rat duodenum, specific antisera against Dyn A (1–17) and Dyn A (1–8) stain two distinct populations of neurons, one which contains both peptides and one with only Dyn A (1–8), indicating that Dyn A (1–8) may be synthesized *via* distinct proteases or at varying rates in distinct neuronal populations (Wolter, 1985a).

FUNCTION OF ENDOGENOUS OPIOID RECEPTOR LIGANDS IN THE GI TRACT

Endogenous opioids play an important regulatory role in normal gut physiology, primarily through activation of ORs on enteric neurons (Wood and Galligan, 2004). When applied exogenously, the physiological effects of endogenous opioids are the same as the effects of other opioids, they hyperpolarize enteric neurons leading to inhibition of GIT motility and secretion and ultimately cause constipation (Miller and Hirning, 2010). On the other hand, the effects of endogenous peptides when released intrinsically under normal physiological conditions are unclear. Release of enkephalin- and dynorphin-derived peptides has been detected in intestinal tissue preparations during peristalsis or after electrical stimulation. These include Leu-enk, Met-enk, Met-enk-Arg-Phe, Met-enk-Arg-Gly-Leu, metorphamide (Schulz et al., 1977; Corbett et al., 1991), α-neoendorphin (Majeed et al., 1987) and Dyn A (Kromer et al., 1981; Donnerer et al., 1984). In addition, studies using opioid antagonists, mainly naloxone, have shown that inhibition of opioid activity increases non-propagating intestinal motility (Sanger and Tuladhar, 2004). Altogether, this shows that endogenous opioids play a subtle but important role in control of GIT motility by suppressing activity. There is also evidence that the endogenous peptides either contribute to, or protect against, the development of pathophysiological conditions. Levels of endogenous opioids in the GIT have been shown to increase under pathological conditions, including inflammatory bowel disease, and not only inhibit gastrointestinal motility, but also provide visceral antinociception. β-endorphin levels have been shown to increase in a

model of chronic inflammatory bowel disease in mice, suppressing inflammation-associated hyperexcitability of colonic primary spinal afferents (Hughes et al., 2013; Valdez-Morales et al., 2013). In addition, T Lymphocytes can release β-endorphin and induce expression of β-endorphin in the myenteric plexus in mice with immunodeficiency-related visceral hyperalgesia (Verma-Gandhu et al., 2006, 2007). Surgical intervention has also been shown to increase dynorphin expression in the dorsal root ganglia of mice (Romero et al., 2012), and stimulate release of opioid peptides from enteric neurons after abdominal surgery in guinea pigs (Patierno et al., 2005). This may contribute in part to post-operative ileus, although sympathetic pathways are likely to play a more significant role. A greater understanding of the involvement of endogenous opioids in GIT pathophysiology is important as the opioid system is not only a potential target for treatment, but the enhanced production and release of endogenous opioids may also alter the effectiveness of opioid-based therapeutics.

Although the global physiological effects of endogenous opioids in the GIT have been widely studied, the role of individual peptides in the control of normal GIT functions or pathophysiological conditions in discrete regions is still not clear. There are specific distributions of endogenous opioids throughout the GIT. However, since all endogenous opioids can activate all ORs, the specific ORs through which endogenous opioids exert their actions or the specific signaling mechanisms behind these functions is unknown. The physiological significance of such diversity and structural organization of opioid peptides suggests that individual endogenous peptides may serve distinct physiological roles. The diversity in physiological effects can in part be achieved by activation of the different ORs. However, as there are far more endogenous opioids than there are receptors and little receptor selectivity, it is probable that the diversity in endogenous opioids exists to fine tune OR-mediated effects through biased agonism.

BIASED AGONISM AT THE OPIOID RECEPTORS

Opioid receptors are prototypical GPCRs where biased agonism displayed by synthetic and exogenous ligands has been widely explored. Indeed, this reflects the extensive knowledge of opioid physiology and the desire to generate opioid-based analgesics devoid of limiting side effects such as respiratory depression or constipation.

In addition to the ideal separation of therapeutic and clinically limiting side effects, two key observations in the actions of morphine at MOPr have sparked the search for biased agonists at this receptor. First, morphine is relatively poor at inducing MOPr internalization, in spite of its efficacy in mediating G-protein activation, and second, morphine-induced respiratory depression and constipation were attenuated in a β-arrestin knock-out mouse, while analgesia was enhanced. Altogether these reports have sparked the search for potentially different signaling mechanisms that mediate the diverse physiological actions of ORs. Similarly, reports of biased agonism by exogenous ligands have also been described for the other OR subtypes, DOPr (Charfi et al., 2014), and KOPr (Melief et al., 2010). However, the potential for endogenous bias at the OR family has not received much attention. This is despite the fact that, as highlighted above, there is significant biological redundancy in the opioid system. In a systematic approach to evaluate biased agonism at the mu-OR, McPherson et al. (2010; Rivero et al., 2012) examined the signaling bias of a wide range of ligands including endogenous opioid peptides and synthetic opioids. In these and subsequent studies, endomorphin-2 as well as endomorphin-1 showed statistically significant bias toward β-arrestin2 recruitment and away from G protein activation. However, as neither the gene nor the precursor protein of endomorphin1 and two has yet been identified, their classification as endogenous opioids is still a matter of debate.

Opioid receptors have also been reported to form homo- and hetero-dimers. Importantly, it has been suggested that these dimers may indeed form a new signaling entity where the intracellular signaling resulting from the activation of heterodimers may be different from that elicited by the individual protomers or homodimers (Waldhoer et al., 2005; Rozenfeld and Devi, 2007; Gomes et al., 2013). Moreover, some of these dimers have been demonstrated to exist *in vivo* (Massotte, 2014). Although such mechanisms of engendering distinct intracellular signals would not fall into the definition of biased agonism, it is another paradigm to take into account in the context of the differential actions of endogenous opioid peptides.

IDENTIFICATION AND QUANTIFICATION OF BIASED AGONISM: CHALLENGES AND LIMITATIONS

Although biased agonism offers the potential of safer and more effective therapeutics, there are still significant limitations for its detection, quantification and, importantly, its translation into differential physiological responses.

QUANTIFICATION OF BIASED AGONISM

Analytical tools for the detection and quantification of biased agonism are necessary in order to effectively inform future drug development efforts aimed in this direction. The majority of studies to date on biased agonism have used largely qualitative observations, such as reversals in agonist potency orders or maximal agonist effects between different pathways. However, such approaches are not optimal. The potency of a ligand is determined by both its affinity for the receptor state coupled to that particular pathway as well as its intrinsic efficacy for generating a response in that pathway. In contrast, the maximal effect of a ligand at saturating concentrations is only determined by intrinsic efficacy. In addition, contributors to system bias, signal amplification, and receptor expression need to be taken into account as they have markedly different effects on potencies and efficacies of differently efficacious ligands. Therefore, the observed response of an agonist at a given pathway is not only the result of unique ligand-induced receptor conformations, rather it is affected by "system bias," which reflects the differing coupling efficiencies of the receptor to a given signaling pathway, and by "observation bias," which results from differing assay sensitivity and conditions (Kenakin et al., 2012; Kenakin and Christopoulos, 2013a). It is the bias imposed by the ligand on the receptor that is the only source of bias that allows the signaling bias profiles of ligands in different cell types to be compared. It is

therefore important to quantify signaling bias in such a way that it excludes system and observation bias, in order to reveal the unique signaling profile that is induced by the different ligands.

Several analytical approaches have been described to quantify biased agonism (reviewed by Kenakin and Christopoulos, 2013b). The relative transduction ratio (Kenakin et al., 2012) is one of the most robust and widely applicable methods for bias quantification. This method applies the operational model of agonism first derived by Black and Leff (1983) to concentration-response curves and estimates a "transduction coefficient" which is comprised of the functional equilibrium dissociation constant (a measure of the affinity for the receptor coupled to a particular effector protein or signaling pathway) and the intrinsic efficacy of the agonist in activating a particular signaling response and receptor density. This coefficient is thus an overall measure of the relative 'power' of an agonist to induce a response. In order to eliminate the effects of system and observation bias, normalization to a reference agonist is required. Finally, these normalized transduction coefficients can be compared across two signaling pathways for a given agonist to obtain the "relative transduction ratio" as measures of agonist bias. It is, however, important to highlight that key factors need to be considered [reference ligand, cellular content and pluridimensionality of efficacy, (Thompson et al., 2014)] which influence the identification and quantification of biased agonism and that need to be taken into account when interpreting information obtained from studying biased signaling *in vitro*.

EXAMINATION OF ENDOGENOUS BIAS IN A PHYSIOLOGICAL SETTING

Potentially insurmountable difficulties may prevent the examination of endogenous ligand bias in tissues and *in vivo*. First and foremost, multiple agonists for the same receptor exist, and these may be coexpressed (e.g., enkephalins), precluding differential release protocols. Selective stimulation of release may be possible in cases where agonists are expressed by distinct cells or neuronal subtypes (e.g., enteric neurons *vs.* enteroendocrine cells). Peptides may differ with respect to their susceptibility to degradation, complicating interpretation of studies of duration or magnitude of effects. Furthermore, these peptides may vary in their relative affinities to receptors of interest. The endpoints that are measured are often indirect and result from activation of complex reflex pathways involving a number of transmitters. For example, suppression of electrically evoked intestinal contractions, such as occurs in response to OR agonists (Wood and Galligan, 2004) may not reveal subtle agonist-dependent differences. Most of the current descriptions of biased agonism rely on direct measurements from cells (e.g., pERK1/2, cAMP accumulation, β-arrestin-recruitment), which are difficult to assay in enteric neurons. Moreover, the effects of exogenous agonist application may not reflect what occurs physiologically, as location of receptors and ligands may mean that such interactions never occur.

Other factors to consider when translating data derived from heterologous cell lines to enteric neurons, tissues, or *in vivo* studies include not only species, but also regional differences, and the relative expression of key regulatory proteins in the cellular environment examined. These factors are most apparent in the case of the ORs. The distribution of ORs in the gut differs between species. For example, there is limited evidence for functional DOPr expression in the guinea pig ileum (Johnson et al., 1987), whereas there is prominent DOPr expression in the mouse ileum (Poole et al., 2011). There may also be differences in the regional distribution of ORs with respect to both the relative numbers of positive neurons and in the neuronal types that express these receptors, as we have previously demonstrated for the DOPr (Poole et al., 2011). Interestingly, this does not appear to be the case for MOPr expression in the guinea pig ileum and colon where similar neuronal populations express the receptor (Poole et al., unpublished). It is worth noting that these differences in distribution are unlikely to have an effect in the detection of bias, as measurements are likely to be performed in the same tissue preparation. However, species and regional differences in OR expression will affect the potential for heterodimerization of ORs, which may influence the pharmacological profiles of any responses to agonists (Rozenfeld and Devi, 2007). Perhaps of greater importance is the relative expression of key modulatory proteins including β-arrestins and GRKs, which influence OR signaling in enteric neurons. This is highlighted by a number of recent studies using knockout mice. β-arrestin 2 deficient mice exhibit reduced constipatory effects of morphine and loperamide based on assays of fecal output and colonic transit (Raehal et al., 2005). Similarly, GRK6$^{-/-}$ mice also display significantly diminished opiate-induced inhibition of colonic transit relative to wildtype mice (Raehal et al., 2009). Deletion of either β-arrestin 2 or GRK6 did not affect morphine-induced inhibition of small intestinal transit, suggesting region-dependent regulation of neuronal MOR. β-arrestins are also integral to the development of opiate tolerance in the intestine, with deletion of β-arrestin 2 promoting acute morphine tolerance in the colon (Maguma et al., 2012; Akbarali et al., 2014). These studies highlight that OR regulation and physiological function can differ markedly between regions of the GIT and the difficulty in translating data obtained from model cell systems to the physiological setting.

In summary, we have provided an overview of the expression and distribution of endogenous ligands for two major therapeutically relevant classes of GPCRs in the GIT. We have provided evidence for functional selectivity of these ligands and have discussed potential issues related to translation of cell line-derived data to the organ and whole animal levels. Therapeutically, the targeting of selective release of endogenous peptides is probably not a realistic goal. However, understanding the fundamental basis for ligand bias and determining whether differences in the expression and release of endogenous ligands underlie the development and maintenance of disease may be more promising avenues to address and to provide mechanistic insight for the development of safer therapies.

ACKNOWLEDGMENTS

NHMRC Australia APP1049730 (Daniel P. Poole, Meritxell Canals), Monash Fellowship (Meritxell Canals), and the Defence Science and Technology Organisation Australia (Georgina L. Thompson). The authors thank Dr. Dane Jensen for assistance with figure preparation.

REFERENCES

Abdu, F., Hicks, G. A., Hennig, G., Allen, J. P., and Grundy, D. (2002). Somatostatin sst(2) receptors inhibit peristalsis in the rat and mouse jejunum. *Am. J. Physiol. Gastrointest. Liver Physiol.* 282, G624–G633. doi: 10.1152/ajpgi.00354.2001

Akbarali, H. I., Inkisar, A., and Dewey, W. L. (2014). Site and mechanism of morphine tolerance in the gastrointestinal tract. *Neurogastroenterol. Motil.* 26, 1361–1367. doi: 10.1111/nmo.12443

Allen, J. P., Canty, A. J., Schulz, S., Humphrey, P. P., Emson, P. C., and Young, H. M. (2002). Identification of cells expressing somatostatin receptor 2 in the gastrointestinal tract of Sstr2 knockout/lacZ knockin mice. *J. Comp. Neurol.* 454, 329–340. doi: 10.1002/cne.10466

Baldissera, F. G., Nielsen, O. V., and Holst, J. J. (1985). The intestinal mucosa preferentially releases somatostatin-28 in pigs. *Regul. Pept.* 11, 251–262. doi: 10.1016/0167-0115(85)90057-6

Baskin, D. G., and Ensinck, J. W. (1984). Somatostatin in epithelial cells of intestinal mucosa is present primarily as somatostatin 28. *Peptides* 5, 615–621. doi: 10.1016/0196-9781(84)90092-5

Benoit, R., Esch, F., Bennett, H. P., Ling, N., Ravazzola, M., Orci, L., et al. (1990). Processing of prosomatostatin. *Metabolism* 39, 22–25. doi: 10.1016/0026-0495(90)90202-N

Benoit, R., Ling, N., and Esch, F. (1987). A new prosomatostatin-derived peptide reveals a pattern for prohormone cleavage at monobasic sites. *Science* 238, 1126–1129. doi: 10.1126/science.2891188

Bersani, M., Thim, L., Baldissera, F. G., and Holst, J. J. (1989). Prosomatostatin 1-64 is a major product of somatostatin gene expression in pancreas and gut. *J. Biol. Chem.* 264, 10633–10636.

Beyer, J., Jabari, S., Rau, T. T., Neuhuber, W., and Brehmer, A. (2013). Substance P- and choline acetyltransferase immunoreactivities in somatostatin-containing, human submucosal neurons. *Histochem. Cell Biol.* 140, 157–167. doi: 10.1007/s00418-013-1078-9

Black, J. W., and Leff, P. (1983). Operational models of pharmacological agonism. *Proc. R. Soc. Lond. B Biol. Sci.* 220, 141–162. doi: 10.1098/rspb.1983.0093

Bohlen, P., Brazeau, P., Benoit, R., Ling, N., Esch, F., and Guillemin, R. (1980). Isolation and amino acid composition of two somatostatin-like peptides from ovine hypothalamus: somatostatin-28 and somatostatin-25. *Biochem. Biophys. Res. Commun.* 96, 725–734. doi: 10.1016/0006-291X(80)91415-1

Bokoch, M. P., Zou, Y., Rasmussen, S. G., Liu, C. W., Nygaard, R., Rosenbaum, D. M., et al. (2010). Ligand-specific regulation of the extracellular surface of a G-protein-coupled receptor. *Nature* 463, 108–112. doi: 10.1038/nature08650

Bornstein, J. C., Costa, M., Furness, J. B., and Lees, G. M. (1984). Electrophysiology and enkephalin immunoreactivity of identified myenteric plexus neurones of guinea-pig small intestine. *J. Physiol.* 351, 313–325.

Boue, J., Basso, L., Cenac, N., Blanpied, C., Rolli-Derkinderen, M., Neunlist, M., et al. (2014). Endogenous regulation of visceral pain via production of opioids by colitogenic CD4(+) T cells in mice. *Gastroenterology* 146, 166–175. doi: 10.1053/j.gastro.2013.09.020

Brazeau, P., Ling, N., Esch, F., Bohlen, P., Benoit, R., and Guillemin, R. (1981). High biological activity of the synthetic replicates of somatostatin-28 and somatostatin-25. *Regul. Pept.* 1, 255–264. doi: 10.1016/0167-0115(81)90048-3

Brazeau, P., Vale, W., Burgus, R., Ling, N., Butcher, M., Rivier, J., et al. (1973). Hypothalamic polypeptide that inhibits the secretion of immunoreactive pituitary growth hormone. *Science* 179, 77–79. doi: 10.1126/science.179.4068.77

Brehmer, A., Lindig, T. M., Schrodl, F., Neuhuber, W., Ditterich, D., Rexer, M., et al. (2005). Morphology of enkephalin-immunoreactive myenteric neurons in the human gut. *Histochem. Cell Biol.* 123, 131–138. doi: 10.1007/s00418-005-0757-6

Bu'Lock, A. J., Vaillant, C., and Dockray, G. J. (1983). Immunohistochemical studies on the gastrointestinal tract using antisera to Met-enkephalin and Met-enkephalin Arg6Phe7. *J. Histochem. Cytochem.* 31, 1356–1362. doi: 10.1177/31.12.6355286

Cescato, R., Loesch, K. A., Waser, B., Macke, H. R., Rivier, J. E., Reubi, J. C., et al. (2010). Agonist-biased signaling at the sst2A receptor: the multi-somatostatin analogs KE108 and SOM230 activate and antagonize distinct signaling pathways. *Mol. Endocrinol.* 24, 240–249. doi: 10.1210/me.2009-0321

Cetin, Y. (1988). Enterochromaffin (EC-) cells of the mammalian gastro-entero-pancreatic (GEP) endocrine system: cellular source of pro-dynorphin-derived peptides. *Cell Tissue Res.* 253, 173–179. doi: 10.1007/BF00221752

Charfi, I., Audet, N., Bagheri Tudashki, H., and Pineyro, G. (2014). Identifying ligand-specific signalling within biased responses: focus on delta opioid receptor ligands. *Br. J. Pharmacol.* doi: 10.1111/bph.12705 [Epub ahead of print].

Cone, R. I., Weber, E., Barchas, J. D., and Goldstein, A. (1983). Regional distribution of dynorphin and neo-endorphin peptides in rat brain, spinal cord, and pituitary. *J. Neurosci.* 3, 2146–2152.

Corbett, A. D., Gillan, M. G., and Kosterlitz, H. W. (1991). Electrically-induced release of opioid peptides from the guinea-pig myenteric plexus preparation. *J. Recept. Res.* 11, 665–673. doi: 10.3109/10799899109066434

Corbett, A. D., Mcknight, A. T., and Kosterlitz, H. W. (1988). Tissue content of opioid peptides in the myenteric plexus-longitudinal muscle of guinea-pig small intestine. *J. Neurochem.* 51, 32–37. doi: 10.1111/j.1471-4159.1988.tb04831.x

Costa, M., Furness, J. B., and Cuello, A. C. (1985). Separate populations of opioid containing neurons in the guinea-pig intestine. *Neuropeptides* 5, 445–448. doi: 10.1016/0143-4179(85)90050-2

Dalm, V. A., Van Hagen, P. M., De Krijger, R. R., Kros, J. M., Van Koetsveld, P. M., Van Der Lely, A. J., et al. (2004). Distribution pattern of somatostatin and cortistatin mRNA in human central and peripheral tissues. *Clin. Endocrinol.* 60, 625–629. doi: 10.1111/j.1365-2265.2004.02024.x

DeBold, C. R., Nicholson, W. E., and Orth, D. N. (1988). Immunoreactive proopiomelanocortin (POMC) peptides and POMC-like messenger ribonucleic acid are present in many rat nonpituitary tissues. *Endocrinology* 122, 2648–2657. doi: 10.1210/endo-122-6-2648

de Lecea, L., Criado, J. R., Prospero-Garcia, O., Gautvik, K. M., Schweitzer, P., Danielson, P. E., et al. (1996). A cortical neuropeptide with neuronal depressant and sleep-modulating properties. *Nature* 381, 242–245. doi: 10.1038/381242a0

Deupi, X., and Kobilka, B. K. (2010). Energy landscapes as a tool to integrate GPCR structure, dynamics, and function. *Physiology (Bethesda)* 25, 293–303. doi: 10.1152/physiol.00002.2010

Donnerer, J., Holzer, P., and Lembeck, F. (1984). Release of dynorphin, somatostatin and substance P from the vascularly perfused small intestine of the guinea-pig during peristalsis. *Br. J. Pharmacol.* 83, 919–925. doi: 10.1111/j.1476-5381.1984.tb16532.x

Eipper, B. A., and Mains, R. E. (1978). Analysis of the common precursor to corticotropin and endorphin. *J. Biol. Chem.* 253, 5732–5744.

Elde, R., Hokfelt, T., Johansson, O., and Terenius, L. (1976). Immunohistochemical studies using antibodies to leucine-enkephalin: initial observations on the nervous system of the rat. *Neuroscience* 1, 349–351. doi: 10.1016/0306-4522(76)90063-4

Ensinck, J. W., Baskin, D. G., Vahl, T. P., Vogel, R. E., Laschansky, E. C., Francis, B. H., et al. (2002). Thrittene, homologous with somatostatin-28((1-13)), is a novel peptide in mammalian gut and circulation. *Endocrinology* 143, 2599–2609. doi: 10.1210/endo.143.7.8904

Ensinck, J. W., Laschansky, E. C., Vogel, R. E., and D'alessio, D. A. (2003). Effect of ingested nutrients on the release of thrittene into the human circulation. *J. Clin. Endocrinol. Metab.* 88, 4798–4804. doi: 10.1210/jc.2003–030063

Esch, F., Bohlen, P., Ling, N., Benoit, R., Brazeau, P., and Guillemin, R. (1980). Primary structure of ovine hypothalamic somatostatin-28 and somatostatin-25. *Proc. Natl. Acad. Sci. U.S.A.* 77, 6827–6831. doi: 10.1073/pnas.77.11.6827

Ferri, G. L., Morreale, R. A., and Dockray, G. J. (1986). Met5-enkephalin-Arg6-Gly7-Leu8 immunoreactivity in the human gut. *Peptides* 7, 735–739. doi: 10.1016/0196-9781(86)90087-2

Ferri, G. L., Watkinson, A., and Dockray, G. J. (1988). Proenkephalin A-derived peptides in the human gut. *Gastroenterology* 95, 1011–1017.

Foong, J. P., Parry, L. J., Gwynne, R. M., and Bornstein, J. C. (2010). 5-HT(1A), SST(1), and SST(2) receptors mediate inhibitory postsynaptic potentials in the submucous plexus of the guinea pig ileum. *Am. J. Physiol. Gastrointest. Liver Physiol.* 298, G384–G394. doi: 10.1152/ajpgi.00438.2009

Francis, B. H., Baskin, D. G., Saunders, D. R., and Ensinck, J. W. (1990). Distribution of somatostatin-14 and somatostatin-28 gastrointestinal-pancreatic cells of rats and humans. *Gastroenterology* 99, 1283–1291.

Furness, J. B., Costa, M., Gibbins, I. L., Llewellyn-Smith, I. J., and Oliver, J. R. (1985). Neurochemically similar myenteric and submucous neurons directly traced to the mucosa of the small intestine. *Cell Tissue Res.* 241, 155–163. doi: 10.1007/BF00214637

Furness, J. B., Costa, M., and Miller, R. J. (1983). Distribution and projections of nerves with enkephalin-like immunoreactivity in the guinea-pig small intestine. *Neuroscience* 8, 653–664. doi: 10.1016/0306-4522(83)90001-5

Galligan, J. J., and Akbarali, H. I. (2014). Molecular physiology of enteric opioid receptors. *Am. J. Gastroenterol.* 2, 17–21. doi: 10.1038/ajgsup.2014.5

Giraud, A. S., Williams, R. G., and Dockray, G. J. (1984). Evidence for different patterns of post-translational processing of pro-enkephalin in the bovine adrenal, colon and striatum indicated by radioimmunoassay using region-specific antisera to Met-Enk-Arg6-Phe7 and Met-Enk-Arg6-Gly7-Leu8. *Neurosci. Lett.* 46, 223–228. doi: 10.1016/0304-3940(84)90446-4

Gomes, I., Fujita, W., Gupta, A., Saldanha, S. A., Negri, A., Pinello, C. E., et al. (2013). Identification of a mu-delta opioid receptor heteromer-biased agonist with antinociceptive activity. *Proc. Natl. Acad. Sci. U.S.A.* 110, 12072–12077. doi: 10.1073/pnas.1222044110

Gonzalez-Rey, E., Varela, N., Sheibanie, A. F., Chorny, A., Ganea, D., and Delgado, M. (2006). Cortistatin, an antiinflammatory peptide with therapeutic action in inflammatory bowel disease. *Proc. Natl. Acad. Sci. U.S.A.* 103, 4228–4233. doi: 10.1073/pnas.0508997103

Grider, J. R. (2003). Neurotransmitters mediating the intestinal peristaltic reflex in the mouse. *J. Pharmacol. Exp. Ther.* 307, 460–467. doi: 10.1124/jpet.103.053512

Hirst, B. H., Conlon, J. M., Coy, D. H., Holland, J., and Shaw, B. (1982). Comparison of the gastric exocrine inhibitory activities and plasma kinetics of somatostatin-28 and somatostatin-14 in cats. *Regul. Pept.* 4, 227–237. doi: 10.1016/0167-0115(82)90115-X

Hofmann, K. P., Scheerer, P., Hildebrand, P. W., Choe, H. W., Park, J. H., Heck, M., et al. (2009). A G protein-coupled receptor at work: the rhodopsin model. *Trends Biochem. Sci.* 34, 540–552. doi: 10.1016/j.tibs.2009.07.005

Horikawa, S., Takai, T., Toyosato, M., Takahashi, H., Noda, M., Kakidani, H., et al. (1983). Isolation and structural organization of the human preproenkephalin B gene. *Nature* 306, 611–614. doi: 10.1038/306611a0

Hughes, J., Kosterlitz, H. W., and Smith, T. W. (1977). The distribution of methionine-enkephalin and leucine-enkephalin in the brain and peripheral tissues. *Br. J. Pharmacol.* 61, 639–647. doi: 10.1111/j.1476-5381.1977.tb07557.x

Hughes, P. A., Harrington, A. M., Castro, J., Liebregts, T., Adam, B., Grasby, D. J., et al. (2013). Sensory neuro-immune interactions differ between irritable bowel syndrome subtypes. *Gut* 62, 1456–1465. doi: 10.1136/gutjnl-2011–301856

Janecka, A., Fichna, J., and Janecki, T. (2004). Opioid receptors and their ligands. *Curr. Top. Med. Chem.* 4, 1–17. doi: 10.2174/1568026043451618

Jessen, K. R., Saffrey, M. J., Van Noorden, S., Bloom, S. R., Polak, J. M., and Burnstock, G. (1980). Immunohistochemical studies of the enteric nervous system in tissue culture and in situ: localization of vascoactive intestinal polypeptide (VIP), substance-P and enkephalin immunoreactive nerves in the guinea-pig gut. *Neuroscience* 5, 1717–1735. doi: 10.1016/0306-4522(80)90091-3

Johnson, S. M., Costa, M., Humphreys, C. M., and Shearman, R. (1987). Inhibitory effects of opioids in a circular muscle-myenteric plexus preparation of guinea-pig ileum. *Naunyn Schmiedebergs Arch. Pharmacol.* 336, 419–424. doi: 10.1007/BF00164876

Keast, J. R., and De Groat, W. C. (1992). Segmental distribution and peptide content of primary afferent neurons innervating the urogenital organs and colon of male rats. *J. Comp. Neurol.* 319, 615–623. doi: 10.1002/cne.903190411

Keast, J. R., Furness, J. B., and Costa, M. (1985). Distribution of certain peptide-containing nerve fibres and endocrine cells in the gastrointestinal mucosa in five mammalian species. *J. Comp. Neurol.* 236, 403–422. doi: 10.1002/cne.902360308

Kenakin, T., and Christopoulos, A. (2013a). Measurements of ligand bias and functional affinity. *Nat. Rev. Drug Discov.* 12, 483. doi: 10.1038/nrd3954-c2

Kenakin, T., and Christopoulos, A. (2013b). Signalling bias in new drug discovery: detection, quantification and therapeutic impact. *Nat. Rev. Drug Discov.* 12, 205–216. doi: 10.1038/nrd3954

Kenakin, T., Watson, C., Muniz-Medina, V., Christopoulos, A., and Novick, S. (2012). A simple method for quantifying functional selectivity and agonist bias. *ACS Chem. Neurosci.* 3, 193–203. doi: 10.1021/cn200111m

Kokrashvili, Z., Rodriguez, D., Yevshayeva, V., Zhou, H., Margolskee, R. F., and Mosinger, B. (2009). Release of endogenous opioids from duodenal enteroendocrine cells requires Trpm5. *Gastroenterology* 137, 598–606; 606.e1–e2. doi: 10.1053/j.gastro.2009.02.070

Kromer, W., Hollt, V., Schmidt, H., and Herz, A. (1981). Release of immunoreactive-dynorphin from the isolated guinea-pig small intestine is reduced during peristaltic activity. *Neurosci. Lett.* 25, 53–56. doi: 10.1016/0304-3940(81)90100-2

Larsson, L. I., Childers, S., and Snyder, S. H. (1979). Met- and Leu-enkephalin immunoreactivity in separate neurones. *Nature* 282, 407–410. doi: 10.1038/282407a0

Larsson, L. I., and Stengaard-Pendersen, K. (1982). Immunocytochemical and ultrastructural differentiation between Met-enkephalin-, Leu-enkephalin-, and Met/Leu-enkephalin-immunoreactive neurons of feline gut. *J. Neurosci.* 2, 861–878.

Laux-Biehlmann, A., Mouheiche, J., Veriepe, J., and Goumon, Y. (2013). Endogenous morphine and its metabolites in mammals: history, synthesis, localization and perspectives. *Neuroscience* 233, 95–117. doi: 10.1016/j.neuroscience.2012.12.013

Leander, S., Ekman, R., Uddman, R., Sundler, F., and Hakanson, R. (1984). Neuronal cholecystokinin, gastrin-releasing peptide, neurotensin, and beta-endorphin in the intestine of the guinea pig. Distribution and possible motor functions. *Cell Tissue Res.* 235, 521–531. doi: 10.1007/BF00226949

Linnoila, R. I., Diaugustine, R. P., Miller, R. J., Chang, K. J., and Cuatrecasas, P. (1978). An immunohistochemical and radioimmunological study of the distribution of [met5]- and [leu5]-enkephalin in the gastrointestinal tract. *Neuroscience* 3, 1187–1196. doi: 10.1016/0306-4522(78)90138-0

Liu, Q., Cescato, R., Dewi, D. A., Rivier, J., Reubi, J. C., and Schonbrunn, A. (2005). Receptor signaling and endocytosis are differentially regulated by somatostatin analogs. *Mol. Pharmacol.* 68, 90–101. doi: 10.1124/mol.105.011767

Liu, Q., Dewi, D. A., Liu, W., Bee, M. S., and Schonbrunn, A. (2008). Distinct phosphorylation sites in the SST2A somatostatin receptor control internalization, desensitization, and arrestin binding. *Mol. Pharmacol.* 73, 292–304. doi: 10.1124/mol.107.038570

Lloyd, K. C., Amirmoazzami, S., Friedik, F., Chew, P., and Walsh, J. H. (1997). Somatostatin inhibits gastrin release and acid secretion by activating sst2 in dogs. *Am. J. Physiol.* 272, G1481–G1488.

Low, M. J. (2004). The somatostatin neuroendocrine system: physiology and clinical relevance in gastrointestinal and pancreatic disorders. *Best Pract. Res. Clin. Endocrinol. Metab.* 18, 607–622. doi: 10.1016/j.beem.2004.08.005

Maguma, H. T., Dewey, W. L., and Akbarali, H. I. (2012). Differences in the characteristics of tolerance to mu-opioid receptor agonists in the colon from wild type and beta-arrestin2 knockout mice. *Eur. J. Pharmacol.* 685, 133–140. doi: 10.1016/j.ejphar.2012.04.001

Majeed, N. H., Silberring, J., and Przewlocki, R. (1987). The in vitro release of immunoreactive dynorphin and alpha-neoendorphin from the perfused rat duodenum. *Life Sci.* 41, 497–504. doi: 10.1016/0024-3205(87)90227-X

Mansour, A., Hoversten, M. T., Taylor, L. P., Watson, S. J., and Akil, H. (1995). The cloned mu, delta and kappa receptors and their endogenous ligands: evidence for two opioid peptide recognition cores. *Brain Res.* 700, 89–98. doi: 10.1016/0006-8993(95)00928-J

Massotte, D. (2014). In vivo opioid receptor heteromerization: where do we stand? *Br. J. Pharmacol.* doi: 10.1111/bph.12702 [Epub ahead of print].

McIntosh, C. H., Bakich, V., Kwok, Y. N., and Brown, J. C. (1986). A comparison of the inhibitory effects of somatostatin-14, -25, and -28 on motility of the guinea pig ileum. *Can. J. Physiol. Pharmacol.* 64, 303–306. doi: 10.1139/y86-048

McPherson, J., Rivero, G., Baptist, M., Llorente, J., Al-Sabah, S., Krasel, C., et al. (2010). mu-opioid receptors: correlation of agonist efficacy for signalling with ability to activate internalization. *Mol. Pharmacol.* 78, 756–766. doi: 10.1124/mol.110.066613

Melief, E. J., Miyatake, M., Bruchas, M. R., and Chavkin, C. (2010). Ligand-directed c-Jun N-terminal kinase activation disrupts opioid receptor signaling. *Proc. Natl. Acad. Sci. U.S.A.* 107, 11608–11613. doi: 10.1073/pnas.1000751107

Miller, R. J., and Hirning, L. D. (2010). "Opioid Peptides of The Gut," in *Comprehensive Physiology*. Hoboken, NJ: John Wiley & Sons, Inc.

Mimoda, T., Kitamura, N., Hondo, E., and Yamada, J. (1998). Immunohistochemical colocalization of serotonin, substance P and Met-enkephalin-Arg6-Gly7-Leu8 in the endocrine cells of the ruminant duodenum. *Anat. Histol. Embryol.* 27, 65–69. doi: 10.1111/j.1439-0264.1998.tb00158.x

Mongardi Fantaguzzi, C., Thacker, M., Chiocchetti, R., and Furness, J. B. (2009). Identification of neuron types in the submucosal ganglia of the mouse ileum. *Cell Tissue Res.* 336, 179–189. doi: 10.1007/s00441-009-0773-2

Mor, A., Delfour, A., Amiche, M., Sagan, S., Nicolas, P., Grassi, J., et al. (1989). Dermorphin and related peptides in rat tissues. *Neuropeptides* 13, 51–57. doi: 10.1016/0143-4179(89)90021-8

Mor, A., Pradelles, P., Delfour, A., Montagne, J. J., Quintero, F. L., Conrath, M., et al. (1990). Evidence for Pro-dermorphin processing products in rat tissues. *Biochem. Biophys. Res. Commun.* 170, 30–38. doi: 10.1016/0006-291X(90)91236-L

Murphy, R., and Turner, C. A. (1990). Isolation and microsequence analysis of guinea pig alpha-neo-endorphin. *Peptides* 11, 65–68. doi: 10.1016/0196-9781(90)90111-H

Nihei, K., and Iwanaga, T. (1985). Localization of Met-enkephalin-Arg6-Gly7-Leu8-like immunoreactivity in the gastrointestinal tract of rat and pig. *J. Histochem. Cytochem.* 33, 1001–1006. doi: 10.1177/33.10.3900192

Noda, M., Teranishi, Y., Takahashi, H., Toyosato, M., Notake, M., Nakanishi, S., et al. (1982). Isolation and structural organization of the human preproenkephalin gene. *Nature* 297, 431–434. doi: 10.1038/297431a0

Nunn, C., Cervia, D., Langenegger, D., Tenaillon, L., Bouhelal, R., and Hoyer, D. (2004). Comparison of functional profiles at human recombinant somatostatin sst2 receptor: simultaneous determination of intracellular Ca2+ and luciferase expression in CHO-K1 cells. *Br. J. Pharmacol.* 142, 150–160. doi: 10.1038/sj.bjp.0705735

Orwoll, E. S., and Kendall, J. W. (1980). Beta-endorphin and adrenocorticotropin in extrapituitary sites: gastrointestinal tract. *Endocrinology* 107, 438–442. doi: 10.1210/endo-107-2-438

Papotti, M., Tarabra, E., Allia, E., Bozzalla-Cassione, F., Broglio, F., Deghenghi, R., et al. (2003). Presence of cortistatin in the human pancreas. *J. Endocrinol. Invest.* 26, RC15–RC18. doi: 10.1007/BF03347348

Patel, Y. C., and Srikant, C. B. (1997). Somatostatin receptors. *Trends Endocrinol. Metab.* 8, 398–405. doi: 10.1016/S1043-2760(97)00168-9

Patierno, S., Zellalem, W., Ho, A., Parsons, C. G., Lloyd, K. C., Tonini, M., et al. (2005). N-methyl-D-aspartate receptors mediate endogenous opioid release in enteric neurons after abdominal surgery. *Gastroenterology* 128, 2009–2019. doi: 10.1053/j.gastro.2005.03.042

Pfannkuche, H., Reiche, D., Firzlaff, U., Sann, H., and Schemann, M. (1998). Enkephalin-immunoreactive subpopulations in the myenteric plexus of the guinea-pig fundus project primarily to the muscle and not to the mucosa. *Cell Tissue Res.* 294, 45–55. doi: 10.1007/s004410051155

Polak, J. M., Bloom, S. R., Sullivan, S. N., Facer, P., and Pearse, A. G. (1977). Enkephalin-like immunoreactivity in the human gastrointestinal tract. *Lancet* 1, 972–974. doi: 10.1016/S0140-6736(77)92277-2

Poole, D. P., Pelayo, J. C., Scherrer, G., Evans, C. J., Kieffer, B. L., and Bunnett, N. W. (2011). Localization and regulation of fluorescently labeled delta opioid receptor, expressed in enteric neurons of mice. *Gastroenterology* 141, 982–991. doi: 10.1053/j.gastro.2011.05.042

Portbury, A. L., Pompolo, S., Furness, J. B., Stebbing, M. J., Kunze, W. A., Bornstein, J. C., et al. (1995). Cholinergic, somatostatin-immunoreactive interneurons in the guinea pig intestine: morphology, ultrastructure, connections and projections. *J. Anat.* 187, 303–321.

Pradayrol, L., Chayvialle, J. A., Carlquist, M., and Mutt, V. (1978). Isolation of a porcine intestinal peptide with C-terminal somatostatin. *Biochem. Biophys. Res. Commun.* 85, 701–708. doi: 10.1016/0006-291X(78)91218-4

Pradayrol, L., Jornvall, H., Mutt, V., and Ribet, A. (1980). N-terminally extended somatostatin: the primary structure of somatostatin-28. *FEBS Lett.* 109, 55–58. doi: 10.1016/0014-5793(80)81310-X

Puebla, L., Mouchantaf, R., Sasi, R., Khare, S., Bennett, H. P., James, S., et al. (1999). Processing of rat preprocortistatin in mouse AtT-20 cells. *J. Neurochem.* 73, 1273–1277. doi: 10.1046/j.1471-4159.1999.0731273.x

Rabbani, S. N., and Patel, Y. C. (1990). Peptides derived by processing of rat prosomatostatin near the amino-terminus: characterization, tissue distribution, and release. *Endocrinology* 126, 2054–2061. doi: 10.1210/endo-126-4-2054

Raehal, K. M., Schmid, C. L., Medvedev, I. O., Gainetdinov, R. R., Premont, R. T., and Bohn, L. M. (2009). Morphine-induced physiological and behavioral responses in mice lacking G protein-coupled receptor kinase 6. *Drug Alcohol Depend.* 104, 187–196. doi: 10.1016/j.drugalcdep.2009.04.011

Raehal, K. M., Walker, J. K., and Bohn, L. M. (2005). Morphine side effects in beta-arrestin 2 knockout mice. *J. Pharmacol. Exp. Ther.* 314, 1195–1201. doi: 10.1124/jpet.105.087254

Rajagopal, S., Bassoni, D. L., Campbell, J. J., Gerard, N. P., Gerard, C., and Wehrman, T. S. (2013). Biased agonism as a mechanism for differential signaling by chemokine receptors. *J. Biol. Chem.* 288, 35039–35048. doi: 10.1074/jbc.M113.479113

Ravazzola, M., Benoit, R., Ling, N., Guillemin, R., and Orci, L. (1983). Immunocytochemical localization of prosomatostatin fragments in maturing and mature secretory granules of pancreatic and gastrointestinal D cells. *Proc. Natl. Acad. Sci. U.S.A.* 80, 215–218. doi: 10.1073/pnas.80.1.215

Ravazzola, M., Benoit, R., Ling, N., and Orci, L. (1989). Prosomatostatin-derived antrin is present in gastric D cells and in portal blood. *J. Clin. Invest.* 83, 362–366. doi: 10.1172/JCI113892

Rivero, G., Llorente, J., Mcpherson, J., Cooke, A., Mundell, S. J., McArdle, C. A., et al. (2012). Endomorphin-2: a biased agonist at the mu-opioid receptor. *Mol. Pharmacol.* 82, 178–188. doi: 10.1124/mol.112.078659

Romero, A., Gonzalez-Cuello, A., Laorden, M. L., Campillo, A., Vasconcelos, N., Romero-Alejo, E., et al. (2012). Effects of surgery and/or remifentanil administration on the expression of pERK1/2, c-Fos and dynorphin in the dorsal root ganglia in mice. *Naunyn Schmiedebergs Arch. Pharmacol.* 385, 397–409. doi: 10.1007/s00210-011-0721-z

Ronai, A. Z., Kiraly, K., Szebeni, A., Szemenyei, E., Prohaszka, Z., Darula, Z., et al. (2009). Immunoreactive endomorphin 2 is generated extracellularly in rat isolated L4,5 dorsal root ganglia by DPP-IV. *Regul. Pept.* 157, 1–2. doi: 10.1016/j.regpep.2009.06.006

Rozenfeld, R., and Devi, L. A. (2007). Receptor heterodimerization leads to a switch in signaling: beta-arrestin2-mediated ERK activation by mu-delta opioid receptor heterodimers. *FASEB J.* 21, 2455–2465. doi: 10.1096/fj.06-7793com

Samson, W. K., Zhang, J. V., Avsian-Kretchmer, O., Cui, K., Yosten, G. L., Klein, C., et al. (2008). Neuronostatin encoded by the somatostatin gene regulates neuronal, cardiovascular, and metabolic functions. *J. Biol. Chem.* 283, 31949–31959. doi: 10.1074/jbc.M804784200

Sanger, G. J., and Tuladhar, B. R. (2004). The role of endogenous opioids in the control of gastrointestinal motility: predictions from in vitro modelling. *Neurogastroenterol. Motil.* 16(Suppl. 2), 38–45. doi: 10.1111/j.1743-3150.2004.00556.x

Schmidt, W. E., Mutt, V., Kratzin, H., Carlquist, M., Conlon, J. M., and Creutzfeldt, W. (1985). Isolation and characterization of proSS1-32, a peptide derived from the N-terminal region of porcine preprosomatostatin. *FEBS Lett.* 192, 141–146. doi: 10.1016/0014-5793(85)80060-0

Schultzberg, M., Hokfelt, T., Nilsson, G., Terenius, L., Rehfeld, J. F., Brown, M., et al. (1980). Distribution of peptide- and catecholamine-containing neurons in the gastro-intestinal tract of rat and guinea-pig: immunohistochemical studies with antisera to substance P, vasoactive intestinal polypeptide, enkephalins, somatostatin, gastrin/cholecystokinin, neurotensin and dopamine beta-hydroxylase. *Neuroscience* 5, 689–744. doi: 10.1016/0306-4522(80)90166-9

Schulz, R., Wuster, M., Simantov, R., Snyder, S., and Herz, A. (1977). Electrically stimulated release of opiate-like material from the myenteric plexus of the guinea pig ileum. *Eur. J. Pharmacol.* 41, 347–348. doi: 10.1016/0014-2999(77)90331-4

Seal, A., Yamada, T., Debas, H., Hollinshead, J., Osadchey, B., Aponte, G., et al. (1982). Somatostatin-14 and -28: clearance and potency on gastric function in dogs. *Am. J. Physiol.* 243, G97–G102.

Shen, K. Z., and Surprenant, A. (1993). Somatostatin-mediated inhibitory postsynaptic potential in sympathetically denervated guinea-pig submucosal neurones. *J. Physiol.* 470, 619–635.

Song, Z. M., Brookes, S. J., Ramsay, G. A., and Costa, M. (1997). Characterization of myenteric interneurons with somatostatin immunoreactivity in the guinea-pig small intestine. *Neuroscience* 80, 907–923. doi: 10.1016/S0306-4522(96)00605-7

Spampinato, S., Ferri, G. L., Candeletti, S., Romualdi, P., Cavicchini, E., Soimero, L., et al. (1988). Regional distribution of immunoreactive dynorphin A in the human gastrointestinal tract. *Neuropeptides* 11, 101–105. doi: 10.1016/0143-4179(88)90077-7

Spampinato, S., Speroni, E., Canossa, M., Sciarretta, G., Malaguti, P., and Ferri, S. (1992). Dynorphin B-like immunoreactivity in gastroduodenal biopsy specimens from gallstone patients. *Regul. Pept.* 41, 131–138. doi: 10.1016/0167-0115(92)90042-S

Steele, P. A., and Costa, M. (1990). Opioid-like immunoreactive neurons in secretomotor pathways of the guinea-pig ileum. *Neuroscience* 38, 771–786. doi: 10.1016/0306-4522(90)90070-K

Steele, P. A., Turner, C. A., and Murphy, R. (1989). Measurement and chromatographic characterization of prodynorphin-derived peptides in the guinea-pig ileum. *Neuropeptides* 13, 207–213. doi: 10.1016/0143-4179(89)90094-2

Sundler, F., Alumets, J., Ekman, R., Hakanson, R., and Van Wimersma Greidanus, T. B. (1981). Immunoreactive adrenocorticotropic hormone (ACTH) in porcine gut and pancreas: fact or artifact? *J. Histochem. Cytochem.* 29, 1328–1335. doi: 10.1177/29.11.6172464

Tang, J., Yang, H. Y., and Costa, E. (1982). Distribution of met5-enkephalin-Arg6-Phe7 (MEAP) in various tissues of rats and guinea pigs. *Life Sci.* 31, 2303–2306. doi: 10.1016/0024-3205(82)90143-6

Terskiy, A., Wannemacher, K. M., Yadav, P. N., Tsai, M., Tian, B., and Howells, R. D. (2007). Search of the human proteome for endomorphin-1 and endomorphin-2 precursor proteins. *Life Sci.* 81, 1593–1601. doi: 10.1016/j.lfs.2007.09.025

Thompson, G. L., Kelly, E., Christopoulos, A., and Canals, M. (2014). Novel GPCR paradigms at the mu-opioid receptor. *Br. J. Pharmacol.* doi: 10.1111/bph.12600 [Epub ahead of print].

Traub, R. J., Hutchcroft, K., and Gebhart, G. F. (1999). The peptide content of colonic afferents decreases following colonic inflammation. *Peptides* 20, 267–273. doi: 10.1016/S0196-9781(98)00157-0

Valdez-Morales, E., Guerrero-Alba, R., Ochoa-Cortes, F., Benson, J., Spreadbury, I., Hurlbut, D., et al. (2013). Release of endogenous opioids during a chronic IBD model suppresses the excitability of colonic DRG neurons. *Neurogastroenterol. Motil.* 25, 39.e4–46.e4. doi: 10.1111/nmo.12008

Van Op den Bosch, J., Adriaensen, D., Van Nassauw, L., and Timmermans, J. P. (2009). The role(s) of somatostatin, structurally related peptides and somatostatin receptors in the gastrointestinal tract: a review. *Regul. Pept.* 156, 1–8. doi: 10.1016/j.regpep.2009.04.003

Verma-Gandhu, M., Bercik, P., Motomura, Y., Verdu, E. F., Khan, W. I., Blennerhassett, P. A., et al. (2006). CD4+ T-cell modulation of visceral nociception in mice. *Gastroenterology* 130, 1721–1728. doi: 10.1053/j.gastro.2006.01.045

Verma-Gandhu, M., Verdu, E. F., Cohen-Lyons, D., and Collins, S. M. (2007). Lymphocyte-mediated regulation of beta-endorphin in the myenteric plexus. *Am. J. Physiol. Gastrointest. Liver Physiol.* 292, G344–G348. doi: 10.1152/ajpgi.00318.2006

Vincent, S. R., Dalsgaard, C. J., Schultzberg, M., Hokfelt, T., Christensson, I., and Terenius, L. (1984). Dynorphin-immunoreactive neurons in the autonomic nervous system. *Neuroscience* 11, 973–987. doi: 10.1016/0306-4522(84)90208-2

Waldhoer, M., Bartlett, S. E., and Whistler, J. L. (2004). Opioid receptors. *Annu. Rev. Biochem.* 73, 953–990. doi: 10.1146/annurev.biochem.73.011303.073940

Waldhoer, M., Fong, J., Jones, R. M., Lunzer, M. M., Sharma, S. K., Kostenis, E., et al. (2005). A heterodimer-selective agonist shows in vivo relevance of G protein-coupled receptor dimers. *Proc. Natl. Acad. Sci. U.S.A.* 102, 9050–9055. doi: 10.1073/pnas.0501112102

Walsh, J. H. (1988). Peptides as regulators of gastric acid secretion. *Annu. Rev. Physiol.* 50, 41–63. doi: 10.1146/annurev.ph.50.030188.000353

Wang, Y. N., and Lindberg, I. (1986). Distribution and characterization of the opioid octapeptide met5-enkephalin-arg6-gly7-leu8 in the gastrointestinal tract of the rat. *Cell Tissue Res.* 244, 77–85. doi: 10.1007/BF00218384

Weinstock, J. V., and Elliott, D. (2000). The somatostatin immunoregulatory circuit present at sites of chronic inflammation. *Eur. J. Endocrinol.* 143(Suppl. 1), S15–S19. doi: 10.1530/eje.0.143S015

Wolter, H. J. (1985a). Colocalization of dynorphin-A(1-17) and dynorphin-A(1-8) within some perikarya of rat duodenum: immunohistochemical evidence for the presence of two separate dynorphinergic systems. *Biochem. Biophys. Res. Commun.* 130, 774–780. doi: 10.1016/0006-291X(85)90483-8

Wolter, H. J. (1985b). Ultrastructural evidence for beta-endorphin-like immunoreactivity in the nervous system of the rat duodenum. *Brain Res.* 334, 194–199. doi: 10.1016/0006-8993(85)90588-8

Wolter, H. J. (1986). Identification of the tridecapeptide dynorphin B (rimorphin) within perikarya of rat duodenum. *Life Sci.* 39, 727–730. doi: 10.1016/0024-3205(86)90020-2

Wood, J. D., and Galligan, J. J. (2004). Function of opioids in the enteric nervous system. *Neurogastroenterol. Motil.* 16(Suppl. 2), 17–28. doi: 10.1111/j.1743-3150.2004.00554.x

Yakovleva, T., Bazov, I., Cebers, G., Marinova, Z., Hara, Y., Ahmed, A., et al. (2006). Prodynorphin storage and processing in axon terminals and dendrites. *FASEB J.* 20, 2124–2126. doi: 10.1096/fj.06-6174fje

Yuferov, V. P., Culpepper-Morgan, J. A., Laforge, K. S., Ho, A., and Kreek, M. J. (1998). Regional quantitation of preprodynorphin mRNA in guinea pig gastrointestinal tract. *Neurochem. Res.* 23, 505–511. doi: 10.1023/A:1022426400545

Zadina, J. E., Hackler, L., Ge, L. J., and Kastin, A. J. (1997). A potent and selective endogenous agonist for the mu-opiate receptor. *Nature* 386, 499–502. doi: 10.1038/386499a0

Zamir, N., Weber, E., Palkovits, M., and Brownstein, M. (1984). Differential processing of prodynorphin and proenkephalin in specific regions of the rat brain. *Proc. Natl. Acad. Sci. U.S.A.* 81, 6886–6889. doi: 10.1073/pnas.81.21.6886

Zhao, P., Canals, M., Murphy, J. E., Klingler, D., Eriksson, E. M., Pelayo, J. C., et al. (2013). Agonist-biased trafficking of somatostatin receptor 2A in enteric neurons. *J. Biol. Chem.* 288, 25689–25700. doi: 10.1074/jbc.M113.496414

Zingg, H. H., and Patel, Y. C. (1983). Processing of somatostatin-28 to somatostatin-14 by rat hypothalamic synaptosomal membranes. *Life Sci.* 33, 1241–1247. doi: 10.1016/0024-3205(83)90004-8

Zweemer, A. J., Toraskar, J., Heitman, L. H., and IJzerman, A. P. (2014). Bias in chemokine receptor signalling. *Trends Immunol.* 35, 243–252. doi: 10.1016/j.it.2014.02.004

Conflict of Interest Statement: The authors declare that the research was conducted in the absence of any commercial or financial relationships that could be construed as a potential conflict of interest.

Received: 29 September 2014; accepted: 12 November 2014; published online: 28 November 2014.

*Citation: Thompson GL, Canals M and Poole DP (2014) Biological redundancy of endogenous GPCR ligands in the gut and the potential for endogenous functional selectivity. Front. Pharmacol. **5**:262. doi: 10.3389/fphar.2014.00262*

This article was submitted to Neuropharmacology, a section of the journal Frontiers in Pharmacology.

B.2 Novel GPCR Paradigms at the μ-Opioid Receptor

BJP British Journal of Pharmacology

DOI:10.1111/bph.12600
www.brjpharmacol.org

Themed Section: Opioids: New Pathways to Functional Selectivity

REVIEW

Novel GPCR paradigms at the μ-opioid receptor

G L Thompson[1], E Kelly[2], A Christopoulos[1] and M Canals[1]

[1]*Drug Discovery Biology and Department of Pharmacology, Monash Institute of Pharmaceutical Sciences, Monash University, Parkville, Vic., Australia, and* [2]*School of Physiology and Pharmacology, University of Bristol, Bristol, UK*

Correspondence
Meritxell Canals, Drug Discovery Biology and Department of Pharmacology, Monash Institute of Pharmaceutical Sciences, Monash University, 399 Royal Parade, Parkville, Vic. 3052, Australia. E-mail: meri.canals@monash.edu

Received
23 October 2013
Revised
12 January 2014
Accepted
19 January 2014

Opioids, such as morphine, are the most clinically useful class of analgesic drugs for the treatment of acute and chronic pain. However, the use of opioids is greatly limited by the development of severe adverse side effects. Consequently, drug discovery efforts have been directed towards improving the therapeutic profile of opioid-based treatments. Opioid receptors are members of the family of GPCRs. As such, the recent GPCR paradigms of biased agonism and allosterism may provide novel avenues for more effective analgesics. Biased agonism (or functional selectivity) has been described for all the opioid receptor family members. Furthermore, the first allosteric modulators of opioid receptors have very recently been described. However, identification and quantification of biased agonism in a manner that is informative to medicinal chemists and drug discovery programmes still remains a challenge. In this review, we examine the progress, to date, towards identification and quantification of biased agonism and allosterism at the μ-opioid receptor in the context of its implications for the discovery of better and safer analgesics.

LINKED ARTICLES

This article is part of a themed section on Opioids: New Pathways to Functional Selectivity. To view the other articles in this section visit http://dx.doi.org/10.1111/bph.2015.172.issue-2

Abbreviations

DAMGO, [D-Ala[2], NMe-Phe[4], Gly-ol[5]]-enkephalin; DOR, δ-opioid receptor; GRK2, GPCR kinase 2; KOR, κ-opioid receptor; MOR, μ-opioid receptor; PAM, positive allosteric modulator; SAR, structure–activity relationship

GPCRs can mediate a spectrum of acute signalling and longer-term regulatory behaviours that can be modulated in a ligand-specific manner. Such functional versatility cannot be explained by a simple 'on–off' switch model of receptor activation, and is more compatible with dynamic and flexible structures. Indeed, during the last decade, we have witnessed the experimental confirmation of previously theoretical concepts demonstrating that GPCRs exist in many, temporally related, micro-conformations (Deupi and Kobilka, 2010). Approaches such as NMR spectroscopy have provided evidence that GPCRs are highly dynamic proteins that exist in several functionally relevant conformational states (Hofmann *et al.*, 2009; Bokoch *et al.*, 2010). Two paradigms that are fundamentally linked to such inherent plasticity of GPCRs are biased agonism (or functional selectivity) and allosterism.

Biased agonism describes the phenomenon whereby the binding of different ligands to the same receptor in an identical cellular background results in differential activation of cell signalling pathways, and eventually, in different physiological outcomes (Kenakin, 2011). At a molecular level, this is a consequence of the fact that different agonists do not activate receptors through stabilization of the same active state; rather, they can stabilize different functionally active states that lead to the engagement of a limited subset of intracellular effectors, and in turn, the activation of specific signalling pathways. The ability of distinct GPCR-agonist complexes to differentially activate intracellular signals provides new avenues for the development of drugs that are not only receptor-specific, but also 'pathway-specific', and has opened the way to the discovery of ligands that selectively activate signalling pathways mediating the desired

physiological effects while minimizing 'on-target' side effects that are elicited by activation of other signalling pathways via the same receptor. However, although this concept is very attractive, there are significant challenges to its translation from the field of medicinal chemistry into effective therapies. On the one hand, the identification of the signalling pathways responsible for therapeutic effects and of those responsible for the deleterious side effects is not straightforward; on the other hand, analytical tools for the detection and quantification of biased agonism are becoming available for drug development efforts aimed in this direction (Kenakin and Christopoulos, 2013).

The phenomenon of allosterism is also a consequence of the conformational plasticity of GPCRs. Allosteric ligands influence receptor activity by binding to sites that are topographically distinct from the site where the endogenous (orthosteric) ligand binds. Classical models of allosterism already postulated the need for multiple conformational states in the absence of ligand as a fundamental characteristic of allosteric proteins (Monod *et al.*, 1965). These states exist in a dynamic equilibrium, and the binding of a ligand to an allosteric protein stabilizes some states at the expense of others (Canals *et al.*, 2011). As such, allosteric ligands mediate their effects by promoting conformational changes in the GPCR protein that are transmitted from the allosteric binding pocket to the orthosteric site, or directly to the effector sites. In terms of drug development, allosteric GPCR ligands offer significant advantages over targeting of the orthosteric site. First, because of the lack of evolutionary pressure on sites other than that where the endogenous ligand binds, allosteric sites have not necessarily been conserved and therefore offer greater potential for receptor subtype selectivity. Second, in the absence of intrinsic efficacy, allosteric modulators will only exert their effect when and where the endogenous ligand is present, therefore tuning cellular responses and maintaining the temporal and spatial characteristics of endogenous signals. Furthermore, as the effect of an allosteric ligand is limited by its cooperativity, such class of ligands may become safer therapies with fewer on-target overdosing risks.

Studies on opioid receptors have provided prototypical examples of ligand-dependent signalling and regulation (Raehal *et al.*, 2011), and recently, allosteric modulators of the μ-opioid receptor (MOR; receptor nomenclature follows Alexander *et al.*, 2013) have been described (Burford *et al.*, 2013). In this review, we examine the progress, to date, towards identification and quantification of biased agonism and allosterism at the MOR, in the context of its implications for the discovery of better and safer analgesics.

Ligand-dependent effects at the MOR

Opioids have been used for millennia for the treatment of moderate to severe pain, and remain the most effective and widely used analgesics to date. Of the four subtypes of opioid receptors, the MOR subtype is the therapeutic target for most currently used opioids as the analgesic effects of morphine were abolished in a MOR knockout mouse (Kieffer and Gavériaux-Ruff, 2002). However, it is well known that opioid analgesics, including morphine, oxycodone and fentanyl, suffer from very limiting side effects such as tolerance, dependence and addiction, respiratory depression, and constipation, which severely limit their clinical use. Therefore, there is a need for new compounds that provide effective analgesia, but without the serious side effects.

As mentioned previously, biased agonism offers such potential, and there are clear indications of the existence of ligand-specific effects on MOR signalling and regulation (see Raehal *et al.*, 2011; Williams *et al.*, 2013). Two key observations on the actions of morphine triggered most of the studies on functional selectivity at the MOR. First, morphine induces relatively less internalization of MORs internalization, in spite of its efficacy in mediating G-protein activation (Keith *et al.*, 1996; Sternini *et al.*, 1996). Second, morphine-induced respiratory depression and constipation are dramatically attenuated in a β-arrestin2 knockout mouse while analgesia is enhanced (Raehal *et al.*, 2005). This latter result also provided clear evidence of the tissue-specific mechanisms of receptor activity and regulation. Taken together, these reports have sparked the search for the potentially different signalling mechanisms that mediate the diverse physiological actions of MOR agonists as well as for ligands that exploit such mechanisms. However, most descriptions of biased agonism at the MOR have been based on qualitative comparisons between ligands. The number of studies quantifying bias is still very low (see later). Yet, in order to apply biased agonism therapeutically and effectively, it is necessary to incorporate parameters that describe the degree of bias in a manner that can inform future drug development.

Quantifying biased agonism

Although biased agonism is now widely accepted, the majority of studies to date on functional selectivity have used largely qualitative observations, such as reversals in agonist potency orders or maximal agonist effects between different pathways, as indicators of biased agonism. However, such approaches are not optimal. The observed response of an agonist at a given pathway is not only the result of unique ligand-induced receptor conformations, but is also affected by 'system bias', which reflects the differing coupling efficiencies of the receptor to a given signalling pathway, and by 'observation bias', which results from differing assay sensitivity and conditions (Kenakin and Christopoulos, 2013). It is the bias imposed by the ligand on the receptor that is the only source of bias that can be chemically optimized to improve the therapeutic profile of a drug. It is therefore important to quantify signalling bias in such a way that it excludes system and observation bias, in order to reveal the unique signalling profile that is induced by the ligand.

The potency of a ligand is determined by both its affinity for the receptor state coupled to that particular pathway, as well as its intrinsic efficacy for generating a response in that pathway. In contrast, the maximal effect of a ligand at saturating concentrations is only determined by intrinsic efficacy. In addition, contributors to system bias, signal amplification and receptor expression need to be taken into account as they have markedly different effects on potencies and efficacies of differently efficacious ligands. Therefore, a rigorous and useful analysis of bias should take into account both potency

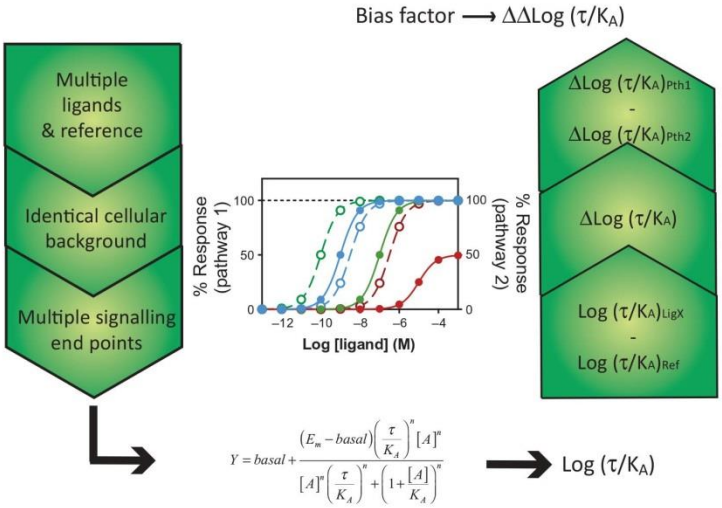

Figure 1

Quantification of biased agonism using relative transduction ratios. In order to quantify the signalling bias of a set of ligands, it is necessary to measure bias in an identical cellular background across several signalling end points. Full concentration–response curves for each pathway are fitted to the Black–Leff operational model to estimate a transduction coefficient (log[τ/K_A]) for each agonist (in the example, solid lines for pathway 1 and dotted lines for pathway 2). Next, the effects of system and observation bias are removed by adjusting these values to a reference ligand to yield the Δlog[τ/K_A]. Finally, the relative transduction ratio (ΔΔlog[τ/K_A]) is obtained by subtraction of the Δlog[τ/K_A] value of two pathways one from another. The ΔΔlog[τ/K_A] values represent ligand bias on a linear scale, which is amenable to statistical analysis. [A], agonist concentration; K_A, operational affinity; τ, efficacy; n, slope of the fitting parameter; E_m, maximal response of the system. For a step-by-step method to measure bias, see Appendix 1 or van der Westhuizen *et al.* (2014).

and maximal effect of a ligand, eliminate effects of system and observation bias, and should be broadly applicable to routinely derived concentration–response data. Such analysis would not only allow the signalling bias profiles of ligands in different cell types to be compared, but would also aid the efforts of medicinal chemists to discover new biased ligands.

Several analytical approaches have been described to quantify biased agonism (see Kenakin and Christopoulos, 2013). Of these, the relative transduction ratio [ΔΔlog(τ/K_A)] is one of the most robust and widely applicable method for bias quantification. This method applies the operational model of agonism first derived by Black and Leff (1983). Application of this model to concentration–response curves estimates a 'transduction coefficient' log(τ/K_A) which is comprised of the functional equilibrium dissociation constant (operational affinity, K_A), a measure of the affinity for the receptor coupled to a particular effector protein or signalling pathway, which is different from the affinity of the ligand for the bare receptor determined in radioligand binding experiments (see later); and τ which encompasses both the intrinsic efficacy of the agonist in activating a particular signalling response and receptor density. The log(τ/K_A) is thus an overall measure of the relative 'power' of an agonist to induce a response. In order to eliminate the effects of system and observation bias, the log(τ/K_A) is normalized to a reference agonist, yielding values of Δlog(τ/K_A). Finally, these values can be compared across two signalling pathways for a given agonist to obtain the relative transduction ratio ΔΔlog(τ/K_A) as measures of agonist bias (Figure 1 and Appendix 1 for a step-by-step method to measure bias).

Quantification of biased agonism at MOR

The effects of morphine in the β-arrestin2 knockout mice (Raehal *et al.*, 2005) together with the substantial evidence of the distinct effects of morphine in MOR desensitization and internalization (Johnson *et al.*, 2006; Dang *et al.*, 2011) suggest that ligands that display bias towards G-protein-mediated pathways and away from β-arrestin2 recruitment, may have improved therapeutic profiles as analgesics. Such ligands offer the potential to provide pain relief with less adverse effects normally associated with the opioid agonists, including tolerance, dependence and addiction, constipation, nausea, and respiratory depression. For this reason, most of the studies focused on detection and quantification of biased agonism have utilized these two pathways, G-protein activation and β-arrestin2 recruitment, albeit using different approaches for such determinations (Borgland, 2003; McPherson *et al.*, 2010; Molinari *et al.*, 2010; Frölich *et al.*, 2011; Rivero *et al.*, 2012).

Using a BRET approach, Molinari *et al.* (2010) investigated the ability of MOR and δ-opioid receptor (DOR) to activate

G-proteins and recruit β-arrestins. G-protein activation by a wide range of opioid ligands was measured as changes in the BRET signal between the receptor and the β1 subunit of the G-protein in cell membranes, while β-arrestin recruitment to the receptor was performed in whole cells. Plotting the relative intrinsic activities (i.e. the maximal response of a given ligand relative to the maximal response of a reference agonist) of all ligands, using the two signalling end points, revealed a hyperbolic relationship between the two pathways. This is in line with the fact that most of the tested ligands displayed full agonism for G-protein activation and that comparison of intrinsic activities fails to differentiate between full agonists (Stallaert *et al.*, 2011). A number of ligands, including morphine, oxymorphone and ethylketocyclazocine clustered as ligands with low intrinsic activities for β-arrestin2 recruitment and high intrinsic activities for G-protein activation. Indeed, this result is also expected when the coupling efficiency of different pathways is taken into consideration, as the response of partial agonists will be lower in less efficiently coupled signalling pathways such as β-arrestin2 recruitment. Estimation of the bias factor $\Delta\Delta\log(\tau/K_A)$ relative to etorphine of the corresponding concentration–response curves reveals that different intrinsic activities (such as oxymorphone vs. etorphine, endomorphin-2 or lofentanyl) do not necessarily translate into significant ligand bias (Figure 2A).

As bias is an intrinsic characteristic of a ligand, it follows that metabolites of a given ligand do not necessarily have to mimic the bias of the original compound. Interestingly, this has been evaluated *in vitro* for morphine, and its metabolites (Frölich *et al.*, 2011) using FRET approaches to detect $G\alpha_{i1}$ activation and β-arrestin2 recruitment. Comparison of relative efficacies of all the metabolites with morphine, suggested that only three metabolites (normorphine, 6-acetylmorphine, morphine-6-glucuronide) showed bias towards β-arrestin2 recruitment. However, when using morphine as the reference ligand to estimate $\Delta\Delta\log(\tau/K_A)$ values, nearly all the metabolites are significantly biased towards β-arrestin2 compared with morphine (Figure 2B). This illustrates additional information that can be obtained by application of the operational model of agonism to detect and quantify bias because, as mentioned previously, comparison of relative efficacies fails to distinguish between full agonists as their activity is limited by the system. In this case, the signalling bias of higher-efficacy agonists may be overlooked or may be mistakenly considered as biased when they are in fact not. Therefore, in the case of the higher-efficacy agonists, a scale that incorporates both the maximal response and potency, such as the transduction coefficient, is required. Such results also suggest that morphine metabolites possess divergent signalling bias, an aspect that will need to be taken into consideration when interpreting the effects of morphine signalling *in vivo*. Finally, it should be noted that in these experiments, GRK2 was only overexpressed when measuring β-arrestin2 recruitment, and as described later, the cellular content of relevant proteins or other agents can also play a role in the direction of bias. It would therefore be very informative to quantify bias of morphine metabolites under similar conditions across different signalling pathways.

In a systematic approach to evaluate biased agonism at the MOR, McPherson *et al.* examined the signalling bias of a wide range of ligands including endogenous opioid peptides and synthetic opioids (McPherson *et al.*, 2010; Rivero *et al.*, 2012). As in the previous reports, G-protein activation and β-arrestin2 recruitment were measured by [^{35}S]GTPγS binding, and an enzymatic complementation assay respectively. In these studies, endomorphin-2 was the only ligand that showed statistically significant bias towards β-arrestin2 recruitment. Agonist bias was determined by fitting concentration–response curves to the Black–Leff operational model to estimate the efficacy parameter τ. However, instead of estimating the functional affinity of the ligand-bound

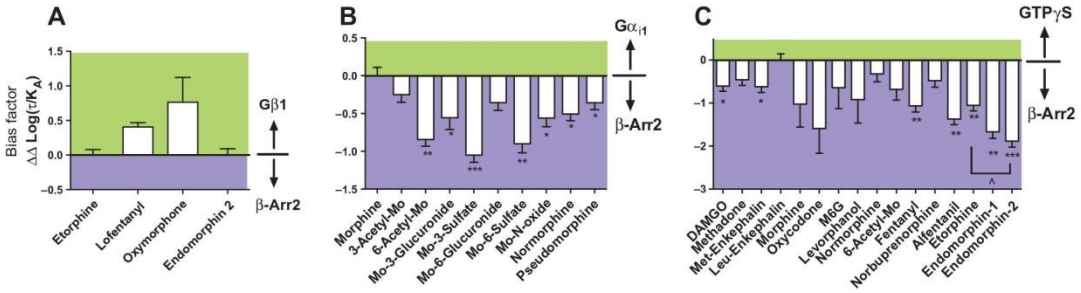

Figure 2

Quantification of signalling bias between G-protein and β-arrestin interactions at the MOR. (A) Relative transduction ratios estimated for data from Molinari *et al.* 2010 between assays for Gβ1 and β-arrestin2 interactions using etorphine as the reference ligand showed no significant bias between ligands (B) Relative transduction ratios between $G\alpha_i1$ and β-arrestin2 recruitment estimated using data from Frölich *et al.* (2011) using morphine as the reference ligand shows that most morphine metabolites are significantly biased towards recruitment of β-arrestin2 compared with morphine (C) Relative transduction ratios between GTPγS binding and β-arrestin2 recruitment from McPherson *et al.* (2010) estimated using Leu-enkephalin as the reference ligand show that in addition to endomorphin-2, endomorphin-1, etorphine and several other ligands are biased towards β-arrestin2 recruitment. The two-tailed *t*-test was used to determine whether transduction ratios were statistically different from the reference ligand * $P \leq 0.05$, ** $P \leq 0.01$, *** $P \leq 0.001$, ^ $P \leq 0.05$.

receptor in each particular pathway, the affinity parameter in these calculations remained constant across pathways and was determined from radioligand binding experiments (Rajagopal *et al.*, 2011). Given that a ligand can have differing affinities for distinct receptor states (e.g., for the G-protein-bound and unbound states), such differing affinities have to be taken into account when measuring biased agonism. Although in some situations, the binding affinity and the functional affinity can be very similar, this will not always be the case (see Kenakin and Christopoulos, 2013; Shonberg *et al.*, 2013). When the dissociation constant is obtained from concentration–response curves using the Black–Leff operational model and bias factors are estimated, it becomes apparent that other ligands, apart from endomorphin-2 also show significant bias towards β-arrestin2 recruitment when compared with Leu-enkephalin as a reference ligand (Figure 2C). Interestingly, some ligands used in this analysis had previously been used in other studies. However, the relative transduction ratio analysis suggests that morphine-6-glucuronide, 6-acetyl-morphine and normorphine did not show significant bias towards β-arrestin2 recruitment when compared with morphine in contrast to previous reports (Frölich *et al.* (2011). Similarly, this analysis also revealed a significant difference between etorphine and endomorphin2 that had not been detected by Molinari *et al.* (2010; Figure 2C).

Finally, the ability of different ligands to mediate G-protein activation, receptor desensitization and receptor internalization has been examined using inhibition of calcium channel currents (I_{Ca}) and immunocytochemistry, respectively, as functional readouts (Borgland, 2003). The relative efficacies of [D-Ala^2, NMe-Phe^4, Gly-ol^5]-enkephalin (DAMGO), morphine, methadone and pentazocine were measured for acute inhibition of calcium currents, for homologous desensitization of these currents and for receptor endocytosis. Importantly, relative efficacies were calculated using functional affinity constants determined experimentally from receptor depletion experiments. These experiments revealed that the efficacy for I_{Ca} inhibition did not correlate with the efficacy of desensitization or receptor internalization, suggesting that morphine and, potentially, pentazocine are biased, relative to DAMGO, and that acute desensitization is not dependent on receptor internalization.

Overall, these studies have provided valuable insight into biased signalling of opioids at MOR although it still remains to be seen whether they are able to predict differential responses *in vivo*. These studies also illustrate the importance of a number of factors that influence the identification and quantification of biased agonism such as cellular content, the pluridimensionality of efficacy and the choice of a reference agonist. It is important to consider these key aspects when interpreting information obtained from studying biased signalling *in vitro*.

Effect of cellular content on biased agonism

The content of signalling effectors among different cells is not identical. As a consequence, biased agonism across different cellular systems is likely to change. This has important implications *in vivo* as, for instance, the effect of the same ligand in primary cells isolated from different tissues can show opposite bias. One relevant example in the case of the MOR-biased agonism is the effect of the levels of GRK2 expression. Overexpression of GRK2 has sometimes been used as a strategy to increase the sensitivity of the detection of β-arrestin2 recruitment to several GPCRs including the MOR (Hoffmann *et al.*, 2008; Allen *et al.*, 2011; Frölich *et al.*, 2011). However, there is substantial evidence to demonstrate that receptor phosphorylation is also subject to bias (ligand-dependent) and that this phosphorylation can have downstream consequences such as differential engagement of signalling kinases or differential receptor regulation (Tobin *et al.*, 2008; Butcher *et al.*, 2011; Doll *et al.*, 2011; Just *et al.*, 2013). Thus, overexpressing a particular kinase may have differential effects on the efficacy of distinct ligands, thus changing the bias profile of the entire set of ligands. One approach to minimize such artificial introduction of bias is to evaluate all the signalling end points under exactly the same cellular conditions and content, for example overexpressing GRK2 when investigating all the pathways in addition to β-arrestin2 recruitment.

However, the issue of differential contents of effector and regulatory proteins in different tissues still remains. For example, high levels of GRK2 are found in brain, leukocytes, heart and spleen, followed by lung and kidney (Aragay *et al.*, 1998). Thus, quantification of signalling bias in recombinant cells can be used to reveal ligands with unique signalling profiles that can then be used as pharmacological tools for studying the consequences of biased agonism *in vivo*. It is therefore important to adopt a global perspective on the concept of bias, that is as an indicator of differential behaviours, fingerprints or activity profiles across ligands at the same receptor that can ultimately translate to different physiological outcomes.

Efficacy is pluridimensional

Most of the descriptions of biased agonism to date have focused on the differential activation of G-protein-mediated events and β-arrestin2 recruitment. However, it is evident that most GPCRs pleiotropically couple to a myriad of signalling effectors. The ability of compounds to promote unique, ligand-selective conformations of GPCRs that are able to engage different transduction pathways or regulatory events underlies the mechanism for the pluridimensionality of efficacy (Galandrin *et al.*, 2007). As such, the detection of bias should be extended beyond differences between G-protein activation and β-arrestin2 recruitment. Additionally, it is now clear that signalling efficacy through GPCRs is not linear, and that multiple mechanisms control the responsiveness of receptor systems such as desensitization and internalization, resulting from receptor phosphorylation (Kenakin, 2007). It is now established in several GPCR models, including the MOR, that not all ligands with similar apparent efficacy towards a given signalling pathway display a similar propensity to trigger these regulatory events (Sternini *et al.*, 1996).

The MOR has been shown to couple to many signalling effectors via G-proteins and β-arrestins (see Law, 2011; Raehal *et al.*, 2011; Georgoussi *et al.*, 2012). Furthermore, the MOR has also been shown to directly interact with phospholipase D2 (Koch *et al.*, 2003), and with proteins that control its localization in lipid raft microdomains (Ge *et al.*, 2009). As such, limiting bias studies to these two proximal events directly limits the detection of functional selectivity. In addition, there is now evidence of biased activation of G-protein subunits by the MOR, which is not detected in proximal

G-protein activation assays (such as cAMP inhibition), but may differentially affect downstream signalling (Massotte *et al.*, 2002; Clark and Traynor, 2006; Saidak *et al.*, 2009). Similarly, biased effects on β-arrestin activity are not completely captured in β-arrestin recruitment assays. β-arrestins have a diverse range of functions that affect signalling and receptor regulation, which are dependent on both cellular content and the ligand itself. The strength of interaction between the receptor and β-arrestin, as measured in a β-arrestin recruitment assay, is not necessarily indicative of the subsequent effects on downstream signalling and receptor regulation.

The systematic analysis of many signalling end points will maximize the information obtained from biased signalling studies *in vitro* as such approaches will provide 'textures' of ligands in cellular models. Different 'textures' *in vitro* may be indicative of distinct physiological fingerprints when translating bias into physiologically relevant systems.

Relevance of the reference ligand

As mentioned earlier, signalling bias is a relative measure; it is always in comparison with another ligand. As such, choosing a reference ligand is a key aspect of the quantification. The reference ligand itself is not unbiased (there is no such thing), but ideally, the reference ligand should show activity in most pathways as well as possess a signalling profile similar to the endogenous ligand or to most ligands that target that particular GPCR. It can be misleading to use a reference agonist such as morphine, which is known to exhibit differential signalling when compared with most endogenous opioid peptides. Under most conditions, morphine will be biased towards G-protein-mediated signalling, so if it is used as a reference agonist, most other ligands will be clustered as β-arrestin biased. This is illustrated in Figure 3, where bias between G-protein activation and β-arrestin2 recruitment measured by Frölich *et al.* (2011), is quantified using two different reference ligands. As shown earlier, when morphine is used as the reference ligand to estimate values of $\Delta\Delta\log(\tau/K_A)$, nearly all the morphine metabolites are biased towards β-arrestin2 recruitment. However, when an agonist with higher efficacy in the β-arrestin2 recruitment assay, such as normorphine, is used as the reference agonist, the calculated bias for many of the metabolites appears to change. This shows that the majority of the metabolites are similar to normorphine, whereas morphine becomes significantly G-protein-biased and there are now only three metabolites that are biased towards β-arrestin2 recruitment. However, it is important to note that while the absolute bias factors ascribed to an agonist will change depending upon the ligand designated as reference, whether or not a significant difference exists between any ligand pair will not change regardless of which ligand is designated as reference.

In order to make direct comparisons of signalling bias among different studies, it is important that the same ligand is used as a reference for quantification. The reference ligand is also very important when attempting to predict bias *in vivo*. As mentioned earlier, ligand bias is cell-dependent, making predictions of *in vivo* bias difficult. However, extensive knowledge of the physiological activity and signalling by the reference ligand, will allow links between signalling profiles and physiological effects to be made. Hence, the reference should ideally be a ligand that has been very widely studied. The obvious choice in most cases would be to use the endogenous ligand; however, that is not straightforward with opioid receptors because of the existence of many endogenous opioid peptides. As DAMGO and Met-enkephalin have been the ligands most widely studied in MOR biology, these two ligands would potentially be ideal 'universal' candidates.

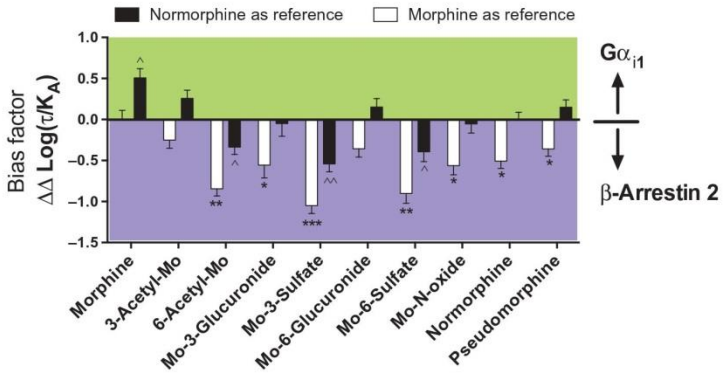

Figure 3

Quantification of bias using different reference ligands. Concentration–response curves from Frölich *et al.* 2011 for G-protein activation and β-arrestin2 recruitment were fitted to the operational model to estimate values of $\Delta\Delta\log(\tau/K_A)$ between the two pathways using either morphine or normorphine as the reference ligand. When morphine is used as the reference ligand most morphine metabolites are biased towards β-arrestin2 recruitment. When normorphine is used as the reference, morphine becomes G-protein-biased and its derivatives, 6-acetyl-morphine (6-acetyl-Mo), Mo-3-sulfate and Mo-6-sulfate are β-arrestin2-biased. The two-tailed t test was used to determine whether transduction ratios were statistically different from the reference ligand, morphine $^*P \le 0.05$, $^{**}P \le 0.01$, $^{***}P \le 0.001$ or normorphine $^{\wedge}P \le 0.05$, $^{\wedge\wedge}P \le 0.01$.

However, the choice of reference ligands will always depend on the question that a particular study is trying to address.

Use of biased agonism in drug discovery to improve pharmacological profiles of analgesics

Quantification and determination of bias *in vitro* can guide medicinal chemists towards the design of biased GPCR ligands for those receptors where the signalling cascades responsible for therapeutic versus side effects are known. Structure–activity relationship (SAR) studies at the angiotensin AT_1 receptor have resulted in a β-arrestin2-biased ligand (TRV120027) that is currently in clinical trials for acute decompensated heart failure (Boerrigter *et al.*, 2011). Similarly, at the dopamine D_2 receptor, biased partial agonists have been identified by exploring the structure of the antipsychotic aripiprazole through a combinatorial chemistry approach (Allen *et al.*, 2011) and, more recently, by classical SAR studies supplemented with parameters of bias and functional affinity determined using the transduction coefficient method (Shonberg *et al.*, 2013).

Given the phenotype of the β-arrestin2 knockout mouse and the accumulated evidence of ligand-directed signalling at the MOR, SAR approaches for the biased activation of this receptor have also been developed and have yielded promising compounds with analgesic function and improved side effect profile (Varamini *et al.*, 2012; DeWire *et al.*, 2013). Recently, new MOR ligands (low MW compounds and endomorphin-1 derivatives) that produce analgesia with less gastrointestinal dysfunction and respiratory depression have been reported. One of these compounds, TRV130, is the result of SAR screening studies by Trevena, Inc. focused on the discovery of G-protein-biased (as opposed to β-arrestin2 biased) ligands at the MOR (Chen *et al.*, 2013). *In vitro*, and compared with morphine, TRV130 displayed markedly different responses when assessed by two different signalling end points – inhibition of forskolin-induced cAMP and β-arrestin2 recruitment. Additionally, TRV130 showed decreased phosphorylation of the receptor at Ser^{375} and failed to internalize receptors. The authors examined bias between adenylate cyclase inhibition and β-arrestin2 recruitment by comparison of relative intrinsic activities (Rajagopal *et al.*, 2011) of TRV130 and morphine, and showed that TRV130 was biased towards adenylate cyclase inhibition. However, statistical comparison of bias using this method was hampered by the low efficacy of TRV130 in β-arrestin2 recruitment. As an alternative approach, the authors constructed a 'bias plot', where the normalized responses as changes in cAMP were shown as a function of the corresponding response in β-arrestin recruitment (Gregory *et al.*, 2010a; Kenakin and Christopoulos, 2013). Bias plots are useful graphical tools for visualizing bias of ligands between two pathways, but they incorporate all three types of bias, observation, system bias and ligand bias. This means ligand bias can only be observed when there are extreme differences between ligands, and also makes bias plots unsuitable for quantifying bias. Estimation of the bias factor using the operational model of agonism described above showed that the relative transduction ratio of TRV130 was not statistically different from morphine. The reduced β-arrestin2 recruitment observed with TRV130 in HEK cells could be attributed to the fact that it is a low-efficacy agonist and hence, poorly stimulates signalling pathways with low coupling efficiency. However, this moderate difference in the bias factors is very likely to be more relevant *in vivo*, which accounts for the improved pharmacological profile of TRV130. A more comprehensive analysis of bias of TRV130 across many signalling pathways, and compared with other opioid ligands will reveal more information about its unique bias profile, and provide insight into how TRV130 exerts its effects *in vivo*.

Finally, it is worth noting that most of the SAR studies performed so far that were focused on the discovery of biased ligands, have utilized differences between G-protein and β-arrestin-mediated pathways. However, it is tempting to anticipate that, in the coming years, there will be an increase in the number of studies that investigate a more diverse array of signalling end points that will reveal differential 'textures' of GPCR ligands.

Allosterism at the MOR

Although topographically distinct, druggable, allosteric sites have been postulated to be present in all GPCRs (May *et al.*, 2007; Gregory *et al.*, 2010b), the discovery of allosteric ligands that bind to the opioid receptors has remained a challenge until recently. Allosteric ligands induce conformational changes that are transmitted from the allosteric binding pocket to the orthosteric binding site. They offer the potential of improved subtype selectivity, decreased risk of overdose and maintained spatial and temporal activity of the target receptor (Keov *et al.*, 2011). All these pharmacological characteristics are of particular relevance for opioid-based therapies, as they may offer the potential to overcome the tolerance and dependence developed upon chronic/prolonged receptor activation. However, several considerations need to be taken into account regarding the effects of allosteric modulators on GPCRs.

The classical view of GPCR allosterism has focused on the change elicited on the properties of the orthosteric ligand; however, the conformational changes induced by the binding of an allosteric modulator can have similar consequences when considering the cytosolic proteins that interact with the receptor and mediate signal transduction. More importantly, this effect can vary depending on the different intracellular effectors. Macroscopically, this translates in some pathways being modulated, in either a positive or negative direction, at the expense of others. Finally, allosteric ligands can also display efficacy in their own right, and as such, they can potentially activate signalling pathways that are distinct from those activated by the orthosteric ligands. It is therefore important that the characterization of allosteric ligands includes the assessment of many relevant signalling pathways as well as the intrinsic efficacy of allosteric ligands on their own.

Interestingly, compared with other family A GPCRs, there have been significantly fewer allosteric ligands discovered for the opioid receptors. This is in contrast with the several descriptions of 'allosteric interactions' across opioid receptor

dimers, whether homodimers or heterodimers (Jordan and Devi, 1999; Wang, 2005; Milligan, 2009; Yekkirala *et al.*, 2012). With regards to the MOR subtype, the crystal structure of the MOR already suggests an oligomeric arrangement of this receptor (Manglik *et al.*, 2012), and allosteric interactions have been described between MOR and mGluR5, CB_1, DOR and κ–opioid receptors (Yekkirala *et al.*, 2011; Metcalf *et al.*, 2012; Akgün *et al.*, 2013; Le Naour *et al.*, 2013).

In terms of – low MW allosteric modulators, Burford *et al.* (2013) recently discovered the first allosteric modulators of the MOR using high throughput screening with a complementation approach to measure β-arrestin2 recruitment. This screening resulted in the identification of two positive allosteric modulators (PAMs) and two silent allosteric modulators (which bind to the allosteric site of the receptor but have neutral cooperativity with the orthosteric ligand). BMS-986121 and BMS-986122 positively modulated the binding of DAMGO to the MOR and potentiated the effects of endomorphin-1, DAMGO and morphine in β-arrestin2 recruitment, G-protein activation and cAMP inhibition. This exciting discovery has provided the tools to investigate the effects of allosterism on ligand-dependent effects at the MOR. For example, how do PAMs affect MOR regulation by different agonist? Do PAMs differently affect synthetic versus endogenous opioid ligands? It will also be extremely interesting to investigate whether PAMs can potentiate the analgesic effects of current opioid drugs or endogenous opioids, without potentiation of the side effects.

Concluding comments

Although GPCRs are coupled to a plethora of signalling pathways, most descriptions of biased agonism have been based on the comparison of two signalling events across different ligands. It is therefore quite likely that the 'relevant' signalling event has been omitted by the initial selection of signalling end points. Additionally, it is unlikely that a response derives from the activation of a very distinct signaling pathway. Rather, physiological responses are likely to reflect complex outputs from a tightly controlled and selective activation of a particular group of intracellular signals. Such a holistic view represents a major challenge for pharmacologists and medicinal chemists. One potential approach to predict physiological outcomes is the thorough investigation of many signaling end points in simple cellular models to generate ligand activity profiles. Subsequently these specific fingerprints can be related to more complex physiological responses. This approach requires not only a robust and systematic quantification method, but also the validation of signaling profiles in more relevant systems. However, once obtained, these fingerprints will represent a framework that will offer the potential to predict the physiological outcome from a novel drug.

Parallel with the discovery of new biased MOR ligands with improved therapeutic windows, the discovery of opioid receptor allosteric modulators will also open new avenues to overcome the current limitations of opioid ligands as analgesics. As such, the evaluation of this new class of compounds *in vivo* will be extremely informative in terms of whether allosterism can be exploited to generate better and safer analgesics.

Acknowledgements

The authors thank Graeme Henderson and Steven J. Charlton for providing complete data sets for analysis and J. Robert Lane for critical discussion of the paper. Work in the authors' laboratory is supported by the National Health and Medical Research Council of Australia (NHMRC) [Programme Grant 519461] A.C., [Project Grant APP1011796] M.C. A.C. is Principal Research Fellow of the NHMRC. G. L. T., PhD, is funded by DSTO Australia.

Conflict of interest

The authors state no conflict of interest.

References

Akgün E, Javed MI, Lunzer MM, Smeester BA, Beitz AJ, Portoghese PS (2013). Ligands that interact with putative MOR-mGluR5 heteromer in mice with inflammatory pain produce potent antinociception. Proc Natl Acad Sci USA 110: 11595–11599.

Alexander SPH, Benson HE, Faccenda E, Pawson AJ, Sharman JL, Spedding M *et al.* (2013). The Concise Guide to PHARMACOLOGY 2013/14: G Protein-Coupled Receptors. Br J Pharmacol 170: 1459–1581.

Allen JA, Yost JM, Setola V, Chen X, Sassano MF, Chen M *et al.* (2011). Discovery of β-arrestin-biased dopamine D2 ligands for probing signal transduction pathways essential for antipsychotic efficacy. Proc Natl Acad Sci USA 108: 18488–18493.

Aragay AM, Ruiz-Gómez A, Penela P, Sarnago S, Elorza A, Jiménez-Sainz MC *et al.* (1998). G protein-coupled receptor kinase 2 (GRK2): mechanisms of regulation and physiological functions. FEBS Lett 430: 37–40.

Black J, Leff P (1983). Operational models of pharmacological agonism. Proc R Soc Lond B Biol Sci 220: 141–162.

Boerrigter G, Lark MW, Whalen EJ, Soergel DG, Violin JD, Burnett JC (2011). Cardiorenal actions of TRV120027, a novel β-arrestin-biased ligand at the angiotensin II type I receptor, in healthy and heart failure canines: a novel therapeutic strategy for acute heart failure. Circ Heart Fail 4: 770–778.

Bokoch M, Zou Y, Rasmussen S, Liu C, Nygaard R, Rosenbaum D *et al.* (2010). Ligand-specific regulation of the extracellular surface of a G-protein-coupled receptor. Nature 463: 108–112.

Borgland SL (2003). Opioid agonists have different efficacy profiles for G protein activation, rapid desensitization, and endocytosis of mu-opioid receptors. J Biol Chem 278: 18776–18784.

Burford NT, Clark MJ, Wehrman TS, Gerritz SW, Banks M, O'Connell J *et al.* (2013). Discovery of positive allosteric modulators and silent allosteric modulators of the μ-opioid receptor. Proc Natl Acad Sci USA 110: 10830–10835.

Butcher AJ, Prihandoko R, Kong KC, McWilliams P, Edwards JM, Bottrill A *et al.* (2011). Differential G-protein-coupled receptor phosphorylation provides evidence for a signaling bar code. J Biol Chem 286: 11506–11518.

Canals M, Sexton PM, Christopoulos A (2011). Allostery in GPCRs: 'MWC' revisited. Trends Biochem Sci 36: 663–672.

Chen X-T, Pitis P, Liu G, Yuan C, Gotchev D, Cowan CL *et al.* (2013). Structure activity relationships and discovery of a G protein biased μ opioid receptor ligand, [(3-methoxythiophen-2-yl)methyl] ([2-[(9 R)-9-(pyridin-2-yl)-6-oxaspiro- [4.5]decan-9-yl]ethyl])-amine (TRV130), for the treatment of acute severe pain. J Med Chem 56: 8019–8031.

Clark MJ, Traynor JR (2006). Mediation of adenylyl cyclase sensitization by PTX-insensitive galpha oA, galphai1, galpha i2 or galpha i3. J Neurochem 99: 1494–1504.

Dang VC, Chieng B, Azriel Y, Christie MJ (2011). Cellular morphine tolerance produced by arrestin-2-dependent impairment of -opioid receptor resensitization. J Neurosci 31: 7122–7130.

Deupi X, Kobilka BK (2010). Energy landscapes as a tool to integrate GPCR structure, dynamics, and function. Physiology 25: 293–303.

DeWire SM, Yamashita DS, Rominger DH, Liu G, Cowan CL, Graczyk TM *et al.* (2013). A G protein-biased ligand at the -opioid receptor is potently analgesic with reduced gastrointestinal and respiratory dysfunction compared with morphine. J Pharmacol Exp Ther 344: 708–717.

Doll C, Konietzko J, Pöll F, Koch T, Höllt V, Schulz S (2011). Agonist-selective patterns of μ-opioid receptor phosphorylation revealed by phosphosite-specific antibodies. Br J Pharmacol 164: 298–307.

Frölich N, Dees C, Paetz C, Ren X, Lohse MJ, Nikolaev VO *et al.* (2011). Distinct pharmacological properties of morphine metabolites at G(i)-protein and β-arrestin signaling pathways activated by the human μ-opioid receptor. Biochem Pharmacol 81: 1248–1254.

Galandrin S, Oligny-Longpré G, Bouvier M (2007). The evasive nature of drug efficacy: implications for drug discovery. Trends Pharmacol Sci 28: 423–430.

Ge X, Qiu Y, Loh HH, Law P-Y (2009). GRIN1 regulates micro-opioid receptor activities by tethering the receptor and G protein in the lipid raft. J Biol Chem 284: 36521–36534.

Georgoussi Z, Georganta E-M, Milligan G (2012). The other side of opioid receptor signalling: regulation by protein-protein interaction. Curr Drug Targets 13: 80–102.

Gregory KJ, Hall NE, Tobin AB, Sexton PM, Christopoulos A (2010a). Identification of orthosteric and allosteric site mutations in M2 muscarinic acetylcholine receptors that contribute to ligand-selective signaling bias. J Biol Chem 285: 7459–7474.

Gregory KJ, Sexton PM, Christopoulos A (2010b). Overview of receptor allosterism. Curr Protoc Pharmacol 51: 1–34.

Hoffmann C, Ziegler N, Reiner S, Krasel C, Lohse M (2008). Agonist-selective, receptor-specific interaction of human P2Y receptors with beta-arrestin-1 and -2. J Biol Chem 283: 30933–30941.

Hofmann K, Scheerer P, Hildebrand P, Choe H-W, Park J, Heck M *et al.* (2009). A G protein-coupled receptor at work: the rhodopsin model. Trends Biochem Sci 34: 540–552.

Johnson EA, Oldfield S, Braksator E, Gonzalez-Cuello A, Couch D, Hall KJ *et al.* (2006). Agonist-selective mechanisms of mu-opioid receptor desensitization in human embryonic kidney 293 cells. Mol Pharmacol 70: 676–685.

Jordan BA, Devi LA (1999). G-protein-coupled receptor heterodimerization modulates receptor function. Nature 399: 697–700.

Just S, Illing S, Trester-Zedlitz M, Lau EK, Kotowski SJ, Miess E *et al.* (2013). Differentiation of opioid drug effects by hierarchical multi-site phosphorylation. Mol Pharmacol 83: 633–639.

Keith DE, Murray SR, Zaki PA, Chu PC, Lissin DV, Kang L *et al.* (1996). Morphine activates opioid receptors without causing their rapid internalization. J Biol Chem 271: 19021–19024.

Kenakin T (2007). Collateral efficacy in drug discovery: taking advantage of the good (allosteric) nature of 7TM receptors. Trends Pharmacol Sci 28: 407–415.

Kenakin T (2011). Functional selectivity and biased receptor signaling. J Pharmacol Exp Ther 336: 296–302.

Kenakin T, Christopoulos A (2013). Signalling bias in new drug discovery: detection, quantification and therapeutic impact. Nat Rev Drug Discov 12: 205–216.

Keov P, Sexton PM, Christopoulos A (2011). Allosteric modulation of G protein-coupled receptors: a pharmacological perspective. Neuropharmacology 60: 24–35.

Kieffer BL, Gavériaux-Ruff C (2002). Exploring the opioid system by gene knockout. Prog Neurobiol 66: 285–306.

Koch T, Brandenburg L-O, Schulz S, Liang Y, Klein J, Höllt V (2003). ADP-ribosylation factor-dependent phospholipase D2 activation is required for agonist-induced mu-opioid receptor endocytosis. J Biol Chem 278: 9979–9985.

Law PY (2011). Opioid receptor signal transduction mechanisms. Opiate Receptors 23: 195–238.

Le Naour M, Akgün E, Yekkirala A, Lunzer MM, Powers MD, Kalyuzhny AE *et al.* (2013). Bivalent ligands that target μ opioid (MOP) and cannabinoid1 (CB 1) receptors are potent analgesics devoid of tolerance. J Med Chem 56: 5505–5513.

Manglik A, Kruse AC, Kobilka TS, Thian FS, Mathiesen JM, Sunahara RK *et al.* (2012). Crystal structure of the μ-opioid receptor bound to a morphinan antagonist. Nature 485: 321–326.

Massotte D, Brillet K, Kieffer B, Milligan G (2002). Agonists activate Gi1 alpha or Gi2 alpha fused to the human mu opioid receptor differently. J Neurochem 81: 1372–1382.

May L, Leach K, Sexton P, Christopoulos A (2007). Allosteric modulation of G protein-coupled receptors. Annu Rev Pharmacol Toxicol 47: 1–51.

McPherson J, Rivero G, Baptist M, Llorente J, Al-Sabah S, Krasel C *et al.* (2010). μ-opioid receptors: correlation of agonist efficacy for signalling with ability to activate internalization. Mol Pharmacol 78: 756–766.

Metcalf MD, Yekkirala AS, Powers MD, Kitto KF, Fairbanks CA, Wilcox GL *et al.* (2012). The δ opioid receptor agonist SNC80 selectively activates heteromeric μ–δ opioid receptors. ACS Chem Neurosci 3: 505–509.

Milligan G (2009). G protein-coupled receptor hetero-dimerization: contribution to pharmacology and function. Br J Pharmacol 158: 5–14.

Molinari P, Vezzi V, Sbraccia M, Gro C, Riitano D, Ambrosio C *et al.* (2010). Morphine-like opiates selectively antagonize receptor-arrestin interactions. J Biol Chem 285: 12522–12535.

Monod J, Wyman J, Changeux J-P (1965). On the nature of allosteric transitions: a plausible model. J Mol Biol 88–118.

Raehal KM, Walker JKL, Bohn LM (2005). Morphine side effects in beta-arrestin 2 knockout mice. J Pharmacol Exp Ther 314: 1195–1201.

Raehal KM, Schmid CL, Groer CE, Bohn LM (2011). Functional selectivity at the μ-opioid receptor: implications for understanding opioid analgesia and tolerance. Pharmacol Rev 63: 1001–1019.

Rajagopal S, Ahn S, Rominger DH, Gowen-MacDonald W, Lam CM, DeWire SM *et al.* (2011). Quantifying ligand bias at seven-transmembrane receptors. Mol Pharmacol 80: 367–377.

Rivero G, Llorente J, McPherson J, Cooke A, Mundell SJ, McArdle CA *et al.* (2012). Endomorphin-2: a biased agonist at the μ-opioid receptor. Mol Pharmacol 82: 178–188.

Saidak Z, Blake-Palmer K, Hay DL, Northup JK, Glass M (2009). Differential activation of G-proteins by μ-opioid receptor agonists. Br J Pharmacol 147: 671–680.

Shonberg J, Klein Herenbrink C, Lopez Munoz L, Christopoulos A, Scammells PJ, Capuano B *et al.* (2013). A structure-activity analysis of biased agonism at the dopamine D2 receptor. J Med Chem 56: 9199–9221.

Stallaert W, Christopoulos A, Bouvier M (2011). Ligand functional selectivity and quantitative pharmacology at G protein-coupled receptors. Expert Opin Drug Discov 6: 811–825.

Sternini C, Spann M, Anton B, Keith DE, Bunnett NW, von Zastrow M *et al.* (1996). Agonist-selective endocytosis of mu opioid receptor by neurons *in vivo*. Proc Natl Acad Sci U S A 93: 9241–9246.

Tobin AB, Butcher AJ, Kong KC (2008). Location, location, location . . . site-specific GPCR phosphorylation offers a mechanism for cell-type-specific signalling. Trends Pharmacol Sci 29: 413–420.

Varamini P, Mansfeld FM, Blanchfield JT, Wyse BD, Smith MT, Toth I (2012). Lipo-endomorphin-1 derivatives with systemic activity against neuropathic pain without producing constipation. PLoS ONE 7: e41909.

Wang D (2005). Opioid receptor homo- and heterodimerization in living cells by quantitative bioluminescence resonance energy transfer. Mol Pharmacol 67: 2173–2184.

van der Westhuizen ET, Breton B, Christopoulos A, Bouvier M (2014). Quantification of ligand bias for clinically relevant 2-adrenergic receptor ligands: implications for drug taxonomy. Mol Pharmacol 85: 492–509.

Williams JT, Ingram SL, Henderson G, Chavkin C, von Zastrow M, Schulz S *et al.* (2013). Regulation of mu-opioid receptors: desensitization, phosphorylation, internalization, and tolerance. Pharmacol Rev 65: 223–254.

Yekkirala AS, Lunzer MM, McCurdy CR, Powers MD, Kalyuzhny AE, Roerig SC *et al.* (2011). N-naphthoyl-beta-naltrexamine (NNTA), a highly selective and potent activator of μ/kappa-opioid heteromers. Proc Natl Acad Sci USA 108: 5098–5103.

Yekkirala AS, Banks ML, Lunzer MM, Negus SS, Rice KC, Portoghese PS (2012). Clinically employed opioid analgesics produce antinociception via μ-δ opioid receptor heteromers in Rhesus monkeys. ACS Chem Neurosci 3: 720–727.

Appendix 1

Step-by-step quantification of bias using the operational model of agonism.

1. Concentration–response data should be normalized to the response of a reference ligand.
2. The operational model is used to determine the transduction ratios (τ/K_A) for the different agonists using the following equation which derives from the standard form of the operational model shown in Figure 1 [for a complete derivation, see van der Westhuizen *et al.* (2014)]

$$E = Basal + \frac{(E_m - Basal)}{1+\left(\frac{\left(\frac{[A]}{10^{\log K_A}}+1\right)}{10^{\log R}\times[A]}\right)^n}$$

   where E is the response of the ligand, $[A]$ is the concentration of agonist, E_m is the maximal possible response of the system, *Basal* is the basal level of response in the absence of agonist, $\log K_A$ denotes the logarithm of the functional equilibrium dissociation constant of the agonist, n is the slope of the transducer function that links occupancy to response, and logR is the logarithm of the 'transduction coefficient' (or 'transduction ratio'), τ/K_A, where τ is an index of the coupling efficiency (or efficacy) of the agonist. For the analysis, all families of agonist curves at each pathway are globally fitted to the model with the parameters, *Basal*, E_m and n shared between all agonists. For full agonists, the $\log K_A$ should be constrained to a value of zero, whereas for partial agonists this is directly estimated by the curve fitting procedure (van der Westhuizen *et al.*, 2014). The logR [i.e. $\log(\tau/K_A)$] parameter is estimated as a unique measure of activity for each agonist.
3. Elimination of system and observation bias is achieved by comparing ligand activity at a given signalling pathway with that of a reference compound. As such, the difference between the $\log\tau/K_A$ of an agonist and the reference ligand is calculated using the equation:

$$\Delta\log\left(\frac{\tau}{K_A}\right) = \log\left(\frac{\tau}{K_A}\right)_{Ligand} - \log\left(\frac{\tau}{K_A}\right)_{Reference}$$

4. Ligand bias is finally calculated as the difference between the $\Delta\log(\tau/K_A)$ values obtained from the previous equation at two different pathways

$$\Delta\Delta\log\left(\frac{\tau}{K_A}\right) = \Delta\log\left(\frac{\tau}{K_A}\right)_{Pathway\ 1} - \Delta\log\left(\frac{\tau}{K_A}\right)_{Pathway\ 2}$$

5. The bias factor is then the anti-logarithm of $\Delta\Delta\log(\tau/K_A)$.

$$\text{bias factor} = 10^{\Delta\Delta\log\left(\frac{\tau}{K_A}\right)}$$

6. For complete GraphPad Prism equations and fitting parameters, see van der Westhuizen *et al.* (2014).

B.3 Biased Agonism of Endogenous Opioid Peptides at the μ-Opioid Receptor

Supplemental material to this article can be found at:
http://molpharm.aspetjournals.org/content/suppl/2015/05/26/mol.115.098848.DC1.html

1521-0111/88/2/335–346$25.00
MOLECULAR PHARMACOLOGY

http://dx.doi.org/10.1124/mol.115.098848
Mol Pharmacol 88:335–346, August 2015

MOLECULAR PHARMACOLOGY

Biased Agonism of Endogenous Opioid Peptides at the μ-Opioid Receptor[S]

Georgina L. Thompson, J. Robert Lane, Thomas Coudrat, Patrick M. Sexton, Arthur Christopoulos, and Meritxell Canals

Drug Discovery Biology, Monash Institute of Pharmaceutical Sciences, Monash University, Parkville, Victoria, Australia (G.L.T., J.R.L., T.C., P.M.S., A.C., M.C.); and Defence Science and Technology Organisation, Department of Defence, Fishermans Bend, Victoria, Australia (G.L.T.)

Received March 4, 2015; accepted May 26, 2015

ABSTRACT

Biased agonism is having a major impact on modern drug discovery, and describes the ability of distinct G protein–coupled receptor (GPCR) ligands to activate different cell signaling pathways, and to result in different physiologic outcomes. To date, most studies of biased agonism have focused on synthetic molecules targeting various GPCRs; however, many of these receptors have multiple endogenous ligands, suggesting that "natural" bias may be an unappreciated feature of these GPCRs. The μ-opioid receptor (MOP) is activated by numerous endogenous opioid peptides, remains an attractive therapeutic target for the treatment of pain, and exhibits biased agonism in response to synthetic opiates. The aim of this study was to rigorously assess the potential for biased agonism in the actions of endogenous opioids at the MOP in a common cellular background, and compare these to the effects of the agonist D-Ala2-*N*-MePhe4-Gly-ol enkephalin (DAMGO). We investigated activation of G proteins, inhibition of cAMP production, extracellular signal-regulated kinase 1 and 2 phosphorylation, β-arrestin 1/2 recruitment, and MOP trafficking, and applied a novel analytical method to quantify biased agonism. Although many endogenous opioids displayed signaling profiles similar to that of DAMGO, α-neoendorphin, Met-enkephalin-Arg-Phe, and the putatively endogenous peptide endomorphin-1 displayed particularly distinct bias profiles. These may represent examples of natural bias if it can be shown that they have different signaling properties and physiologic effects in vivo compared with other endogenous opioids. Understanding how endogenous opioids control physiologic processes through biased agonism can reveal vital information required to enable the design of biased opioids with improved pharmacological profiles and treat diseases involving dysfunction of the endogenous opioid system.

Introduction

Opioids are the most widely used and most effective analgesics available. However, their use is associated with a large array of side effects (Benyamin et al., 2008). Opioids that are currently used as therapeutics, such as morphine, predominantly exert both their analgesic effects and undesirable effects through activation of the μ-opioid receptor (MOP) subtype (Matthes et al., 1996; Cox et al., 2015). It is now accepted that chemically distinct ligands binding to the same G protein–coupled receptor (GPCR) can stabilize the receptor in multiple active conformations, which results in differential activation of cell signaling pathways and, eventually, in different physiologic outcomes, a phenomenon known as biased agonism (Kenakin et al., 2012). Biased agonism can be exploited to design drugs that selectively activate signaling pathways, leading to the desired physiologic effects while minimizing on-target side effects elicited by activation of other signaling pathways via the same receptor subtype (Gesty-Palmer et al., 2009; Walters et al., 2009; Valant et al., 2014).

Biased agonism at the MOP has been extensively studied (McPherson et al., 2010; Al-Hasani and Bruchas, 2011; Raehal et al., 2011; Pradhan et al., 2012; Rivero et al., 2012; Kelly, 2013; Williams et al., 2013; Thompson et al., 2015). However, evidence of biased agonism at the MOP is mostly limited to qualitative analyses of two signaling events with a limited number of ligands. Evidence of the involvement of β-arrestin 2 (β-arr2) in the mediation of the adverse effects of morphine has prompted the search for opioids that do not induce β-arr2 recruitment. Indeed, enhanced morphine

M.C. is a Monash Fellow. A.C. and P.M.S. are Principal Research Fellows of the National Health and Medical Research Council (NHMRC) of Australia. J.R.L. is a Monash University Larkins Fellow and an RD Wright Biomedical Career Development Fellow (NHMRC). This work was funded in part by the NHMRC [Program Grant APP1055134 to A.C. and P.M.S.] and the Monash Institute of Pharmaceutical Sciences Large Grant Support Scheme (M.C.). G.L.T. scholarship was funded by the Australian Commonwealth Government Department of Defence.
dx.doi.org/10.1124/mol.115.098848.
[S] This article has supplemental material available at molpharm.aspetjournals.org.

ABBREVIATIONS: AC, adenylyl cyclase; BRET, bioluminescence resonance energy transfer; BSA, bovine serum albumin; CHO, Chinese hamster ovary; DAMGO, D-Ala2-*N*-MePhe4-Gly-ol enkephalin; DMEM, Dulbecco's modified Eagle's medium; dynA, dynorphin A; endo-1, endomorphin-1; endo-2, endomorphin-2; GPCR, G protein–coupled receptor; GTPγS, guanosine 5′*O*-(γ-thio)triphosphate; Met-enk, Met-enkephalin; MOP, μ-opioid receptor; α-neo, α-neoendorphin; PC, principal component; PCA, principal component analysis; pERK, ERK1/2 phosphorylation; PKC, protein kinase C; Rluc, *Renilla* Luciferase; YFP, yellow fluorescent protein.

analgesia with reduced respiratory and gastrointestinal side effects was reported in β-arr2 knockout mice (Bohn et al., 1999; Raehal et al., 2005; Maguma et al., 2012). Recently, ligands with impaired β-arr2 recruitment have been reported to provide potent analgesia with less severe side effects (Groer et al., 2007; DeWire et al., 2013; Soergel et al., 2014). However, the improved pharmacological profiles of these ligands may still be due to their partial agonism, with lower overall efficacy than morphine, rather than true "bias" away from β-arr2 recruitment (Thompson et al., 2015).

To guide discovery efforts to generate drugs with therapeutically relevant biased agonism profiles, it is necessary to quantify this phenomenon. In any system, the observed biased agonism can be confounded by "system bias," which reflects the differing coupling efficiencies of the receptor for each signaling pathway, and by "observational bias," which results from differing assay sensitivities and conditions (Kenakin and Christopoulos, 2013). Bias imposed by the ligand on the conformation of the receptor is the only source of bias that can be chemically optimized to improve its therapeutic profile. Therefore, it is important to quantify biased agonism in such a way that excludes system and observational bias to reveal the unique signaling profile that is induced by the ligand. Several analytical methods to quantify biased agonism have been developed. The method recently described by Kenakin et al. (2012), based on the Black and Leff (1983) operational model, can be applied to concentration-response curves to obtain a single parameter that describes bias between signaling pathways in a system-independent manner.

Several studies have quantified biased agonism at the MOP, but these have been limited to comparison of efficacies for G protein activation versus β-arr2 recruitment (McPherson et al., 2010; Molinari et al., 2010; Frolich et al., 2011; Rivero et al., 2012). However, differential activation of other signaling events including receptor internalization, mitogen-activated protein kinase, and protein kinase C (PKC) activation has been reported (Williams et al., 2013), but these signaling events are rarely considered when describing bias of the MOP, or when attempting to link biased agonism with physiologic effects. Moreover, bias between G protein activation and β-arrestin recruitment may not necessarily predict differential activation of such downstream signaling events. Therefore, it is important to study biased agonism at multiple signaling pathways to encompass multiple aspects of the signaling properties of a ligand.

To date, descriptions of biased agonism have mainly focused upon the actions of synthetic ligands. However, the existence of multiple endogenous ligands targeting the same GPCR suggests the potential for "endogenous" biased agonism. Indeed, biased agonism by endogenous peptide ligands has been observed at several GPCRs (Zidar, 2011; Rajagopal et al., 2013; Zhao et al., 2013). Such observations may explain, in part, the apparent redundancy of such systems. However, the potential for bias within the endogenous opioid system has not been explored extensively. The endogenous ligands for opioid receptors are small peptides generated by cleavage of precursor proteins: pro-enkephalin, pro-opiomelanocortin, and pro-dynorphin. Pro-enkephalin–derived and pro-opiomelanocortin–derived peptides, enkephalins, and endorphins, respectively, are generally localized to regions with MOP or δ-opioid receptor expression and are involved in the numerous physiologic processes mediated by these receptors. Similarly, the pro-dynorphin–derived peptides, the dynorphins and neoendorphins, are generally localized to similar regions as the κ-opioid receptor; however, it is likely that, in some regions, dynorphins may also activate the MOP. All of the opioid peptides have varying affinities for all three opioid receptors, and none are significantly selective for one receptor subtype (Mansour et al., 1995; Janecka et al., 2004). Finally, the precursor genes for endomorphin-1 (endo-1) and endomorphin-2 (endo-2) are still unknown, and therefore, these two ligands remain "putatively endogenous"; however, they are the most selective and potent opioid peptides for the MOP (Zadina et al., 1997). Such diversity in the endogenous opioid system suggests that biased agonism may play a role in control of normal MOP-mediated physiologic processes. Understanding the fundamental basis for ligand bias at the MOP and determining whether differences in the expression and release of endogenous opioids can underlie the development and maintenance of disease may offer promising avenues to address and provide mechanistic insight for the development of safer opioid-based therapies.

In the current study, we investigated the existence of biased agonism at the MOP by endogenous and putatively endogenous opioids. The ability to activate several signal transduction pathways for a range of opioid peptides and three reference ligands was assessed. Bias between each signaling pathway was quantified to obtain unique biased agonism profiles for these ligands. The results show that, although most endogenous opioids possess similar biased agonism profiles to one another, α-neoendorphin (α-neo) and the putative endogenous opioid endo-1 display unique biased agonism profiles. Our studies also provide a foundation for future studies aimed at linking these profiles to physiology of the opioid system.

Materials and Methods

Chinese hamster ovary (CHO) FlpIn cells and Dulbecco's modified Eagle's medium (DMEM) were purchased from Invitrogen (Mulgrave, VIC, Australia). Fetal bovine serum was purchased from ThermoTrace (Melbourne, VIC, Australia). Hygromycin-B was purchased from Roche Applied Science (Dee Why, NSW, Australia). Sure-Fire cellular extracellular signal-regulated kinase 1/2 (ERK1/2) assay kits were a generous gift from TGR BioSciences (Adelaide, SA, Australia). AlphaScreen reagents for ERK1/2 assays, [^{35}S]guanosine 5′-O-[γ-thio] triphosphate ([^{35}S]GTPγS; >1000 Ci/mmol), [^{3}H]diprenorphine, and Ultima Gold scintillation cocktail were purchased from PerkinElmer Life Sciences (Melbourne, VIC, Australia). All endogenous opioid peptides were purchased from Mimotopes (Melbourne, VIC, Australia). All other chemicals were purchased from Sigma-Aldrich (St. Louis, MO). Morphine HCl was from GlaxoSmithKline (Boronia, VIC, Australia). *Renilla* Luciferase (Rluc)–tagged MOPr (MOP-Rluc) was a gift from Laura Bohn (Scripps Research Institute, Jupiter, Florida).

Cell Culture and Generation of Stable Cell Line. Cells were maintained and cultured in high-glucose DMEM containing 10% fetal bovine serum and 600 μg/ml hygromycin B at 37°C under a humidified atmosphere containing 5% CO_2. cDNA encoding the wild-type human MOP was obtained from the Missouri University of Science and Technology (http://www.cdna.org) and was provided in pcDNA3.1+. Sequence of the human MOP was amplified by polymerase chain reaction and cloned into the Gateway entry vector pENTR/D-TOPO, using the pENTR directional TOPO cloning kit, according to the manufacturer's instructions (Life Technologies, Mulgrave, VIC, Australia). The construct was subsequently transferred into the

Gateway destination vector pEF5/frt/V5/dest using the LR Clonase enzyme mix (Invitrogen), and the constructs were used to transfect FlpIn CHO cells (Invitrogen), which ensure constant expression of the MOP across a cell population. Cells were selected using 600 μg/ml hygromycin B to generate cell lines stably expressing MOP.

Membrane Preparation. Cells from 10 175-cm^2 flasks were grown until approximately 90% confluence and harvested using 2 mM EDTA in phosphate-buffered saline (137 mM NaCl, 2.7 mM KCl, 4.3 mM Na_2HPO_4, and 1.5 mM KH_2PO_4). Cells were pelleted by centrifugation for 10 minutes at 1200*g*, and the pellets were resuspended in 20 ml of phosphate-buffered saline containing 20 mM HEPES and 10 mM EDTA at pH 7.4. All subsequent steps were performed at 4°C. The cell suspension was homogenized using a Polytron homogenizer (PT 1200 CL; Kinematica, Basel, Switzerland), with three 10-second bursts separated by cooling on ice. The cell homogenate was centrifuged for 5 minutes at 1700*g*, and the supernatant was transferred to new tubes and further centrifuged (90 minutes, 38,000*g*). The pellet was resuspended in 5 ml of buffer (20 mM HEPES and 0.1 mM EDTA, pH 7.4) and briefly homogenized to ensure uniform consistency. Membranes were aliquoted and stored at −80°C. The protein concentration was determined using a Bradford assay and bovine serum albumin as a standard.

Saturation Radioligand Binding Assay. Cell membranes (20 μg) were incubated in buffer (50 mM Tris, 100 mM NaCl, 3 mM $MgCl_2$, pH 7.4) containing increasing concentrations of [^{3}H]diprenorphine (0.01–10 nM) at 25°C for 60 minutes. The reaction was terminated by rapid filtration through glass fiber filters (GF/B) with a Brandel cell harvester (Brandel Inc, Gaithersburg, MD) and washing with cold saline. Nonspecific binding was determined using 1 mM naloxone, and radioactivity was determined by liquid scintillation counting using Ultima Gold scintillation cocktail and a Tri-Carb 2900TR liquid scintillation counter (PerkinElmer).

[^{35}S]GTPγS Binding Assay. Cell membranes (10 μg) were incubated in buffer (20 mM HEPES, 100 mM NaCl, 4 mM $MgCl_2$, pH 7.4) containing 1 μm GDP, 0.01% bovine serum albumin (BSA), protease inhibitors (1 μM captopril, 1 μM phosphoramidon, and 1 μM amastatin), and increasing concentrations of agonist for 30 minutes at 30°C. A 100-μl volume of [^{35}S]GTPγS (0.1 nM final concentration) was then added, and the incubation was continued for a further 30 minutes. The reaction was terminated by rapid filtration through glass fiber filters (GF/B) with a Brandel cell harvester and washing with cold saline. Radioactivity was determined by liquid scintillation counting using Ultima Gold scintillation cocktail and a Tri-Carb 2900TR liquid scintillation counter (PerkinElmer). All experiments were performed in triplicate.

Inhibition of Forskolin-Induced cAMP Levels. The ability of ligands to inhibit forskolin-induced cAMP production was assessed in FlpIn CHO-MOP cells transiently transfected to express the CAMYEL cAMP bioluminescence resonance energy transfer (BRET) biosensor (Jiang et al., 2007). FlpIn CHO-MOP cells were grown overnight in 10-cm dishes. Transient transfection was performed using polyethylenimine at a 6:1 ratio of DNA. Twenty-four hours after transfection, FlpIn CHO-MOP cells were seeded in white 96-well plates (Culturplates; PerkinElmer) and incubated overnight. The following day, cells were rinsed and preincubated in Hanks' balanced saline solution with 0.01% BSA and protease inhibitors (1 μM captopril, 1 μM phosphoramidon, and 1 μM amastatin) for 30 minutes at 37°C. Cells were then incubated with the Rluc substrate coelenterazine-*h*, final concentration 5 μM, for 5 minutes, followed by a further 5-minute incubation with increasing concentrations of agonists. Forskolin was added to a final concentration of 10 μM. After 5 minutes, the yellow fluorescent protein (YFP) and the Rluc emissions were measured using a LumiSTAR Omega instrument (BMG Labtech, Ortenberg, Germany), which allows for sequential integration of the signals detected at 475 ± 30 and 535 ± 30 nm, using filters with the appropriate band pass. Data are presented as a BRET ratio, calculated as the ratio of YFP to Rluc signals, and expressed as the percentage of the forskolin-induced signal.

BRET Assays. Agonist-induced recruitment of β-arrestins to the MOP and MOP proximity to the plasma membrane maker KRas were examined using a BRET-based method. Parental FlpIn CHO cells were transfected to coexpress MOP C-terminally tagged with Rluc and β-arr1–Venus, β-arr2–Venus, or KRas-Venus at a 1:4 DNA ratio. The assay was performed as described earlier for the cAMP BRET-based assay. For β-arrestin recruitment assays, agonists were added after 5 minutes of preincubation with coelenterazine-*h* and then incubated for an additional 5 minutes, and the BRET ratio was determined. For receptor trafficking (KRas BRET) assays, cells were incubated with agonists for 60 minutes in the presence of protease inhibitors, and coelenterazine-*h* added 10 minutes prior to detection of BRET. Data are expressed as D-Ala2-*N*-MePhe4-Gly-ol enkephalin (DAMGO) response for β-arrestin assays and percent vehicle response for KRas assays.

ERK1/2 Phosphorylation Assay. Cells were seeded at 4×10^4 cells/well in clear 96-well plates and grown for 5 hours. Cells were washed twice with 200 μl of phosphate-buffered saline and incubated in serum-free DMEM overnight at 37°C in 5% CO_2. ERK1/2 phosphorylation (pERK) was detected using the AlphaScreen ERK1/2 SureFire protocol (TGR Biosciences). The assay was performed at 37°C, and cells were preincubated with 0.01% BSA and protease inhibitors (1 μM captopril, 1 μM phosphoramidon, and 1 μM amastatin) followed by addition of ligands to a final volume of 200 μl. Time course experiments were initially performed to determine the time at which maximal pERK was detected following agonist stimulation (5 minutes). Ligand-stimulated pERK was terminated by removal of media and drugs, followed by the addition of 100 μl of SureFire lysis buffer per well and agitation of lysates for 5 minutes at room temperature. Five microliters of lysate was added in a 384-well white ProxiPlate (PerkinElmer). A mixture of SureFire activation buffer, SureFire reaction buffer, and AlphaScreen beads was prepared in a ratio of 100:600:3 (v/v/v) and added to the lysate for a lysate:mixture ratio of 5:8 (v/v). Plates were incubated for 1–1.5 hours at 37°C before the fluorescence signal was measured on a Fusion-α plate reader (PerkinElmer) using standard AlphaScreen settings. For all experiments, 10 μM DAMGO (100%) and vehicle (0%) were used to normalize pERK curves.

Data Analysis. Agonist concentration-response curves were fitted empirically to a three-parameter logistic equation using Prism 6.0 (GraphPad Software Inc., La Jolla, CA) where bottom and top are the lower and upper plateaus, respectively, of the concentration-response curve, [*A*] is the molar concentration of agonist, and EC_{50} is the molar concentration of agonist required to generate a response halfway between the top and the bottom:

$$Y = \text{bottom} + \frac{\text{top} - \text{bottom}}{1 + 10^{(\log EC_{50} - \log[A])}}. \quad (1)$$

To compare agonist profiles and to quantify stimulus bias, agonist concentration-response data were fitted to the following form of the operational model of agonism (Black and Leff, 1983):

$$Y = \text{basal} + \frac{(E_m - \text{basal})\left(\frac{\tau}{K_A}\right)^n [A]^n}{[A]^n \left(\frac{\tau}{K_A}\right)^n + \left(1 + \frac{[A]^n}{K_A}\right)} \quad (2)$$

where E_m is the maximal possible response of the system, basal is the basal level of response, K_A denotes the functional equilibrium dissociation constant of the agonist (A) for the receptor, τ is an index of the signaling efficacy of the agonist and is defined as R_T/K_E (where R_T is the total number of receptors and K_E is the coupling efficiency of each agonist-occupied receptor), and n is the slope of the transducer function that links occupancy to response. The analysis assumes that the maximal system responsiveness (E_m) and the transduction machinery used for a given cellular pathway are the same for all agonists, such that the E_m and transducer slope (n) are shared between agonists. Data for all compounds for each pathway were fit globally to determine values of K_A and τ.

The ratio τ/K_A was determined as a logarithm [i.e., $\log(\tau/K_A)$] and is referred to herein as the transduction coefficient which represents a single fitted parameter sufficient to describe agonism and bias for a given pathway [i.e., biased agonism can result from either a selective affinity (K_A) of an agonist for a given receptor state(s) and/or a differential coupling efficacy (τ) toward certain pathways].

To cancel the impact of cell-dependent effects on the observed agonism at each pathway, the $\log(\tau/K_A)$ values were then normalized to that determined for DAMGO at each pathway to yield a normalized transduction coefficient, $\Delta\log(\tau/K_A)$, which was calculated as follows:

$$\Delta \log\left(\frac{\tau}{K_A}\right) = \log\left(\frac{\tau}{K_A}\right)_{\substack{\text{test}\\ \text{compund}}} - \log\left(\frac{\tau}{K_A}\right)_{\text{DAMGO}}. \quad (3)$$

Finally, to determine the actual bias of each agonist between different signaling pathways, the $\Delta\log(\tau/K_A)$ values were evaluated statistically between the pathways. The ligand bias of an agonist for one pathway, $j1$, over another, $j2$, is given as:

$$\Delta\Delta\log(\tau/K_A)_{j1-j2} = \Delta\log\left(\frac{\tau}{K_A}\right)_{j1} - \Delta\log\left(\frac{\tau}{K_A}\right)_{j2}. \quad (4)$$

A lack of biased agonism as compared with the reference agonist DAMGO will result in values of $\Delta\Delta\log(\tau/K_A)$ not significantly different from 0 between pathways. To account for the propagation of error associated with the determination of composite parameters using eqs. 3 and 4, the following equation was used:

$$\text{Pooled\_S.E.M.} = \sqrt{(\text{S.E}j1)^2 + (\text{S.E}j2)^2} \quad (5)$$

All potency (pEC_{50}) and transduction ratio [$\Delta\Delta\log(\tau/K_A)$] parameters were estimated as logarithms. Fold changes in bias were calculated by first converting values of $\Delta\Delta\log(\tau/K_A)$ to the corresponding antilog value:

$$\text{Bias} = 10^{\Delta\Delta\log\left(\frac{\tau}{K_A}\right)}. \quad (6)$$

The distribution of antilog values does not conform to a normal (Gaussian) distribution, whereas the logarithm of the measure is approximately Gaussian (Motulsky and Ransnas, 1987; Leff et al., 1990; Christopoulos, 1998). Thus, as the application of t tests and analyses of variance assume Gaussian distribution, estimating the parameters as logarithms allows valid statistical comparison. All results are expressed as the mean ± S.E.M. Statistical analysis was performed using a two-way unpaired Student's t test to make pairwise comparisons between bias factors for a given ligand and DAMGO, where $P < 0.05$ was considered to be statistically significant.

To visualize bias between multiple pathways at once, webs of bias were constructed. $\Delta\Delta\tau/K_A$ values between a reference pathway, cAMP, and all other pathways were obtained using DAMGO as the reference ligand as follows:

$$\Delta\tau/K_A = \frac{\tau/K_{A\ \text{test compound}}}{\tau/K_{A\ \text{DAMGO}}} \quad (7)$$

$$\Delta\Delta\tau/K_A = \frac{\Delta\tau/K_{A_{j1}}}{\Delta\tau/K_{A_{j2}}} \quad (8)$$

Principal Component Analysis. Principal component analysis (PCA) is a dimensionality reduction method that uses transformations to project a high-dimensional set of data into a lower dimensional set of variables called principal components (PCs). The PCs extract the important information from the data, revealing the data's internal structure in a way that best explains its variance (Wold et al., 1987). PCs are ranked according to the percentage of total variance in the data they explain. The first PC explains a maximal amount of total variance in the data. Each succeeding PC explains a maximal amount of the remaining variation, without being correlated with the preceding components. PCA was applied using singular value decomposition as implemented in the package scikit-learn (Pedregosa et al., 2011); the script used for the analysis and plotting can be found at https://github.com/thomas-coudrat/pca_analysis.

Results

The ability of the MOP to activate several signal transduction pathways in response to 10 endogenous peptides, endo-1, endo-2, and three synthetic ligands was assessed in FlpIn CHO cells stably expressing the human MOP. Receptor expression levels were determined by saturation binding assays with [^{3}H]diprenorphine (B_{max} 0.72 ±0.04 pmol/mg protein; Supplemental Fig. 1). The selected opioid peptides included members of all three of the main classes of endogenous opioids (enkephalins, dynorphins, and endorphins) as well as the putative endogenous ligands, the endomorphins (Table 1). Quantification of bias between each pathway was performed using DAMGO as the reference ligand. Morphine was included as an additional control ligand, as the literature suggests that it may be a biased

TABLE 1
Endogenous and selective opioid peptides used in this study

Peptide	Sequence
Enkephalins	
Leu-enk	Tyr-Gly-Gly-Phe-Leu
Met-enk	Tyr-Gly-Gly-Phe-Met
Met-enk-RF	Tyr-Gly-Gly-Phe-Met-Arg-Phe
Dynorphins	
Dynorphin A (DynA)	Tyr-Gly-Gly-Phe-Leu-Arg-Arg-Ile-Arg-Pro-Lys-Leu-Lys-Trp-Asp-Asn-Gln
Dynorphin B	Tyr-Gly-Gly-Phe-Leu-Arg-Arg-Gln-Phe-Lys-Val-Val-Thr
DynA 1–13	Tyr-Gly-Gly-Phe-Leu-Arg-Arg-Ile-Arg-Pro-Lys-Leu-Lys
DynA 1–8	Tyr-Gly-Gly-Phe-Leu-Arg-Arg-Ile
DynA 1–6	Tyr-Gly-Gly-Phe-Leu-Arg
α-Neo	Tyr-Gly-Gly-Phe-Leu-Arg-Lys-Tyr-Pro-Lys
Endorphins	
β-Endorphin	Tyr-Gly-Gly-Phe-Met-Thr-Ser-Glu-Lys-Ser-Gln-Thr-Pro-Val-Thr-Leu-Phe-Lys-Asn-Ile-Ile-Lys-Asn-Ala-Tyr-Lys-Lys-Gly-Glu
Endomorphins	
Endo-1	Tyr-Pro-Trp-Phe
Endo-2	Tyr-Pro-Phe-Phe

agonist at the MOP compared with DAMGO (Raehal et al., 2011; Pradhan et al., 2012; Williams et al., 2013), and finally, the signaling profile of the peripherally restricted MOP agonist loperamide was also investigated. All incubations in the different signaling assays were performed in the presence of endopeptidase inhibitors (see *Materials and Methods*) to prevent peptide degradation.

Endogenous Opioids Differentially Inhibit Adenylyl Cyclase and Recruit β-Arrestin 2. MOPs are primarily coupled to $G\alpha_i$ G proteins that mediate inhibition of adenylyl cyclase (AC), resulting in a decrease in the levels of intracellular cAMP. The ability of ligands to inhibit forskolin-induced cAMP production was assessed in FlpIn CHO-MOP cells transiently transfected to express the CAMYEL cAMP BRET-based biosensor (Fig. 1, A and B; Supplemental Table 1). All ligands inhibited forskolin-induced cAMP stimulation. Such inhibition was abolished by incubation of the cells with pertussis toxin (unpublished data) demonstrating the $G\alpha_i$ dependence of this effect. However, concentration-response curves could not be obtained for dynorphin A (dynA) and dynA 1–13. Although these two peptides stimulated the production of cAMP at high concentrations (Fig. 1B), this effect was not mediated by the MOP, as it was not blocked by the MOP antagonist naloxone, and was still observed in untransfected FlpIn CHO cells (Supplemental Fig. 2).

We then examined recruitment of β-arr2 to the MOP using a BRET assay. CHO FlpIn cells were cotransfected with Rluc-tagged MOP and YFP-tagged β-arr2. All endogenous opioids as well as DAMGO and loperamide stimulated recruitment of β-arr2. In contrast, morphine displayed partial agonism by only stimulating 28% of the DAMGO-mediated response (Fig. 1, C and D; Supplemental Table 1).

To quantify biased agonism at these two signaling pathways, bias factors were calculated as described in *Materials and Methods* (Fig. 1E; Supplemental Table 2). Both loperamide

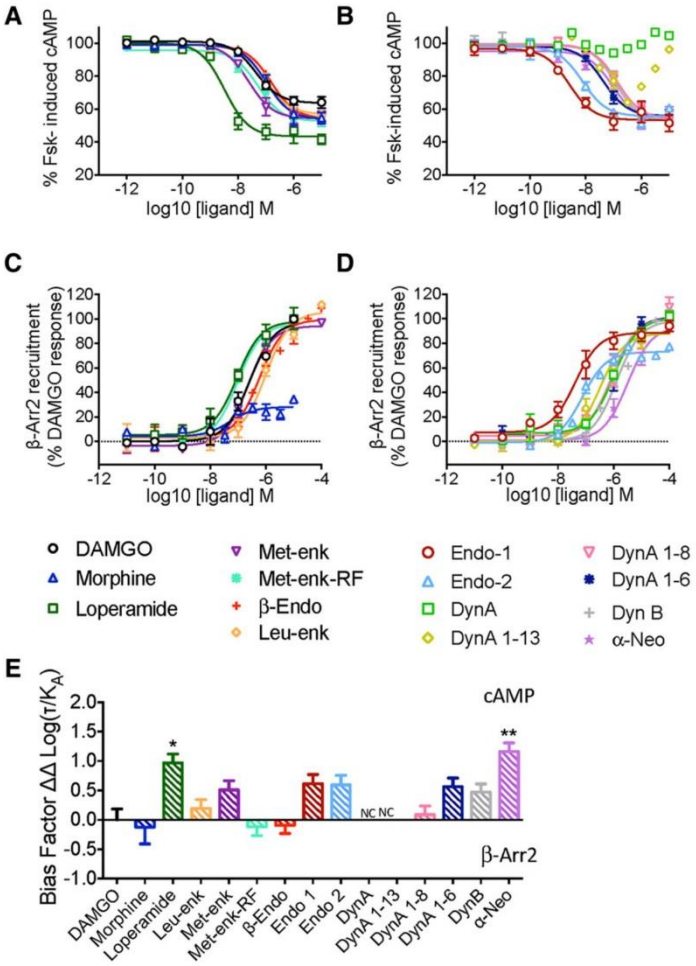

Fig. 1. Biased agonism of endogenous opioids between inhibition of forskolin-induced cAMP and β-arr2 recruitment. (A and B) Inhibition of forskolin (Fsk)-induced cAMP in CHO-MOP cells. (C and D) Recruitment of β-arr2 in FlpIn CHO cells. Data normalized to the 10 μM DAMGO response. Data are expressed as the mean ± S.E.M. of at least three separate experiments. (E) Bias factors for all agonists between cAMP and β-arr2 recruitment (Supplemental Table 2). $^*P \leq 0.05$; $^{**}P \leq 0.005$, different from DAMGO, as determined by two-tailed *t* test. Bias factors for DynA and DynA 1–13 not shown as $\log[\tau/K_A]$ values could not be calculated for the cAMP assay. NC, not calculable.

and the endogenous opioid, α-neo, showed significant bias toward inhibition of AC over recruitment of β-arr2 compared with the reference ligand DAMGO. Morphine and all the other opioid peptides tested were not significantly biased compared with DAMGO.

Differential Recruitment of β-Arrestin Isoforms by Opioid Ligands. Morphine has previously been shown to preferentially stimulate recruitment of β-arr2 over β-arr1 (Bohn et al., 2004). Differential recruitment of arrestins may have significant effects on downstream signaling, as different β-arrestin isoforms have different functions (DeWire et al., 2007; Nobles et al., 2011). We examined the potential for endogenous opioids to stimulate differential recruitment of β-arrestin isoforms to the MOP. For this, β-arrestin recruitment assays were repeated using YFP-tagged β-arr1. All the ligands tested stimulated recruitment of β-arr1, with the exception of morphine, which did not stimulate any detectable recruitment (Fig. 2, A and B; Supplemental Table 1). Of note, the BRET signal was much lower for the β-arr1 assays compared with the BRET signal obtained for β-arr2. Although this could be interpreted as a compromised recruitment of β-arr1 for all the ligands, we cannot exclude the possibility that this is due to lower BRET efficiency between the different arrestin isoforms and the Rluc-tagged receptor. Bias factors between recruitment of β-arr1 and β-arr2 showed that, in addition to morphine, endo-1 differentially recruits β-arrestins in comparison with the reference ligand DAMGO (Fig. 2C; Supplemental Table 2). Endo-1 showed significant bias toward recruitment of β-arr2 over β-arr1. Since morphine did not stimulate any detectable β-arr1 recruitment, a bias factor could not be calculated. However, this does not necessarily indicate that morphine is biased toward β-arr2 recruitment. Since all the ligands showed a lower response in the β-arr1 assay than for β-arr2, a partial agonist such as morphine is expected to stimulate little to no response in the β-arr1 assay. Hence, our results suggest that bias between β-arrestin isoforms can be due to the lower sensitivity of β-arr1 assays and/or lower coupling efficiency of β-arr1 recruitment to the MOP.

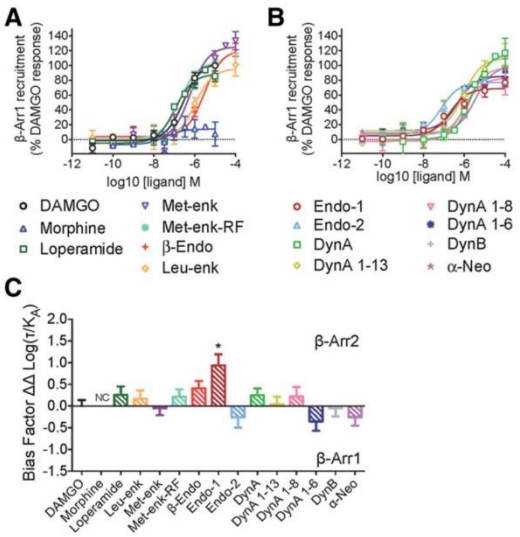

Fig. 2. Bias between β-arr1 and β-arr2 recruitment. (A and B) Recruitment of β-arr1 in FlpIn CHO cells. Data are normalized to the 10 μM DAMGO response and expressed as means ± S.E.M. of three separate experiments. (C) Bias factors for all agonists between β-arr1 and β-arr2 (Supplemental Table 2). *$P \leq 0.05$, different from DAMGO as determined by two-tailed t test. NC, not calculable.

Biased ERK1/2 Phosphorylation Correlates with Bias between cAMP and β-Arrestin Recruitment. Next, we examined activation of ERK1/2. Agonist-induced stimulation of pERK was measured in FlpIn CHO-MOP cells using the AlphaScreen phospho ERK1/2 assay. All agonists strongly stimulated pERK in CHO-MOP cells (Fig. 3, A and B; Supplemental Table 1). This effect was blocked by naloxone and was absent in untransfected CHO cells (unpublished data). Bias factors between pERK and all the previous signaling pathways (inhibition of cAMP production, β-arr1 and β-arr2 recruitment) were calculated (Fig. 3, C and D; Supplemental Table 2). There were several ligands that displayed biased agonism toward cAMP inhibition over pERK compared with DAMGO, including morphine, loperamide, endo-1, α-neo, and dynorphin B. In line with this result, there was also a strong correlation between bias toward cAMP inhibition over pERK and the bias toward cAMP inhibition over β-arr2 recruitment (Pearson $r = 0.893$, $P < 0.0001$; Fig. 3E). However, β-arrestin–dependent pERK may not be specifically mediated via β-arr2 only, as a similar correlation was observed for bias between pERK and β-arr1 recruitment (Supplemental Fig. 3). The lack of bias between pERK and β-arr1 or 2 recruitment for nearly all of the ligands suggests that a component of pERK in CHO cells is β-arrestin–dependent. The only exception to this was morphine, which was biased toward β-arr2 and cAMP and away from pERK.

Differential Activation of G Protein–Mediated Signaling. Although we used the inhibition of AC as a measure of G protein–mediated signaling, AC activity is regulated by numerous other signaling effectors in addition to $G\alpha_i$ subunits. These include Ca^{2+}, $G\beta\gamma$ subunits, and A-kinase anchoring protein. In addition to this, AC is differentially regulated by various $G\alpha$ subunits (Willoughby and Cooper, 2007), which in turn are differentially modified by regulators of G protein signaling (Traynor, 2012). We measured direct G protein activation in FlpIn CHO-MOP membrane preparations using [^{35}S]GTPγS binding assays and quantified bias between [^{35}S]GTPγS binding and inhibition of forskolin-induced cAMP (Fig. 4). Several ligands showed bias toward cAMP over [^{35}S]GTPγS binding in comparison with DAMGO, including morphine, Met-enkephalin (Met-enk), endo-1, endo-2, and α-neo. Interestingly, some of these, endo-1 and α-neo, consistently showed bias toward cAMP over all other signaling pathways, whereas Met-enk and endo-2 did not. This suggests that bias toward cAMP by these two sets of ligands may be driven by different effectors. Modulation of AC activity by βγ subunits and A-kinase anchoring protein did not contribute to bias between the cAMP and [^{35}S]GTPγS binding, as inhibitors for these proteins had no effect on endo-1 or DAMGO inhibition of cAMP stimulation (Supplemental Fig. 4).

Receptor Localization/Trafficking. The inability of morphine to induce MOP internalization was the first

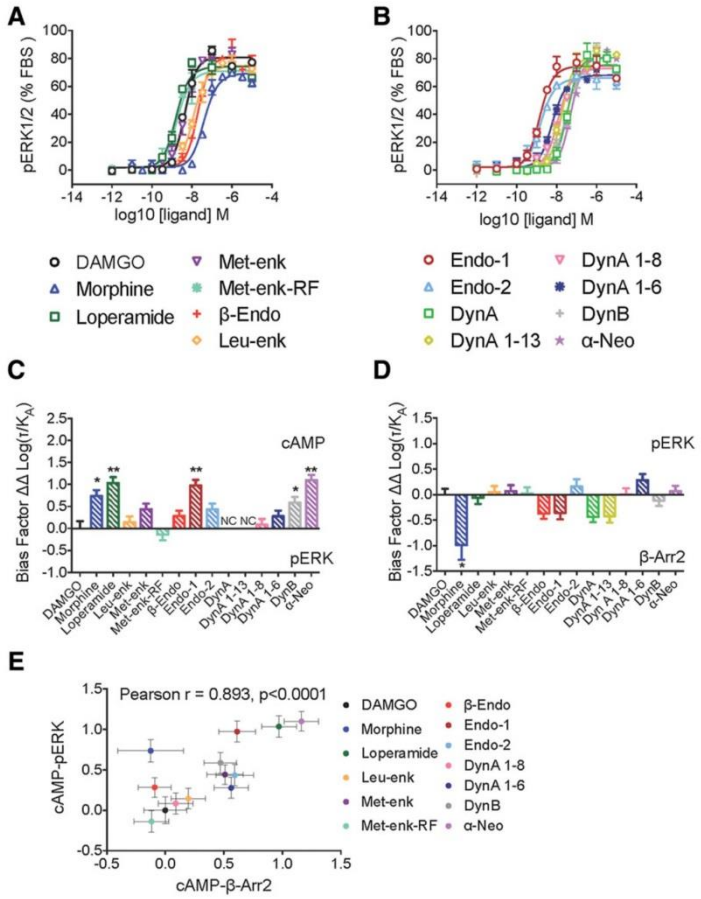

Fig. 3. Bias toward β-arrestin recruitment determines pERK bias. (A and B) pERK in FlpIn CHO-MOP cells. Data are normalized to the 10% fetal bovine serum (FBS) response and expressed as means ± S.E.M. of at least three separate experiments. Bias factors between pERK and cAMP (C) and β-arr2 (D). $^{*}P \leq 0.05$; $^{**}P \leq 0.005$, as determined by two-tailed t test compared with DAMGO. (E) Two-tailed Pearson correlation was calculated between bias factors for cAMP–β-arr2 in Fig. 1E and cAMP-pERK excluding morphine. NC, not calculable.

indication of differential actions of MOP agonists (Arden et al., 1995; Keith et al., 1996). It is now apparent that this compromised internalization is associated with different modes of desensitization for internalizing versus noninternalizing agonists. MOP trafficking was examined using BRET to measure the proximity between the Rluc-tagged MOP and Venus-tagged KRas construct, used as a plasma membrane marker. Before stimulation with agonists, MOP and KRas are in close proximity, allowing BRET to occur. Upon MOP activation, receptor redistribution, clustering, and internalization, the distance between these two proteins increases and results in a reduction in the BRET signal. A time-course experiment was initially performed to determine the time at which a maximal reduction in BRET was observed following agonist stimulation, which occurred at 60 minutes (unpublished data). All ligands except morphine induced a reduction in BRET between the MOP and KRas at 60 minutes (Fig. 5; Supplemental Table 1). Bias between receptor trafficking and the other signaling pathways for Met-enkephalin-Arg-Phe (Met-enk-RF) could not be quantified since a full concentration-response curve could not be obtained for this ligand in the KRas BRET assay. As Met-enk-RF gave similar responses to Met-enk in all the signaling pathways interrogated previously, this result suggests that Met-enk-RF is biased away from this pathway. Since receptor trafficking is dependent on recruitment of β-arrestins, bias factors were calculated between KRas BRET and β-arr1 and 2 recruitment. No ligands showed bias between KRas BRET and recruitment of β-arr1. Only endo-1 showed significant bias toward recruitment of β-arr2 and away from receptor trafficking. This result is in line with the fact that this ligand had previously shown significant bias toward β-arr2 over β-arr1 when these two pathways were compared (Fig. 2; Supplemental Table 2).

We next compared the bias between KRas BRET and other signaling pathways. Endo-1 and α-neo, which previously showed bias toward cAMP inhibition over β-arr1 and 2 recruitment, now displayed significant bias toward cAMP over receptor trafficking. Surprisingly, endo-2, which previously showed no bias between cAMP and recruitment of β-arrestins, was now biased toward cAMP over KRas BRET. This shows that endo-2 is slightly biased toward β-arrestin recruitment over receptor trafficking, and this has significant

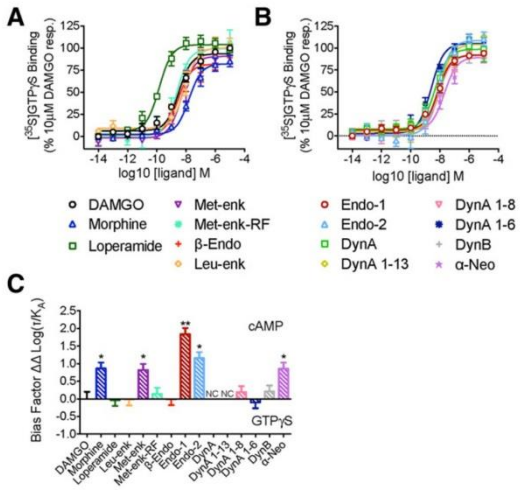

Fig. 4. Bias between G protein activation and AC inhibition. (A and B) Agonist-induced [^{35}S]GTPγS binding in CHO-MOP membrane preparations. Data are normalized to the 10 μM DAMGO response and expressed as means ± S.E.M. of three separate experiments. (C) Bias factors between cAMP and GTPγS assays. $^{*}P \leq 0.05$; $^{**}P \leq 0.005$, as determined by two-tailed t test compared with DAMGO. NC, not calculable; resp., response.

consequences on downstream signaling. Bias between recruitment of β-arrestins and KRas BRET indicates that the β-arrestins recruited to endo-2–activated MOP receptors may be mediating activation of an alternative signaling pathway that has not been captured by the signaling pathways interrogated in this study. Interestingly, the differences in bias between cAMP and KRas BRET or [^{35}S]GTPγS and KRas BRET track with the bias between cAMP and [^{35}S]GTPγS binding. Therefore, these results highlight the fact that the bias between G protein signaling and receptor trafficking depends on the endpoint measured for G protein signaling.

Comprehensive Biased Agonism Profiles. In the context of biased agonism, given the complex signaling pathways that lie downstream of the MOP, it is evident that the comparison of ligand action between two pathways gives only a limited picture of drug action. Thus, to allow visualization of the action of different ligands across all the pathways tested in this study, "webs of bias" were generated. These webs of bias allow the clustering of ligands into different activity profiles across the entire data set. For this, bias factors between cAMP and all other pathways were calculated using DAMGO as the reference ligand ($\Delta\Delta\tau/K_A$) and represented in a single multiaxial graph. Morphine and loperamide are already known to possess different signaling properties compared with DAMGO; hence, they were included in this study as positive controls to validate our analytical tools. As expected, morphine and loperamide each showed characteristic fingerprints, different from that of DAMGO (Fig. 6B). Importantly, two additional opioids, endo-1 and α-neo, also displayed unique signaling profiles, and showed bias across multiple different signaling pathways when compared with DAMGO. Met-enk and endo-2 also showed bias compared with DAMGO, but were similar to one another. Met-enk-RF also displayed a unique signaling profile. Despite its bias profile being very similar to DAMGO at most signaling pathways, Met-enk-RF only stimulated a very small response in the KRas BRET assay, which indicates that Met-enk-RF is biased away from receptor trafficking; however, the degree of bias could not be quantified. All other endogenous ligands displayed activity profiles that were very similar to DAMGO (Fig. 6A).

Another method to visualize and evaluate the overall signaling profiles is to perform PCA (see *Materials and Methods*). PCA identifies values in the data set that contribute the most variability, the principal components, which in this case are the bias factors that reveal the largest differences between ligands. Ligands that show similar biased agonism to one another will cluster together. PCA of all the bias factors (Fig. 6C; Supplemental Table 2) showed that most of the endogenous ligands cluster closely with DAMGO. In contrast, loperamide, α-neo and endo-1, and to a smaller extent Met-enk and endo-2 are separated, indicating that these ligands display an overall unique pattern of bias, consistent with their signaling profiles in the webs of bias. Of note, the first principal component (PC1) of the analysis, which accounts for the greatest source of variability between ligands, only accounts for 56% of the variability (Fig. 6C; Supplemental Table 3). PC2 contributes 26% to the variability between ligands. Indeed, PC1 and PC2 together only account for 82% of the variability. Interestingly, both of the first two principal components are composed mainly of bias factors between G protein– and β-arrestin–mediated signaling endpoints (Supplemental Table 4). This shows that bias between G protein activation and β-arrestin recruitment is a major determinant of the biased agonism characteristics of a ligand. However, as these bias factors are separated into two uncorrelated principal components, this also means that there is a diverse spectrum of bias between G protein– and β-arrestin–mediated signaling pathways. Altogether, this highlights the multidimensional nature of biased agonism and the fact that quantification of bias should be expanded beyond examination of only two pathways, such as G proteins versus β-arrestins, to cover the whole spectrum of possible signaling characteristics.

Discussion

The data presented here show that endogenous opioids acting on the MOP can exhibit diverse signaling profiles. Examining bias across multiple pathways has highlighted the complex nature of biased agonism at the MOP, and has revealed another level of complexity of bias that extends beyond differential activation of G proteins and β-arrestin recruitment. Several endogenous opioids, including α-neo, Met-enk, Met-enk-RF, and the putative endogenous opioids endo-1 and endo-2, displayed biased agonism compared with DAMGO across multiple signaling pathways, whereas the rest of the endogenous ligands displayed profiles that were similar to that of DAMGO. In particular, endo-1 and α-neo displayed markedly different signaling profiles. α-Neo is considered a κ-opioid receptor agonist, and as such, no studies have examined its actions at the MOP. The physiologic actions and signaling endo-1 at the MOP, conversely, have been extensively studied (Fichna et al., 2007). Endo-1 produces physiologic effects similar to most opioids, such as analgesia, inhibition of gut motility, respiratory depression,

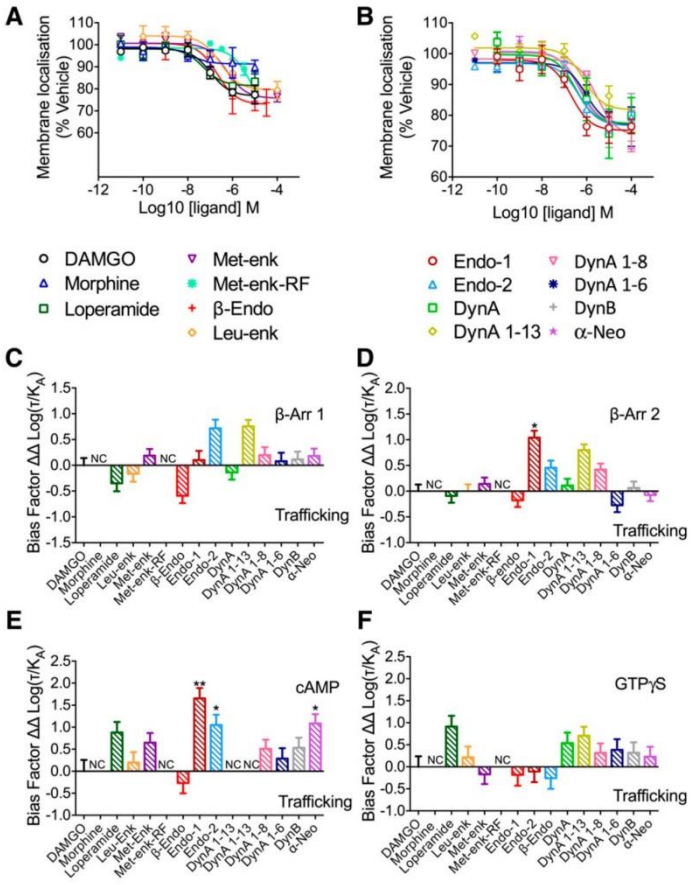

Fig. 5. Endogenous opioids decrease the association of the MOP with KRas. (A and B) BRET between MOR-Rluc and KRas-Venus. Data are expressed as the percentage of vehicle, and as means ± S.E.M. of at least three separate experiments. Bias factors between internalization measured using KRas BRET assay and β-arr1 (C), β-arr2 (D), cAMP (E), and GTPγS (F). $^{*}P \leq 0.05$; $^{**}P \leq 0.005$, as determined by two-tailed t test compared with DAMGO. NC, not calculable.

and the development of tolerance (Goldberg et al., 1998; Tonini et al., 1998; Lonergan et al., 2003; Yu et al., 2007). Differences between the physiologic effects of endo-1 and endo-2 have been described. However, these differences are usually small, and it cannot be ruled out that they are due to different degradation rates of the peptides rather than biased agonism (Sakurada et al., 2002; Terashvili et al., 2007). Interestingly, endo-1 has been shown to produce antinociceptive cross-tolerance to morphine whereas endo-2 does not, suggesting potential differences in the mechanisms of tolerance produced by these two ligands. As both endo-1 and endo-2 stimulate receptor internalization (McConalogue et al., 1999), they would both be expected to produce tolerance via a similar mechanism to that of DAMGO. This suggests that tolerance produced by endo-1 and endo-2 may involve differential activation of signaling pathways unrelated to receptor internalization, or alternatively, that the mechanisms of development of tolerance to these ligands are cell type–dependent.

Few other studies have examined biased agonism of endogenous opioids, and the results from these different studies are not consistent. Morse et al. (2011) examined a range of endogenous and exogenous opioids in HEK293 cells using dynamic mass redistribution to measure MOP global responses. In that study, all endogenous opioids, except dynA 1–13, exhibited similar profiles. Our analysis suggests that, although dynA 1–13 displayed some bias compared with the other endogenous ligands, this is limited evidence to suggest that dynA 1–13 is particularly unique compared with the other endogenous opioids. Rivero et al. (2012) quantified bias between [^{35}S]GTPγS binding and β-arr2 recruitment in HEK293 cells for some endogenous ligands, and found that endo-1 and endo-2 were biased toward β-arr2 recruitment compared with leu-enkephalin (McPherson et al., 2010; Rivero et al., 2012; Thompson et al., 2015). In our study, only endo-1 was biased toward β-arr2 over [^{35}S]GTPγS binding (Supplemental Fig. 5). Various reasons can explain the different results. First, the different methodologies and time points used to measure β-arr2 recruitment may affect bias, since at later time points differential rates and modes of desensitization may affect the level of β-arr2 recruitment. In addition, the different cell backgrounds used in each study may also change the bias of a ligand, as the expression levels of the various proteins involved in the activation of the

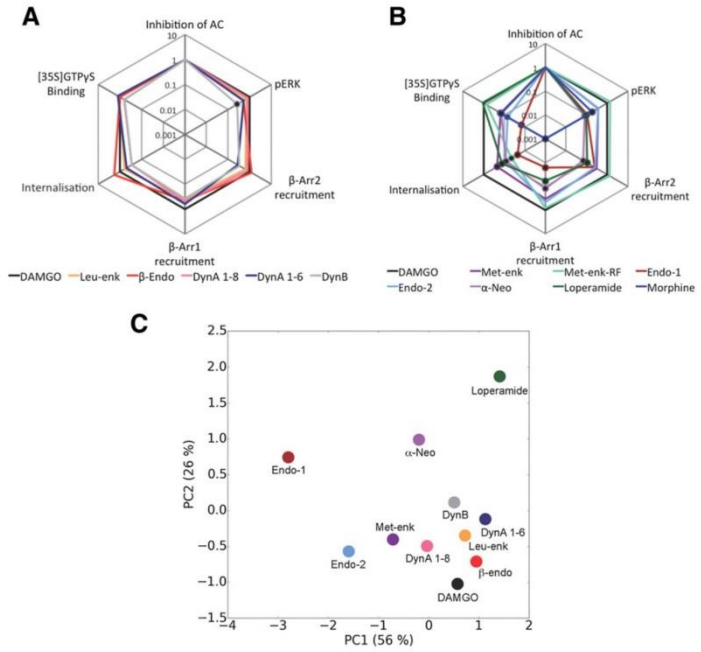

Fig. 6. Webs of bias of endogenous opioid peptides and reference ligands at the MOP. (A) Ligands with profiles similar to DAMGO. (B) Ligands with profiles that differ from that of DAMGO. τ/K_A values were normalized to the reference ligand DAMGO and to the cAMP assay. Statistically significant differences ($P \leq 0.05$) are denoted by black circles as determined by two-tailed t test. For the purposes of visualization only, a τ/K_A for Met-enk-RF in the internalization assay was estimated using the incomplete KRas concentration-response curve. (C) PCA of all bias factors excluding morphine, DynA, DynA 1–13, and Met-enk-RF.

signaling pathways examined may differ across cell lines and have an impact in the measures of bias (Thompson et al., 2015).

Morphine is often described as a ligand with compromised ability to recruit β-arrestins (Whistler and von Zastrow, 1998; Bohn et al., 2004; Molinari et al., 2010; Chen et al., 2013). As a partial agonist, morphine is expected to give a lower response in signaling pathways with low coupling efficiency and/or assays with low sensitivity. However, understanding whether these observations refer to a biased action requires systematic quantification of biased agonism. In our study, morphine did not show significant bias between β-arr2 and cAMP, although it was significantly biased toward β-arr2 when compared with [^{35}S]GTPγS binding. This is similar to results obtained by Rivero et al. (2012), where morphine was slightly biased toward β-arr2, although not significantly (Thompson et al., 2015).

We observed a correlation between pERK and β-arrestin recruitment, suggesting that β-arrestin recruitment is involved in pERK in CHO cells. This correlation was seen with both β-arr1 and β-arr2, indicating that both β-arrestins are capable of mediating a component of ERK activation. β-Arrestin–dependent pERK has also been shown previously in transgenic cell lines and primary cells (Macey et al., 2006; Miyatake et al., 2009). The one exception to this correlation was morphine. This indicates that morphine stimulates pERK via a different pathway that is independent of β-arrestins. A likely candidate is PKC, as morphine-stimulated pERK in HEK293 cells has been suggested to be PKC-dependent (Zheng et al., 2008). However, to date this has not been demonstrated in CHO cells.

In our study, endo-1 preferentially recruited β-arr2 over β-arr1. Differential recruitment of β-arrestins to the MOP by endo-1 has not been shown previously, but has been demonstrated for morphine, which promotes recruitment of β-arr2 and little or no recruitment of β-arr1 (Bohn et al., 2004; Groer et al., 2007). However, as mentioned previously, as all ligands gave a lower response in the β-arr1 assay, a partial agonist is expected to have a very low to undetectable signal. Biased activation of β-arrestins may result in differential activation of downstream signaling, as different β-arrestins can act as scaffolds for different signaling complexes (DeWire et al., 2007; Nobles et al., 2011). β-Arr1, but not β-arr2, is required for MOP ubiquitination, and has also been shown to promote MOP dephosphorylation more rapidly than β-arr2 (Groer et al., 2011). In addition, the downstream functions of β-arrestins may vary with different ligands. Differential engagement of G protein receptor–coupled kinases and different patterns of ligand-induced MOP phosphorylation have been demonstrated previously (Schulz et al., 2004; Doll et al., 2011; Lau et al., 2011; Chen et al., 2013). These receptor phosphorylation patterns play a vital role in determining receptor interactions with β-arrestins and may direct β-arrestin functions (Zidar et al., 2009). The differential role of β-arr2 recruitment in response to morphine compared with other opioids has been shown in the β-arr2 knockout mice, where the improved pharmacological profile is only observed with morphine (Bohn et al., 1999; Raehal et al., 2005). Although morphine-induced β-arrestin recruitment results in activation of different signaling pathways, whether the differential recruitment of β-arrestins induced by endo-1 mediates biased activation of signaling pathways downstream of β-arrestin is still unknown.

Agonists were assessed for bias between G protein activation and inhibition of AC, a classic downstream G

protein–mediated effect. Several ligands showed bias toward inhibition of AC over [^{35}S]GTPγS binding in comparison with DAMGO, indicating differential activation of G protein–mediated signaling pathways. There are not many examples where [^{35}S]GTPγS assays have been performed in conjunction with cAMP assays in the same cellular background to assess MOP function (Zaki et al., 2000; Vigano et al., 2003). Zaki et al. (2000) reported differing relative potencies of some agonists between the two assays, but concluded that this was due to the different coupling efficiencies. There is also some evidence of ligand-dependent engagement of different G_α subunits with MOP (Sanchez-Blazquez et al., 2001; Massotte et al., 2002; Clark et al., 2006; Saidak et al., 2006). However, these differences are small, and since most methods used in these studies require overexpression or addition of purified G proteins, the real preferences for different subunits may be masked by differences in stoichiometry between receptor and G proteins. It is also possible that the bias observed between these signaling effectors is due to differences in signaling kinetics. As measurements for [^{35}S]GTPγS binding assays are usually taken after longer incubations with the ligand than for cAMP assays, ligands with slower association kinetics or that stimulate different rates of desensitization can display bias between two signaling endpoints. Further experiments are required to elucidate whether bias between [^{35}S]GTPγS binding and AC inhibition or other signaling pathways is due to differential regulation of G protein–mediated signaling pathways, different signaling kinetics, or different ligand association/dissociation rates.

The bias between cAMP inhibition and [^{35}S]GTPγS also correlates with the bias observed between MOP trafficking and these signaling pathways. Several ligands showed bias between trafficking and cAMP, but not between trafficking and [^{35}S]GTPγS. Morphine and possibly Met-enk-RF may also be biased toward cAMP inhibition and [^{35}S]GTPγS binding over trafficking. However, as bias factors could not be quantified for morphine and Met-enk-RF between trafficking and other signaling pathways, we cannot exclude the possibility that these ligands simply have lower efficacy, in which case the lower response in a low-sensitivity assay, such as trafficking, is to be expected. There were no ligands showing significant bias between trafficking and recruitment of β-arr1, and only endo-1 was biased toward β-arr2 over receptor trafficking. This result is in line with the fact that receptor trafficking is highly dependent on recruitment of β-arrestins.

In summary, we have performed a systematic quantitative analysis of biased agonism at the MOP by endogenous and putatively endogenous opioid peptides across multiple different signaling pathways. This work has revealed that opioid peptides display a variety of different biased agonism profiles, some of which are unique. α-Neo and endo-1 display particularly distinct biased agonism profiles, and may have different signaling properties and physiologic effects in vivo compared with other endogenous opioids. Biased agonism profiles, combined with different degradation rates, expression patterns in the body, and differing selectivities for opioid receptor subtypes, may engender tremendous diversity in endogenous opioid activity and lead to finely tuned physiologic processes. Although the impact of MOP-biased agonism in the control of normal physiologic processes still remains to be explored, our findings provide a pharmacological framework to progress our understanding of ligand redundancy of the opioid system. A greater understanding of how endogenous opioids control physiologic processes through biased agonism will reveal vital information required to enable the design of biased opioids with improved pharmacological profiles.

Authorship Contributions

Participated in research design: Thompson, Lane, Christopoulos, Canals.

Conducted experiments: Thompson.

Performed data analysis: Thompson, Coudrat.

Wrote or contributed to the writing of the manuscript: Thompson, Lane, Sexton, Christopoulos, Canals.

References

Al-Hasani R and Bruchas MR (2011) Molecular mechanisms of opioid receptor-dependent signaling and behavior. *Anesthesiology* **115**:1363–1381.

Arden JR, Segredo V, Wang Z, Lameh J, and Sadée W (1995) Phosphorylation and agonist-specific intracellular trafficking of an epitope-tagged μ-opioid receptor expressed in HEK 293 cells. *J Neurochem* **65**:1636–1645.

Benyamin R, Trescot AM, Datta S, Buenaventura R, Adlaka R, Sehgal N, Glaser SE, and Vallejo R (2008) Opioid complications and side effects. *Pain Physician* **11**(2, Suppl)S105–S120.

Black JW and Leff P (1983) Operational models of pharmacological agonism. *Proc R Soc Lond B Biol Sci* **220**:141–162.

Bohn LM, Dykstra LA, Lefkowitz RJ, Caron MG, and Barak LS (2004) Relative opioid efficacy is determined by the complements of the G protein-coupled receptor desensitization machinery. *Mol Pharmacol* **66**:106–112.

Bohn LM, Lefkowitz RJ, Gainetdinov RR, Peppel K, Caron MG, and Lin FT (1999) Enhanced morphine analgesia in mice lacking beta-arrestin 2. *Science* **286**: 2495–2498.

Chen Y-J, Oldfield S, Butcher AJ, Tobin AB, Saxena K, Gurevich VV, Benovic JL, Henderson G, and Kelly E (2013) Identification of phosphorylation sites in the COOH-terminal tail of the μ-opioid receptor. *J Neurochem* **124**:189–199.

Christopoulos A (1998) Assessing the distribution of parameters in models of ligand-receptor interaction: to log or not to log. *Trends Pharmacol Sci* **19**:351–357.

Clark MJ, Furman CA, Gilson TD, and Traynor JR (2006) Comparison of the relative efficacy and potency of mu-opioid agonists to activate Galpha(i/o) proteins containing a pertussis toxin-insensitive mutation. *J Pharmacol Exp Ther* **317**: 858–864.

Cox BM, Christie MJ, Devi L, Toll L, and Traynor JR (2015) Challenges for opioid receptor nomenclature: IUPHAR Review 9. *Br J Pharmacol* **172**:317–323.

DeWire SM, Ahn S, Lefkowitz RJ, and Shenoy SK (2007) Beta-arrestins and cell signaling. *Annu Rev Physiol* **69**:483–510.

DeWire SM, Yamashita DS, Rominger DH, Liu G, Cowan CL, Graczyk TM, Chen XT, Pitis PM, Gotchev D, and Yuan C et al. (2013) A G protein-biased ligand at the μ-opioid receptor is potently analgesic with reduced gastrointestinal and respiratory dysfunction compared with morphine. *J Pharmacol Exp Ther* **344**: 708–717.

Doll C, Konietzko J, Pöll F, Koch T, Höllt V, and Schulz S (2011) Agonist-selective patterns of μ-opioid receptor phosphorylation revealed by phosphosite-specific antibodies. *Br J Pharmacol* **164**:298–307.

Fichna J, Janecka A, Costentin J, and Do Rego J-C (2007) The endomorphin system and its evolving neurophysiological role. *Pharmacol Rev* **59**:88–123.

Frölich N, Dees C, Paetz C, Ren X, Lohse MJ, Nikolaev VO, and Zenk MH (2011) Distinct pharmacological properties of morphine metabolites at G(i)-protein and β-arrestin signaling pathways activated by the human μ-opioid receptor. *Biochem Pharmacol* **81**:1248–1254.

Gesty-Palmer D, Flannery P, Yuan L, Corsino L, Spurney R, Lefkowitz RJ, and Luttrell LM (2009) A beta-arrestin-biased agonist of the parathyroid hormone receptor (PTH1R) promotes bone formation independent of G protein activation. *Sci Transl Med* **1**:1ra1.

Goldberg IE, Rossi GC, Letchworth SR, Mathis JP, Ryan-Moro J, Leventhal L, Su W, Emmel D, Bolan EA, and Pasternak GW (1998) Pharmacological characterization of endomorphin-1 and endomorphin-2 in mouse brain. *J Pharmacol Exp Ther* **286**: 1007–1013.

Groer CE, Schmid CL, Jaeger AM, and Bohn LM (2011) Agonist-directed interactions with specific beta-arrestins determine mu-opioid receptor trafficking, ubiquitination, and dephosphorylation. *J Biol Chem* **286**:31731–31741.

Groer CE, Tidgewell K, Moyer RA, Harding WW, Rothman RB, Prisinzano TE, and Bohn LM (2007) An opioid agonist that does not induce mu-opioid receptor—arrestin interactions or receptor internalization. *Mol Pharmacol* **71**:549–557.

Janecka A, Fichna J, and Janecki T (2004) Opioid receptors and their ligands. *Curr Top Med Chem* **4**:1–17.

Jiang LI, Collins J, Davis R, Lin KM, DeCamp D, Roach T, Hsueh R, Rebres RA, Ross EM, and Taussig R et al. (2007) Use of a cAMP BRET sensor to characterize a novel regulation of cAMP by the sphingosine 1-phosphate/G13 pathway. *J Biol Chem* **282**:10576–10584.

Keith DE, Murray SR, Zaki PA, Chu PC, Lissin DV, Kang L, Evans CJ, and von Zastrow M (1996) Morphine activates opioid receptors without causing their rapid internalization. *J Biol Chem* **271**:19021–19024.

Kelly E (2013) Ligand bias at the μ-opioid receptor. *Biochem Soc Trans* **41**:218–224.

Kenakin T and Christopoulos A (2013) Signalling bias in new drug discovery: detection, quantification and therapeutic impact. *Nat Rev Drug Discov* **12**:205–216.

Kenakin T, Watson C, Muniz-Medina V, Christopoulos A, and Novick S (2012) A simple method for quantifying functional selectivity and agonist bias. *ACS Chem Neurosci* **3**:193–203.

Lau EK, Trester-Zedlitz M, Trinidad JC, Kotowski SJ, Krutchinsky AN, Burlingame AL, and von Zastrow M (2011) Quantitative encoding of the effect of a partial agonist on individual opioid receptors by multisite phosphorylation and threshold detection. *Sci Signal* **4**:ra52.

Leff P, Prentice DJ, Giles H, Martin GR, and Wood J (1990) Estimation of agonist affinity and efficacy by direct, operational model-fitting. *J Pharmacol Methods* **23**: 225–237.

Lonergan T, Goodchild AK, Christie MJ, and Pilowsky PM (2003) Mu opioid receptors in rat ventral medulla: effects of endomorphin-1 on phrenic nerve activity. *Respir Physiol Neurobiol* **138**:165–178.

Macey TA, Bobeck EN, Hegarty DM, Aicher SA, Ingram SL, and Morgan MM (2006) Extracellular signal-regulated kinase 1/2 activation counteracts morphine tolerance in the periaqueductal gray of the rat. *J Pharmacol Exp Ther* **331**: 412–418.

Maguma HT, Dewey WL, and Akbarali HI (2012) Differences in the characteristics of tolerance to μ-opioid receptor agonists in the colon from wild type and β-arrestin2 knockout mice. *Eur J Pharmacol* **685**:133–140.

Mansour A, Hoversten MT, Taylor LP, Watson SJ, and Akil H (1995) The cloned mu, delta and kappa receptors and their endogenous ligands: evidence for two opioid peptide recognition cores. *Brain Res* **700**:89–98.

Massotte D, Brillet K, Kieffer B, and Milligan G (2002) Agonists activate Gi1 alpha or Gi2 alpha fused to the human mu opioid receptor differently. *J Neurochem* **81**: 1372–1382.

Matthes HW, Maldonado R, Simonin F, Valverde O, Slowe S, Kitchen I, Befort K, Dierich A, Le Meur M, and Dollé P et al. (1996) Loss of morphine-induced analgesia, reward effect and withdrawal symptoms in mice lacking the mu-opioid-receptor gene. *Nature* **383**:819–823.

McConalogue K, Grady EF, Minnis J, Balestra B, Tonini M, Brecha NC, Bunnett NW, and Sternini C (1999) Activation and internalization of the μ-opioid receptor by the newly discovered endogenous agonists, endomorphin-1 and endomorphin-2. *Neuroscience* **90**:1051–1059.

McPherson J, Rivero G, Baptist M, Llorente J, Al-Sabah S, Krasel C, Dewey WL, Bailey CP, Rosethorne EM, and Charlton SJ et al. (2010) μ-opioid receptors: correlation of agonist efficacy for signalling with ability to activate internalization. *Mol Pharmacol* **78**:756–766.

Miyatake M, Rubinstein TJ, McLennan GP, Belcheva MM, and Coscia CJ (2009) Inhibition of EGF-induced ERK/MAP kinase-mediated astrocyte proliferation by mu opioids: integration of G protein and beta-arrestin 2-dependent pathways. *J Neurochem* **110**:662–674.

Molinari P, Vezzi V, Sbraccia M, Grò C, Riitano D, Ambrosio C, Casella I, and Costa T (2010) Morphine-like opiates selectively antagonize receptor-arrestin interactions. *J Biol Chem* **285**:12522–12535.

Morse M, Tran E, Sun H, Levenson R, and Fang Y (2011) Ligand-directed functional selectivity at the mu opioid receptor revealed by label-free integrative pharmacology on-target. *PLoS ONE* **6**:e25643.

Motulsky HJ and Ransnas LA (1987) Fitting curves to data using nonlinear regression: a practical and nonmathematical review. *FASEB J* **1**:365–374.

Nobles KN, Xiao K, Ahn S, Shukla AK, Lam CM, Rajagopal S, Strachan RT, Huang TY, Bressler EA, and Hara MR et al. (2011) Distinct phosphorylation sites on the β(2)-adrenergic receptor establish a barcode that encodes differential functions of β-arrestin. *Sci Signal* **4**:ra51.

Pedregosa F, Varoquaux G, Gramfort A, Michel V, Thirion B, Grisel O, Blondel M, Prettenhofer P, Weiss R, and Dubourg V et al. (2011) Scikit-learn: Machine Learning in Python. *J Mach Learn Res* **12**:2825–2830.

Pradhan AA, Smith ML, Kieffer BL, and Evans CJ (2012) Ligand-directed signalling within the opioid receptor family. *Br J Pharmacol* **167**:960–969.

Raehal KM, Schmid CL, Groer CE, and Bohn LM (2011) Functional selectivity at the μ-opioid receptor: implications for understanding opioid analgesia and tolerance. *Pharmacol Rev* **63**:1001–1019.

Raehal KM, Walker JK, and Bohn LM (2005) Morphine side effects in beta-arrestin 2 knockout mice. *J Pharmacol Exp Ther* **314**:1195–1201.

Rajagopal S, Bassoni DL, Campbell JJ, Gerard NP, Gerard C, and Wehrman TS (2013) Biased agonism as a mechanism for differential signaling by chemokine receptors. *J Biol Chem* **288**:35039–35048.

Rivero G, Llorente J, McPherson J, Cooke A, Mundell SJ, McArdle CA, Rosethorne EM, Charlton SJ, Krasel C, and Bailey CP et al. (2012) Endomorphin-2: a biased agonist at the μ-opioid receptor. *Mol Pharmacol* **82**:178–188.

Saidak Z, Blake-Palmer K, Hay DL, Northup JK, and Glass M (2006) Differential activation of G-proteins by mu-opioid receptor agonists. *Br J Pharmacol* **147**: 671–680.

Sakurada S, Hayashi T, and Yuhki M (2002) Differential antinociceptive effects induced by intrathecally-administered endomorphin-1 and endomorphin-2 in mice. *Jpn J Pharmacol* **89**:221–223.

Sánchez-Blázquez P, Gómez-Serranillos P, and Garzón J (2001) Agonists determine the pattern of G-protein activation in mu-opioid receptor-mediated supraspinal analgesia. *Brain Res Bull* **54**:229–235.

Schulz S, Mayer D, Pfeiffer M, Stumm R, Koch T, and Höllt V (2004) Morphine induces terminal micro-opioid receptor desensitization by sustained phosphorylation of serine-375. *EMBO J* **23**:3282–3289.

Soergel DG, Subach RA, Burnham N, Lark MW, James IE, Sadler BM, Skobieranda F, Violin JD, and Webster LR (2014) Biased agonism of the μ-opioid receptor by TRV130 increases analgesia and reduces on-target adverse effects versus morphine: A randomized, double-blind, placebo-controlled, crossover study in healthy volunteers. *Pain* **155**:1829–1835.

Terashvili M, Wu HE, Schwasinger E, and Tseng LF (2007) Paradoxical hyperalgesia induced by mu-opioid receptor agonist endomorphin-2, but not endomorphin-1, microinjected into the centromedial amygdala of the rat. *Eur J Pharmacol* **554**:137–144.

Thompson GL, Kelly E, Christopoulos A, and Canals M (2015) Novel GPCR paradigms at the μ-opioid receptor. *Br J Pharmacol* **172**:287–296.

Tonini M, Fiori E, Balestra B, Spelta V, D'Agostino G, Di Nucci A, Brecha NC, and Sternini C (1998) Endomorphin-1 and endomorphin-2 activate μ-opioid receptors in myenteric neurons of the guinea-pig small intestine. *Naunyn Schmiedebergs Arch Pharmacol* **358**:686–689.

Traynor J (2012) μ-Opioid receptors and regulators of G protein signaling (RGS) proteins: from a symposium on new concepts in mu-opioid pharmacology. *Drug Alcohol Depend* **121**:173–180.

Valant C, May LT, Aurelio L, Chuo CH, White PJ, Baltos JA, Sexton PM, Scammells PJ, and Christopoulos A (2014) Separation of on-target efficacy from adverse effects through rational design of a bitopic adenosine receptor agonist. *Proc Natl Acad Sci USA* **111**:4614–4619.

Viganò D, Rubino T, Di Chiara G, Ascari I, Massi P, and Parolaro D (2003) Mu opioid receptor signaling in morphine sensitization. *Neuroscience* **117**:921–929.

Walters RW, Shukla AK, Kovacs JJ, Violin JD, DeWire SM, Lam CM, Chen JR, Muehlbauer MJ, Whalen EJ, and Lefkowitz RJ (2009) beta-Arrestin1 mediates nicotinic acid-induced flushing, but not its antilipolytic effect, in mice. *J Clin Invest* **119**:1312–1321.

Whistler JL and von Zastrow M (1998) Morphine-activated opioid receptors elude desensitization by beta-arrestin. *Proc Natl Acad Sci USA* **95**:9914–9919.

Williams JT, Ingram SL, Henderson G, Chavkin C, von Zastrow M, Schulz S, Koch T, Evans CJ, and Christie MJ (2013) Regulation of μ-opioid receptors: desensitization, phosphorylation, internalization, and tolerance. *Pharmacol Rev* **65**:223–254.

Willoughby D and Cooper DM (2007) Organization and Ca2+ regulation of adenylyl cyclases in cAMP microdomains. *Physiol Rev* **87**:965–1010.

Wold S, Esbensen K, and Geladi P (1987) Principal component analysis. *Chemom Intell Lab Syst* **2**:37–52.

Yu Y, Cui Y, Wang X, Lai LH, Wang C-L, Fan YZ, Liu J, and Wang R (2007) In vitro characterization of the effects of endomorphin 1 and 2, endogenous ligands for μ-opioid receptors, on mouse colonic motility. *Biochem Pharmacol* **73**:1384–1393.

Zadina JE, Hackler L, Ge LJ, and Kastin AJ (1997) A potent and selective endogenous agonist for the μ-opiate receptor. *Nature* **386**:499–502.

Zaki PA, Keith DE, Jr, Brine GA, Carroll FI, and Evans CJ (2000) Ligand-induced changes in surface mu-opioid receptor number: relationship to G protein activation? *J Pharmacol Exp Ther* **292**:1127–1134.

Zhao P, Canals M, Murphy JE, Klingler D, Eriksson EM, Pelayo JC, Hardt M, Bunnett NW, and Poole DP (2013) Agonist-biased trafficking of somatostatin receptor 2A in enteric neurons. *J Biol Chem* **288**:25689–25700.

Zheng H, Loh HH, and Law PY (2008) Beta-arrestin-dependent mu-opioid receptor-activated extracellular signal-regulated kinases (ERKs) Translocate to Nucleus in Contrast to G protein-dependent ERK activation. *Mol Pharmacol* **73**:178–190.

Zidar DA (2011) Endogenous ligand bias by chemokines: implications at the front lines of infection and leukocyte trafficking. *Endocr Metab Immune Disord Drug Targets* **11**:120–131.

Zidar DA, Violin JD, Whalen EJ, and Lefkowitz RJ (2009) Selective engagement of G protein coupled receptor kinases (GRKs) encodes distinct functions of biased ligands. *Proc Natl Acad Sci USA* **106**:9649–9654.

Address correspondence to: Meritxell Canals, Drug Discovery Biology, Monash Institute of Pharmaceutical Sciences, Monash University, Parkville, VIC 3052, Australia. E-mail: meri.canals@monash.edu or Arthur Christopoulos, Drug Discovery Biology, Monash Institute of Pharmaceutical Sciences, Monash University, Parkville, VIC 3052, Australia. E-mail: arthur.christopoulos@monash.edu

B.4 Systematic Analysis of Factors Influencing Observations of Biased Agonism at the μ Opioid Receptor

Biochemical Pharmacology 113 (2016) 70–87

Contents lists available at ScienceDirect

Biochemical Pharmacology

journal homepage: www.elsevier.com/locate/biochempharm

Systematic analysis of factors influencing observations of biased agonism at the mu-opioid receptor

Georgina L. Thompson [a,b], J. Robert Lane [a], Thomas Coudrat [a], Patrick M. Sexton [a], Arthur Christopoulos [a,*], Meritxell Canals [a,*]

[a] Drug Discovery Biology, Monash Institute of Pharmaceutical Sciences, Monash University, Parkville, VIC 3052, Australia
[b] Defence Science and Technology Organisation, Department of Defence, Fishermans Bend, VIC 3207, Australia

ARTICLE INFO

Article history:
Received 25 April 2016
Accepted 31 May 2016
Available online 7 June 2016

Keywords:
Opioid receptor
Biased agonism
G protein-coupled receptors
Cell signalling

ABSTRACT

Biased agonism describes the ability of distinct G protein-coupled receptor (GPCR) ligands to stabilise distinct receptor conformations leading to the activation of different cell signalling pathways that can deliver different physiologic outcomes. This phenomenon is having a major impact on modern drug discovery as it offers the potential to design ligands that selectively activate or inhibit the signalling pathways linked to therapeutic effects with minimal activation or blockade of signalling pathways that are linked to the development of adverse on-target effects. However, the explosion in studies of biased agonism at multiple GPCR families in recombinant cell lines has revealed a high degree of variability on descriptions of biased ligands at the same GPCR and raised the question of whether biased agonism is a fixed attribute of a ligand in all cell types. The current study addresses this question at the mu-opioid receptor (MOP). Here, we have systematically assessed the impact of differential cellular protein complement (and cellular background), signalling kinetics and receptor species on our previous descriptions of biased agonism at MOP by several opioid peptides and synthetic opioids. Our results show that all these factors need to be carefully determined and reported when considering biased agonism. Nevertheless, our studies also show that, despite changes in overall signalling profiles, ligands that previously showed distinct bias profiles at MOP retained their uniqueness across different cell backgrounds.

1. Introduction

G protein-coupled receptors (GPCRs) are involved in the control of virtually every physiological process. They are a major target of currently used medicines, and represent valuable targets for the design of new therapeutics. However, most GPCRs are ubiquitously expressed in multiple tissues and exert their effects through activation of a wide variety of signalling pathways. Many drugs that target GPCRs produce side effects mediated through the activation of "unwanted" signalling pathways by the GPCR of interest, or by the activation of the same GPCR in different non-target tissues. The former "on-target" side effects can be minimised by designing drugs that selectively activate the signalling pathways required to produce the therapeutic response. This pathway-specific drug design is based on a property of GPCRs known as "biased agonism", "ligand-directed signalling" or "functional selectivity" [1]. Biased agonism describes how chemically distinct ligands targeting the same GPCR in an identical cellular background, stabilise the receptor in different conformations, resulting in differential activation of downstream signalling, which in turn can induce different physiological effects. Therefore, biased agonism offers the potential to design ligands that selectively activate or inhibit the signalling pathways linked to the desired therapeutic effects with minimal activation or blockade of signalling pathways that are linked to the development of side effects.

In order to develop strategies to design a biased ligand with the desired selectivity for particular signalling pathways, methods for quantifying biased agonism are essential. To achieve this, it is important to consider that the observed response that is induced

Abbreviations: AC, adenylyl cyclase; α-neo, α-neoendorphin; β-arr1 and β-arr2, β-arrestin 1 and 2; BRET, bioluminescence resonance energy transfer; CHO, Chinese hamster ovary; DAMGO, D-Ala2-*N*-MePhe4-Gly-ol enkephalin; endo, endomorphin; pERK, extracellular signal regulated kinases 1/2 phosphorylation; GIRK, G protein-gated inwardly rectifying K^+ channel; GPCR, G protein-coupled receptor; GRK, G protein-coupled receptor kinase; enk, enkephalin; MOP, μ-opioid receptor; PKC, protein kinase C; PCA, principal component analysis; RGS, regulator of G protein signalling; RLuc, renilla luciferase; YFP, yellow fluorescent protein.

* Corresponding authors.
E-mail addresses: arthur.christopoulos@monash.edu (A. Christopoulos), meri.canals@monash.edu (M. Canals).

http://dx.doi.org/10.1016/j.bcp.2016.05.014
0006-2952/

by a ligand at a particular signalling pathway is not solely determined by the affinity and intrinsic efficacy of such ligand. Rather, the differing coupling efficiencies of the signalling pathways, and the different conditions and sensitivities of the detection methods, also contribute to the overall observed response, and are termed "system bias" and "observational bias", respectively [2]. Therefore, biased agonism engendered solely by conformational effects of the ligand–receptor interaction, must be quantified using a method that excludes both system and observational bias. Although several analytical methods to quantify biased agonism have been developed, most can only be applied in specific circumstances (as reviewed in [2]). The method recently described by Kenakin et al. [3], or "transduction coefficient" method, based on the Black and Leff (1983) [4] operational model of agonism, can be applied to concentration–response curves to obtain a single parameter that describes bias between signalling pathways in a system independent manner [2].

In the last decade, biased agonism has been quantified at numerous GPCRs including; opioid receptors [5–8], chemokine receptors [3,9,10], adrenoceptors [11,12], and many others [13–16]. Most studies have focused on discovery of ligands with differential receptor signalling versus regulation characteristics, specifically by quantifying bias between G protein-mediated signalling and β-arrestin recruitment or receptor internalisation [5,7,8,10]. However, it has become increasingly apparent that biased agonism can result in the differential activation of a plethora of signalling pathways downstream of receptor activation, not only G protein activation and β-arrestin recruitment, supporting the concept of the pluridimensionality of efficacy [17]. For this reason, more recent studies are extending assessment of bias to a wider array of signalling pathways to obtain comprehensive descriptions of ligand action that can predict the differential effects of GPCR ligands [6,9,12,14].

Most descriptions of biased agonism have been initially based on studies in recombinant cell systems, where consistent and robust responses of different signalling pathways can be obtained, ensuring a high degree of accuracy and sensitivity. However, it is still unclear whether quantification of biased agonism in recombinant cell lines can truly predict biased agonism *in vivo* [18]. The potential for inconsistencies in biased agonism determinations is exemplified by conflicting results reported in different studies of the same GPCR that have examined this phenomenon in different cell backgrounds. At the μ opioid receptor (MOP), for instance, several studies have examined bias between G protein activation and β-arrestin recruitment [6,8,19,20]. Most notably, endomorphin 2 (endo-2) may exhibit differential bias towards β-arrestin 2 (β-arr2) recruitment and away from G protein activation in different studies [6,8,19]. Similar discrepancies have been observed for bias of aripiprazole between extracellular signal regulated kinase 1/2 (ERK1/2) phosphorylation and adenylyl cyclase (AC) inhibition at the dopamine D_2 receptor [16,21], and bias between receptor internalisation and G protein-mediated signalling pathways mediated by CCL4 and CCL3L1 at CCR5 receptors [3,10]. Altogether, such discrepancies between studies raise important questions about the determination and quantification of biased agonism, specifically, is biased agonism a fixed attribute of a ligand in all cell types?

Because GPCR function is determined by at least three molecular partners, i.e. ligand, receptor, and transducer or effector protein, it follows that an agonist-bound active receptor state cannot be defined outside the context of a specific receptor–transducer interaction [22]. Such active receptor state will be dependent on the cellular complement of transducers (or intracellular effector proteins) of a particular cell type. Thus, altering the cellular complement of intracellular binding proteins by overexpressing specific signalling components, or changing cell background, will likely affect bias. When the change in expression of a signalling effector(s) has equal effects on the agonism of all ligands, this results in a change in "system bias" which is eliminated when quantifying bias relative to the reference ligand using the "transduction coefficient" method (see above and [3]). However, altered expression of signalling effectors may have unequal effects on different ligands and, as a consequence, the observed biased agonism will not necessarily be maintained in different systems. Ligands may preferentially activate different isoforms of signalling effectors that are expressed in different cell types such as G protein subunits or G protein-coupled receptor kinases (GRKs). Moreover, in addition to potentially altering ligand bias, the cell background also dictates which signalling pathways can be practically used to quantify bias. GPCRs will be more efficiently coupled to some signalling pathways than others (system bias). This may require alterations of assay conditions to optimise detection of poorly coupled signalling pathways, and may entail changing the signalling effectors examined altogether. This makes it prohibitively difficult to measure the same signalling events under identical conditions in different cells, increasing the likelihood of obtaining different results when quantifying bias in different cell backgrounds. Alterations in the assays conditions may include overexpression of a signalling effector to enhance detection of the desired signalling pathway, such as the overexpression of a GRK to enhance β-arrestin recruitment [23,24]. Altering the balance between signalling effectors that are in competition with each other, such as G proteins and β-arrestins or different GRK isoforms, may enhance interactions with signalling effectors that a ligand–receptor complex naturally has little affinity for. This change in signalling effector expression may again affect the descriptions of biased agonism.

Quantifying bias in a different cell background may alternatively require substitution of a poorly coupled signalling pathway for another closely related signalling pathway, such as different G protein-mediated signalling pathways. However, even closely related signalling pathways are differentially regulated by distinct signalling effectors, and therefore are subject to the same limitations in determining biased agonism. For example, differential activation of G protein-mediated signalling pathways can occur as a result of differential activation of G protein subunits [25], which may preferentially activate some signalling pathways, and may in turn be differentially controlled by regulators of G protein signalling (RGS) [26–28]. Additionally, different G protein-mediated signalling pathways, such as AC stimulation or inhibition, are regulated by numerous other signalling effectors [29].

Finally, another factor that may alter observed bias when measured under different experimental conditions is the kinetics of all processes involved; ligand binding, activation and desensitisation of the signalling pathways [30]. Biased agonism is generally described as a difference in the magnitude of activation of signalling pathways compared to a reference ligand, when measured at its peak or steady state activation. However, this limited measure of biased agonism largely excludes the differential effects biased agonists may have on the spatiotemporal properties of the signalling pathways. Every signalling pathway has different activation and desensitisation kinetics that will be differentially regulated by different ligands, i.e. ligands may have similar bias when considering the maximal response of the signalling pathway, but due to differential desensitisation their bias may change at later time points. This means that the observed bias of a ligand will be time dependent, and consequently different results may be obtained when measuring the same signalling pathway using different assay techniques that require different incubation times [30].

Altogether, cell background and signalling kinetics add additional layers of complexity to defining the biased agonism of a ligand, and to ascertain the profile that is required to produce the desired therapeutic effects. Previously, we systematically quantified biased agonism of a range of both exogenous and

endogenous opioids at MOP across multiple different signalling pathways in CHO cells [6]. This study revealed a number of ligands that possess unique biased agonism profiles, including the endogenous ligands Met-enkephalin-Arg-Phe (Met-enk-RF) and α-neoendorphin (α-neo). Here, we have used this initial characterisation to extend our studies towards understanding the impact of cell background and signalling dynamics on the detection and quantification of bias. Our results illustrate that when assessing biased agonism, both of these factors need to be taken under consideration. However, our studies at MOP also show that, despite changes in directions of bias, and overall signalling profiles, ligands with distinct bias profiles retained their differentiation across different cell backgrounds.

2. Methods

2.1. Materials

Chinese hamster ovary (CHO) FlpIn cells and Dulbecco's modified Eagle's medium (DMEM) were purchased from Invitrogen (Mulgrave, VIC, Australia). Foetal bovine serum (FBS) was purchased from ThermoTrace (Melbourne, Australia). Hygromycin-B was purchased from Roche Applied Science (Dee Why, NSW, Australia). All endogenous opioid peptides were purchased from Mimotopes (Melbourne, Australia). Morphine HCl was from GlaxoSmithKline (Boronia, Victoria, Australia). All other chemicals were purchased from Sigma Aldrich (Castle Hill, NSW, Australia). AtT20 and AtT20-FLAG-MOP cells were a gift from Prof. Macdonald Christie (University of Sydney, Australia). MOP-RLuc was a gift of Prof. Laura Bohn (Scripps Research Institute, Florida, USA).

2.2. Cell culture and generation of stable cell line

Cells were maintained and cultured in high-glucose DMEM containing 10% FBS and 600 μg/ml hygromycin B for CHO-MOP cells, and 500 μg/ml G418 for AtT20-MOP, at 37 °C under a humidified atmosphere containing 5% CO_2. cDNA encoding the wild-type human MOP was obtained from the Missouri University of Science and Technology (http://www.cdna.org) and was provided in pcDNA3.1+. Sequence of the human MOP was amplified by polymerase chain reaction and cloned into the Gateway entry vector pENTR/D-TOPO, using the pENTR directional TOPO cloning kit, according to the manufacturer's instructions (Invitrogen, Mulgrave, Australia). The construct was subsequently transferred into the Gateway destination vector pEF5/frt/V5/dest using the LR Clonase enzyme mix (Invitrogen), and the constructs were used to transfect FlpIn CHO cells (Invitrogen). Cells were selected using 600 μg/ml hygromycin B to generate cell lines stably expressing MOP. AtT20 cells stably expressing a FLAG tagged MOP were generated as described previously [31].

2.3. Inhibition of forskolin-induced cAMP levels

The ability of ligands to inhibit forskolin-induced cAMP production was assessed in AtT20-MOP and FlpIn CHO-MOP cells transiently transfected to express the CAMYEL cAMP BRET biosensor [32]. CHO-MOP cells were grown overnight in white 96-well plates (Culturplates, Perkin Elmer, Melbourne, Australia). Transient transfection of FlpIn CHO-MOP cells was performed using polyethylenimine (PEI, Polysciences, Warrington, PA, USA) at a 6:1 ratio of DNA. AtT20-MOP cells were grown in 10 cm dishes and transient transfection was performed using lipofectamine (Invitrogen). After 24 h AtT20-MOP cells were transferred to white 96-well plates. 48 h after transfection cells were rinsed and pre-incubated in Hank's Balanced Saline Solution (HBSS) with 0.01% BSA and protease inhibitors (1 μM captopril, 1 μM phosphoramidon, 1 μM amastatin, 1 μM actinonin and 1 μM Diprotin A) for 30 min at 37 °C. Cells were then incubated with the Rluc substrate coelenterazine-h, final concentration 5 μM, for 5 min, followed by a further 5 min incubation with increasing concentrations of agonists. Forskolin was then added to a final concentration of 10 μM. After 5 min the YFP and the Rluc emissions were measured using a LumiSTAR Omega (BMG Labtech, Ortenberg, Germany) that allows for sequential integration of the signals detected at 475 ± 30 and 535 ± 30 nm, using filters with the appropriate band pass. For cAMP kinetic experiments baseline readings were taken every 30 s for 3 min before addition of forskolin, and measurements taken every 30 s for 30 min after addition of forskolin. Data are presented as a BRET ratio, calculated as the ratio of YFP to Rluc signals, and expressed as the percentage of the forskolin-induced signal.

2.4. Bioluminescence resonance energy transfer (BRET) assays

Agonist-induced recruitment of β-arrestins to the MOP was examined using a BRET-based method. AtT20 cells and parental FlpIn CHO cells were transfected as described above to co-express MOP C-terminally tagged with Rluc, G protein coupled receptor kinase 2 (GRK2) and β-arr1- or β-arr2-YFP, at a 1:2:4 DNA ratio. To measure G protein activation in FlpIn CHO cells, 1×10^6 cell were seeded in white 96 well plates. The next day cells were transfected using PEI as above with 1 μg MOP, 1.2 μg Gβ1, and either 1.35 μg Gγ-Venus with 0.6 μg of $G\alpha_{i1}$-Rluc8, $G\alpha_{i2}$-Rluc8 or $G\alpha_{i3}$-Rluc8, or 0.6 μg Gγ2-Venus with 0.14 μg $G\alpha_{ob}$-Rluc8. For β-arrestin recruitment assays, agonists were added after 5 min of pre-incubation with coelenterazine-h, and then incubated for an additional 5 min before the BRET ratio was determined. For G protein assays, agonists were added after 10 min pre-incubation with coelenterazine-h, and readings were taken after 5 min incubation with the ligand. For G protein assays with 60 min agonist stimulation, coelenterazine-h was added 10 min prior to detection. Data are expressed as the percentage of the maximum DAMGO response for β-arrestin assays, and the maximum Loperamide response for G protein assays.

2.5. Membrane potential

Agonist-induced membrane hyperpolarisation in AtT20-MOP cells was measured using the FLIPR membrane potential assay kit (Molecular devices, CA, USA). AtT20-MOP cells were plated in clear bottom black half area 96-well plates (Corning, Clayton, Australia). Cells were allowed to adhere, the media were changed to low serum media (1% FBS), and cells allowed to grow overnight. 1 bottle of red membrane potential dye was dissolved in 10 ml K^+ free HBSS (0.388 mM $NaHPO_4$, 4.17 mM $NaHCO_3$, 0.441 mM KH_2PO_4, 145 mM NaCl, 22 mM HEPES, 0.407 mM $MgSO_4$, 0.493 mM $MgCl_2$, 1.26 mM $CaCl_2$ and 5.56 mM glucose). Dye was added to cells to a 1:1 ratio of dye to low serum media, and cells allowed to recover for 30 min. Membrane hyperpolarisation was measured at 37 °C using a Flexstation®3 (Molecular Devices; Sunnyvale, CA, USA). Fluorescence was detected for every 2 s for 90 s at 530 nm excitation and 565 nm emission. Baseline readings were taken for 30 s before addition of agonists. Data are expressed as ΔMP, which is the area under the curve units normalised to the maximum response obtained with DAMGO.

2.6. Receptor internalisation

AtT20-MOP cells were plated and grown overnight in 48-well culture plates. Cells were incubated with increasing concentrations of agonists in DMEM for 30 min, then washed gently 3 times with TBS and fixed in 3.7% v/v paraformaldehyde. Surface or total FLAG-MOP receptors were detected in intact or (Nonidet P-40

equivalent)-detergent permeabilised cells, respectively, using the mouse anti-FLAG antibody (1:2000) followed by HRP-conjugated goat anti-mouse IgG (1:2000). After washing with TBS, the peroxidase substrate (SIGMAFAST™ OPD, Sigma Aldrich) was added at a final concentration of 0.4 mg/ml, and the reaction was terminated by the addition of 1 M HCl. The coloured reaction product was detected at 490 nm in a multi-label plate reader (EnVision, PerkinElmer Life Sciences). The absorbance values for transfected cells were normalised to those of mock-transfected cells, and receptor density was reported relative to vehicle-treated wells.

2.7. Data analysis

Agonist concentration–response curves were fitted empirically to a three-parameter logistic equation using Prism 6.0 (GraphPad Software Inc.) where bottom and top are the lower and upper plateaus, respectively, of the concentration–response curve, [A] is the molar concentration of agonist, and EC_{50} is the molar concentration of agonist required to generate a response halfway between the top and the bottom.

$$Y = bottom + \frac{top - bottom}{1 + 10^{(\log EC_{50} - \log[A])}} \quad (1)$$

To compare agonist profiles and to quantify biased agonism, agonist concentration–response data were fitted to the following form of the operational model of agonism [2,4]

$$Y = basal + \frac{(E_m - basal)\left(\frac{\tau}{K_A}\right)^n [A]^n}{[A]^n\left(\frac{\tau}{K_A}\right)^n + \left(1 + \frac{[A]}{K_A}\right)^n} \quad (2)$$

where E_m is the maximal possible response of the system, *basal* is the basal level of response, K_A denotes the functional equilibrium dissociation constant of the agonist (A) for the receptor, τ is an index of the signalling efficacy of the agonist and is defined as R_T/K_E, where R_T is the total number of receptors and K_E is the coupling efficiency of each agonist-occupied receptor, and n is the slope of the transducer function that links occupancy to response. The analysis assumes that the maximal system responsiveness (E_m) and the transduction machinery utilised for a given cellular pathway are the same for all agonists, such that the E_m and transducer slope (n) are shared between agonists. Data for all compounds for each pathway were fitted globally to determine values of K_A and τ; for partial agonists, analysis of the concentration response curves using the operational model of agonism allowed for the direct estimation of the individual Log τ and Log K_A parameters, whereas for full agonists, only the Log(τ/K_A) ratio could be determined.

The aforementioned ratio, τ/K_A (determined as a single fitted value and estimated as a logarithm) is referred to herein as the "transduction coefficient", which represents a single parameter sufficient to describe agonism for a given pathway (biased agonism can result from either a selective affinity (K_A) of an agonist for a given receptor state(s) and/or a differential coupling efficacy (τ) towards certain pathways).

To cancel the impact of cell-dependent effects on the observed agonism at each pathway, the log(τ/K_A) values were then normalised to that determined for DAMGO at each pathway to yield a normalised transduction coefficient, $\Delta\log(\tau/K_A)$, which was calculated as follows

$$\Delta \log\left(\frac{\tau}{K_A}\right) = \log\left(\frac{\tau}{K_A}\right)_{test\ compound} - \log\left(\frac{\tau}{K_A}\right)_{DAMGO} \quad (3)$$

Finally, to determine the actual bias of each agonist between different signalling pathways, the $\Delta\log(\tau/K_A)$ values were evaluated statistically between the pathways. The ligand bias of an agonist for one pathway, j1, over another, j2, is given as

$$\Delta\Delta \log\left(\frac{\tau}{K_A}\right)_{j1-j2} = \Delta \log\left(\frac{\tau}{K_A}\right)_{j1} - \log\left(\frac{\tau}{K_A}\right)_{j2} \quad (4)$$

Lack of biased agonism as compared to the reference agonist DAMGO will result in values of $\Delta\Delta\log(\tau/K_A)$ not significantly different from 0 between pathways. To account for the propagation of error associated with the determination of composite parameters using Eqs. (3) and (4), the following equation was used

$$Pooled\ SEM = \sqrt{(SEj1)^2 + (SEj2)^2} \quad (5)$$

All potency (pEC_{50}), K_A, and transduction ratio ($\Delta\Delta\log(\tau/K_A)$) parameters were estimated as logarithms. When fold-changes in bias are described, this was calculated by first converting values of $\Delta\Delta\log(\tau/K_A)$ to the corresponding antilog value.

$$Bias = 10^{\Delta\Delta \log\left(\frac{\tau}{K_A}\right)} \quad (6)$$

The distribution of antilogs of affinity and potency values does not conform to a normal (Gaussian) distribution, whereas the logarithm of the measure is approximately Gaussian [33–35]. Thus, as the application of t tests and analyses of variance assume Gaussian distribution, estimating the parameters as logarithms allows valid statistical comparison. All results are expressed as mean ± SEM. Statistical analysis was performed using a one-way ANOVA with Dunnett's multiple comparison test to make pairwise comparisons between bias factors for a given ligand and DAMGO, where $P < 0.05$ was considered to be statistically significant.

To visualise bias between multiple pathways at once, webs of bias were constructed. $\Delta\Delta\tau/K_A$ values between a reference endpoint, membrane hyperpolarisation (ΔMP), and all other pathways were obtained using DAMGO as the reference ligand as follows

$$\Delta\tau/K_A = \frac{\tau/K_{A\ test\ compound}}{\tau/K_{ADAMGO}} \quad (7)$$

$$\Delta\Delta\tau/K_A = \frac{\Delta\tau/K_{A_{j1}}}{\Delta\tau/K_{A_{j2}}} \quad (8)$$

2.8. Principal component analysis

Principal component analysis (PCA) is a dimensionality reduction method that uses transformations to project a high-dimensional set of data into a lower dimensional set of variables called principal components (PCs). The PCs extract the important information from the data, revealing its internal structure in a way that best explains its variance [36]. PCs are ranked according to the percentage of total variance in the data they explain. The first PC explains a maximal amount of total variance in the data. Each succeeding PC explains a maximal amount of the remaining variation, without being correlated with the preceding components. PCA was applied using singular value decomposition as implemented in the package scikit-learn [37], the script used for the analysis and plotting can be found at https://github.com/thomas-coudrat/pca_analysis.

3. Results

We recently quantified biased agonism at the MOP in FlpIn CHO cells stably expressing the human MOP [6] and identified several opioids that display unique biased agonism profiles compared to the reference ligand D-Ala^2-*N*-MePhe^4-Gly-ol enkephalin (DAMGO). These include morphine, endo-1 and endo-2, which had previously been reported to display biased agonism at the MOP [8,19], the peripherally restricted MOP agonist, loperamide, as well as three endogenous opioids, Met-enk, met-enk-RF and

α-neo. In the current study, we investigated whether the biased agonism profiles for these eight MOP ligands remain consistent across different cell lines, examined the effect of different cellular protein complement on bias, and assessed the time dependency of biased agonism.

3.1. Opioids show differential G_α subunit activation

To investigate the effect of the different G protein complement on biased agonism we have examined the activation of different G proteins by MOP agonists. MOPs are primarily coupled to G proteins containing $G_{\alpha i}$ or $G_{\alpha o}$ subunits, and there is some evidence that opioid ligands show differential preference for some subtypes [38–40]. The ability of ligands to activate G proteins was assessed using a BRET-based assay. CHO FlpIn MOP cells were co-transfected with $G_{\gamma 2}$-Venus, $G_{\beta 1}$ and either RLuc8-tagged $G_{\alpha i1}$, $G_{\alpha i2}$, $G_{\alpha i3}$ or $G_{\alpha ob}$. All ligands activated the four G protein subtypes after 5 min in a concentration-dependent manner (Fig. 1). The greatest changes in BRET were observed with $G_{\alpha i1}$ and $G_{\alpha ob}$ (data not shown), which may indicate that MOP has a greater ability to couple to G proteins containing $G_{\alpha i1}$ or $G_{\alpha ob}$ subunits, however we cannot exclude the possibility that this is due to differences in BRET efficiency between the different RLuc8-G_α constructs and the G_γ-Venus. DAMGO and Met-enk stimulated most G_α subtypes to at least 80% of the response to loperamide at 5 min, whereas morphine, endo-1, endo-2, Met-enk-RF and α-neo were, in general, less efficacious than loperamide (Fig. 1).

Bias factors ($\Delta\Delta\log(\tau/K_A)$, see materials and methods) between activation of different G_α subtypes were quantified for all ligands using DAMGO as the reference ligand (Fig. 2, Table 1). When compared to DAMGO, Met-enk-RF and α-neo were biased away from $G_{\alpha i1}$ activation relative to at least one of the other G_α subunits (Fig. 2a–c). This is largely due to the fact that DAMGO-stimulated MOP is more efficiently coupled to $G_{\alpha i1}$ than to the other G_α subunits, which is apparent when comparing the $\log(\tau/K_A)$ values of DAMGO vs other ligands for each G_α subunit (Table 1). Additionally, Met-enk-RF, which exhibited similar activation of $G_{\alpha i1}$, $G_{\alpha i2}$ and $G_{\alpha ob}$ relative to DAMGO, showed increased $G_{\alpha i3}$ activation when compared to DAMGO at 5 min, resulting in bias towards $G_{\alpha i3}$ over $G_{\alpha i1}$ (Fig. 2b). This bias is partly attributable to a small increase in the K_A of Met-enk-RF for $G_{\alpha i3}$ (Table 1). Interestingly, no ligands showed bias between $G_{\alpha i2}$ and $G_{\alpha i3}$, $G_{\alpha i3}$ and $G_{\alpha ob}$ or $G_{\alpha i2}$ and $G_{\alpha ob}$ (Fig. 2d–f).

We next quantified bias between activation of the different G_α subunits and recruitment of β-arr2 (Fig. 2g). α-Neo showed bias towards $G_{\alpha i2}$ which is in line with previous results that showed α-neo was biased towards inhibition of cAMP production when compared to β-arr2 [6]. In addition to this, morphine and endo-1 were biased towards β-arr2 over $G_{\alpha i1}$ and $G_{\alpha i3}$ respectively. This was unexpected since morphine and endo-1 previously showed no bias between inhibition of cAMP production and β-arr2. The different bias observed when comparing β-arr2 to either inhibition of cAMP production or G protein activation illustrates that the level of G protein activation is not always indicative of the level of activation of downstream G protein-mediated signalling.

3.2. Changes in GRK2 expression levels alter the bias between β-arr1 and β-arr2

Recruitment of β-arrestins to MOP is dependent on preceding phosphorylation of the receptor. Different GRKs and other kinases such as PKC have been shown to phosphorylate residues on the receptor, and several studies have demonstrated that phosphorylation of the C-tail of MOP is ligand-dependent [41,42]. As diverse cell types express different kinase levels, this may, in turn, change the ability of ligands to recruit β-arrestins in different cells. Indeed, overexpression of GRK2 has been shown to enhance recruitment of β-arrestins to MOP [43]. We have found that endo-1 is biased towards recruitment of β-arr2 over β-arr1 in CHO-MOP cells with endogenous levels of GRKs [6]. To investigate whether this bias

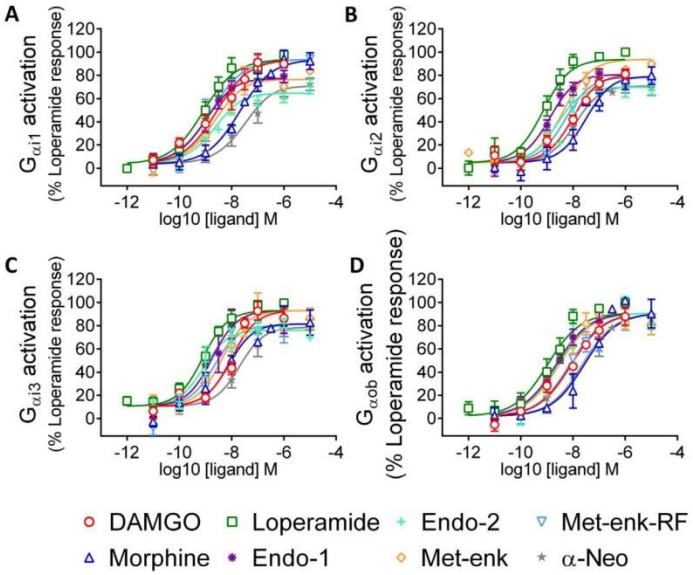

Fig. 1. Activation of $G_{\alpha i/o}$ subunits by MOP agonists. Activation of (a) $G_{\alpha i1}$, (b) $G_{\alpha i2}$, (c) $G_{\alpha i3}$ and (d) $G_{\alpha ob}$ in FlpIn CHO cells after 5 min of agonist stimulation. Data normalised to the 1 μM Loperamide response. Data expressed as mean ± SEM of at least 3 separate experiments.

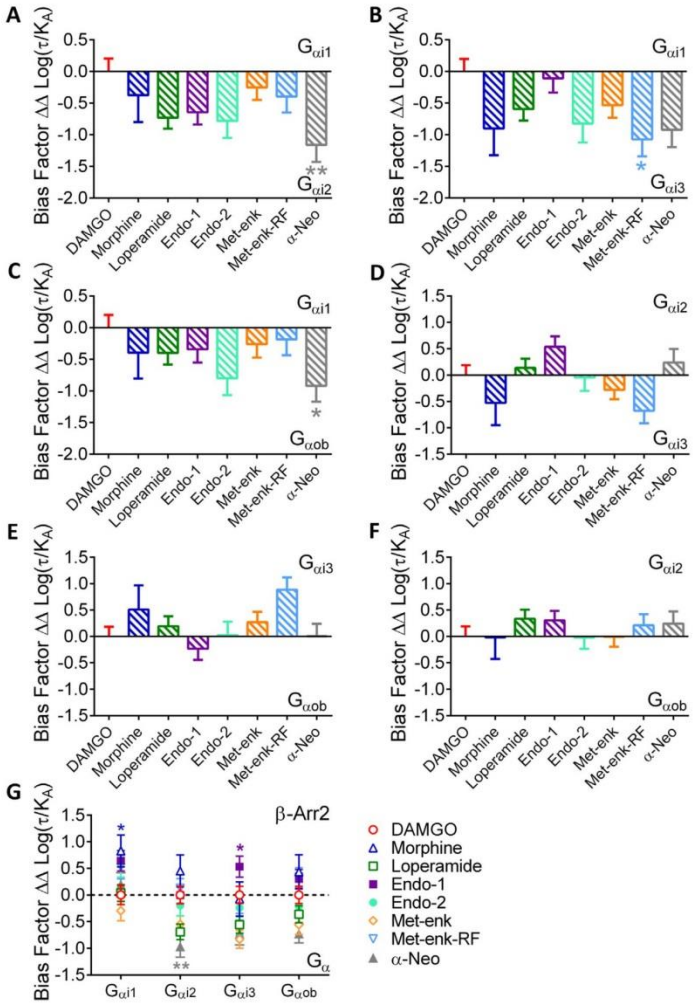

Fig. 2. Quantification of biased agonism of MOP agonists between activation of different $G_{\alpha i/o}$ subunits. (a–f) Bias factors for all agonists between activation of $G_{\alpha i1}$, $G_{\alpha i2}$, $G_{\alpha i3}$ and $G_{\alpha ob}$ after 5 min of agonist stimulation. (g) Bias factors between recruitment of β-arr2 and activation of $G_{\alpha i1}$, $G_{\alpha i2}$, $G_{\alpha i3}$ and $G_{\alpha ob}$ after 5 min agonist stimulation. Data expressed as mean ± SEM of at least 3 separate experiments. $^{*}p \leqslant 0.05$ $^{**}p \leqslant 0.005$, different from DAMGO as determined by a one-way ANOVA with Dunnett's multiple comparison test.

was altered upon changes in GRK expression levels, we repeated this experiment with overexpression of GRK2. CHO FlpIn cells were co-transfected with GRK2, RLuc-tagged MOP and YFP-tagged β-arr1 or β-arr2. Upon overexpression of GRK2, all the ligands tested stimulated recruitment of β-arr1 and β-arr2 in CHO-MOP-GRK2 cells (Fig. 3a and b, Table 2), and all stimulated greater β-arrestin recruitment than measured previously in CHO-MOP cells with endogenous levels of GRKs [6]. In agreement with previous reports, even the weak partial agonist morphine was now able to significantly recruit β-arrestins to MOP. Quantification of bias factors between recruitment of β-arr1 and β-arr2 upon GRK2 overexpression showed that under these conditions, endo-1 no longer differentially recruits β-arrestins when compared to the reference ligand DAMGO (Fig. 3c).

Next, we investigated whether different levels of GRK2 expression affect the biased agonism between recruitment of β-arrestins and G protein-mediated signalling that we had previously observed for some opioid ligands (loperamide, endo-1 and α-neo). Enhancing β-arrestin recruitment would be expected to correlate with a decrease in G protein activation. However, this change may not affect all ligands equally. To test this we measured the MOP-induced inhibition of AC in CHO-MOP-GRK2 cells using a cAMP BRET biosensor and compared this to our results upon endogenous GRK2 expression levels [6] (Fig. 3d–f). All ligands inhibited forskolin induced cAMP production, however, the maximum response was greatly reduced upon GRK2 overexpression, when compared to endogenous levels of GRK2 (less than 30% inhibition compared to 58% inhibition by DAMGO) (Fig. 3d, Table 2).

Table 1
Quantification of biased agonism between activation of different G protein subtypes at two time points. Transduction coefficients [Log(τ/K_A)], normalised transduction coefficients [ΔLog(τ/K_A)] and Log(bias factors) [$\Delta\Delta$Log(τ/K_A)]. Values represent mean ± SEM of three to five independent experiments.

		5 mins						60mins					
		log K_A	SEM	Log τ/K_A	SEM	Δlog τ/K_{AA}	SEM	log K_A	SEM	Log τ/K_A	SEM	Δlog τ/K_A	SEM
$G_{\alpha i1}$	DAMGO	NC	NC	8.575	0.150	0.000	0.212	−6.89	0.29	7.759†	0.110	0.000	0.155
	Morphine	NC	NC	7.686	0.149	−0.889	0.211	−6.76	0.26	7.445	0.157	−0.315	0.191
	Loperamide	NC	NC	9.082	0.128	0.507	0.197	NC	NC	8.948	0.092	1.189	0.143
	Endo-1	−7.89	0.32	8.813	0.157	0.239	0.217	NC	NC	8.516	0.107	0.756	0.153
	Endo-2	−7.85	0.29	8.309	0.221	−0.266	0.267	NC	NC	8.328	0.153	0.569	0.188
	Met-enk	−7.56	0.36	8.781	0.153	0.207	0.214	−7.21	0.32	8.001†	0.151	0.242	0.187
	Met-enk-RF	NC	NC	8.448	0.200	−0.127	0.250	−6.78	0.33	7.543†	0.138	−0.217	0.176
	α-Neo	−6.58	0.32	7.238	0.201	−1.336	0.251	−6.79	0.30	7.767†	0.140	0.007	0.178
$G_{\alpha i2}$	DAMGO	−7.01	0.36	7.908	0.138	0.000	0.195	−6.74	0.40	7.619	0.120	0.000	0.170
	Morphine	−6.57	0.31	7.396	0.149	−0.512	0.203	NC	NC	7.293	0.112	−0.326	0.164
	Loperamide	NC	NC	9.147	0.113	1.239	0.178	NC	NC	8.816	0.096	1.198	0.154
	Endo-1	−7.89	0.28	8.790	0.115	0.883	0.179	−7.85	0.28	8.599	0.135	0.980	0.181
	Endo-2	−7.91	0.22	8.424	0.156	0.516	0.208	−7.74	0.28	8.428	0.171	0.809	0.209
	Met-enk	NC	NC	8.368	0.119	0.460	0.182	NC	NC	8.517	0.133	0.898	0.179
	Met-enk-RF	−7.38	0.31	8.178	0.153	0.270	0.206	−7.08	0.31	7.589†	0.171	−0.030	0.209
	α-Neo	−7.19	0.26	7.734	0.177	−0.174	0.224	−6.75	0.33	7.226†	0.218	−0.392	0.249
$G_{\alpha i3}$	DAMGO	NC	NC	8.006	0.128	0.000	0.181	−7.30	0.33	7.970	0.167	0.000	0.237
	Morphine	−7.15	0.36	8.021	0.192	0.015	0.231	−7.22	0.27	7.627	0.196	−0.343	0.258
	Loperamide	NC	NC	9.107	0.132	1.102	0.184	NC	NC	8.969	0.132	0.999	0.213
	Endo-1	NC	NC	8.746	0.131	0.741	0.183	−7.65	0.29	8.224	0.157	0.254	0.230
	Endo-2	−8.31	0.27	8.952	0.181	0.946	0.222	−8.08	0.34	8.369†	0.278	0.399	0.324
	Met-enk	NC	NC	8.354	0.161	0.348	0.206	−7.47	0.35	8.107	0.193	0.137	0.255
	Met-enk-RF	−7.76	0.39	8.564	0.205	0.559	0.242	−7.30	0.39	7.835†	0.218	−0.135	0.275
	α-Neo	−6.86	0.33	7.593	0.184	−0.413	0.225	−7.35	0.31	7.691	0.235	−0.279	0.289
$G_{\alpha ob}$	DAMGO	NC	NC	8.037	0.128	0.000	0.181	−6.94	0.38	8.099	0.145	0.000	0.204
	Morphine	NC	NC	7.546	0.179	−0.491	0.220	−6.73	0.29	7.460	0.185	−0.639	0.235
	Loperamide	NC	NC	8.946	0.126	0.910	0.180	NC	NC	8.959	0.140	0.860	0.201
	Endo-1	NC	NC	8.626	0.134	0.590	0.186	−7.47	0.28	8.300	0.152	0.201	0.209
	Endo-2	NC	NC	8.584	0.147	0.547	0.195	−7.85	0.23	8.423	0.179	0.324	0.230
	Met-enk	NC	NC	8.508	0.139	0.471	0.189	−7.62	0.27	8.525	0.160	0.426	0.216
	Met-enk-RF	NC	NC	8.289	0.182	0.252	0.223	−7.00	0.32	7.905	0.149	−0.194	0.208
	α-Neo	NC	NC	7.622	0.145	−0.415	0.193	−6.77	0.26	7.542	0.169	−0.557	0.223

		$G_{\alpha i1}$–$G_{\alpha i2}$		$G_{\alpha i1}$–$G_{\alpha i3}$		$G_{\alpha i1}$–$G_{\alpha ob}$		$G_{\alpha i2}$–$G_{\alpha i3}$		$G_{\alpha i2}$–$G_{\alpha ob}$		$G_{\alpha i3}$–$G_{\alpha ob}$	
		$\Delta\Delta$Logτ/K_A	SEM	$\Delta\Delta$Logτ/K_A	SEM	$\Delta\Delta$Logτ/K_A	SEM	$\Delta\Delta$Logτ/K_A	SEM	$\Delta\Delta$Logτ/K_A	SEM	$\Delta\Delta$Logτ/K_A	SEM
5mins	DAMGO	0.000	0.288	0	0.279	0.000	0.279	0.000	0.266	0.000	0.266	0.000	0.256
	Morphine	−0.377	0.293	−0.904	0.313	−0.398	0.305	−0.527	0.307	−0.021	0.299	0.506	0.319
	Loperamide	−0.732	0.266	−0.594	0.270	−0.402	0.267	0.138	0.256	0.330	0.253	0.192	0.257
	Endo-1	−0.644	0.282	−0.109	0.284	−0.351	0.286	0.535	0.274	0.293	0.258	−0.242	0.261
	Endo-2	−0.782	0.338	−0.824	0.347	−0.813	0.330	−0.043	0.317	−0.031	0.285	0.012	0.295
	Met-enk	−0.254	0.281	−0.534	0.297	−0.264	0.286	−0.280	0.256	−0.011	0.262	0.270	0.279
	Met-enk-RF	−0.397	0.323	−1.073*	0.347	−0.379	0.335	−0.676	0.304	0.018	0.303	0.694	0.329
	α-Neo	−1.162**	0.337	−0.923	0.337	−0.921*	0.317	0.239	0.317	0.241	0.296	0.002	0.296
60mins	DAMGO	0.000	0.230	0.000	0.283	0.000	0.257	0.000	0.292	0.000	0.266	0.000	0.313
	Morphine	0.011	0.252	0.028	0.321	0.324	0.303	0.017	0.306	0.313	0.287	0.296	0.349
	Loperamide	−0.009	0.210	0.190	0.257	0.329	0.247	0.199	0.263	0.338	0.253	0.139	0.293
	Endo-1	−0.224	0.237	0.502	0.276	0.555	0.260	0.726	0.292	0.779	0.277	0.053	0.311
	Endo-2	−0.241	0.281	0.169	0.375	0.245	0.297	0.410	0.386	0.485	0.311	0.076	0.397
	Met-enk	−0.657	0.259	0.104	0.316	−0.184	0.285	0.761	0.312	0.473	0.280	−0.288	0.334
	Met-enk-RF	−0.187	0.273	−0.082	0.327	−0.023	0.272	0.105	0.345	0.164	0.295	0.059	0.344
	α-Neo	0.400	0.306	0.286	0.339	0.564	0.285	−0.114	0.381	0.164	0.334	0.278	0.364

*$p \leqslant 0.05$ **$p \leqslant 0.005$, different from DAMGO as determined by ANOVA with Dunnett's multiple comparison test. †$p \leqslant 0.05$ as determined by two-tailed t-test compared to same ligand at 5min. NC: not calculated due to full agonism.

Despite this, calculation of bias factors between cAMP and β-arr1 and β-arr2 in CHO-MOP-GRK2 cells showed that the bias of most ligands in these cells was similar to the bias they showed in CHO-MOP cells (Fig. 3e–f, Table 2). The only exception was endo-1, which showed a significant reduction in the bias between cAMP and β-arr1 in the CHO-MOP-GRK2 cells (Fig. 3e). This means that overexpression of GRK2 caused a greater reduction in the inhibition of cAMP induced by endo-1 than expected. This could, in part, be due to the enhanced recruitment of β-arr1 detected upon GRK2 overexpression.

3.3. The differential kinetics of adenylyl cyclase inhibition by opioids changes bias

Most quantifications of biased agonism are calculated at a single time point for each signalling pathway which usually corresponds to the maximum activation of that pathway, or when the signal reaches a steady state. As such, this time point can significantly vary across different signalling pathways. However, it is now apparent that ligands can elicit differential kinetics of activation and deactivation of each signalling pathway. MOP activation

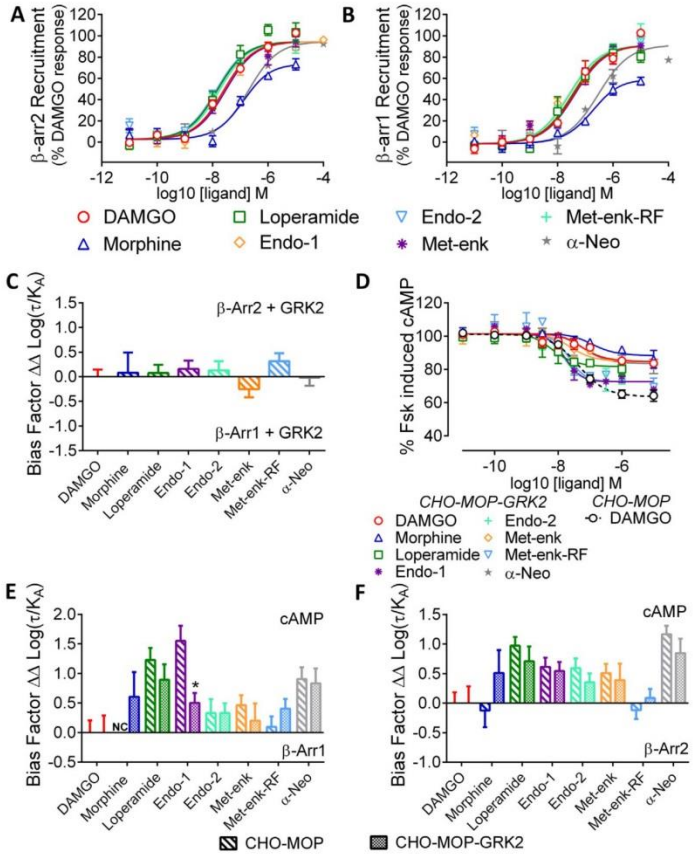

Fig. 3. Overexpression of GRK2 changes bias between recruitment of β-arrestins and AC inhibition. Recruitment of (a) β-arr2 and (b) β-arr1 in FlpIn CHO-MOP-GRK2 cells. Data normalised to the 10 μM DAMGO response and expressed as mean ± SEM of at least 3 separate experiments. (c) Bias factors between recruitment of β-arr1 and β-arr2 in CHO-MOP-GRK2 cells. (d) Inhibition of fsk- induced cAMP in FlpIn CHO-MOP-GRK2 cells. Data expressed as the % fsk-induced cAMP response in the absence of agonist, and expressed as mean ± SEM of 2-3 separate experiments. Bias factors between cAMP and (e) β-arr1 and (f) β-arr2 in CHO-MOP [6] and CHO-MOP-GRK2 cells. $^{*}p \leqslant 0.05$, as determined by a one-way ANOVA with Dunnett's multiple comparison test compared to bias factor for same ligand in CHO-MOP. NC = not calculable.

results in inhibition of AC, which is detectable within minutes, and is also known to produce prolonged inhibition of AC [44,45]. Inhibition of cAMP production is usually measured using accumulation assays, requiring long incubation times, up to 60 min, thereby detecting both acute and prolonged signalling. However, the kinetics of AC inhibition over this time period may vary significantly for different agonists, which means bias between cAMP and other signalling pathways can also change over time. To test this we examined the inhibition of AC using the CAMYEL BRET biosensor for 30 min. An initial experiment using EC_{50} concentrations of the ligands (as determined previously [6]) showed that most ligands inhibit cAMP production with a similar profile to that of DAMGO, where maximum cAMP inhibition is reached between 5 and 10 min after forskolin (fsk) addition, and remains constant for up to 30 min (Fig. 4a). However, we observed that whilst Met-enk-RF also reached maximum cAMP inhibition between 5 and 10 min, by 30 min such inhibition was no longer detected (Fig. 4a). This effect was not due to degradation of the peptide, as protease inhibitors used in all experiments (see Materials and Methods) provided adequate protection from proteases, and the same effect was observed in the presence of a protease inhibitor cocktail (Fig. 4b).

We then examined the cAMP inhibition kinetics for Met-enk-RF, DAMGO, loperamide and endo-1 at a full range of concentrations (Fig. 4c–f). DAMGO, loperamide and endo-1 showed the same cAMP kinetic profiles regardless of concentration, they all reached their maximum signal at 5 min and remained constant for the duration of the experiment. However, Met-enk-RF only displayed this profile at the highest concentrations tested (1–10 μM), and at lower concentrations the AC inhibition was gradually lost over time. This difference in the kinetics of inhibition of cAMP production could impact the quantification of bias between AC inhibition and other signalling pathways, especially if cAMP production is measured at different times and/or by different methods. We plotted concentration response curves using the BRET values obtained at 5 min and 30 min, and quantified bias between these two time points (Fig. 4g and h). As expected from its observed kinetic profile, Met-enk-RF demonstrated relatively greater efficacy for inhibition of cAMP production at 5 min versus 30 min that led to altered bias with respect to DAMGO for this pathway across the two time

Table 2
Quantification of biased agonism upon overexpression of GRK2. Transduction coefficients [Log(τ/K_A)], normalised transduction coefficients [ΔLog(τ/K_A)] and Log(bias factors) [$\Delta\Delta$Log(τ/K_A)]. Values represent mean ± SEM of three to five independent experiments.

	β-Arr1 + GRK2				β-Arr2 + GRK2				cAMP + GRK2			
	Log τ/K_A	SEM	Δlog τ/K_A	SEM	Log τ/K_A	SEM	Δlog τ/K_A	SEM	Log τ/K_A	SEM	Δlog τ/K_A	SEM
DAMGO	7.410	0.113	0.000	0.160	7.599	0.097	0.000	0.137	7.309	0.267	0.000	0.377
Morphine	6.437	0.205	−0.973	0.234	6.721	0.131	−0.878	0.163	6.943	0.363	−0.366	0.450
Loperamide	7.458	0.128	0.048	0.171	7.831	0.096	0.232	0.137	8.251	0.227	0.942	0.351
Endo-1	7.381	0.128	−0.029	0.170	7.529	0.111	−0.070	0.147	7.783	0.105	0.474	0.287
Endo-2	7.587	0.128	0.177	0.171	7.755	0.110	0.156	0.146	7.818	0.105	0.509	0.287
Met-enk	7.564	0.128	0.154	0.171	7.564	0.097	−0.035	0.137	7.664	0.262	0.355	0.374
Met-enk-RF	7.370	0.128	−0.040	0.170	7.875	0.109	0.276	0.146	7.674	0.105	0.365	0.287
α-Neo	6.530	0.128	−0.880	0.171	6.703	0.110	−0.896	0.147	7.263	0.215	−0.047	0.343

	β-Arr2 + GRK2 − β-Arr1 + GRK2		cAMP + GRK2 − β-Arr1 + GRK2		cAMP + GRK2 − β-Arr2 + GRK2	
	$\Delta\Delta$Log τ/K_A	SEM	$\Delta\Delta$Log τ/K_A	SEM	$\Delta\Delta$Log τ/K_A	SEM
DAMGO	0.000	0.211	0.000	0.410	0.000	0.402
Morphine	0.095	0.285	0.607	0.508	0.512	0.479
Loperamide	0.184	0.218	0.894	0.390	0.710	0.376
Endo-1	−0.041	0.225	0.503	0.334	0.544	0.322
Endo-2	−0.021	0.225	0.332	0.334	0.353	0.322
Met-enk	−0.189	0.219	0.201	0.411	0.390	0.399
Met-enk-RF	0.316	0.224	0.405	0.334	0.089	0.322
α-Neo	−0.016	0.225	0.833	0.383	0.849	0.373

	β-Arr1 + GRK2				β-Arr2 + GRK2				cAMP + GRK2			
	Log EC50	SEM	Emax	SEM	Log EC50	SEM	Emax	SEM	Log EC50	SEM	Emax	SEM
DAMGO	−7.39	0.12	93.3	4.2	−7.59	0.09	95.4	2.9	−7.00	0.24	16.2	1.8
Morphine	−6.73	0.16	58.4	4.0	−6.92	0.13	72.4	3.8	−6.73	0.28	12.5	1.8
Loperamide	−7.73	0.16	81.3	4.5	−7.73	0.12	103.6	4.0	−7.92	0.32	19.6	2.8
Endo-1	−7.34	0.14	88.3	4.3	−7.65	0.13	88.0	3.8	−7.88	0.13	29.7	1.6
Endo-2	−7.54	0.17	93.0	5.4	−7.81	0.08	88.1	2.2	−7.86	0.18	28.9	2.1
Met-enk	−7.77	0.16	78.5	3.9	−7.78	0.11	87.9	3.3	−7.19	0.31	16.8	2.3
Met-enk-RF	−7.30	0.13	93.5	4.3	−7.90	0.12	88.9	3.1	−7.80	0.23	27.0	2.9
α-Neo	−6.63	0.15	86.5	5.2	−6.74	0.11	88.7	3.4	−7.20	0.26	16.9	2.2

points. Consequently, the bias of Met-enk-RF, but not the other ligands, will change when quantifying bias between cAMP and other signalling pathways, depending on the time point chosen to measure cAMP inhibition.

3.4. Differential G protein desensitisation alters bias

Since the kinetics of a G protein-mediated signalling pathway are ligand dependent, it follows that G protein activation kinetics may also be ligand dependent. It is also well established that neither the initial level of G protein activation, nor the level of desensitisation of G protein-mediated signalling of MOP correlate with the level β-arrestin recruitment and receptor internalisation [31]. Therefore, quantifying bias between acute G protein activation and receptor regulatory events reveals only limited information about the differential desensitisation mechanisms initiated by different ligands. Alternatively, quantifying bias between G protein activation and regulatory events at the same time point can reveal ligands that have divergent mechanisms of receptor regulation. Additionally, the divergent mechanisms of receptor desensitisation and regulation initiated by different ligands can potentially have differential effects on G_α subtypes thereby altering bias between various G_α subtypes at different time points. To examine this, the G protein activation assay described above was repeated after 60 min of agonist stimulation (Fig. 5). As expected, most ligands stimulated less G_α subunit activation at 60 min compared to 5 min, which is apparent in the reduction of log(τ/K_A) values at 60 min (Table 1), however only small changes were observed with $G_{\alpha ob}$. Interestingly, the greatest reductions in relative efficacy between 5 and 60 min for all G_α subunits were observed for Met-enk-RF. This enhanced desensitisation of Met-enk-RF induced G_α subunit activation is in line with the increased desensitisation of the inhibition of cAMP production observed at later time points (Fig. 4g). DAMGO and Met-enk also showed a significant reduction in activation of $G_{\alpha i1}$ at 60 min, whereas α-neo surprisingly showed an increase in activation of $G_{\alpha i1}$. Calculation of bias factors between each G protein at 60 min showed that α-neo and Met-enk-RF were no longer biased between $G_{\alpha i1}$ and $G_{\alpha i2}$, $G_{\alpha i3}$ or $G_{\alpha ob}$. (Fig. 6, Table 1). Together these results show the variability in the level of desensitisation of different G_α subunits by different ligands.

Next we examined the effect of G protein desensitisation on bias between G protein activation and receptor trafficking. Previously, we measured MOP trafficking at 60 min using a BRET assay to measure the reduction in MOP proximity to the membrane marker KRas, which revealed that endo-1, endo-2 and α-neo were all biased towards the acute inhibition of cAMP production (at 10 min) over MOP trafficking at 60 min [6]. In order to identify whether these ligands are still G protein biased after desensitisation of G protein activation, we quantified bias between G protein activation and receptor trafficking when both pathways were measured at 60 min. Endo-1, and Met-enk showed bias towards activation of $G_{\alpha i2}$ over receptor trafficking (Fig. 6e). Surprisingly, Met-enk-RF, which showed the greatest reductions in G protein activation at 60 min, also stimulated very little receptor trafficking, as a result a bias factor could not be quantified. This may suggest that desensitisation and trafficking induced by Met-enk-RF are completely independent mechanisms. Alternatively, the rapid desensitisation of cAMP inhibition by Met-enk-RF observed at 30 min (Fig. 4d), suggests that the kinetics of receptor trafficking induced by Met-enk-RF may also be more rapid than for the other ligands, and no longer detectable at 60 min due to rapid receptor recycling. Altogether, quantifying bias between the G protein activation and receptor trafficking at the same time point has revealed ligands that may have differential desensitisation mechanisms or kinetics.

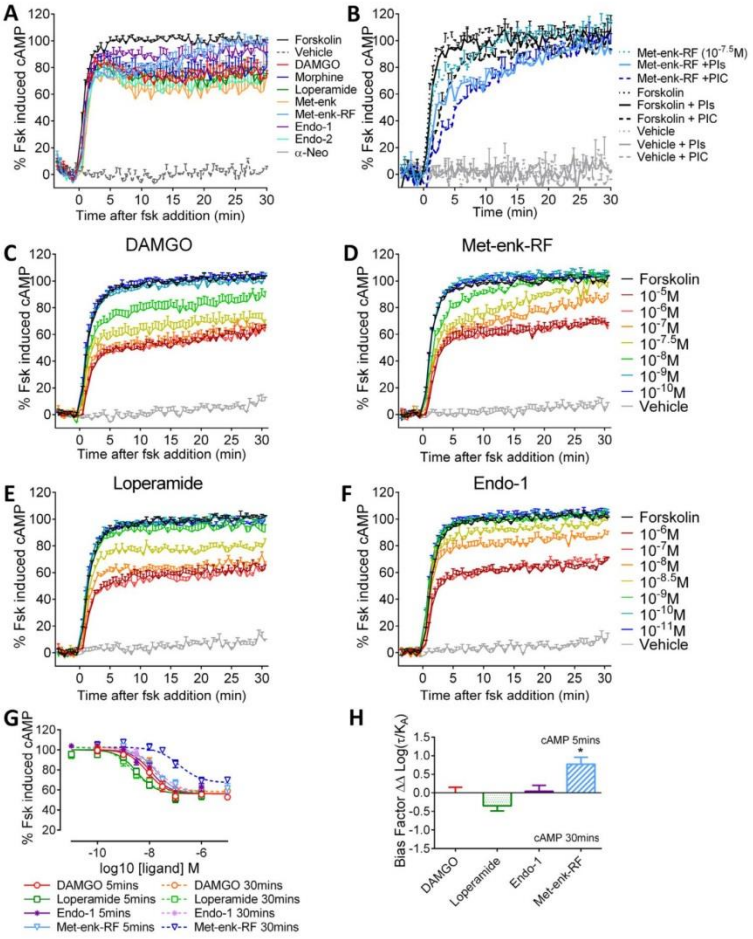

Fig. 4. Kinetics of AC inhibition. (a–f) Kinetic profiles of agonist-induced inhibition of fsk-induced cAMP production in FlpIn CHO-MOP up to 30 min after fsk addition. (a) Kinetic traces of ligands at EC_{50} concentrations, (b) Met-enk-RF kinetic profile of AC inhibition in the presence of protease inhibitor mix (PIs; 1 μM captopril, 1 μM phosphoramidon, 1 μM amastatin, 1 μM actinonin and 1 μM Diprotin A) or protease inhibitor cocktail (PIC, from Sigma Aldrich). (c–f) Kinetic profile of AC inhibition by increasing concentrations of DAMGO (c), Met-enk-RF (d), Loperamide (e) or endo-1 (f). Data expressed as the %fsk induced cAMP response (mean fsk response between 10 and 30 min) in the absence of agonist, and expressed as mean ± SEM of 3 separate experiments. (g) Concentration response curves of inhibition of fsk-induced cAMP production at 5 min and 30 min post fsk addition constructed from kinetic profiles. (h) Bias factors between inhibition of fsk-induced cAMP production at 5 min and 30 min. $^{*}p \leqslant 0.05$, as determined by a one-way ANOVA with Dunnett's multiple comparison test compared to DAMGO.

3.5. Impact of cell background in determinations of biased agonism at MOP

We next investigated whether the biased agonism detected in CHO FlpIn hMOP cells was retained at the mMOP, and whether such biased agonism changes in a different cell background, where different endpoints and assay conditions may be necessary to obtain robust signals. For this we determined comprehensive biased agonism profiles for the same eight ligands in AtT20 mouse pituitary tumour cells stably expressing mMOP.

We first quantified bias between inhibition of AC and recruitment of β-arr1 and β-arr2. β-arr1 and β-arr2 recruitment was measured using BRET in cells co-transfected with GRK2 (Fig. 7a and b), as β-arrestin recruitment in AtT20-mMOP cells was barely detectable in the absence of this kinase. Loperamide, endo-1, endo-2 and α-neo stimulated less β-arr1 recruitment compared to DAMGO and the other ligands (75–85%). Morphine only stimulated 39.9% of DAMGO induced β-arr1 recruitment. All ligands stimulated a similar level of β-arr2 recruitment as DAMGO, except α-neo and morphine, which only stimulated 81% and 62%, respectively. In agreement with the bias profiles obtained in CHO MOP cells overexpressing GRK2, no ligands were biased between the two β-arrestins (Fig. 7c, Table 3).

Inhibition of cAMP production was measured using the CAMYEL BRET-based biosensor (Fig. 7d), without additional co-transfection of GRK2 as this would compromise the cAMP response as shown in the CHO cells. All ligands produced between 55% and 65% inhibition of forskolin-induced cAMP production. Our previous study in CHO–hMOP cells showed that endo-1 was biased towards cAMP over recruitment of β-arr1, whilst loperamide and α-neo were biased towards cAMP over β-arr1 and β-arr2 when compared to the reference ligand DAMGO [6]. In contrast, in AtT20-mMOP cells,

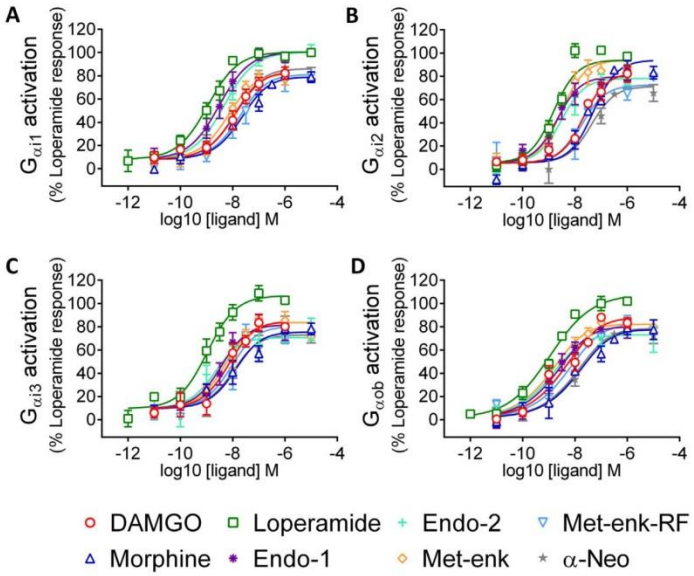

Fig. 5. Activation of $G_{\alpha i/o}$ subunits by MOP agonists at 60min. Activation of (a) $G_{\alpha i1}$, (b) $G_{\alpha i2}$, (c) $G_{\alpha i3}$ and (d) $G_{\alpha ob}$ in FlpIn CHO cells after 60 min agonist stimulation. Data normalised to the 1 μM Loperamide response. Data expressed as mean ± SEM of at least 3 separate experiments.

no ligands showed significant bias towards cAMP over β-arr1 or β-arr2 (Fig. 7e and f, Table 3). This may be due, in part, to the fact that GRK2 needed to be overexpressed in β-arrestin recruitment assays but not the cAMP assays. Moreover, in AtT20 cells and relative to DAMGO, loperamide, endo-1 and α-neo are less efficacious at inhibiting cAMP production than in CHO cells (which is apparent when comparing the $\Delta\log(\tau/K_A)$ values for the cAMP assays between these cell lines). Such changes in efficacy, thus, may explain the loss of bias towards cAMP of these ligands in AtT20 cells.

FLAG-MOP internalisation after 30 min of agonist exposure was measured using anti-FLAG ELISA. All ligands, except morphine, induced a reduction MOP at the cell surface after 30 min in AtT20 cells (Fig. 8a). Bias factors were calculated between internalisation and inhibition of cAMP production, β-arr1 and β-arr2 (Fig. 8b and c, Table 3). Loperamide, Met-enk and Met-enk-RF all showed significant bias towards receptor internalisation over inhibition of cAMP, β-arr1 and β-arr2. This is in contrast to our previous results in CHO-MOR cells where these ligands showed no bias towards receptor trafficking. The bias towards internalisation of Met-enk-RF is particularly surprising, since Met-enk-RF stimulated very little receptor trafficking in CHO-MOP cells. However, this result is difficult to interpret as this discrepancy may be due to the use of different methods (membrane localisation vs ELISA) or time points in the two cells types.

We next examined the bias between activation of two canonical G protein-mediated signalling pathways; inhibition of cAMP production (predominantly $G_{\alpha i/o}$-mediated) and cell hyperpolarisation (predominantly $G_{\beta\gamma}$-mediated) [46]. Hyperpolarisation in AtT20-mMOR cells was measured using the FLIPR membrane potential assay [47]. Opioids hyperpolarise AtT20 cells primarily through G protein mediated activation of G protein-gated inwardly rectifying K^+ channels (GIRKs). In agreement with this, all ligands stimulated AtT20-mMOR hyperpolarisation (Fig. 8d and e). Quantification of bias factors between hyperpolarisation (ΔMP) and inhibition of cAMP production showed that no ligands were significantly biased between these two signalling pathways compared to DAMGO (Fig. 8f, Table 3). In agreement with this, the bias between receptor internalisation and ΔMP was very similar to bias between internalisation and cAMP (Table 3), with loperamide and Met-enk being significantly biased towards internalisation. The only exception was Met-enk-RF, which was no longer significantly biased towards internalisation when compared to ΔMP.

Finally, we assessed whether biased agonism between hyperpolarisation and β-arr1or β-arr2 recruitment also reflected the results obtained when using inhibition of cAMP as a G protein-mediated pathway (Fig. 7e and f, Fig. 8g and Table 3). Interestingly, Met-enk was biased towards cell hyperpolarisation (Fig. 8g and Table 3).

3.6. Ligand clustering by biased agonism profiles in AtT20 cells

As shown above, quantification of bias in different cell lines requires the use of different assay conditions and signalling endpoints. Thus, directly comparing individual bias factors between two pathways obtained in two different cell lines can be difficult to interpret. For this reason, an overall bias profile of the ligands across all of the signalling pathways can provide information about ligand clustering and, consequently allow the comparison of different clusters across cell lines. To obtain an overall picture of the bias profiles of the ligands in AtT20-mMOP cells we constructed webs of bias. For this, the bias factors between ΔMP and all of the other signalling pathways were calculated ($\Delta\Delta\tau/K_A$) and plotted on a single multiaxial graph (Fig. 9a). This shows that all ligands (morphine, loperamide, α-neo, Met-enk-RF and Met-enk) are biased compared to DAMGO at one or more signalling pathways, and that no ligands under study show the same pattern of bias as one another. Importantly, these results also highlight that, although the absolute bias of each ligand between individual signalling pathways has changed compared to the bias that we had previously determined in CHO cells [6], ligands that displayed bias still do so across all cell backgrounds.

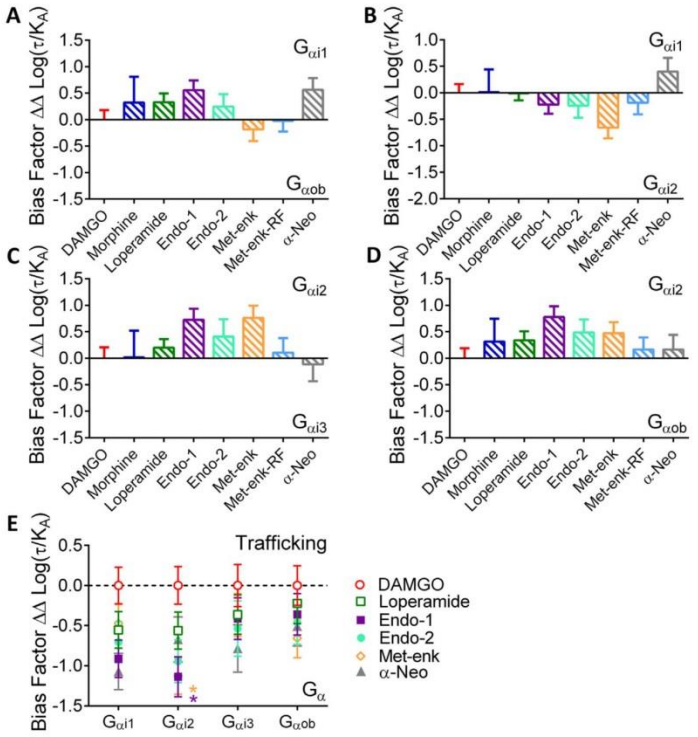

Fig. 6. Quantification of biased agonism of MOP agonists between activation of different $G_{\alpha i/o}$ subunits at 60 min. (a–d) Bias factors for all agonists between activation of $G_{\alpha i1}$, $G_{\alpha i2}$, $G_{\alpha i3}$ and $G_{\alpha ob}$ after 60 min agonist stimulation (Table 1). (e) Bias factors between MOP trafficking measured using BRET between MOP-Rluc and KRas-Venus [6] and activation of $G_{\alpha i1}$, $G_{\alpha i2}$, $G_{\alpha i3}$ and $G_{\alpha ob}$ after 60 min agonist stimulation. Data expressed as mean ± SEM of at least 3 separate experiments.

The overall bias profile of a ligand can also be visualised using Principal Component Analysis (PCA). PCA identifies which bias factors are correlated with one another, and collectively contribute the greatest variation in bias between the ligands, called principal components. PCA of all the bias factors revealed that the bias between receptor internalisation and recruitment of β-arr1 and β-arr2 contributes the greatest variability in bias between all the ligands, contributing to 54% of the overall observed bias. Bias between G protein-mediated signalling and β-arrestin recruitment and internalisation only contributed to ~ 37% of the observed bias. When these principal components are plotted against one another ligands with similar bias will cluster together (Fig. 9b). PCA analysis of our data in AtT20 cells showed that loperamide, Met-enk and Met-enk-RF are separated from DAMGO, and hence have unique patterns of bias, whereas endo-1, endo-2 and α-neo cluster more closely to DAMGO. These results are in contrast to our previous data in CHO cells, where endo-1 and α-neo did not cluster with DAMGO, whilst Met-enk did. This illustrates that biased agonism profiles have not changed uniformly across the group of ligands, but, rather, that the impact of cell background on bias determinations is different for each agonist.

4. Discussion

In the present study we have extended our determinations of biased agonism at MOP to systematically assess the impact of differential cellular protein complement, signalling kinetics and receptor species. Examination of biased agonism at MOP across multiple different signalling pathways in two different cell backgrounds, one expressing hMOP and the other mMOP, has shown that although the biased agonism profiles of most ligands changed between the different cell types, ligands that displayed distinct bias profiles were still unique across different cell backgrounds. Specifically, we show that despite changes in directions of bias and overall signalling profiles, ligands that displayed unique bias profiles relative to DAMGO at MOP in CHO cells (e.g. endo-1, met-enk-RF and α-neo) still displayed unique bias fingerprints, when evaluated in a different cell background [6]. Our previous study in CHO cells showed that ligands such as loperamide, endo-1, Met-enk-RF and α-neo displayed signalling profiles different to that of DAMGO. In the present study, such ligands still generate signalling profiles that are different from the same reference agonist. This is illustrated by the individual bias factors across different pathways (Figs. 2, 3, 6 and 8) as well as by the web of bias presented in Fig. 9 (and compared to that of [6]).

However, our results also demonstrate that the direction of bias (i.e. towards different signalling endpoints) can change across different cell lines, as can the clustering of these ligands based on these bias profiles. Therefore, at least for this example, whilst biased agonism is maintained across different cell lines, the *directionality* of this bias appears to be context dependent. Thus an 'absolute' ascription of directionality to bias, such as labelling a ligand as 'G protein biased', may be an inadequate description of its action unless this description is qualified with the context of experimental conditions and cell background. Thus, our results also highlight the importance of the experimental conditions used for the

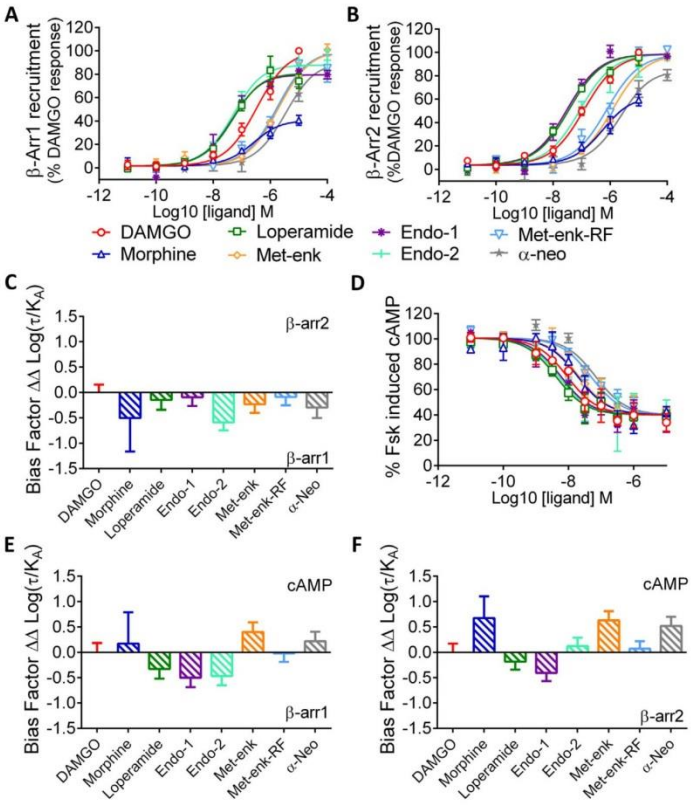

Fig. 7. Bias between AC inhibition and recruitment of β-arrestins is cell dependent. Recruitment of (a) β-arr1 and (b) β-arr2 in AtT20-mMOP-GRK2 cells. Data normalised to the 10 μM DAMGO response and expressed as mean ± SEM of 3 separate experiments. (c) Bias factors for all agonists between β-arr1 and β-arr2 (Table 3). (d) Inhibition of fsk-induced cAMP in AtT20-mMOP cells. Data expressed as the %fsk-induced cAMP response in the absence of agonist, and expressed as mean ± SEM of at least 3 separate experiments. Bias factors for all agonists between cAMP and (e) β-arr1 and (f) β-arr2 in AtT20 cells is shown in Table 3.

measurement of activation of various signalling pathways, and show that these conditions need to be carefully and systematically determined when reporting biased agonism at GPCRs.

We illustrate how biased agonism is influenced by the cellular protein complement by altering the expression of receptor kinases involved in the regulation of MOP. The bias of endo-1 between inhibition of cAMP and β-arr1/2 recruitment changed when the levels of GRK2 expression were increased in CHO cells. In addition to this, α-neo and Met-enk-RF showed bias compared to DAMGO between activation of different $G_{\alpha i/o}$ subunits, indicating that the overall level of G protein activation, and consequently bias between G protein-mediated signalling and other signalling pathways may change depending on the G protein subunit content in a particular cell type. This shows that changes in the expression of a single protein can change the relative bias of a set of ligands, hence the direction of biased agonism can change in different cell types. Notably, changes in proteins other than intracellular signalling effectors can also determine changes in biased agonism. For instance, opioid receptors and other GPCRs have been shown to form homo- or heterodimers. It is therefore possible that the formation of oligomeric structures in specific cell types, could lead to differences in the observed biased agonism.

The temporal dependence of biased agonism is demonstrated by the unusually rapid desensitisation of cAMP inhibition induced by Met-enk-RF. Whilst the different cAMP kinetic profile may not directly result in significantly different physiological effects, the differential kinetics may be an indicator of differential activation of other signalling pathways that will produce distinctive physiological effects. There are numerous factors that could contribute to the altered cAMP kinetics of Met-enk-RF. Different signalling kinetics could result from differing association and dissociation rates of the ligand (which is currently unexplored at MOP) or from unique conformations of the receptor induced by the ligand which possess altered receptor-effector activation dynamics. As mentioned earlier, differential receptor trafficking may also alter the cAMP kinetic profile. Indeed, receptor endocytosis has been shown to affect the initial cAMP inhibition kinetics at DOP [48]. Another factor that can affect the kinetic profile of cAMP signalling is the activation of other signalling effectors that regulate or desensitise cAMP signalling. Such signalling effectors include Ca^{2+}, PKC and several other kinases [29]. Differential activation of these signalling pathways by Met-enk-RF has not been examined to date, however Ca^{2+} mobilisation and PKC activation have been shown to be differentially activated by MOP ligands [49,50]. In addition to this, cAMP

Table 3
Quantification of biased agonism in AtT20-mMOP cells. Transduction coefficients [Log(τ/K_A)], normalised transduction coefficients [ΔLog(τ/K_A)] and Log(bias factors) [$\Delta\Delta$Log(τ/K_A)]. Values represent mean ± SEM of three to five independent experiments.

	cAMP				Membrane potential				β-Arr1				β-Arr2				Internalisation			
	Log τ/K_A	SEM	$\Delta\Delta$log τ/K_A	SEM	Log τ/K_A	SEM	Δlog τ/K_A	SEM	Log τ/K_A	SEM	Δlog τ/K_A	SEM	Log τ/K_A	SEM	$\Delta\Delta$log τ/K_A	SEM	Log τ/K_A	SEM	Δlog τ/K_A	SEM
DAMGO	8.041	0.139	0.000	0.197	8.282	0.086	0.000	0.121	6.475	0.120	0.000	0.170	6.912	0.100	0.000	0.142	5.106	0.130	0.000	0.000
Morphine	7.718	0.145	−0.323	0.201	7.806	0.086	−0.476	0.122	5.979	0.326	−0.495	0.347	5.914	0.201	−0.998	0.225	NC	NC	NC	NC
Loperamide	8.385	0.109	0.344	0.176	8.165	0.100	−0.117	0.132	7.149	0.156	0.674	0.196	7.439	0.115	0.527	0.152	6.864	0.135	1.758	1.758
Endo-1	8.232	0.121	0.192	0.184	8.334	0.096	0.052	0.129	7.168	0.138	0.693	0.183	7.511	0.101	0.599	0.143	5.675	0.128	0.570	0.570
Endo-2	8.299	0.134	0.259	0.193	8.342	0.085	0.060	0.121	7.201	0.124	0.726	0.172	7.049	0.101	0.137	0.142	5.584	0.103	0.479	0.479
Met-enk	7.676	0.139	−0.365	0.196	8.135	0.099	−0.147	0.131	5.709	0.132	−0.766	0.178	5.916	0.114	−0.996	0.152	5.592	0.099	0.487	0.487
Met-enk-RF	7.316	0.110	−0.725	0.177	8.134	0.132	−0.148	0.157	5.768	0.132	−0.707	0.178	6.117	0.100	−0.795	0.142	5.388	0.099	0.283	0.283
α-Neo	7.172	0.117	−0.869	0.182	7.265	0.073	−1.017	0.113	5.387	0.149	−1.087	0.191	5.526	0.142	−1.387	0.174	4.505	0.121	−0.601	−0.601

	MP-cAMP		cAMP − β-Arr1		cAMP − β-Arr2		cAMP − Int		MP − β-Arr1		MP − β-Arr2		MP − Int		β-Arr2 − β-Arr1		Int − β-Arr1		Int − β-Arr2	
	$\Delta\Delta$Log τ/K_A		$\Delta\Delta$Log τ/K_A	SEM	$\Delta\Delta$Log τ/K_A	SEM	$\Delta\Delta$Log τ/K_A	SEM	$\Delta\Delta$Log τ/K_A	SEM	$\Delta\Delta$Log τ/K_A	SEM	$\Delta\Delta$Log τ/K_A	SEM	$\Delta\Delta$Log τ/K_A	SEM	$\Delta\Delta$Log τ/K_A	SEM	$\Delta\Delta$Log τ/K_A	SEM
DAMGO	0.000	0.231	0.000	0.260	0.000	0.243	0.000	0.197	0.000	0.209	0.000	0.187	0.000	0.121	0.000	0.221	0.000	0.170	0.000	0.142
Morphine	−0.153	0.235	0.172	0.401	0.675	0.301	NC	NC	0.020	0.368	0.522	0.256	NC	NC	−0.503	0.414	NC	NC	NC	NC
Loperamide	−0.4614	0.220	−0.330	0.264	−0.183	0.233	−1.414***	1.767	−0.791	0.237	−0.644	0.202	−1.875***	1.763	−0.147	0.249	1.084**	1.769	1.231***	1.765
Endo-1	−0.140	0.225	−0.502	0.260	−0.407	0.233	−0.3781	0.599	−0.642	0.224	−0.547	0.192	−0.518	0.584	−0.094	0.232	−0.124	0.598	−0.029	0.587
Endo-2	−0.199	0.228	−0.467	0.259	0.122	0.240	−0.2198	0.516	−0.666	0.211	−0.077	0.187	−0.419	0.494	−0.589	0.223	−0.248	0.509	0.342	0.499
Met-enk	0.218	0.236	0.401	0.265	0.631	0.248	−0.852*	0.525	0.618	0.221	0.849**	0.200	−0.633*	0.504	−0.230	0.234	1.252**	0.518	1.482***	0.510
Met-enk-RF	0.577	0.237	−0.018	0.251	0.070	0.227	−1.007**	0.333	0.559	0.238	0.648	0.212	−0.430	0.323	−0.089	0.228	0.989**	0.334	1.078**	0.316
α-Neo	−0.148	0.214	0.218	0.263	0.518	0.251	−0.268	0.628	0.070	0.222	0.370	0.207	−0.416	0.612	−0.299	0.258	0.486	0.631	0.786*	0.626

*$p \leqslant 0.05$ **$p \leqslant 0.005$ ***$p \leqslant 0.005$, different from DAMGO as determined by ANOVA with Dunnett's multiple comparison test. NC: not calculated due to full agonism.

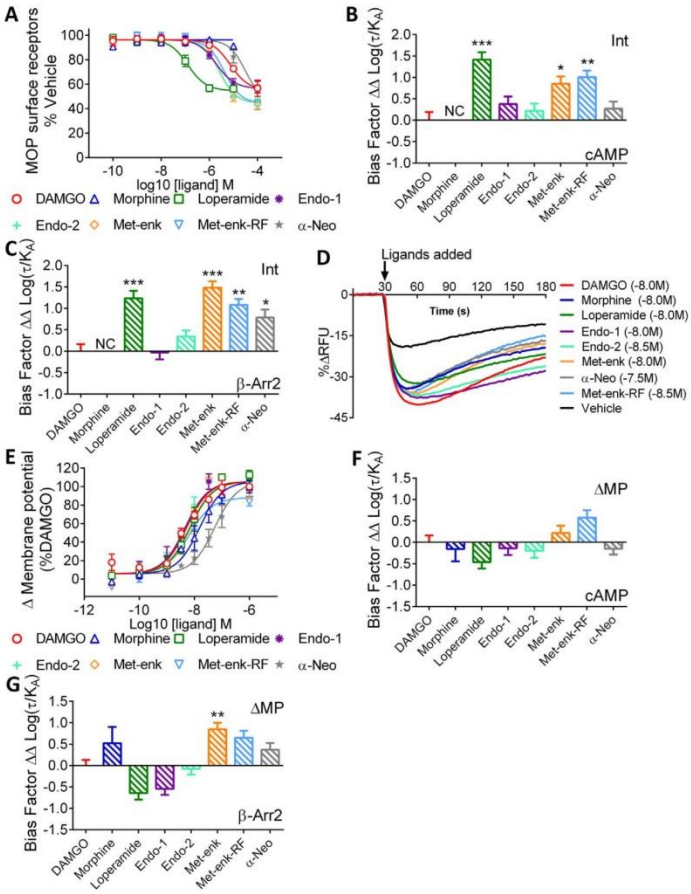

Fig. 8. Quantification of biased agonism in AtT20 cells. (a) FLAG-mMOP internalisation in AtT20 cells. Data expressed as percentage of vehicle, and expressed as mean ± SEM of at least 3 separate experiments. Bias factors between internalisation (Int) and (b) cAMP and (c) β-arr2. (d) Representative kinetic trace of AtT20 cells hyperpolarisation measured using FLIPR membrane potential kit. Data expressed as %change in relative fluorescence units. (e) Concentration–response curves of cell hyperpolarisation (ΔMP) in AtT20-mMOP cells. Data normalised to the area under the curve of the 1 μM DAMGO response and expressed as mean ± SEM of at least 3 separate experiments. Bias factors between cell hyperpolarisation and (f) cAMP and (g) β-arr2. $^{*}p \leqslant 0.05$, $^{**}p \leqslant 0.005$, $^{***}p \leqslant 0.001$ different from DAMGO as determined by a one-way ANOVA with Dunnett's multiple comparison test compared to DAMGO. NC = not calculable.

assays typically measure total AC activity throughout the whole cell, but cAMP signalling can occur selectively in spatially distinct regions of the cell such as at the membrane or cytosol or even from internalised receptors in endosomes [51,52]. Regulation of AC activity, and consequently the kinetics of cAMP signalling, can vary between different areas of the cell [53], hence differential activation of cAMP in different cellular compartments may also result in different cAMP signalling kinetics.

To quantify bias between G protein activation and other signalling pathways, measuring G protein activation directly using GTPγS or BRET/FRET based assays is thought to be the most direct approach that avoids complex signalling kinetics of downstream signalling effectors. However, nearly all ligands examined in this study, showed a change in bias between activation of different G_{α} subunits in CHO-MOP, when comparing acute activation of G proteins at 5 min to G protein activation at 60 min (time point at which substantial levels of receptor regulatory processes can be detected). This suggests that G protein activation and deactivation kinetics are also ligand-dependent, hence measuring G protein activation directly instead of measuring downstream signalling pathways may only provide a partial picture of the differential signalling mechanisms. Altogether, the ligand-dependent kinetics of G protein activation and downstream G protein-mediated signalling indicate that bias is likely to be frequently observed between these two signalling endpoints. This was observed previously between cAMP and G protein-activation measured by [^{35}S] GTPγS binding assays in CHO-MOP [6], and to a lesser extent between cAMP and ΔMP in AtT20-MOP, in the current study. This has shown that the level of G protein activation does not necessarily have to be indicative of the level of activation of G protein-mediated downstream signalling, and that the level of activation of one G protein-mediated pathway is not necessarily representative of all G protein-mediated signalling.

Another factor that may contribute to bias between G protein activation and G protein-mediated signalling pathways is the bias between activation of different subtypes of G protein subunits. All

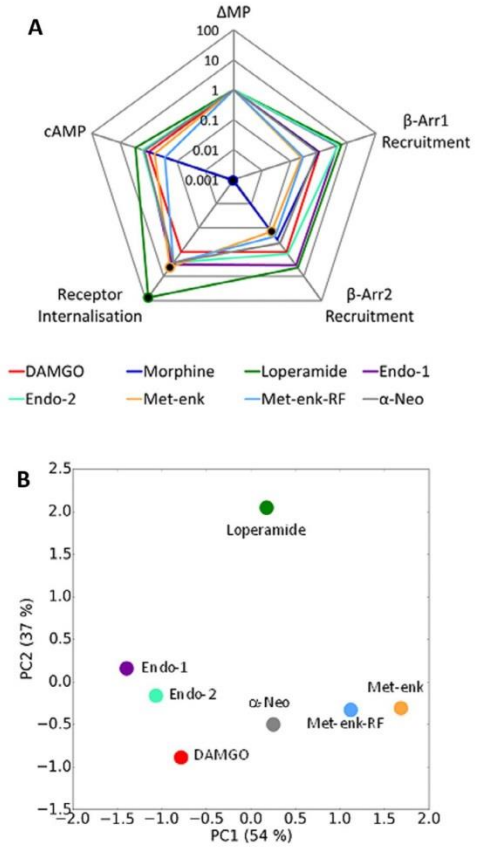

Fig. 9. Biased agonism profiles of MOP agonists in AtT20-mMOP cells. (a) Webs of bias for all ligands. τ/K_A values were normalised to the reference ligand DAMGO, and to the membrane polarisation assay. Statistically significant differences ($p < 0.05$) are denoted by black circles as determined by a one-way ANOVA with Dunnett's multiple comparison test compared to DAMGO. (b) Principal component analysis (PCA) of all bias factors.

ligands showed some bias compared to DAMGO between activation of different $G_{\alpha i/o}$ subtypes in CHO-MOP after 5 min or 60 min of agonist stimulation. Small differences in the level of activation of different $G_{\alpha i/o}$ subtypes at MOP by endo-1, endo-2 and morphine have also been reported previously [38–40,54], however none of these reports are consistent with the bias observed in this study. Such inconsistencies could be due to differences in the cell background, measurement of G protein activation at different time points, or factors related to the different experimental conditions. Selective G protein activation could cause unequal activation of downstream signalling pathways, as not all G_α subtypes have the same downstream effectors. Different $G_{\alpha i/o}$ subtypes have been shown to differentially inhibit AC isoforms [55–57], and are more susceptible to inactivation by different RGS subtypes [26–28]. Altogether, the differential activity and regulation of $G_{\alpha i/o}$ subunits could contribute to bias between G protein-mediated signalling pathways. Additionally, selective activation of particular $G_{\alpha i/o}$ subtypes and differential interactions with signalling effector isoforms will depend on the expression specific subtypes/isoforms and their localisation in signalling complexes.

The dependence of biased agonism on the cellular protein content was also clearly demonstrated by the change in bias of endo-1 between cAMP and β-arr1/2 recruitment in CHO-MOP when GRK2 was overexpressed. As a consequence, biased agonism of endo-1 is likely to change in different tissues which express different levels of GRK2, and be cAMP biased in some tissues and β-arrestin biased in others. It remains to be seen whether this change in bias is significant enough to produce marked differences in physiological effects. However, different cell types typically show altered expression of numerous signalling effectors, since changing the expression of a single protein can cause such a notable change in bias, it is likely that the cumulative effects of all changes in protein expression could induce considerable differences in bias across different cell types.

Altogether, the impact of the cellular complement on determinations of biased agonism, combined with the kinetics of the signalling pathways suggest that caution must be taken when interpreting bias quantifications in different cell backgrounds. The altered expression and localisation of proteins in a different cell background can result in changes in signalling kinetics, as well as changes in experimental conditions required to obtain concentration–response curves. Microarray analysis of genes expressed in AtT20 cells have shown that these cells have a very limited range of signalling proteins compared to other commonly used cell lines [58]. AtT20 cells only express detectable levels of GRK2, β-arr2, and $G_{\alpha i2}$, and also a very limited number of RGS subtypes and AC isoforms. With only a single GRK isoform and no endogenously expressed β-arr1, there will be less variation in receptor phosphorylation patterns that govern subsequent MOP regulation and trafficking events. Additionally, the expression of a single $G_{\alpha i/o}$ subtype, $G_{\alpha i2}$, and the low levels of a small subset of AC isoforms and RGS subtypes indicates that the level AC inhibition induced by the ligands and regulation of AC activity in these cells is likely to be different from that observed in the CHO cells. Overall, this may account for many of the changes in bias compared to CHO-MOP observed for endo-1, loperamide and α-neo between cAMP, β-arr1/2 recruitment and receptor internalisation. Moreover, the difference between biased agonism in AtT20 and CHO cells may also be due to the difference in species, mouse and human MOP, as has been recently observed at KOP [59]. Overall, this indicates that ligands will not only exhibit different biased agonism characteristics in different tissues, but that this can also change due to cellular adaptations that cause changes in protein expression and localisation, such as during the development of opioid tolerance.

Since the unique conformations of the receptor induced by the ligand are more likely to be consistent between cell types, some studies have bypassed the complications of signalling kinetics and cell background by directly measuring receptor conformational changes using BRET or FRET-based sensors [60]. Whilst this approach can identify novel biased ligands that stabilise the receptor into unique conformations, there is still a requirement to link these unique conformations to specific signalling characteristics, and hence cell specific complications of biased agonism remain. However, the cell-dependent aspect of biased agonism may be an advantage in some cases, such as when the therapeutic effects and the side effects are mediated by activation of the same signalling pathways in different tissues. In such cases, a ligand that displays a distinct bias profile in different cells can selectively activate the desired signalling pathways in the desired tissue. In the case of MOP, a ligand which shows marked cell-dependent bias may produce less desensitisation and tolerance in cells involved in nociception and more in other cell types which are linked to limited side effects (those controlling respiration or gut motility), even if the mechanisms of desensitisation and tolerance are the same in different cells.

In summary the data presented here demonstrate the complex nature of biased agonism. Biased agonism is not an absolute

quality, it is a dynamic and multi-faceted phenomenon; it is always relative to a reference ligand, and it is dependent on both cellular protein complement as well as the spatiotemporal properties of the different signalling pathways [30]. Our results highlight that biased agonism cannot be described in isolation of conformational, kinetic and cellular context. As mentioned above, it is vital to use a reference ligand that is likely to be subject to the same kinetic and cellular context than the other ligands. Ideally, such reference ligand is an endogenous agonist, although when multiple endogenous agonists exist, one may need to consider the potential of biased agonism and the effect of the so-called conformational and kinetic context amongst these.

Nevertheless, quantification of biased agonism in different cell backgrounds has also shown that despite the dramatic changes in the biased agonism profiles of the ligands between the cell backgrounds, the ligands under study still possessed distinct biased agonism profiles. This shows that despite such caveats, the diversity of biased agonism characteristics can be captured by examining bias across several signalling pathways. Ultimately, in order to establish links between distinct biased agonism traits and specific physiological responses, a greater understanding about biased signalling in native tissue and *in vivo* is essential. This complexity in biased agonism determination presents a significant current challenge when attempting to predict biased signalling *in vivo*. For drug discovery programs, this means that preclinical measurements of efficacy and bias in a model cell system may not be predictive of the efficacy of a drug *in vivo*, in the relevant tissue, cell or signalling pathway and must be acknowledged as such. Nonetheless, this should not preclude a judicious clustering of biased molecules for subsequent testing in more relevant (native) environments but, rather, a more cautious approach towards assuming absolute directionality of bias across different cellular systems. Moreover, the cell-dependent characteristics of biased agonism may prove to be an advantage in the development of biased ligands, as this facilitates the design of drugs that are more targeted to specific tissues.

Authorship contributions

Participated in research design: Thompson, Lane, Christopoulos, Canals. *Conducted experiments*: Thompson. *Performed data analysis*: Thompson, Coudrat. *Wrote or contributed to the writing of the manuscript*: Thompson, Lane, Sexton, Christopoulos, Canals.

Acknowledgements

We thank Prof. M. J. Christie for providing AtT20 and AtT20-MOP cells; and Profs. L. Bohn and M. Caron for providing DNAs. G.L.T. scholarship was funded by the Australian Commonwealth Government Department of Defence. T.C. acknowledges a Victorian Life Sciences Computation Initiative PhD top-up scholarship. M.C. is a Monash Fellow. A.C. is a Senior Principal Research Fellow and P.M.S. is a Principal Research Fellow of the National Health and Medical Research Council (NHMRC) of Australia. J.R.L. is a Monash University Larkins Fellow and an RD Wright Biomedical Career Development Fellow (NHMRC). This work was funded in part by the NHMRC [Program Grant APP1055134 to A.C. and P.M.S.] and the Monash Institute of Pharmaceutical Sciences Large Grant Support Scheme (M.C.).

References

[1] J.D. Urban, W.P. Clarke, M. von Zastrow, D.E. Nichols, B. Kobilka, H. Weinstein, J. A. Javitch, B.L. Roth, A. Christopoulos, P.M. Sexton, K.J. Miller, M. Spedding, R.B. Mailman, Functional selectivity and classical concepts of quantitative pharmacology, J. Pharmacol. Exp. Ther. 320 (1) (2007) 1–13.

[2] T. Kenakin, A. Christopoulos, Signalling bias in new drug discovery: detection, quantification and therapeutic impact, Nat. Rev. Drug. Discov. 12 (3) (2013) 205–216.

[3] T. Kenakin, C. Watson, V. Muniz-Medina, A. Christopoulos, S. Novick, A simple method for quantifying functional selectivity and agonist bias, ACS Chem. Neurosci. 3 (3) (2012) 193–203.

[4] J.W. Black, P. Leff, Operational models of pharmacological agonism, Proc. R. Soc. Lond. B. Biol. Sci. 220 (1219) (1983) 141–162.

[5] K.L. White, A.P. Scopton, M.L. Rives, R.V. Bikbulatov, P.R. Polepally, P.J. Brown, T. Kenakin, J.A. Javitch, J.K. Zjawiony, B.L. Roth, Identification of novel functionally selective kappa-opioid receptor scaffolds, Mol. Pharmacol. 85 (1) (2014) 83–90.

[6] G.L. Thompson, J.R. Lane, T. Coudrat, P.M. Sexton, A. Christopoulos, M. Canals, Biased agonism of endogenous opioid peptides at the mu-opioid receptor, Mol. Pharmacol. 88 (2) (2015) 335–346.

[7] I. Charfi, K. Nagi, O. Mnie-Filali, D. Thibault, G. Balboni, P.W. Schiller, L.E. Trudeau, G. Pineyro, Ligand- and cell-dependent determinants of internalization and cAMP modulation by delta opioid receptor (DOR) agonists, Cel. Mol. Life Sci. 71 (8) (2014) 1529–1546.

[8] G. Rivero, J. Llorente, J. McPherson, A. Cooke, S.J. Mundell, C.A. McArdle, E.M. Rosethorne, S.J. Charlton, C. Krasel, C.P. Bailey, G. Henderson, E. Kelly, Endomorphin-2: a biased agonist at the mu-opioid receptor, Mol. Pharmacol. 82 (2) (2012) 178–188.

[9] J. Corbisier, C. Gales, A. Huszagh, M. Parmentier, J.Y. Springael, Biased signaling at chemokine receptors, J. Biol. Chem. 290 (15) (2015) 9542–9554.

[10] S. Rajagopal, D.L. Bassoni, J.J. Campbell, N.P. Gerard, C. Gerard, T.S. Wehrman, Biased agonism as a mechanism for differential signaling by chemokine receptors, J. Biol. Chem. 288 (49) (2013) 35039–35048.

[11] B.A. Evans, N. Broxton, J. Merlin, M. Sato, D.S. Hutchinson, A. Christopoulos, R.J. Summers, Quantification of functional selectivity at the human alpha(1A)-adrenoceptor, Mol. Pharmacol. 79 (2) (2011) 298–307.

[12] E.T. van der Westhuizen, B. Breton, A. Christopoulos, M. Bouvier, Quantification of ligand bias for clinically relevant beta2-adrenergic receptor ligands: implications for drug taxonomy, Mol. Pharmacol. 85 (3) (2014) 492–509.

[13] Y. Namkung, O. Radresa, S. Armando, D. Devost, A. Beautrait, C. Le-Gouill, S.A. Laporte, Quantifying biased signaling in GPCRs using BRET-based biosensors, Methods (San Diego, Calif.) (2015).

[14] D. Wootten, E.E. Savage, F.S. Willard, A.B. Bueno, K.W. Sloop, A. Christopoulos, P.M. Sexton, Differential activation and modulation of the glucagon-like peptide-1 receptor by small molecule ligands, Mol. Pharmacol. 83 (4) (2013) 822–834.

[15] A.G. Soto, T.H. Smith, B. Chen, S. Bhattacharya, I.C. Cordova, T. Kenakin, N. Vaidehi, J. Trejo, N-linked glycosylation of protease-activated receptor-1 at extracellular loop 2 regulates G-protein signaling bias, Proc. Natl. Acad. Sci. U. S.A. (2015).

[16] M. Szabo, C. Klein Herenbrink, A. Christopoulos, J.R. Lane, B. Capuano, Structure–activity relationships of privileged structures lead to the discovery of novel biased ligands at the dopamine D(2) receptor, J. Med. Chem. 57 (11) (2014) 4924–4939.

[17] S. Galandrin, M. Bouvier, Distinct signaling profiles of beta1 and beta2 adrenergic receptor ligands toward adenylyl cyclase and mitogen-activated protein kinase reveals the pluridimensionality of efficacy, Mol. Pharmacol. 70 (5) (2006) 1575–1584.

[18] T. Kenakin, The effective application of biased signaling to new drug discovery, Mol. Pharmacol. (2015).

[19] G.L. Thompson, E. Kelly, A. Christopoulos, M. Canals, Novel GPCR paradigms at the mu-opioid receptor, Br. J. Pharmacol. 172 (2) (2014) 287–296.

[20] P. Molinari, V. Vezzi, M. Sbraccia, C. Gr, D. Riitano, C. Ambrosio, I. Casella, T. Costa, Morphine-like opiates selectively antagonize receptor–arrestin interactions, J. Biol. Chem. 285 (17) (2010) 12522–12535.

[21] N. Tschammer, S. Bollinger, T. Kenakin, P. Gmeiner, Histidine 6.55 is a major determinant of ligand-biased signaling in dopamine D2L receptor, Mol. Pharmacol. 79 (3) (2011) 575–585.

[22] H.O. Onaran, S. Rajagopal, T. Costa, What is biased efficacy? Defining the relationship between intrinsic efficacy and free energy coupling, Trends Pharmacol. Sci. 35 (12) (2014) 639–647.

[23] J.A. Allen, J.M. Yost, V. Setola, X. Chen, M.F. Sassano, M. Chen, S. Peterson, P.N. Yadav, X.P. Huang, B. Feng, N.H. Jensen, X. Che, X. Bai, S.V. Frye, W.C. Wetsel, M. G. Caron, J.A. Javitch, B.L. Roth, J. Jin, Discovery of beta-arrestin-biased dopamine D2 ligands for probing signal transduction pathways essential for antipsychotic efficacy, Proc. Natl. Acad. Sci. USA 108 (45) (2011) 18488–18493.

[24] C. Hoffmann, N. Ziegler, S. Reiner, C. Krasel, M.J. Lohse, Agonist-selective, receptor-specific interaction of human P2Y receptors with beta-arrestin-1 and -2, J. Biol. Chem. 283 (45) (2008) 30933–30941.

[25] G. Pineyro, E. Archer-Lahlou, Ligand-specific receptor states: implications for opiate receptor signalling and regulation, Cell. Signal. 19 (1) (2007) 8–19.

[26] L.J. Leontiadis, M.P. Papakonstantinou, Z. Georgoussi, Regulator of G protein signaling 4 confers selectivity to specific G proteins to modulate mu- and delta-opioid receptor signaling, Cell. Signal. 21 (7) (2009) 1218–1228.

[27] K.L. Lan, H. Zhong, M. Nanamori, R.R. Neubig, Rapid kinetics of regulator of G-protein signaling (RGS)-mediated Galphai and Galphao deactivation. Galpha specificity of RGS4 AND RGS7, J. Biol. Chem. 275 (43) (2000) 33497–33503.

[28] J.N. Talbot, D.L. Roman, M.J. Clark, R.A. Roof, J.J. Tesmer, R.R. Neubig, J.R. Traynor, Differential modulation of mu-opioid receptor signaling to adenylyl cyclase by regulators of G protein signaling proteins 4 or 8 and 7 in

permeabilised C6 cells is Galpha subtype dependent, J. Neurochem. 112 (4) (2010) 1026–1034.
[29] R.S. Ostrom, A.S. Bogard, R. Gros, R.D. Feldman, Choreographing the adenylyl cyclase signalosome: sorting out the partners and the steps, Naunyn Schmiedebergs Arch. Pharmacol. 385 (1) (2012) 5–12.
[30] C. Klein Herenbrink, D.A. Sykes, P. Donthamsetti, M. Canals, T. Coudrat, J. Shonberg, P.J. Scammells, B. Capuano, P.M. Sexton, S.J. Charlton, J.A. Javitch, A. Christopoulos, J.R. Lane, The role of kinetic context in apparent biased agonism at GPCRs, Nat. Commun. 7 (2016) 10842.
[31] S.L. Borgland, M. Connor, P.B. Osborne, J.B. Furness, M.J. Christie, Opioid agonists have different efficacy profiles for G protein activation, rapid desensitization, and endocytosis of mu-opioid receptors, J. Biol. Chem. 278 (21) (2003) 18776–18784.
[32] L.I. Jiang, J. Collins, R. Davis, K.M. Lin, D. DeCamp, T. Roach, R. Hsueh, R.A. Rebres, E.M. Ross, R. Taussig, I. Fraser, P.C. Sternweis, Use of a cAMP BRET sensor to characterize a novel regulation of cAMP by the sphingosine 1-phosphate/G13 pathway, J. Biol. Chem. 282 (14) (2007) 10576–10584.
[33] A. Christopoulos, Assessing the distribution of parameters in models of ligand-receptor interaction: to log or not to log, Trends Pharmacol. Sci. 19 (9) (1998) 351–357.
[34] P. Leff, D.J. Prentice, H. Giles, G.R. Martin, J. Wood, Estimation of agonist affinity and efficacy by direct, operational model-fitting, J. Pharmacol. Meth. 23 (3) (1990) 225–237.
[35] H.J. Motulsky, L.A. Ransnas, Fitting curves to data using nonlinear regression: a practical and nonmathematical review, FASEB J. 1 (5) (1987) 365–374.
[36] S. Wold, K. Esbensen, P. Geladi, Principal component analysis, Chemometr. Intell. Lab. Syst. 2 (1–3) (1987) 37–52.
[37] F. Pedregosa, G. Varoquaux, A. Gramfort, V. Michel, B. Thirion, O. Grisel, M. Blondel, P. Prettenhofer, R. Weiss, V. Dubourg, J. Vanderplas, A. Passos, D. Cournapeau, M. Brucher, M. Perrot, E. Duchesnay, Scikit-learn: machine learning in python, J. Mach. Learn. Res. 12 (2011) 2825–2830.
[38] M.J. Clark, C.A. Furman, T.D. Gilson, J.R. Traynor, Comparison of the relative efficacy and potency of mu-opioid agonists to activate Galpha(i/o) proteins containing a pertussis toxin-insensitive mutation, J. Pharmacol. Exp. Ther. 317 (2) (2006) 858–864.
[39] D. Massotte, K. Brillet, B. Kieffer, G. Milligan, Agonists activate Gi1 alpha or Gi2 alpha fused to the human mu opioid receptor differently, J. Neurochem. 81 (6) (2002) 1372–1382.
[40] Z. Saidak, K. Blake-Palmer, D.L. Hay, J.K. Northup, M. Glass, Differential activation of G-proteins by mu-opioid receptor agonists, Br. J. Pharmacol. 147 (6) (2006) 671–680.
[41] C. Doll, F. Poll, K. Peuker, A. Loktev, L. Gluck, S. Schulz, Deciphering micro-opioid receptor phosphorylation and dephosphorylation in HEK293 cells, Br. J. Pharmacol. 167 (6) (2012) 1259–1270.
[42] S. Just, S. Illing, M. Trester-Zedlitz, E.K. Lau, S.J. Kotowski, E. Miess, A. Mann, C. Doll, J.C. Trinidad, A.L. Burlingame, M. von Zastrow, S. Schulz, Differentiation of opioid drug effects by hierarchical multi-site phosphorylation, Mol. Pharmacol. 83 (3) (2013) 633–639.
[43] J. Zhang, S.S. Ferguson, L.S. Barak, S.R. Bodduluri, S.A. Laporte, P.Y. Law, M.G. Caron, Role for G protein-coupled receptor kinase in agonist-specific regulation of mu-opioid receptor responsiveness, Proc. Natl. Acad. Sci. U.S.A. 95 (12) (1998) 7157–7162.
[44] M.J. Clark, J.J. Linderman, J.R. Traynor, Endogenous regulators of g protein signaling differentially modulate full and partial μ-opioid agonists at adenylyl cyclase as predicted by a collision coupling model, Mol. Pharmacol. 73 (5) (2008) 1538–1548.
[45] T. Koch, S. Schulz, H. Schroder, R. Wolf, E. Raulf, V. Hollt, Carboxyl-terminal splicing of the rat mu opioid receptor modulates agonist-mediated internalization and receptor resensitization, J. Biol. Chem. 273 (22) (1998) 13652–13657.
[46] R.A. North, J.T. Williams, A. Surprenant, M.J. Christie, Mu and delta receptors belong to a family of receptors that are coupled to potassium channels, Proc. Natl. Acad. Sci. U.S.A. 84 (15) (1987) 5487–5491.
[47] A. Knapman, M. Santiago, Y.P. Du, P.R. Bennallack, M.J. Christie, M. Connor, A. Continuous, Fluorescence-based assay of mu-opioid receptor activation in AtT-20 cells, J. Biomol. Screen 26 (2012) 26.
[48] H.B. Tudashki, D.N. Robertson, P.W. Schiller, G. Pineyro, Endocytic profiles of delta-opioid receptor ligands determine the duration of rapid but not sustained cAMP responses, Mol. Pharmacol. 85 (1) (2014) 148–161.
[49] J.M. Quillan, K. Carlson, C. Song, D. Wang, W. Sade, Differential effects of mu-opioid receptor ligands on Ca(2+) signaling, J. Pharmacol. Exp. Ther. 302 (3) (2002) 1002–1012.
[50] E.A. Johnson, S. Oldfield, E. Braksator, A. Gonzalez-Cuello, D. Couch, K.J. Hall, S.J. Mundell, C.P. Bailey, E. Kelly, G. Henderson, Agonist-selective mechanisms of mu-opioid receptor desensitization in human embryonic kidney 293 cells, Mol. Pharmacol. 70 (2) (2006) 676–685.
[51] R. Irannejad, J.C. Tomshine, J.R. Tomshine, M. Chevalier, J.P. Mahoney, J. Steyaert, S.G. Rasmussen, R.K. Sunahara, H. El-Samad, B. Huang, M. von Zastrow, Conformational biosensors reveal GPCR signalling from endosomes, Nature 495 (7442) (2013) 534–538.
[52] D. Calebiro, V.O. Nikolaev, M.C. Gagliani, T. de Filippis, C. Dees, C. Tacchetti, L. Persani, M.J. Lohse, Persistent cAMP-signals triggered by internalized G-protein-coupled receptors, PLoS Biol. 7 (8) (2009) e1000172.
[53] R.K. Perera, V.O. Nikolaev, Compartmentation of cAMP signalling in cardiomyocytes in health and disease, Acta Physiol. (Oxford, England) 207 (4) (2013) 650–662.
[54] L. Stanasila, W.K. Lim, R.R. Neubig, F. Pattus, Coupling efficacy and selectivity of the human μ-opioid receptor expressed as receptor—Gα fusion proteins in *Escherichia coli*, J. Neurochem. 75 (3) (2000) 1190–1199.
[55] R. Taussig, W.J. Tang, J.R. Hepler, A.G. Gilman, Distinct patterns of bidirectional regulation of mammalian adenylyl cyclases, J. Biol. Chem. 269 (8) (1994) 6093–6100.
[56] R. Taussig, J.A. Iniguez-Lluhi, A.G. Gilman, Inhibition of adenylyl cyclase by Gi alpha, Science (New York, N.Y.) 261 (5118) (1993) 218–221.
[57] J. Chen, R. Iyengar, Inhibition of cloned adenylyl cyclases by mutant-activated Gi-alpha and specific suppression of type 2 adenylyl cyclase inhibition by phorbol ester treatment, J. Biol. Chem. 268 (17) (1993) 12253–12256.
[58] B.K. Atwood, J. Lopez, J. Wager-Miller, K. Mackie, A. Straiker, Expression of G protein-coupled receptors and related proteins in HEK293, AtT20, BV2, and N18 cell lines as revealed by microarray analysis, BMC Genom. 12 (2011) 14.
[59] K.M. DiMattio, F.J. Ehlert, L.Y. Liu-Chen, Intrinsic relative activities of kappa opioid agonists in activating Galpha proteins and internalizing receptor: differences between human and mouse receptors, Eur. J. Pharmacol. 761 (2015) 235–244.
[60] M.J. Lohse, S. Nuber, C. Hoffmann, Fluorescence/bioluminescence resonance energy transfer techniques to study G-protein-coupled receptor activation and signaling, Pharmacol. Rev. 64 (2) (2012) 299–336.

B.5 Plasma Membrane Localization of the μ-Opioid Receptor Controls Spatiotemporal Signaling

RESEARCH ARTICLE

GPCR SIGNALING

Plasma membrane localization of the μ-opioid receptor controls spatiotemporal signaling

Michelle L. Halls,[1]* Holly R. Yeatman,[1] Cameron J. Nowell,[1] Georgina L. Thompson,[1] Arisbel Batista Gondin,[1] Srgjan Civciristov,[1] Nigel W. Bunnett,[1,2,3,4] Nevin A. Lambert,[5] Daniel P. Poole,[1,6] Meritxell Canals[1,2]*

Differential regulation of the μ-opioid receptor (MOR), a G protein (heterotrimeric guanine nucleotide–binding protein)–coupled receptor, contributes to the clinically limiting effects of opioid analgesics, such as morphine. We used biophysical approaches to quantify spatiotemporal MOR signaling in response to different ligands. In human embryonic kidney (HEK) 293 cells overexpressing MOR, morphine caused a Gβγ-dependent increase in plasma membrane–localized protein kinase C (PKC) activity, which resulted in a restricted distribution of MOR within the plasma membrane and induced sustained cytosolic extracellular signal–regulated kinase (ERK) signaling. In contrast, the synthetic opioid peptide DAMGO ([D-Ala^2,N-Me-Phe^4, Gly^5-ol]-enkephalin) enabled receptor redistribution within the plasma membrane, resulting in transient increases in cytosolic and nuclear ERK activity, and, subsequently, receptor internalization. When Gβγ subunits or PKCα activity was inhibited or when the carboxyl-terminal phosphorylation sites of MOR were mutated, morphine-activated MOR was released from its restricted plasma membrane localization and stimulated a transient increase in cytosolic and nuclear ERK activity in the absence of receptor internalization. Thus, these data suggest that the ligand-induced redistribution of MOR within the plasma membrane, and not its internalization, controls its spatiotemporal signaling.

INTRODUCTION

Heterotrimeric guanine nucleotide–binding protein (G protein)–coupled receptors (GPCRs) are the largest family of cell surface signaling proteins encoded by the human genome. These receptors enable cells to respond to structurally diverse endogenous and environmental signals, and they are the targets of more than 30% of marketed drugs. It is increasingly recognized that the uniform increase in the abundance of second messengers throughout the cell cannot explain the diversity of GPCR-mediated effects. Rather, spatial (location) and temporal (duration) control of signaling play an important role (*1*, *2*). Spatial compartmentalization of signaling can be achieved by the formation of GPCR-dependent protein complexes, which restrict the diffusion of second messengers to induce extremely localized signals (*3*). In addition, multiple regulatory mechanisms (including receptor phosphorylation, desensitization, and internalization) control the duration of GPCR activation. Therefore, the spatial and temporal distribution of both receptors and signaling effectors are critical for the generation of distinct and highly specialized GPCR-mediated responses.

The μ-opioid receptor (MOR) has been extensively studied because of its physiological importance in mediating the effects of endogenous opioids as well as its prominence as the target of opioid analgesics, such as morphine. However, chronic use of opioid analgesics is still clinically limited by the development of tolerance, addiction, constipation, and respiratory depression (*4*). At the cellular level, stimulation of MOR by all opioids activates the same G protein–dependent signaling pathways. MOR activates $G\alpha_{i/o}$ proteins, leading to inhibition of cyclic adenosine monophosphate (cAMP) generation, increased extracellular signal–regulated kinase (ERK) phosphorylation and activation, activation of G protein–regulated inwardly rectifying potassium channels (GIRKs), and inhibition of voltage-gated calcium channels (*5*). However, different MOR agonists induce distinct patterns of receptor regulation and internalization. In particular, morphine causes limited receptor phosphorylation and recruitment of the scaffolding protein β-arrestin, which results in compromised receptor internalization and resensitization (*6*–*10*). These observations have prompted intensive studies of the ability of MOR ligands to differentially activate G proteins and β-arrestins in an effort to explain their divergent biological effects (*11*–*13*).

It is now apparent that the spatiotemporal characteristics of a signal can specify the outcome of receptor activation (*1*, *2*). Most opioids, including morphine, result in the phosphorylation and activation of cytosolic ERK (*14*–*16*); however, unlike other opioids, morphine is unable to promote nuclear ERK activation (*15*). Together with its impaired ability to induce the internalization of MOR, this finding suggests that morphine may stimulate a spatiotemporal cellular response distinct from those induced by other opioids. To investigate this hypothesis, we used complimentary biophysical techniques and superresolution microscopy. We report that morphine and DAMGO activated distinct spatial and temporal signaling profiles that were controlled by the plasma membrane localization of MOR induced by the two ligands. Subcellular targeted Förster resonance energy transfer (FRET) biosensors showed that only morphine-dependent stimulation of MOR induced sustained cytosolic ERK phosphorylation and plasma membrane–localized protein kinase C (PKC) activation, which restricted the localization of MOR. In contrast, DAMGO caused the redistribution of MOR within the plasma membrane as well as the transient activation of both cytosolic and nuclear ERK. Thus, not only did morphine and DAMGO stimulate different signaling pathways, but they also activated signals in distinct subcellular compartments with distinct temporal profiles. Furthermore, we altered the spatiotemporal signaling profile of morphine to

[1]Drug Discovery Biology Theme, Monash Institute of Pharmaceutical Sciences, Monash University, Parkville, Victoria 3052, Australia. [2]ARC Centre of Excellence in Convergent Bio-Nano Science and Technology, Monash Institute of Pharmaceutical Sciences, Monash University, Parkville, Victoria 3052, Australia. [3]Department of Anesthesia and Perioperative Medicine, Monash University, Melbourne, Victoria 3004, Australia. [4]Department of Pharmacology, The University of Melbourne, Parkville, Victoria 3052, Australia. [5]Department of Toxicology and Pharmacology, Georgia Regents University, Augusta, GA 30912, USA. [6]Department of Anatomy and Neuroscience, The University of Melbourne, Parkville, Victoria 3052, Australia.
*Corresponding author. E-mail: michelle.halls@monash.edu (M.L.H.); meri.canals@monash.edu (M.C.)

RESEARCH ARTICLE

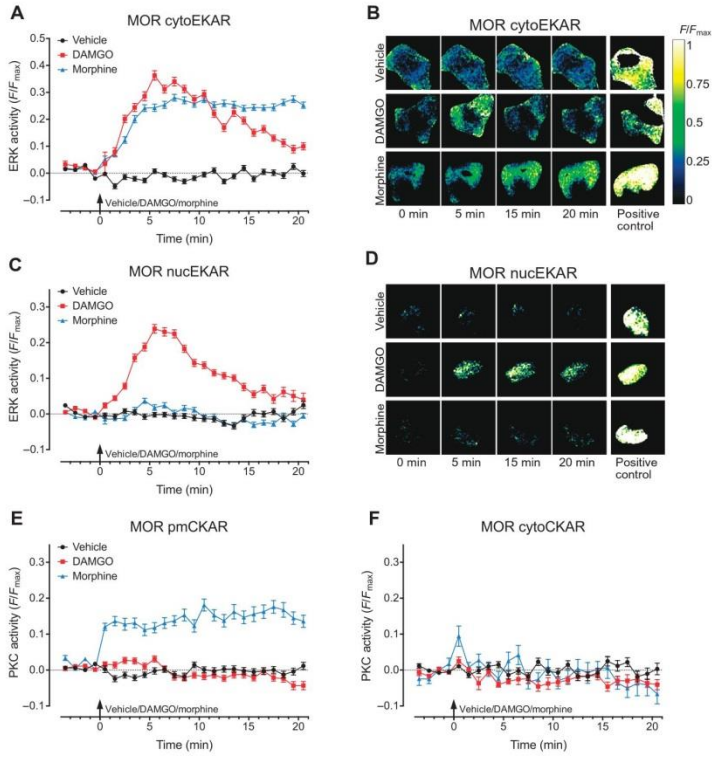

Fig. 1. Ligand-dependent spatiotemporal signaling of MOR. (A to D) Spatiotemporal activation of ERK in transfected HEK 293 cells treated with vehicle, DAMGO, or morphine for the indicated times. (A) Analysis of cytosolic ERK activity. Data are means ± SEM of 416 to 606 cells from five experiments. (B) Representative pseudocolor ratiometric images of cytoEKAR. (C) Analysis of nuclear ERK activity. Data are means ± SEM of 561 to 810 cells from five experiments. (D) Representative pseudocolor ratiometric images of nucEKAR. Pseudocolor scale as in (B). (E and F) Spatiotemporal activation of PKC in transfected HEK 293 cells after treatment with vehicle, DAMGO, or morphine for the indicated times. (E) Analysis of plasma membrane–localized PKC activity. Data are means ± SEM of 155 to 220 cells from three experiments. (F) Analysis of cytosolic PKC activity. Data are means ± SEM of 45 to 115 cells from three experiments.

mimic that of DAMGO by enabling the redistribution of MOR within the plasma membrane in the absence of β-arrestin recruitment or receptor internalization. Thus, these data suggest that receptor localization within the plasma membrane determines the spatiotemporal signals activated by MOR in response to different ligands.

RESULTS

Ligand-dependent spatiotemporal signaling of MOR

To gain spatial and temporal resolution of MOR signaling in live cells, we used FRET biosensors for ERK and PKC (EKAR and CKAR, respectively), which localized to different subcellular compartments (*17*, *18*). In human embryonic kidney (HEK) 293 cells cotransfected with plasmids encoding MOR and either a cytosolic or a nuclear ERK biosensor (cytoEKAR and nucEKAR, respectively), DAMGO and morphine at EC_{50} concentrations (concentration that provokes 50% of the maximal response of the receptor; 10 nM DAMGO and 100 nM morphine, fig. S1A) caused distinct temporal profiles of ERK activation, shown as changes in the corresponding FRET signal. Whereas DAMGO caused a transient increase in cytosolic ERK activity, morphine induced a sustained increase (Fig. 1, A and B). Moreover, only DAMGO caused a transient increase in nuclear ERK activity (Fig. 1, C and D). Ligand-dependent responses were also observed when assessing the direct activation of PKC. In cells cotransfected with plasmids encoding MOR and a plasma membrane–localized biosensor of PKC activity (pmCKAR), only morphine caused a sustained increase in PKC activity (Fig. 1E). DAMGO did not affect the activity of plasma membrane–localized PKC, even at maximal concentrations (1 μM, fig. S1B), and neither ligand stimulated the activity of cytosolic PKC (Fig. 1F).

The distinct internalization profiles of MOR in response to DAMGO and morphine (*6*, *10*) were quantified with a bioluminescence resonance energy transfer (BRET) assay that detects the proximity between BRET partners in defined subcellular compartments in live cells (*19*, *20*). Consistent with previous reports, incubation of HEK 293 cells with 1 μM DAMGO (concentration corresponding to its EC_{50} of β-arrestin recruitment using BRET; fig. S2A) induced MOR internalization, as shown by the increase in the BRET signal between a *Renilla* luciferase–tagged MOR (MOR-RLuc) and a Venus-tagged marker of early endosomes (Rab5a-Venus) (Fig. 2A). In contrast, morphine produced no substantial change in BRET (Fig. 2A and fig. S2B). These results were validated by automated, high-content image analysis (fig. S2C). DAMGO-mediated MOR endocytosis was unaffected by the inhibition of $G\alpha_{i/o}$ activity with NF023 or pertussis toxin (PTx) (*21*, *22*) but was abolished by the clathrin-dependent endocytosis inhibitor PitStop2 (*23*), by the expression of a dominant-negative dynamin mutant (K44E) (*24*), or by knockdown of β-arrestins [combined small interfering RNAs (siRNAs) specific for β-arrestin-1 and β-arrestin-2] (Fig. 2, A and B, and fig. S2, D to H). These data suggest that β-arrestin recruitment and MOR endocytosis are independent of $G\alpha_{i/o}$ coupling.

Previous studies have linked PKC activation to cytosolic ERK activity and β-arrestin activation to increased nuclear ERK activity to conclude that G protein– and β-arrestin–dependent pathways activate distinct modes of ERK signaling (*15*). By inhibiting $G\alpha_{i/o}$ proteins, we demonstrated that cytosolic ERK activation in response to DAMGO and morphine was dependent on $G\alpha_{i/o}$ (Fig. 2C). In agreement with previous studies, cytosolic ERK activity was unaffected by knockdown of β-arrestins (Fig. 2C). However, inhibition of receptor endocytosis by PitStop2 or by expression of the dynamin K44E mutant transformed the profile of DAMGO-induced cytosolic

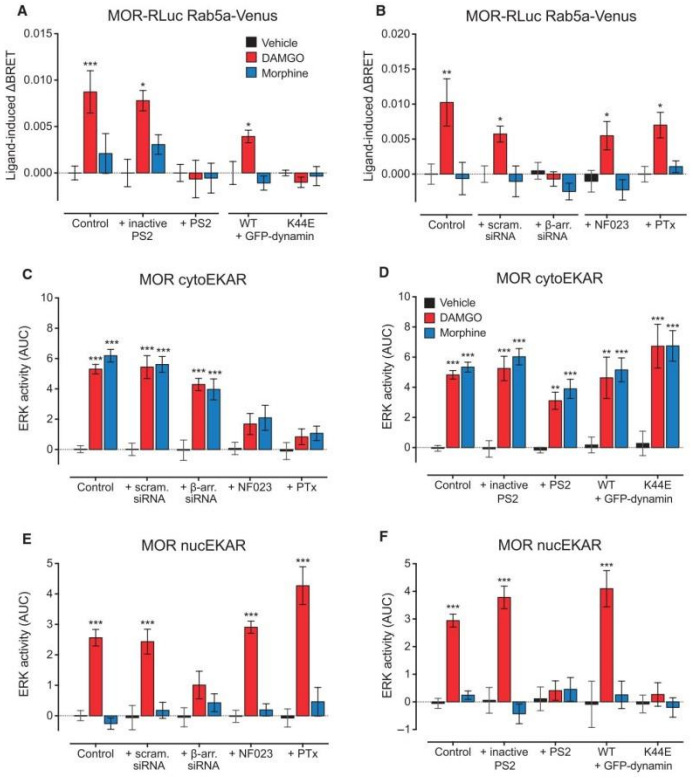

Fig. 2. Effect of $G\alpha_{i/o}$ protein inhibition, β-arrestin knockdown, or inhibition of endocytosis on MOR-stimulated cytosolic and nuclear ERK activities. (A and B) The trafficking of MOR to early endosomes in transfected HEK 293 cells in response to treatment with vehicle, DAMGO, or morphine for 30 min was determined by BRET analysis between MOR-RLuc and Rab5a-Venus. (A) Cells were treated with the clathrin-mediated endocytosis inhibitor PitStop2 (PS2) or its inactive control, or transfected to express wild-type (WT) dynamin or a dominant-negative dynamin K44E mutant. (B) Cells were treated with or without siRNAs specific for β-arrestins or were preincubated with the indicated $G\alpha_{i/o}$ protein inhibitors. Data are means ± SEM from five experiments. (C to F) Analysis of the spatial activation of ERK in HEK 293 cells in response to vehicle, DAMGO, or morphine in the presence or absence of β-arrestin–specific siRNA, $G\alpha_{i/o}$ protein inhibitors, PitStop2 or its inactive control, or upon expression of WT or K44E mutant dynamin. (C) Analysis of cytosolic ERK activity. Data are means ± SEM of 96 to 168 cells from three experiments. (D) Analysis of cytosolic ERK activity in cells in which endocytosis was inhibited. Data are means ± SEM of 35 to 606 cells from three experiments. (E) Analysis of nuclear ERK activity in cells treated with $G\alpha_{i/o}$ protein inhibitors or β-arrestin–specific siRNAs. Data are means ± SEM of 52 to 258 cells from three experiments. (F) Analysis of nuclear ERK activity in cells in which endocytosis was inhibited. Data are means ± SEM of 51 to 306 cells from three experiments. $^*P < 0.05$, $^{**}P < 0.01$, and $^{***}P < 0.001$ versus vehicle control. Data were analyzed by two-way analysis of variance (ANOVA) with Tukey's multiple comparison test. AUC, area under the curve; scram., scrambled.

ERK activity from a transient to a sustained signal, consistent with the retention of MOR at the plasma membrane (Fig. 2D and fig. S2, I and J). As expected, the increase in nuclear ERK activity in response to DAMGO was dependent on β-arrestins and receptor internalization (Fig. 2, E and F). Thus, our results suggest that $G\alpha_{i/o}$ activation by MOR mediates increases in cytosolic ERK activity in response to DAMGO and morphine, and confirm that the increases in nuclear ERK activity in response to DAMGO are dependent on β-arrestins and receptor endocytosis.

Role of PKC activation in the spatiotemporal profile of ERK in response to morphine

Inhibition of the activity of $G\alpha_{i/o}$ subunits (with NF023 or PTx) or of Gβγ subunits [with the cell-permeable N-myristoylated Gβγ-selective peptide mSIRK or by expression of βARKct, a GPCR kinase 2 (GRK2) C-terminal peptide that interferes with Gβγ function] (*25*, *26*) abolished the response of plasma membrane–localized PKC to morphine (Fig. 3A); however, knockdown of β-arrestins and negative controls (inactive mSIRK L9A and scrambled siRNA) had no such effects (Fig. 3A and fig. S3A). Thus, the sustained increase in plasma membrane–localized PKC activity that was stimulated by morphine was mediated by $G\alpha_{i/o}$ and Gβγ subunits.

Previous studies reported that PKC activity mediates the increased activity of cytosolic ERK in response to morphine (*15*). We therefore investigated whether the $G\alpha_{i/o}$-Gβγ-PKC pathway influenced the distinct ERK spatiotemporal signaling profiles of MOR. Rather than decreasing ERK activity, and in contrast to previous reports, inhibition of Gβγ subunits or of PKC (with GF109203X or Gö6983) (*27*, *28*) transformed the temporal profile of morphine-stimulated cytosolic ERK activity to resemble the transient response induced by DAMGO (Fig. 3B and fig. S3, B and C). Moreover, inhibition of the Gβγ-PKC pathway also enabled morphine to increase the activity of nuclear ERK (Fig. 3, C and D). Previous studies implicated PKCα, PKCγ, and PKCε as the PKC isoforms that contribute to morphine signaling and to the development of morphine tolerance (*16*, *29*–*32*). Of these, only the mRNAs of PKCα and PKCε were present in our HEK 293 cell line (fig. S3D). Inhibition of PKCα (with Gö6976, which targets PKCα and $PKC\beta_1$) (*33*), but not PKCε (with iPKCε, a cell-permeable PKCε inhibitory peptide) (*34*), transformed the temporal profile of morphine-stimulated cytosolic ERK activity from being sustained to be being transient and also facilitated an increase in nuclear ERK activity (fig. S3, E and F). There were no effects of inactive controls or these inhibitors on the responses of cells to DAMGO (Fig. 3, B to D, and fig. S3, C and F).

As expected, the inhibition of Gβγ subunits or PKC did not substantially affect the recruitment of β-arrestin-2 or MOR internalization in response to DAMGO, as determined by BRET analysis and high-content imaging (Fig. 3E and fig. S3, G to I). In contrast, upon inhibition of Gβγ subunits or PKC,

RESEARCH ARTICLE

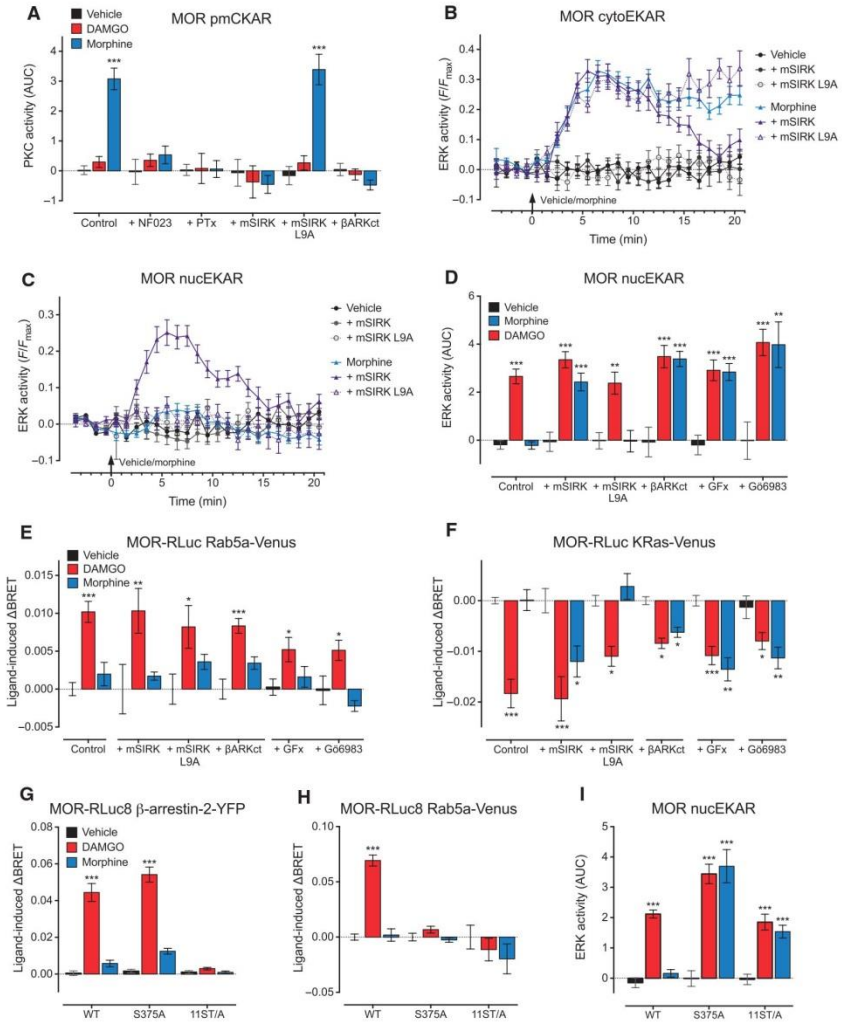

Fig. 3. The role of PKC activation by morphine in the spatiotemporal control of ERK activity. (**A**) The effects of the indicated G protein inhibitors or inactive controls on plasma membrane PKC activity in HEK 293 cells treated with vehicle, DAMGO, or morphine were determined with the pmCKAR FRET biosensor. Data are means ± SEM of 39 to 229 cells from three experiments. (**B** to **D**) Analysis of the MOR-stimulated spatiotemporal activation of ERK in response to vehicle, DAMGO, or morphine in cells in which Gβγ or PKC signaling was inhibited. (B) Analysis of cytosolic ERK activity over time. Data are means ± SEM of 31 to 101 cells from three experiments. (C) Analysis of nuclear ERK activity over time. Data are means ± SEM of 74 to 126 cells from three experiments. (D) Nuclear ERK activity was analyzed as the AUC. Data are means ± SEM of 22 to 360 cells from three experiments. (**E** and **F**) MOR trafficking in response to vehicle, DAMGO, or morphine was monitored in HEK 293 cells in the presence or absence of the indicated Gβγ and PKC inhibitors. (E) Analysis of BRET between MOR-RLuc and Rab5a-Venus. Data are means ± SEM of three to seven experiments. (F) Analysis of BRET between MOR-RLuc and KRas-Venus. Data are means ± SEM of three to seven experiments. (**G** to **I**) Effect of the indicated phosphorylation site mutations on MOR trafficking and nuclear ERK activity. (G) Analysis of BRET between MOR-RLuc8 and β-arrestin-2–YFP (yellow fluorescent protein). Data are means ± SEM of three to seven experiments. (H) Analysis of BRET between MOR-RLuc8 and Rab5a-Venus. Data are means ± SEM of three or four experiments. (I) Analysis of nuclear ERK activity over time. Data are means ± SEM of 87 to 359 cells from three to five experiments. **P* < 0.05, ***P* < 0.01, and ****P* < 0.001 versus vehicle control. Data were analyzed by two-way ANOVA with Tukey's (A and D) or Dunnett's (E to I) multiple comparison tests. GFx, GF109203X.

the activation of MOR by morphine resulted in a decrease in BRET between MOR-RLuc and the plasma membrane marker KRas-Venus (Fig. 3F), which suggested that there was an increase in the distance between these two proteins. In the absence of MOR internalization (Fig. 3E and fig. S3, G and H), the morphine-stimulated change in BRET between MOR and KRas may indicate a movement of the receptor away from KRas within the plasma membrane. Thus, the transient activation of cytosolic and nuclear ERK elicited by morphine did not require MOR internalization but may instead depend on the translocation of MOR within the plasma membrane.

The importance of the localization of MOR within the plasma membrane for the control of spatiotemporal signaling was also supported by the effects of the expression of a phosphorylation-deficient MOR mutant (S375A) (*35*). DAMGO still induced the recruitment of β-arrestin-2 to MOR S375A; however, the receptor was not internalized as determined by high-content imaging or analysis of BRET between the receptor and Rab5a (Fig. 3, G and H, and fig. S3, G and H). There was no change in the BRET between MOR S375A and KRas in response to DAMGO or morphine (fig. S3J); however, stimulation of MOR S375A by either DAMGO or morphine induced transient increases in cytosolic and nuclear ERK activity (Fig. 3I and fig. S3K).

To confirm that receptor phosphorylation was key for the control of the plasma membrane localization of MOR and its spatiotemporal signaling, we used a phosphorylation-deficient MOR mutant in which all of the C-terminal serine and threonine residues were mutated to alanines (11ST/A) (*9*). Consistent with previous reports, MOR 11ST/A was not internalized, as determined by measurement of BRET with Rab5a, nor did it recruit β-arrestin-2 in response to DAMGO (Fig. 3, G and H). However, stimulation of MOR 11ST/A by either DAMGO or morphine induced a transient increase in nuclear ERK activity, with no accompanying change in BRET between the receptor and KRas (Fig. 3I and fig. S3J). Phosphorylation of Ser^{375} therefore appears to be critical for the control of the spatiotemporal signaling by MOR in response to morphine. Together, these data suggest that the impaired trafficking of MOR mutants results in an altered signaling profile and support the hypothesis that the plasma membrane localization of MOR, and not β-arrestin recruitment or receptor internalization, plays a key role in the spatiotemporal control of receptor signaling.

Ligand-dependent redistribution of MOR within the plasma membrane

To investigate the changes in MOR distribution elicited by morphine upon inhibition of the Gβγ-PKCα pathway, we assessed receptor localization at the plasma membrane by confocal microscopy and subcellular fractionation. After 10 min of stimulation of the MOR (when all signaling pathways are activated), there was no substantial colocalization between the receptor and immunolabeled clathrin as determined by confocal microscopy analysis under any condition tested (fig. S4, A and B). However, 60 min of stimulation with DAMGO, but not morphine, caused substantial colocalization between MOR and clathrin (fig. S4C). In contrast, activation of the fast internalizing β_2-adrenergic receptor (β_2AR) by isoprenaline caused substantial receptor-clathrin colocalization after only 10 min of stimulation (fig. S4, A to C). Similarly, there was no effect of DAMGO or morphine on the location of FLAG-tagged MOR (FLAG-MOR) within non–lipid-rich (that is, Triton X-100–soluble) plasma membrane domains through basic lipid fractionation analysis (fig. S4D). Therefore, the distinct spatiotemporal signaling profiles of morphine and DAMGO do not reflect either ligand-dependent MOR clustering in clathrin-coated pits or translocation of the receptor to different lipid domains.

To investigate the localization of MOR within the plasma membrane with increased resolution, we used ground-state depletion (GSD) super-resolution microscopy in total internal reflection fluorescence (TIRF) mode. GSD-TIRF enables the detection of events within the plane of the plasma membrane to an axial resolution of 100 nm. This approach can measure the distance between an event (for example, a receptor or receptor clusters) and its nearest neighbor across a population. Stimulation of FLAG-MOR with DAMGO for 10 min increased the average distance between detected events (Fig. 4, A and B), which suggested the redistribution of MOR within the plasma membrane. This increase in distance occurred before, and was independent of, receptor internalization, because the dominant-negative dynamin K44E mutant had no effect (fig. S4, E and F).

The stimulation of cells expressing FLAG-MOR with morphine for 10 min did not change the average distance between events (Fig. 4, A and B); however, after the inhibition of Gβγ subunits, morphine increased the distance between detected MOR events (Fig. 4, C and D, and fig. S4, E and G), suggesting that activation of this pathway by morphine normally restricts MOR localization. Furthermore, the distance between MOR events under basal conditions in cells expressing MOR S375A was also increased when compared to that in cells expressing the wild-type receptor (Fig. 4, E and F). This increase in distance between events was not a result of decreased receptor abundance at the plasma membrane (MOR S375A 510,000 sites per cell, MOR wild-type 121,000 sites per cell measured by whole-cell [^{3}H]diprenorphine binding; table S1), confirming that MOR S375A was differentially distributed compared to the wild-type receptor.

Thus, our results suggest that the activation of MOR by morphine restricts receptor localization, whereas DAMGO stimulates the redistribution of MOR within the plasma membrane. Disruption of the Gβγ-PKCα pathway enabled morphine to stimulate a DAMGO-like redistribution of MOR but did not result in receptor internalization. Receptor redistribution preceded endocytosis (in the case of DAMGO) or occurred independently of endocytosis (in the case of morphine), and it appeared to control the ability of MOR to transiently activate cytosolic and nuclear ERK.

Effect of plasma membrane organization on MOR spatiotemporal signaling

To confirm the importance of membrane organization in the control of compartmentalized MOR signaling, we depleted cholesterol from the plasma membrane with methyl-β-cyclodextrin (MβCD) (*36*) or filipin III (*37*). Neither reagent had any substantial effect on MOR internalization, as determined by high-content imaging (fig. S5, A and B); however, both MβCD and filipin III abolished the distinct spatiotemporal signaling profiles of morphine and DAMGO (Fig. 5 and fig. S5). Upon cholesterol depletion, both morphine and DAMGO increased PKC activity at the plasma membrane and caused a transient increase in both cytosolic and nuclear ERK activity (Fig. 5 and fig. S5, C to F). Indeed, replenishment of membrane cholesterol by incubation of the cells with MβCD-cholesterol complexes completely restored the original spatiotemporal signaling profiles of DAMGO and morphine (Fig. 5 and fig. S5). Thus, disruption of membrane organization altered the spatiotemporal signaling profiles of MOR, with no change in the ability of the receptor to be internalized, suggesting that the plasma membrane localization of MOR plays an important role in determining its spatiotemporal signaling.

MOR compartmentalized signaling in dorsal root ganglion neurons

To confirm the physiological relevance of the spatiotemporal signaling patterns of MOR that we determined in HEK 293 cells, we used nucleofection to transfect isolated neurons from mouse dorsal root ganglions (DRGs) with the FRET biosensors. DRG neurons are the principal mediators of nociception from the periphery to the spinal cord, and activation of endogenous MOR in these neurons partially mediates the analgesic actions of opioids (*38*).

Activation of MOR in DRG neurons stimulated ERK and PKC activity with spatiotemporal profiles that were identical to those observed in HEK 293 cells. DAMGO caused a transient increase in both cytosolic and nuclear ERK activities, whereas morphine elicited a sustained increase in the activities of cytosolic ERK and plasma membrane–localized PKC (Fig. 6, A to C). Inhibition of PKC decreased the percentage of neurons (from 75 to 49%) that exhibited sustained cytosolic ERK activity in response to morphine and increased the percentage of neurons (from 25 to 51%) that exhibited a transient increase in cytosolic ERK activity (Fig. 6, D and E). There was no effect of PKC inhibition on the temporal profile of cytosolic ERK activity after stimulation with DAMGO (Fig. 6, D and E). As was observed in HEK 293 cells, inhibition of PKC enabled morphine to stimulate nuclear ERK activity in DRG neurons (Fig. 6F).

We also assessed the distribution of endogenous MOR at the plasma membrane of DRG neurons by GSD-TIRF microscopy (Fig. 6G). As was observed in HEK 293 cells, stimulation of endogenous MOR in DRG neurons with DAMGO increased the distance between detected events at the plasma membrane (Fig. 6, H and I). In contrast, there was no change in the distance between MOR events in response to morphine. Thus, in DRG neurons, as in HEK 293 cells, receptor redistribution at the plasma membrane correlated with transient increases in cytosolic and nuclear ERK activities in response to DAMGO. Moreover, inhibition of PKC enabled morphine to cause transient increases in cytosolic and nuclear ERK activities. As such, the spatiotemporal regulation of MOR activation and signaling identified in recombinant expression systems also occurred in DRG neurons endogenously expressing this receptor.

DISCUSSION

The use of biophysical approaches to assess MOR signaling in real time and in live cells revealed a previously uncharacterized mechanism that contributes to the control of differential MOR activation. Here, we showed that the activation of MOR by DAMGO stimulated the translocation of the receptor within the plasma membrane. This translocation preceded receptor trafficking to clathrin-containing domains and internalization, and is likely dependent on receptor phosphorylation (Fig. 7A). This translocation, but

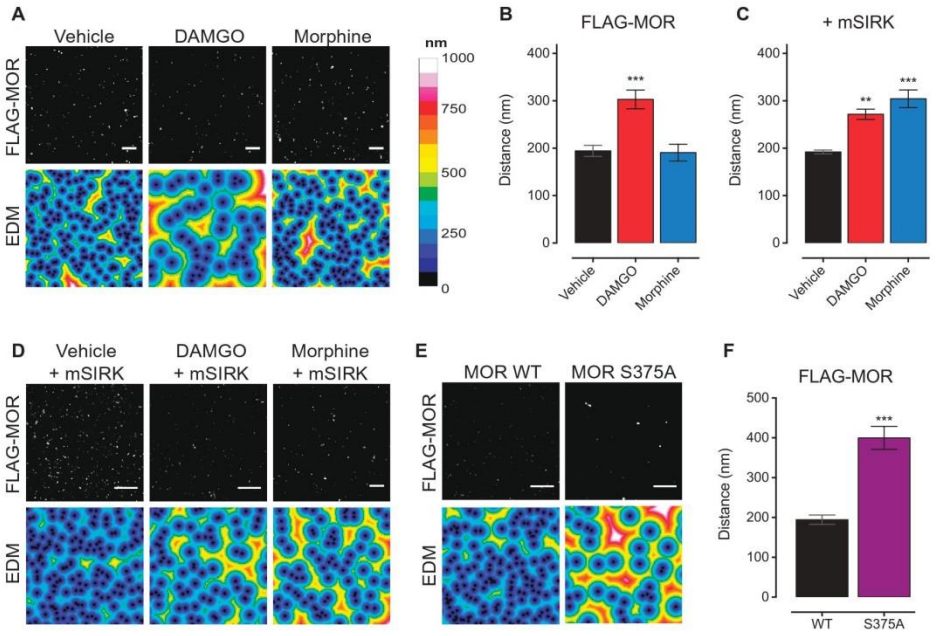

Fig. 4. DAMGO induces a distinct MOR distribution at the plasma membrane. GSD-TIRF microscopy was used to monitor the plasma membrane distribution of FLAG-MOR in HEK 293 cells in response to treatment with vehicle, DAMGO, or morphine for 10 min. (**A**) Representative GSD-TIRF images and Euclidean distance maps (EDMs) from cells under the indicated conditions. Scale bars, 1 μm. (**B**) Average distances to nearest neighbors in the cells shown in (A). Data are means ± SEM of three to nine experiments. (**C**) Average distances to nearest neighbors in cells subjected to Gβγ inhibition by preincubation with mSIRK and then treated with vehicle, DAMGO, or morphine. Data are means ± SEM of three to nine experiments. (**D**) Representative GSD-TIRF images and EDMs from cells preincubated with mSIRK to inhibit Gβγ and then subjected to the indicated treatments. Scale bars, 1 μm. Pseudocolor scale is as described in (A). (**E**) Representative GSD-TIRF images and EDMs of unstimulated cells expressing either WT MOR or the MOR S375A mutant. Scale bars, 1 μm. Pseudocolor scale is as described in (A). (**F**) Average distances to nearest neighbors in the cells shown in (E). Data are means ± SEM of three to nine experiments. $^{**}P < 0.01$ and $^{***}P < 0.001$ versus vehicle control. Data were analyzed by one-way ANOVA with Dunnett's multiple comparison test (B and C) or unpaired *t* test (E).

not internalization, of MOR determined the transient cytosolic ERK activity profile and the activation of nuclear ERK (Fig. 7A). In contrast, morphine activated plasma membrane–localized PKCα through Gβγ subunits, which prevented receptor translocation within the plasma membrane. This resulted in the sustained activity of cytosolic ERK, but not nuclear ERK (Fig. 7B). Inhibition of this Gβγ-PKCα pathway enabled the morphine-activated MOR to translocate within the plasma membrane, thus transforming its spatiotemporal signaling profile (Fig. 7B). Furthermore, this altered signaling profile mimicked that of the internalizing ligand DAMGO (that is, it was characterized by transient cytosolic and nuclear ERK activity) but occurred in the absence of β-arrestin-2 recruitment and receptor internalization.

These results add details to previous descriptions of ligand-dependent differences in ERK signaling (*14*–*16*). Previous studies used Western blotting analysis to show that etorphine-induced ERK phosphorylation was dependent on β-arrestins, whereas morphine activated ERK through a PKC-dependent pathway (*15*). However, we showed that upon PKC inhibition, morphine stimulated ERK phosphorylation, although this signal had different temporal dynamics and occurred in both the cytosol and the nucleus (Figs. 3 and 7B). Therefore, the activation of cytosolic ERK by morphine is not PKC-dependent, but rather PKC, by controlling the localization of MOR, likely determines the dynamics and location of this response. It is interesting to consider that in the context of a whole cell after its solubilization (with a relatively greater contribution of cytosolic compared to nuclear ERK), this altered temporal profile could appear as an apparent decrease in morphine-stimulated ERK activity. This illustrates the extra mechanistic detail that can be obtained by resolving spatial and temporal signaling dynamics in live cells. We therefore propose that the plasma membrane organization of MOR, and not just the recruitment of β-arrestin and subsequent receptor internalization, determines the spatiotemporal outcome of receptor activation. Furthermore, these mechanisms appear to operate in nociceptive neurons and may thus contribute to the analgesic actions of opioids.

The ability of DAMGO, but not morphine, to cause receptor redistribution may relate to differential patterns of MOR phosphorylation. Although all opioids cause the phosphorylation of MOR at Ser^{375}, this event is mediated by different kinases depending on the ligand (*9*, *39*). Previous studies showed that the DAMGO-activated MOR is phosphorylated by GRK2 and GRK3 and that internalizing ligands stimulate the higher-order phosphorylation of flanking residues, which results in efficient β-arrestin recruitment and receptor internalization (*9*). Here, we showed that the recruitment of β-arrestin-2, translocation of MOR, and activation of nuclear ERK in response to DAMGO preceded receptor internalization. As such, we hypothesize that the differential recruitment of regulatory proteins (including GRKs and β-arrestins) to MOR

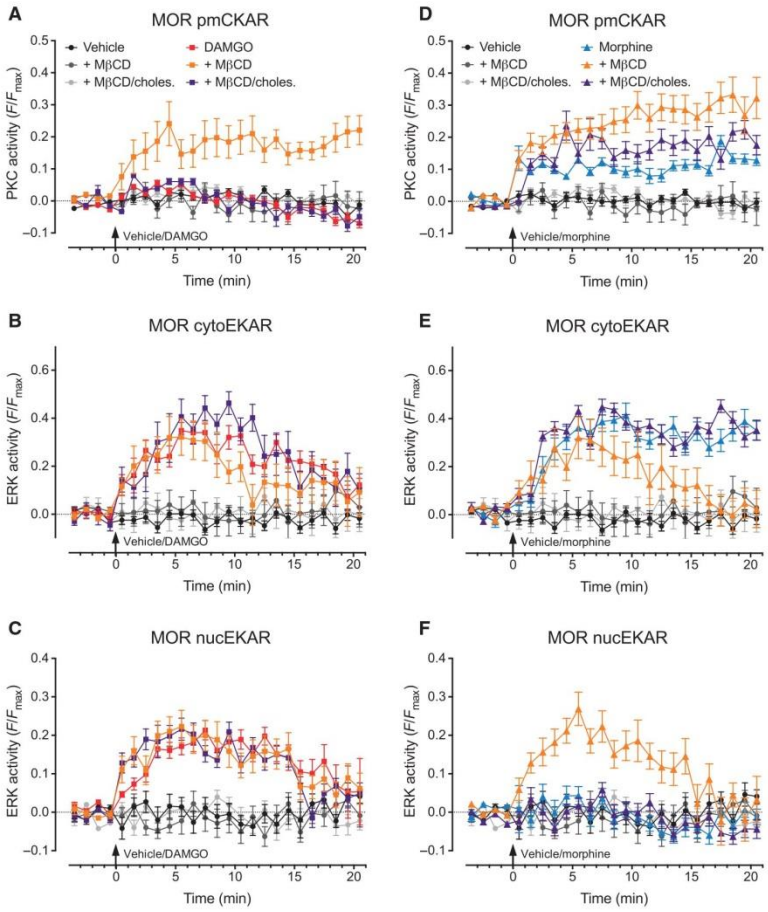

Fig. 5. Disruption of membrane architecture alters MOR signaling profiles. (A to F) HEK 293 cells were pretreated with vehicle, MβCD, or MβCD-cholesterol complexes (MβCD/choles.) before being treated with vehicle, DAMGO, or morphine. The spatiotemporal activation of plasma membrane–localized PKC and either cytoplasmic or nuclear ERK was then measured. (A) Plasma membrane–localized PKC activity in response to DAMGO. Data are means ± SEM of 40 to 174 cells from three experiments. (B) Cytosolic ERK activity in response to DAMGO. Data are means ± SEM of 30 to 167 cells from three experiments. (C) Nuclear ERK activity in response to DAMGO. Data are means ± SEM of 68 to 230 cells from three experiments. (D) Plasma membrane–localized PKC activity in response to morphine. Data are means ± SEM of 41 to 195 cells from three experiments. (E) Cytosolic ERK activity in response to morphine. Data are means ± SEM of 32 to 194 cells from three experiments. (F) Nuclear ERK activity in response to morphine. Data are means ± SEM of 80 to 217 cells from three experiments.

RESEARCH ARTICLE

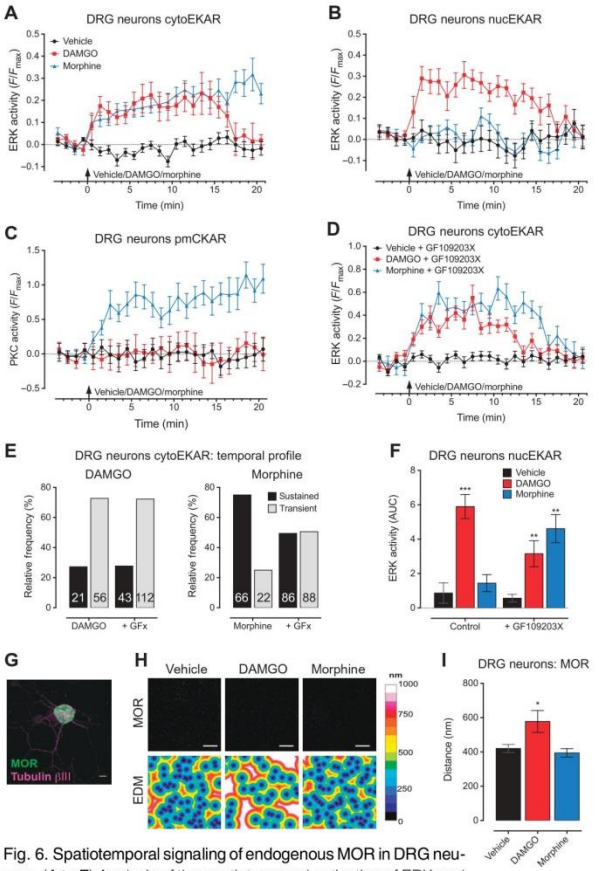

Fig. 6. Spatiotemporal signaling of endogenous MOR in DRG neurons. (**A** to **F**) Analysis of the spatiotemporal activation of ERK and PKC in DRG neurons treated with vehicle, DAMGO, or morphine. (A) Cytosolic ERK activity. Data are means ± SEM of 56 to 120 neurons from three experiments. (B) Nuclear ERK activity. Data are means ± SEM of 45 to 64 neurons from three experiments. (C) Plasma membrane–localized PKC activity. Data are means ± SEM of 40 to 55 neurons from three experiments. (D) Effect of PKC inhibition on cytosolic ERK activity. Data are means ± SEM of 86 to 99 neurons from three experiments. (E) Population analysis of the temporal profile of cytosolic ERK activity. The numbers of neurons in each group are indicated. (F) Effect of PKC inhibition on nuclear ERK activity. Data are means ± SEM of 25 to 73 neurons from three experiments. (**G** to **I**) GSD-TRIF–based analysis of the plasma membrane distribution of endogenous MOR in DRG neurons in response to treatment with vehicle, DAMGO, or morphine for 10 min. Data are means ± SEM of 9 to 15 cells from three experiments. (G) Isolated DRG neuron immunostained for MOR (green) and tubulin βIII (magenta). Scale bar, 10 μm. (H) Representative GSD-TIRF images and EDMs of DRG neurons under the indicated conditions. Scale bars, 1 μm. (I) Average distances to nearest neighbors. Data are means ± SEM of 9 to 15 cells from three experiments. *$P < 0.05$, **$P < 0.01$, and ***$P < 0.001$ versus vehicle control. Data were analyzed by two-way ANOVA with Tukey's multiple comparison test (F) or one-way ANOVA with Dunnett's multiple comparison test (I).

may underlie receptor redistribution at the plasma membrane, and thus indirectly control spatiotemporal signaling. This hypothesis is supported by the finding that mutation of the key hierarchical phosphorylation site of MOR (to generate the MOR S375A mutant) affected the localization of the receptor within the plasma membrane and its spatiotemporal signaling. In this context, β-arrestins are increasingly recognized as scaffolding proteins for signaling complexes, in addition to their traditional roles in the regulation of receptor desensitization and internalization (*40*). Furthermore, evidence suggests that GRKs can also have important scaffolding functions, particularly in the control of ERK activation (*41*, *42*). We hypothesize that the differential assembly of receptor kinases and other signaling mediators in response to morphine versus DAMGO determines MOR redistribution, transient signaling profiles, and the activation of nuclear ERK. Furthermore, this hypothesis entails that the responses of opioid ligands will be highly dependent on the specific protein content of opioid-responsive cells (*6*, *7*, *43*, *44*).

Our results also highlight the importance of PKCα in governing the spatiotemporal signaling profiles of MOR. Previous studies showed that the phosphorylation and desensitization of MOR after stimulation with morphine is partially dependent on PKC (*39*, *45*, *46*). Moreover, there are indications that PKC plays a substantial role in the initiation and maintenance of tolerance to morphine analgesia (*47*, *48*). To date, evidence for morphine-induced activation of PKC comes from coimmunoprecipitation studies showing the recruitment of overexpressed PKCε to MOR (*16*) and increased PKC activity in cell lysates (*49*). By measuring endogenous PKC activity at the subcellular level, we demonstrated that morphine, but not DAMGO, stimulated the sustained activation of PKC at the plasma membrane. Whereas PKC can phosphorylate MOR directly (*32*, *50*), it can also phosphorylate proteins that participate in MOR signaling, such as $G\alpha_i$ (*51*) or GRK2 (*52*), and could therefore restrict receptor redistribution by modulating the function, association, or both of such signaling and scaffolding proteins with MOR.

It is clear that plasma membrane organization plays a critical role in the control of MOR spatiotemporal signaling. Whether MOR resides within biochemically defined, lipid-rich plasma membrane regions is controversial (*53*–*55*). However, and consistent with our findings, previous studies provided evidence for the restricted plasma membrane localization of the receptor as well as the agonist-regulated diffusion of MOR within the plasma membrane (*56*–*59*). Protein-protein interactions were hypothesized to mediate the restricted and slow diffusion of agonist-stimulated, noninternalizing MOR (*60*). Together with this hypothesis, the results presented here suggest that the dynamic organization of MOR within the plasma membrane, rather than the association of MOR with a predefined lipid-rich domain, may control ligand-dependent receptor redistribution and distinct spatiotemporal signaling profiles. The dependence of MOR signaling on plasma membrane localization extends previous studies that demonstrated distinct control of spatiotemporal signaling by endosomally localized GPCRs (*2*, *61*). In the context of MOR, mechanistic insight into the actions of morphine at the cellular level is of particular therapeutic relevance because of the severe side effects induced by this opiate. Whether chronic exposure to opiates differentially alters the spatiotemporal signaling, plasma membrane distribution, or both of MOR remains to be investigated.

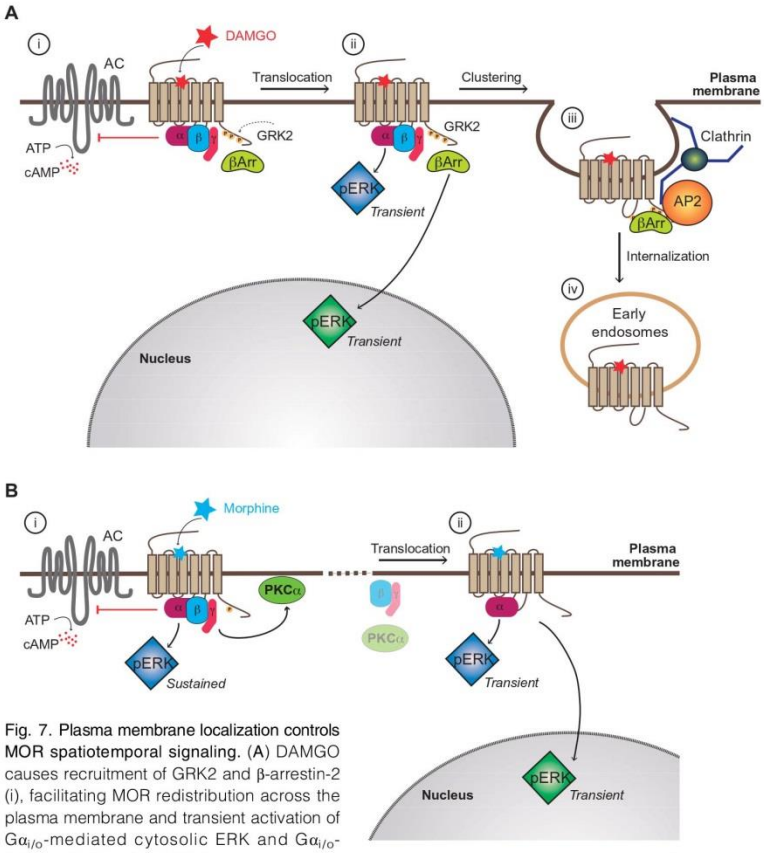

Fig. 7. Plasma membrane localization controls MOR spatiotemporal signaling. (**A**) DAMGO causes recruitment of GRK2 and β-arrestin-2 (i), facilitating MOR redistribution across the plasma membrane and transient activation of $G\alpha_{i/o}$-mediated cytosolic ERK and $G\alpha_{i/o}$-independent nuclear ERK (ii). Upon prolonged stimulation of MOR, DAMGO stimulates MOR clustering and receptor internalization through clathrin-coated pits (iii) to early endosomes (iv). (**B**) Morphine stimulates the plasma membrane–localized Gβγ-PKCα pathway, which prevents receptor translocation within the plasma membrane. This causes a sustained activation of $G\alpha_{i/o}$-mediated cytosolic ERK (i). Inhibition of the Gβγ-PKCα pathway or alteration of the organization of the plasma membrane facilitates MOR translocation and the activation of nuclear ERK by morphine (ii) in the absence of receptor internalization.

MATERIALS AND METHODS

Reagents

DAMGO was obtained from Mimotopes. Morphine and anti–FLAG M2 were from Sigma-Aldrich. Coelenterazine h was obtained from Promega. β-Arrestin-1– and β-arrestin-2–specific siRNAs were purchased from GE-Dharmacon. Mouse anti–early endosome antigen 1 was from BD Transduction Laboratories; rabbit anti-MOR (UMB-3) was from Abcam; mouse anti–tubulin βIII isoform for confocal imaging was from Merck Millipore; Alexa Fluor–conjugated goat anti-mouse secondary antibodies were from Jackson ImmunoResearch; anti–caveolin 1, anti–β-actin, and anti–clathrin heavy chain were from Abcam; anti–β-tubulin for Western blotting was from Santa Cruz Biotechnology; antibodies against β-arrestin-1/2 were from Cell Signaling Technology; and fluorescent IRDye–conjugated goat anti-rabbit (800 channel) and anti-mouse (680 channel) secondary antibodies were from LI-COR Biotechnology.

Complementary DNAs

Plasmids encoding KRas-Venus, Rab5a-Venus, green fluorescent protein (GFP)–dynamin, and GFP-dynamin K44E have been previously described (*19*, *61*, *62*). MOR-RLuc was from L. Bohn (Scripps, Jupiter, FL); FLAG-MOR was from M. Christie (University of Sydney, Sydney, New South Wales, Australia); β-arrestin-2–YFP was from M. Caron (University of North Carolina); and FLAG-MOR 11ST/A was from S. Schulz (Friedrich Schiller University, Jena, Germany). The following constructs were obtained from Addgene: cytoEKAR GFP/RFP (plasmid 18680), cytoEKAR Cerulean/Venus (plasmid 18679), nucEKAR GFP/RFP (plasmid 18682) and nucEKAR Cerulean/Venus (plasmid 18681) (*17*), and cytoCKAR (plasmid 14870) and pmCKAR (plasmid 14862) (*18*). MOR S375A has a mutation of the essential site governing hierarchical phosphorylation (human, S377A; mouse, S375A) (*9*) and was generated with the QuikChange site-directed mutagenesis kit. RLuc8-tagged MOR was generated by subcloning MOR into the pcDNA3-RLuc8 vector.

Cell culture and inhibitors

HEK 293 cells were cultured in Dulbecco's modified Eagle's medium (DMEM) supplemented with 5% (v/v) fetal bovine serum (FBS). Cells were transfected with linear polyethyleneimine (*63*). For siRNAs, cells were transfected with scrambled or combined β-arrestin-1 and β-arrestin-2 SMARTpool ON-TARGETplus siRNAs (25 nM) with Lipofectamine 2000, 24 hours before the cells were transfected with plasmids encoding receptor and biosensors. Cells were pretreated with inhibitors for 30 min at 37°C, except for filipin III, MβCD, or MβCD-cholesterol complexes (45-min pretreatment) or PTx (16-hour pretreatment). MβCD-cholesterol complexes were formed as described previously (*64*). Inhibitors were used at the following concentrations: 30 μM PitStop2 or inactive PitStop2, 10 μM NF023, PTx at 100 ng/ml, 5 μM mSIRK or mSIRK L9A, 1 μM GF109203X or Gö6983, 10 nM Gö6976, 10 μM Myr-EAVSLKPT-OH (a PKCε translocation inhibitor peptide), filipin III at 1 μg/ml, 10 mM MβCD, and 2 mM MβCD with 0.2 mM cholesterol (MβCD-cholesterol complexes). All experiments were performed in live cells at 37°C. For all regulation and trafficking experiments, cells were stimulated with an EC_{50} concentration of DAMGO or morphine (both 1 μM) as defined by β-arrestin-2 concentration-response curves (fig. S2A). For all signaling experiments, cells were stimulated with an

EC_{50} concentration of DAMGO (10 nM) or morphine (100 nM) as defined by AlphaScreen pERK assays (fig. S1A).

RNA sequencing

RNA was extracted from two passages of HEK 293 cells (P0 and P37) with the RNeasy Mini Kit (Qiagen). Transcriptome sequencing was performed by the Beijing Genomics Institute.

DRG isolation and culture

All procedures involving mice were approved by the Monash Institute of Pharmaceutical Sciences animal ethics committee. DRG neurons were isolated and transfected with 600 ng of cytoEKAR Cerulean/Venus, nucEKAR Cerulean/Venus, or pmCKAR with the Nucleofector system (Lonza). Detailed protocols of DRG isolation and nucleofection were described previously (*63*).

BRET assays

HEK 293 cells were transfected with 1 μg of MOR-RLuc and 4 μg of KRas-Venus, Rab5a-Venus, or β-arrestin-2-YFP. For coexpression, cells were transfected with an additional 2 μg of βARKct, GFP-dynamin, or GFP-dynamin K44E. After 24 hours, cells were plated in poly-D-lysine–coated 96-well plates (CulturPlate, PerkinElmer) and allowed to adhere. Forty-eight hours after transfection, the cells were equilibrated in Hanks' balanced salt solution (HBSS) and then were incubated with vehicle [0.1% dimethyl sulfoxide (DMSO)], DAMGO, or morphine for 30 min. Coelenterazine h (Promega) was added at a final concentration of 5 μM, and the cells were incubated for a further 10 min. BRET measurements were obtained with the PHERAstar Omega microplate reader (BMG Labtech), which enabled sequential integration of the signals detected at 475 ± 30 nm and 535 ± 30 nm with filters with the appropriate band pass. Data were presented as a BRET ratio (calculated as the ratio of the YFP signal to the *Renilla* luciferase signal) corrected for vehicle.

High-content image analysis

HEK 293 cells were plated in poly-D-lysine–coated, black, optically clear 96-well plates (ViewPlate, PerkinElmer) and transfected with plasmid encoding MOR-GFP (20 ng per well). Forty-eight hours after transfection, the cells were incubated with inhibitors and treated with vehicle (0.1% DMSO), DAMGO (1 μM), or morphine (1 μM) for 30 min. Cells were fixed with 4% paraformaldehyde (PFA) and washed three times with phosphate-buffered saline (PBS). Nuclei were stained with Hoechst (1 μg/ml). Images of four fields of view were collected with a GE Healthcare INCell 2000 Analyzer with a Nikon Plan Fluor ELWD 40× [numerical aperture (NA), 0.6] objective. Analysis was performed with the granularity application module in MetaMorph imaging software (v7.8.6, Molecular Devices). Granule detection was set at 4 to 8 μm, nuclei detection was set at 35 to 60 μm, and the total number of cytosolic granules per cell was calculated. The effect of vehicle was subtracted, and the data were expressed relative to the DAMGO-stimulated response (in the absence of inhibitors).

Förster resonance energy transfer

HEK 293 cells were transfected with plasmid encoding MOR (55 ng per well) and with plasmid encoding cytoEKAR GFP/RFP, nucEKAR GFP/RFP, cytoCKAR, or pmCKAR (40 ng per well). For coexpression, cells were transfected with plasmid encoding βARKct, GFP-dynamin, or GFP-dynamin K44E (50 ng per well). Experiments in which GFP-dynamin or GFP-dynamin K44E were coexpressed used the Cerulean-Venus FRET sensors. FRET was measured with a high-content GE Healthcare INCell 2000 Analyzer as described previously (*63*). Briefly, fluorescence imaging was performed with a Nikon Plan Fluor ELWD 40× (NA, 0.6) objective and FRET module. For GFP-RFP emission ratio analysis, cells were sequentially excited with a fluorescein isothiocyanate (FITC) filter (490/20) with emission measured with dsRed (RFP from *Discosoma* sp.) (605/52) and FITC (525/36) filters and a polychroic mirror, optimized for the FITC-dsRed filter pair (Quad4). For cyan fluorescent protein (CFP)–YFP or Cerulean-Venus emission ratio analysis, cells were sequentially excited with a CFP filter (430/24) with emission measured with YFP (535/30) and CFP (470/24) filters and a polychroic mirror, optimized for the CFP-YFP filter pair (Quad3). HEK 293 cells were imaged every 1 min, which enabled image capture at 14 wells/min; DRG neurons were imaged every 1 min with four fields of view per well, which enabled the capture of 3 wells/min. At the end of every experiment, the same cells were stimulated for 10 min with the positive control [200 nM phorbol 12,13-dibutyrate for ERK or 200 nM phorbol 12,13-dibutyrate with phosphatase inhibitor cocktail 2 (Sigma Aldrich) for PKC] to generate a maximal FRET change, and positive emission ratio images were captured for 4 min. Data were analyzed with the FIJI distribution of ImageJ (*65*). The three emission ratio image stacks (baseline, stimulated, and positive) were collated and aligned with the StackCreator script (*63*). Cells were selected, and fluorescence intensity was measured over the combined stack. Background intensity was subtracted, and then the FRET data were plotted as the change in FRET emission ratio relative to the maximal response for each cell [FRET ratio/maximum FRET ratio (F/F_{max})]. For HEK 293 cells, only cells that showed more than a 10% change relative to baseline after stimulation with the positive control were considered for analysis. For DRG neurons, all cells that showed more than a 3% change relative to baseline after stimulation with the positive control were considered for analysis. Ratiometric pseudocolor images were generated as previously described (*66*). The Green Fire Blue LUT was applied, and the brightness and contrast range was set to the minimum and maximum FRET ratios within the image stack (0.13 to 0.23).

GSD-TIRF microscopy

HEK 293 cells and DRG neurons were treated with vehicle (0.1% DMSO), DAMGO, or morphine as indicated in the figure legends; fixed in 4% PFA for 20 min at 4°C; washed for 15 min with PBS; blocked in PBS with 1% normal goat serum and 0.1% saponin for 1 hour at room temperature; and incubated overnight at 4°C with mouse anti-FLAG (at a 1:1000 dilution) for HEK 293 cells or with rabbit anti-MOR (UMB-3, 1:250) and anti–tubulin βIII (1:1000) for DRG neurons. Cells were washed and incubated with Alexa Fluor 568– or Alexa Fluor 647–conjugated goat anti-mouse or anti-rabbit secondary antibodies (1:400; for 2 hours at room temperature). Coverslips were mounted on a concave slide containing 100 mM cysteamine (MEA) and sealed. Cells were observed with a Leica GSD microscope with HCX PL APO 160× (NA, 1.43) objective, SuMo stage, Andor iXon Ultra 897 camera, and LAS AF software. Pumping occurred at 100% laser power until the frame correlation dropped to 0.25. Data were acquired at 50% laser power, and up to 30,000 frames were captured. TIRF penetration was at 110 nm. Only neurons with positive staining for β-tubulin were analyzed. Images were analyzed with FIJI software (*65*). Individual particles were selected with Find Maxima (noise tolerance 5) to generate a binary output of the single points. The average distance between events was calculated by generating a centroid list with the Analyze Particles command and was processed by the Nearest Neighbor Distance (NND) macro (Yuxiong Mao). EDMs were generated from the single-point binary image with the Euclidean distance option.

Whole-cell radioligand binding assays

Cells were plated in a 96-well isoplate (20,000 cells per well; PerkinElmer) and allowed to adhere for 24 hours. The cells were then washed three

times with assay buffer [146 mM NaCl, 10 mM D-glucose, 5 mM KCl, 1 mM $MgSO_4$, 2 mM $CaCl_2$, 1.5 mM $NaHCO_3$, 10 mM Hepes (pH 7.45)] and incubated for 3 hours at 4°C with increasing concentrations of [^{3}H]diprenorphine (specific activity, 36.1 Ci/mmol). Nonspecific binding was determined by the coaddition of 1 μM naloxone. After being washed in cold saline, the cells were solubilized in Optiphase scintillant, and radioactivity was measured in a MicroBeta counter (PerkinElmer).

AlphaScreen pERK signaling assays

ERK1/2 phosphorylation was detected with the AlphaScreen ERK1/2 SureFire protocol (TGR Biosciences). Briefly, cells were seeded in clear 96-well plates (40,000 cells per well) and allowed to adhere for 8 hours. Cells were washed twice with PBS and incubated in serum-free DMEM overnight at 37°C and 5% CO_2. Cells were stimulated for 5 min, and then the medium was replaced with lysis buffer in which the cells were incubated for 5 min at room temperature with agitation. Lysates were transferred to a 384-well white ProxiPlate (PerkinElmer), and then a mixture of activation buffer, reaction buffer, and AlphaScreen beads (100:600:3) was added to generate a final lysate/mixture ratio of 5:8. Plates were incubated for 1.5 hours at 37°C and then were read on a Fusion-α plate reader (PerkinElmer). Data were expressed relative to the responses of cells to vehicle (0%) and 10% (v/v) FBS (100%).

Confirmation of β-arrestin knockdown

Cells were transfected with combined β-arrestin-1– and β-arrestin-2–specific siRNAs or scrambled siRNA (25 nM) in a six-well plate. After 72 hours, cells were washed with ice-cold PBS, harvested by scraping in 1 ml of PBS, and then centrifuged at 500*g* for 5 min at 4°C. Cells were then lysed in 100 μl of lysis buffer [50 mM Tris-HCl (pH 7.4), 150 mM NaCl, 0.1 mM EDTA, 0.6% Tween 20, protease inhibitor cocktail] for 30 min on ice by passing through a 26-gauge needle 10 times. Lysates were then centrifuged at 700*g* for 5 min at 4°C; the supernatants were incubated with 50 U of deoxyribonuclease I for 1 hour at 37°C, and then Laemmli sample buffer was added.

Basic membrane fractionation

Cells transfected with 5 μg of plasmid encoding FLAG-MOR (in confluent 10-cm dishes) were treated with 0.1% DMSO (vehicle), 10 μM DAMGO, or 10 μM morphine for 10 min at 37°C; washed with ice-cold MES buffer [25 mM MES (pH 6.5), 150 mM NaCl]; and then incubated in 1 ml of ice-cold MBS buffer (MES containing 1 mM EDTA and protease inhibitor cocktail) for 10 min on ice. The cells were scraped, centrifuged at 500*g* for 5 min at 4°C, and then resuspended in 0.5 ml of MBS buffer containing 1% Triton X-100. After a 20-min incubation on ice, samples were homogenized with a 2-ml Dounce homogenizer and centrifuged at 16,000*g* for 5 min at 4°C. The supernatants were collected as the Triton X-100–soluble fractions. The pellets (the Triton X-100–insoluble fractions) were resuspended in 225 μl of MBS containing 1% Triton X-100 by sonication three times (30 s, 20% amplitude, 2-mm microprobe) with a Q125 sonicator (Qsonica). Laemmli sample buffer was added, and the samples were incubated at 37°C for 10 min.

Western blotting analysis

Samples were resolved by SDS-PAGE with 10% tris-glycine gels and then were transferred onto 0.45-μm Bio-Rad low-fluorescence polyvinylidene difluoride membranes with a Trans-Blot SD Semi-Dry Transfer Cell (Bio-Rad). Membranes were blocked for 1 hour at room temperature with Odyssey Blocking Buffer (LI-COR Biotechnology) and then were incubated with primary antibody overnight at 4°C. The membranes were washed three times in PBS containing 0.1% Tween 20, incubated with secondary antibody for 1 hour at room temperature, and then were washed three times in PBS containing 0.1% Tween 20. Secondary antibody fluorescence was detected with an Odyssey Classic Infrared Imager (LI-COR Biotechnology) with the intensity setting adjusted to be in the linear range for infrared fluorescence detection. Antibodies were used at the following dilutions: mouse anti–FLAG M2, 1:1000; rabbit anti–caveolin 1, 1:1000; rabbit anti–β-tubulin, 1:5000; rabbit anti–β-arrestin-1/2, 1:2000; mouse anti–β-actin, 1:2000; goat anti-rabbit IRDye800, 1:5000; and goat anti-mouse IRDye680, 1:10,000.

Localization of MOR or β_2AR by confocal microscopy

Cells expressing MOR-GFP were treated with vehicle (0.1% DMSO), DAMGO (1 μM), or morphine (1 μM), whereas cells expressing β_2AR-GFP were treated with vehicle (0.1% ascorbic acid) or 1 μM isoprenaline for the times indicated in the figure legends. After stimulation, the cells were fixed with 4% PFA in PBS for 20 min at 4°C and then were washed for 15 min with PBS. Cells were blocked in PBS containing 1% normal goat serum and 0.1% saponin for 1 hour at room temperature and then were incubated with rabbit anti–clathrin heavy chain (1:1000) overnight at 4°C. Cells were washed and incubated with Alexa Fluor 568–conjugated goat anti-rabbit secondary antibody (1:400) for 2 hours at room temperature. To visualize the colocalization of MOR-GFP or β_2AR-GFP with clathrin in HEK 293 cells or of MOR with β-tubulin in DRG neurons, cells were observed with a Leica SP8 confocal microscope and HCX PL APO 63× CS2 (NA, 1.40) oil objective. Images were collected at a zoom of 1 to 3, and three to five optical sections were taken at intervals of 0.39 μm. Colocalization between receptor and clathrin was quantified with the colocalization threshold command in FIJI (*65*) after background intensity was subtracted from the corresponding images.

SUPPLEMENTARY MATERIALS

www.sciencesignaling.org/cgi/content/full/9/414/ra16/DC1

Fig. S1. Ligand-dependent spatiotemporal signaling of MOR.

Fig. S2. MOR regulation and its effect on cytosolic ERK activity.

Fig. S3. Roles of PKC and receptor phosphorylation on the MOR-dependent spatiotemporal profiles of ERK signaling.

Fig. S4. MOR localization within the plasma membrane is ligand-dependent.

Fig. S5. Effect of membrane disruption on MOR trafficking and spatiotemporal signaling.

Table S1. Expression of wild-type MOR and the MOR S375A mutant.

REFERENCES AND NOTES

1. N. G. Tsvetanova, M. von Zastrow, Spatial encoding of cyclic AMP signaling specificity by GPCR endocytosis. *Nat. Chem. Biol.* **10**, 1061–1065 (2014).
2. D. Calebiro, V. O. Nikolaev, M. C. Gagliani, T. de Filippis, C. Dees, C. Tacchetti, L. Persani, M. J. Lohse, Persistent cAMP-signals triggered by internalized G-protein–coupled receptors. *PLOS Biol.* **7**, e1000172 (2009).
3. V. O. Nikolaev, M. Bünemann, E. Schmitteckert, M. J. Lohse, S. Engelhardt, Cyclic AMP imaging in adult cardiac myocytes reveals far-reaching β_1-adrenergic but locally confined β_2-adrenergic receptor–mediated signaling. *Circ. Res.* **99**, 1084–1091 (2006).
4. K. Ahlbeck, Opioids: A two-faced Janus. *Curr. Med. Res. Opin.* **27**, 439–448 (2011).
5. R. Al-Hasani, M. R. Bruchas, Molecular mechanisms of opioid receptor-dependent signaling and behavior. *Anesthesiology* **115**, 1363–1381 (2011).
6. J. L. Whistler, M. von Zastrow, Morphine-activated opioid receptors elude desensitization by β-arrestin. *Proc. Natl. Acad. Sci. U.S.A.* **95**, 9914–9919 (1998).
7. J. Zhang, S. S. G. Ferguson, L. S. Barak, S. R. Bodduluri, S. A. Laporte, P.-Y. Law, M. G. Caron, Role for G protein-coupled receptor kinase in agonist-specific regulation of μ-opioid receptor responsiveness. *Proc. Natl. Acad. Sci. U.S.A.* **95**, 7157–7162 (1998).
8. N. Quillinan, E. K. Lau, M. Virk, M. von Zastrow, J. T. Williams, Recovery from μ-opioid receptor desensitization after chronic treatment with morphine and methadone. *J. Neurosci.* **31**, 4434–4443 (2011).
9. S. Just, S. Illing, M. Trester-Zedlitz, E. K. Lau, S. J. Kotowski, E. Miess, A. Mann, C. Doll, J. C. Trinidad, A. L. Burlingame, M. von Zastrow, S. Schulz, Differentiation of opioid drug effects by hierarchical multi-site phosphorylation. *Mol. Pharmacol.* **83**, 633–639 (2013).

10. D. E. Keith, S. R. Murray, P. A. Zaki, P. C. Chu, D. V. Lissin, L. Kang, C. J. Evans, M. von Zastrow, Morphine activates opioid receptors without causing their rapid internalization. *J. Biol. Chem.* **271**, 19021–19024 (1996).
11. L. M. Bohn, R. J. Lefkowitz, R. R. Gainetdinov, K. Peppel, M. G. Caron, F.-T. Lin, Enhanced morphine analgesia in mice lacking β-arrestin 2. *Science* **286**, 2495–2498 (1999).
12. C. E. Groer, K. Tidgewell, R. A. Moyer, W. W. Harding, R. B. Rothman, T. E. Prisinzano, L. M. Bohn, An opioid agonist that does not induce μ-opioid receptor—Arrestin interactions or receptor internalization. *Mol. Pharmacol.* **71**, 549–557 (2007).
13. S. M. DeWire, D. S. Yamashita, D. H. Rominger, G. Liu, C. L. Cowan, T. M. Graczyk, X.-T. Chen, P. M. Pitis, D. Gotchev, C. Yuan, M. Koblish, M. W. Lark, J. D. Violin, A G protein-biased ligand at the μ-opioid receptor is potently analgesic with reduced gastrointestinal and respiratory dysfunction compared with morphine. *J. Pharmacol. Exp. Ther.* **344**, 708–717 (2013).
14. H. Zheng, J. Chu, Y. Qiu, H. H. Loh, P.-Y. Law, Agonist-selective signaling is determined by the receptor location within the membrane domains. *Proc. Natl. Acad. Sci. U.S.A.* **105**, 9421–9426 (2008).
15. H. Zheng, H. H. Loh, P.-Y. Law, β-Arrestin-dependent μ-opioid receptor-activated extracellular signal-regulated kinases (ERKs) translocate to nucleus in contrast to G protein-dependent ERK activation. *Mol. Pharmacol.* **73**, 178–190 (2008).
16. H. Zheng, J. Chu, Y. Zhang, H. H. Loh, P.-Y. Law, Modulating μ-opioid receptor phosphorylation switches agonist-dependent signaling as reflected in PKCε activation and dendritic spine stability. *J. Biol. Chem.* **286**, 12724–12733 (2011).
17. C. D. Harvey, A. G. Ehrhardt, C. Cellurale, H. Zhong, R. Yasuda, R. J. Davis, K. Svoboda, A genetically encoded fluorescent sensor of ERK activity. *Proc. Natl. Acad. Sci. U.S.A.* **105**, 19264–19269 (2008).
18. J. D. Violin, J. Zhang, R. Y. Tsien, A. C. Newton, A genetically encoded fluorescent reporter reveals oscillatory phosphorylation by protein kinase C. *J. Cell Biol.* **161**, 899–909 (2003).
19. T.-H. Lan, Q. Liu, C. Li, G. Wu, N. A. Lambert, Sensitive and high resolution localization and tracking of membrane proteins in live cells with BRET. *Traffic* **13**, 1450–1456 (2012).
20. D. D. Jensen, C. B. Godfrey, C. Niklas, M. Canals, M. Kocan, D. P. Poole, J. E. Murphy, F. Alemi, G. S. Cottrell, C. Korbmacher, N. A. Lambert, N. W. Bunnett, C. U. Corvera, The bile acid receptor TGR5 does not interact with β-arrestins or traffic to endosomes but transmits sustained signals from plasma membrane rafts. *J. Biol. Chem.* **288**, 22942–22960 (2013).
21. M. Freissmuth, S. Boehm, W. Beindl, P. Nickel, A. P. IJzerman, M. Hohenegger, C. Nanoff, Suramin analogues as subtype-selective G protein inhibitors. *Mol. Pharmacol.* **49**, 602–611 (1996).
22. T. Katada, M. Ui, Direct modification of the membrane adenylate cyclase system by islet-activating protein due to ADP-ribosylation of a membrane protein. *Proc. Natl. Acad. Sci. U.S.A.* **79**, 3129–3133 (1982).
23. L. von Kleist, W. Stahlschmidt, H. Bulut, K. Gromova, D. Puchkov, M. J. Robertson, K. A. MacGregor, N. Tomilin, A. Pechstein, N. Chau, M. Chircop, J. Sakoff, J. P. von Kries, W. Saenger, H.-G. Kräusslich, O. Shupliakov, P. J. Robinson, A. McCluskey, V. Haucke, Role of the clathrin terminal domain in regulating coated pit dynamics revealed by small molecule inhibition. *Cell* **146**, 471–484 (2011).
24. J. S. Herskovits, C. C. Burgess, R. A. Obar, R. B. Vallee, Effects of mutant rat dynamin on endocytosis. *J. Cell Biol.* **122**, 565–578 (1993).
25. J. K. Scott, S.-F. Huang, B. P. Gangadhar, G. M. Samoriski, P. Clapp, R. A. Gross, R. Taussig, A. V. Smrcka, Evidence that a protein-protein interaction "hot spot on heterotrimeric G protein βγ subunits is used for recognition of a subclass of effectors. *EMBO J.* **20**, 767–776 (2001).
26. W. J. Koch, B. E. Hawes, J. Inglese, L. M. Luttrell, R. J. Lefkowitz, Cellular expression of the carboxyl terminus of a G protein-coupled receptor kinase attenuates $G_{\beta\gamma}$-mediated signaling. *J. Biol. Chem.* **269**, 6193–6197 (1994).
27. D. Toullec, P. Pianetti, H. Coste, P. Bellevergue, T. Grand-Perret, M. Ajakane, V. Baudet, P. Boissin, E. Boursier, F. Loriolle, L. Duhamel, D. Charon, J. Kirilovsky, The bisindolylmaleimide GF 109203X is a potent and selective inhibitor of protein kinase C. *J. Biol. Chem.* **266**, 15771–15781 (1991).
28. M. Gschwendt, S. Dieterich, J. Rennecke, W. Kittstein, H.-J. Mueller, F.-J. Johannes, Inhibition of protein kinase C μ by various inhibitors. Inhibition from protein kinase c isoenzymes. *FEBS Lett.* **392**, 77–80 (1996).
29. C. P. Bailey, S. Oldfield, J. Llorente, C. J. Caunt, A. G. Teschemacher, L. Roberts, C. A. McArdle, F. L. Smith, W. L. Dewey, E. Kelly, G. Henderson, Involvement of PKCα and G-protein-coupled receptor kinase 2 in agonist-selective desensitization of μ-opioid receptors in mature brain neurons. *Br. J. Pharmacol.* **158**, 157–164 (2009).
30. M. Inoue, H. Ueda, Protein kinase C-mediated acute tolerance to peripheral μ-opioid analgesia in the bradykinin-nociception test in mice. *J. Pharmacol. Exp. Ther.* **293**, 662–669 (2000).
31. F. L. Smith, B. H. Gabra, P. A. Smith, M. C. Redwood, W. L. Dewey, Determination of the role of conventional, novel and atypical PKC isoforms in the expression of morphine tolerance in mice. *Pain* **127**, 129–139 (2007).
32. S. Illing, A. Mann, S. Schulz, Heterologous regulation of agonist-independent μ-opioid receptor phosphorylation by protein kinase C. *Br. J. Pharmacol.* **171**, 1330–1340 (2014).
33. G. Martiny-Baron, M. G. Kazanietz, H. Mischak, P. M. Blumberg, G. Kochs, H. Hug, D. Marmé, C. Schächtele, Selective inhibition of protein kinase C isozymes by the indolocarbazole Gö 6976. *J. Biol. Chem.* **268**, 9194–9197 (1993).
34. J. A. Johnson, M. O. Gray, C.-H. Chen, D. Mochly-Rosen, A protein kinase C translocation inhibitor as an isozyme-selective antagonist of cardiac function. *J. Biol. Chem.* **271**, 24962–24966 (1996).
35. S. Schulz, D. Mayer, M. Pfeiffer, R. Stumm, T. Koch, V. Höllt, Morphine induces terminal μ-opioid receptor desensitization by sustained phosphorylation of serine-375. *EMBO J.* **23**, 3282–3289 (2004).
36. Y. Ohtani, T. Irie, K. Uekama, K. Fukunaga, J. Pitha, Differential effects of α-, β- and γ-cyclodextrins on human erythrocytes. *Eur. J. Biochem.* **186**, 17–22 (1989).
37. A. W. Norman, R. A. Demel, B. de Kruyff, L. L. M. van Deenen, Studies on the biological properties of polyene antibiotics. Evidence for the direct interaction of filipin with cholesterol. *J. Biol. Chem.* **247**, 1918–1929 (1972).
38. A. I. Basbaum, D. M. Bautista, G. Scherrer, D. Julius, Cellular and molecular mechanisms of pain. *Cell* **139**, 267–284 (2009).
39. C. Doll, J. Konietzko, F. Pöll, T. Koch, V. Höllt, S. Schulz, Agonist-selective patterns of μ-opioid receptor phosphorylation revealed by phosphosite-specific antibodies. *Br. J. Pharmacol.* **164**, 298–307 (2011).
40. K. A. DeFea, β-Arrestins as regulators of signal termination and transduction: How do they determine what to scaffold? *Cell. Signal.* **23**, 621–629 (2011).
41. J. D. Robinson, J. A. Pitcher, G protein-coupled receptor kinase 2 (GRK2) is a Rho-activated scaffold protein for the ERK MAP kinase cascade. *Cell. Signal.* **25**, 2831–2839 (2013).
42. P. Penela, C. Ribas, I. Aymerich, N. Eijkelkamp, O. Barreiro, C. Heijnen, A. Kavelaars, F. Sánchez-Madrid, F. Mayor, G protein-coupled receptor kinase 2 positively regulates epithelial cell migration. *EMBO J.* **27**, 1206–1218 (2008).
43. H. Haberstock-Debic, M. Wein, M. Barrot, E. E. O. Colago, Z. Rahman, R. L. Neve, V. M. Pickel, E. J. Nestler, M. von Zastrow, A. L. Svingos, Morphine acutely regulates opioid receptor trafficking selectively in dendrites of nucleus accumbens neurons. *J. Neurosci.* **23**, 4324–4332 (2003).
44. H. Haberstock-Debic, K.-A. Kim, Y. J. Yu, M. von Zastrow, Morphine promotes rapid, arrestin-dependent endocytosis of μ-opioid receptors in striatal neurons. *J. Neurosci.* **25**, 7847–7857 (2005).
45. C. P. Bailey, F. L. Smith, E. Kelly, W. L. Dewey, G. Henderson, How important is protein kinase C in μ-opioid receptor desensitization and morphine tolerance? *Trends Pharmacol. Sci.* **27**, 558–565 (2006).
46. E. A. Johnson, S. Oldfield, E. Braksator, A. Gonzalez-Cuello, D. Couch, K. J. Hall, S. J. Mundell, C. P. Bailey, E. Kelly, G. Henderson, Agonist-selective mechanisms of μ-opioid receptor desensitization in human embryonic kidney 293 cells. *Mol. Pharmacol.* **70**, 676–685 (2006).
47. X.-Y. Hua, A. Moore, S. Malkmus, S. F. Murray, N. Dean, T. L. Yaksh, M. Butler, Inhibition of spinal protein kinase Cα expression by an antisense oligonucleotide attenuates morphine infusion-induced tolerance. *Neuroscience* **113**, 99–107 (2002).
48. F. L. Smith, A. B. Lohmann, W. L. Dewey, Involvement of phospholipid signal transduction pathways in morphine tolerance in mice. *Br. J. Pharmacol.* **128**, 220–226 (1999).
49. Y. Qiu, W. Zhao, Y. Wang, J.-R. Xu, E. Huie, S. Jiang, Y.-H. Yan, H. H. Loh, H.-Z. Chen, P.-Y. Law, FK506-binding protein 12 modulates μ-opioid receptor phosphorylation and protein kinase Cε–dependent signaling by its direct interaction with the receptor. *Mol. Pharmacol.* **85**, 37–49 (2014).
50. B. Feng, Z. Li, J. B. Wang, Protein kinase C-mediated phosphorylation of the μ-opioid receptor and its effects on receptor signaling. *Mol. Pharmacol.* **79**, 768–775 (2011).
51. J. Chu, H. Zheng, Y. Zhang, H. H. Loh, P.-Y. Law, Agonist-dependent μ-opioid receptor signaling can lead to heterologous desensitization. *Cell. Signal.* **22**, 684–696 (2010).
52. R. Winstel, S. Freund, C. Krasel, E. Hoppe, M. J. Lohse, Protein kinase cross-talk: Membrane targeting of the β-adrenergic receptor kinase by protein kinase C. *Proc. Natl. Acad. Sci. U.S.A.* **93**, 2105–2109 (1996).
53. P. Huang, W. Xu, S.-l. Yoon, C. Chen, P. L.-G. Chong, E. M. Unterwald, L.-Y. Liu-Chen, Agonist treatment did not affect association of mu opioid receptors with lipid rafts and cholesterol reduction had opposite effects on the receptor-mediated signaling in rat brain and CHO cells. *Brain Res.* **1184**, 46–56 (2007).
54. G. Gaibelet, C. Millot, C. Lebrun, S. Ravault, A. Saulière, A. André, B. Lagane, A. Lopez, Cholesterol content drives distinct pharmacological behaviours of μ-opioid receptor in different microdomains of the CHO plasma membrane. *Mol. Membr. Biol.* **25**, 423–435 (2008).
55. L. Moulédous, S. Merker, J. Neasta, B. Roux, J.-M. Zajac, C. Mollereau, Neuropeptide FF-sensitive confinement of mu opioid receptor does not involve lipid rafts in SH-SY5Y cells. *Biochem. Biophys. Res. Commun.* **373**, 80–84 (2008).
56. K. Suzuki, K. Ritchie, E. Kajikawa, T. Fujiwara, A. Kusumi, Rapid hop diffusion of a G protein-coupled receptor in the plasma membrane as revealed by single-molecule techniques. *Biophys. J.* **88**, 3659–3680 (2005).

57. F. Daumas, N. Destainville, C. Millot, A. Lopez, D. Dean, L. Salomé, Confined diffusion without fences of a G protein-coupled receptor as revealed by single particle tracking. *Biophys. J.* **84**, 356–366 (2003).
58. F. Daumas, N. Destainville, C. Millot, A. Lopez, D. Dean, L. Salomé, Interprotein interactions are responsible for the confined diffusion of a G-protein-coupled receptor at the cell surface. *Biochem. Soc. Trans.* **31**, 1001–1005 (2003).
59. A. Saulière, G. Gaibelet, C. Millot, S. Mazères, A. Lopez, L. Salomé, Diffusion of the mu opioid receptor at the surface of human neuroblastoma SH-SY5Y cells is restricted to permeable domains. *FEBS Lett.* **580**, 5227–5231 (2006).
60. A. Lopez, L. Salomé, Membrane functional organisation and dynamic of μ-opioid receptors. *Cell. Mol. Life Sci.* **66**, 2093–2108 (2009).
61. D. D. Jensen, M. L. Halls, J. E. Murphy, M. Canals, F. Cattaruzza, D. P. Poole, T. Lieu, H.-W. Koon, C. Pothoulakis, N. W. Bunnett, Endothelin-converting enzyme 1 and β-arrestins exert spatiotemporal control of substance P-induced inflammatory signals. *J. Biol. Chem.* **289**, 20283–20294 (2014).
62. F. Schmidlin, O. Déry, K. O. DeFea, L. Slice, S. Patierno, C. Stemini, E. F. Grady, N. W. Bunnett, Dynamin and Rab5a-dependent trafficking and signaling of the neurokinin 1 receptor. *J. Biol. Chem.* **276**, 25427–25437 (2001).
63. M. L. Halls, D. P. Poole, A. M. Ellisdon, C. J. Nowell, M. Canals, in *Methods in Molecular Biology* (Springer, New York, 2015), vol. 1335, pp. 131–161.
64. U. Klein, G. Gimpl, F. Fahrenholz, Alteration of the myometrial plasma membrane cholesterol content with β-cyclodextrin modulates the binding affinity of the oxytocin receptor. *Biochemistry* **34**, 13784–13793 (1995).
65. J. Schindelin, I. Arganda-Carreras, E. Frise, V. Kaynig, M. Longair, T. Pietzsch, S. Preibisch, C. Rueden, S. Saalfeld, B. Schmid, J.-Y. Tinevez, D. J. White, V. Hartenstein, K. Eliceiri, P. Tomancak, A. Cardona, Fiji: An open-source platform for biological-image analysis. *Nat. Methods* **9**, 676–682 (2012).
66. E. Kardash, J. Bandemer, E. Raz, Imaging protein activity in live embryos using fluorescence resonance energy transfer biosensors. *Nat. Protoc.* **6**, 1835–1846 (2011).

Acknowledgments: We thank D. D. Jensen for technical assistance; M. J. Christie for critical discussion; R. J. Summers, J. R. Lane, and A. M. Ellisdon for careful review of this manuscript; and L. Bohn, S. Schulz, and M. Caron for providing DNAs. **Funding:** This work was supported by a Monash Fellowship to M.C.; National Health and Medical Research Council (NHMRC) RD Wright Fellowship to M.L.H. (1061687); NHMRC Australia Fellowship to N.W.B. (63303); NHMRC Project Grants (1011796, 1047633, 1049682, and 1031886) to M.C., M.L.H., and N.W.B.; ARC Centre of Excellence in Convergent Bio-Nano Science and Technology, Monash Institute of Pharmaceutical Sciences Large Grant Support Scheme grants to M.C. and M.L.H.; and Monash University support to N.W.B. G.L.T. is funded by DSTO (Defence Science and Technology Organisation) Australia. **Author contributions:** M.L.H. and M.C. designed the study; M.L.H., H.R.Y., C.J.N., G.L.T., A.B.G., S.C., D.P.P., and M.C. performed the experiments; M.L.H. and M.C. analyzed and interpreted the data; M.L.H. and M.C. drafted and wrote the manuscript; all authors reviewed the manuscript; and N.W.B. and N.A.L. provided reagents. **Competing interests:** The authors declare that they have no competing interests.

Submitted 28 June 2015
Accepted 25 January 2016
Final Publication 9 February 2016
10.1126/scisignal.aac9177
Citation: M. L. Halls, H. R. Yeatman, C. J. Nowell, G. L. Thompson, A. B. Gondin, S. Civciristov, N. W. Bunnett, N. A. Lambert, D. P. Poole, M. Canals, Plasma membrane localization of the μ-opioid receptor controls spatiotemporal signaling. *Sci. Signal.* **9**, ra16 (2016).

REFERENCES

[1] R. Fredriksson, M.C. Lagerstrom, L.G. Lundin, H.B. Schioth, The G-protein-coupled receptors in the human genome form five main families. Phylogenetic analysis, paralogon groups, and fingerprints, Mol Pharmacol 63(6) (2003) 1256-72.
[2] H.G. Dohlman, M.G. Caron, R.J. Lefkowitz, Structure and function of the beta 2-adrenergic receptor--homology with rhodopsin, Kidney international. Supplement 23 (1987) S2-13.
[3] K. Palczewski, T. Kumasaka, T. Hori, C.A. Behnke, H. Motoshima, B.A. Fox, I. Le Trong, D.C. Teller, T. Okada, R.E. Stenkamp, M. Yamamoto, M. Miyano, Crystal structure of rhodopsin: A G protein-coupled receptor, Science 289(5480) (2000) 739-45.
[4] V. Cherezov, D.M. Rosenbaum, M.A. Hanson, S.G. Rasmussen, F.S. Thian, T.S. Kobilka, H.J. Choi, P. Kuhn, W.I. Weis, B.K. Kobilka, R.C. Stevens, High-resolution crystal structure of an engineered human beta2-adrenergic G protein-coupled receptor, Science 318(5854) (2007) 1258-65.
[5] S. Kaushal, K.D. Ridge, H.G. Khorana, Structure and function in rhodopsin: the role of asparagine-linked glycosylation, Proc Natl Acad Sci U S A 91(9) (1994) 4024-8.
[6] S.T. George, A.E. Ruoho, C.C. Malbon, N-glycosylation in expression and function of beta-adrenergic receptors, J Biol Chem 261(35) (1986) 16559-64.
[7] M. Kahn, K. Ishii, W.L. Kuo, M. Piper, A. Connolly, Y.P. Shi, R. Wu, C.C. Lin, S.R. Coughlin, Conserved structure and adjacent location of the thrombin receptor and protease-activated receptor 2 genes define a protease-activated receptor gene cluster, Molecular medicine (Cambridge, Mass.) 2(3) (1996) 349-57.
[8] T.K. Vu, D.T. Hung, V.I. Wheaton, S.R. Coughlin, Molecular cloning of a functional thrombin receptor reveals a novel proteolytic mechanism of receptor activation, Cell 64(6) (1991) 1057-68.
[9] C.R. Grace, M.H. Perrin, M.R. DiGruccio, C.L. Miller, J.E. Rivier, W.W. Vale, R. Riek, NMR structure and peptide hormone binding site of the first extracellular domain of a type B1 G protein-coupled receptor, Proc Natl Acad Sci U S A 101(35) (2004) 12836-41.
[10] U. Grauschopf, H. Lilie, K. Honold, M. Wozny, D. Reusch, A. Esswein, W. Schafer, K.P. Rucknagel, R. Rudolph, The N-terminal fragment of human parathyroid hormone receptor 1 constitutes a hormone binding domain and reveals a distinct disulfide pattern, Biochemistry 39(30) (2000) 8878-87.
[11] M.H. Perrin, S. Sutton, D.L. Bain, W.T. Berggren, W.W. Vale, The first extracellular domain of corticotropin releasing factor-R1 contains major binding determinants for urocortin and astressin, Endocrinology 139(2) (1998) 566-70.
[12] Y.J. Cao, G. Gimpl, F. Fahrenholz, The amino-terminal fragment of the adenylate cyclase activating polypeptide (PACAP) receptor functions as a high affinity PACAP binding domain, Biochemical and biophysical research communications 212(2) (1995) 673-80.
[13] H. Brauner-Osborne, A.A. Jensen, P.O. Sheppard, P. O'Hara, P. Krogsgaard-Larsen, The agonist-binding domain of the calcium-sensing receptor is located at the amino-terminal domain, J Biol Chem 274(26) (1999) 18382-6.
[14] T. Okamoto, N. Sekiyama, M. Otsu, Y. Shimada, A. Sato, S. Nakanishi, H. Jingami, Expression and purification of the extracellular ligand binding region of metabotropic glutamate receptor subtype 1, J Biol Chem 273(21) (1998) 13089-96.
[15] P.J. O'Hara, P.O. Sheppard, H. Thogersen, D. Venezia, B.A. Haldeman, V. McGrane, K.M. Houamed, C. Thomsen, T.L. Gilbert, E.R. Mulvihill, The ligand-binding

domain in metabotropic glutamate receptors is related to bacterial periplasmic binding proteins, Neuron 11(1) (1993) 41-52.
[16] J.P. Dijksterhuis, J. Petersen, G. Schulte, WNT/Frizzled signalling: receptor-ligand selectivity with focus on FZD-G protein signalling and its physiological relevance: IUPHAR Review 3, Br J Pharmacol 171(5) (2014) 1195-209.
[17] T. Langenhan, G. Aust, J. Hamann, Sticky signaling--adhesion class G protein-coupled receptors take the stage, Sci Signal 6(276) (2013) re3.
[18] F.Y. Siu, M. He, C. de Graaf, G.W. Han, D. Yang, Z. Zhang, C. Zhou, Q. Xu, D. Wacker, J.S. Joseph, W. Liu, J. Lau, V. Cherezov, V. Katritch, M.-W. Wang, R.C. Stevens, Structure of the class B human glucagon G protein coupled receptor, Nature 499(7459) (2013) 10.1038/nature12393.
[19] C. Wang, H. Wu, V. Katritch, G.W. Han, X.P. Huang, W. Liu, F.Y. Siu, B.L. Roth, V. Cherezov, R.C. Stevens, Structure of the human smoothened receptor bound to an antitumour agent, Nature 497(7449) (2013) 338-43.
[20] H. Wu, C. Wang, K.J. Gregory, G.W. Han, H.P. Cho, Y. Xia, C.M. Niswender, V. Katritch, J. Meiler, V. Cherezov, P.J. Conn, R.C. Stevens, Structure of a class C GPCR metabotropic glutamate receptor 1 bound to an allosteric modulator(), Science (New York, N.Y.) 344(6179) (2014) 58-64.
[21] V.M. Unger, P.A. Hargrave, J.M. Baldwin, G.F.X. Schertler, Arrangement of rhodopsin transmembrane [alpha]-helices, Nature 389(6647) (1997) 203-206.
[22] T. Mizobe, M. Maze, V. Lam, S. Suryanarayana, B.K. Kobilka, Arrangement of Transmembrane Domains in Adrenergic Receptors: SIMILARITY TO BACTERIORHODOPSIN, Journal of Biological Chemistry 271(5) (1996) 2387-2389.
[23] E. Pebay-Peyroula, G. Rummel, J.P. Rosenbusch, E.M. Landau, X-ray Structure of Bacteriorhodopsin at 2.5 Angstroms from Microcrystals Grown in Lipidic Cubic Phases, Science 277(5332) (1997) 1676-1681.
[24] R.A. Dixon, I.S. Sigal, E. Rands, R.B. Register, M.R. Candelore, A.D. Blake, C.D. Strader, Ligand binding to the beta-adrenergic receptor involves its rhodopsin-like core, Nature 326(6108) (1987) 73-7.
[25] M.R. Tota, C.D. Strader, Characterization of the binding domain of the beta-adrenergic receptor with the fluorescent antagonist carazolol. Evidence for a buried ligand binding site, J Biol Chem 265(28) (1990) 16891-7.
[26] B.K. Kobilka, T.S. Kobilka, K. Daniel, J.W. Regan, M.G. Caron, R.J. Lefkowitz, Chimeric alpha 2-,beta 2-adrenergic receptors: delineation of domains involved in effector coupling and ligand binding specificity, Science 240(4857) (1988) 1310-6.
[27] V. Katritch, V. Cherezov, R.C. Stevens, Diversity and Modularity of G Protein-Coupled Receptor Structures, Trends in Pharmacological Sciences 33(1) (2012) 17-27.
[28] M. Wheatley, D. Wootten, M.T. Conner, J. Simms, R. Kendrick, R.T. Logan, D.R. Poyner, J. Barwell, Lifting the lid on GPCRs: the role of extracellular loops, Br J Pharmacol 165(6) (2012) 1688-703.
[29] A. Manglik, A.C. Kruse, T.S. Kobilka, F.S. Thian, J.M. Mathiesen, R.K. Sunahara, L. Pardo, W.I. Weis, B.K. Kobilka, S. Granier, Crystal structure of the micro-opioid receptor bound to a morphinan antagonist, Nature 485(7398) (2012) 321-6.
[30] J.M. Taylor, G.G. Jacob-Mosier, R.G. Lawton, A.E. Remmers, R.R. Neubig, Binding of an alpha 2 adrenergic receptor third intracellular loop peptide to G beta and the amino terminus of G alpha, J Biol Chem 269(44) (1994) 27618-24.
[31] M. Havlickova, J. Blahos, I. Brabet, J. Liu, B. Hruskova, L. Prezeau, J.P. Pin, The second intracellular loop of metabotropic glutamate receptors recognizes C termini of G-protein alpha-subunits, J Biol Chem 278(37) (2003) 35063-70.
[32] S.G. Rasmussen, B.T. DeVree, Y. Zou, A.C. Kruse, K.Y. Chung, T.S. Kobilka, F.S. Thian, P.S. Chae, E. Pardon, D. Calinski, J.M. Mathiesen, S.T. Shah, J.A. Lyons, M. Caffrey, S.H. Gellman, J. Steyaert, G. Skiniotis, W.I. Weis, R.K. Sunahara, B.K. Kobilka,

Crystal structure of the beta2 adrenergic receptor-Gs protein complex, Nature 477(7366) (2011) 549-55.
[33] R. Franke, B. Konig, T. Sakmar, H. Khorana, K. Hofmann, Rhodopsin mutants that bind but fail to activate transducin, Science 250(4977) (1990) 123-125.
[34] E.A. Jewell-Motz, K.M. Small, C.T. Theiss, S.B. Liggett, alpha 2A/alpha 2C-adrenergic receptor third loop chimera show that agonist interaction with receptor subtype backbone establishes G protein-coupled receptor kinase phosphorylation, J Biol Chem 275(37) (2000) 28989-93.
[35] R. Sounier, C. Mas, J. Steyaert, T. Laeremans, A. Manglik, W. Huang, B.K. Kobilka, H. Demene, S. Granier, Propagation of conformational changes during mu-opioid receptor activation, Nature 524(7565) (2015) 375-8.
[36] R.G. Kaye, J.W. Saldanha, Z.L. Lu, E.C. Hulme, Helix 8 of the M1 muscarinic acetylcholine receptor: scanning mutagenesis delineates a G protein recognition site, Mol Pharmacol 79(4) (2011) 701-9.
[37] N.M. Delos Santos, L.A. Gardner, S.W. White, S.W. Bahouth, Characterization of the residues in helix 8 of the human beta1-adrenergic receptor that are involved in coupling the receptor to G proteins, J Biol Chem 281(18) (2006) 12896-907.
[38] O.P. Ernst, C.K. Meyer, E.P. Marin, P. Henklein, W.Y. Fu, T.P. Sakmar, K.P. Hofmann, Mutation of the fourth cytoplasmic loop of rhodopsin affects binding of transducin and peptides derived from the carboxyl-terminal sequences of transducin alpha and gamma subunits, J Biol Chem 275(3) (2000) 1937-43.
[39] R. Moukhametzianov, T. Warne, P.C. Edwards, M.J. Serrano-Vega, A.G. Leslie, C.G. Tate, G.F. Schertler, Two distinct conformations of helix 6 observed in antagonist-bound structures of a beta1-adrenergic receptor, Proc Natl Acad Sci U S A 108(20) (2011) 8228-32.
[40] G. Swaminath, X. Deupi, T.W. Lee, W. Zhu, F.S. Thian, T.S. Kobilka, B. Kobilka, Probing the beta2 adrenoceptor binding site with catechol reveals differences in binding and activation by agonists and partial agonists, J Biol Chem 280(23) (2005) 22165-71.
[41] G. Swaminath, Y. Xiang, T.W. Lee, J. Steenhuis, C. Parnot, B.K. Kobilka, Sequential binding of agonists to the beta2 adrenoceptor. Kinetic evidence for intermediate conformational states, J Biol Chem 279(1) (2004) 686-91.
[42] X. Yao, C. Parnot, X. Deupi, V.R. Ratnala, G. Swaminath, D. Farrens, B. Kobilka, Coupling ligand structure to specific conformational switches in the beta2-adrenoceptor, Nature chemical biology 2(8) (2006) 417-22.
[43] A. Zurn, U. Zabel, J.P. Vilardaga, H. Schindelin, M.J. Lohse, C. Hoffmann, Fluorescence resonance energy transfer analysis of alpha 2a-adrenergic receptor activation reveals distinct agonist-specific conformational changes, Mol Pharmacol 75(3) (2009) 534-41.
[44] X.J. Yao, G. Velez Ruiz, M.R. Whorton, S.G. Rasmussen, B.T. DeVree, X. Deupi, R.K. Sunahara, B. Kobilka, The effect of ligand efficacy on the formation and stability of a GPCR-G protein complex, Proc Natl Acad Sci U S A 106(23) (2009) 9501-6.
[45] T. Costa, A. Herz, Antagonists with negative intrinsic activity at delta opioid receptors coupled to GTP-binding proteins, Proc Natl Acad Sci U S A 86(19) (1989) 7321-5.
[46] J.P. Vilardaga, R. Steinmeyer, G.S. Harms, M.J. Lohse, Molecular basis of inverse agonism in a G protein-coupled receptor, Nature chemical biology 1(1) (2005) 25-8.
[47] N. Audet, C. Gales, E. Archer-Lahlou, M. Vallieres, P.W. Schiller, M. Bouvier, G. Pineyro, Bioluminescence resonance energy transfer assays reveal ligand-specific conformational changes within preformed signaling complexes containing delta-opioid receptors and heterotrimeric G proteins, J Biol Chem 283(22) (2008) 15078-88.

[48] C. Altenbach, A.K. Kusnetzow, O.P. Ernst, K.P. Hofmann, W.L. Hubbell, High-resolution distance mapping in rhodopsin reveals the pattern of helix movement due to activation, Proc Natl Acad Sci U S A 105(21) (2008) 7439-44.
[49] W. Huang, A. Manglik, A.J. Venkatakrishnan, T. Laeremans, E.N. Feinberg, A.L. Sanborn, H.E. Kato, K.E. Livingston, T.S. Thorsen, R.C. Kling, S. Granier, P. Gmeiner, S.M. Husbands, J.R. Traynor, W.I. Weis, J. Steyaert, R.O. Dror, B.K. Kobilka, Structural insights into micro-opioid receptor activation, Nature 524(7565) (2015) 315-21.
[50] H.W. Choe, Y.J. Kim, J.H. Park, T. Morizumi, E.F. Pai, N. Krauss, K.P. Hofmann, P. Scheerer, O.P. Ernst, Crystal structure of metarhodopsin II, Nature 471(7340) (2011) 651-5.
[51] A.C. Kruse, A.M. Ring, A. Manglik, J. Hu, K. Hu, K. Eitel, H. Hubner, E. Pardon, C. Valant, P.M. Sexton, A. Christopoulos, C.C. Felder, P. Gmeiner, J. Steyaert, W.I. Weis, K.C. Garcia, J. Wess, B.K. Kobilka, Activation and allosteric modulation of a muscarinic acetylcholine receptor, Nature 504(7478) (2013) 101-6.
[52] M.P. Bokoch, Y. Zou, S.G. Rasmussen, C.W. Liu, R. Nygaard, D.M. Rosenbaum, J.J. Fung, H.J. Choi, F.S. Thian, T.S. Kobilka, J.D. Puglisi, W.I. Weis, L. Pardo, R.S. Prosser, L. Mueller, B.K. Kobilka, Ligand-specific regulation of the extracellular surface of a G-protein-coupled receptor, Nature 463(7277) (2010) 108-12.
[53] T.W. Schwartz, T.M. Frimurer, B. Holst, M.M. Rosenkilde, C.E. Elling, Molecular mechanism of 7TM receptor activation--a global toggle switch model, Annu Rev Pharmacol Toxicol 46 (2006) 481-519.
[54] F. Xu, H. Wu, V. Katritch, G.W. Han, K.A. Jacobson, Z.-G. Gao, V. Cherezov, R.C. Stevens, Structure of an agonist-bound human A(2A) adenosine receptor, Science (New York, N.Y.) 332(6027) (2011) 322-327.
[55] R. Nygaard, Y. Zou, R.O. Dror, T.J. Mildorf, D.H. Arlow, A. Manglik, A.C. Pan, C.W. Liu, J.J. Fung, M.P. Bokoch, F.S. Thian, T.S. Kobilka, D.E. Shaw, L. Mueller, R.S. Prosser, B.K. Kobilka, The dynamic process of beta(2)-adrenergic receptor activation, Cell 152(3) (2013) 532-42.
[56] U. Gether, S. Lin, P. Ghanouni, J.A. Ballesteros, H. Weinstein, B.K. Kobilka, Agonists induce conformational changes in transmembrane domains III and VI of the beta2 adrenoceptor, The EMBO journal 16(22) (1997) 6737-47.
[57] B.J. Ebersole, I. Visiers, H. Weinstein, S.C. Sealfon, Molecular basis of partial agonism: orientation of indoleamine ligands in the binding pocket of the human serotonin 5-HT2A receptor determines relative efficacy, Mol Pharmacol 63(1) (2003) 36-43.
[58] W.L. Hubbell, C. Altenbach, C.M. Hubbell, H.G. Khorana, Rhodopsin structure, dynamics, and activation: a perspective from crystallography, site-directed spin labeling, sulfhydryl reactivity, and disulfide cross-linking, Advances in protein chemistry 63 (2003) 243-90.
[59] B.G. Tehan, A. Bortolato, F.E. Blaney, M.P. Weir, J.S. Mason, Unifying family A GPCR theories of activation, Pharmacol Ther 143(1) (2014) 51-60.
[60] L. Pardo, X. Deupi, N. Dolker, M.L. Lopez-Rodriguez, M. Campillo, The role of internal water molecules in the structure and function of the rhodopsin family of G protein-coupled receptors, Chembiochem : a European journal of chemical biology 8(1) (2007) 19-24.
[61] J.A. Ballesteros, A.D. Jensen, G. Liapakis, S.G. Rasmussen, L. Shi, U. Gether, J.A. Javitch, Activation of the beta 2-adrenergic receptor involves disruption of an ionic lock between the cytoplasmic ends of transmembrane segments 3 and 6, J Biol Chem 276(31) (2001) 29171-7.
[62] C. Prioleau, I. Visiers, B.J. Ebersole, H. Weinstein, S.C. Sealfon, Conserved helix 7 tyrosine acts as a multistate conformational switch in the 5HT2C receptor. Identification

of a novel "locked-on" phenotype and double revertant mutations, J Biol Chem 277(39) (2002) 36577-84.
[63] I.D. Alves, Z. Salamon, E. Varga, H.I. Yamamura, G. Tollin, V.J. Hruby, Direct observation of G-protein binding to the human delta-opioid receptor using plasmon-waveguide resonance spectroscopy, J Biol Chem 278(49) (2003) 48890-7.
[64] A. Manglik, T.H. Kim, M. Masureel, C. Altenbach, Z. Yang, D. Hilger, M.T. Lerch, T.S. Kobilka, F.S. Thian, W.L. Hubbell, R.S. Prosser, B.K. Kobilka, Structural Insights into the Dynamic Process of beta2-Adrenergic Receptor Signaling, Cell 161(5) (2015) 1101-11.
[65] P. Ghanouni, Z. Gryczynski, J.J. Steenhuis, T.W. Lee, D.L. Farrens, J.R. Lakowicz, B.K. Kobilka, Functionally different agonists induce distinct conformations in the G protein coupling domain of the beta 2 adrenergic receptor, J Biol Chem 276(27) (2001) 24433-6.
[66] Y. Kofuku, T. Ueda, J. Okude, Y. Shiraishi, K. Kondo, M. Maeda, H. Tsujishita, I. Shimada, Efficacy of the beta(2)-adrenergic receptor is determined by conformational equilibrium in the transmembrane region, Nature communications 3 (2012) 1045.
[67] A. De Lean, J.M. Stadel, R.J. Lefkowitz, A ternary complex model explains the agonist-specific binding properties of the adenylate cyclase-coupled beta-adrenergic receptor, J Biol Chem 255(15) (1980) 7108-17.
[68] T.H. Kim, K.Y. Chung, A. Manglik, A.L. Hansen, R.O. Dror, T.J. Mildorf, D.E. Shaw, B.K. Kobilka, R.S. Prosser, The role of ligands on the equilibria between functional states of a G protein-coupled receptor, Journal of the American Chemical Society 135(25) (2013) 9465-74.
[69] S. Mary, M. Damian, M. Louet, N. Floquet, J.A. Fehrentz, J. Marie, J. Martinez, J.L. Baneres, Ligands and signaling proteins govern the conformational landscape explored by a G protein-coupled receptor, Proc Natl Acad Sci U S A 109(21) (2012) 8304-9.
[70] W. Liu, E. Chun, A.A. Thompson, P. Chubukov, F. Xu, V. Katritch, G.W. Han, C.B. Roth, L.H. Heitman, A.P. Ijzerman, V. Cherezov, R.C. Stevens, Structural Basis for Allosteric Regulation of GPCRs by Sodium Ions(), Science (New York, N.y.) 337(6091) (2012) 232-236.
[71] J.A. Schetz, D.R. Sibley, Zinc allosterically modulates antagonist binding to cloned D1 and D2 dopamine receptors, J Neurochem 68(5) (1997) 1990-7.
[72] C.B. Pert, G. Pasternak, S.H. Snyder, Opiate agonists and antagonists discriminated by receptor binding in brain, Science 182(4119) (1973) 1359-61.
[73] A.D. Conigrave, S.J. Quinn, E.M. Brown, L-amino acid sensing by the extracellular Ca2+-sensing receptor, Proc Natl Acad Sci U S A 97(9) (2000) 4814-9.
[74] G. Fillion, J.C. Rousselle, O. Massot, E. Zifa, M.P. Fillion, N. Prudhomme, A new peptide, 5-HT-moduline, isolated and purified from mammalian brain specifically interacts with 5-HT1B/1D receptors, Behav Brain Res 73(1-2) (1996) 313-17.
[75] G. Gimpl, K. Burger, F. Fahrenholz, Cholesterol as modulator of receptor function, Biochemistry 36(36) (1997) 10959-74.
[76] M.A. Hanson, V. Cherezov, M.T. Griffith, C.B. Roth, V.P. Jaakola, E.Y. Chien, J. Velasquez, P. Kuhn, R.C. Stevens, A specific cholesterol binding site is established by the 2.8 A structure of the human beta2-adrenergic receptor, Structure (London, England : 1993) 16(6) (2008) 897-905.
[77] S.M. Patra, S. Chakraborty, G. Shahane, X. Prasanna, D. Sengupta, P.K. Maiti, A. Chattopadhyay, Differential dynamics of the serotonin1A receptor in membrane bilayers of varying cholesterol content revealed by all atom molecular dynamics simulation, Molecular membrane biology 32(4) (2015) 127-37.
[78] V.V. Gurevich, R. Pals-Rylaarsdam, J.L. Benovic, M.M. Hosey, J.J. Onorato, Agonist-receptor-arrestin, an alternative ternary complex with high agonist affinity, J Biol Chem 272(46) (1997) 28849-52.

[79] K. Burger, G. Gimpl, F. Fahrenholz, Regulation of receptor function by cholesterol, Cell Mol Life Sci 57(11) (2000) 1577-92.
[80] E.S. Levitt, M.J. Clark, P.M. Jenkins, J.R. Martens, J.R. Traynor, Differential effect of membrane cholesterol removal on mu- and delta-opioid receptors: a parallel comparison of acute and chronic signaling to adenylyl cyclase, J Biol Chem 284(33) (2009) 22108-22.
[81] G. Khelashvili, A. Grossfield, S.E. Feller, M.C. Pitman, H. Weinstein, Structural and dynamic effects of cholesterol at preferred sites of interaction with rhodopsin identified from microsecond length molecular dynamics simulations, Proteins 76(2) (2009) 403-17.
[82] D. Sengupta, A. Chattopadhyay, Molecular dynamics simulations of GPCR-cholesterol interaction: An emerging paradigm, Biochim Biophys Acta 1848(9) (2015) 1775-82.
[83] K.A. Jones, B. Borowsky, J.A. Tamm, D.A. Craig, M.M. Durkin, M. Dai, W.J. Yao, M. Johnson, C. Gunwaldsen, L.Y. Huang, C. Tang, Q. Shen, J.A. Salon, K. Morse, T. Laz, K.E. Smith, D. Nagarathnam, S.A. Noble, T.A. Branchek, C. Gerald, GABA(B) receptors function as a heteromeric assembly of the subunits GABA(B)R1 and GABA(B)R2, Nature 396(6712) (1998) 674-9.
[84] M.J. Robbins, A.R. Calver, A.K. Filippov, W.D. Hirst, R.B. Russell, M.D. Wood, S. Nasir, A. Couve, D.A. Brown, S.J. Moss, M.N. Pangalos, GABA(B2) is essential for g-protein coupling of the GABA(B) receptor heterodimer, J Neurosci 21(20) (2001) 8043-52.
[85] M. Margeta-Mitrovic, Y.N. Jan, L.Y. Jan, A trafficking checkpoint controls GABA(B) receptor heterodimerization, Neuron 27(1) (2000) 97-106.
[86] R. Kuner, G. Kohr, S. Grunewald, G. Eisenhardt, A. Bach, H.C. Kornau, Role of heteromer formation in GABAB receptor function, Science 283(5398) (1999) 74-7.
[87] N. Kunishima, Y. Shimada, Y. Tsuji, T. Sato, M. Yamamoto, T. Kumasaka, S. Nakanishi, H. Jingami, K. Morikawa, Structural basis of glutamate recognition by a dimeric metabotropic glutamate receptor, Nature 407(6807) (2000) 971-7.
[88] D. El Moustaine, S. Granier, E. Doumazane, P. Scholler, R. Rahmeh, P. Bron, B. Mouillac, J.L. Baneres, P. Rondard, J.P. Pin, Distinct roles of metabotropic glutamate receptor dimerization in agonist activation and G-protein coupling, Proc Natl Acad Sci U S A 109(40) (2012) 16342-7.
[89] S. Ferre, V. Casado, L.A. Devi, M. Filizola, R. Jockers, M.J. Lohse, G. Milligan, J.P. Pin, X. Guitart, G protein-coupled receptor oligomerization revisited: functional and pharmacological perspectives, Pharmacol Rev 66(2) (2014) 413-34.
[90] M.R. Whorton, M.P. Bokoch, S.G. Rasmussen, B. Huang, R.N. Zare, B. Kobilka, R.K. Sunahara, A monomeric G protein-coupled receptor isolated in a high-density lipoprotein particle efficiently activates its G protein, Proc Natl Acad Sci U S A 104(18) (2007) 7682-7.
[91] A.J. Kuszak, S. Pitchiaya, J.P. Anand, H.I. Mosberg, N.G. Walter, R.K. Sunahara, Purification and functional reconstitution of monomeric mu-opioid receptors: allosteric modulation of agonist binding by Gi2, J Biol Chem 284(39) (2009) 26732-41.
[92] K. Herrick-Davis, E. Grinde, A. Cowan, J.E. Mazurkiewicz, Fluorescence correlation spectroscopy analysis of serotonin, adrenergic, muscarinic, and dopamine receptor dimerization: the oligomer number puzzle, Mol Pharmacol 84(4) (2013) 630-42.
[93] W. Guo, E. Urizar, M. Kralikova, J.C. Mobarec, L. Shi, M. Filizola, J.A. Javitch, Dopamine D2 receptors form higher order oligomers at physiological expression levels, The EMBO journal 27(17) (2008) 2293-304.
[94] B. Wu, E.Y. Chien, C.D. Mol, G. Fenalti, W. Liu, V. Katritch, R. Abagyan, A. Brooun, P. Wells, F.C. Bi, D.J. Hamel, P. Kuhn, T.M. Handel, V. Cherezov, R.C. Stevens,

Structures of the CXCR4 chemokine GPCR with small-molecule and cyclic peptide antagonists, Science 330(6007) (2010) 1066-71.
[95] H. Wu, D. Wacker, M. Mileni, V. Katritch, G.W. Han, E. Vardy, W. Liu, A.A. Thompson, X.P. Huang, F.I. Carroll, S.W. Mascarella, R.B. Westkaemper, P.D. Mosier, B.L. Roth, V. Cherezov, R.C. Stevens, Structure of the human kappa-opioid receptor in complex with JDTic, Nature 485(7398) (2012) 327-32.
[96] R. Maggio, Z. Vogel, J. Wess, Coexpression studies with mutant muscarinic/adrenergic receptors provide evidence for intermolecular "cross-talk" between G-protein-linked receptors, Proc Natl Acad Sci U S A 90(7) (1993) 3103-7.
[97] T.E. Hebert, S. Moffett, J.P. Morello, T.P. Loisel, D.G. Bichet, C. Barret, M. Bouvier, A peptide derived from a beta2-adrenergic receptor transmembrane domain inhibits both receptor dimerization and activation, J Biol Chem 271(27) (1996) 16384-92.
[98] J. Huang, S. Chen, J.J. Zhang, X.Y. Huang, Crystal structure of oligomeric beta1-adrenergic G protein-coupled receptors in ligand-free basal state, Nature structural & molecular biology 20(4) (2013) 419-25.
[99] R.S. Kasai, K.G. Suzuki, E.R. Prossnitz, I. Koyama-Honda, C. Nakada, T.K. Fujiwara, A. Kusumi, Full characterization of GPCR monomer-dimer dynamic equilibrium by single molecule imaging, The Journal of cell biology 192(3) (2011) 463-80.
[100] J.A. Hern, A.H. Baig, G.I. Mashanov, B. Birdsall, J.E. Corrie, S. Lazareno, J.E. Molloy, N.J. Birdsall, Formation and dissociation of M1 muscarinic receptor dimers seen by total internal reflection fluorescence imaging of single molecules, Proc Natl Acad Sci U S A 107(6) (2010) 2693-8.
[101] D. Calebiro, F. Rieken, J. Wagner, T. Sungkaworn, U. Zabel, A. Borzi, E. Cocucci, A. Zurn, M.J. Lohse, Single-molecule analysis of fluorescently labeled G-protein-coupled receptors reveals complexes with distinct dynamics and organization, Proc Natl Acad Sci U S A 110(2) (2013) 743-8.
[102] A. Salahpour, S. Angers, J.F. Mercier, M. Lagace, S. Marullo, M. Bouvier, Homodimerization of the beta2-adrenergic receptor as a prerequisite for cell surface targeting, J Biol Chem 279(32) (2004) 33390-7.
[103] T. Kenakin, L.J. Miller, Seven transmembrane receptors as shapeshifting proteins: the impact of allosteric modulation and functional selectivity on new drug discovery, Pharmacol Rev 62(2) (2010) 265-304.
[104] M. Orru, J. Bakesova, M. Brugarolas, C. Quiroz, V. Beaumont, S.R. Goldberg, C. Lluis, A. Cortes, R. Franco, V. Casado, E.I. Canela, S. Ferre, Striatal pre- and postsynaptic profile of adenosine A(2A) receptor antagonists, PLoS One 6(1) (2011) e16088.
[105] I. Gomes, A. Gupta, J. Filipovska, H.H. Szeto, J.E. Pintar, L.A. Devi, A role for heterodimerization of mu and delta opiate receptors in enhancing morphine analgesia, Proc Natl Acad Sci U S A 101(14) (2004) 5135-9.
[106] R. Franco, V. Casado, J. Mallol, S. Ferre, K. Fuxe, A. Cortes, F. Ciruela, C. Lluis, E.I. Canela, Dimer-based model for heptaspanning membrane receptors, Trends Biochem Sci 30(7) (2005) 360-6.
[107] L.P. Pellissier, G. Barthet, F. Gaven, E. Cassier, E. Trinquet, J.P. Pin, P. Marin, A. Dumuis, J. Bockaert, J.L. Baneres, S. Claeysen, G protein activation by serotonin type 4 receptor dimers: evidence that turning on two protomers is more efficient, J Biol Chem 286(12) (2011) 9985-97.
[108] D.R. Brandt, E.M. Ross, GTPase activity of the stimulatory GTP-binding regulatory protein of adenylate cyclase, Gs. Accumulation and turnover of enzyme-nucleotide intermediates, J Biol Chem 260(1) (1985) 266-72.

[109] D. Cassel, Z. Selinger, Mechanism of adenylate cyclase activation through the beta-adrenergic receptor: catecholamine-induced displacement of bound GDP by GTP, Proc Natl Acad Sci U S A 75(9) (1978) 4155-9.
[110] J.P. Noel, H.E. Hamm, P.B. Sigler, The 2.2 A crystal structure of transducin-alpha complexed with GTP gamma S, Nature 366(6456) (1993) 654-63.
[111] M.B. Mixon, E. Lee, D.E. Coleman, A.M. Berghuis, A.G. Gilman, S.R. Sprang, Tertiary and quaternary structural changes in Gi alpha 1 induced by GTP hydrolysis, Science 270(5238) (1995) 954-60.
[112] R.O. Dror, T.J. Mildorf, D. Hilger, A. Manglik, D.W. Borhani, D.H. Arlow, A. Philippsen, N. Villanueva, Z. Yang, M.T. Lerch, W.L. Hubbell, B.K. Kobilka, R.K. Sunahara, D.E. Shaw, SIGNAL TRANSDUCTION. Structural basis for nucleotide exchange in heterotrimeric G proteins, Science 348(6241) (2015) 1361-5.
[113] M.A. Wall, B.A. Posner, S.R. Sprang, Structural basis of activity and subunit recognition in G protein heterotrimers, Structure (London, England : 1993) 6(9) (1998) 1169-83.
[114] L. De Vries, B. Zheng, T. Fischer, E. Elenko, M.G. Farquhar, The regulator of G protein signaling family, Annu Rev Pharmacol Toxicol 40 (2000) 235-71.
[115] D.M. Berman, T.M. Wilkie, A.G. Gilman, GAIP and RGS4 Are GTPase-Activating Proteins for the Gi Subfamily of G Protein α Subunits, Cell 86(3) (1996) 445-452.
[116] S. Yokoyama, W.T. Starmer, Phylogeny and evolutionary rates of G protein alpha subunit genes, Journal of molecular evolution 35(3) (1992) 230-8.
[117] E.W. Sutherland, T.W. Rall, T. Menon, Adenyl cylase. I. Distribution, preparation, and properties, J Biol Chem 237 (1962) 1220-7.
[118] T. Pfeuffer, GTP-binding proteins in membranes and the control of adenylate cyclase activity, J Biol Chem 252(20) (1977) 7224-34.
[119] J. Codina, J. Hildebrandt, R. Iyengar, L. Birnbaumer, R.D. Sekura, C.R. Manclark, Pertussis toxin substrate, the putative Ni component of adenylyl cyclases, is an alpha beta heterodimer regulated by guanine nucleotide and magnesium, Proc Natl Acad Sci U S A 80(14) (1983) 4276-80.
[120] R.S. Ostrom, A.S. Bogard, R. Gros, R.D. Feldman, Choreographing the adenylyl cyclase signalosome: sorting out the partners and the steps, Naunyn Schmiedebergs Arch Pharmacol 385(1) (2012) 5-12.
[121] W.E. Theurkauf, R.B. Vallee, Molecular characterization of the cAMP-dependent protein kinase bound to microtubule-associated protein 2, J Biol Chem 257(6) (1982) 3284-90.
[122] J. de Rooij, H. Rehmann, M. van Triest, R.H. Cool, A. Wittinghofer, J.L. Bos, Mechanism of regulation of the Epac family of cAMP-dependent RapGEFs, J Biol Chem 275(27) (2000) 20829-36.
[123] S.L. Ingram, J.T. Williams, Opioid inhibition of Ih via adenylyl cyclase, Neuron 13(1) (1994) 179-86.
[124] D.A. Walsh, J.P. Perkins, E.G. Krebs, An adenosine 3',5'-monophosphate-dependant protein kinase from rabbit skeletal muscle, J Biol Chem 243(13) (1968) 3763-5.
[125] P.B. Daniel, W.H. Walker, J.F. Habener, Cyclic AMP signaling and gene regulation, Annual review of nutrition 18 (1998) 353-83.
[126] F.D. Smith, B.K. Samelson, J.D. Scott, Discovery of cellular substrates for protein kinase A using a peptide array screening protocol, Biochemical Journal 438(1) (2011) 103-110.
[127] S.J. Taylor, J.H. Exton, Two alpha subunits of the Gq class of G proteins stimulate phosphoinositide phospholipase C-beta 1 activity, FEBS letters 286(1-2) (1991) 214-6.
[128] M.J. Berridge, Inositol trisphosphate and calcium signalling, Nature 361(6410) (1993) 315-25.

[129] A.V. Smrcka, J.R. Hepler, K.O. Brown, P.C. Sternweis, Regulation of polyphosphoinositide-specific phospholipase C activity by purified Gq, Science 251(4995) (1991) 804-7.
[130] L.E. Rameh, L.C. Cantley, The Role of Phosphoinositide 3-Kinase Lipid Products in Cell Function, Journal of Biological Chemistry 274(13) (1999) 8347-8350.
[131] M.J. Berridge, P. Lipp, M.D. Bootman, The versatility and universality of calcium signalling, Nature reviews. Molecular cell biology 1(1) (2000) 11-21.
[132] A.E. Lacerda, D. Rampe, A.M. Brown, Effects of protein kinase C activators on cardiac Ca2+ channels, Nature 335(6187) (1988) 249-251.
[133] T.P. Abeyweera, X. Chen, S.A. Rotenberg, Phosphorylation of α6-Tubulin by Protein Kinase Cα Activates Motility of Human Breast Cells, Journal of Biological Chemistry 284(26) (2009) 17648-17656.
[134] W. Kolch, G. Heidecker, G. Kochs, R. Hummel, H. Vahidi, H. Mischak, G. Finkenzeller, D. Marme, U.R. Rapp, Protein kinase C[alpha] activates RAF-1 by direct phosphorylation, Nature 364(6434) (1993) 249-252.
[135] M. Bouvier, L.M. Leeb-Lundberg, J.L. Benovic, M.G. Caron, R.J. Lefkowitz, Regulation of adrenergic receptor function by phosphorylation. II. Effects of agonist occupancy on phosphorylation of alpha 1- and beta 2-adrenergic receptors by protein kinase C and the cyclic AMP-dependent protein kinase, Journal of Biological Chemistry 262(7) (1987) 3106-3113.
[136] M.J. Hart, X. Jiang, T. Kozasa, W. Roscoe, W.D. Singer, A.G. Gilman, P.C. Sternweis, G. Bollag, Direct stimulation of the guanine nucleotide exchange activity of p115 RhoGEF by Galpha13, Science 280(5372) (1998) 2112-4.
[137] A.J. Ridley, A. Hall, The small GTP-binding protein rho regulates the assembly of focal adhesions and actin stress fibers in response to growth factors, Cell 70(3) 389-399.
[138] T. Leung, X.Q. Chen, E. Manser, L. Lim, The p160 RhoA-binding kinase ROK alpha is a member of a kinase family and is involved in the reorganization of the cytoskeleton, Molecular and Cellular Biology 16(10) (1996) 5313-27.
[139] D.S. Evanko, M.M. Thiyagarajan, D.P. Siderovski, P.B. Wedegaertner, Gbeta gamma isoforms selectively rescue plasma membrane localization and palmitoylation of mutant Galphas and Galphaq, J Biol Chem 276(26) (2001) 23945-53.
[140] L. Robillard, N. Ethier, M. Lachance, T.E. Hebert, Gbetagamma subunit combinations differentially modulate receptor and effector coupling in vivo, Cell Signal 12(9-10) (2000) 673-82.
[141] M.B. Jones, D.P. Siderovski, S.B. Hooks, The G betagamma dimer as a novel source of selectivity in G-protein signaling: GGL-ing at convention, Molecular interventions 4(4) (2004) 200-14.
[142] D.E. Logothetis, Y. Kurachi, J. Galper, E.J. Neer, D.E. Clapham, The beta gamma subunits of GTP-binding proteins activate the muscarinic K+ channel in heart, Nature 325(6102) (1987) 321-6.
[143] S. Herlitze, D.E. Garcia, K. Mackie, B. Hille, T. Scheuer, W.A. Catterall, Modulation of Ca2+ channels [beta][gamma] G-protein py subunits, Nature 380(6571) (1996) 258-262.
[144] S.R. Ikeda, Voltage-dependent modulation of N-type calcium channels by G-protein [beta] [gamma]subunits, Nature 380(6571) (1996) 255-258.
[145] G.G. Holz, S.G. Rane, K. Dunlap, GTP-binding proteins mediate transmitter inhibition of voltage-dependent calcium channels, Nature 319(6055) (1986) 670-672.
[146] R.A. North, J.T. Williams, A. Surprenant, M.J. Christie, Mu and delta receptors belong to a family of receptors that are coupled to potassium channels, Proc Natl Acad Sci U S A 84(15) (1987) 5487-91.

[147] M. Camps, A. Carozzi, P. Schnabel, A. Scheer, P.J. Parker, P. Gierschik, Isozyme-selective stimulation of phospholipase C-beta 2 by G protein beta gamma-subunits, Nature 360(6405) (1992) 684-6.
[148] L. Stephens, A. Smrcka, F.T. Cooke, T.R. Jackson, P.C. Sternweis, P.T. Hawkins, A novel phosphoinositide 3 kinase activity in myeloid-derived cells is activated by G protein beta gamma subunits, Cell 77(1) (1994) 83-93.
[149] W.J. Tang, A.G. Gilman, Type-specific regulation of adenylyl cyclase by G protein beta gamma subunits, Science 254(5037) (1991) 1500-3.
[150] S.K. DebBurman, J. Ptasienski, J.L. Benovic, M.M. Hosey, G protein-coupled receptor kinase GRK2 is a phospholipid-dependent enzyme that can be conditionally activated by G protein betagamma subunits, J Biol Chem 271(37) (1996) 22552-62.
[151] J.S. Gutkind, Regulation of mitogen-activated protein kinase signaling networks by G protein-coupled receptors, Science's STKE : signal transduction knowledge environment 2000(40) (2000) re1.
[152] M.M. Belcheva, C.J. Coscia, Diversity of G protein-coupled receptor signaling pathways to ERK/MAP kinase, Neuro-Signals 11(1) (2002) 34-44.
[153] W.J. Koch, B.E. Hawes, L.F. Allen, R.J. Lefkowitz, Direct evidence that Gi-coupled receptor stimulation of mitogen-activated protein kinase is mediated by G beta gamma activation of p21ras, Proc Natl Acad Sci U S A 91(26) (1994) 12706-10.
[154] B.E. Hawes, S. Fried, X. Yao, B. Weig, M.P. Graziano, Nociceptin (ORL-1) and mu-opioid receptors mediate mitogen-activated protein kinase activation in CHO cells through a Gi-coupled signaling pathway: evidence for distinct mechanisms of agonist-mediated desensitization, J Neurochem 71(3) (1998) 1024-33.
[155] M. Faure, T.A. Voyno-Yasenetskaya, H.R. Bourne, cAMP and beta gamma subunits of heterotrimeric G proteins stimulate the mitogen-activated protein kinase pathway in COS-7 cells, J Biol Chem 269(11) (1994) 7851-4.
[156] L.M. Luttrell, G.J. Della Rocca, T. van Biesen, D.K. Luttrell, R.J. Lefkowitz, Gbetagamma subunits mediate Src-dependent phosphorylation of the epidermal growth factor receptor. A scaffold for G protein-coupled receptor-mediated Ras activation, J Biol Chem 272(7) (1997) 4637-44.
[157] M. Lopez-Ilasaca, P. Crespo, P.G. Pellici, J.S. Gutkind, R. Wetzker, Linkage of G protein-coupled receptors to the MAPK signaling pathway through PI 3-kinase gamma, Science 275(5298) (1997) 394-7.
[158] B.E. Hawes, T. van Biesen, W.J. Koch, L.M. Luttrell, R.J. Lefkowitz, Distinct pathways of Gi- and Gq-mediated mitogen-activated protein kinase activation, J Biol Chem 270(29) (1995) 17148-53.
[159] T. van Biesen, B.E. Hawes, D.K. Luttrell, K.M. Krueger, K. Touhara, E. Porfiri, M. Sakaue, L.M. Luttrell, R.J. Lefkowitz, Receptor-tyrosine-kinase- and G beta gamma-mediated MAP kinase activation by a common signalling pathway, Nature 376(6543) (1995) 781-4.
[160] H. Daub, F.U. Weiss, C. Wallasch, A. Ullrich, Role of transactivation of the EGF receptor in signalling by G-protein-coupled receptors, Nature 379(6565) (1996) 557-60.
[161] J. Dong, L.K. Opresko, P.J. Dempsey, D.A. Lauffenburger, R.J. Coffey, H.S. Wiley, Metalloprotease-mediated ligand release regulates autocrine signaling through the epidermal growth factor receptor, Proc Natl Acad Sci U S A 96(11) (1999) 6235-40.
[162] H. Chong, H.G. Vikis, K.L. Guan, Mechanisms of regulating the Raf kinase family, Cell Signal 15(5) (2003) 463-9.
[163] Y. Chen, D. Grall, A.E. Salcini, P.G. Pelicci, J. Pouyssegur, E. Van Obberghen-Schilling, Shc adaptor proteins are key transducers of mitogenic signaling mediated by the G protein-coupled thrombin receptor, The EMBO journal 15(5) (1996) 1037-44.
[164] J. Chen, R. Iyengar, Interactions between the Gs/protein kinase A and the Ras/MAP-kinase signalling pathways, Biochem Soc Trans 23(1) (1995) 129-33.

[165] N. Mochizuki, Y. Ohba, E. Kiyokawa, T. Kurata, T. Murakami, T. Ozaki, A. Kitabatake, K. Nagashima, M. Matsuda, Activation of the ERK/MAPK pathway by an isoform of rap1GAP associated with G alpha(i), Nature 400(6747) (1999) 891-4.
[166] T.D. Werry, P.M. Sexton, A. Christopoulos, "Ins and outs" of seven-transmembrane receptor signalling to ERK, Trends in endocrinology and metabolism: TEM 16(1) (2005) 26-33.
[167] T.K. Harden, Y.F. Su, J.P. Perkins, Catecholamine-induced desensitization involves an uncoupling of beta-adrenergic receptors and adenylate cyclase, Journal of cyclic nucleotide research 5(2) (1979) 99-106.
[168] D.R. Sibley, R.H. Strasser, M.G. Caron, R.J. Lefkowitz, Homologous desensitization of adenylate cyclase is associated with phosphorylation of the beta-adrenergic receptor, J Biol Chem 260(7) (1985) 3883-6.
[169] M.R. Wessels, D. Mullikin, R.J. Lefkowitz, Selective alteration in high affinity agonist binding: a mechanism of beta-adrenergic receptor desensitization, Mol Pharmacol 16(1) (1979) 10-20.
[170] M.J. Lohse, Molecular mechanisms of membrane receptor desensitization, Biochim Biophys Acta 1179(2) (1993) 171-88.
[171] J.R. Arden, V. Segredo, Z. Wang, J. Lameh, W. Sadée, Phosphorylation and Agonist-Specific Intracellular Trafficking of an Epitope-Tagged μ-Opioid Receptor Expressed in HEK 293 Cells, Journal of Neurochemistry 65(4) (1995) 1636-1645.
[172] M. Bouvier, L.M. Leeb-Lundberg, J.L. Benovic, M.G. Caron, R.J. Lefkowitz, Regulation of adrenergic receptor function by phosphorylation. II. Effects of agonist occupancy on phosphorylation of alpha 1- and beta 2-adrenergic receptors by protein kinase C and the cyclic AMP-dependent protein kinase, J Biol Chem 262(7) (1987) 3106-13.
[173] R.T. Premont, J. Inglese, R.J. Lefkowitz, Protein kinases that phosphorylate activated G protein-coupled receptors, Faseb j 9(2) (1995) 175-82.
[174] J.L. Benovic, R.H. Strasser, M.G. Caron, R.J. Lefkowitz, Beta-adrenergic receptor kinase: identification of a novel protein kinase that phosphorylates the agonist-occupied form of the receptor, Proc Natl Acad Sci U S A 83(9) (1986) 2797-801.
[175] C. Ambrose, M. James, G. Barnes, C. Lin, G. Bates, M. Altherr, M. Duyao, N. Groot, D. Church, J.J. Wasmuth, et al., A novel G protein-coupled receptor kinase gene cloned from 4p16.3, Human molecular genetics 1(9) (1992) 697-703.
[176] M. Weller, N. Virmaux, P. Mandel, Light-stimulated phosphorylation of rhodopsin in the retina: the presence of a protein kinase that is specific for photobleached rhodopsin, Proc Natl Acad Sci U S A 72(1) (1975) 381-5.
[177] O. Hisatomi, S. Matsuda, T. Satoh, S. Kotaka, Y. Imanishi, F. Tokunaga, A novel subtype of G-protein-coupled receptor kinase, GRK7, in teleost cone photoreceptors, FEBS letters 424(3) (1998) 159-64.
[178] P. Kunapuli, J.L. Benovic, Cloning and expression of GRK5: a member of the G protein-coupled receptor kinase family, Proceedings of the National Academy of Sciences of the United States of America 90(12) (1993) 5588-5592.
[179] J.A. Pitcher, J. Inglese, J.B. Higgins, J.L. Arriza, P.J. Casey, C. Kim, J.L. Benovic, M.M. Kwatra, M.G. Caron, R.J. Lefkowitz, Role of beta gamma subunits of G proteins in targeting the beta-adrenergic receptor kinase to membrane-bound receptors, Science 257(5074) (1992) 1264-7.
[180] K.T. Homan, A. Glukhova, J.J. Tesmer, Regulation of G protein-coupled receptor kinases by phospholipids, Current medicinal chemistry 20(1) (2013) 39-46.
[181] D.T. Lodowski, J.A. Pitcher, W.D. Capel, R.J. Lefkowitz, J.J. Tesmer, Keeping G proteins at bay: a complex between G protein-coupled receptor kinase 2 and Gbetagamma, Science 300(5623) (2003) 1256-62.

[182] C.V. Carman, J.L. Parent, P.W. Day, A.N. Pronin, P.M. Sternweis, P.B. Wedegaertner, A.G. Gilman, J.L. Benovic, T. Kozasa, Selective regulation of Galpha(q/11) by an RGS domain in the G protein-coupled receptor kinase, GRK2, J Biol Chem 274(48) (1999) 34483-92.
[183] A.K. Shukla, G.H. Westfield, K. Xiao, R.I. Reis, L.-Y. Huang, P. Tripathi-Shukla, J. Qian, S. Li, A. Blanc, A.N. Oleskie, A.M. Dosey, M. Su, C.-R. Liang, L.-L. Gu, J.-M. Shan, X. Chen, R. Hanna, M. Choi, X.J. Yao, B.U. Klink, A.W. Kahsai, S.S. Sidhu, S. Koide, P.A. Penczek, A.A. Kossiakoff, V.L.W. Jr, B.K. Kobilka, G. Skiniotis, R.J. Lefkowitz, Visualization of arrestin recruitment by a G Protein-Coupled Receptor, Nature 512(7513) (2014) 218-222.
[184] S. Just, S. Illing, M. Trester-Zedlitz, E.K. Lau, S.J. Kotowski, E. Miess, A. Mann, C. Doll, J.C. Trinidad, A.L. Burlingame, M. von Zastrow, S. Schulz, Differentiation of opioid drug effects by hierarchical multi-site phosphorylation, Mol Pharmacol 83(3) (2013) 633-9.
[185] M.G. Eason, S.P. Moreira, S.B. Liggett, Four consecutive serines in the third intracellular loop are the sites for beta-adrenergic receptor kinase-mediated phosphorylation and desensitization of the alpha 2A-adrenergic receptor, J Biol Chem 270(9) (1995) 4681-8.
[186] U. Wilden, S.W. Hall, H. Kuhn, Phosphodiesterase activation by photoexcited rhodopsin is quenched when rhodopsin is phosphorylated and binds the intrinsic 48-kDa protein of rod outer segments, Proc Natl Acad Sci U S A 83(5) (1986) 1174-8.
[187] J.L. Benovic, H. Kuhn, I. Weyand, J. Codina, M.G. Caron, R.J. Lefkowitz, Functional desensitization of the isolated beta-adrenergic receptor by the beta-adrenergic receptor kinase: potential role of an analog of the retinal protein arrestin (48-kDa protein), Proc Natl Acad Sci U S A 84(24) (1987) 8879-82.
[188] M.J. Lohse, J.L. Benovic, J. Codina, M.G. Caron, R.J. Lefkowitz, beta-Arrestin: a protein that regulates beta-adrenergic receptor function, Science 248(4962) (1990) 1547-50.
[189] J.G. Krupnick, V.V. Gurevich, J.L. Benovic, Mechanism of quenching of phototransduction. Binding competition between arrestin and transducin for phosphorhodopsin, J Biol Chem 272(29) (1997) 18125-31.
[190] H. Attramadal, J.L. Arriza, C. Aoki, T.M. Dawson, J. Codina, M.M. Kwatra, S.H. Snyder, M.G. Caron, R.J. Lefkowitz, Beta-arrestin2, a novel member of the arrestin/beta-arrestin gene family, J Biol Chem 267(25) (1992) 17882-90.
[191] K.L. Pierce, R.J. Lefkowitz, Classical and new roles of beta-arrestins in the regulation of G-protein-coupled receptors, Nat Rev Neurosci 2(10) (2001) 727-33.
[192] M. von Zastrow, B.K. Kobilka, Ligand-regulated internalization and recycling of human beta 2-adrenergic receptors between the plasma membrane and endosomes containing transferrin receptors, Journal of Biological Chemistry 267(5) (1992) 3530-3538.
[193] O.B. Goodman, Jr., J.G. Krupnick, F. Santini, V.V. Gurevich, R.B. Penn, A.W. Gagnon, J.H. Keen, J.L. Benovic, Beta-arrestin acts as a clathrin adaptor in endocytosis of the beta2-adrenergic receptor, Nature 383(6599) (1996) 447-50.
[194] S.A. Laporte, R.H. Oakley, J. Zhang, J.A. Holt, S.S.G. Ferguson, M.G. Caron, L.S. Barak, The β(2)-adrenergic receptor/βarrestin complex recruits the clathrin adaptor AP-2 during endocytosis, Proceedings of the National Academy of Sciences of the United States of America 96(7) (1999) 3712-3717.
[195] S.S.G. Ferguson, W.E. Downey, III, A.-M. Colapietro, L.S. Barak, et al., Role of beta-arrestin in mediating agonist-promoted G protein-coupled receptor internalization, Science 271(5247) (1996) 363.

[196] I. Gaidarov, J.G. Krupnick, J.R. Falck, J.L. Benovic, J.H. Keen, Arrestin function in G protein-coupled receptor endocytosis requires phosphoinositide binding, The EMBO journal 18(4) (1999) 871-881.
[197] F.T. Lin, K.M. Krueger, H.E. Kendall, Y. Daaka, Z.L. Fredericks, J.A. Pitcher, R.J. Lefkowitz, Clathrin-mediated endocytosis of the beta-adrenergic receptor is regulated by phosphorylation/dephosphorylation of beta-arrestin1, J Biol Chem 272(49) (1997) 31051-7.
[198] P. Tsao, T. Cao, M. von Zastrow, Role of endocytosis in mediating downregulation of G-protein-coupled receptors, Trends Pharmacol Sci 22(2) (2001) 91-6.
[199] R.C. Doss, J.P. Perkins, T.K. Harden, Recovery of beta-adrenergic receptors following long term exposure of astrocytoma cells to catecholamine. Role of protein synthesis, J Biol Chem 256(23) (1981) 12281-6.
[200] K.A. DeFea, J. Zalevsky, M.S. Thoma, O. Dery, R.D. Mullins, N.W. Bunnett, beta-arrestin-dependent endocytosis of proteinase-activated receptor 2 is required for intracellular targeting of activated ERK1/2, The Journal of cell biology 148(6) (2000) 1267-81.
[201] K.A. DeFea, Z.D. Vaughn, E.M. O'Bryan, D. Nishijima, O. Dery, N.W. Bunnett, The proliferative and antiapoptotic effects of substance P are facilitated by formation of a beta -arrestin-dependent scaffolding complex, Proc Natl Acad Sci U S A 97(20) (2000) 11086-91.
[202] L.M. Luttrell, S.S. Ferguson, Y. Daaka, W.E. Miller, S. Maudsley, G.J. Della Rocca, F. Lin, H. Kawakatsu, K. Owada, D.K. Luttrell, M.G. Caron, R.J. Lefkowitz, Beta-arrestin-dependent formation of beta2 adrenergic receptor-Src protein kinase complexes, Science 283(5402) (1999) 655-61.
[203] K. Eichel, D. Jullie, M. von Zastrow, beta-Arrestin drives MAP kinase signalling from clathrin-coated structures after GPCR dissociation, Nature cell biology (2016).
[204] J.E. Murphy, B.E. Padilla, B. Hasdemir, G.S. Cottrell, N.W. Bunnett, Endosomes: a legitimate platform for the signaling train, Proc Natl Acad Sci U S A 106(42) (2009) 17615-22.
[205] L.M. Luttrell, F.L. Roudabush, E.W. Choy, W.E. Miller, M.E. Field, K.L. Pierce, R.J. Lefkowitz, Activation and targeting of extracellular signal-regulated kinases by β-arrestin scaffolds, Proceedings of the National Academy of Sciences of the United States of America 98(5) (2001) 2449-2454.
[206] S. Ahn, S.K. Shenoy, H. Wei, R.J. Lefkowitz, Differential kinetic and spatial patterns of beta-arrestin and G protein-mediated ERK activation by the angiotensin II receptor, J Biol Chem 279(34) (2004) 35518-25.
[207] S.K. Shenoy, M.T. Drake, C.D. Nelson, D.A. Houtz, K. Xiao, S. Madabushi, E. Reiter, R.T. Premont, O. Lichtarge, R.J. Lefkowitz, beta-arrestin-dependent, G protein-independent ERK1/2 activation by the beta2 adrenergic receptor, J Biol Chem 281(2) (2006) 1261-73.
[208] H. Zheng, H.H. Loh, P.Y. Law, Beta-arrestin-dependent mu-opioid receptor-activated extracellular signal-regulated kinases (ERKs) Translocate to Nucleus in Contrast to G protein-dependent ERK activation, Mol Pharmacol 73(1) (2008) 178-90.
[209] A. Tohgo, K.L. Pierce, E.W. Choy, R.J. Lefkowitz, L.M. Luttrell, beta-Arrestin scaffolding of the ERK cascade enhances cytosolic ERK activity but inhibits ERK-mediated transcription following angiotensin AT1a receptor stimulation, J Biol Chem 277(11) (2002) 9429-36.
[210] P.H. McDonald, C.W. Chow, W.E. Miller, S.A. Laporte, M.E. Field, F.T. Lin, R.J. Davis, R.J. Lefkowitz, Beta-arrestin 2: a receptor-regulated MAPK scaffold for the activation of JNK3, Science 290(5496) (2000) 1574-7.

[211] W.E. Miller, P.H. McDonald, S.F. Cai, M.E. Field, R.J. Davis, R.J. Lefkowitz, Identification of a motif in the carboxyl terminus of beta -arrestin2 responsible for activation of JNK3, J Biol Chem 276(30) (2001) 27770-7.
[212] Y. Sun, Z. Cheng, L. Ma, G. Pei, Beta-arrestin2 is critically involved in CXCR4-mediated chemotaxis, and this is mediated by its enhancement of p38 MAPK activation, J Biol Chem 277(51) (2002) 49212-9.
[213] M.R. Bruchas, T.A. Macey, J.D. Lowe, C. Chavkin, Kappa opioid receptor activation of p38 MAPK is GRK3- and arrestin-dependent in neurons and astrocytes, J Biol Chem 281(26) (2006) 18081-9.
[214] W.E. Miller, D.A. Houtz, C.D. Nelson, P.E. Kolattukudy, R.J. Lefkowitz, G-protein-coupled receptor (GPCR) kinase phosphorylation and beta-arrestin recruitment regulate the constitutive signaling activity of the human cytomegalovirus US28 GPCR, J Biol Chem 278(24) (2003) 21663-71.
[215] W.G. Barnes, E. Reiter, J.D. Violin, X.R. Ren, G. Milligan, R.J. Lefkowitz, beta-Arrestin 1 and Galphaq/11 coordinately activate RhoA and stress fiber formation following receptor stimulation, J Biol Chem 280(9) (2005) 8041-50.
[216] T.J. Povsic, T.A. Kohout, R.J. Lefkowitz, Beta-arrestin1 mediates insulin-like growth factor 1 (IGF-1) activation of phosphatidylinositol 3-kinase (PI3K) and anti-apoptosis, J Biol Chem 278(51) (2003) 51334-9.
[217] R. Goel, P.J. Phillips-Mason, D.M. Raben, J.J. Baldassare, alpha-Thrombin induces rapid and sustained Akt phosphorylation by beta-arrestin1-dependent and -independent mechanisms, and only the sustained Akt phosphorylation is essential for G1 phase progression, J Biol Chem 277(21) (2002) 18640-8.
[218] J.M. Beaulieu, T.D. Sotnikova, S. Marion, R.J. Lefkowitz, R.R. Gainetdinov, M.G. Caron, An Akt/beta-arrestin 2/PP2A signaling complex mediates dopaminergic neurotransmission and behavior, Cell 122(2) (2005) 261-73.
[219] D.S. Witherow, T.R. Garrison, W.E. Miller, R.J. Lefkowitz, beta-Arrestin inhibits NF-kappaB activity by means of its interaction with the NF-kappaB inhibitor IkappaBalpha, Proc Natl Acad Sci U S A 101(23) (2004) 8603-7.
[220] H. Gao, Y. Sun, Y. Wu, B. Luan, Y. Wang, B. Qu, G. Pei, Identification of beta-arrestin2 as a G protein-coupled receptor-stimulated regulator of NF-kappaB pathways, Molecular cell 14(3) (2004) 303-17.
[221] D. Calebiro, V.O. Nikolaev, M.C. Gagliani, T. de Filippis, C. Dees, C. Tacchetti, L. Persani, M.J. Lohse, Persistent cAMP-signals triggered by internalized G-protein-coupled receptors, PLoS biology 7(8) (2009) e1000172.
[222] S. Ferrandon, T.N. Feinstein, M. Castro, B. Wang, R. Bouley, J.T. Potts, T.J. Gardella, J.P. Vilardaga, Sustained cyclic AMP production by parathyroid hormone receptor endocytosis, Nature chemical biology 5(10) (2009) 734-42.
[223] R. Irannejad, J.C. Tomshine, J.R. Tomshine, M. Chevalier, J.P. Mahoney, J. Steyaert, S.G.F. Rasmussen, R.K. Sunahara, H. El-Samad, B. Huang, M. von Zastrow, Conformational biosensors reveal adrenoceptor signalling from endosomes, Nature 495(7442) (2013) 10.1038/nature12000.
[224] P. Samama, S. Cotecchia, T. Costa, R.J. Lefkowitz, A mutation-induced activated state of the beta 2-adrenergic receptor. Extending the ternary complex model, J Biol Chem 268(7) (1993) 4625-36.
[225] P. Samama, G. Pei, T. Costa, S. Cotecchia, R.J. Lefkowitz, Negative antagonists promote an inactive conformation of the beta 2-adrenergic receptor, Mol Pharmacol 45(3) (1994) 390-4.
[226] S. Robb, T.R. Cheek, F.L. Hannan, L.M. Hall, J.M. Midgley, P.D. Evans, Agonist-specific coupling of a cloned Drosophila octopamine/tyramine receptor to multiple second messenger systems, The EMBO journal 13(6) (1994) 1325-30.

[227] D. Spengler, C. Waeber, C. Pantaloni, F. Holsboer, J. Bockaert, P.H. Seeburg, L. Journot, Differential signal transduction by five splice variants of the PACAP receptor, Nature 365(6442) (1993) 170-5.
[228] A. Fisher, E. Heldman, D. Gurwitz, R. Haring, D. Barak, H. Meshulam, D. Marciano, R. Brandeis, Z. Pittel, M. Segal, et al., Selective signaling via unique M1 muscarinic agonists, Ann N Y Acad Sci 695 (1993) 300-3.
[229] S. Galandrin, M. Bouvier, Distinct signaling profiles of beta1 and beta2 adrenergic receptor ligands toward adenylyl cyclase and mitogen-activated protein kinase reveals the pluridimensionality of efficacy, Mol Pharmacol 70(5) (2006) 1575-84.
[230] K.A. Berg, S. Maayani, J. Goldfarb, C. Scaramellini, P. Leff, W.P. Clarke, Effector pathway-dependent relative efficacy at serotonin type 2A and 2C receptors: evidence for agonist-directed trafficking of receptor stimulus, Mol Pharmacol 54(1) (1998) 94-104.
[231] P. De Deurwaerdere, S. Navailles, K.A. Berg, W.P. Clarke, U. Spampinato, Constitutive activity of the serotonin2C receptor inhibits in vivo dopamine release in the rat striatum and nucleus accumbens, J Neurosci 24(13) (2004) 3235-41.
[232] G. Bardi, M. Lipp, M. Baggiolini, P. Loetscher, The T cell chemokine receptor CCR7 is internalized on stimulation with ELC, but not with SLC, Eur J Immunol 31(11) (2001) 3291-7.
[233] T. Kenakin, Functional Selectivity and Biased Receptor Signaling, Journal of Pharmacology and Experimental Therapeutics 336(2) (2011) 296-302.
[234] S. Reiner, M. Ambrosio, C. Hoffmann, M.J. Lohse, Differential signaling of the endogenous agonists at the beta2-adrenergic receptor, J Biol Chem 285(46) (2010) 36188-98.
[235] P. Zhao, M. Canals, J.E. Murphy, D. Klingler, E.M. Eriksson, J.C. Pelayo, M. Hardt, N.W. Bunnett, D.P. Poole, Agonist-biased trafficking of somatostatin receptor 2A in enteric neurons, J Biol Chem 288(36) (2013) 25689-700.
[236] M. Oppermann, M. Mack, A.E. Proudfoot, H. Olbrich, Differential effects of CC chemokines on CC chemokine receptor 5 (CCR5) phosphorylation and identification of phosphorylation sites on the CCR5 carboxyl terminus, J Biol Chem 274(13) (1999) 8875-85.
[237] S. Rajagopal, D.L. Bassoni, J.J. Campbell, N.P. Gerard, C. Gerard, T.S. Wehrman, Biased agonism as a mechanism for differential signaling by chemokine receptors, J Biol Chem 288(49) (2013) 35039-48.
[238] J. Corbisier, C. Gales, A. Huszagh, M. Parmentier, J.Y. Springael, Biased signaling at chemokine receptors, J Biol Chem 290(15) (2015) 9542-54.
[239] S.A. Nickolls, B. Fleck, S.R. Hoare, R.A. Maki, Functional selectivity of melanocortin 4 receptor peptide and nonpeptide agonists: evidence for ligand-specific conformational states, J Pharmacol Exp Ther 313(3) (2005) 1281-8.
[240] D.A. Deshpande, B.S. Theriot, R.B. Penn, J.K.L. Walker, β-Arrestins specifically constrain β2-adrenergic receptor signaling and function in airway smooth muscle, FASEB journal : official publication of the Federation of American Societies for Experimental Biology 22(7) (2008) 2134-2141.
[241] W.C.H. Wang, K.A. Mihlbachler, A.C. Brunnett, S.B. Liggett, Targeted transgenesis reveals discrete attenuator functions of GRK and PKA in airway β(2)-adrenergic receptor physiologic signaling, Proceedings of the National Academy of Sciences of the United States of America 106(35) (2009) 15007-15012.
[242] L.S. Barak, R.H. Oakley, S.A. Laporte, M.G. Caron, Constitutive arrestin-mediated desensitization of a human vasopressin receptor mutant associated with nephrogenic diabetes insipidus, Proceedings of the National Academy of Sciences of the United States of America 98(1) (2001) 93-98.
[243] T. Noma, A. Lemaire, S.V. Naga Prasad, L. Barki-Harrington, D.G. Tilley, J. Chen, P. Le Corvoisier, J.D. Violin, H. Wei, R.J. Lefkowitz, H.A. Rockman, β-Arrestin–

mediated β(1)-adrenergic receptor transactivation of the EGFR confers cardioprotection, The Journal of Clinical Investigation 117(9) (2007) 2445-2458.
[244] K. Balabanian, B. Lagane, J.L. Pablos, L. Laurent, T. Planchenault, O. Verola, C. Lebbe, D. Kerob, A. Dupuy, O. Hermine, J.F. Nicolas, V. Latger-Cannard, D. Bensoussan, P. Bordigoni, F. Baleux, F. Le Deist, J.L. Virelizier, F. Arenzana-Seisdedos, F. Bachelerie, WHIM syndromes with different genetic anomalies are accounted for by impaired CXCR4 desensitization to CXCL12, Blood 105(6) (2005) 2449-57.
[245] B. Poulin, A. Butcher, P. McWilliams, J.M. Bourgognon, R. Pawlak, K.C. Kong, A. Bottrill, S. Mistry, J. Wess, E.M. Rosethorne, S.J. Charlton, A.B. Tobin, The M3-muscarinic receptor regulates learning and memory in a receptor phosphorylation/arrestin-dependent manner, Proc Natl Acad Sci U S A 107(20) (2010) 9440-5.
[246] H. Yagi, W. Tan, P. Dillenburg-Pilla, S. Armando, P. Amornphimoltham, M. Simaan, R. Weigert, A.A. Molinolo, M. Bouvier, J.S. Gutkind, A synthetic biology approach reveals a CXCR4-G13-Rho signaling axis driving transendothelial migration of metastatic breast cancer cells, Sci Signal 4(191) (2011) ra60.
[247] J.D. Violin, S.M. DeWire, D. Yamashita, D.H. Rominger, L. Nguyen, K. Schiller, E.J. Whalen, M. Gowen, M.W. Lark, Selectively engaging beta-arrestins at the angiotensin II type 1 receptor reduces blood pressure and increases cardiac performance, J Pharmacol Exp Ther 335(3) (2010) 572-9.
[248] D. Gesty-Palmer, P. Flannery, L. Yuan, L. Corsino, R. Spurney, R.J. Lefkowitz, L.M. Luttrell, A beta-arrestin-biased agonist of the parathyroid hormone receptor (PTH1R) promotes bone formation independent of G protein activation, Science translational medicine 1(1) (2009) 1ra1.
[249] D.M. Kurrasch-Orbaugh, V.J. Watts, E.L. Barker, D.E. Nichols, Serotonin 5-Hydroxytryptamine2A Receptor-Coupled Phospholipase C and Phospholipase A2 Signaling Pathways Have Different Receptor Reserves, Journal of Pharmacology and Experimental Therapeutics 304(1) (2003) 229-237.
[250] B. Tchernychev, Y. Ren, P. Sachdev, J.M. Janz, L. Haggis, A. O'Shea, E. McBride, R. Looby, Q. Deng, T. McMurry, M.A. Kazmi, T.P. Sakmar, S. Hunt, 3rd, K.E. Carlson, Discovery of a CXCR4 agonist pepducin that mobilizes bone marrow hematopoietic cells, Proc Natl Acad Sci U S A 107(51) (2010) 22255-9.
[251] P.R. Moya, K.A. Berg, M.A. Gutierrez-Hernandez, P. Saez-Briones, M. Reyes-Parada, B.K. Cassels, W.P. Clarke, Functional selectivity of hallucinogenic phenethylamine and phenylisopropylamine derivatives at human 5-hydroxytryptamine (5-HT)2A and 5-HT2C receptors, J Pharmacol Exp Ther 321(3) (2007) 1054-61.
[252] J.G. Richman, M. Kanemitsu-Parks, I. Gaidarov, J.S. Cameron, P. Griffin, H. Zheng, N.C. Guerra, L. Cham, D. Maciejewski-Lenoir, D.P. Behan, D. Boatman, R. Chen, P. Skinner, P. Ornelas, M.G. Waters, S.D. Wright, G. Semple, D.T. Connolly, Nicotinic acid receptor agonists differentially activate downstream effectors, J Biol Chem 282(25) (2007) 18028-36.
[253] T. Georgieva, S. Devanathan, D. Stropova, C.K. Park, Z. Salamon, G. Tollin, V.J. Hruby, W.R. Roeske, H.I. Yamamura, E. Varga, Unique agonist-bound cannabinoid CB1 receptor conformations indicate agonist specificity in signaling, Eur J Pharmacol 581(1-2) (2008) 19-29.
[254] S. Galandrin, G. Oligny-Longpre, H. Bonin, K. Ogawa, C. Gales, M. Bouvier, Conformational rearrangements and signaling cascades involved in ligand-biased mitogen-activated protein kinase signaling through the beta1-adrenergic receptor, Mol Pharmacol 74(1) (2008) 162-72.

[255] A.W. Kahsai, K. Xiao, S. Rajagopal, S. Ahn, A.K. Shukla, J. Sun, T.G. Oas, R.J. Lefkowitz, Multiple ligand-specific conformations of the beta2-adrenergic receptor, Nature chemical biology 7(10) (2011) 692-700.
[256] S. Granier, S. Kim, A.M. Shafer, V.R. Ratnala, J.J. Fung, R.N. Zare, B. Kobilka, Structure and conformational changes in the C-terminal domain of the beta2-adrenoceptor: insights from fluorescence resonance energy transfer studies, J Biol Chem 282(18) (2007) 13895-905.
[257] A. Bisello, M. Chorev, M. Rosenblatt, L. Monticelli, D.F. Mierke, S.L. Ferrari, Selective ligand-induced stabilization of active and desensitized parathyroid hormone type 1 receptor conformations, J Biol Chem 277(41) (2002) 38524-30.
[258] J.P. Vilardaga, M. Frank, C. Krasel, C. Dees, R.A. Nissenson, M.J. Lohse, Differential conformational requirements for activation of G proteins and the regulatory proteins arrestin and G protein-coupled receptor kinase in the G protein-coupled receptor for parathyroid hormone (PTH)/PTH-related protein, J Biol Chem 276(36) (2001) 33435-43.
[259] K.J. Gregory, P.M. Sexton, A.B. Tobin, A. Christopoulos, Stimulus bias provides evidence for conformational constraints in the structure of a G protein-coupled receptor, J Biol Chem 287(44) (2012) 37066-77.
[260] R. Rahmeh, M. Damian, M. Cottet, H. Orcel, C. Mendre, T. Durroux, K.S. Sharma, G. Durand, B. Pucci, E. Trinquet, J.M. Zwier, X. Deupi, P. Bron, J.L. Baneres, B. Mouillac, S. Granier, Structural insights into biased G protein-coupled receptor signaling revealed by fluorescence spectroscopy, Proc Natl Acad Sci U S A 109(17) (2012) 6733-8.
[261] J.L. Whistler, B.O. Gerber, E.C. Meng, T.J. Baranski, M. von Zastrow, H.R. Bourne, Constitutive activation and endocytosis of the complement factor 5a receptor: evidence for multiple activated conformations of a G protein-coupled receptor, Traffic (Copenhagen, Denmark) 3(12) (2002) 866-77.
[262] A.K. Shukla, J.D. Violin, E.J. Whalen, D. Gesty-Palmer, S.K. Shenoy, R.J. Lefkowitz, Distinct conformational changes in β-arrestin report biased agonism at seven-transmembrane receptors, Proceedings of the National Academy of Sciences 105(29) (2008) 9988-9993.
[263] V.O. Nikolaev, C. Hoffmann, M. Bunemann, M.J. Lohse, J.P. Vilardaga, Molecular basis of partial agonism at the neurotransmitter alpha2A-adrenergic receptor and Gi-protein heterotrimer, J Biol Chem 281(34) (2006) 24506-11.
[264] J. Okude, T. Ueda, Y. Kofuku, M. Sato, N. Nobuyama, K. Kondo, Y. Shiraishi, T. Mizumura, K. Onishi, M. Natsume, M. Maeda, H. Tsujishita, T. Kuranaga, M. Inoue, I. Shimada, Identification of a Conformational Equilibrium That Determines the Efficacy and Functional Selectivity of the mu-Opioid Receptor, Angewandte Chemie (International ed. in English) (2015).
[265] H. Wei, S. Ahn, S.K. Shenoy, S.S. Karnik, L. Hunyady, L.M. Luttrell, R.J. Lefkowitz, Independent beta-arrestin 2 and G protein-mediated pathways for angiotensin II activation of extracellular signal-regulated kinases 1 and 2, Proc Natl Acad Sci U S A 100(19) (2003) 10782-7.
[266] M. Azzi, P.G. Charest, S. Angers, G. Rousseau, T. Kohout, M. Bouvier, G. Pineyro, Beta-arrestin-mediated activation of MAPK by inverse agonists reveals distinct active conformations for G protein-coupled receptors, Proc Natl Acad Sci U S A 100(20) (2003) 11406-11.
[267] A. Steen, S. Thiele, D. Guo, L.S. Hansen, T.M. Frimurer, M.M. Rosenkilde, Biased and constitutive signaling in the CC-chemokine receptor CCR5 by manipulating the interface between transmembrane helices 6 and 7, J Biol Chem 288(18) (2013) 12511-21.

[268] S.J. Peroutka, S.H. Snyder, Regulation of serotonin2 (5-HT2) receptors labeled with [3H]spiroperidol by chronic treatment with the antidepressant amitriptyline, J Pharmacol Exp Ther 215(3) (1980) 582-7.
[269] B.F. Roettger, D. Ghanekar, R. Rao, C. Toledo, J. Yingling, D. Pinon, L.J. Miller, Antagonist-stimulated internalization of the G protein-coupled cholecystokinin receptor, Mol Pharmacol 51(3) (1997) 357-62.
[270] J.W. Wisler, S.M. DeWire, E.J. Whalen, J.D. Violin, M.T. Drake, S. Ahn, S.K. Shenoy, R.J. Lefkowitz, A unique mechanism of beta-blocker action: carvedilol stimulates beta-arrestin signaling, Proc Natl Acad Sci U S A 104(42) (2007) 16657-62.
[271] D. Wacker, C. Wang, V. Katritch, G.W. Han, X.P. Huang, E. Vardy, J.D. McCorvy, Y. Jiang, M. Chu, F.Y. Siu, W. Liu, H.E. Xu, V. Cherezov, B.L. Roth, R.C. Stevens, Structural features for functional selectivity at serotonin receptors, Science 340(6132) (2013) 615-9.
[272] J.J. Liu, R. Horst, V. Katritch, R.C. Stevens, K. Wuthrich, Biased signaling pathways in beta2-adrenergic receptor characterized by 19F-NMR, Science 335(6072) (2012) 1106-10.
[273] G. Fenalti, P.M. Giguere, V. Katritch, X.P. Huang, A.A. Thompson, V. Cherezov, B.L. Roth, R.C. Stevens, Molecular control of delta-opioid receptor signalling, Nature 506(7487) (2014) 191-6.
[274] J.L. Whistler, M. von Zastrow, Morphine-activated opioid receptors elude desensitization by beta-arrestin, Proc Natl Acad Sci U S A 95(17) (1998) 9914-9.
[275] J. Zhang, S.S. Ferguson, P.Y. Law, L.S. Barak, M.G. Caron, Agonist-specific regulation of delta-opioid receptor trafficking by G protein-coupled receptor kinase and beta-arrestin, Journal of receptor and signal transduction research 19(1-4) (1999) 301-13.
[276] T.A. Kohout, S.L. Nicholas, S.J. Perry, G. Reinhart, S. Junger, R.S. Struthers, Differential desensitization, receptor phosphorylation, beta-arrestin recruitment, and ERK1/2 activation by the two endogenous ligands for the CC chemokine receptor 7, J Biol Chem 279(22) (2004) 23214-22.
[277] M.M. Lewis, V.J. Watts, C.P. Lawler, D.E. Nichols, R.B. Mailman, Homologous desensitization of the D1A dopamine receptor: efficacy in causing desensitization dissociates from both receptor occupancy and functional potency, J Pharmacol Exp Ther 286(1) (1998) 345-53.
[278] Z.-G. Gao, K.A. Jacobson, Translocation of Arrestin Induced by Human A(3) Adenosine Receptor Ligands in an Engineered Cell Line: Comparison with G Protein-dependent Pathways, Pharmacological research : the official journal of the Italian Pharmacological Society 57(4) (2008) 303-311.
[279] V. Wehbi, T. Tranchant, G. Durand, A. Musnier, J. Decourtye, V. Piketty, V.Y. Butnev, G.R. Bousfield, P. Crepieux, M.C. Maurel, E. Reiter, Partially deglycosylated equine LH preferentially activates beta-arrestin-dependent signaling at the follicle-stimulating hormone receptor, Molecular endocrinology (Baltimore, Md.) 24(3) (2010) 561-73.
[280] D. Gesty-Palmer, M. Chen, E. Reiter, S. Ahn, C.D. Nelson, S. Wang, A.E. Eckhardt, C.L. Cowan, R.F. Spurney, L.M. Luttrell, R.J. Lefkowitz, Distinct beta-arrestin- and G protein-dependent pathways for parathyroid hormone receptor-stimulated ERK1/2 activation, J Biol Chem 281(16) (2006) 10856-64.
[281] A.C. Holloway, H. Qian, L. Pipolo, J. Ziogas, S. Miura, S. Karnik, B.R. Southwell, M.J. Lew, W.G. Thomas, Side-chain substitutions within angiotensin II reveal different requirements for signaling, internalization, and phosphorylation of type 1A angiotensin receptors, Mol Pharmacol 61(4) (2002) 768-77.

[282] N. Marie, I. Lecoq, P. Jauzac, S. Allouche, Differential sorting of human delta-opioid receptors after internalization by peptide and alkaloid agonists, J Biol Chem 278(25) (2003) 22795-804.
[283] A.J. Butcher, R. Prihandoko, K.C. Kong, P. McWilliams, J.M. Edwards, A. Bottrill, S. Mistry, A.B. Tobin, Differential G-protein-coupled receptor phosphorylation provides evidence for a signaling bar code, J Biol Chem 286(13) (2011) 11506-18.
[284] K.N. Nobles, K. Xiao, S. Ahn, A.K. Shukla, C.M. Lam, S. Rajagopal, R.T. Strachan, T.Y. Huang, E.A. Bressler, M.R. Hara, S.K. Shenoy, S.P. Gygi, R.J. Lefkowitz, Distinct phosphorylation sites on the beta(2)-adrenergic receptor establish a barcode that encodes differential functions of beta-arrestin, Sci Signal 4(185) (2011).
[285] D.A. Zidar, J.D. Violin, E.J. Whalen, R.J. Lefkowitz, Selective engagement of G protein coupled receptor kinases (GRKs) encodes distinct functions of biased ligands, Proc Natl Acad Sci U S A 106(24) (2009) 9649-54.
[286] J. Quoyer, J.M. Janz, J. Luo, Y. Ren, S. Armando, V. Lukashova, J.L. Benovic, K.E. Carlson, S.W. Hunt, 3rd, M. Bouvier, Pepducin targeting the C-X-C chemokine receptor type 4 acts as a biased agonist favoring activation of the inhibitory G protein, Proc Natl Acad Sci U S A 110(52) (2013) E5088-97.
[287] K. Xiao, S.K. Shenoy, K. Nobles, R.J. Lefkowitz, Activation-dependent conformational changes in {beta}-arrestin 2, J Biol Chem 279(53) (2004) 55744-53.
[288] F. Yang, X. Yu, C. Liu, C.-X. Qu, Z. Gong, H.-D. Liu, F.-H. Li, H.-M. Wang, D.-F. He, F. Yi, C. Song, C.-L. Tian, K.-H. Xiao, J.-Y. Wang, J.-P. Sun, Phospho-selective mechanisms of arrestin conformations and functions revealed by unnatural amino acid incorporation and (19)F-NMR, Nature communications 6 (2015) 8202.
[289] S. Nuber, U. Zabel, K. Lorenz, A. Nuber, G. Milligan, A.B. Tobin, M.J. Lohse, C. Hoffmann, beta-Arrestin biosensors reveal a rapid, receptor-dependent activation/deactivation cycle, Nature 531(7596) (2016) 661-4.
[290] M. Ghosh, A. Schonbrunn, Differential temporal and spatial regulation of somatostatin receptor phosphorylation and dephosphorylation, J Biol Chem 286(15) (2011) 13561-73.
[291] L. Bray, C. Froment, P. Pardo, C. Candotto, O. Burlet-Schiltz, J.M. Zajac, C. Mollereau, L. Mouledous, Identification and functional characterization of the phosphorylation sites of the neuropeptide FF2 receptor, J Biol Chem 289(49) (2014) 33754-66.
[292] R. El Kouhen, A.L. Burd, L.J. Erickson-Herbrandson, C.Y. Chang, P.Y. Law, H.H. Loh, Phosphorylation of Ser363, Thr370, and Ser375 residues within the carboxyl tail differentially regulates mu-opioid receptor internalization, J Biol Chem 276(16) (2001) 12774-80.
[293] J.D. Violin, X.R. Ren, R.J. Lefkowitz, G-protein-coupled receptor kinase specificity for beta-arrestin recruitment to the beta2-adrenergic receptor revealed by fluorescence resonance energy transfer, J Biol Chem 281(29) (2006) 20577-88.
[294] J. Kim, S. Ahn, X.R. Ren, E.J. Whalen, E. Reiter, H. Wei, R.J. Lefkowitz, Functional antagonism of different G protein-coupled receptor kinases for beta-arrestin-mediated angiotensin II receptor signaling, Proc Natl Acad Sci U S A 102(5) (2005) 1442-7.
[295] E. Kara, P. Crepieux, C. Gauthier, N. Martinat, V. Piketty, F. Guillou, E. Reiter, A phosphorylation cluster of five serine and threonine residues in the C-terminus of the follicle-stimulating hormone receptor is important for desensitization but not for beta-arrestin-mediated ERK activation, Molecular endocrinology (Baltimore, Md.) 20(11) (2006) 3014-26.
[296] X.R. Ren, E. Reiter, S. Ahn, J. Kim, W. Chen, R.J. Lefkowitz, Different G protein-coupled receptor kinases govern G protein and beta-arrestin-mediated signaling of V2 vasopressin receptor, Proc Natl Acad Sci U S A 102(5) (2005) 1448-53.

[297] J.M. Busillo, S. Armando, R. Sengupta, O. Meucci, M. Bouvier, J.L. Benovic, Site-specific phosphorylation of CXCR4 is dynamically regulated by multiple kinases and results in differential modulation of CXCR4 signaling, J Biol Chem 285(10) (2010) 7805-17.
[298] W.G. Thomas, H. Qian, C.S. Chang, S. Karnik, Agonist-induced phosphorylation of the angiotensin II (AT(1A)) receptor requires generation of a conformation that is distinct from the inositol phosphate-signaling state, J Biol Chem 275(4) (2000) 2893-900.
[299] G.A. Santos, D.A. Duarte, L.T. Parreiras-e-Silva, F.R. Teixeira, R. Silva-Rocha, E.B. Oliveira, M. Bouvier, C.M. Costa-Neto, Comparative analyses of downstream signal transduction targets modulated after activation of the AT(1) receptor by two β-arrestin-biased agonists, Frontiers in pharmacology 6 (2015) 131.
[300] K.H. Ahn, M.M. Mahmoud, J.Y. Shim, D.A. Kendall, Distinct roles of beta-arrestin 1 and beta-arrestin 2 in ORG27569-induced biased signaling and internalization of the cannabinoid receptor 1 (CB1), J Biol Chem 288(14) (2013) 9790-800.
[301] S. Allouche, J. Polastron, A. Hasbi, V. Homburger, P. Jauzac, Differential G-protein activation by alkaloid and peptide opioid agonists in the human neuroblastoma cell line SK-N-BE, Biochemical Journal 342(1) (1999) 71-78.
[302] K.L. Laugwitz, S. Offermanns, K. Spicher, G. Schultz, mu and delta opioid receptors differentially couple to G protein subtypes in membranes of human neuroblastoma SH-SY5Y cells, Neuron 10(2) (1993) 233-42.
[303] M.G. Eason, H. Kurose, B.D. Holt, J.R. Raymond, S.B. Liggett, Simultaneous coupling of alpha 2-adrenergic receptors to two G-proteins with opposing effects. Subtype-selective coupling of alpha 2C10, alpha 2C4, and alpha 2C2 adrenergic receptors to Gi and Gs, J Biol Chem 267(22) (1992) 15795-801.
[304] Y. Daaka, L.M. Luttrell, R.J. Lefkowitz, Switching of the coupling of the beta2-adrenergic receptor to different G proteins by protein kinase A, Nature 390(6655) (1997) 88-91.
[305] R.P. Xiao, X. Ji, E.G. Lakatta, Functional coupling of the beta 2-adrenoceptor to a pertussis toxin-sensitive G protein in cardiac myocytes, Mol Pharmacol 47(2) (1995) 322-9.
[306] I.D. Alves, K.A. Ciano, V. Boguslavski, E. Varga, Z. Salamon, H.I. Yamamura, V.J. Hruby, G. Tollin, Selectivity, cooperativity, and reciprocity in the interactions between the delta-opioid receptor, its ligands, and G-proteins, J Biol Chem 279(43) (2004) 44673-82.
[307] M.G. Eason, M.T. Jacinto, S.B. Liggett, Contribution of ligand structure to activation of alpha 2-adrenergic receptor subtype coupling to Gs, Molecular Pharmacology 45(4) (1994) 696-702.
[308] Y. Tian, D.C. New, L.Y. Yung, R.A. Allen, P.M. Slocombe, B.M. Twomey, M.M. Lee, Y.H. Wong, Differential chemokine activation of CC chemokine receptor 1-regulated pathways: ligand selective activation of Galpha 14-coupled pathways, Eur J Immunol 34(3) (2004) 785-95.
[309] R.P. Xiao, S.J. Zhang, K. Chakir, P. Avdonin, W. Zhu, R.A. Bond, C.W. Balke, E.G. Lakatta, H. Cheng, Enhanced G(i) signaling selectively negates beta2-adrenergic receptor (AR)--but not beta1-AR-mediated positive inotropic effect in myocytes from failing rat hearts, Circulation 108(13) (2003) 1633-9.
[310] J.R. Lane, B. Powney, A. Wise, S. Rees, G. Milligan, Protean agonism at the dopamine D2 receptor: (S)-3-(3-hydroxyphenyl)-N-propylpiperidine is an agonist for activation of Go1 but an antagonist/inverse agonist for Gi1,Gi2, and Gi3, Mol Pharmacol 71(5) (2007) 1349-59.

[311] M. Kocan, M. Sarwar, M.A. Hossain, J.D. Wade, R.J. Summers, Signalling profiles of H3 relaxin, H2 relaxin and R3(BΔ23–27)R/I5 acting at the relaxin family peptide receptor 3 (RXFP3), British Journal of Pharmacology 171(11) (2014) 2827-2841.
[312] T.W. Gettys, T.A. Fields, J.R. Raymond, Selective Activation of Inhibitory G-Protein .alpha.-Subunits by Partial Agonists of the Human 5-HT1A Receptor, Biochemistry 33(14) (1994) 4283-4290.
[313] B. Sivertsen, M. Lang, T.M. Frimurer, N.D. Holliday, A. Bach, S. Els, M.S. Engelstoft, P.S. Petersen, A.N. Madsen, T.W. Schwartz, A.G. Beck-Sickinger, B. Holst, Unique interaction pattern for a functionally biased ghrelin receptor agonist, J Biol Chem 286(23) (2011) 20845-60.
[314] D.M. Kurrasch-Orbaugh, J.C. Parrish, V.J. Watts, D.E. Nichols, A complex signaling cascade links the serotonin2A receptor to phospholipase A2 activation: the involvement of MAP kinases, J Neurochem 86(4) (2003) 980-91.
[315] B.L. Roth, T. Nakaki, D.M. Chuang, E. Costa, Aortic recognition sites for serotonin (5HT) are coupled to phospholipase C and modulate phosphatidylinositol turnover, Neuropharmacology 23(10) (1984) 1223-5.
[316] S. Blattermann, L. Peters, P.A. Ottersbach, A. Bock, V. Konya, C.D. Weaver, A. Gonzalez, R. Schroder, R. Tyagi, P. Luschnig, J. Gab, S. Hennen, T. Ulven, L. Pardo, K. Mohr, M. Gutschow, A. Heinemann, E. Kostenis, A biased ligand for OXE-R uncouples Galpha and Gbetagamma signaling within a heterotrimer, Nature chemical biology 8(7) (2012) 631-8.
[317] P. Chidiac, RGS proteins destroy spare receptors: Effects of GPCR-interacting proteins and signal deamplification on measurements of GPCR agonist potency, Methods (San Diego, Calif.) 92 (2016) 87-93.
[318] K.Y. Chung, P.W. Day, G. Vélez-Ruiz, R.K. Sunahara, B.K. Kobilka, Identification of GPCR-Interacting Cytosolic Proteins Using HDL Particles and Mass Spectrometry-Based Proteomic Approach, PLoS ONE 8(1) (2013) e54942.
[319] Z. Georgoussi, E.M. Georganta, G. Milligan, The other side of opioid receptor signalling: regulation by protein-protein interaction, Curr Drug Targets 13(1) (2012) 80-102.
[320] D.L. Hay, D.R. Poyner, P.M. Sexton, GPCR modulation by RAMPs, Pharmacol Ther 109(1-2) (2006) 173-97.
[321] J. Bockaert, P. Marin, A. Dumuis, L. Fagni, The 'magic tail' of G protein-coupled receptors: an anchorage for functional protein networks, FEBS letters 546(1) (2003) 65-72.
[322] S.L. Ritter, R.A. Hall, Fine-tuning of GPCR activity by receptor-interacting proteins, Nature reviews. Molecular cell biology 10(12) (2009) 819-830.
[323] P. Huang, D. Steplock, E.J. Weinman, R.A. Hall, Z. Ding, J. Li, Y. Wang, L.Y. Liu-Chen, kappa Opioid receptor interacts with Na(+)/H(+)-exchanger regulatory factor-1/Ezrin-radixin-moesin-binding phosphoprotein-50 (NHERF-1/EBP50) to stimulate Na(+)/H(+) exchange independent of G(i)/G(o) proteins, J Biol Chem 279(24) (2004) 25002-9.
[324] R.A. Hall, R.T. Premont, C.W. Chow, J.T. Blitzer, J.A. Pitcher, A. Claing, R.H. Stoffel, L.S. Barak, S. Shenolikar, E.J. Weinman, S. Grinstein, R.J. Lefkowitz, The beta2-adrenergic receptor interacts with the Na+/H+-exchanger regulatory factor to control Na+/H+ exchange, Nature 392(6676) (1998) 626-30.
[325] M.B. Marrero, V.J. Venema, H. Ju, D.C. Eaton, R.C. Venema, Regulation of angiotensin II-induced JAK2 tyrosine phosphorylation: roles of SHP-1 and SHP-2, The American journal of physiology 275(5 Pt 1) (1998) C1216-23.
[326] C. Bousquet, J. Guillermet-Guibert, N. Saint-Laurent, E. Archer-Lahlou, F. Lopez, M. Fanjul, A. Ferrand, D. Fourmy, C. Pichereaux, B. Monsarrat, L. Pradayrol, J.P.

Esteve, C. Susini, Direct binding of p85 to sst2 somatostatin receptor reveals a novel mechanism for inhibiting PI3K pathway, The EMBO journal 25(17) (2006) 3943-54.
[327] M.S. Ali, P.P. Sayeski, L.B. Dirksen, D.J. Hayzer, M.B. Marrero, K.E. Bernstein, Dependence on the Motif YIPP for the Physical Association of Jak2 Kinase with the Intracellular Carboxyl Tail of the Angiotensin II AT1 Receptor, Journal of Biological Chemistry 272(37) (1997) 23382-23388.
[328] T.N. Doan, M.S. Ali, K.E. Bernstein, Tyrosine Kinase Activation by the Angiotensin II Receptor in the Absence of Calcium Signaling, Journal of Biological Chemistry 276(24) (2001) 20954-20958.
[329] A.A. Thompson, W. Liu, E. Chun, V. Katritch, H. Wu, E. Vardy, X.P. Huang, C. Trapella, R. Guerrini, G. Calo, B.L. Roth, V. Cherezov, R.C. Stevens, Structure of the nociceptin/orphanin FQ receptor in complex with a peptide mimetic, Nature 485(7398) (2012) 395-9.
[330] J.C. Meunier, C. Mollereau, L. Toll, C. Suaudeau, C. Moisand, P. Alvinerie, J.L. Butour, J.C. Guillemot, P. Ferrara, B. Monsarrat, et al., Isolation and structure of the endogenous agonist of opioid receptor-like ORL1 receptor, Nature 377(6549) (1995) 532-5.
[331] J.E. Lachowicz, Y. Shen, F.J. Monsma, Jr., D.R. Sibley, Molecular cloning of a novel G protein-coupled receptor related to the opiate receptor family, J Neurochem 64(1) (1995) 34-40.
[332] A. Janecka, J. Fichna, T. Janecki, Opioid receptors and their ligands, Curr Top Med Chem 4(1) (2004) 1-17.
[333] A. Mansour, M.T. Hoversten, L.P. Taylor, S.J. Watson, H. Akil, The cloned mu, delta and kappa receptors and their endogenous ligands: evidence for two opioid peptide recognition cores, Brain Res 700(1-2) (1995) 89-98.
[334] J.E. Zadina, L. Hackler, L.J. Ge, A.J. Kastin, A potent and selective endogenous agonist for the μ-opiate receptor, Nature 386(6624) (1997) 499-502.
[335] A. Terskiy, K.M. Wannemacher, P.N. Yadav, M. Tsai, B. Tian, R.D. Howells, Search of the human proteome for endomorphin-1 and endomorphin-2 precursor proteins, Life sciences 81(23-24) (2007) 1593-601.
[336] A.Z. Ronai, K. Kiraly, A. Szebeni, E. Szemenyei, Z. Prohaszka, Z. Darula, G. Toth, I. Till, B. Szalay, E. Kato, I. Barna, Immunoreactive endomorphin 2 is generated extracellularly in rat isolated L4,5 dorsal root ganglia by DPP-IV, Regul Pept 157(1-3) (2009) 1-2.
[337] A. Lesniak, A.W. Lipkowski, Opioid peptides in peripheral pain control, Acta Neurobiol Exp 71(1) (2011) 129-38.
[338] M.J. Millan, Descending control of pain, Prog Neurobiol 66(6) (2002) 355-474.
[339] B.L. Kieffer, C. Gaveriaux-Ruff, Exploring the opioid system by gene knockout, Prog Neurobiol 66(5) (2002) 285-306.
[340] A.R. Light, E.R. Perl, Reexamination of the dorsal root projection to the spinal dorsal horn including observations on the differential termination of coarse and fine fibers, The Journal of comparative neurology 186(2) (1979) 117-131.
[341] K.K. Rau, R.M. Caudle, B.Y. Cooper, R.D. Johnson, Diverse immunocytochemical expression of opioid receptors in electrophysiologically defined cells of rat dorsal root ganglia, J Chem Neuroanat 29(4) (2005) 255-64.
[342] G. Scherrer, N. Imamachi, Y.Q. Cao, C. Contet, F. Mennicken, D. O'Donnell, B.L. Kieffer, A.I. Basbaum, Dissociation of the opioid receptor mechanisms that control mechanical and heat pain, Cell 137(6) (2009) 1148-59.
[343] B.Y. Cooper, C.J. Vierck, Jr., D.C. Yeomans, Selective reduction of second pain sensations by systemic morphine in humans, Pain 24(1) (1986) 93-116.

[344] U. Arvidsson, M. Riedl, S. Chakrabarti, J.H. Lee, A.H. Nakano, R.J. Dado, H.H. Loh, P.Y. Law, M.W. Wessendorf, R. Elde, Distribution and targeting of a mu-opioid receptor (MOR1) in brain and spinal cord, J Neurosci 15(5 Pt 1) (1995) 3328-41.
[345] E. Erbs, L. Faget, G. Scherrer, A. Matifas, D. Filliol, J.-L. Vonesch, M. Koch, P. Kessler, D. Hentsch, M.-C. Birling, M. Koutsourakis, L. Vasseur, P. Veinante, B.L. Kieffer, D. Massotte, A mu–delta opioid receptor brain atlas reveals neuronal co-occurrence in subcortical networks, Brain Structure & Function 220(2) (2015) 677-702.
[346] A. Moriwaki, J.B. Wang, A. Svingos, E. van Bockstaele, P. Cheng, V. Pickel, G.R. Uhl, mu Opiate receptor immunoreactivity in rat central nervous system, Neurochemical research 21(11) (1996) 1315-31.
[347] S. Irwin, D.R. Bennett, L.C. Hendershot, M.H. Seevers, R.W. Houde, THE EFFECTS OF MORPHINE, METHADONE AND MEPERIDINE ON SOME REFLEX RESPONSES OF SPINAL ANIMALS TO NOCICEPTIVE STIMULATION, Journal of Pharmacology and Experimental Therapeutics 101(2) (1951) 132-143.
[348] R.H.t. Kline, R.G. Wiley, Spinal mu-opioid receptor-expressing dorsal horn neurons: role in nociception and morphine antinociception, J Neurosci 28(4) (2008) 904-13.
[349] J.C. Willer, B. Bussel, Evidence for a direct spinal mechanism in morphine-induced inhibition of nociceptive reflexes in humans, Brain Res 187(1) (1980) 212-5.
[350] A.D. Craig, L.P. Serrano, Effects of systemic morphine on lamina I spinothalamic tract neurons in the cat, Brain Res 636(2) (1994) 233-44.
[351] D. Le Bars, J.P. Rivot, G. Guilbaud, D. Menetrey, J.M. Besson, The depressive effects of morphine on the C fibre response of dorsal horn neurones in the spinal rat pretreated or not by pCPA, Brain Res 176(2) (1979) 337-53.
[352] D. Le Bars, D. Menetrey, C. Conseiller, J.M. Besson, Depressive effects of morphine upon lamina V cells activities in the dorsal horn of the spinal cat, Brain Res 98(2) (1975) 261-77.
[353] F.J. Einspahr, M.F. Piercey, Morphine depresses dorsal horn neuron responses to controlled noxious and non-noxious cutaneous stimulation, J Pharmacol Exp Ther 213(3) (1980) 456-61.
[354] W. Zieglgansberger, H. Bayerl, The mechanism of inhibition of neuronal activity by opiates in the spinal cord of cat, Brain Res 115(1) (1976) 111-28.
[355] J. Yang, Y. Yang, J. Chu, G. Wang, H. Xu, W.Y. Liu, C.H. Wang, B.C. Lin, Endogenous opiate peptides in the spinal cord are involved in the analgesia of hypothalamic paraventricular nucleus in the rat, Peptides 30(4) (2009) 740-4.
[356] T.L. Yaksh, L. Terenius, F. Nyberg, K. Jhamandas, J.Y. Wang, Studies on the release by somatic stimulation from rat and cat spinal cord of active materials which displace dihydromorphine in an opiate-binding assay, Brain Res 268(1) (1983) 119-28.
[357] D. Le Bars, S. Bourgoin, A.M. Clot, M. Hamon, F. Cesselin, Noxious mechanical stimuli increase the release of Met-enkephalin-like material heterosegmentally in the rat spinal cord, Brain Res 402(1) (1987) 188-92.
[358] R. Elde, T. Hokfelt, O. Johansson, L. Terenius, Immunohistochemical studies using antibodies to leucine-enkephalin: initial observations on the nervous system of the rat, Neuroscience 1(4) (1976) 349-51.
[359] M. Tsuchiya, H. Yamazaki, Y. Hori, Enkephalinergic neurons express 5-HT3 receptors in the spinal cord dorsal horn: single cell RT-PCR analysis, Neuroreport 10(13) (1999) 2749-53.
[360] K. Tsou, H. Khachaturian, H. Akil, S.J. Watson, Immunocytochemical localization of pro-opiomelanocortin-derived peptides in the adult rat spinal cord, Brain Res 378(1) (1986) 28-35.

[361] B. Song, J.C. Marvizon, Dorsal horn neurons firing at high frequency, but not primary afferents, release opioid peptides that produce micro-opioid receptor internalization in the rat spinal cord, J Neurosci 23(27) (2003) 9171-84.
[362] L. Lao, B. Song, W. Chen, J.C.G. Marvizón, Noxious mechanical stimulation evokes the segmental release of opioid peptides that induce μ-opioid receptor internalization in the presence of peptidase inhibitors, Brain Research 1197(0) (2008) 85-93.
[363] J.A. Trafton, C. Abbadie, K. Marek, A.I. Basbaum, Postsynaptic signaling via the [mu]-opioid receptor: responses of dorsal horn neurons to exogenous opioids and noxious stimulation, J Neurosci 20(23) (2000) 8578-84.
[364] S. Martin-Schild, J.E. Zadina, A.A. Gerall, S. Vigh, A.J. Kastin, Localization of endomorphin-2-like immunoreactivity in the rat medulla and spinal cord, Peptides 18(10) (1997) 1641-9.
[365] S. Martin-Schild, A.A. Gerall, A.J. Kastin, J.E. Zadina, Endomorphin-2 is an endogenous opioid in primary sensory afferent fibers, Peptides 19(10) (1998) 1783-9.
[366] K. Sanderson Nydahl, K. Skinner, D. Julius, A.I. Basbaum, Co-localization of endomorphin-2 and substance P in primary afferent nociceptors and effects of injury: a light and electron microscopic study in the rat, Eur J Neurosci 19(7) (2004) 1789-99.
[367] S.Y. Wu, S.L. Dun, M.T. Wright, J.K. Chang, N.J. Dun, Endomorphin-like immunoreactivity in the rat dorsal horn and inhibition of substantia gelatinosa neurons in vitro, Neuroscience 89(2) (1999) 317-21.
[368] T.L. Lisi, K.A. Sluka, A new electrochemical HPLC method for analysis of enkephalins and endomorphins, J Neurosci Methods 150(1) (2006) 74-9.
[369] A. Mansour, H. Khachaturian, M.E. Lewis, H. Akil, S.J. Watson, Autoradiographic differentiation of mu, delta, and kappa opioid receptors in the rat forebrain and midbrain, J Neurosci 7(8) (1987) 2445-64.
[370] J. Le Merrer, J.A. Becker, K. Befort, B.L. Kieffer, Reward processing by the opioid system in the brain, Physiol Rev 89(4) (2009) 1379-412.
[371] A.C. Gray, I.M. Coupar, P.J. White, Comparison of opioid receptor distributions in the rat central nervous system, Life sciences 79(7) (2006) 674-85.
[372] E. Carstens, B. Stelzer, M. Zimmermann, Microinjections of glutamate or morphine at coincident midbrain sites have different effects on nociceptive dorsal horn neurons in the rat, Neurosci Lett 95(1-3) (1988) 185-91.
[373] D.S. Baskin, W.R. Mehler, Y. Hosobuchi, D.E. Richardson, J.E. Adams, M.A. Flitter, Autopsy analysis of the safety, efficacy and cartography of electrical stimulation of the central gray in humans, Brain Res 371(2) (1986) 231-6.
[374] Y. Hosobuchi, J.E. Adams, R. Linchitz, Pain relief by electrical stimulation of the central gray matter in humans and its reversal by naloxone, Science 197(4299) (1977) 183-6.
[375] M.B. Llewelyn, J. Azami, M.H. Roberts, Brainstem mechanisms of antinociception. Effects of electrical stimulation and injection of morphine into the nucleus raphe magnus, Neuropharmacology 25(7) (1986) 727-35.
[376] J.L. Oliveras, F. Redjemi, G. Guilbaud, J.M. Besson, Analgesia induced by electrical stimulation of the inferior centralis nucleus of the raphe in the cat, Pain 1(2) (1975) 139-45.
[377] S.L. Jones, G.F. Gebhart, Inhibition of spinal nociceptive transmission from the midbrain, pons and medulla in the rat: activation of descending inhibition by morphine, glutamate and electrical stimulation, Brain Res 460(2) (1988) 281-96.
[378] R.J. Bodnar, C.L. Williams, S.J. Lee, G.W. Pasternak, Role of mu 1-opiate receptors in supraspinal opiate analgesia: a microinjection study, Brain Res 447(1) (1988) 25-34.

[379] H. Takagi, M. Satoh, A. Akaike, T. Shibata, H. Yajima, H. Ogawa, Analgesia by enkephalins injected into the nucleus reticularis gigantocellularis of rat medulla oblongata, Eur J Pharmacol 49(1) (1978) 113-6.
[380] G.J. Bennett, D.J. Mayer, Inhibition of spinal cord interneurons by narcotic microinjection and focal electrical stimulation in the periaqueductal central gray matter, Brain Res 172(2) (1979) 243-57.
[381] F. Fang, H.K. Proudfit, Spinal cholinergic and monoamine receptors mediate the antinociceptive effect of morphine microinjected in the periaqueductal gray on the rat tail, but not the feet, Brain Res 722(1-2) (1996) 95-108.
[382] J.E. Holden, H.K. Proudfit, Enkephalin neurons that project to the A7 catecholamine cell group are located in nuclei that modulate nociception: ventromedial medulla, Neuroscience 83(3) (1998) 929-47.
[383] S.P. Hunt, T.A. Lovick, The distribution of serotonin, met-enkephalin and beta-lipotropin-like immunoreactivity in neuronal perikarya of the cat brainstem, Neurosci Lett 30(2) (1982) 139-45.
[384] F.G. Williams, M.A. Mullet, A.J. Beitz, Basal release of Met-enkephalin and neurotensin in the ventrolateral periaqueductal gray matter of the rat: a microdialysis study of antinociceptive circuits, Brain Res 690(2) (1995) 207-16.
[385] D.E. Millhorn, T. Hokfelt, A.A. Verhofstad, L. Terenius, Individual cells in the raphe nuclei of the medulla oblongata in rat that contain immunoreactivities for both serotonin and enkephalin project to the spinal cord, Experimental brain research 75(3) (1989) 536-42.
[386] D. Menetrey, A.I. Basbaum, The distribution of substance P-, enkephalin- and dynorphin-immunoreactive neurons in the medulla of the rat and their contribution to bulbospinal pathways, Neuroscience 23(1) (1987) 173-87.
[387] V. Hollt, F.C. Tulunay, S.K. Woo, H.H. Loh, A. Herz, Opioid peptides derived from pro-enkephalin A but not that from pro-enkephalin B are substantial analgesics after administration into brain of mice, Eur J Pharmacol 85(3-4) (1982) 355-6.
[388] M. Rubinstein, J.S. Mogil, M. Japon, E.C. Chan, R.G. Allen, M.J. Low, Absence of opioid stress-induced analgesia in mice lacking beta-endorphin by site-directed mutagenesis, Proc Natl Acad Sci U S A 93(9) (1996) 3995-4000.
[389] C.A. Porro, F. Facchinetti, P. Pozzo, C. Benassi, G.P. Biral, A.R. Genazzani, Tonic pain time-dependently affects beta-endorphin-like immunoreactivity in the ventral periaqueductal gray matter of the rat brain, Neurosci Lett 86(1) (1988) 89-93.
[390] M. Hiramatsu, K. Inoue, A. Ambo, Y. Sasaki, T. Kameyama, Long-lasting antinociceptive effects of a novel dynorphin analogue, Tyr-D-Ala-Phe-Leu-Arg psi (CH(2)NH) Arg-NH(2), in mice, Br J Pharmacol 132(8) (2001) 1948-56.
[391] F. Bloom, E. Battenberg, J. Rossier, N. Ling, R. Guillemin, Neurons containing beta-endorphin in rat brain exist separately from those containing enkephalin: immunocytochemical studies, Proc Natl Acad Sci U S A 75(3) (1978) 1591-5.
[392] J.C. Finley, P. Lindstrom, P. Petrusz, Immunocytochemical localization of beta-endorphin-containing neurons in the rat brain, Neuroendocrinology 33(1) (1981) 28-42.
[393] S. Martin-Schild, A.A. Gerall, A.J. Kastin, J.E. Zadina, Differential distribution of endomorphin 1- and endomorphin 2-like immunoreactivities in the CNS of the rodent, The Journal of comparative neurology 405(4) (1999) 450-71.
[394] M. Gu, M. Wessendorf, Endomorphin-2-immunoreactive fibers selectively appose serotonergic neuronal somata in the rostral ventral medial medulla, The Journal of comparative neurology 502(5) (2007) 701-13.
[395] S.J. Watson, H. Akil, V.E. Ghazarossian, A. Goldstein, Dynorphin immunocytochemical localization in brain and peripheral nervous system: preliminary studies, Proc Natl Acad Sci U S A 78(2) (1981) 1260-3.

[396] C. Gramsch, V. Hollt, A. Pasi, P. Mehraein, A. Herz, Immunoreactive dynorphin in human brain and pituitary, Brain Res 233(1) (1982) 65-74.
[397] A. Herz, V. Hollt, C. Gramsch, B.R. Seizinger, Differential distribution, release, and modulation of dynorphin and beta-endorphin, Advances in biochemical psychopharmacology 33 (1982) 51-9.
[398] H.B. Wang, B. Zhao, Y.Q. Zhong, K.C. Li, Z.Y. Li, Q. Wang, Y.J. Lu, Z.N. Zhang, S.Q. He, H.C. Zheng, S.X. Wu, T.G. Hokfelt, L. Bao, X. Zhang, Coexpression of delta- and mu-opioid receptors in nociceptive sensory neurons, Proc Natl Acad Sci U S A 107(29) (2010) 13117-22.
[399] W. Truong, C. Cheng, Q.G. Xu, X.Q. Li, D.W. Zochodne, Mu opioid receptors and analgesia at the site of a peripheral nerve injury, Ann Neurol 53(3) (2003) 366-75.
[400] W.S. Young, 3rd, J.K. Wamsley, M.A. Zarbin, M.J. Kuhar, Opioid receptors undergo axonal flow, Science 210(4465) (1980) 76-8.
[401] C. Stein, A.H. Hassan, R. Przewlocki, C. Gramsch, K. Peter, A. Herz, Opioids from immunocytes interact with receptors on sensory nerves to inhibit nociception in inflammation, Proc Natl Acad Sci U S A 87(15) (1990) 5935-9.
[402] M. Bigliardi-Qi, L.T. Sumanovski, S. Buchner, T. Rufli, P.L. Bigliardi, Mu-opiate receptor and Beta-endorphin expression in nerve endings and keratinocytes in human skin, Dermatology 209(3) (2004) 183-9.
[403] H. Machelska, Control of neuropathic pain by immune cells and opioids, CNS Neurol Disord Drug Targets 10(5) (2011) 559-70.
[404] A.H. Hassan, A. Ableitner, C. Stein, A. Herz, Inflammation of the rat paw enhances axonal transport of opioid receptors in the sciatic nerve and increases their density in the inflamed tissue, Neuroscience 55(1) (1993) 185-95.
[405] R.R. Ji, Q. Zhang, P.Y. Law, H.H. Low, R. Elde, T. Hokfelt, Expression of mu-, delta-, and kappa-opioid receptor-like immunoreactivities in rat dorsal root ganglia after carrageenan-induced inflammation, J Neurosci 15(12) (1995) 8156-66.
[406] M. Schafer, Y. Imai, G.R. Uhl, C. Stein, Inflammation enhances peripheral mu-opioid receptor-mediated analgesia, but not mu-opioid receptor transcription in dorsal root ganglia, Eur J Pharmacol 279(2-3) (1995) 165-9.
[407] O. Pol, M.M. Puig, Expression of opioid receptors during peripheral inflammation, Curr Top Med Chem 4(1) (2004) 51-61.
[408] Q. Zhang, M. Schaffer, R. Elde, C. Stein, Effects of neurotoxins and hindpaw inflammation on opioid receptor immunoreactivities in dorsal root ganglia, Neuroscience 85(1) (1998) 281-91.
[409] W. Puehler, C. Zollner, A. Brack, M.A. Shaqura, H. Krause, M. Schafer, C. Stein, Rapid upregulation of mu opioid receptor mRNA in dorsal root ganglia in response to peripheral inflammation depends on neuronal conduction, Neuroscience 129(2) (2004) 473-9.
[410] I. Antonijevic, S.A. Mousa, M. Schafer, C. Stein, Perineurial defect and peripheral opioid analgesia in inflammation, J Neurosci 15(1 Pt 1) (1995) 165-72.
[411] Y. Olsson, Microenvironment of the peripheral nervous system under normal and pathological conditions, Crit Rev Neurobiol 5(3) (1990) 265-311.
[412] S.J. Lolait, J.A. Clements, A.J. Markwick, C. Cheng, M. McNally, A.I. Smith, J.W. Funder, Pro-opiomelanocortin messenger ribonucleic acid and posttranslational processing of beta endorphin in spleen macrophages, J Clin Invest 77(6) (1986) 1776-9.
[413] G. Zurawski, M. Benedik, B.J. Kamb, J.S. Abrams, S.M. Zurawski, F.D. Lee, Activation of mouse T-helper cells induces abundant preproenkephalin mRNA synthesis, Science 232(4751) (1986) 772-5.
[414] E.M. Smith, A.C. Morrill, W.J. Meyer, 3rd, J.E. Blalock, Corticotropin releasing factor induction of leukocyte-derived immunoreactive ACTH and endorphins, Nature 321(6073) (1986) 881-2.

[415] S.A. Mousa, H. Machelska, M. Schafer, C. Stein, Immunohistochemical localization of endomorphin-1 and endomorphin-2 in immune cells and spinal cord in a model of inflammatory pain, J Neuroimmunol 126(1-2) (2002) 5-15.
[416] G.M. Denning, L.W. Ackermann, T.J. Barna, J.G. Armstrong, L.L. Stoll, N.L. Weintraub, E.W. Dickson, Proenkephalin expression and enkephalin release are widely observed in non-neuronal tissues, Peptides 29(1) (2008) 83-92.
[417] H.L. Rittner, A. Brack, H. Machelska, S.A. Mousa, M. Bauer, M. Schafer, C. Stein, Opioid peptide-expressing leukocytes: identification, recruitment, and simultaneously increasing inhibition of inflammatory pain, Anesthesiology 95(2) (2001) 500-8.
[418] P.J. Cabot, Immune-derived opioids and peripheral antinociception, Clin Exp Pharmacol Physiol 28(3) (2001) 230-2.
[419] M. Verma-Gandhu, E.F. Verdu, D. Cohen-Lyons, S.M. Collins, Lymphocyte-mediated regulation of β-endorphin in the myenteric plexus, American Journal of Physiology - Gastrointestinal and Liver Physiology 292(1) (2007) G344-G348.
[420] E. Valdez-Morales, R. Guerrero-Alba, F. Ochoa-Cortes, J. Benson, I. Spreadbury, D. Hurlbut, M. Miranda-Morales, A.E. Lomax, S. Vanner, Release of endogenous opioids during a chronic IBD model suppresses the excitability of colonic DRG neurons, Neurogastroenterol Motil 25(1) (2013) 39-46.
[421] A. Romero, A. Gonzalez-Cuello, M.L. Laorden, A. Campillo, N. Vasconcelos, E. Romero-Alejo, M.M. Puig, Effects of surgery and/or remifentanil administration on the expression of pERK1/2, c-Fos and dynorphin in the dorsal root ganglia in mice, Naunyn Schmiedebergs Arch Pharmacol 385(4) (2012) 397-409.
[422] S. Patierno, W. Zellalem, A. Ho, C.G. Parsons, K.C. Lloyd, M. Tonini, C. Sternini, N-methyl-D-aspartate receptors mediate endogenous opioid release in enteric neurons after abdominal surgery, Gastroenterology 128(7) (2005) 2009-19.
[423] S.J. Panchal, P. Muller-Schwefe, J.I. Wurzelmann, Opioid-induced bowel dysfunction: prevalence, pathophysiology and burden, International journal of clinical practice 61(7) (2007) 1181-7.
[424] M. Pappagallo, Incidence, prevalence, and management of opioid bowel dysfunction, American journal of surgery 182(5A Suppl) (2001) 11s-18s.
[425] G.R. Ross, B.H. Gabra, W.L. Dewey, H.I. Akbarali, Morphine tolerance in the mouse ileum and colon, J Pharmacol Exp Ther 327(2) (2008) 561-72.
[426] G.S. Ling, D. Paul, R. Simantov, G.W. Pasternak, Differential development of acute tolerance to analgesia, respiratory depression, gastrointestinal transit and hormone release in a morphine infusion model, Life sciences 45(18) (1989) 1627-36.
[427] C.S. Yuan, J.F. Foss, M. O'Connor, J. Moss, M.F. Roizen, Gut motility and transit changes in patients receiving long-term methadone maintenance, Journal of clinical pharmacology 38(10) (1998) 931-5.
[428] C. Sternini, S. Patierno, I.S. Selmer, A. Kirchgessner, The opioid system in the gastrointestinal tract, Neurogastroenterol Motil 2 (2004) 3-16.
[429] J.J. Galligan, H.I. Akbarali, Molecular Physiology of Enteric Opioid Receptors, The American journal of gastroenterology 2(1) (2014) 17-21.
[430] R.J. Miller, L.D. Hirning, Opioid Peptides of The Gut, Comprehensive Physiology, John Wiley & Sons, Inc.2010.
[431] W.D. Paton, The action of morphine and related substances on contraction and on acetylcholine output of coaxially stimulated guinea-pig ileum, British journal of pharmacology and chemotherapy 12(1) (1957) 119-27.
[432] G.L. Thompson, M. Canals, D.P. Poole, Biological redundancy of endogenous GPCR ligands in the gut and the potential for endogenous functional selectivity, Frontiers in pharmacology 5 (2014) 262.

[433] M. Noda, Y. Teranishi, H. Takahashi, M. Toyosato, M. Notake, S. Nakanishi, S. Numa, Isolation and structural organization of the human preproenkephalin gene, Nature 297(5865) (1982) 431-4.
[434] J. Hughes, H.W. Kosterlitz, T.W. Smith, The distribution of methionine-enkephalin and leucine-enkephalin in the brain and peripheral tissues, Br J Pharmacol 61(4) (1977) 639-47.
[435] R.I. Linnoila, R.P. DiAugustine, R.J. Miller, K.J. Chang, P. Cuatrecasas, An immunohistochemical and radioimmunological study of the distribution of [met5]- and [leu5]-enkephalin in the gastrointestinal tract, Neuroscience 3(12) (1978) 1187-96.
[436] J. Tang, H.Y. Yang, E. Costa, Distribution of met5-enkephalin-Arg6-Phe7 (MEAP) in various tissues of rats and guinea pigs, Life sciences 31(20-21) (1982) 2303-6.
[437] A.S. Giraud, R.G. Williams, G.J. Dockray, Evidence for different patterns of post-translational processing of pro-enkephalin in the bovine adrenal, colon and striatum indicated by radioimmunoassay using region-specific antisera to Met-Enk-Arg6-Phe7 and Met-Enk-Arg6-Gly7-Leu8, Neurosci Lett 46(2) (1984) 223-8.
[438] J.M. Polak, S.R. Bloom, S.N. Sullivan, P. Facer, A.G. Pearse, Enkephalin-like immunoreactivity in the human gastrointestinal tract, Lancet 1(8019) (1977) 972-4.
[439] G.L. Ferri, R.A. Morreale, G.J. Dockray, Met5-enkephalin-Arg6-Gly7-Leu8 immunoreactivity in the human gut, Peptides 7(5) (1986) 735-9.
[440] G.L. Ferri, A. Watkinson, G.J. Dockray, Proenkephalin A-derived peptides in the human gut, Gastroenterology 95(4) (1988) 1011-7.
[441] J.R. Keast, J.B. Furness, M. Costa, Distribution of certain peptide-containing nerve fibres and endocrine cells in the gastrointestinal mucosa in five mammalian species, The Journal of comparative neurology 236(3) (1985) 403-22.
[442] J.B. Furness, M. Costa, R.J. Miller, Distribution and projections of nerves with enkephalin-like immunoreactivity in the guinea-pig small intestine, Neuroscience 8(4) (1983) 653-664.
[443] K.R. Jessen, M.J. Saffrey, S. Van Noorden, S.R. Bloom, J.M. Polak, G. Burnstock, Immunohistochemical studies of the enteric nervous system in tissue culture and in situ: localization of vascoactive intestinal polypeptide (VIP), substance-P and enkephalin immunoreactive nerves in the guinea-pig gut, Neuroscience 5(10) (1980) 1717-35.
[444] M. Schultzberg, T. Hokfelt, G. Nilsson, L. Terenius, J.F. Rehfeld, M. Brown, R. Elde, M. Goldstein, S. Said, Distribution of peptide- and catecholamine-containing neurons in the gastro-intestinal tract of rat and guinea-pig: immunohistochemical studies with antisera to substance P, vasoactive intestinal polypeptide, enkephalins, somatostatin, gastrin/cholecystokinin, neurotensin and dopamine beta-hydroxylase, Neuroscience 5(4) (1980) 689-744.
[445] L.I. Larsson, K. Stengaard-Pedersen, Enkephalin/endorphin-related peptides in antropyloric gastrin cells, The journal of histochemistry and cytochemistry : official journal of the Histochemistry Society 29(9) (1981) 1088-98.
[446] L.I. Larsson, S. Childers, S.H. Snyder, Met- and Leu-enkephalin immunoreactivity in separate neurones, Nature 282(5737) (1979) 407-10.
[447] J.C. Bornstein, M. Costa, J.B. Furness, G.M. Lees, Electrophysiology and enkephalin immunoreactivity of identified myenteric plexus neurones of guinea-pig small intestine, The Journal of physiology 351 (1984) 313-25.
[448] M. Costa, J.B. Furness, A.C. Cuello, Separate populations of opioid containing neurons in the guinea-pig intestine, Neuropeptides 5(4-6) (1985) 445-8.
[449] H. Pfannkuche, D. Reiche, U. Firzlaff, H. Sann, M. Schemann, Enkephalin-immunoreactive subpopulations in the myenteric plexus of the guinea-pig fundus project primarily to the muscle and not to the mucosa, Cell and tissue research 294(1) (1998) 45-55.

[450] A. Brehmer, T.M. Lindig, F. Schrodl, W. Neuhuber, D. Ditterich, M. Rexer, H. Rupprecht, Morphology of enkephalin-immunoreactive myenteric neurons in the human gut, Histochemistry and cell biology 123(2) (2005) 131-8.
[451] J.B. Furness, M. Costa, I.L. Gibbins, I.J. Llewellyn-Smith, J.R. Oliver, Neurochemically similar myenteric and submucous neurons directly traced to the mucosa of the small intestine, Cell and tissue research 241(1) (1985) 155-63.
[452] T. Mimoda, N. Kitamura, E. Hondo, J. Yamada, Immunohistochemical colocalization of serotonin, substance P and Met-enkephalin-Arg6-Gly7-Leu8 in the endocrine cells of the ruminant duodenum, Anatomia, histologia, embryologia 27(1) (1998) 65-9.
[453] A.J. Bu'Lock, C. Vaillant, G.J. Dockray, Immunohistochemical studies on the gastrointestinal tract using antisera to Met-enkephalin and Met-enkephalin Arg6Phe7, The journal of histochemistry and cytochemistry : official journal of the Histochemistry Society 31(12) (1983) 1356-62.
[454] Y.N. Wang, I. Lindberg, Distribution and characterization of the opioid octapeptide met5-enkephalin-arg6-gly7-leu8 in the gastrointestinal tract of the rat, Cell and tissue research 244(1) (1986) 77-85.
[455] K. Nihei, T. Iwanaga, Localization of Met-enkephalin-Arg6-Gly7-Leu8-like immunoreactivity in the gastrointestinal tract of rat and pig, The journal of histochemistry and cytochemistry : official journal of the Histochemistry Society 33(10) (1985) 1001-6.
[456] Z. Kokrashvili, D. Rodriguez, V. Yevshayeva, H. Zhou, R.F. Margolskee, B. Mosinger, Release of endogenous opioids from duodenal enteroendocrine cells requires Trpm5, Gastroenterology 137(2) (2009) 598-606, 606.e1-2.
[457] P.A. Steele, M. Costa, Opioid-like immunoreactive neurons in secretomotor pathways of the guinea-pig ileum, Neuroscience 38(3) (1990) 771-86.
[458] J. Boue, L. Basso, N. Cenac, C. Blanpied, M. Rolli-Derkinderen, M. Neunlist, N. Vergnolle, G. Dietrich, Endogenous regulation of visceral pain via production of opioids by colitogenic CD4(+) T cells in mice, Gastroenterology 146(1) (2014) 166-75.
[459] V.P. Yuferov, J.A. Culpepper-Morgan, K.S. LaForge, A. Ho, M.J. Kreek, Regional quantitation of preprodynorphin mRNA in guinea pig gastrointestinal tract, Neurochemical research 23(4) (1998) 505-11.
[460] S. Horikawa, T. Takai, M. Toyosato, H. Takahashi, M. Noda, H. Kakidani, T. Kubo, T. Hirose, S. Inayama, H. Hayashida, et al., Isolation and structural organization of the human preproenkephalin B gene, Nature 306(5943) (1983) 611-4.
[461] S.R. Vincent, C.J. Dalsgaard, M. Schultzberg, T. Hokfelt, I. Christensson, L. Terenius, Dynorphin-immunoreactive neurons in the autonomic nervous system, Neuroscience 11(4) (1984) 973-87.
[462] H.J. Wolter, Identification of the tridecapeptide dynorphin B (rimorphin) within perikarya of rat duodenum, Life sciences 39(8) (1986) 727-30.
[463] S. Spampinato, E. Speroni, M. Canossa, G. Sciarretta, P. Malaguti, S. Ferri, Dynorphin B-like immunoreactivity in gastroduodenal biopsy specimens from gallstone patients, Regul Pept 41(2) (1992) 131-8.
[464] P.A. Steele, C.A. Turner, R. Murphy, Measurement and chromatographic characterization of prodynorphin-derived peptides in the guinea-pig ileum, Neuropeptides 13(3) (1989) 207-13.
[465] R. Murphy, C.A. Turner, Isolation and microsequence analysis of guinea pig alpha-neo-endorphin, Peptides 11(1) (1990) 65-8.
[466] S. Spampinato, G.L. Ferri, S. Candeletti, P. Romualdi, E. Cavicchini, L. Soimero, G. Labo, S. Ferri, Regional distribution of immunoreactive dynorphin A in the human gastrointestinal tract, Neuropeptides 11(3) (1988) 101-5.

[467] Y. Cetin, Enterochromaffin (EC-) cells of the mammalian gastro-entero-pancreatic (GEP) endocrine system: cellular source of pro-dynorphin-derived peptides, Cell and tissue research 253(1) (1988) 173-9.
[468] B.A. Eipper, R.E. Mains, Analysis of the common precursor to corticotropin and endorphin, J Biol Chem 253(16) (1978) 5732-44.
[469] E.S. Orwoll, J.W. Kendall, Beta-endorphin and adrenocorticotropin in extrapituitary sites: gastrointestinal tract, Endocrinology 107(2) (1980) 438-42.
[470] C.R. DeBold, W.E. Nicholson, D.N. Orth, Immunoreactive proopiomelanocortin (POMC) peptides and POMC-like messenger ribonucleic acid are present in many rat nonpituitary tissues, Endocrinology 122(6) (1988) 2648-57.
[471] S. Leander, R. Ekman, R. Uddman, F. Sundler, R. Hakanson, Neuronal cholecystokinin, gastrin-releasing peptide, neurotensin, and beta-endorphin in the intestine of the guinea pig. Distribution and possible motor functions, Cell and tissue research 235(3) (1984) 521-31.
[472] H.J. Wolter, Ultrastructural evidence for beta-endorphin-like immunoreactivity in the nervous system of the rat duodenum, Brain Res 334(1) (1985) 194-9.
[473] M. Verma-Gandhu, P. Bercik, Y. Motomura, E.F. Verdu, W.I. Khan, P.A. Blennerhassett, L. Wang, R.T. El-Sharkawy, S.M. Collins, CD4+ T-cell modulation of visceral nociception in mice, Gastroenterology 130(6) (2006) 1721-8.
[474] P.A. Hughes, A.M. Harrington, J. Castro, T. Liebregts, B. Adam, D.J. Grasby, N.J. Isaacs, L. Maldeniya, C.M. Martin, J. Persson, J.M. Andrews, G. Holtmann, L.A. Blackshaw, S.M. Brierley, Sensory neuro-immune interactions differ between irritable bowel syndrome subtypes, Gut 62(10) (2013) 1456-65.
[475] F. Sundler, J. Alumets, R. Ekman, R. Hakanson, T.B. Van Wimersma Greidanus, Immunoreactive adrenocorticotropic hormone (ACTH) in porcine gut and pancreas: Fact or artifact?, The journal of histochemistry and cytochemistry : official journal of the Histochemistry Society 29(11) (1981) 1328-35.
[476] R.I. Cone, E. Weber, J.D. Barchas, A. Goldstein, Regional distribution of dynorphin and neo-endorphin peptides in rat brain, spinal cord, and pituitary, J Neurosci 3(11) (1983) 2146-52.
[477] N. Zamir, E. Weber, M. Palkovits, M. Brownstein, Differential processing of prodynorphin and proenkephalin in specific regions of the rat brain, Proc Natl Acad Sci U S A 81(21) (1984) 6886-9.
[478] T. Yakovleva, I. Bazov, G. Cebers, Z. Marinova, Y. Hara, A. Ahmed, M. Vlaskovska, B. Johansson, U. Hochgeschwender, I.N. Singh, A.J. Bruce-Keller, Y.L. Hurd, T. Kaneko, L. Terenius, T.J. Ekstrom, K.F. Hauser, V.M. Pickel, G. Bakalkin, Prodynorphin storage and processing in axon terminals and dendrites, Faseb J 20(12) (2006) 2124-6.
[479] H.J. Wolter, Colocalization of dynorphin-A(1-17) and dynorphin-A(1-8) within some perikarya of rat duodenum: immunohistochemical evidence for the presence of two separate dynorphinergic systems, Biochemical and biophysical research communications 130(2) (1985) 774-80.
[480] J.D. Wood, J.J. Galligan, Function of opioids in the enteric nervous system, Neurogastroenterol Motil 2 (2004) 17-28.
[481] R. Schulz, M. Wuster, R. Simantov, S. Snyder, A. Herz, Electrically stimulated release of opiate-like material from the myenteric plexus of the guinea pig ileum, Eur J Pharmacol 41(3) (1977) 347-8.
[482] A.D. Corbett, M.G. Gillan, H.W. Kosterlitz, Electrically-induced release of opioid peptides from the guinea-pig myenteric plexus preparation, Journal of receptor research 11(1-4) (1991) 665-73.

[483] N.H. Majeed, J. Silberring, R. Przewlocki, The in vitro release of immunoreactive dynorphin and alpha-neoendorphin from the perfused rat duodenum, Life sciences 41(4) (1987) 497-504.
[484] W. Kromer, V. Hollt, H. Schmidt, A. Herz, Release of immunoreactive-dynorphin from the isolated guinea-pig small intestine is reduced during peristaltic activity, Neurosci Lett 25(1) (1981) 53-6.
[485] J. Donnerer, P. Holzer, F. Lembeck, Release of dynorphin, somatostatin and substance P from the vascularly perfused small intestine of the guinea-pig during peristalsis, Br J Pharmacol 83(4) (1984) 919-25.
[486] G.J. Sanger, B.R. Tuladhar, The role of endogenous opioids in the control of gastrointestinal motility: predictions from in vitro modelling, Neurogastroenterol Motil 16 Suppl 2 (2004) 38-45.
[487] B.D. Carter, F. Medzihradsky, Go mediates the coupling of the mu opioid receptor to adenylyl cyclase in cloned neural cells and brain, Proc Natl Acad Sci U S A 90(9) (1993) 4062-6.
[488] J.S. Chan, T.T. Chiu, Y.H. Wong, Activation of type II adenylyl cyclase by the cloned mu-opioid receptor: coupling to multiple G proteins, J Neurochem 65(6) (1995) 2682-9.
[489] Y.H. Wong, C.D. Demoliou-Mason, E.A. Barnard, Opioid receptors in magnesium-digitonin-solubilized rat brain membranes are tightly coupled to a pertussis toxin-sensitive guanine nucleotide-binding protein, J Neurochem 52(4) (1989) 999-1009.
[490] S. Offermanns, M.I. Simon, G alpha 15 and G alpha 16 couple a wide variety of receptors to phospholipase C, J Biol Chem 270(25) (1995) 15175-80.
[491] H.O. Collier, A.C. Roy, Morphine-like drugs inhibit the stimulation of E prostaglandins of cyclic AMP formation by rat brain homogenate, Nature 248(443) (1974) 24-7.
[492] E. Seward, C. Hammond, G. Henderson, Mu-opioid-receptor-mediated inhibition of the N-type calcium-channel current, Proc Biol Sci 244(1310) (1991) 129-35.
[493] H. Rhim, R.J. Miller, Opioid receptors modulate diverse types of calcium channels in the nucleus tractus solitarius of the rat, J Neurosci 14(12) (1994) 7608-15.
[494] E. Bourinet, T.W. Soong, A. Stea, T.P. Snutch, Determinants of the G protein-dependent opioid modulation of neuronal calcium channels, Proc Natl Acad Sci U S A 93(4) (1996) 1486-91.
[495] M. Torrecilla, C.L. Marker, S.C. Cintora, M. Stoffel, J.T. Williams, K. Wickman, G-protein-gated potassium channels containing Kir3.2 and Kir3.3 subunits mediate the acute inhibitory effects of opioids on locus ceruleus neurons, J Neurosci 22(11) (2002) 4328-34.
[496] R.A. North, L.V. Vitek, A study of the role of cyclic adenosine 3',5'-monophosphate in the depression by opiates and opioid peptides of excitatory junction potentials in the mouse vas deferens, Br J Pharmacol 71(1) (1980) 307-13.
[497] G. Henderson, J. Hughes, H.W. Kosterlitz, A new example of a morphine-sensitive neuro-effector junction: adrenergic transmission in the mouse vas deferens, Br J Pharmacol 46(4) (1972) 764-6.
[498] D.V. Madison, R.A. Nicoll, Enkephalin hyperpolarizes interneurones in the rat hippocampus, The Journal of physiology 398 (1988) 123-30.
[499] C.M. Pepper, G. Henderson, Opiates and opioid peptides hyperpolarize locus coeruleus neurons in vitro, Science 209(4454) (1980) 394-5.
[500] L.F. Chuang, K.F. Killam, Jr., R.Y. Chuang, Induction and activation of mitogen-activated protein kinases of human lymphocytes as one of the signaling pathways of the immunomodulatory effects of morphine sulfate, J Biol Chem 272(43) (1997) 26815-7.

[501] J.L. Whistler, M. von Zastrow, Dissociation of Functional Roles of Dynamin in Receptor-mediated Endocytosis and Mitogenic Signal Transduction, Journal of biological chemistry 274(35) (1999) 24575-24578.
[502] A.Y. Kam, A.S. Chan, Y.H. Wong, Phosphatidylinositol-3 kinase is distinctively required for mu-, but not kappa-opioid receptor-induced activation of c-Jun N-terminal kinase, J Neurochem 89(2) (2004) 391-402.
[503] E.J. Melief, M. Miyatake, M.R. Bruchas, C. Chavkin, Ligand-directed c-Jun N-terminal kinase activation disrupts opioid receptor signaling, Proc Natl Acad Sci U S A 107(25) (2010) 11608-13.
[504] N. Mittal, M. Tan, O. Egbuta, N. Desai, C. Crawford, C.-W. Xie, C. Evans, W. Walwyn, Evidence that behavioral phenotypes of morphine in β-arr2-/- mice are due to the unmasking of JNK signaling, Neuropsychopharmacology 37(8) (2012) 1953-1962.
[505] M.B. Yuill, M.L. Zee, D. Marcus, D.J. Morgan, Tolerance to the antinociceptive and hypothermic effects of morphine is mediated by multiple isoforms of c-Jun N-terminal kinase, Neuroreport (2016).
[506] W. Ma, W.H. Zheng, K. Powell, K. Jhamandas, R. Quirion, Chronic morphine exposure increases the phosphorylation of MAP kinases and the transcription factor CREB in dorsal root ganglion neurons: an in vitro and in vivo study, Eur J Neurosci 14(7) (2001) 1091-104.
[507] G. Mace, M. Miaczynska, M. Zerial, A. Nebreda, Phosphorylation of EEA1 by p38 MAP kinase regulates mu opioid receptor endocytosis, EMBO journal 24(18) (2005) 3235-3246.
[508] M. Tan, W. Walwyn, C. Evans, C.-W. Xie, p38 MAPK and beta-arrestin 2 mediate functional interactions between endogenous micro-opioid and alpha2A-adrenergic receptors in neurons, Journal of biological chemistry 284(10) (2009) 6270-6281.
[509] H.M. Lesscher, J.P. Burbach, J.M. van Ree, M.A. Gerrits, ERK1/2 activation in rat ventral tegmental area by the mu-opioid agonist fentanyl: an in vitro study, Neuroscience 116(1) (2003) 139-44.
[510] M. Miyatake, T.J. Rubinstein, G.P. McLennan, M.M. Belcheva, C.J. Coscia, Inhibition of EGF-induced ERK/MAP kinase-mediated astrocyte proliferation by mu opioids: integration of G protein and beta-arrestin 2-dependent pathways, J Neurochem 110(2) (2009) 662-74.
[511] T.A. Macey, J.D. Lowe, C. Chavkin, Mu opioid receptor activation of ERK1/2 is GRK3 and arrestin dependent in striatal neurons, J Biol Chem 281(45) (2006) 34515-24.
[512] M.M. Belcheva, Y. Tan, V.M. Heaton, A.L. Clark, C.J. Coscia, Mu opioid transactivation and down-regulation of the epidermal growth factor receptor in astrocytes: implications for mitogen-activated protein kinase signaling, Molecular Pharmacology 64(6) (2003) 1391-1401.
[513] M.M. Belcheva, Z. Vogel, E. Ignatova, T. Avidor-Reiss, R. Zippel, R. Levy, E.C. Young, J. Barg, C.J. Coscia, Opioid modulation of extracellular signal-regulated protein kinase activity is ras-dependent and involves Gbetagamma subunits, Journal Of Neurochemistry 70(2) (1998) 635-645.
[514] K. Fukuda, S. Kato, H. Morikawa, T. Shoda, K. Mori, Functional coupling of the delta-, mu-, and kappa-opioid receptors to mitogen-activated protein kinase and arachidonate release in Chinese hamster ovary cells, J Neurochem 67(3) (1996) 1309-16.
[515] M.M. Belcheva, A.L. Clark, P.D. Haas, J.S. Serna, J.W. Hahn, A. Kiss, C.J. Coscia, Mu and kappa opioid receptors activate ERK/MAPK via different protein kinase C isoforms and secondary messengers in astrocytes, J Biol Chem 280(30) (2005) 27662-9.

[516] M.M. Belcheva, M. Szùcs, D. Wang, W. Sadee, C.J. Coscia, mu-Opioid receptor-mediated ERK activation involves calmodulin-dependent epidermal growth factor receptor transactivation, The Journal Of Biological Chemistry 276(36) (2001) 33847-33853.
[517] R.D. Polakiewicz, S.M. Schieferl, L.F. Dorner, V. Kansra, M.J. Comb, A mitogen-activated protein kinase pathway is required for mu-opioid receptor desensitization, J Biol Chem 273(20) (1998) 12402-6.
[518] E.G. Ignatova, M.M. Belcheva, L.M. Bohn, M.C. Neuman, C.J. Coscia, Requirement of receptor internalization for opioid stimulation of mitogen-activated protein kinase: biochemical and immunofluorescence confocal microscopic evidence, The Journal of neuroscience 19(1) (1999) 56-63.
[519] H.K. Kramer, E.J. Simon, mu and delta-opioid receptor agonists induce mitogen-activated protein kinase (MAPK) activation in the absence of receptor internalization, Neuropharmacology 39(10) (2000) 1707-1719.
[520] H. Zheng, J. Chu, Y. Qiu, H.H. Loh, P.-Y. Law, Agonist-selective signaling is determined by the receptor location within the membrane domains, Proceedings Of The National Academy Of Sciences Of The United States Of America 105(27) (2008) 9421-9426.
[521] J.R. Kuhar, A. Bedini, E.J. Melief, Y.C. Chiu, H.N. Striegel, C. Chavkin, Mu opioid receptor stimulation activates c-Jun N-terminal kinase 2 by distinct arrestin-dependent and independent mechanisms, Cell Signal 27(9) (2015) 1799-806.
[522] P.C. Singhal, M. Bhaskaran, J. Patel, K. Patel, B.S. Kasinath, S. Duraisamy, N. Franki, K. Reddy, A.A. Kapasi, Role of p38 mitogen-activated protein kinase phosphorylation and Fas-Fas ligand interaction in morphine-induced macrophage apoptosis, J Immunol 168(8) (2002) 4025-33.
[523] L. Yang, A. Seifert, D. Wu, X. Wang, V. Rankovic, H. Schroder, L.O. Brandenburg, V. Hollt, T. Koch, Role of phospholipase D2/phosphatidic acid signal transduction in micro- and delta-opioid receptor endocytosis, Mol Pharmacol 78(1) (2010) 105-13.
[524] T. Koch, L.O. Brandenburg, Y. Liang, S. Schulz, A. Beyer, H. Schroder, V. Hollt, Phospholipase D2 modulates agonist-induced mu-opioid receptor desensitization and resensitization, J Neurochem 88(3) (2004) 680-8.
[525] J. Zhang, S.S. Ferguson, L.S. Barak, S.R. Bodduluri, S.A. Laporte, P.Y. Law, M.G. Caron, Role for G protein-coupled receptor kinase in agonist-specific regulation of mu-opioid receptor responsiveness, Proc Natl Acad Sci U S A 95(12) (1998) 7157-62.
[526] A.H. Li, H.L. Wang, G protein-coupled receptor kinase 2 mediates mu-opioid receptor desensitization in GABAergic neurons of the nucleus raphe magnus, J Neurochem 77(2) (2001) 435-44.
[527] A. Yousuf, E. Miess, S. Sianati, Y.P. Du, S. Schulz, M.J. Christie, Role of Phosphorylation Sites in Desensitization of micro-Opioid Receptor, Mol Pharmacol 88(4) (2015) 825-35.
[528] J.P. Celver, J. Lowe, A. Kovoor, V.V. Gurevich, C. Chavkin, Threonine 180 is required for G-protein-coupled receptor kinase 3- and beta-arrestin 2-mediated desensitization of the mu-opioid receptor in Xenopus oocytes, J Biol Chem 276(7) (2001) 4894-900.
[529] T. Koch, T. Kroslak, P. Mayer, E. Raulf, V. Hollt, Site mutation in the rat mu-opioid receptor demonstrates the involvement of calcium/calmodulin-dependent protein kinase II in agonist-mediated desensitization, J Neurochem 69(4) (1997) 1767-70.
[530] E.A. Johnson, S. Oldfield, E. Braksator, A. Gonzalez-Cuello, D. Couch, K.J. Hall, S.J. Mundell, C.P. Bailey, E. Kelly, G. Henderson, Agonist-selective mechanisms of mu-opioid receptor desensitization in human embryonic kidney 293 cells, Mol Pharmacol 70(2) (2006) 676-85.

[531] A. Kovoor, V. Nappey, B.L. Kieffer, C. Chavkin, Mu and delta opioid receptors are differentially desensitized by the coexpression of beta-adrenergic receptor kinase 2 and beta-arrestin 2 in xenopus oocytes, J Biol Chem 272(44) (1997) 27605-11.
[532] J. Zhang, S.S. Ferguson, L.S. Barak, L. Menard, M.G. Caron, Dynamin and beta-arrestin reveal distinct mechanisms for G protein-coupled receptor internalization, J Biol Chem 271(31) (1996) 18302-5.
[533] D.E. Keith, S.R. Murray, P.A. Zaki, P.C. Chu, D.V. Lissin, L. Kang, C.J. Evans, M. von Zastrow, Morphine Activates Opioid Receptors without Causing Their Rapid Internalization, Journal of Biological Chemistry 271(32) (1996) 19021-19024.
[534] D.B. Bennett, J.W. Spain, M.B. Laskowski, B.L. Roth, C.J. Coscia, Stereospecific opiate-binding sites occur in coated vesicles, J Neurosci 5(11) (1985) 3010-5.
[535] C. Sternini, M. Spann, B. Anton, D.E. Keith, Jr., N.W. Bunnett, M. von Zastrow, C. Evans, N.C. Brecha, Agonist-selective endocytosis of mu opioid receptor by neurons in vivo, Proc Natl Acad Sci U S A 93(17) (1996) 9241-6.
[536] C.E. Groer, C.L. Schmid, A.M. Jaeger, L.M. Bohn, Agonist-directed interactions with specific beta-arrestins determine mu-opioid receptor trafficking, ubiquitination, and dephosphorylation, J Biol Chem 286(36) (2011) 31731-41.
[537] J.N. Hislop, A.G. Henry, M. von Zastrow, Ubiquitination in the first cytoplasmic loop of mu-opioid receptors reveals a hierarchical mechanism of lysosomal down-regulation, J Biol Chem 286(46) (2011) 40193-204.
[538] A.B. Tobin, A.J. Butcher, K.C. Kong, Location, location, location...site-specific GPCR phosphorylation offers a mechanism for cell-type-specific signalling, Trends Pharmacol Sci 29(8) (2008) 413-20.
[539] J. Chu, H. Zheng, H.H. Loh, P.Y. Law, Morphine-induced mu-opioid receptor rapid desensitization is independent of receptor phosphorylation and beta-arrestins, Cell Signal 20(9) (2008) 1616-24.
[540] G. Grecksch, S. Just, C. Pierstorff, A.K. Imhof, L. Gluck, C. Doll, A. Lupp, A. Becker, T. Koch, R. Stumm, V. Hollt, S. Schulz, Analgesic tolerance to high-efficacy agonists but not to morphine is diminished in phosphorylation-deficient S375A mu-opioid receptor knock-in mice, J Neurosci 31(39) (2011) 13890-6.
[541] S. Schulz, D. Mayer, M. Pfeiffer, R. Stumm, T. Koch, V. Hollt, Morphine induces terminal micro-opioid receptor desensitization by sustained phosphorylation of serine-375, The EMBO journal 23(16) (2004) 3282-9.
[542] L. Mouledous, C. Froment, O. Burlet-Schiltz, S. Schulz, C. Mollereau, Phosphoproteomic analysis of the mouse brain mu-opioid (MOP) receptor, FEBS letters 589(18) (2015) 2401-8.
[543] C. Doll, J. Konietzko, F. Poll, T. Koch, V. Hollt, S. Schulz, Agonist-selective patterns of micro-opioid receptor phosphorylation revealed by phosphosite-specific antibodies, Br J Pharmacol 164(2) (2011) 298-307.
[544] Y.-J. Chen, S. Oldfield, A.J. Butcher, A.B. Tobin, K. Saxena, V.V. Gurevich, J.L. Benovic, G. Henderson, E. Kelly, Identification of phosphorylation sites in the COOH-terminal tail of the μ-opioid receptor, Journal of Neurochemistry 124(2) (2012) 189-99.
[545] E.K. Lau, M. Trester-Zedlitz, J.C. Trinidad, S.J. Kotowski, A.N. Krutchinsky, A.L. Burlingame, M. von Zastrow, Quantitative encoding of the effect of a partial agonist on individual opioid receptors by multisite phosphorylation and threshold detection, Sci Signal 4(185) (2011) ra52.
[546] C. Doll, F. Poll, K. Peuker, A. Loktev, L. Gluck, S. Schulz, Deciphering micro-opioid receptor phosphorylation and dephosphorylation in HEK293 cells, Br J Pharmacol 167(6) (2012) 1259-70.
[547] H.L. Wang, A cluster of Ser/Thr residues at the C-terminus of mu-opioid receptor is required for G protein-coupled receptor kinase 2-mediated desensitization, Neuropharmacology 39(3) (2000) 353-63.

[548] H.L. Wang, W.T. Chang, C.Y. Hsu, P.C. Huang, Y.W. Chow, A.H. Li, Identification of two C-terminal amino acids, Ser(355) and Thr(357), required for short-term homologous desensitization of mu-opioid receptors, Biochem Pharmacol 64(2) (2002) 257-66.
[549] W.T. Birdsong, S. Arttamangkul, J.R. Bunzow, J.T. Williams, Agonist Binding and Desensitization of the μ-Opioid Receptor Is Modulated by Phosphorylation of the C-Terminal Tail Domain, Molecular Pharmacology 88(4) (2015) 816-824.
[550] H. Wang, W. Guang, E. Barbier, P. Shapiro, J.B. Wang, Mu opioid receptor mutant, T394A, abolishes opioid-mediated adenylyl cyclase superactivation, Neuroreport 18(18) (2007) 1969-73.
[551] Y. Pak, B.F. O'Dowd, S.R. George, Agonist-induced desensitization of the mu opioid receptor is determined by threonine 394 preceded by acidic amino acids in the COOH-terminal tail, J Biol Chem 272(40) (1997) 24961-5.
[552] R. Wolf, T. Koch, S. Schulz, M. Klutzny, H. Schroder, E. Raulf, F. Buhling, V. Hollt, Replacement of threonine 394 by alanine facilitates internalization and resensitization of the rat mu opioid receptor, Mol Pharmacol 55(2) (1999) 263-8.
[553] W.T. Birdsong, S. Arttamangkul, M.J. Clark, K. Cheng, K.C. Rice, J.R. Traynor, J.T. Williams, Increased Agonist Affinity at the mu-Opioid Receptor Induced by Prolonged Agonist Exposure, J Neurosci 33(9) (2013) 4118-27.
[554] B. Feng, Z. Li, J.B. Wang, Protein kinase C-mediated phosphorylation of the mu-opioid receptor and its effects on receptor signaling, Mol Pharmacol 79(4) (2011) 768-75.
[555] S. Chakrabarti, P.Y. Law, H.H. Loh, Distinct differences between morphine- and [D-Ala2,N-MePhe4,Gly-ol5]-enkephalin-mu-opioid receptor complexes demonstrated by cyclic AMP-dependent protein kinase phosphorylation, J Neurochem 71(1) (1998) 231-9.
[556] H. Schmidt, S. Schulz, M. Klutzny, T. Koch, M. Händel, V. Höllt, Involvement of mitogen-activated protein kinase in agonist-induced phosphorylation of the mu-opioid receptor in HEK 293 cells, Journal Of Neurochemistry 74(1) (2000) 414-422.
[557] S. Illing, A. Mann, S. Schulz, Heterologous regulation of agonist-independent mu-opioid receptor phosphorylation by protein kinase C, Br J Pharmacol 171(5) (2014) 1330-40.
[558] A. Mestek, J.H. Hurley, L.S. Bye, A.D. Campbell, Y. Chen, M. Tian, J. Liu, H. Schulman, L. Yu, The human mu opioid receptor: modulation of functional desensitization by calcium/calmodulin-dependent protein kinase and protein kinase C, J Neurosci 15(3 Pt 2) (1995) 2396-406.
[559] G.H. Fan, L.Z. Wang, H.C. Qiu, L. Ma, G. Pei, Inhibition of calcium/calmodulin-dependent protein kinase II in rat hippocampus attenuates morphine tolerance and dependence, Mol Pharmacol 56(1) (1999) 39-45.
[560] S. Arttamangkul, E.K. Lau, H.-W. Lu, J.T. Williams, Desensitization and Trafficking of μ-Opioid Receptors in Locus Ceruleus Neurons: Modulation by Kinases, Molecular Pharmacology 81(3) (2012) 348-355.
[561] N. Quillinan, E.K. Lau, M. Virk, M. von Zastrow, J.T. Williams, Recovery from mu-opioid receptor desensitization after chronic treatment with morphine and methadone, J Neurosci 31(12) (2011) 4434-43.
[562] V.C. Dang, I.A. Napier, M.J. Christie, Two distinct mechanisms mediate acute mu-opioid receptor desensitization in native neurons, The Journal Of Neuroscience: The Official Journal Of The Society For Neuroscience 29(10) (2009) 3322-3327.
[563] A. Raveh, A. Cooper, L. Guy-David, E. Reuveny, Nonenzymatic rapid control of GIRK channel function by a G protein-coupled receptor kinase, Cell 143(5) (2010) 750-60.

[564] J. Chu, H. Zheng, Y. Zhang, H.H. Loh, P.Y. Law, Agonist-dependent mu-opioid receptor signaling can lead to heterologous desensitization, Cell Signal 22(4) (2010) 684-96.
[565] S.K. Sharma, W.A. Klee, M. Nirenberg, Dual regulation of adenylate cyclase accounts for narcotic dependence and tolerance, Proceedings of the National Academy of Sciences 72(8) (1975) 3092-3096.
[566] D.S. Samways, G. Henderson, Opioid elevation of intracellular free calcium: possible mechanisms and physiological relevance, Cell Signal 18(2) (2006) 151-61.
[567] D. Smart, G. Smith, D.G. Lambert, Mu-opioids activate phospholipase C in SH-SY5Y human neuroblastoma cells via calcium-channel opening, The Biochemical journal 305(Pt 2) (1995) 577-81.
[568] J.W. Lee, S. Joshi, J.S. Chan, Y.H. Wong, Differential coupling of mu-, delta-, and kappa-opioid receptors to G alpha16-mediated stimulation of phospholipase C, J Neurochem 70(5) (1998) 2203-11.
[569] S. Offermanns, M.I. Simon, Gα15 and Gα16 Couple a Wide Variety of Receptors to Phospholipase C, Journal of Biological Chemistry 270(25) (1995) 15175-15180.
[570] R.D. Polakiewicz, S.M. Schieferl, A.C. Gingras, N. Sonenberg, M.J. Comb, mu-Opioid receptor activates signaling pathways implicated in cell survival and translational control, J Biol Chem 273(36) (1998) 23534-41.
[571] B.E. Kane, B. Svensson, D.M. Ferguson, Molecular recognition of opioid receptor ligands, Aaps J 8(1) (2006) E126-37.
[572] C.K. Surratt, P.S. Johnson, A. Moriwaki, B.K. Seidleck, C.J. Blaschak, J.B. Wang, G.R. Uhl, -mu opiate receptor. Charged transmembrane domain amino acids are critical for agonist recognition and intrinsic activity, Journal of Biological Chemistry 269(32) (1994) 20548-53.
[573] K. Befort, L. Tabbara, D. Kling, B. Maigret¶, B.L. Kieffer, Role of Aromatic Transmembrane Residues of the -Opioid Receptor in Ligand Recognition, Journal of Biological Chemistry 271(17) (1996) 10161-10168.
[574] H. Xu, Y.F. Lu, J.S. Partilla, Q.X. Zheng, J.B. Wang, G.A. Brine, F.I. Carroll, K.C. Rice, K.X. Chen, Z.Q. Chi, R.B. Rothman, Opioid peptide receptor studies, 11: involvement of Tyr148, Trp318 and His319 of the rat mu-opioid receptor in binding of mu-selective ligands, Synapse (New York, N.Y.) 32(1) (1999) 23-8.
[575] K. Fukuda, S. Kato, K. Mori, Location of Regions of the Opioid Receptor Involved in Selective Agonist Binding, Journal of Biological Chemistry 270(12) (1995) 6702-6709.
[576] D.E. Keith, B. Anton, S.R. Murray, P.A. Zaki, P.C. Chu, D.V. Lissin, G. Monteillet Agius, P.L. Stewart, C.J. Evans, M. von Zastrow, mu-Opioid receptor internalization: opiate drugs have differential effects on a conserved endocytic mechanism in vitro and in the mammalian brain, Molecular pharmacology 53(3) (1998) 377-384.
[577] V.A. Alvarez, S. Arttamangkul, V. Dang, A. Salem, J.L. Whistler, M. Von Zastrow, D.K. Grandy, J.T. Williams, mu-Opioid receptors: Ligand-dependent activation of potassium conductance, desensitization, and internalization, J Neurosci 22(13) (2002) 5769-76.
[578] K. McConalogue, E.F. Grady, J. Minnis, B. Balestra, M. Tonini, N.C. Brecha, N.W. Bunnett, C. Sternini, Activation and internalization of the μ-opioid receptor by the newly discovered endogenous agonists, endomorphin-1 and endomorphin-2, Neuroscience 90(3) (1999) 1051-1059.
[579] L.M. Bohn, L.A. Dykstra, R.J. Lefkowitz, M.G. Caron, L.S. Barak, Relative opioid efficacy is determined by the complements of the G protein-coupled receptor desensitization machinery, Mol Pharmacol 66(1) (2004) 106-12.
[580] C.E. Groer, K. Tidgewell, R.A. Moyer, W.W. Harding, R.B. Rothman, T.E. Prisinzano, L.M. Bohn, An opioid agonist that does not induce mu-opioid receptor--arrestin interactions or receptor internalization, Mol Pharmacol 71(2) (2007) 549-57.

[581] S.M. DeWire, D.S. Yamashita, D.H. Rominger, G. Liu, C.L. Cowan, T.M. Graczyk, X.T. Chen, P.M. Pitis, D. Gotchev, C. Yuan, M. Koblish, M.W. Lark, J.D. Violin, A G protein-biased ligand at the mu-opioid receptor is potently analgesic with reduced gastrointestinal and respiratory dysfunction compared with morphine, J Pharmacol Exp Ther 344(3) (2013) 708-17.
[582] R.H. Oakley, S.A. Laporte, J.A. Holt, M.G. Caron, L.S. Barak, Differential Affinities of Visual Arrestin, βArrestin1, and βArrestin2 for G Protein-coupled Receptors Delineate Two Major Classes of Receptors, Journal of Biological Chemistry 275(22) (2000) 17201-17210.
[583] L.C. Hull, J. Llorente, B.H. Gabra, F.L. Smith, E. Kelly, C. Bailey, G. Henderson, W.L. Dewey, The effect of protein kinase C and G protein-coupled receptor kinase inhibition on tolerance induced by mu-opioid agonists of different efficacy, J Pharmacol Exp Ther 332(3) (2010) 1127-35.
[584] C.P. Bailey, S. Oldfield, J. Llorente, C.J. Caunt, A.G. Teschemacher, L. Roberts, C.A. McArdle, F.L. Smith, W.L. Dewey, E. Kelly, G. Henderson, Involvement of PKC alpha and G-protein-coupled receptor kinase 2 in agonist-selective desensitization of mu-opioid receptors in mature brain neurons, Br J Pharmacol 158(1) (2009) 157-64.
[585] G.W. Terman, W. Jin, Y.P. Cheong, J. Lowe, M.G. Caron, R.J. Lefkowitz, C. Chavkin, G-protein receptor kinase 3 (GRK3) influences opioid analgesic tolerance but not opioid withdrawal, Br J Pharmacol 141(1) (2004) 55-64.
[586] J.D. Lowe, H.S. Sanderson, A.E. Cooke, M. Ostovar, E. Tsisanova, S.L. Withey, C. Chavkin, S.M. Husbands, E. Kelly, G. Henderson, C.P. Bailey, Role of G Protein-Coupled Receptor Kinases 2 and 3 in mu-Opioid Receptor Desensitization and Internalization, Mol Pharmacol 88(2) (2015) 347-56.
[587] V.C. Dang, B. Chieng, Y. Azriel, M.J. Christie, Cellular morphine tolerance produced by betaarrestin-2-dependent impairment of mu-opioid receptor resensitization, J Neurosci 31(19) (2011) 7122-30.
[588] D.J. Marcus, M. Zee, A. Hughes, M.B. Yuill, A.G. Hohmann, K. Mackie, J. Guindon, D.J. Morgan, Tolerance to the antinociceptive effects of chronic morphine requires c-Jun N-terminal kinase, Mol Pain 11 (2015) 34.
[589] M.M. Morgan, R.A. Reid, K.A. Saville, Functionally selective signaling for morphine and fentanyl antinociception and tolerance mediated by the rat periaqueductal gray, PLoS One 9(12) (2014) e114269.
[590] C.P. Bailey, E. Kelly, G. Henderson, Protein kinase C activation enhances morphine-induced rapid desensitization of mu-opioid receptors in mature rat locus ceruleus neurons, Mol Pharmacol 66(6) (2004) 1592-8.
[591] D.J. Mayer, J. Mao, D.D. Price, The development of morphine tolerance and dependence is associated with translocation of protein kinase C, Pain 61(3) (1995) 365-74.
[592] M. Inoue, H. Ueda, Protein Kinase C-Mediated Acute Tolerance to Peripheral μ-Opioid Analgesia in the Bradykinin-Nociception Test in Mice, Journal of Pharmacology and Experimental Therapeutics 293(2) (2000) 662-669.
[593] H. Zheng, J. Chu, Y. Zhang, H.H. Loh, P.-Y. Law, Modulating micro-opioid receptor phosphorylation switches agonist-dependent signaling as reflected in PKCepsilon activation and dendritic spine stability, The Journal Of Biological Chemistry 286(14) (2011) 12724-12733.
[594] E.N. Bobeck, S.L. Ingram, S.M. Hermes, S.A. Aicher, M.M. Morgan, Ligand-biased activation of extracellular signal-regulated kinase 1/2 leads to differences in opioid induced antinociception and tolerance, Behav Brain Res (2015).
[595] P.A. Zaki, D.E. Keith, Jr., G.A. Brine, F.I. Carroll, C.J. Evans, Ligand-induced changes in surface mu-opioid receptor number: relationship to G protein activation?, J Pharmacol Exp Ther 292(3) (2000) 1127-34.

[596] J. McPherson, G. Rivero, M. Baptist, J. Llorente, S. Al-Sabah, C. Krasel, W.L. Dewey, C.P. Bailey, E.M. Rosethorne, S.J. Charlton, G. Henderson, E. Kelly, mu-opioid receptors: correlation of agonist efficacy for signalling with ability to activate internalization, Mol Pharmacol 78(4) (2010) 756-66.
[597] Y. Yu, L. Zhang, X. Yin, H. Sun, G.R. Uhl, J.B. Wang, Mu opioid receptor phosphorylation, desensitization, and ligand efficacy, J Biol Chem 272(46) (1997) 28869-74.
[598] S.L. Borgland, M. Connor, P.B. Osborne, J.B. Furness, M.J. Christie, Opioid agonists have different efficacy profiles for G protein activation, rapid desensitization, and endocytosis of mu-opioid receptors, J Biol Chem 278(21) (2003) 18776-84.
[599] T. Koch, A. Widera, K. Bartzsch, S. Schulz, L.O. Brandenburg, N. Wundrack, A. Beyer, G. Grecksch, V. Hollt, Receptor endocytosis counteracts the development of opioid tolerance, Mol Pharmacol 67(1) (2005) 280-7.
[600] J.R. Traynor, S.R. Nahorski, Modulation by mu-opioid agonists of guanosine-5'-O-(3-[35S]thio)triphosphate binding to membranes from human neuroblastoma SH-SY5Y cells, Mol Pharmacol 47(4) (1995) 848-54.
[601] M.M. Morgan, M.J. Christie, Analysis of opioid efficacy, tolerance, addiction and dependence from cell culture to human, Br J Pharmacol 164(4) (2011) 1322-34.
[602] J.M. Quillan, K. Carlson, C. Song, D. Wang, W. Sade, Differential effects of mu-opioid receptor ligands on Ca(2+) signaling, The journal of pharmacology and experimental therapeutics 302(3) (2002) 1002-1012.
[603] Z. Saidak, K. Blake-Palmer, D.L. Hay, J.K. Northup, M. Glass, Differential activation of G-proteins by mu-opioid receptor agonists, Br J Pharmacol 147(6) (2006) 671-80.
[604] D. Massotte, K. Brillet, B. Kieffer, G. Milligan, Agonists activate Gi1 alpha or Gi2 alpha fused to the human mu opioid receptor differently, Journal Of Neurochemistry 81(6) (2002) 1372-1382.
[605] M.J. Clark, C.A. Furman, T.D. Gilson, J.R. Traynor, Comparison of the relative efficacy and potency of mu-opioid agonists to activate Galpha(i/o) proteins containing a pertussis toxin-insensitive mutation, J Pharmacol Exp Ther 317(2) (2006) 858-64.
[606] L. Stanasila, W.K. Lim, R.R. Neubig, F. Pattus, Coupling Efficacy and Selectivity of the Human μ-Opioid Receptor Expressed as Receptor—Gα Fusion Proteins in Escherichia coli, Journal of Neurochemistry 75(3) (2000) 1190-1199.
[607] A.W. Lipkowski, S.W. Tam, P.S. Portoghese, Peptides as receptor selectivity modulators of opiate pharmacophores, J Med Chem 29(7) (1986) 1222-5.
[608] J.B. Wang, P.S. Johnson, J.M. Wu, W.F. Wang, G.R. Uhl, Human kappa opiate receptor second extracellular loop elevates dynorphin's affinity for human mu/kappa chimeras, Journal of Biological Chemistry 269(42) (1994) 25966-25969.
[609] M. Minami, T. Onogi, T. Nakagawa, Y. Katao, Y. Aoki, S. Katsumata, M. Satoh, DAMGO, a mu-opioid receptor selective ligand, distinguishes between mu-and kappa-opioid receptors at a different region from that for the distinction between mu- and delta-opioid receptors, FEBS letters 364(1) (1995) 23-7.
[610] F. Meng, M.T. Hoversten, R.C. Thompson, L. Taylor, S.J. Watson, H. Akil, A Chimeric Study of the Molecular Basis of Affinity and Selectivity of the κ and the δ Opioid Receptors.: POTENTIAL ROLE OF EXTRACELLULAR DOMAINS, Journal of Biological Chemistry 270(21) (1995) 12730-12736.
[611] F. Wieberneit, A. Korste, H.B. Albada, N. Metzler-Nolte, R. Stoll, Structural and biological implications of the binding of Leu-enkephalin and its metal derivatives to opioid receptors, Dalton Trans 42(27) (2013) 9799-802.
[612] P. Molinari, V. Vezzi, M. Sbraccia, C. Gr, D. Riitano, C. Ambrosio, I. Casella, T. Costa, Morphine-like opiates selectively antagonize receptor-arrestin interactions, Journal of biological chemistry 285(17) (2010) 12522-12535.

[613] M. Morse, E. Tran, H. Sun, R. Levenson, Y. Fang, Ligand-directed functional selectivity at the mu opioid receptor revealed by label-free integrative pharmacology on-target, PLoS One 6(10) (2011) 7.
[614] D. Winpenny, M. Clark, D. Cawkill, Biased ligand quantification in drug discovery: from theory to high throughput screening to identify New biased mu opioid receptor agonists, Br J Pharmacol (2016).
[615] G. Rivero, J. Llorente, J. McPherson, A. Cooke, S.J. Mundell, C.A. McArdle, E.M. Rosethorne, S.J. Charlton, C. Krasel, C.P. Bailey, G. Henderson, E. Kelly, Endomorphin-2: a biased agonist at the mu-opioid receptor, Mol Pharmacol 82(2) (2012) 178-88.
[616] G.L. Thompson, E. Kelly, A. Christopoulos, M. Canals, Novel GPCR paradigms at the mu-opioid receptor, Br J Pharmacol 172(2) (2015) 287-96.
[617] M.P. Del Borgo, J.T. Blanchfield, I. Toth, Internalisation of the μ-opioid receptor by endomorphin-1 and leu-enkephalin is dependant on aromatic amino acid residues, Bioorganic & Medicinal Chemistry 16(8) (2008) 4341-4346.
[618] S. Arttamangkul, N. Quillinan, M.J. Low, M. von Zastrow, J. Pintar, J.T. Williams, Differential activation and trafficking of micro-opioid receptors in brain slices, Mol Pharmacol 74(4) (2008) 972-9.
[619] K.R. Svoboda, C.R. Lupica, Opioid inhibition of hippocampal interneurons via modulation of potassium and hyperpolarization-activated cation (Ih) currents, J Neurosci 18(18) (1998) 7084-98.
[620] S. Ingram, T.J. Wilding, E.W. McCleskey, J.T. Williams, Efficacy and kinetics of opioid action on acutely dissociated neurons, Mol Pharmacol 52(1) (1997) 136-43.
[621] M. Alreja, G.K. Aghajanian, Opiates suppress a resting sodium-dependent inward current and activate an outward potassium current in locus coeruleus neurons, J Neurosci 13(8) (1993) 3525-32.
[622] M. Miyake, M.J. Christie, R.A. North, Single potassium channels opened by opioids in rat locus ceruleus neurons, Proc Natl Acad Sci U S A 86(9) (1989) 3419-22.
[623] M. Connor, S.L. Borgland, M.J. Christie, Continued morphine modulation of calcium channel currents in acutely isolated locus coeruleus neurons from morphine-dependent rats, Br J Pharmacol 128(7) (1999) 1561-9.
[624] H.C. Moises, K.I. Rusin, R.L. Macdonald, Mu- and kappa-opioid receptors selectively reduce the same transient components of high-threshold calcium current in rat dorsal root ganglion sensory neurons, J Neurosci 14(10) (1994) 5903-16.
[625] Y.O. Taiwo, L.K. Bjerknes, E.J. Goetzl, J.D. Levine, Mediation of primary afferent peripheral hyperalgesia by the cAMP second messenger system, Neuroscience 32(3) (1989) 577-80.
[626] M.S. Gold, J.D. Levine, DAMGO inhibits prostaglandin E2-induced potentiation of a TTX-resistant Na+ current in rat sensory neurons in vitro, Neuroscience Letters 212(2) (1996) 83-86.
[627] J.E. Schroeder, P.S. Fischbach, D. Zheng, E.W. McCleskey, Activation of mu opioid receptors inhibits transient high- and low-threshold Ca2+ currents, but spares a sustained current, Neuron 6(1) (1991) 13-20.
[628] M. Ocana, E. Del Pozo, M. Barrios, J.M. Baeyens, Subgroups among mu-opioid receptor agonists distinguished by ATP-sensitive K+ channel-acting drugs, Br J Pharmacol 114(6) (1995) 1296-302.
[629] W. Masocha, L.G. Gonzalez, A. Agil, Distinguishing subgroups among mu-opioid receptor agonists using na,K-ATPase as an effector mechanism, Eur J Pharmacol (2016).
[630] P. Sanchez-Blazquez, I. Ulibarri, J. Garzon, Intracerebroventricular N-ethylmaleimide differentially reduces supraspinal opioid analgesia in mice, Eur J Pharmacol 166(2) (1989) 193-200.

[631] L. Statile, M.M. Puig, W. Warner, M. Bansinath, M. Lovitz, H. Turndorf, Droperidol enhances fentanyl and sufentanil, but not morphine, analgesia, General pharmacology 19(3) (1988) 451-4.
[632] E. Rojewska, K. Popiolek-Barczyk, N. Kolosowska, A. Piotrowska, M. Zychowska, W. Makuch, B. Przewlocka, J. Mika, PD98059 Influences Immune Factors and Enhances Opioid Analgesia in Model of Neuropathy, PLoS One 10(10) (2015) e0138583.
[633] M.D. Sanna, C. Ghelardini, N. Galeotti, Regionally selective activation of ERK and JNK in morphine paradoxical hyperalgesia: a step toward improving opioid pain therapy, Neuropharmacology 86 (2014) 67-77.
[634] K.T. Pattinson, Opioids and the control of respiration, Br J Anaesth 100(6) (2008) 747-58.
[635] J.M. Trigo, E. Martin-Garcia, F. Berrendero, P. Robledo, R. Maldonado, The endogenous opioid system: a common substrate in drug addiction, Drug Alcohol Depend 108(3) (2010) 183-94.
[636] H. Haberstock-Debic, K.-A. Kim, Y.J. Yu, M. von Zastrow, Morphine Promotes Rapid, Arrestin-Dependent Endocytosis of μ-Opioid Receptors in Striatal Neurons, The Journal of Neuroscience 25(34) (2005) 7847-7857.
[637] L. Mouledous, M.F. Diaz, H.B. Gutstein, Extracellular signal-regulated kinase (ERK) inhibition does not prevent the development or expression of tolerance to and dependence on morphine in the mouse, Pharmacology, biochemistry, and behavior 88(1) (2007) 39-46.
[638] T.A. Macey, E.N. Bobeck, D.M. Hegarty, S.A. Aicher, S.L. Ingram, M.M. Morgan, Extracellular signal-regulated kinase 1/2 activation counteracts morphine tolerance in the periaqueductal gray of the rat, J Pharmacol Exp Ther 331(2) (2009) 412-8.
[639] Y. Chen, C. Geis, C. Sommer, Activation of TRPV1 contributes to morphine tolerance: involvement of the mitogen-activated protein kinase signaling pathway, J Neurosci 28(22) (2008) 5836-45.
[640] K.M. Raehal, J.K. Walker, L.M. Bohn, Morphine side effects in beta-arrestin 2 knockout mice, J Pharmacol Exp Ther 314(3) (2005) 1195-201.
[641] L.M. Bohn, R.J. Lefkowitz, R.R. Gainetdinov, K. Peppel, M.G. Caron, F.T. Lin, Enhanced morphine analgesia in mice lacking beta-arrestin 2, Science 286(5449) (1999) 2495-8.
[642] K.M. Raehal, L.M. Bohn, The role of beta-arrestin2 in the severity of antinociceptive tolerance and physical dependence induced by different opioid pain therapeutics, Neuropharmacology 60(1) (2011) 58-65.
[643] L.M. Bohn, R.J. Lefkowitz, M.G. Caron, Differential mechanisms of morphine antinociceptive tolerance revealed in (beta)arrestin-2 knock-out mice, J Neurosci 22(23) (2002) 10494-500.
[644] D.G. Soergel, R.A. Subach, N. Burnham, M.W. Lark, I.E. James, B.M. Sadler, F. Skobieranda, J.D. Violin, L.R. Webster, Biased agonism of the mu-opioid receptor by TRV130 increases analgesia and reduces on-target adverse effects versus morphine: A randomized, double-blind, placebo-controlled, crossover study in healthy volunteers, Pain 155(9) (2014) 1829-35.
[645] E.R. Viscusi, L. Webster, M. Kuss, S. Daniels, J.A. Bolognese, S. Zuckerman, D.G. Soergel, R.A. Subach, E. Cook, F. Skobieranda, A randomized, phase 2 study investigating TRV130, a biased ligand of the mu-opioid receptor, for the intravenous treatment of acute pain, Pain 157(1) (2016) 264-72.
[646] X. Deupi, B.K. Kobilka, Energy landscapes as a tool to integrate GPCR structure, dynamics, and function, Physiology (Bethesda, Md.) 25(5) (2010) 293-303.

[647] K.P. Hofmann, P. Scheerer, P.W. Hildebrand, H.W. Choe, J.H. Park, M. Heck, O.P. Ernst, A G protein-coupled receptor at work: the rhodopsin model, Trends Biochem Sci 34(11) (2009) 540-52.
[648] T. Kenakin, A. Christopoulos, Signalling bias in new drug discovery: detection, quantification and therapeutic impact, Nat Rev Drug Discov 12(3) (2013) 205-216.
[649] J. Monod, J. Wyman, J.P. Changeux, ON THE NATURE OF ALLOSTERIC TRANSITIONS: A PLAUSIBLE MODEL, Journal of molecular biology 12 (1965) 88-118.
[650] M. Canals, P.M. Sexton, A. Christopoulos, Allostery in GPCRs: 'MWC' revisited, Trends Biochem Sci 36(12) (2011) 663-72.
[651] K.M. Raehal, C.L. Schmid, C.E. Groer, L.M. Bohn, Functional selectivity at the mu-opioid receptor: implications for understanding opioid analgesia and tolerance, Pharmacol Rev 63(4) (2011) 1001-19.
[652] N.T. Burford, M.J. Clark, T.S. Wehrman, S.W. Gerritz, M. Banks, J. O'Connell, J.R. Traynor, A. Alt, Discovery of positive allosteric modulators and silent allosteric modulators of the mu-opioid receptor, Proc Natl Acad Sci U S A 110(26) (2013) 10830-5.
[653] J.T. Williams, S.L. Ingram, G. Henderson, C. Chavkin, M. von Zastrow, S. Schulz, T. Koch, C.J. Evans, M.J. Christie, Regulation of mu-opioid receptors: desensitization, phosphorylation, internalization, and tolerance, Pharmacol Rev 65(1) (2013) 223-54.
[654] E.T. van der Westhuizen, B. Breton, A. Christopoulos, M. Bouvier, Quantification of ligand bias for clinically relevant beta2-adrenergic receptor ligands: implications for drug taxonomy, Mol Pharmacol 85(3) (2014) 492-509.
[655] J.W. Black, P. Leff, Operational models of pharmacological agonism, Proc R Soc Lond B Biol Sci 220(1219) (1983) 141-62.
[656] N. Frolich, C. Dees, C. Paetz, X. Ren, M.J. Lohse, V.O. Nikolaev, M.H. Zenk, Distinct pharmacological properties of morphine metabolites at G(i)-protein and beta-arrestin signaling pathways activated by the human mu-opioid receptor, Biochem Pharmacol 81(10) (2011) 1248-54.
[657] W. Stallaert, A. Christopoulos, M. Bouvier, Ligand functional selectivity and quantitative pharmacology at G protein-coupled receptors, Expert Opin Drug Discov 6(8) (2011) 811-25.
[658] S. Rajagopal, S. Ahn, D.H. Rominger, W. Gowen-MacDonald, C.M. Lam, S.M. Dewire, J.D. Violin, R.J. Lefkowitz, Quantifying ligand bias at seven-transmembrane receptors, Mol Pharmacol 80(3) (2011) 367-77.
[659] J. Shonberg, C.K. Herenbrink, L. Lopez, A. Christopoulos, P.J. Scammells, B. Capuano, J.R. Lane, A structure-activity analysis of biased agonism at the dopamine D2 receptor, J Med Chem 56(22) (2013) 9199-221.
[660] C. Hoffmann, N. Ziegler, S. Reiner, C. Krasel, M.J. Lohse, Agonist-selective, receptor-specific interaction of human P2Y receptors with beta-arrestin-1 and -2, J Biol Chem 283(45) (2008) 30933-41.
[661] J.A. Allen, J.M. Yost, V. Setola, X. Chen, M.F. Sassano, M. Chen, S. Peterson, P.N. Yadav, X.P. Huang, B. Feng, N.H. Jensen, X. Che, X. Bai, S.V. Frye, W.C. Wetsel, M.G. Caron, J.A. Javitch, B.L. Roth, J. Jin, Discovery of beta-arrestin-biased dopamine D2 ligands for probing signal transduction pathways essential for antipsychotic efficacy, Proc Natl Acad Sci U S A 108(45) (2011) 18488-93.
[662] A.M. Aragay, A. Ruiz-Gomez, P. Penela, S. Sarnago, A. Elorza, M.C. Jimenez-Sainz, F. Mayor, Jr., G protein-coupled receptor kinase 2 (GRK2): mechanisms of regulation and physiological functions, FEBS letters 430(1-2) (1998) 37-40.
[663] S. Galandrin, G. Oligny-Longpre, M. Bouvier, The evasive nature of drug efficacy: implications for drug discovery, Trends Pharmacol Sci 28(8) (2007) 423-30.
[664] T. Kenakin, Collateral efficacy in drug discovery: taking advantage of the good (allosteric) nature of 7TM receptors, Trends Pharmacol Sci 28(8) (2007) 407-15.

[665] P.-Y. Law, Opioid Receptor Signal Transduction Mechanisms, in: W.G. Pasternak (Ed.), The Opiate Receptors, Humana Press, Totowa, NJ, 2011, pp. 195-238.
[666] T. Koch, L.O. Brandenburg, S. Schulz, Y. Liang, J. Klein, V. Hollt, ADP-ribosylation factor-dependent phospholipase D2 activation is required for agonist-induced mu-opioid receptor endocytosis, J Biol Chem 278(11) (2003) 9979-85.
[667] X. Ge, Y. Qiu, H.H. Loh, P.Y. Law, GRIN1 regulates micro-opioid receptor activities by tethering the receptor and G protein in the lipid raft, J Biol Chem 284(52) (2009) 36521-34.
[668] G. Boerrigter, M.W. Lark, E.J. Whalen, D.G. Soergel, J.D. Violin, J.C. Burnett, Jr., Cardiorenal actions of TRV120027, a novel ss-arrestin-biased ligand at the angiotensin II type I receptor, in healthy and heart failure canines: a novel therapeutic strategy for acute heart failure, Circulation. Heart failure 4(6) (2011) 770-8.
[669] P. Varamini, W.H. Goh, F.M. Mansfeld, J.T. Blanchfield, B.D. Wyse, M.T. Smith, I. Toth, Peripherally acting novel lipo-endomorphin-1 peptides in neuropathic pain without producing constipation, Bioorg Med Chem 31(13) (2013) 00083-7.
[670] X.T. Chen, P. Pitis, G. Liu, C. Yuan, D. Gotchev, C.L. Cowan, D.H. Rominger, M. Koblish, S.M. Dewire, A.L. Crombie, J.D. Violin, D.S. Yamashita, Structure-activity relationships and discovery of a G protein biased mu opioid receptor ligand, [(3-methoxythiophen-2-yl)methyl]({2-[(9R)-9-(pyridin-2-yl)-6-oxaspiro-[4.5]decan- 9-yl]ethyl})amine (TRV130), for the treatment of acute severe pain, J Med Chem 56(20) (2013) 8019-31.
[671] K.J. Gregory, N.E. Hall, A.B. Tobin, P.M. Sexton, A. Christopoulos, Identification of orthosteric and allosteric site mutations in M2 muscarinic acetylcholine receptors that contribute to ligand-selective signaling bias, J Biol Chem 285(10) (2010) 7459-74.
[672] L.T. May, K. Leach, P.M. Sexton, A. Christopoulos, Allosteric modulation of G protein-coupled receptors, Annu Rev Pharmacol Toxicol 47 (2007) 1-51.
[673] K.J. Gregory, P.M. Sexton, A. Christopoulos, Overview of receptor allosterism, Current protocols in pharmacology / editorial board, S.J. Enna (editor-in-chief) ... [et al.] Chapter 1 (2010) Unit 1.21.
[674] P. Keov, P.M. Sexton, A. Christopoulos, Allosteric modulation of G protein-coupled receptors: a pharmacological perspective, Neuropharmacology 60(1) (2011) 24-35.
[675] B.A. Jordan, L.A. Devi, G-protein-coupled receptor heterodimerization modulates receptor function, Nature 399(6737) (1999) 697-700.
[676] D. Wang, X. Sun, L.M. Bohn, W. Sadee, Opioid receptor homo- and heterodimerization in living cells by quantitative bioluminescence resonance energy transfer, Mol Pharmacol 67(6) (2005) 2173-84.
[677] G. Milligan, G protein-coupled receptor hetero-dimerization: contribution to pharmacology and function, Br J Pharmacol 158(1) (2009) 5-14.
[678] A.S. Yekkirala, M.L. Banks, M.M. Lunzer, S.S. Negus, K.C. Rice, P.S. Portoghese, Clinically employed opioid analgesics produce antinociception via mu-delta opioid receptor heteromers in Rhesus monkeys, ACS Chem Neurosci 3(9) (2012) 720-7.
[679] M.D. Metcalf, A.S. Yekkirala, M.D. Powers, K.F. Kitto, C.A. Fairbanks, G.L. Wilcox, P.S. Portoghese, The delta opioid receptor agonist SNC80 selectively activates heteromeric mu-delta opioid receptors, ACS Chem Neurosci 3(7) (2012) 505-9.
[680] E. Akgun, M.I. Javed, M.M. Lunzer, B.A. Smeester, A.J. Beitz, P.S. Portoghese, Ligands that interact with putative MOR-mGluR5 heteromer in mice with inflammatory pain produce potent antinociception, Proc Natl Acad Sci U S A 110(28) (2013) 11595-9.
[681] M. Le Naour, E. Akgun, A. Yekkirala, M.M. Lunzer, M.D. Powers, A.E. Kalyuzhny, P.S. Portoghese, Bivalent ligands that target mu opioid (MOP) and cannabinoid1 (CB1) receptors are potent analgesics devoid of tolerance, J Med Chem 56(13) (2013) 5505-13.

[682] R. Benyamin, A.M. Trescot, S. Datta, R. Buenaventura, R. Adlaka, N. Sehgal, S.E. Glaser, R. Vallejo, Opioid complications and side effects, Pain physician 11(2 Suppl) (2008) S105-20.
[683] B.M. Cox, M.J. Christie, L. Devi, L. Toll, J.R. Traynor, Challenges for opioid receptor nomenclature: IUPHAR Review 9, Br J Pharmacol (2014).
[684] H.W. Matthes, R. Maldonado, F. Simonin, O. Valverde, S. Slowe, I. Kitchen, K. Befort, A. Dierich, M. Le Meur, P. Dolle, E. Tzavara, J. Hanoune, B.P. Roques, B.L. Kieffer, Loss of morphine-induced analgesia, reward effect and withdrawal symptoms in mice lacking the mu-opioid-receptor gene, Nature 383(6603) (1996) 819-23.
[685] T. Kenakin, C. Watson, V. Muniz-Medina, A. Christopoulos, S. Novick, A simple method for quantifying functional selectivity and agonist bias, ACS Chem Neurosci 3(3) (2012) 193-203.
[686] C. Valant, L.T. May, L. Aurelio, C.H. Chuo, P.J. White, J.A. Baltos, P.M. Sexton, P.J. Scammells, A. Christopoulos, Separation of on-target efficacy from adverse effects through rational design of a bitopic adenosine receptor agonist, Proc Natl Acad Sci U S A 111(12) (2014) 4614-9.
[687] R.W. Walters, A.K. Shukla, J.J. Kovacs, J.D. Violin, S.M. DeWire, C.M. Lam, J.R. Chen, M.J. Muehlbauer, E.J. Whalen, R.J. Lefkowitz, beta-Arrestin1 mediates nicotinic acid-induced flushing, but not its antilipolytic effect, in mice, J Clin Invest 119(5) (2009) 1312-21.
[688] R. Al-Hasani, M.R. Bruchas, Molecular mechanisms of opioid receptor-dependent signaling and behavior, Anesthesiology 115(6) (2011) 1363-81.
[689] E. Kelly, Ligand bias at the mu-opioid receptor, Biochem Soc Trans 41(1) (2013) 218-24.
[690] A.A. Pradhan, M.L. Smith, B.L. Kieffer, C.J. Evans, Ligand-directed signalling within the opioid receptor family, Br J Pharmacol 167(5) (2012) 960-9.
[691] H.T. Maguma, W.L. Dewey, H.I. Akbarali, Differences in the characteristics of tolerance to mu-opioid receptor agonists in the colon from wild type and beta-arrestin2 knockout mice, Eur J Pharmacol 685(1-3) (2012) 133-40.
[692] D.A. Zidar, Endogenous ligand bias by chemokines: implications at the front lines of infection and leukocyte trafficking, Endocr Metab Immune Disord Drug Targets 11(2) (2011) 120-31.
[693] L.I. Jiang, J. Collins, R. Davis, K.M. Lin, D. DeCamp, T. Roach, R. Hsueh, R.A. Rebres, E.M. Ross, R. Taussig, I. Fraser, P.C. Sternweis, Use of a cAMP BRET sensor to characterize a novel regulation of cAMP by the sphingosine 1-phosphate/G13 pathway, J Biol Chem 282(14) (2007) 10576-84.
[694] A. Christopoulos, Assessing the distribution of parameters in models of ligand-receptor interaction: to log or not to log, Trends Pharmacol Sci 19(9) (1998) 351-7.
[695] P. Leff, D.J. Prentice, H. Giles, G.R. Martin, J. Wood, Estimation of agonist affinity and efficacy by direct, operational model-fitting, Journal of pharmacological methods 23(3) (1990) 225-37.
[696] H.J. Motulsky, L.A. Ransnas, Fitting curves to data using nonlinear regression: a practical and nonmathematical review, Faseb j 1(5) (1987) 365-74.
[697] S. Wold, K. Esbensen, P. Geladi, Principal component analysis, Chemometrics and Intelligent Laboratory Systems 2(1–3) (1987) 37-52.
[698] F. Pedregosa, Ga, #235, l. Varoquaux, A. Gramfort, V. Michel, B. Thirion, O. Grisel, M. Blondel, P. Prettenhofer, R. Weiss, V. Dubourg, J. Vanderplas, A. Passos, D. Cournapeau, M. Brucher, M. Perrot, #201, d. Duchesnay, Scikit-learn: Machine Learning in Python, J. Mach. Learn. Res. 12 (2011) 2825-2830.
[699] S.M. DeWire, S. Ahn, R.J. Lefkowitz, S.K. Shenoy, Beta-arrestins and cell signaling, Annual review of physiology 69 (2007) 483-510.

[700] D. Willoughby, D.M. Cooper, Organization and Ca2+ regulation of adenylyl cyclases in cAMP microdomains, Physiol Rev 87(3) (2007) 965-1010.
[701] J. Traynor, mu-Opioid receptors and regulators of G protein signaling (RGS) proteins: from a symposium on new concepts in mu-opioid pharmacology, Drug Alcohol Depend 121(3) (2012) 173-80.
[702] J. Fichna, A. Janecka, J. Costentin, J.-C. Do Rego, The Endomorphin System and Its Evolving Neurophysiological Role, Pharmacological Reviews 59(1) (2007) 88-123.
[703] T. Lonergan, A.K. Goodchild, M.J. Christie, P.M. Pilowsky, Mu opioid receptors in rat ventral medulla: effects of endomorphin-1 on phrenic nerve activity, Respir Physiol Neurobiol 138(2-3) (2003) 165-78.
[704] I.E. Goldberg, G.C. Rossi, S.R. Letchworth, J.P. Mathis, J. Ryan-Moro, L. Leventhal, W. Su, D. Emmel, E.A. Bolan, G.W. Pasternak, Pharmacological characterization of endomorphin-1 and endomorphin-2 in mouse brain, Journal of Pharmacology and Experimental Therapeutics 286(2) (1998) 1007-1013.
[705] Y. Yu, Y. Cui, X. Wang, L.-h. Lai, C.-L. Wang, Y.-z. Fan, J. Liu, R. Wang, In vitro characterization of the effects of endomorphin 1 and 2, endogenous ligands for μ-opioid receptors, on mouse colonic motility, Biochemical Pharmacology 73(9) (2007) 1384-1393.
[706] M. Tonini, E. Fiori, B. Balestra, V. Spelta, G. D'Agostino, A. Di Nucci, N.C. Brecha, C. Sternini, Endomorphin-1 and endomorphin-2 activate μ-opioid receptors in myenteric neurons of the guinea-pig small intestine, Naunyn-Schmiedeberg's Archives of Pharmacology 358(6) (1998) 686-689.
[707] S. Sakurada, T. Hayashi, M. Yuhki, Differential antinociceptive effects induced by intrathecally-administered endomorphin-1 and endomorphin-2 in mice, Jpn J Pharmacol 89(3) (2002) 221-3.
[708] M. Terashvili, H.E. Wu, E. Schwasinger, L.F. Tseng, Paradoxical hyperalgesia induced by mu-opioid receptor agonist endomorphin-2, but not endomorphin-1, microinjected into the centromedial amygdala of the rat, Eur J Pharmacol 554(2-3) (2007) 137-44.
[709] D. Vigano, T. Rubino, G. Di Chiara, I. Ascari, P. Massi, D. Parolaro, Mu opioid receptor signaling in morphine sensitization, Neuroscience 117(4) (2003) 921-9.
[710] P. Sanchez-Blazquez, P. Gomez-Serranillos, J. Garzon, Agonists determine the pattern of G-protein activation in mu-opioid receptor-mediated supraspinal analgesia, Brain Res Bull 54(2) (2001) 229-35.
[711] J.D. Urban, W.P. Clarke, M. von Zastrow, D.E. Nichols, B. Kobilka, H. Weinstein, J.A. Javitch, B.L. Roth, A. Christopoulos, P.M. Sexton, K.J. Miller, M. Spedding, R.B. Mailman, Functional Selectivity and Classical Concepts of Quantitative Pharmacology, Journal of Pharmacology and Experimental Therapeutics 320(1) (2007) 1-13.
[712] K.L. White, A.P. Scopton, M.L. Rives, R.V. Bikbulatov, P.R. Polepally, P.J. Brown, T. Kenakin, J.A. Javitch, J.K. Zjawiony, B.L. Roth, Identification of novel functionally selective kappa-opioid receptor scaffolds, Mol Pharmacol 85(1) (2014) 83-90.
[713] G.L. Thompson, J.R. Lane, T. Coudrat, P.M. Sexton, A. Christopoulos, M. Canals, Biased Agonism of Endogenous Opioid Peptides at the mu-Opioid Receptor, Mol Pharmacol 88(2) (2015) 335-46.
[714] I. Charfi, K. Nagi, O. Mnie-Filali, D. Thibault, G. Balboni, P.W. Schiller, L.E. Trudeau, G. Pineyro, Ligand- and cell-dependent determinants of internalization and cAMP modulation by delta opioid receptor (DOR) agonists, Cell Mol Life Sci 71(8) (2014) 1529-46.
[715] B.A. Evans, N. Broxton, J. Merlin, M. Sato, D.S. Hutchinson, A. Christopoulos, R.J. Summers, Quantification of functional selectivity at the human alpha(1A)-adrenoceptor, Mol Pharmacol 79(2) (2011) 298-307.

[716] Y. Namkung, O. Radresa, S. Armando, D. Devost, A. Beautrait, C. Le Gouill, S.A. Laporte, Quantifying biased signaling in GPCRs using BRET-based biosensors, Methods (San Diego, Calif.) (2015).
[717] D. Wootten, E.E. Savage, F.S. Willard, A.B. Bueno, K.W. Sloop, A. Christopoulos, P.M. Sexton, Differential activation and modulation of the glucagon-like peptide-1 receptor by small molecule ligands, Mol Pharmacol 83(4) (2013) 822-34.
[718] A.G. Soto, T.H. Smith, B. Chen, S. Bhattacharya, I.C. Cordova, T. Kenakin, N. Vaidehi, J. Trejo, N-linked glycosylation of protease-activated receptor-1 at extracellular loop 2 regulates G-protein signaling bias, Proc Natl Acad Sci U S A (2015).
[719] M. Szabo, C. Klein Herenbrink, A. Christopoulos, J.R. Lane, B. Capuano, Structure-activity relationships of privileged structures lead to the discovery of novel biased ligands at the dopamine D(2) receptor, J Med Chem 57(11) (2014) 4924-39.
[720] T. Kenakin, The Effective Application of Biased Signaling to New Drug Discovery, Mol Pharmacol (2015).
[721] N. Tschammer, S. Bollinger, T. Kenakin, P. Gmeiner, Histidine 6.55 is a major determinant of ligand-biased signaling in dopamine D2L receptor, Mol Pharmacol 79(3) (2011) 575-85.
[722] H.O. Onaran, S. Rajagopal, T. Costa, What is biased efficacy? Defining the relationship between intrinsic efficacy and free energy coupling, Trends Pharmacol Sci 35(12) (2014) 639-47.
[723] G. Pineyro, E. Archer-Lahlou, Ligand-specific receptor states: implications for opiate receptor signalling and regulation, Cell Signal 19(1) (2007) 8-19.
[724] L.J. Leontiadis, M.P. Papakonstantinou, Z. Georgoussi, Regulator of G protein signaling 4 confers selectivity to specific G proteins to modulate mu- and delta-opioid receptor signaling, Cell Signal 21(7) (2009) 1218-28.
[725] K.L. Lan, H. Zhong, M. Nanamori, R.R. Neubig, Rapid kinetics of regulator of G-protein signaling (RGS)-mediated Galphai and Galphao deactivation. Galpha specificity of RGS4 AND RGS7, J Biol Chem 275(43) (2000) 33497-503.
[726] J.N. Talbot, D.L. Roman, M.J. Clark, R.A. Roof, J.J. Tesmer, R.R. Neubig, J.R. Traynor, Differential modulation of mu-opioid receptor signaling to adenylyl cyclase by regulators of G protein signaling proteins 4 or 8 and 7 in permeabilised C6 cells is Galpha subtype dependent, J Neurochem 112(4) (2010) 1026-34.
[727] C. Klein Herenbrink, D.A. Sykes, P. Donthamsetti, M. Canals, T. Coudrat, J. Shonberg, P.J. Scammells, B. Capuano, P.M. Sexton, S.J. Charlton, J.A. Javitch, A. Christopoulos, J.R. Lane, The role of kinetic context in apparent biased agonism at GPCRs, Nature communications 7 (2016) 10842.
[728] M.J. Clark, J.J. Linderman, J.R. Traynor, Endogenous Regulators of G Protein Signaling Differentially Modulate Full and Partial μ-Opioid Agonists at Adenylyl Cyclase as Predicted by a Collision Coupling Model, Molecular Pharmacology 73(5) (2008) 1538-1548.
[729] T. Koch, S. Schulz, H. Schroder, R. Wolf, E. Raulf, V. Hollt, Carboxyl-terminal splicing of the rat mu opioid receptor modulates agonist-mediated internalization and receptor resensitization, J Biol Chem 273(22) (1998) 13652-7.
[730] A. Knapman, M. Santiago, Y.P. Du, P.R. Bennallack, M.J. Christie, M. Connor, A Continuous, Fluorescence-based Assay of mu-Opioid Receptor Activation in AtT-20 Cells, J Biomol Screen 26 (2012) 26.
[731] H.B. Tudashki, D.N. Robertson, P.W. Schiller, G. Pineyro, Endocytic profiles of delta-opioid receptor ligands determine the duration of rapid but not sustained cAMP responses, Mol Pharmacol 85(1) (2014) 148-61.
[732] R. Irannejad, J.C. Tomshine, J.R. Tomshine, M. Chevalier, J.P. Mahoney, J. Steyaert, S.G. Rasmussen, R.K. Sunahara, H. El-Samad, B. Huang, M. von Zastrow,

Conformational biosensors reveal GPCR signalling from endosomes, Nature 495(7442) (2013) 534-8.
[733] R.K. Perera, V.O. Nikolaev, Compartmentation of cAMP signalling in cardiomyocytes in health and disease, Acta physiologica (Oxford, England) 207(4) (2013) 650-62.
[734] R. Taussig, W.J. Tang, J.R. Hepler, A.G. Gilman, Distinct patterns of bidirectional regulation of mammalian adenylyl cyclases, J Biol Chem 269(8) (1994) 6093-100.
[735] R. Taussig, J.A. Iniguez-Lluhi, A.G. Gilman, Inhibition of adenylyl cyclase by Gi alpha, Science 261(5118) (1993) 218-21.
[736] J. Chen, R. Iyengar, Inhibition of cloned adenylyl cyclases by mutant-activated Gi-alpha and specific suppression of type 2 adenylyl cyclase inhibition by phorbol ester treatment, J Biol Chem 268(17) (1993) 12253-6.
[737] B.K. Atwood, J. Lopez, J. Wager-Miller, K. Mackie, A. Straiker, Expression of G protein-coupled receptors and related proteins in HEK293, AtT20, BV2, and N18 cell lines as revealed by microarray analysis, BMC genomics 12 (2011) 14.
[738] K.M. DiMattio, F.J. Ehlert, L.Y. Liu-Chen, Intrinsic relative activities of kappa opioid agonists in activating Galpha proteins and internalizing receptor: Differences between human and mouse receptors, Eur J Pharmacol 761 (2015) 235-244.
[739] M.J. Lohse, S. Nuber, C. Hoffmann, Fluorescence/bioluminescence resonance energy transfer techniques to study G-protein-coupled receptor activation and signaling, Pharmacol Rev 64(2) (2012) 299-336.
[740] N.G. Tsvetanova, M. von Zastrow, Spatial encoding of cyclic AMP signaling specificity by GPCR endocytosis, Nature chemical biology 10(12) (2014) 1061-1065.
[741] V.O. Nikolaev, M. Bünemann, E. Schmitteckert, M.J. Lohse, S. Engelhardt, Cyclic AMP Imaging in Adult Cardiac Myocytes Reveals Far-Reaching β1-Adrenergic but Locally Confined β2-Adrenergic Receptor–Mediated Signaling, Circulation Research 99(10) (2006) 1084-1091.
[742] K. Ahlbeck, Opioids: a two-faced Janus, Current Medical Research and Opinion 27(2) (2011) 439-448.
[743] T.-H. Lan, Q. Liu, C. Li, G. Wu, N.A. Lambert, Sensitive and High Resolution Localization and Tracking of Membrane Proteins in Live Cells with BRET, Traffic (Copenhagen, Denmark) 13(11) (2012) 1450-1456.
[744] D.D. Jensen, M.L. Halls, J.E. Murphy, M. Canals, F. Cattaruzza, D.P. Poole, T. Lieu, H.W. Koon, C. Pothoulakis, N.W. Bunnett, Endothelin-converting enzyme 1 and beta-arrestins exert spatiotemporal control of substance P-induced inflammatory signals, J Biol Chem 289(29) (2014) 20283-94.
[745] F. Schmidlin, O. Déry, K.O. DeFea, L. Slice, S. Patierno, C. Sternini, E.F. Grady, N.W. Bunnett, Dynamin and Rab5a-dependent Trafficking and Signaling of the Neurokinin 1 Receptor, Journal of Biological Chemistry 276(27) (2001) 25427-25437.
[746] C.D. Harvey, A.G. Ehrhardt, C. Cellurale, H. Zhong, R. Yasuda, R.J. Davis, K. Svoboda, A genetically encoded fluorescent sensor of ERK activity, Proc Natl Acad Sci U S A 105(49) (2008) 19264-9.
[747] J.D. Violin, J. Zhang, R.Y. Tsien, A.C. Newton, A genetically encoded fluorescent reporter reveals oscillatory phosphorylation by protein kinase C, The Journal of cell biology 161(5) (2003) 899-909.
[748] U. Klein, G. Gimpl, F. Fahrenholz, Alteration of the Myometrial Plasma Membrane Cholesterol Content with .beta.-Cyclodextrin Modulates the Binding Affinity of the Oxytocin Receptor, Biochemistry 34(42) (1995) 13784-13793.
[749] M.L. Halls, D.P. Poole, A.M. Ellisdon, C.J. Nowell, M. Canals, Methods in Molecular Biology, Springer, New York2015, pp. 131–161.
[750] J. Schindelin, I. Arganda-Carreras, E. Frise, V. Kaynig, M. Longair, T. Pietzsch, S. Preibisch, C. Rueden, S. Saalfeld, B. Schmid, J.-Y. Tinevez, D.J. White, V. Hartenstein,

K. Eliceiri, P. Tomancak, A. Cardona, Fiji: an open-source platform for biological-image analysis, Nat Meth 9(7) (2012) 676-682.
[751] E. Kardash, J. Bandemer, E. Raz, Imaging protein activity in live embryos using fluorescence resonance energy transfer biosensors, Nat. Protocols 6(12) (2011) 1835-1846.
[752] D.D. Jensen, C.B. Godfrey, C. Niklas, M. Canals, M. Kocan, D.P. Poole, J.E. Murphy, F. Alemi, G.S. Cottrell, C. Korbmacher, N.A. Lambert, N.W. Bunnett, C.U. Corvera, The Bile Acid Receptor TGR5 Does Not Interact with β-Arrestins or Traffic to Endosomes but Transmits Sustained Signals from Plasma Membrane Rafts, Journal of Biological Chemistry 288(32) (2013) 22942-22960.
[753] M. Freissmuth, S. Boehm, W. Beindl, P. Nickel, A.P. Ijzerman, M. Hohenegger, C. Nanoff, Suramin analogues as subtype-selective G protein inhibitors, Molecular Pharmacology 49(4) (1996) 602-611.
[754] T. Katada, M. Ui, Direct modification of the membrane adenylate cyclase system by islet-activating protein due to ADP-ribosylation of a membrane protein, Proceedings of the National Academy of Sciences 79(10) (1982) 3129-3133.
[755] L. von Kleist, W. Stahlschmidt, H. Bulut, K. Gromova, D. Puchkov, Mark J. Robertson, Kylie A. MacGregor, N. Tomilin, A. Pechstein, N. Chau, M. Chircop, J. Sakoff, Jens P. von Kries, W. Saenger, H.-G. Kräusslich, O. Shupliakov, Phillip J. Robinson, A. McCluskey, V. Haucke, Role of the Clathrin Terminal Domain in Regulating Coated Pit Dynamics Revealed by Small Molecule Inhibition, Cell 146(3) (2011) 471-484.
[756] J. Herskovits, C. Burgess, R. Obar, R. Vallee, Effects of mutant rat dynamin on endocytosis, The Journal of cell biology 122(3) (1993) 565-578.
[757] J.K. Scott, S.F. Huang, B.P. Gangadhar, G.M. Samoriski, P. Clapp, R.A. Gross, R. Taussig, A.V. Smrcka, Evidence that a protein-protein interaction 'hot spot' on heterotrimeric G protein βγ subunits is used for recognition of a subclass of effectors, The EMBO journal 20(4) (2001) 767-776.
[758] W.J. Koch, B.E. Hawes, J. Inglese, L.M. Luttrell, R.J. Lefkowitz, Cellular expression of the carboxyl terminus of a G protein-coupled receptor kinase attenuates G beta gamma-mediated signaling, Journal of Biological Chemistry 269(8) (1994) 6193-6197.
[759] D. Toullec, P. Pianetti, H. Coste, P. Bellevergue, T. Grand-Perret, M. Ajakane, V. Baudet, P. Boissin, E. Boursier, F. Loriolle, The bisindolylmaleimide GF 109203X is a potent and selective inhibitor of protein kinase C, Journal of Biological Chemistry 266(24) (1991) 15771-15781.
[760] M. Gschwendt, S. Dieterich, J. Rennecke, W. Kittstein, H.-J. Mueller, F.-J. Johannes, Inhibition of protein kinase C μ by various inhibitors. Inhibition from protein kinase c isoenzymes, FEBS letters 392(2) (1996) 77-80.
[761] F.L. Smith, B.H. Gabra, P.A. Smith, M.C. Redwood, W.L. Dewey, Determination of the role of conventional, novel and atypical PKC isoforms in the expression of morphine tolerance in mice, Pain 127(1-2) (2007) 129-39.
[762] G. Martiny-Baron, M.G. Kazanietz, H. Mischak, P.M. Blumberg, G. Kochs, H. Hug, D. Marmé, C. Schächtele, Selective inhibition of protein kinase C isozymes by the indolocarbazole Gö 6976, Journal of Biological Chemistry 268(13) (1993) 9194-7.
[763] J.A. Johnson, M.O. Gray, C.-H. Chen, D. Mochly-Rosen, A Protein Kinase C Translocation Inhibitor as an Isozyme-selective Antagonist of Cardiac Function, Journal of Biological Chemistry 271(40) (1996) 24962-24966.
[764] Y. Ohtani, T. Irie, K. Uekama, K. Fukunaga, J. Pitha, Differential effects of α-, β- and γ-cyclodextrins on human erythrocytes, European Journal of Biochemistry 186(1-2) (1989) 17-22.

[765] A.W. Norman, R.A. Demel, B. de Kruyff, L.L.M. van Deenen, Studies on the Biological Properties of Polyene Antibiotics: EVIDENCE FOR THE DIRECT INTERACTION OF FILIPIN WITH CHOLESTEROL, Journal of Biological Chemistry 247(6) (1972) 1918-1929.
[766] A.I. Basbaum, D.M. Bautista, G. Scherrer, D. Julius, Cellular and Molecular Mechanisms of Pain, Cell 139(2) (2009) 267-284.
[767] K.A. DeFea, Beta-arrestins as regulators of signal termination and transduction: How do they determine what to scaffold?, Cellular Signalling 23(4) (2011) 621-629.
[768] J.D. Robinson, J.A. Pitcher, G protein-coupled receptor kinase 2 (GRK2) is a Rho-activated scaffold protein for the ERK MAP kinase cascade, Cellular Signalling 25(12) (2013) 2831-2839.
[769] P. Penela, C. Ribas, I. Aymerich, N. Eijkelkamp, O. Barreiro, C.J. Heijnen, A. Kavelaars, F. Sánchez-Madrid, F. Mayor, G protein-coupled receptor kinase 2 positively regulates epithelial cell migration, The EMBO journal 27(8) (2008) 1206-1218.
[770] H. Haberstock-Debic, M. Wein, M. Barrot, E.E. Colago, Z. Rahman, R.L. Neve, V.M. Pickel, E.J. Nestler, M. von Zastrow, A.L. Svingos, Morphine acutely regulates opioid receptor trafficking selectively in dendrites of nucleus accumbens neurons, J Neurosci 23(10) (2003) 4324-32.
[771] C.P. Bailey, F.L. Smith, E. Kelly, W.L. Dewey, G. Henderson, How important is protein kinase C in μ-opioid receptor desensitization and morphine tolerance?, Trends in Pharmacological Sciences 27(11) (2006) 558-565.
[772] X.Y. Hua, A. Moore, S. Malkmus, S.F. Murray, N. Dean, T.L. Yaksh, M. Butler, Inhibition of spinal protein kinase Calpha expression by an antisense oligonucleotide attenuates morphine infusion-induced tolerance, Neuroscience 113(1) (2002) 99-107.
[773] F.L. Smith, A.B. Lohmann, W.L. Dewey, Involvement of phospholipid signal transduction pathways in morphine tolerance in mice, British Journal of Pharmacology 128(1) (1999) 220-226.
[774] Y. Qiu, W. Zhao, Y. Wang, J.-R. Xu, E. Huie, S. Jiang, Y.-H. Yan, H.H. Loh, H.-Z. Chen, P.-Y. Law, FK506-Binding Protein 12 Modulates μ-Opioid Receptor Phosphorylation and Protein Kinase Cε–Dependent Signaling by Its Direct Interaction with the Receptor, Molecular Pharmacology 85(1) (2014) 37-49.
[775] R. Winstel, S. Freund, C. Krasel, E. Hoppe, M.J. Lohse, Protein kinase cross-talk: membrane targeting of the beta-adrenergic receptor kinase by protein kinase C, Proceedings of the National Academy of Sciences 93(5) (1996) 2105-2109.
[776] P. Huang, W. Xu, S.-I. Yoon, C. Chen, P.L.-G. Chong, E.M. Unterwald, L.-Y. Liu-Chen, Agonist treatment did not affect association of mu opioid receptors with lipid rafts and cholesterol reduction had opposite effects on the receptor-mediated signaling in rat brain and CHO cells, Brain Research 1184 (2007) 46-56.
[777] G. Gaibelet, C. Millot, C. Lebrun, S. Ravault, A. Saulière, A. André, B. Lagane, A. Lopez, Cholesterol content drives distinct pharmacological behaviours of μ-opioid receptor in different microdomains of the CHO plasma membrane, Molecular membrane biology 25(5) (2008) 423-435.
[778] L. Moulédous, S. Merker, J. Neasta, B. Roux, J.-M. Zajac, C. Mollereau, Neuropeptide FF-sensitive confinement of mu opioid receptor does not involve lipid rafts in SH-SY5Y cells, Biochemical and biophysical research communications 373(1) (2008) 80-84.
[779] K. Suzuki, K. Ritchie, E. Kajikawa, T. Fujiwara, A. Kusumi, Rapid hop diffusion of a G-protein-coupled receptor in the plasma membrane as revealed by single-molecule techniques, Biophysical journal 88(5) (2005) 3659-80.
[780] F. Daumas, N. Destainville, C. Millot, A. Lopez, D. Dean, L. Salomé, Confined Diffusion Without Fences of a G-Protein-Coupled Receptor as Revealed by Single Particle Tracking, Biophysical journal 84(1) (2003) 356-366.

[781] F. Daumas, N. Destainville, C. Millot, A. Lopez, D. Dean, L. Salomé, Interprotein interactions are responsible for the confined diffusion of a G-protein-coupled receptor at the cell surface, Biochemical Society Transactions 31(5) (2003) 1001-1005.
[782] A. Saulière, G. Gaibelet, C. Millot, S. Mazères, A. Lopez, L. Salomé, Diffusion of the mu opioid receptor at the surface of human neuroblastoma SH-SY5Y cells is restricted to permeable domains, FEBS letters 580(22) (2006) 5227-5231.
[783] A. Lopez, L. Salomé, Membrane functional organisation and dynamic of μ-opioid receptors, Cellular and Molecular Life Sciences 66(13) (2009) 2093-2108.
[784] A.I. Basbaum, H.L. Fields, Endogenous pain control systems: brainstem spinal pathways and endorphin circuitry, Annual review of neuroscience 7 (1984) 309-38.
[785] P. Mosinska, M. Zielinska, J. Fichna, Expression and physiology of opioid receptors in the gastrointestinal tract, Current opinion in endocrinology, diabetes, and obesity 23(1) (2016) 3-10.
[786] J. Guthrie, A.I. Basbaum, Colocalization of immunoreactive proenkephalin and prodynorphin products in medullary neurons of the rat, Neuropeptides 4(6) (1984) 437-45.
[787] R.K. Sunahara, C.W. Dessauer, A.G. Gilman, Complexity and diversity of mammalian adenylyl cyclases, Annu Rev Pharmacol Toxicol 36 (1996) 461-80.
[788] B.C. Chieng, D.J. Lee, Y.P. Du, P.B. Osborne, M.J. Christie, D. Massotte, Functional coupling of mu-receptor-Galphai-tethered proteins in AtT20 cells, Neuroreport 19(18) (2008) 1793-6.
[789] M.L. Halls, H.R. Yeatman, C.J. Nowell, G.L. Thompson, A.B. Gondin, S. Civciristov, N.W. Bunnett, N.A. Lambert, D.P. Poole, M. Canals, Plasma membrane localization of the μ-opioid receptor controls spatiotemporal signaling, Science Signaling 9(414) (2016).
[790] E.M. Rosethorne, M.E. Bradley, K. Gherbi, D.A. Sykes, A. Sattikar, J.D. Wright, E. Renard, A. Trifilieff, R.A. Fairhurst, S.J. Charlton, Long Receptor Residence Time of C26 Contributes to Super Agonist Activity at the Human beta2 Adrenoceptor, Mol Pharmacol 89(4) (2016) 467-75.
[791] D.J. Unett, J. Gatlin, T.L. Anthony, D.J. Buzard, S. Chang, C. Chen, X. Chen, H.T. Dang, J. Frazer, M.K. Le, A.J. Sadeque, C. Xing, I. Gaidarov, Kinetics of 5-HT2B receptor signaling: profound agonist-dependent effects on signaling onset and duration, J Pharmacol Exp Ther 347(3) (2013) 645-59.
[792] J.D. Hothersall, A.J. Brown, I. Dale, P. Rawlins, Can residence time offer a useful strategy to target agonist drugs for sustained GPCR responses?, Drug Discovery Today 21(1) (2016) 90-96.
[793] T. Koch, V. Hollt, Role of receptor internalization in opioid tolerance and dependence, Pharmacol Ther 117(2) (2008) 199-206.
[794] L. Martini, J.L. Whistler, The role of mu opioid receptor desensitization and endocytosis in morphine tolerance and dependence, Curr Opin Neurobiol 17(5) (2007) 556-64.
[795] R.H. Oakley, S.A. Laporte, J.A. Holt, L.S. Barak, M.G. Caron, §, Association of β-Arrestin with G Protein-coupled Receptors during Clathrin-mediated Endocytosis Dictates the Profile of Receptor Resensitization, Journal of Biological Chemistry 274(45) (1999) 32248-32257.
[796] E.F. Grady, A.M. Garland, P.D. Gamp, M. Lovett, D.G. Payan, N.W. Bunnett, Delineation of the endocytic pathway of substance P and its seven-transmembrane domain NK1 receptor, Molecular biology of the cell 6(5) (1995) 509-524.
[797] D.A. Sykes, D.M. Riddy, C. Stamp, M.E. Bradley, N. McGuiness, A. Sattikar, D. Guerini, I. Rodrigues, A. Glaenzel, M.R. Dowling, F. Mullershausen, S.J. Charlton, Investigating the molecular mechanisms through which FTY720-P causes persistent S1P1 receptor internalization, Br J Pharmacol 171(21) (2014) 4797-807.

[798] K.V. Andreassen, S.T. Hjuler, S.G. Furness, P.M. Sexton, A. Christopoulos, O. Nosjean, M.A. Karsdal, K. Henriksen, Prolonged calcitonin receptor signaling by salmon, but not human calcitonin, reveals ligand bias, PLoS One 9(3) (2014) e92042.
[799] C. Regnard, R. Twycross, M. Mihalyo, A. Wilcock, Loperamide, Journal of Pain and Symptom Management 42(2) (2011) 319-323.
[800] G. Gaudriault, D. Nouel, C. Dal Farra, A. Beaudet, J.P. Vincent, Receptor-induced internalization of selective peptidic mu and delta opioid ligands, J Biol Chem 272(5) (1997) 2880-8.
[801] S. Arttamangkul, V. Alvarez-Maubecin, G. Thomas, J.T. Williams, D.K. Grandy, Binding and internalization of fluorescent opioid peptide conjugates in living cells, Mol Pharmacol 58(6) (2000) 1570-80.
[802] M.C. Lee, C.M. Cahill, J.P. Vincent, A. Beaudet, Internalization and trafficking of opioid receptor ligands in rat cortical neurons, Synapse (New York, N.Y.) 43(2) (2002) 102-11.
[803] D. Roosterman, G.S. Cottrell, B.E. Padilla, L. Muller, C.B. Eckman, N.W. Bunnett, M. Steinhoff, Endothelin-converting enzyme 1 degrades neuropeptides in endosomes to control receptor recycling, Proceedings of the National Academy of Sciences of the United States of America 104(28) (2007) 11838-11843.
[804] G.S. Cottrell, B.E. Padilla, S. Amadesi, D.P. Poole, J.E. Murphy, M. Hardt, D. Roosterman, M. Steinhoff, N.W. Bunnett, Endosomal endothelin-converting enzyme-1. A regulator of β-arrestin-dependent ERK signaling, Journal of Biological Chemistry 284(33) (2009) 22411-22425.
[805] S. Oldfield, E. Braksator, I. Rodriguez-Martin, C.P. Bailey, L.F. Donaldson, G. Henderson, E. Kelly, C-terminal splice variants of the mu-opioid receptor: existence, distribution and functional characteristics, J Neurochem 104(4) (2008) 937-45.
[806] R.M. van Rijn, J.L. Whistler, M. Waldhoer, Opioid-receptor-heteromer-specific trafficking and pharmacology, Current opinion in pharmacology 10(1) (2010) 73-9.
[807] W. Fujita, I. Gomes, L.A. Devi, Revolution in GPCR signalling: opioid receptor heteromers as novel therapeutic targets: IUPHAR review 10, Br J Pharmacol 171(18) (2014) 4155-76.
[808] R. Rozenfeld, L.A. Devi, Receptor heterodimerization leads to a switch in signaling: beta-arrestin2-mediated ERK activation by mu-delta opioid receptor heterodimers, Faseb j 21(10) (2007) 2455-65.
[809] I. Gomes, A.P. Ijzerman, K. Ye, E.L. Maillet, L.A. Devi, G protein-coupled receptor heteromerization: a role in allosteric modulation of ligand binding, Mol Pharmacol 79(6) (2011) 1044-52.
[810] I. Gomes, W. Fujita, A. Gupta, S.A. Saldanha, A. Negri, C.E. Pinello, C. Eberhart, E. Roberts, M. Filizola, P. Hodder, L.A. Devi, Identification of a μ-δ opioid receptor heteromer-biased agonist with antinociceptive activity, Proceedings of the National Academy of Sciences of the United States of America 110(29) (2013) 12072-12077.
[811] A.M. Bender, N.W. Griggs, J.P. Anand, J.R. Traynor, E.M. Jutkiewicz, H.I. Mosberg, Asymmetric synthesis and in vitro and in vivo activity of tetrahydroquinolines featuring a diverse set of polar substitutions at the 6 position as mixed-efficacy mu opioid receptor/delta opioid receptor ligands, ACS Chem Neurosci 6(8) (2015) 1428-35.
[812] A.A. Harland, L. Yeomans, N.W. Griggs, J.P. Anand, I.D. Pogozheva, E.M. Jutkiewicz, J.R. Traynor, H.I. Mosberg, Further Optimization and Evaluation of Bioavailable, Mixed-Efficacy mu-Opioid Receptor (MOR) Agonists/delta-Opioid Receptor (DOR) Antagonists: Balancing MOR and DOR Affinities, J Med Chem 58(22) (2015) 8952-69.
[813] J.T. Lamberts, C.E. Smith, M.H. Li, S.L. Ingram, R.R. Neubig, J.R. Traynor, Differential control of opioid antinociception to thermal stimuli in a knock-in mouse

expressing regulator of G-protein signaling-insensitive Galphao protein, J Neurosci 33(10) (2013) 4369-77.
[814] P. Bisignano, N.T. Burford, Y. Shang, B. Marlow, K.E. Livingston, A.M. Fenton, K. Rockwell, L. Budenholzer, J.R. Traynor, S.W. Gerritz, A. Alt, M. Filizola, Ligand-Based Discovery of a New Scaffold for Allosteric Modulation of the mu-Opioid Receptor, Journal of chemical information and modeling 55(9) (2015) 1836-43.